



# Spatial Modulation for MIMO Wireless Systems

**Marco Di Renzo<sup>(1)</sup>, Harald Haas<sup>(2)</sup> and Ali Ghrayeb<sup>(3)</sup>**

<sup>(1)</sup> Laboratory of Signals and Systems (L2S), CNRS – SUPÉLEC – University of Paris-Sud XI  
3 rue Joliot-Curie, 91192 Gif-sur-Yvette, France  
[marco.direnzo@lss.supelec.fr](mailto:marco.direnzo@lss.supelec.fr)

<sup>(2)</sup> The University of Edinburgh, Institute for Digital Communications (IDCOM)  
Mayfield Road, Edinburgh, EH9 3JL, UK  
[h.haas@ed.ac.uk](mailto:h.haas@ed.ac.uk)

<sup>(3)</sup> Concordia University, Department of Electrical and Computer Engineering  
1455 de Maisonneuve West, Montreal, H3G 1M8, Canada  
[aghrayeb@ece.concordia.ca](mailto:aghrayeb@ece.concordia.ca)



**greenet**

<http://www.fp7-greenet.eu>

*IEEE Tutorial Presented at:  
WCNC, EW, VTC-Spring, ICC, VTC-Fall, CAMAD 2013*

# *Outline*

---

1. Introduction and Motivation behind SM-MIMO
2. History of SM Research and Research Groups Working on SM
3. Transmitter Design – Encoding
4. Receiver Design – Demodulation
5. Error Performance (Numerical Results and Main Trends)
6. Achievable Capacity
7. Channel State Information at the Transmitter
8. Imperfect Channel State Information at the Receiver
9. Multiple Access Interference
10. Energy Efficiency
11. Transmit-Diversity for SM
12. Spatially-Modulated Space-Time-Coded MIMO
13. Relay-Aided SM
14. SM in Heterogeneous Cellular Networks
15. SM for Visible Light Communications
16. Experimental Evaluation of SM
17. The Road Ahead – Open Research Challenges/Opportunities
18. Implementation Challenges of SM-MIMO

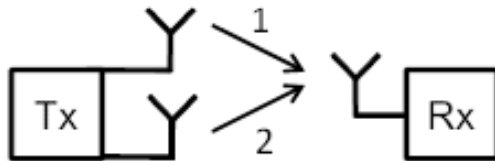
# *Outline*

---

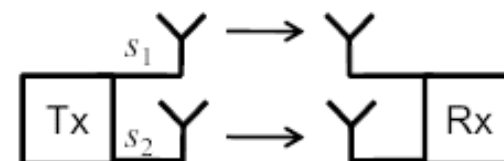
1. Introduction and Motivation behind SM-MIMO
2. History of SM Research and Research Groups Working on SM
3. Transmitter Design – Encoding
4. Receiver Design – Demodulation
5. Error Performance (Numerical Results and Main Trends)
6. Achievable Capacity
7. Channel State Information at the Transmitter
8. Imperfect Channel State Information at the Receiver
9. Multiple Access Interference
10. Energy Efficiency
11. Transmit-Diversity for SM
12. Spatially-Modulated Space-Time-Coded MIMO
13. Relay-Aided SM
14. SM in Heterogeneous Cellular Networks
15. SM for Visible Light Communications
16. Experimental Evaluation of SM
17. The Road Ahead – Open Research Challenges/Opportunities
18. Implementation Challenges of SM-MIMO

# Why MIMO?

•Diversity – STBC, etc.



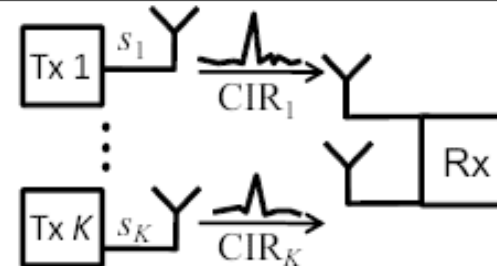
•Multiplexing – BLAST, etc.



•Beamforming



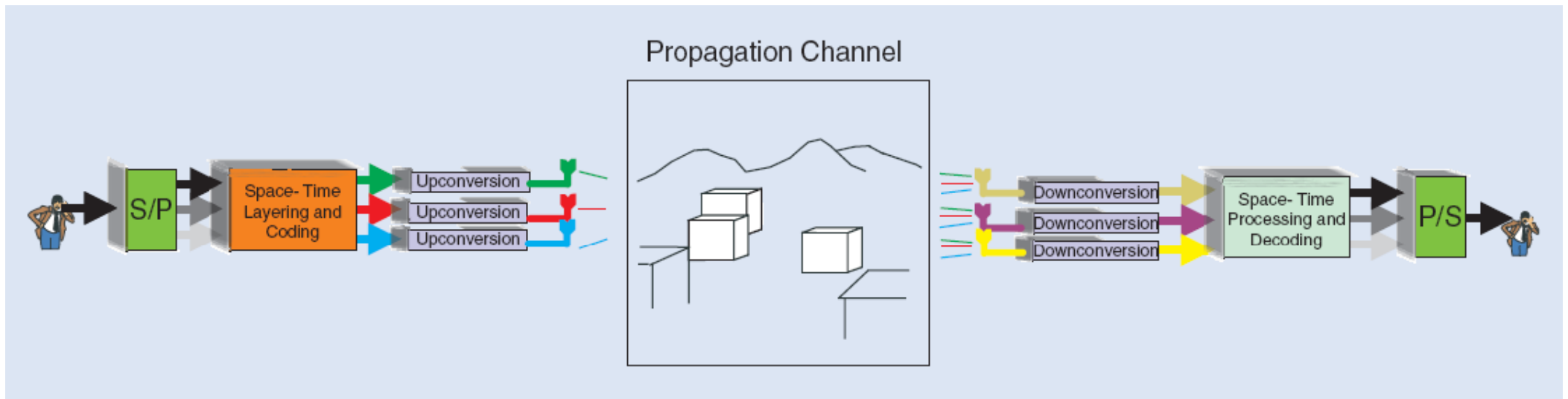
•Space Division Multiple Access



- ❑ Array gain (beamforming), spatial division multiple access
- ❑ Spatial multiplexing:  $\text{Rate} = \min(N_t, N_r) \log_2(1 + \text{SNR})$
- ❑ Reliability:  $\text{BEP} \sim \text{SNR}^{-(N_t N_r)}$



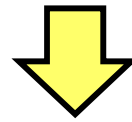
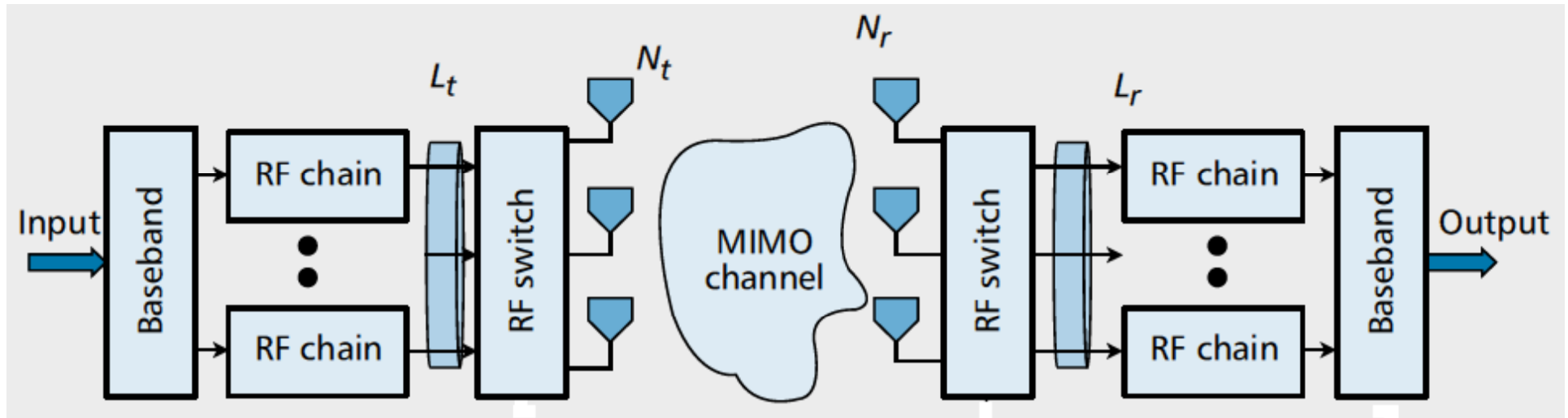
# Very Good, But...



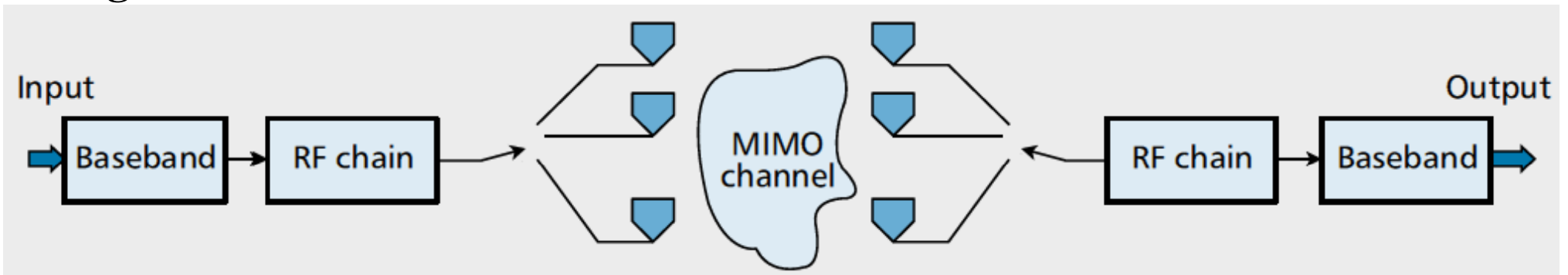
- ❑ Regardless of the use as diversity or spatial multiplexing system, the main drawback of conventional MIMO systems is the increased complexity, increased power/energy consumption, and high cost. **Why?**
  - **Inter-channel interference (ICI):** Introduced by coupling multiple symbols in time and space – signal processing complexity.
  - **Inter-antenna synchronization (IAS):** Detection algorithms require that all symbols are transmitted at the same time.
  - **Multiple radio frequency (RF) chains:** RF elements are expensive, bulky, no simple to implement, and do not follow Moore's law.
  - **Energy consumption:** The energy efficiency decreases linearly with the number of active antennas (RF chains) and it mostly depends on the Power Amplifiers (>60%) – EARTH model.

# Conventional vs. Single-RF MIMO

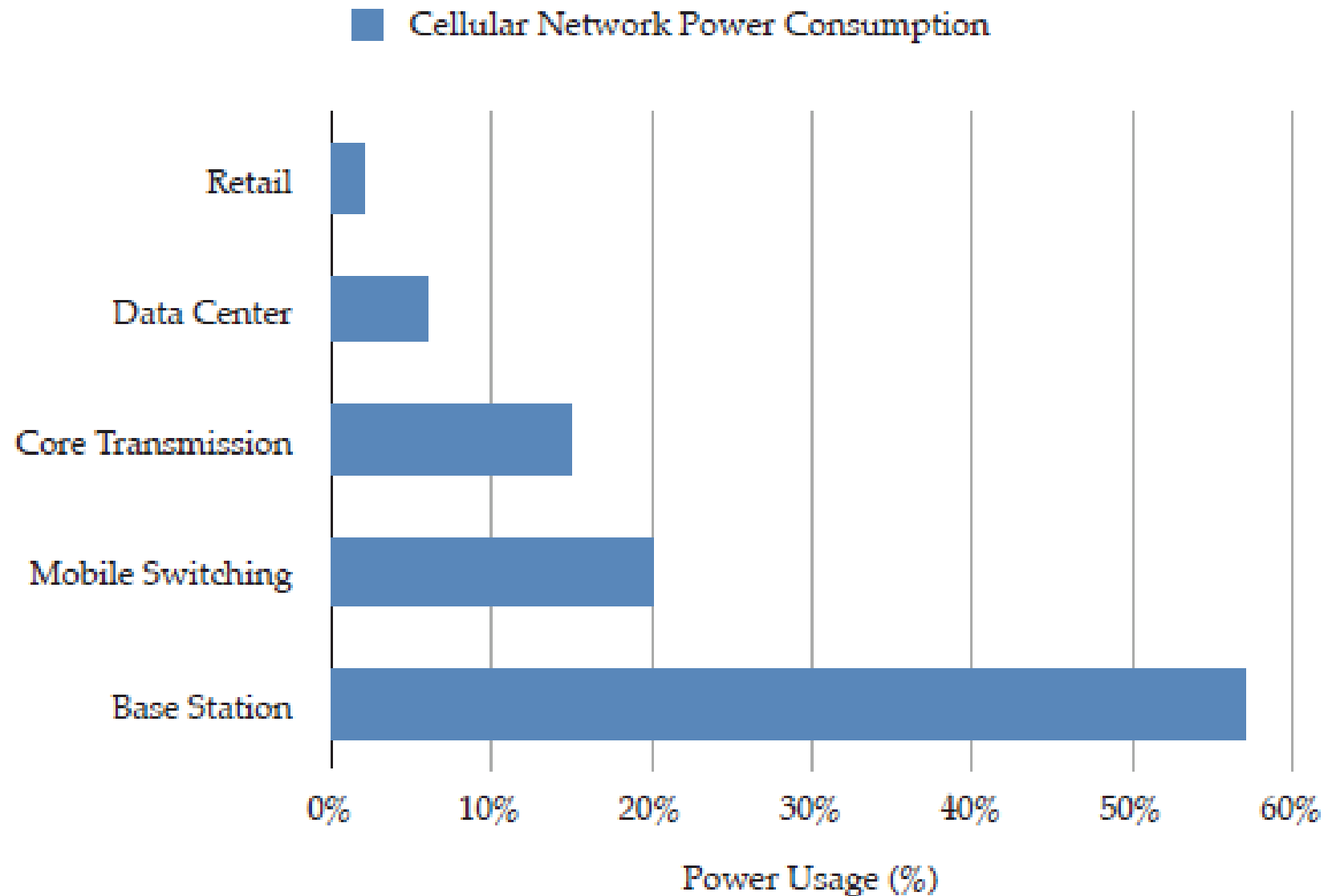
## Conventional MIMO



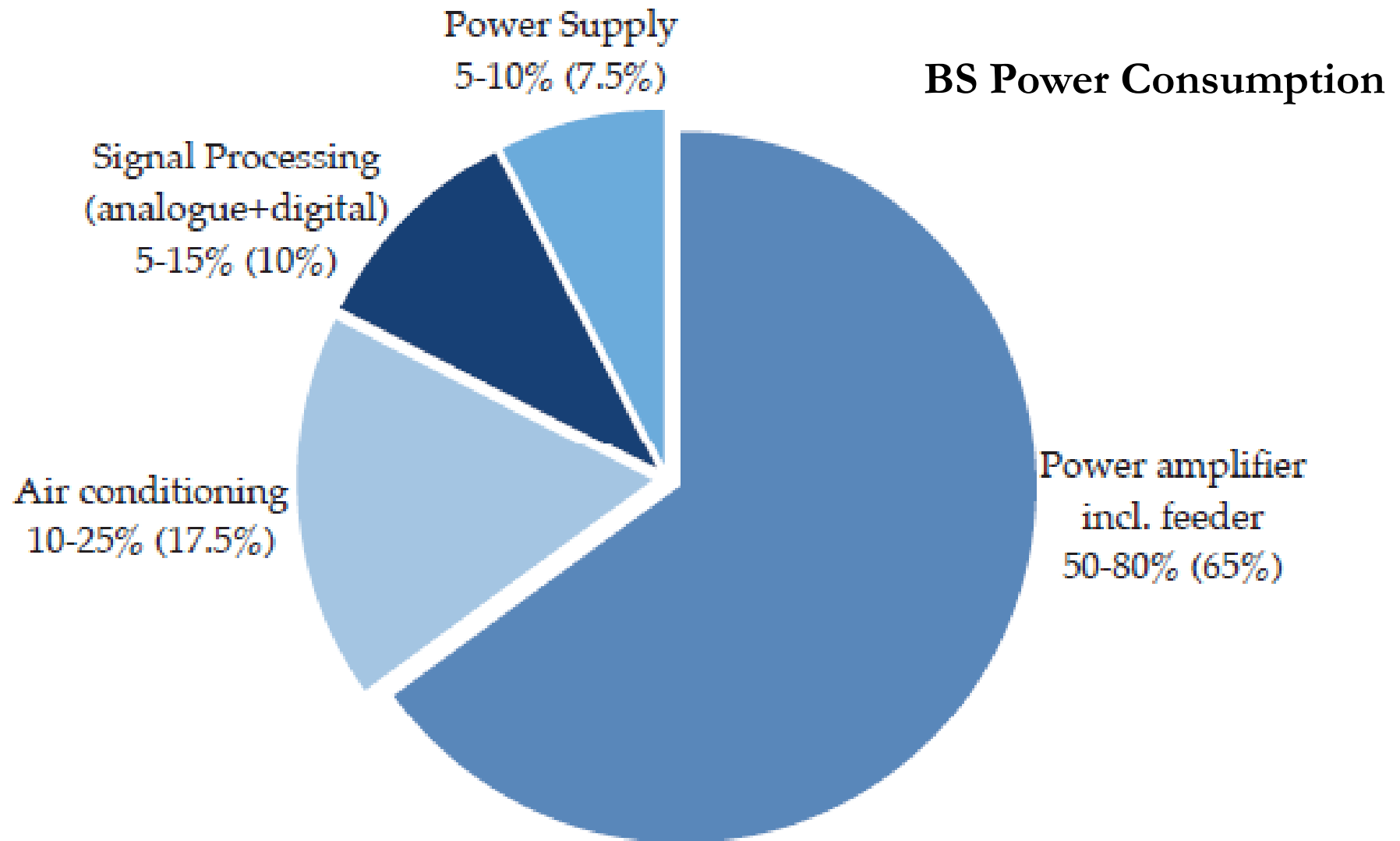
## Single-RF MIMO



# *The Energy Efficiency (EE) Challenge (1/3)*



## *The Energy Efficiency (EE) Challenge (2/3)*



# The Energy Efficiency (EE) Challenge (3/3)

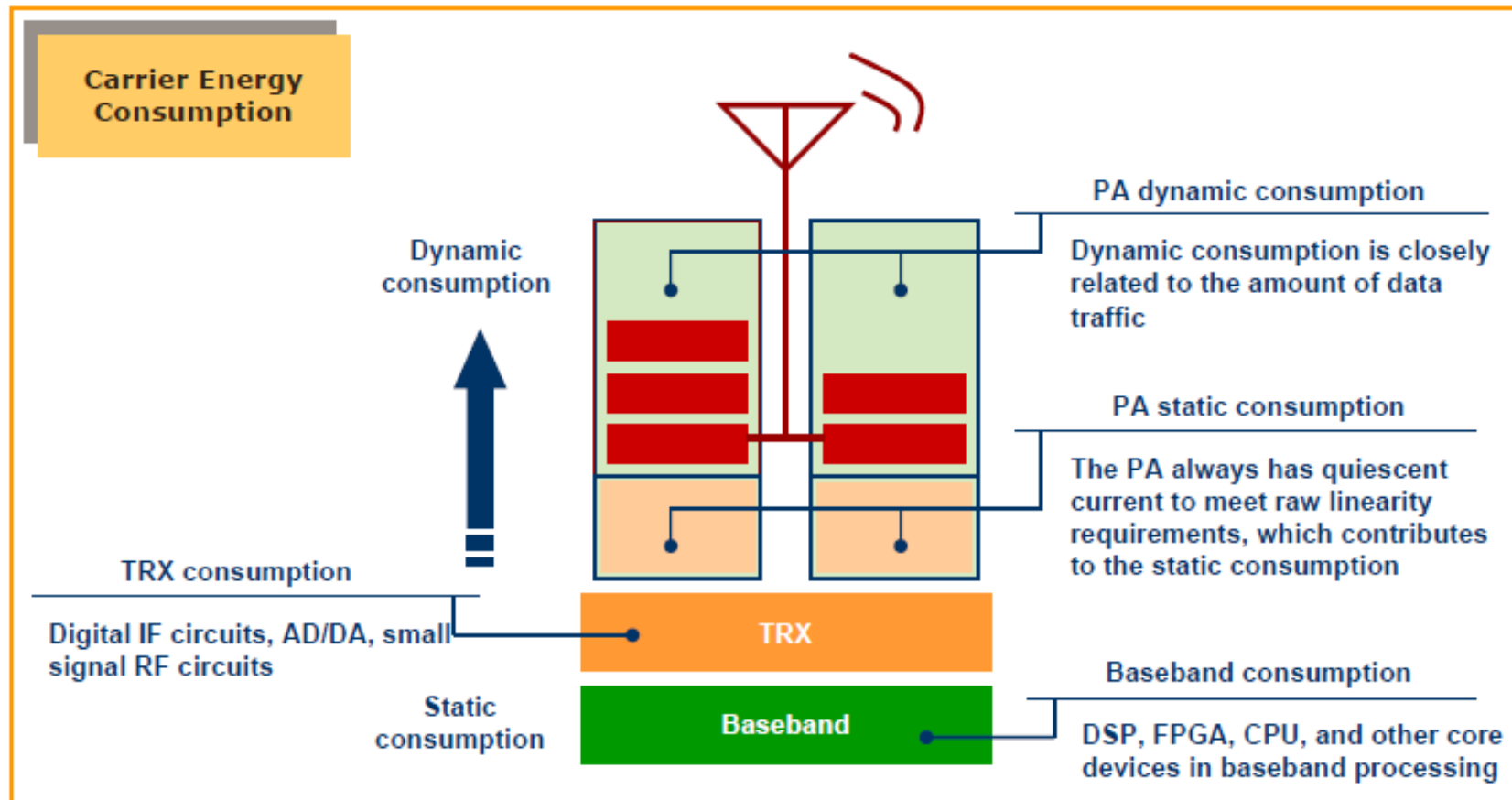
## Base Station Energy



### Energy Consumption Modeling

3E System Modeling

Basic Modeling  
(E for BTS/Site/  
Network levels, etc)



S. D. Gray, "Theoretical and Practical Considerations for the Design of Green Radio Networks", **IEEE VTC-2011 Spring**, Budapest, Hungary, May 2011.

3GPP TSG-RAN WG2 #67, "eNB power saving by changing antenna number", **R2-094677 from Huawei**:  
[http://www.3gpp.org/ftp/tsg\\_ran/WG2\\_RL2/TSGR2\\_67/Tdoclist/History/ADN\\_Tdoc\\_List\\_RAN2\\_67.htm](http://www.3gpp.org/ftp/tsg_ran/WG2_RL2/TSGR2_67/Tdoclist/History/ADN_Tdoc_List_RAN2_67.htm).

# Static Power: How Much Is It Important ?(1/2)

## MIMO Gain WITHOUT Considering Circuit Power

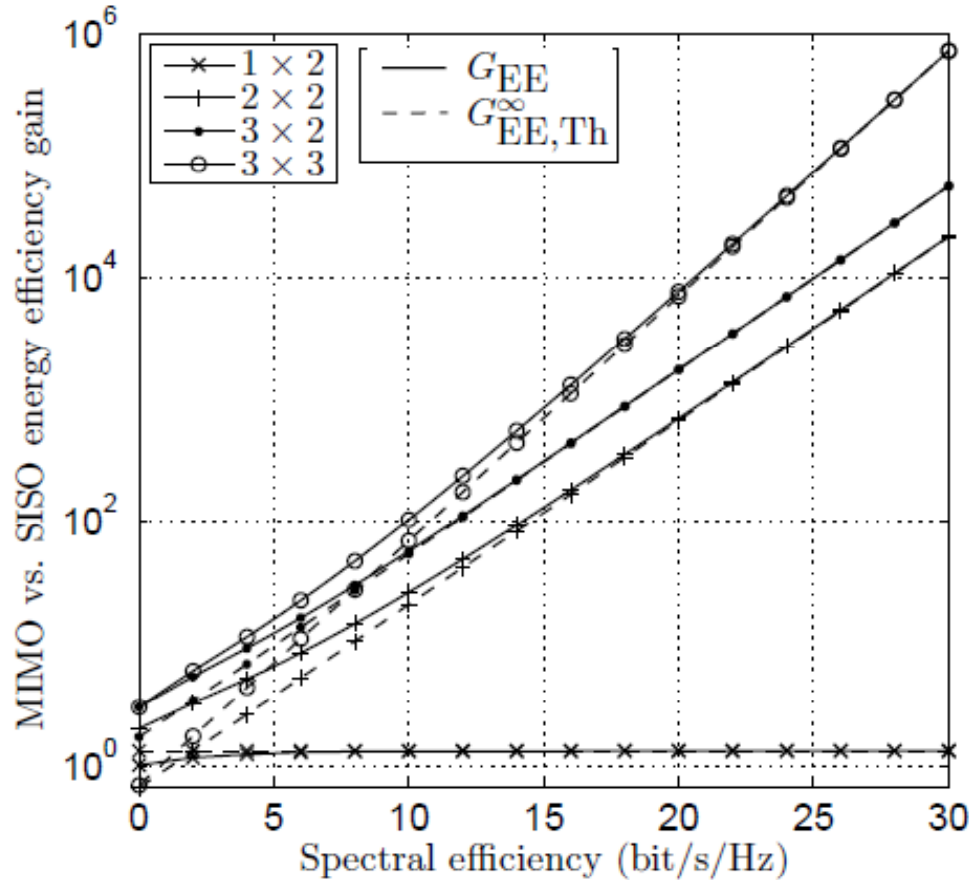


Fig. 6. MIMO vs. SISO EE gain against the SE when considering the theoretical PCM.

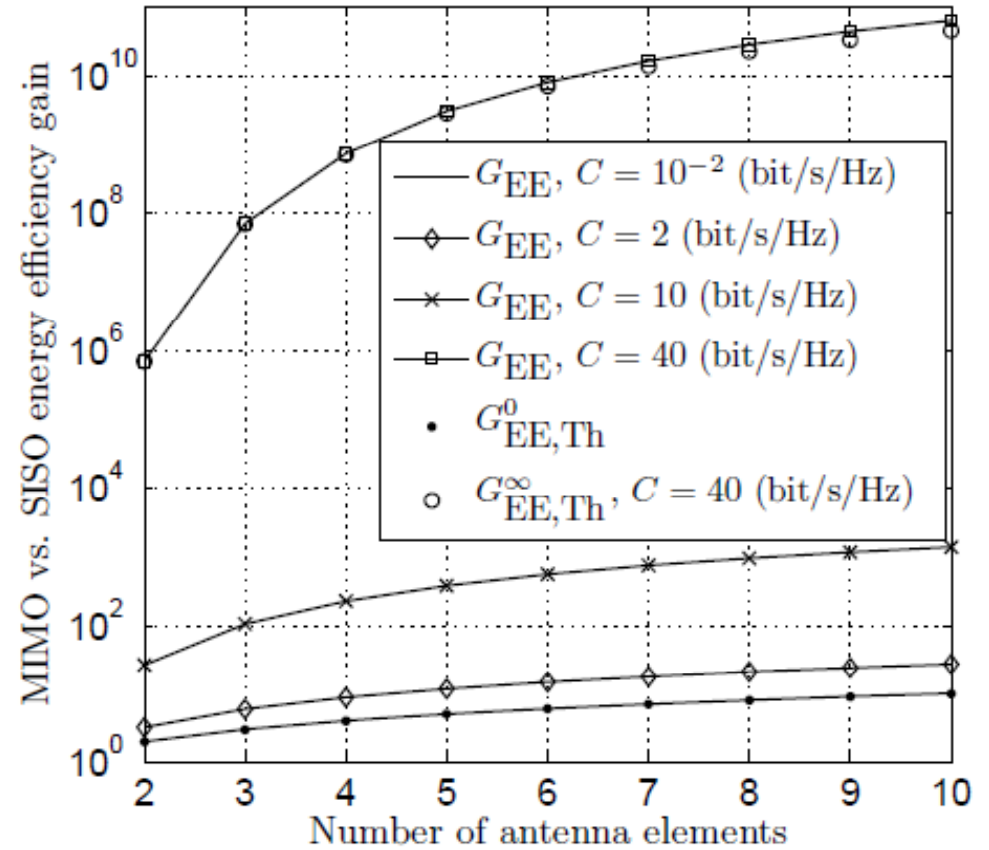


Fig. 8. MIMO vs. SISO EE gain against the number of antenna elements  $n_{\text{ant}} = t = r$  when considering the theoretical PCM.

# Static Power: How Much Is It Important ?(2/2)

## MIMO Gain Considering Circuit Power

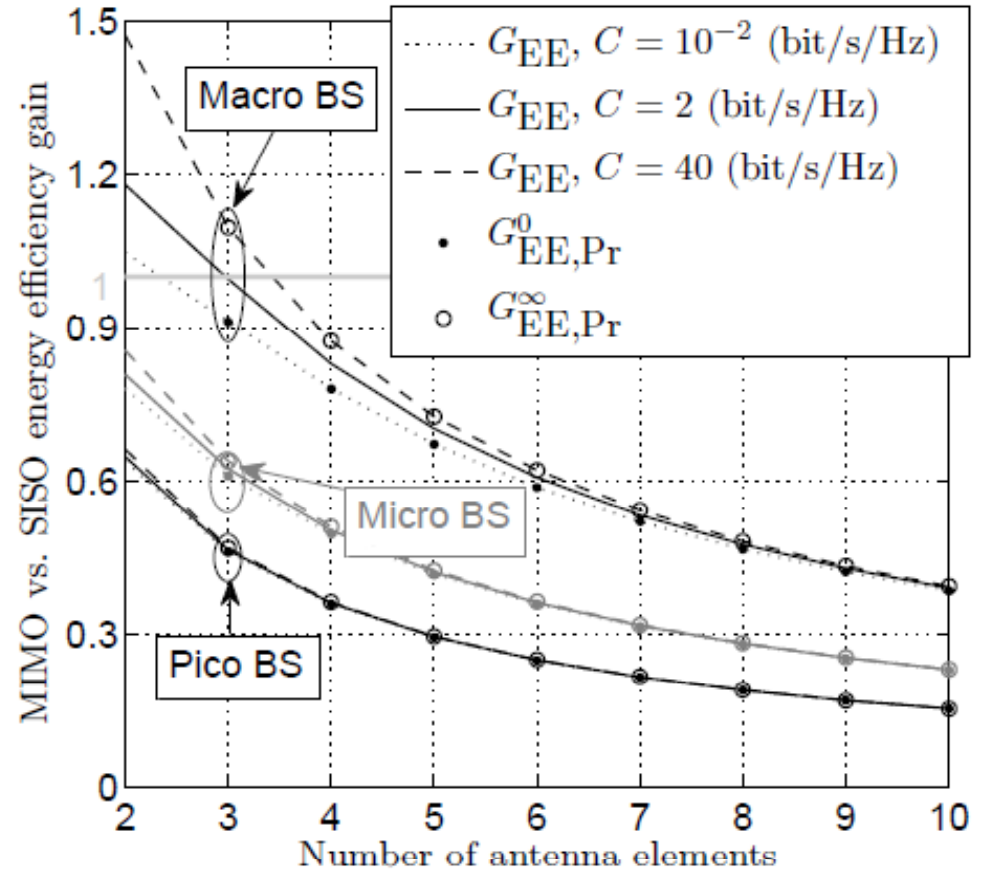
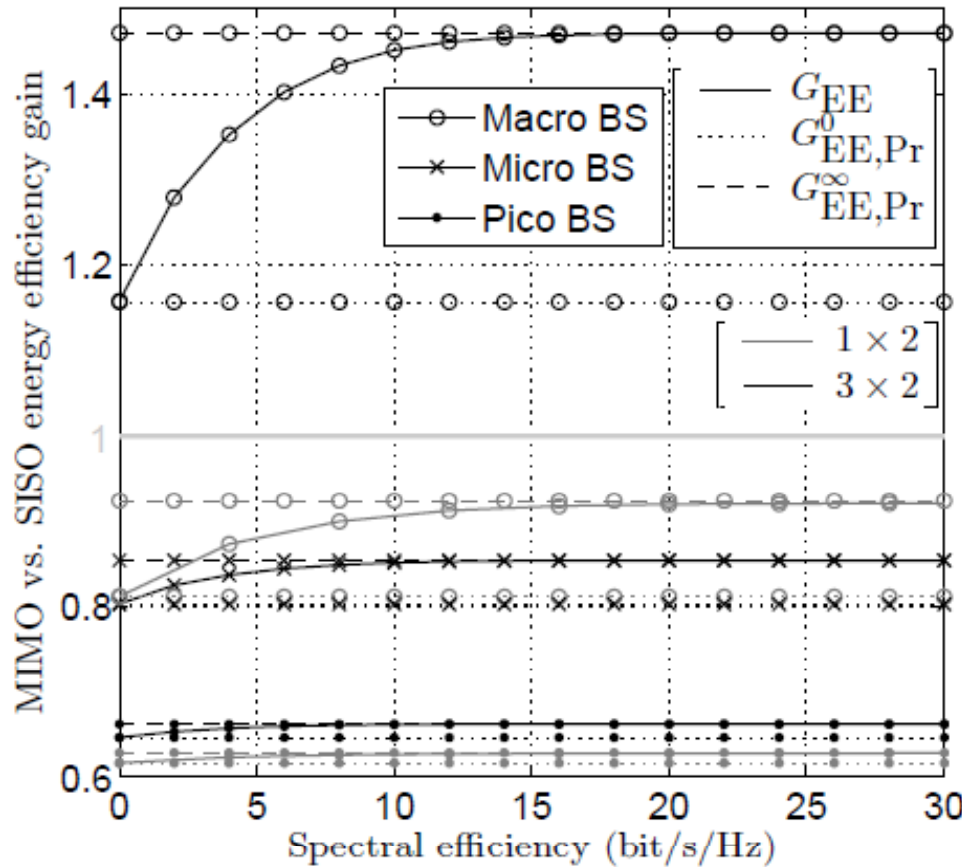


Fig. 7. MIMO vs. SISO EE gain against the SE for different types of BS when considering the double linear PCM of (6).

Fig. 9. MIMO vs. SISO EE gain against the number of antennas  $n_{\text{ant}} = t = r$  for different types of BS when considering the double linear PCM of (6).

## *SE vs. EE Tradeoff (1/2)*

- ❑ **SE-oriented systems are designed to maximize the capacity under peak or average power constraints**, which may lead to transmitting with the maximum allowed power for long periods, thus deviate from EE design.
- ❑ **EE is commonly defined as information bits per unit of transmit energy**. It has been studied from the information-theoretic perspective for various scenarios.
- ❑ For an additive white Gaussian noise (AWGN) channel, it is well known that for a given transmit power,  $P$ , and system bandwidth,  $B$ , the channel capacity is:

$$R = (1/2) \log_2 \left( 1 + \frac{P}{N_0 B} \right) = (1/2) \eta_{SE}$$

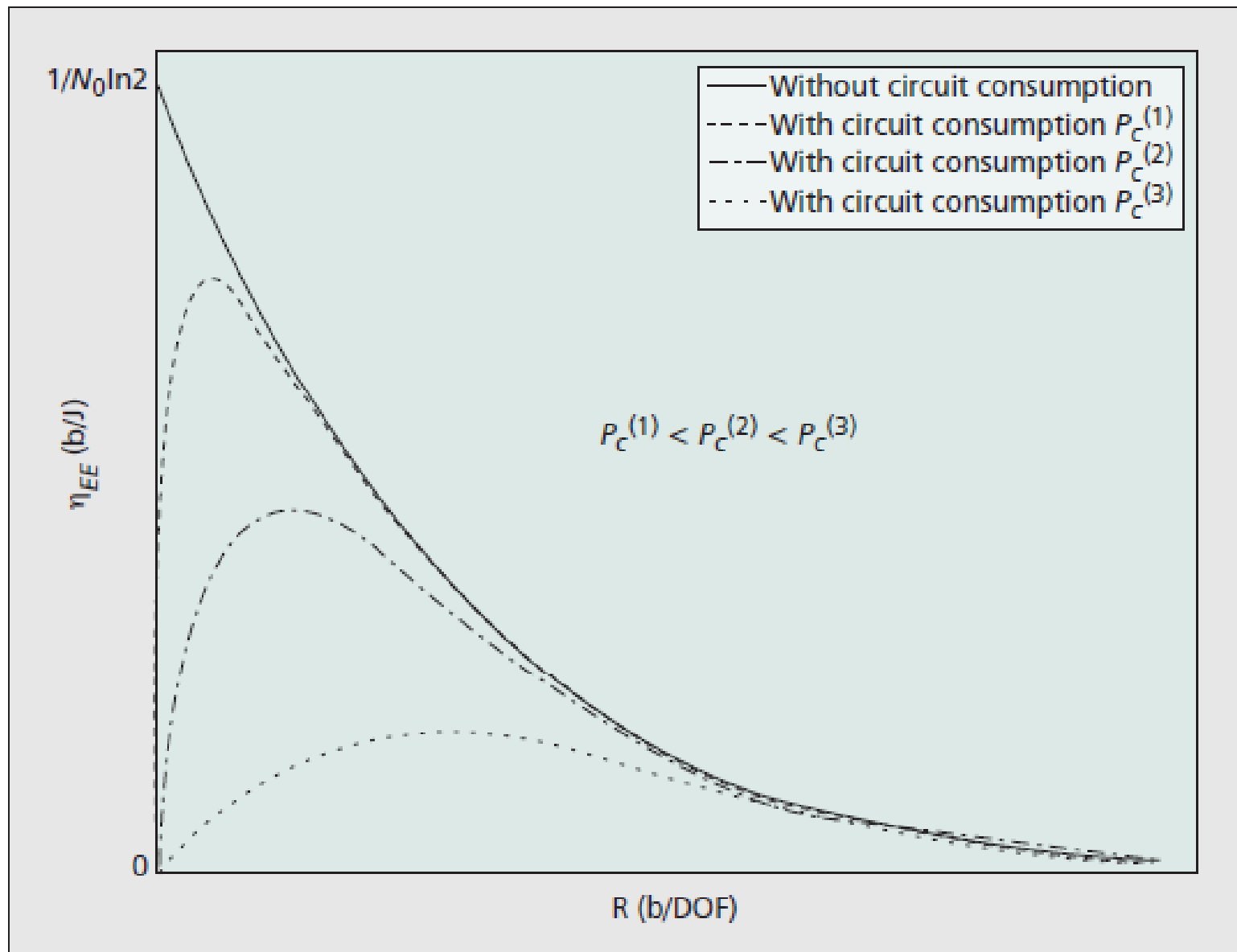
- ❑ bits per real dimension or degrees of freedom (DOF), where  $N_0$  is the noise power spectral density. According to the Nyquist sampling theory, DOF per second is  $2B$ . Therefore, the channel capacity is  $C = 2BR$  b/s. Consequently, the EE is:

$$\eta_{EE} = \frac{C}{P} = \frac{2R}{N_0 (2^{2R} - 1)} = \frac{\eta_{SE}}{N_0 (2^{\eta_{SE}} - 1)}$$

- ❑ **It follows that the EE decreases monotonically with  $R$  (i.e., with SE).**



## *SE vs. EE Tradeoff (2/2)*



## *Now, Imagine a New Modulation for MIMOs:*

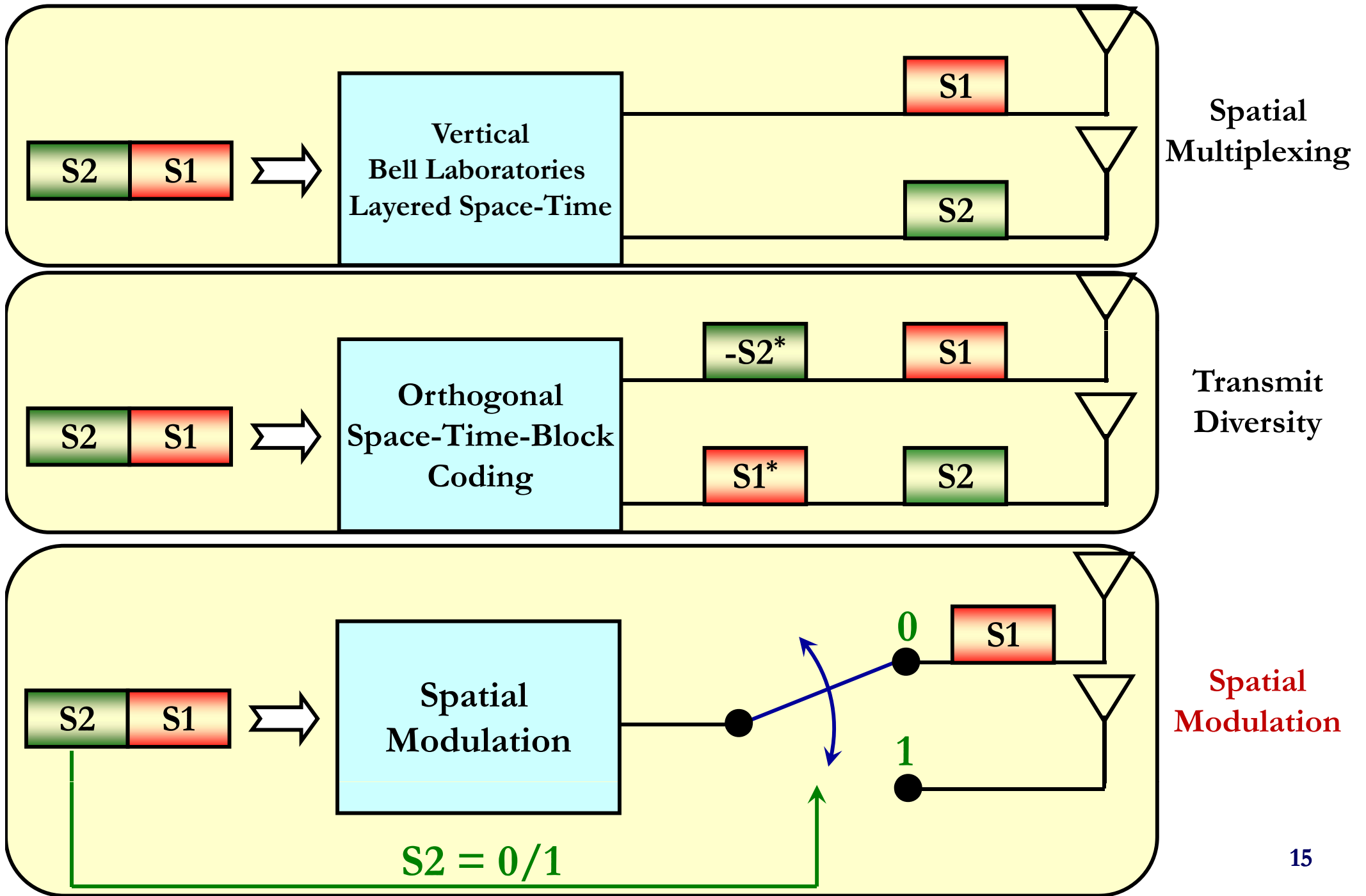
---

- ❑ Having one (or few) active RF chains but still being able to exploit all transmit-antenna elements for multiplexing and transmit-diversity gains
- ❑ Offering Maximum-Likelihood (ML) optimum decoding performance with single-stream decoding complexity
- ❑ Working without the need of (power inefficient) linear modulation schemes (QAM) or allowing us to use constant-envelope modulation (PSK) with negligible performance degradation

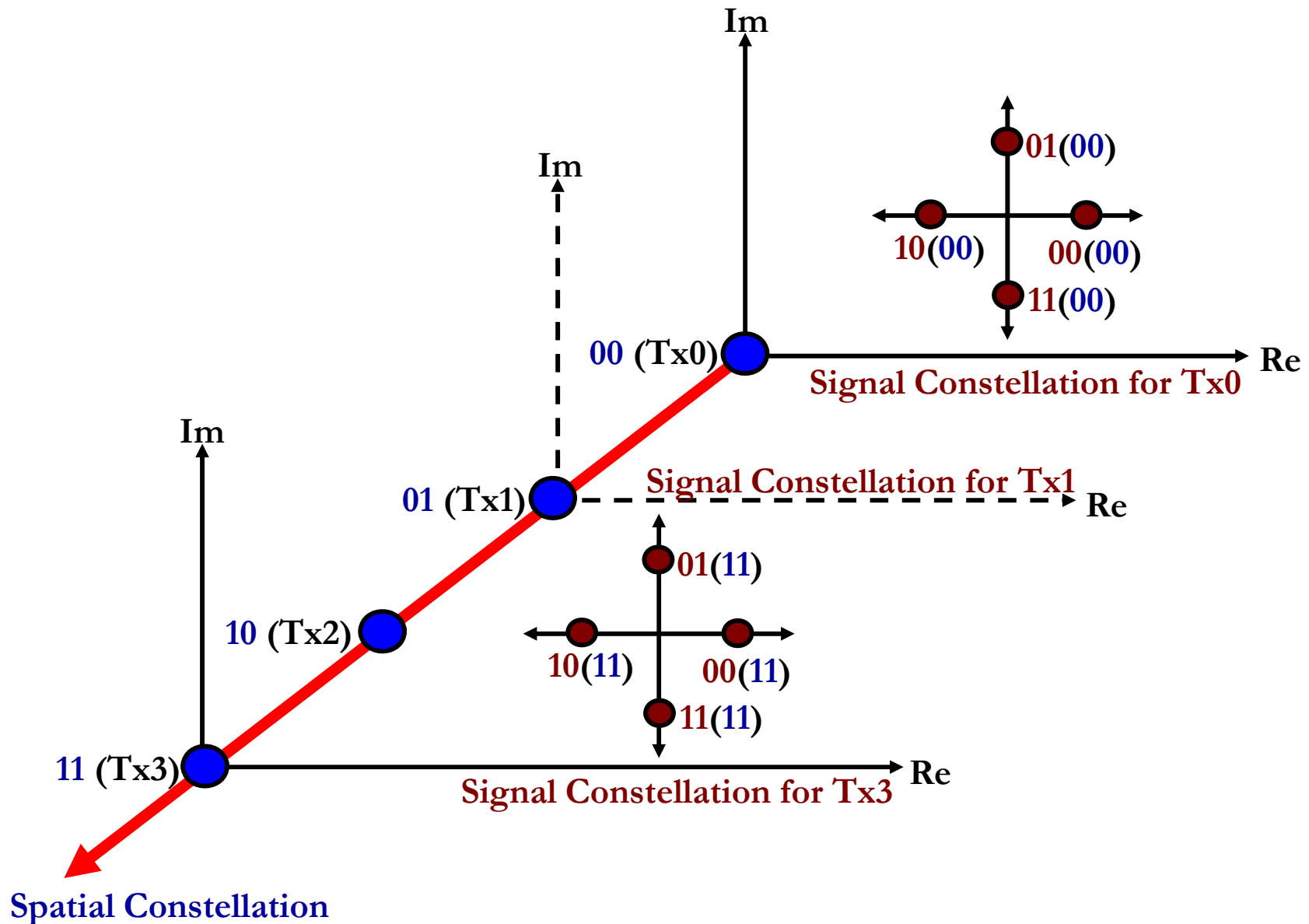
**Spatial Modulation (SM)**

**has the inherent potential to meet these goals**

## *SM – In a Nutshell*

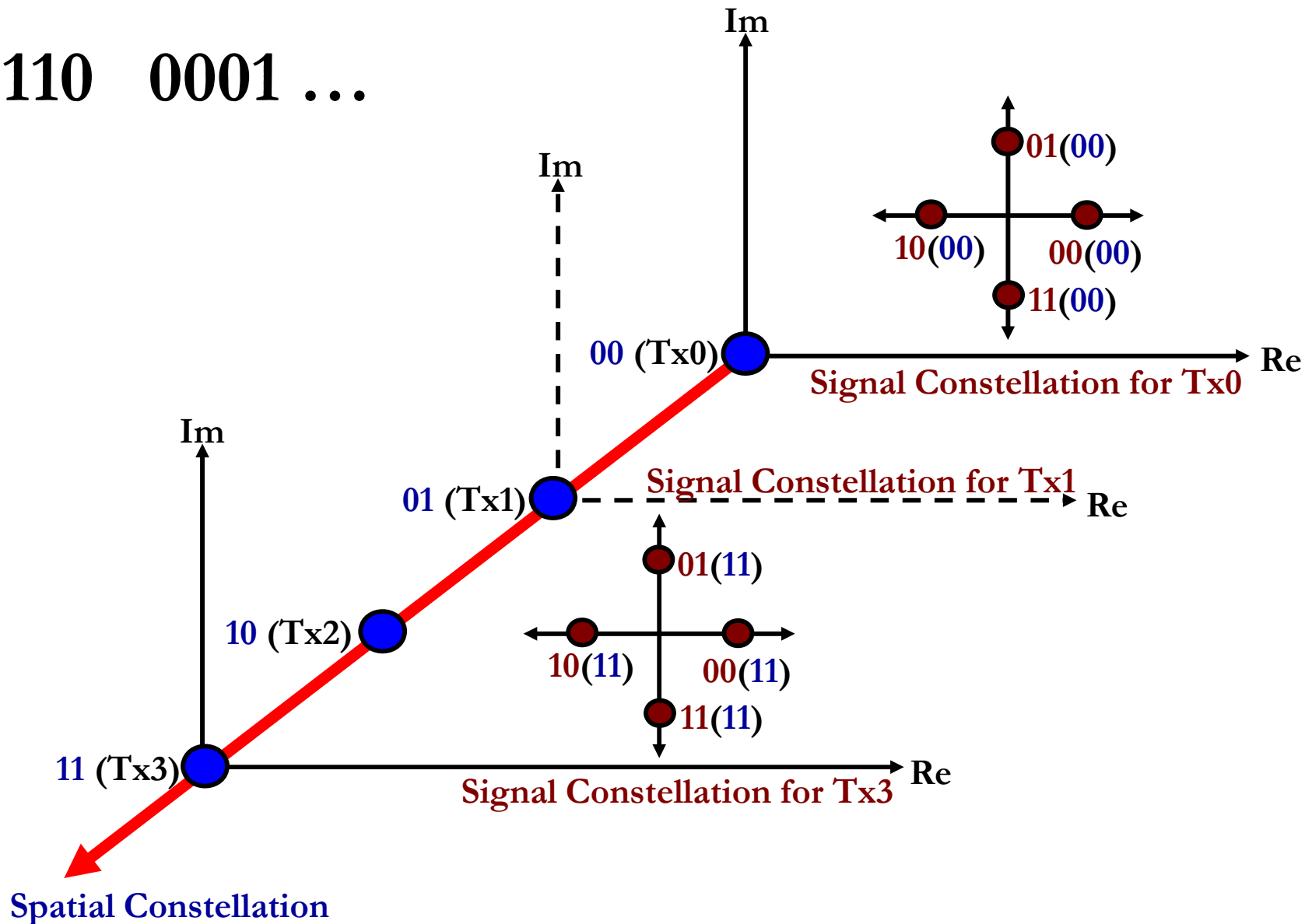


# *SM – How It Works (3D Constellation Diagram)*



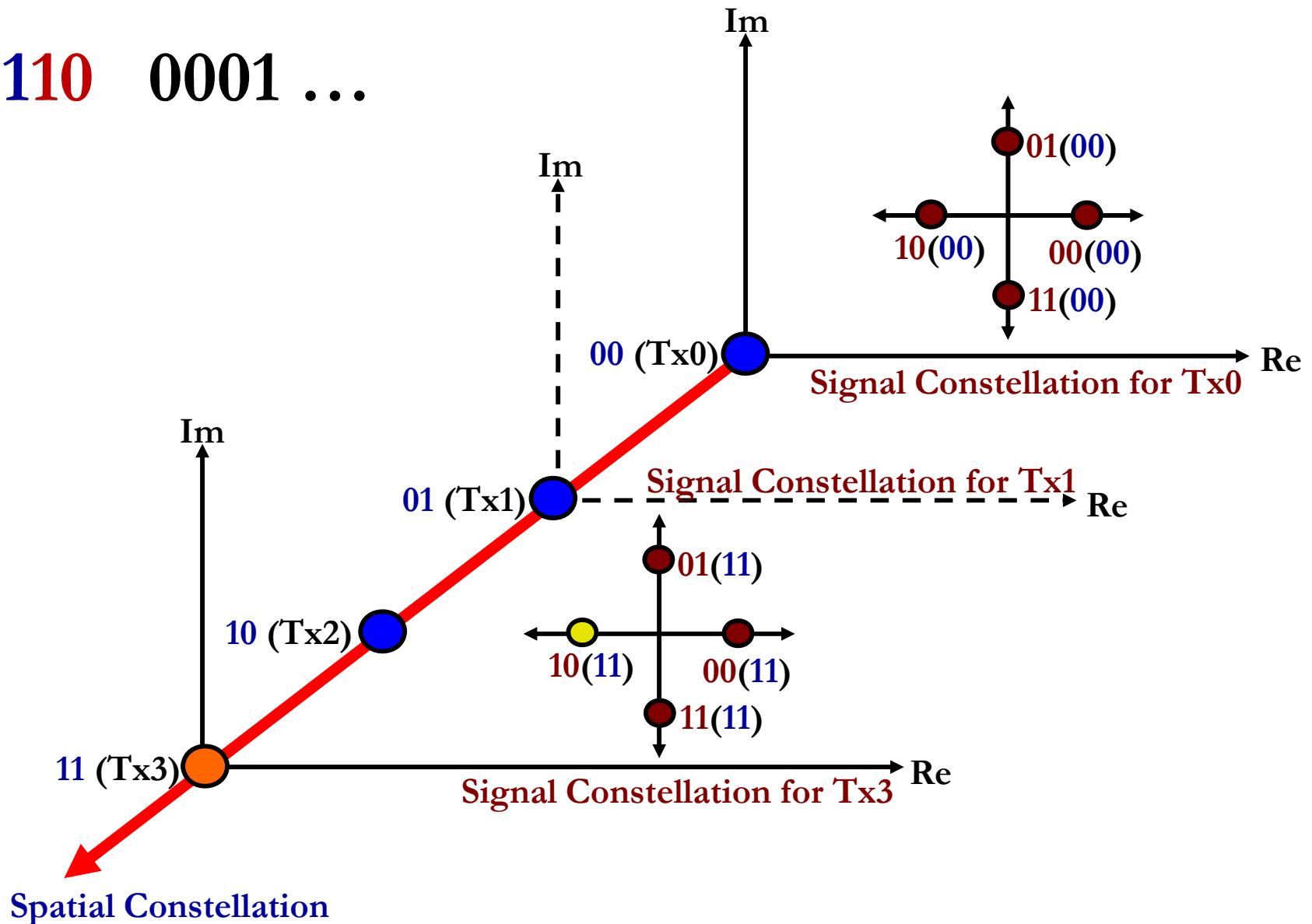
# *SM – How It Works (1/3)*

... 1110 0001 ...



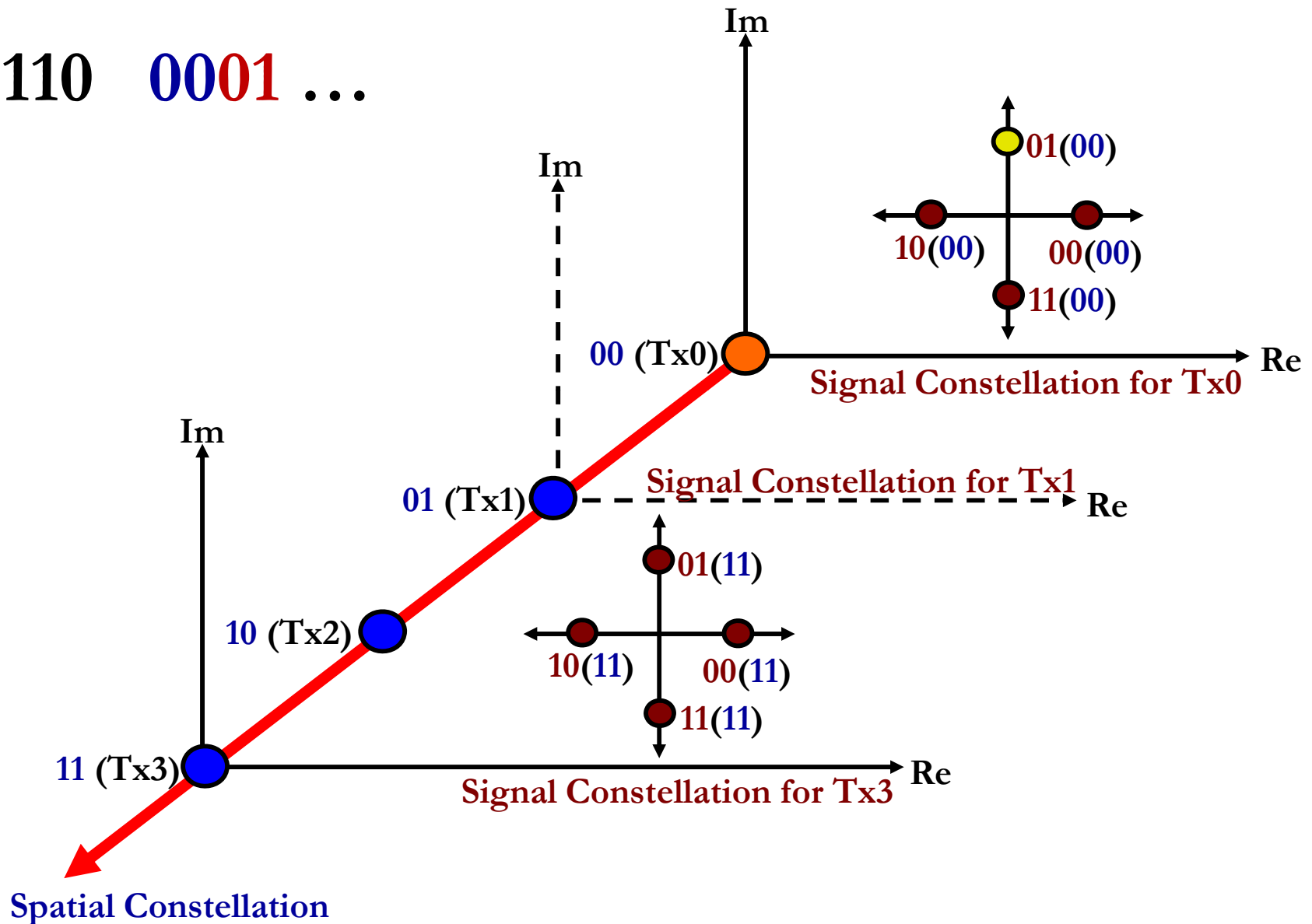
## SM – How It Works (2/3)

... 1110 0001 ...

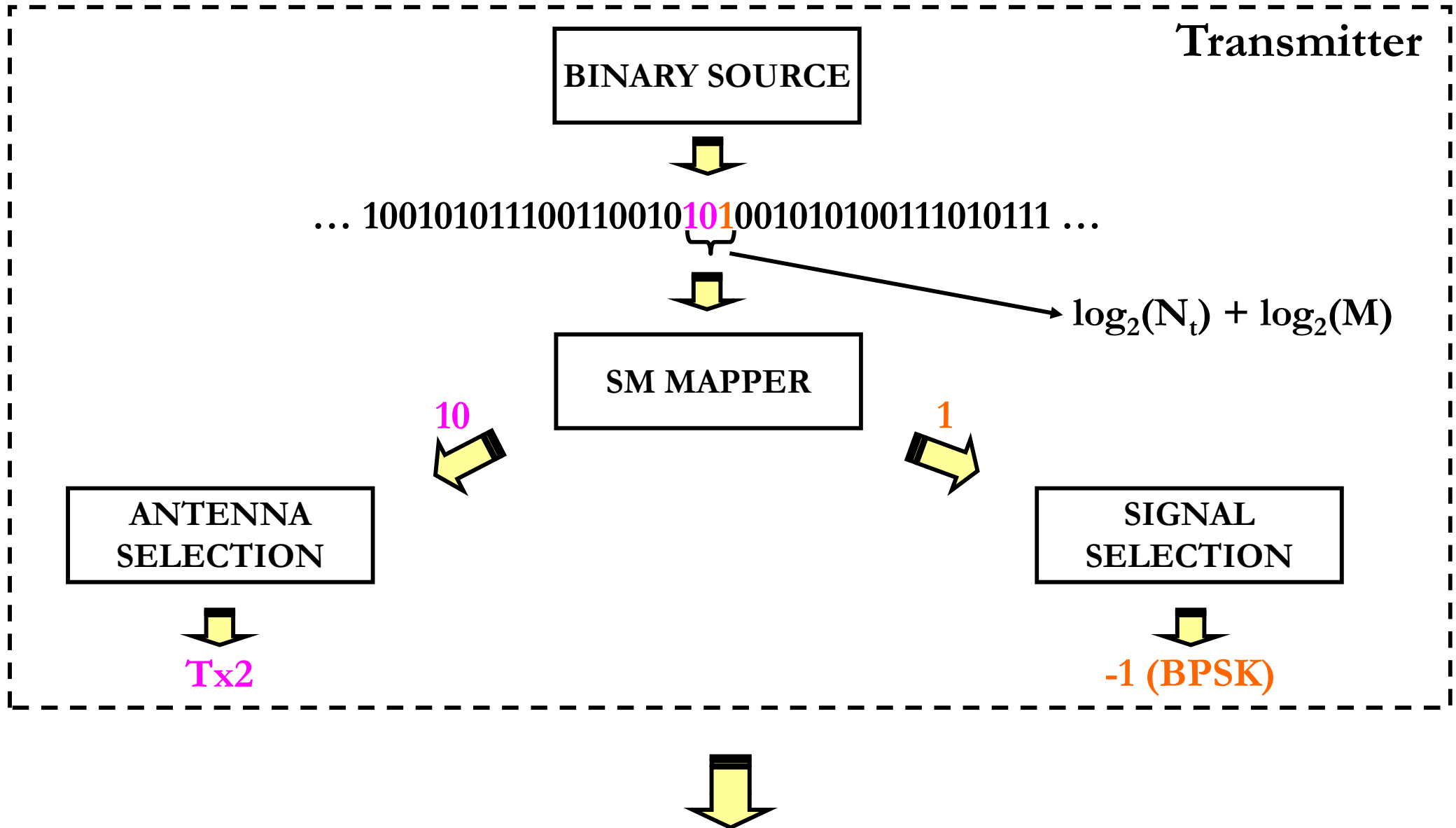


## SM – How It Works (3/3)

... 1110 **0001** ...

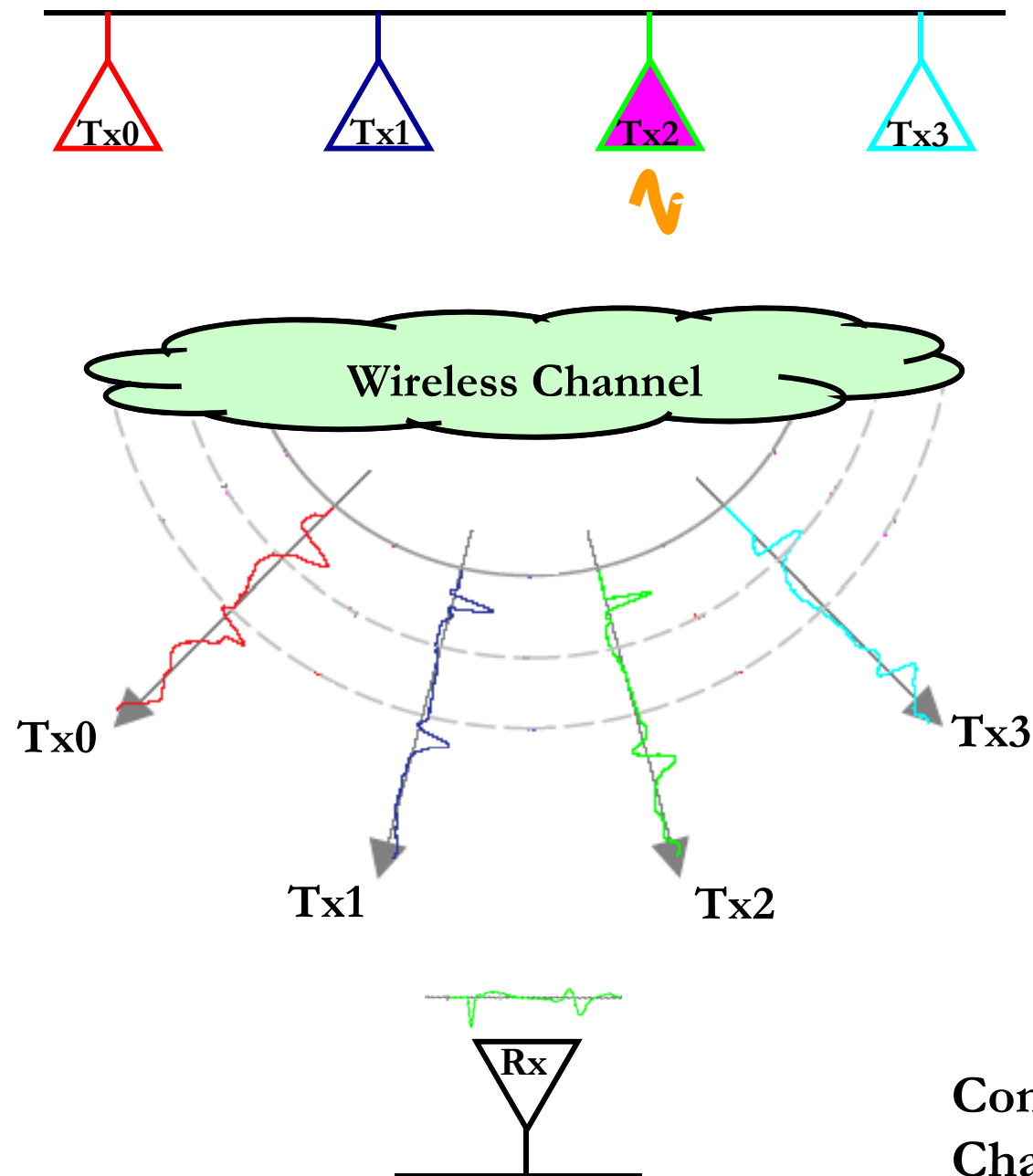


# *SM – Transmitter*

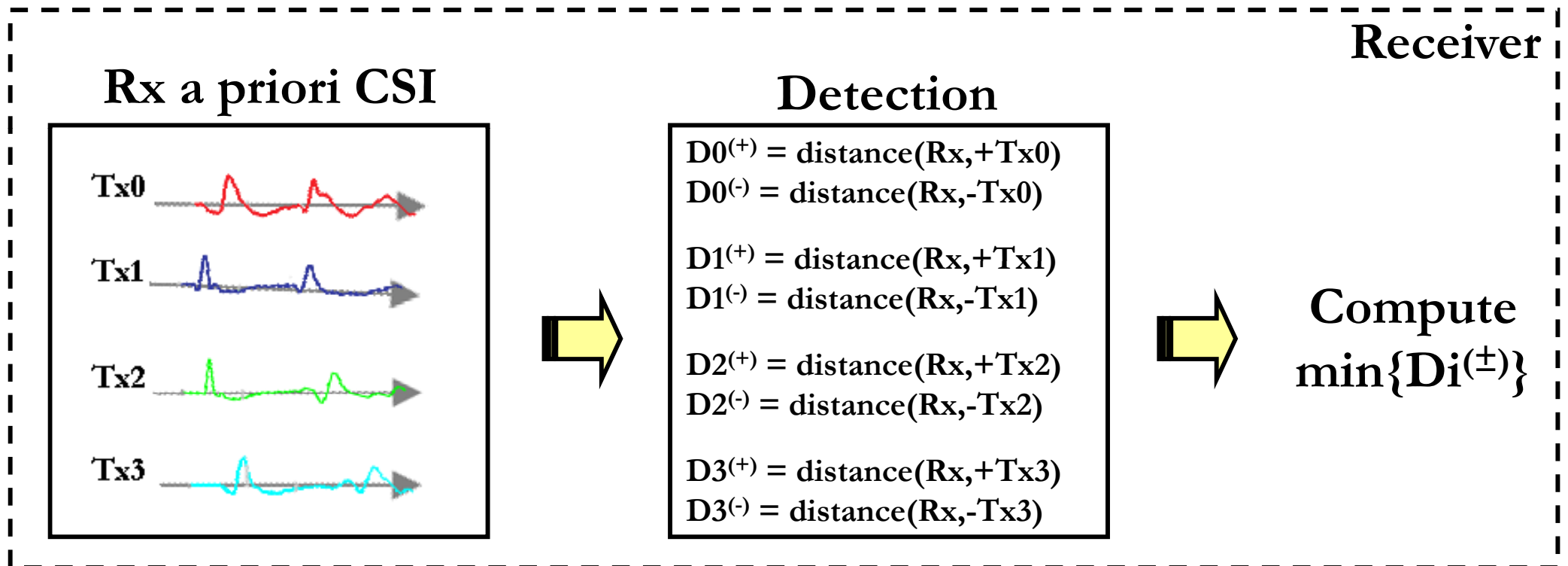




# *SM – Wireless Channel*



## *SM – Receiver*



# Common Misunderstandings

- ❑ **What is the difference with Transmit Antenna Selection (TAS)?**
  - TAS is closed-loop (transmit-diversity). SM is open-loop (spatial-multiplexing).
  - In TAS, antenna switching depends on the end-to-end performance. In SM, antenna switching depends on the incoming bit-stream.
- ❑ **SIMO:  $\log_2(M)$  bpcu – MIMO:  $N_t \log_2(M)$  bpcu – SM:  $\log_2(N_t) + \log_2(M)$  bpcu. So, SM is spectral efficiency (SE) sub-optimal. Why using it?**
  - Correct. But what about signal processing complexity, cost, total power consumption, and energy efficiency (EE)?
  - Are we looking for SE-MIMO? For EE-MIMO? Or for a good SE/EE tradeoff?
- ❑ **SM needs many more transmit-antennas than conventional MIMO for the same SE. Is the comparison fair? Is having so many antennas practical?**
  - What does fair mean? Same transmit-antennas? Same RF chains?
  - What about massive MIMOs? What about mm-Wave communications?
- ❑ **Due to the encoding mechanism, is SM more sensitive to channel estimation errors than conventional MIMO?**
  - No, it is as/more robust as/than MIMO and we have results proving it.

# *Our Proposal: Single-RF Large-Scale SM-MIMO*

---

- The rationale behind SM–MIMO communications for the design of spectral and energy efficient cellular networks is based upon two main pillars:
  - 1) **Minimize**, given some performance constraints, the **number of active antenna–elements** in order to **increase the EE by reducing the circuit power consumption** (single–RF MIMO principle).
  - 2) **Maximize**, given some implementation and size constraints, the **number of passive antenna–elements** in order to **increase both the SE and the EE by reducing the transmit power consumption** (large–scale MIMO principle). This is realized by capitalizing on the multiplexing gain introduced by the “spatial-constellation diagram”.

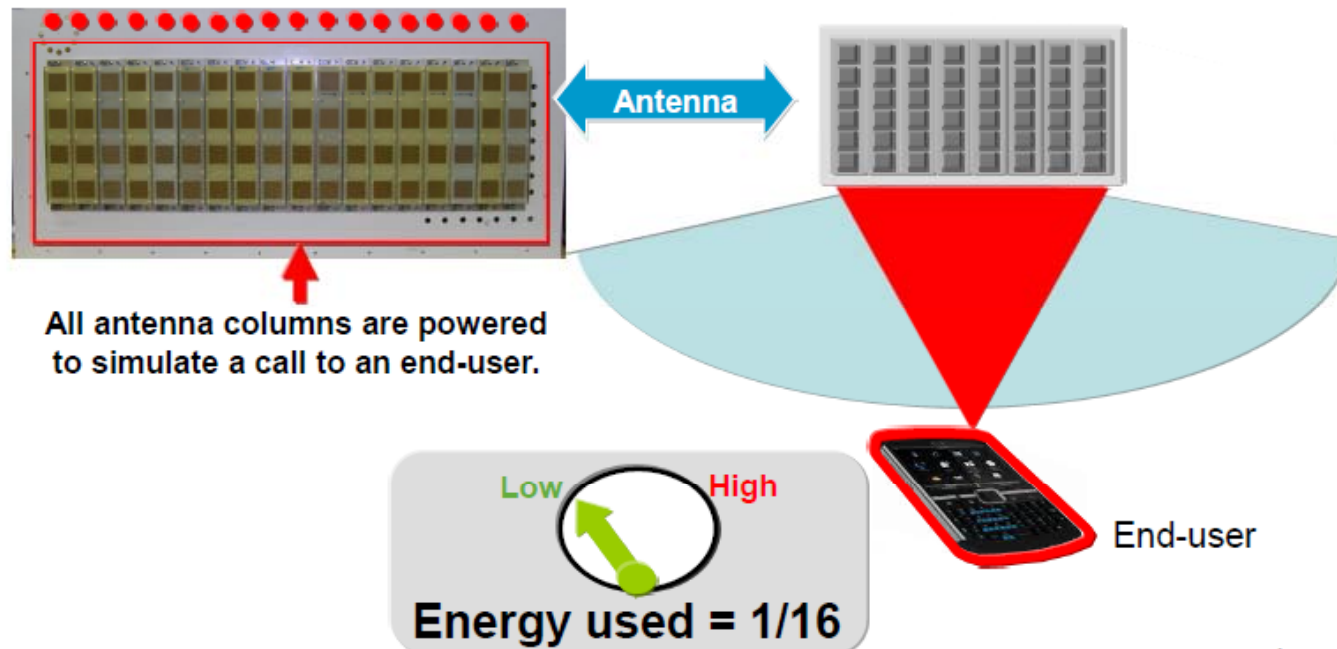
# Massive MIMO (1/5)



## Large Scale Antenna Systems Demonstration

Simulated action of the prototype  
Large Scale Antenna Systems.

Large Scale Antenna Systems focus  
the wireless signal to the end-user.  
**Energy efficiency is improved 16X!**



G. Wright “GreenTouch Initiative: Large Scale Antenna Systems Demonstration”, 2011 Spring meeting, Seoul, South Korea. Available at: <http://www.youtube.com/watch?v=U3euDDr0uvo>.

T. L. Marzetta, “Noncooperative Cellular Wireless with Unlimited Numbers of Base Station Antennas”, *IEEE Trans. Wireless Commun.*, vol. 9, no. 11, pp. 3590-3600, Nov. 2010.

## *Massive MIMO (2/5)*

---

- ❑ With very large MIMO, we think of systems that use antenna arrays with an order of magnitude more elements than in systems being built today, say a hundred antennas or more.
- ❑ Very large MIMO entails an unprecedented number of antennas simultaneously serving a much smaller number of terminals.
- ❑ In very large MIMO systems, each antenna unit uses extremely low power, of the order of mW.
- ❑ As a bonus, several expensive and bulky items, such as large coaxial cables, can be eliminated altogether. (The coaxial cables used for tower-mounted base stations today are up to four centimeters in diameter).
- ❑ Very-large MIMO designs can be made extremely robust in that the failure of one or a few of the antenna units would not appreciably affect the system. Malfunctioning individual antennas may be hotswapped.

<http://www.commsys.isy.liu.se/~egl/vlm/vlm.html>.

F. Rusek, D. Persson, B. K. Lau, E. G. Larsson, T. L. Marzetta, O. Edfors, and F. Tufvesson, “Scaling up MIMO: Opportunities and Challenges with Very Large Arrays”, *IEEE Signal Proces. Mag.*, vol. 30, no. 1, pp. 40–46, Jan. 2013.

## *Massive MIMO (3/5)*

---

- ❑ The main effect of scaling up the dimensions is that uncorrelated thermal noise and fast fading can be averaged out and vanish so that the system is predominantly limited by interference from other transmitters.
- ❑ If we could assign an orthogonal pilot sequence to every terminal in every cell then large numbers of base station antennas would eventually defeat all noise and fading, and eliminate both intra-and inter-cell interference.
- ❑ But there are not enough orthogonal pilot sequences for all terminals. Pilot sequences have to be reused. The performance of a very large array becomes limited by interference arising from re-using pilots in neighboring cells (pilot contamination problem).
- ❑ With an infinite number of antennas, the simplest forms of user detection and precoding, i.e., matched filtering (MF) and eigenbeamforming, become optimal.
- ❑ Spectral efficiency is independent of bandwidth, and the required transmitted energy per bit vanishes.

## *Massive MIMO (4/5) – In Formulas*

- Consider a MIMO Multiple Access (MAC - UPLINK) system with  $N$  antennas per BS and  $K$  users per cell:

$$\mathbf{y} = \sum_{k=1}^K \mathbf{h}_k x_k + \mathbf{n}$$

where channel and noise are i.i.d. RVs with zero mean and unit variance.

- By the strong law of large numbers:

$$\frac{1}{N} \mathbf{h}_m^H \mathbf{y} \xrightarrow[N \rightarrow \infty \text{ and } K = \text{const}]{} \mathbf{x}_m$$

- Thus, with an unlimited number of BS antennas:
  - Uncorrelated interference and noise vanish
  - The matched filter is optimal
  - The transmit power can be made arbitrarily small



## Massive MIMO (5/5) – In Formulas

- Assume now that transmitter **m** and **j** use the same pilot:

$$\hat{\mathbf{h}}_m = \mathbf{h}_m + \underbrace{\mathbf{h}_j}_{\text{pilot contamination}} + \underbrace{\mathbf{n}_m}_{\text{estimation noise}}$$

- Thus, by the strong law of large numbers:

$$\frac{1}{N} \hat{\mathbf{h}}_m^H \mathbf{y} \xrightarrow[N \rightarrow \infty \text{ and } K = \text{const}]{} \mathbf{x}_m + \mathbf{x}_j$$

- Thus, with an unlimited number of BS antennas:

- Uncorrelated interference, noise, and estimation errors vanish
- The performance of the matched filter receiver is limited by pilot contamination
- Matched filter and minimum mean square receivers provide the same limiting performance

# *Massive MIMO vs. SM-MIMO (downlink)*

---

## □ Massive MIMO:

- Many (hundreds or more) transmit-antennas
- All transmit-antennas are simultaneously-active: multi-RF MIMO but antennas are less expensive and more EE than state-of-the-art
- EE: reduction of transmit (RF) power

## □ SM-MIMO:

- Many (hundreds or more) transmit-antennas
- One (or few) transmit-antennas are simultaneously-active: single-RF MIMO
- EE: reduction of transmit (RF) power and circuits power

# *Power-Amplifier Aware MISO Design*

---

## ❑ Motivation:

... the **mutual information was maximized** under an assumption of a **limited output power**. However, in many applications it is desirable to instead limit the **total consumed power, consisting of both output power and losses in the transmitter chain**. The scientific literature agrees that the power amplifier is the largest source of losses in the transmitter.

## ❑ Contribution:

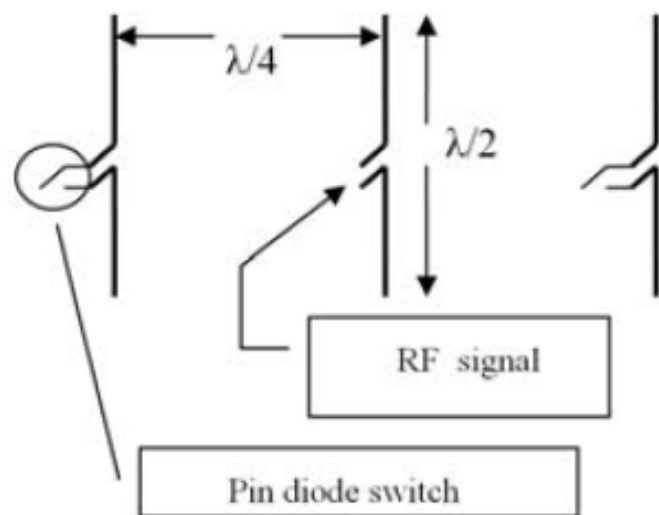
...we utilize the analytic expression of amplifier losses to design MIMO beamforming schemes. We observe that our **MISO solution**, **different from the traditional MRT beamforming**, is such that **some antennas in general are turned off**.

## ❑ Takeaway Message:

The proposed procedure allows us to **turn off antennas while operating optimally**, which is **beneficial in cases where dissipated power per antenna is significant**. This also gives us the possibility to turn off whole radio frequency chains with filters and mixers, which saves additional power.

# Transmission Concepts Related to SM (1/5)

New multiple antenna designs based on **compact parasitic architectures** have been proposed to **enable multiplexing gains with a single active RF element and many passive antenna elements**. The key idea is to change the radiation pattern of the array **at each symbol time instance**, and to encode independent information streams onto angular variations of the far-field in the wave-vector domain.



$s_\theta$	$s_\pi$	Radiation Pattern
0	0	
0	1	

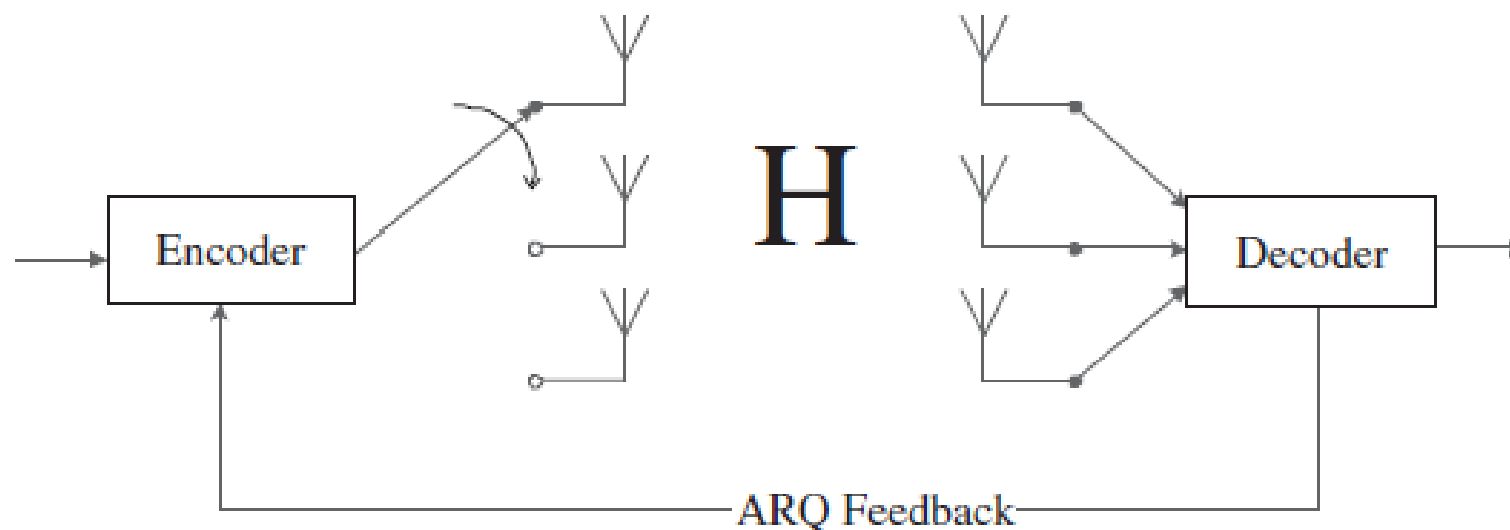
1	0	
1	1	

A. Kalis, A. G. Kanatas, and C. B. Papadias, “**A novel approach to MIMO transmission using a single RF front end**”, **IEEE J. Select. Areas Commun.**, vol. 26, no. 6, pp. 972–980, Aug. 2008.

O. N. Alrabadi, C. Divarathne, P. Tragas, A. Kalis, N. Marchetti, C. B. Papadias, and R. Prasad, “**Spatial multiplexing with a single radio: Proof-of-concept experiments in an indoor environment with a 2.6 GHz prototypes**”, **IEEE Commun. Lett.**, vol. 15, no. 2, pp. 178–180, Feb. 2011.

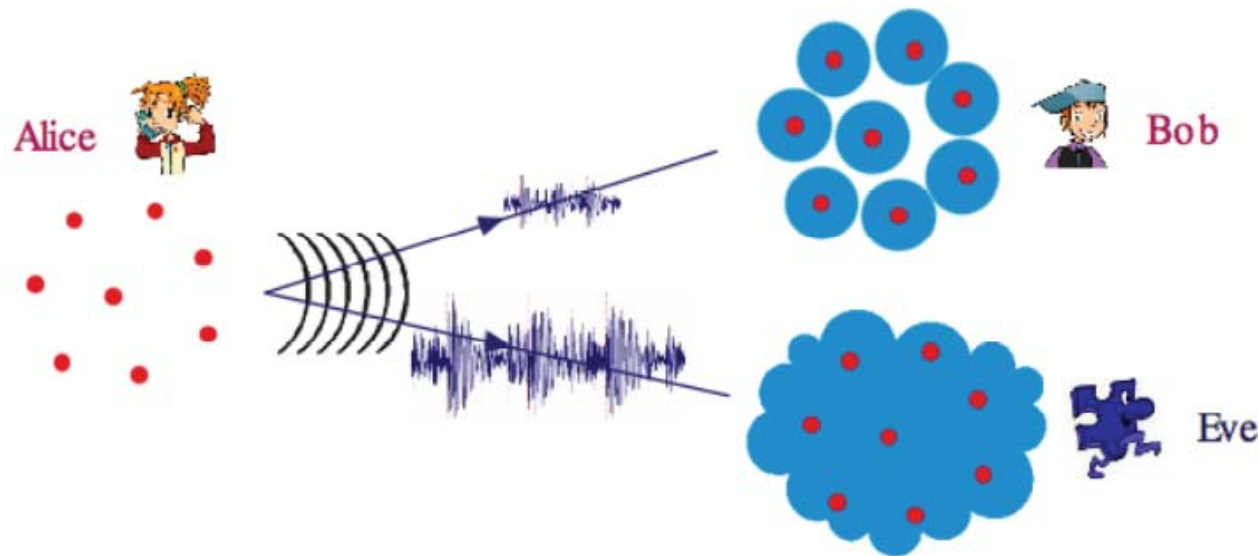
## *Transmission Concepts Related to SM (2/5)*

New MIMO schemes jointly combining multiple-antenna transmission and Automatic Repeat reQuest (ARQ) feedback have been **proposed to avoid to keep all available antennas on**, thus enabling MIMO gains with a single RF chain and a single power amplifier. This solution is named **Incremental MIMO**. The main idea is to reduce complexity and to improve the energy efficiency by **having one active antenna at a time, but to exploit ARQ feedback to randomly cycle through the available antennas at the transmitter in case of incorrect data reception**.

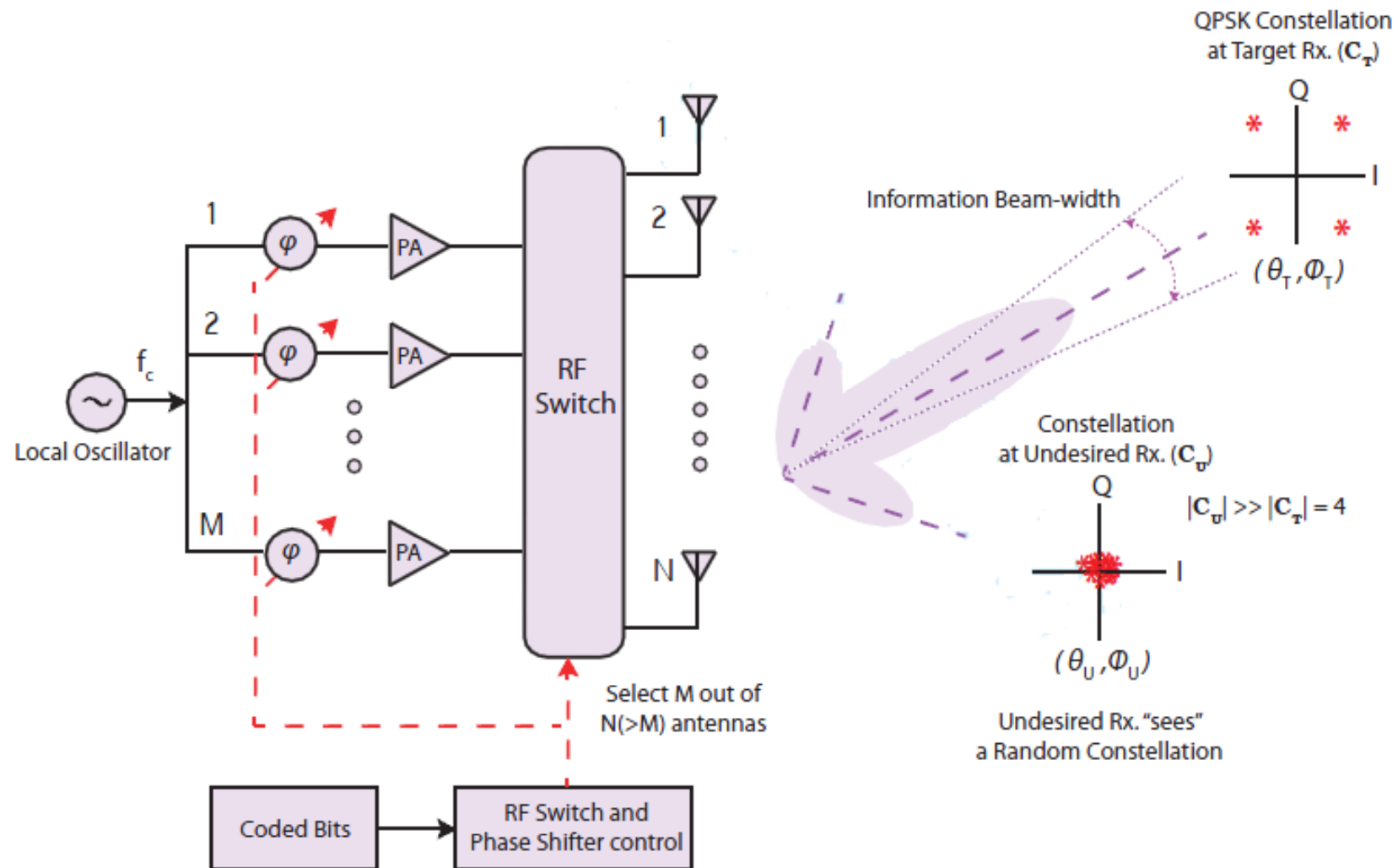


## *Transmission Concepts Related to SM (3/5)*

New **directional modulation schemes** for **mm-Wave frequencies** have been proposed to **enable secure and low-complexity wireless communications**. The solution is named **Antenna Subset Modulation (ASM)**. The main idea in ASM is to **modulate the radiation pattern at the symbol rate** by driving only a **subset of antennas in the array**. While randomly switching antenna subsets does not affect the symbol modulation for a desired receiver along the main direction, it effectively randomizes the amplitude and phase of the received symbol for an eavesdropper along a sidelobe.

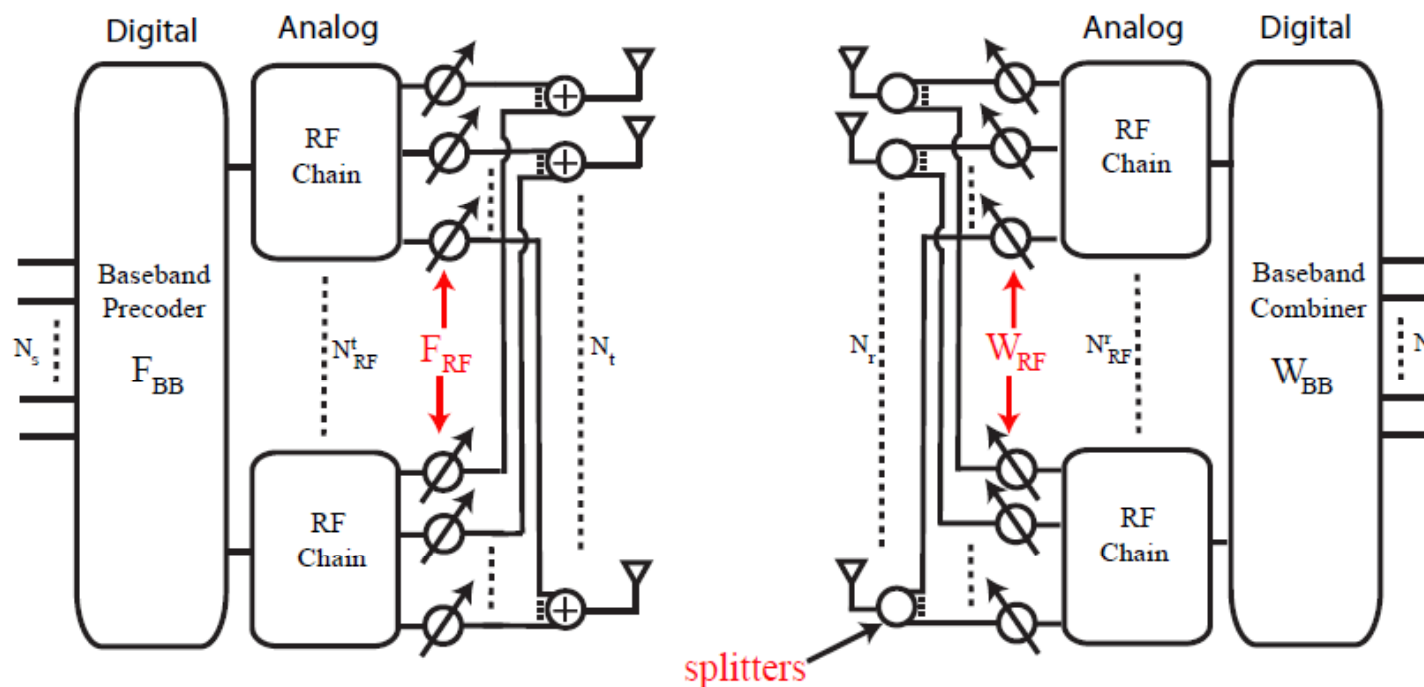


# Transmission Concepts Related to SM (4/5)



## Transmission Concepts Related to SM (5/5)

In Millimeter-wave Mobile Broadband (MMB) system design, the **cost of implementing one RF chain per transmit-antenna can be prohibitive**. For this reason, analog baseband beamforming or RF beamforming with **one or a few active RF chains can be promising low-complexity solutions**. Proposal: low-complexity hybrid RF/baseband precoding schemes where large antenna-arrays are driven by a limited number of transmit/receive chains.



O. El Ayach, S. Rajagopal, S. Abu-Surra, Z. Pi, and R. W. Heath Jr., “Spatially sparse precoding in millimeter wave MIMO systems”, *IEEE Trans. Wireless Commun.*, submitted, May 2013. [Online]. Available: <http://arxiv.org/pdf/1305.2460.pdf>.



## *To Summarize: SM-MIMO Advantages...*

---

- ❑ Higher throughput
- ❑ Simpler receiver design
- ❑ Simpler transmitter design
- ❑ Lower transmit power supply
- ❑ Better efficiency of the power amplifiers

## *... and Some Disadvantages/Trade-Offs*

---

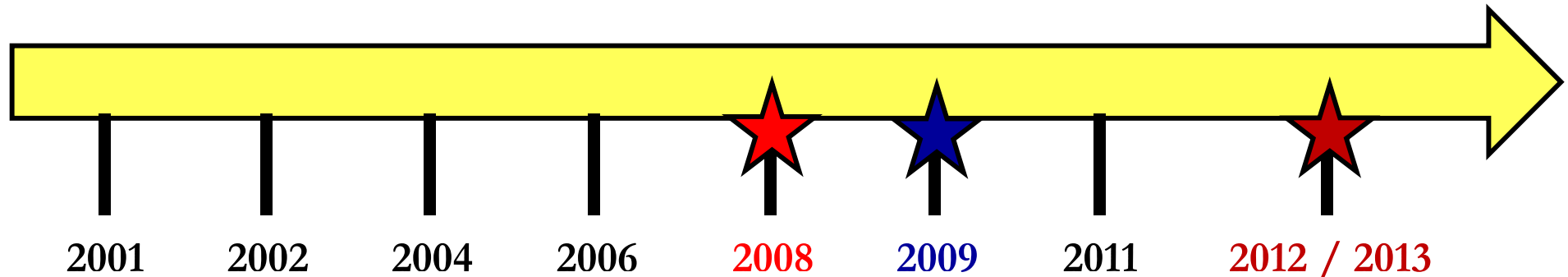
- ❑ Spectral efficiency sub-optimality
- ❑ Fast antenna switching
- ❑ Time-limited pulse shaping
- ❑ Favorable propagation conditions
- ❑ Training overhead
- ❑ Directional beamforming (for mmWave applications)

# Outline

---

1. Introduction and Motivation behind SM-MIMO
2. **History of SM Research and Research Groups Working on SM**
3. Transmitter Design – Encoding
4. Receiver Design – Demodulation
5. Error Performance (Numerical Results and Main Trends)
6. Achievable Capacity
7. Channel State Information at the Transmitter
8. Imperfect Channel State Information at the Receiver
9. Multiple Access Interference
10. Energy Efficiency
11. Transmit-Diversity for SM
12. Spatially-Modulated Space-Time-Coded MIMO
13. Relay-Aided SM
14. SM in Heterogeneous Cellular Networks
15. SM for Visible Light Communications
16. Experimental Evaluation of SM
17. The Road Ahead – Open Research Challenges/Opportunities
18. Implementation Challenges of SM-MIMO

# *A Glimpse into the History of SM*



[2001] Y. Chau, S.-H. Yu, “Space Modulation on Wireless Fading Channels”, IEEE VTC-Fall

[2002] H. Haas, E. Costa, E. Schultz, “Increasing Spectral Efficiency by Data Multiplexing Using Antennas Arrays”, IEEE PIMRC

[2004] S. Song, et al., “A Channel Hopping Technique I: Theoretical Studies on Band Efficiency and Capacity”, IEEE ISCA

[2006] R. Y. Mesleh, H. Haas, et al., “Spatial modulation - A New Low Complexity Spectral Efficiency Enhancing Technique”, ChinaCom

[2008] Y. Yang and B. Jiao, “Information-Guided Channel-Hopping for High Data Rate Wireless Communication”, IEEE Commun. Lett.

[2008] R. Y. Mesleh, H. Haas, et al., “Spatial Modulation”, IEEE Trans. Veh. Technol.

[2009] J. Jeganathan, A. Ghrayeb, et al., “Space Shift Keying Modulation for MIMO Channels”, IEEE Trans. Wireless Commun.

[2011] M. Di Renzo, H. Haas, P. M. Grant, “Spatial Modulation for Multiple-Antenna Wireless Systems - A Survey”, IEEE Commun. Mag.

[2012/2013] N. Serafimovski, A. Younis, M. Di Renzo, H. Haas, et al., "Practical Implementation of Spatial Modulation", IEEE Trans. Veh. Technol., (to appear, IEEE Early Access)

## *Research Groups Working on SM*

---

- ❑ University of Edinburgh, UK (H. Haas)
- ❑ CNRS – SUPELEC – University of Paris-Sud XI, France (M. Di Renzo)
- ❑ Concordia University, Canada (A. Ghrayeb)
- ❑ University of Tabuk, Saudi Arabia (R. Y. Mesleh)
- ❑ University of Southampton, UK (L. Hanzo)
- ❑ Princeton University, US (V. Poor)
- ❑ Istanbul Technical University, Turkey (E. Basar, E. Panayirci)
- ❑ Tokyo University, Japan (S. Sugiura)
- ❑ Indian Institute of Science, India (K. V. S. Hari and A. Chockalingam)
- ❑ Québec University - INRS, Canada (S. Aissa)
- ❑ The University of Akron, US (H. R. Bahrami)
- ❑ Academia Sinica, Taiwan (a large group)
- ❑ Tsinghua University and many other universities, China (many groups)
- ❑ Le Quy Don Technical University, Vietnam (T. X. Nam)
- ❑ etc., etc., etc...
  
- ❑ Collaborations with: Univ. of L'Aquila (Italy), CTTC (Spain), Univ. of Bristol (UK), Heriot-Watt Univ. (UK), EADS (Germany), etc...

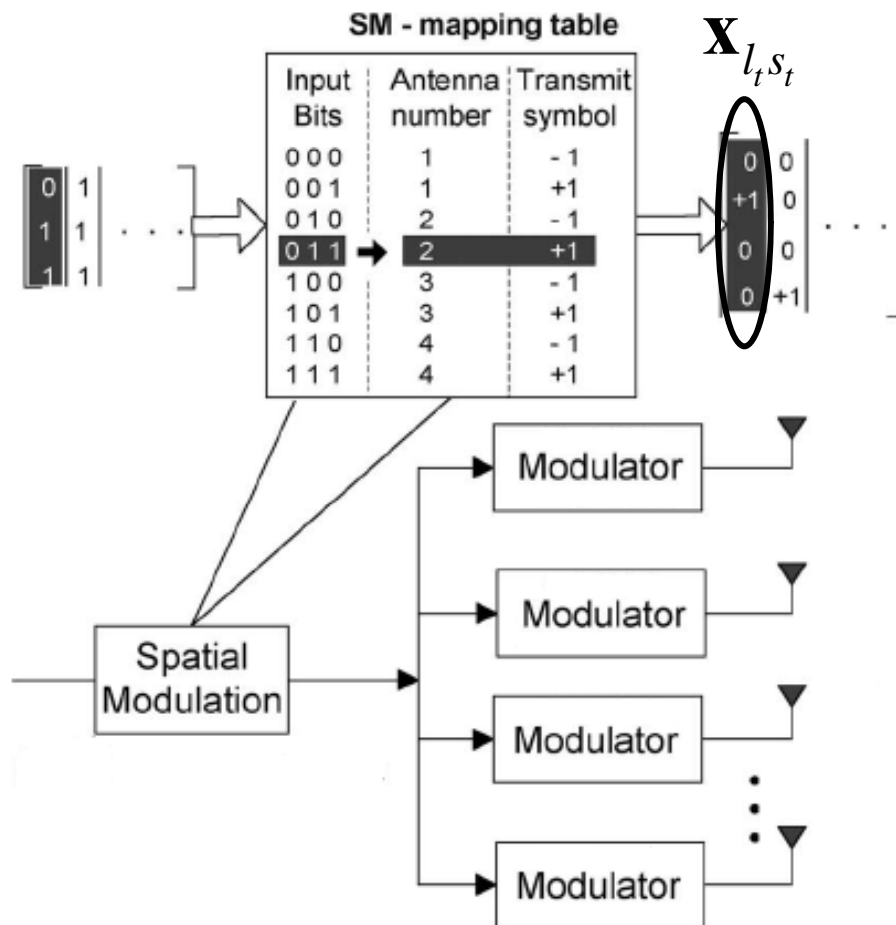
# *Outline*

---

1. Introduction and Motivation behind SM-MIMO
2. History of SM Research and Research Groups Working on SM
3. **Transmitter Design – Encoding**
4. Receiver Design – Demodulation
5. Error Performance (Numerical Results and Main Trends)
6. Achievable Capacity
7. Channel State Information at the Transmitter
8. Imperfect Channel State Information at the Receiver
9. Multiple Access Interference
10. Energy Efficiency
11. Transmit-Diversity for SM
12. Spatially-Modulated Space-Time-Coded MIMO
13. Relay-Aided SM
14. SM in Heterogeneous Cellular Networks
15. SM for Visible Light Communications
16. Experimental Evaluation of SM
17. The Road Ahead – Open Research Challenges/Opportunities
18. Implementation Challenges of SM-MIMO

# Transmitter Design – Encoding (1/7)

## Spatial Modulation (SM)



3 bpcu

Input bits	$N_t=2, M=4$		$N_t=4, M=2$	
	Antenna number	Transmit symbol	Antenna number	Transmit symbol
000	1	+1+j	1	-1
001	1	-1+j	1	+1
010	1	-1-j	2	-1
011	1	+1-j	2	+1
100	2	+1+j	3	-1
101	2	-1+j	3	+1
110	2	-1-j	4	-1
111	2	+1-j	4	+1

$$\mathbf{y} = \mathbf{H}\mathbf{x}_{l_t, s_t} + \mathbf{n}$$

$$= \mathbf{h}^l s_t + \mathbf{n}$$

# Transmitter Design – Encoding (2/7)

## Space Shift Keying (SSK)

- Information is conveyed only by the Spatial-Constellation diagram
  - No signal modulation → more efficient power amplifiers (no linearity constraints)
  - Simplified demodulation
  - Larger antenna-arrays are needed for the same spectral efficiency

$\mathbf{b} = [b_1 \quad b_2]$	symbol	antenna index $j$	$\mathbf{x} = [x_1 \quad \cdots \quad x_4]^T$
$[0 \quad 0]$	0	1	$[1 \quad 0 \quad 0 \quad 0]^T$
$[0 \quad 1]$	1	2	$[0 \quad 1 \quad 0 \quad 0]^T$
$[1 \quad 0]$	2	3	$[0 \quad 0 \quad 1 \quad 0]^T$
$[1 \quad 1]$	3	4	$[0 \quad 0 \quad 0 \quad 1]^T$

$$\mathbf{y} = \mathbf{H}\mathbf{x}_{l_t} + \mathbf{n} = \mathbf{h}^l + \mathbf{n}$$



# *Transmitter Design – Encoding (3/7)*

---

## Generalized SM and SSK

- ❑ SM and SSK are appealing because of their single RF design which greatly simplifies the transmitter.
- ❑ However, their rates are:
  - $\log_2(N_t) + \log_2(M)$  bpcu for SM
  - $\log_2(N_t)$  bpcu for SSK
- ❑ Rate and complexity can be traded-off by allowing more than one active antenna in each time instance, as well as by allowing different numbers of active antennas per time slots:
  - Generalized SSK
  - Generalized SM
  - Variable Generalized SSK/SM

# Transmitter Design – Encoding (4/7)

## Generalized SSK (GSSK)

$\mathbf{b} = [b_1 \ b_2 \ b_3]$	$\mathbf{j}$	$\mathbf{x} = [x_1 \ x_2 \ \cdots \ x_5]^T$
$[0 \ 0 \ 0]$	(1,2)	$\left[\frac{1}{\sqrt{2}} \ \frac{1}{\sqrt{2}} \ 0 \ 0 \ 0\right]^T$
$[0 \ 0 \ 1]$	(1,3)	$\left[\frac{1}{\sqrt{2}} \ 0 \ \frac{1}{\sqrt{2}} \ 0 \ 0\right]^T$
$[0 \ 1 \ 0]$	(1,4)	$\left[\frac{1}{\sqrt{2}} \ 0 \ 0 \ \frac{1}{\sqrt{2}} \ 0\right]^T$
$[0 \ 1 \ 1]$	(1,5)	$\left[\frac{1}{\sqrt{2}} \ 0 \ 0 \ 0 \ \frac{1}{\sqrt{2}}\right]^T$
$[1 \ 0 \ 0]$	(2,3)	$\left[0 \ \frac{1}{\sqrt{2}} \ \frac{1}{\sqrt{2}} \ 0 \ 0\right]^T$
$[1 \ 0 \ 1]$	(2,4)	$\left[0 \ \frac{1}{\sqrt{2}} \ 0 \ \frac{1}{\sqrt{2}} \ 0\right]^T$
$[1 \ 1 \ 0]$	(2,5)	$\left[0 \ \frac{1}{\sqrt{2}} \ 0 \ 0 \ \frac{1}{\sqrt{2}}\right]^T$
$[1 \ 1 \ 1]$	(3,4)	$\left[0 \ 0 \ \frac{1}{\sqrt{2}} \ \frac{1}{\sqrt{2}} \ 0\right]^T$

Rate = 3bpcu

$N_t = 5$

$n_t = 2$

$$\mathbf{x}_j \triangleq \underbrace{\left[\frac{1}{\sqrt{n_t}} \ 0 \ \cdots \ 0 \ \frac{1}{\sqrt{n_t}} \ \cdots \ \frac{1}{\sqrt{n_t}} \ 0\right]^T}_{n_t \text{ of } N_t \text{ non-zero values}}$$

$$\text{Rate} = \left\lfloor \log_2 \binom{N_t}{n_t} \right\rfloor$$

# Transmitter Design – Encoding (5/7)

## Generalized SM (GSM)

Grouped Bits	Antenna Combination ( $\ell$ )	Symbol ( $s$ )
0000	(1,2)	-1
0001	(1,2)	+1
0010	(1,3)	-1
0011	(1,3)	+1
0100	(1,4)	-1
0101	(1,4)	+1
0110	(1,5)	-1
0111	(1,5)	+1
1000	(2,3)	-1
1001	(2,3)	+1
1010	(2,4)	-1
1011	(2,4)	+1
1100	(3,5)	-1
1101	(3,5)	+1
1110	(4,5)	-1
1111	(4,5)	+1

Rate = 4bpcu

$N_t = 5$

$n_t = 2$

BPSK

$$\text{Rate} = \left\lfloor \log_2 \binom{N_t}{n_t} \right\rfloor + \log_2(M)$$

# Transmitter Design – Encoding (6/7)

## Variable Generalized SSK/SM (VGSM/VGSSK)

Grouped Bits	Antenna Combination ( $\Upsilon^{\text{VGSM}}$ )
000	(1)
001	(2)
010	(3)
011	(4)
100	(1,2)
101	(1,3)
110	(1,4)
111	(2,3)

$$\text{Rate} = 3\text{bpcu} + \log_2(M)$$

$$N_t = 4$$

$$n_t = 1 \text{ and } 2$$

MQAM/MPSK

$$\left\{ \begin{array}{l} \text{Rate}_{\text{VGSM}} = \log_2(M) + \left\lfloor \log_2 \left( \sum_{n_t=1}^{N_t} \binom{N_t}{n_t} \right) \right\rfloor = \log_2(M) + \lfloor 2^{N_t} - 1 \rfloor = \log_2(M) + (N_t - 1) \\ \text{Rate}_{\text{VGSSK}} = \left\lfloor \log_2 \left( \sum_{n_t=0}^{N_t} \binom{N_t}{n_t} \right) \right\rfloor = \lfloor 2^{N_t} \rfloor = N_t \end{array} \right.$$

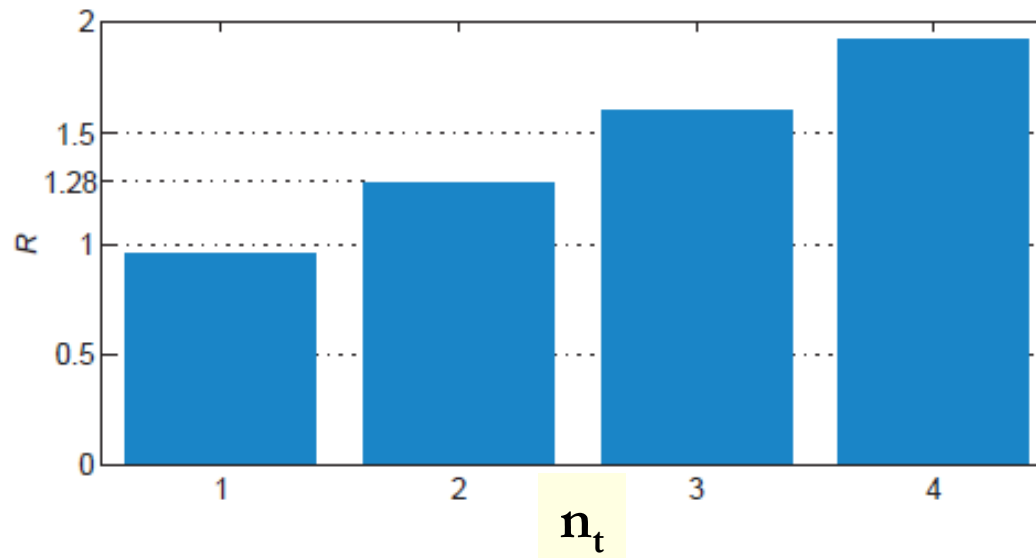
# Transmitter Design – Encoding (7/7)

## Reasoning on the Tradeoffs

### □ Performance

$$\text{PEP} \propto Q\left(\sqrt{\text{SNR} \|\mathbf{H}\mathbf{x}_k - \mathbf{H}\mathbf{x}_h\|^2}\right)$$

### □ Signal processing complexity (detection)



$$R = \frac{\text{Complexity GSM}}{\text{Complexity SM}}$$

### □ Total vs. active (RF chains) number of transmit-antennas

# *Outline*

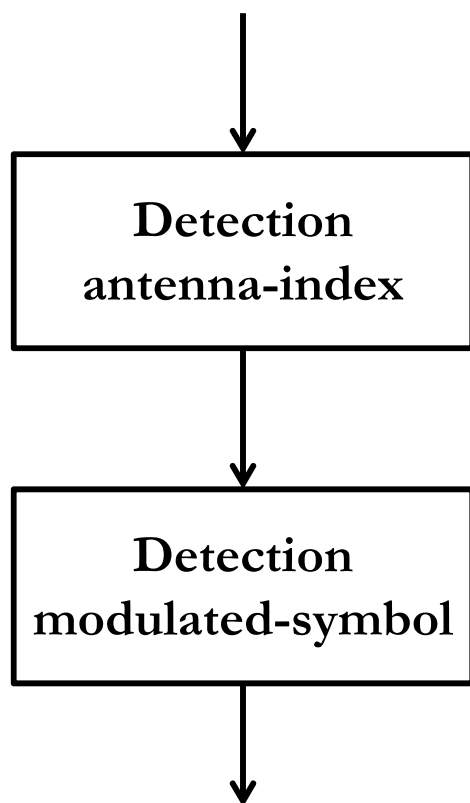
---

1. Introduction and Motivation behind SM-MIMO
2. History of SM Research and Research Groups Working on SM
3. Transmitter Design – Encoding
4. **Receiver Design – Demodulation**
5. Error Performance (Numerical Results and Main Trends)
6. Achievable Capacity
7. Channel State Information at the Transmitter
8. Imperfect Channel State Information at the Receiver
9. Multiple Access Interference
10. Energy Efficiency
11. Transmit-Diversity for SM
12. Spatially-Modulated Space-Time-Coded MIMO
13. Relay-Aided SM
14. SM in Heterogeneous Cellular Networks
15. SM for Visible Light Communications
16. Experimental Evaluation of SM
17. The Road Ahead – Open Research Challenges/Opportunities
18. Implementation Challenges of SM-MIMO

# Receiver Design – Demodulation (1/12)

□ The first proposed demodulator for SM is based on a two-step approach:

- Detection of the antenna index (spatial-constellation diagram)
- Detection of the modulated symbol (signal-constellation diagram)



$$\hat{l} = \arg \max_l \left\{ \frac{|\mathbf{h}_l^H \mathbf{y}|}{\|\mathbf{h}_l\|_F^2} \right\}$$

$$\hat{s} = \arg \min_s \left\{ \|\mathbf{y} - \mathbf{h}_{\hat{l}}^H s\|_F^2 \right\}$$

## *Receiver Design – Demodulation (2/12)*

- Maximum-Likelihood (ML) optimum decoding:
  - Spatial- and signal-constellation diagrams are jointly decoded

$$\begin{aligned} (\hat{l}, \hat{s}) &= \arg \min_{(l,s)} \left\{ \left\| \mathbf{y} - \mathbf{H} \mathbf{x}_{l,s} \right\|_F^2 \right\} \\ &\stackrel{\text{SM}}{=} \arg \min_{(l,s)} \left\{ \left\| \mathbf{y} - \mathbf{h}_l \mathbf{x}_s \right\|_F^2 \right\} \end{aligned}$$



## *Receiver Design – Demodulation (3/12)*

---

- ❑ Many other sub-optimal demodulators have been proposed recently.
- ❑ In general, they offer a trade-off between complexity and performance.
- ❑ Sometimes, they provide good performance for low/medium SNRs, while their performance degrades for high SNRs.
- ❑ We consider two examples:
  - The application of Compressed Sensing to SM
  - The application of Sphere Decoding to SM

C.-M. Yu, S.-H. Hsieh, H.-W. Liang, C.-S. Lu, W.-H. Chung, S.-Y. Kuo, and S.-C. Pei, "Compressed Sensing Detector Design for Space Shift Keying in MIMO Systems", *IEEE Commun. Lett.*, vol. 16, no. 10, pp. 1556-1559, Oct. 2012.

A. Younis, S. Sinanovic, M. Di Renzo, and H. Haas, "Generalized Sphere Decoding for Spatial Modulation", *IEEE Trans. Commun.*, Vol. 61, No. 7, pp. 2805–2815, July 2013.

# Receiver Design – Demodulation (4/12)

## Compressed Sensing (CS) Generalized Space Shift Keying

- ❑ The idea is to leverage the inherent sparsity of SSK modulation: **the number of active antennas is much less than the radiating elements** ( $n_t < N_t$ )
- ❑ SSK demodulation is re-formulated as **a convex program via CS**
- ❑ **CS-SSK uses 1-norm metric** instead of 2-norm of ML demodulation
- ❑ The demodulation complexity is:

$$\begin{cases} \text{ML} : O\left(N_r N_t^{n_t}\right) \\ \text{CS} : O\left(N_r N_t n_t\right) \end{cases}$$

# Receiver Design – Demodulation (5/12)

## Compressed Sensing (CS) Generalized Space Shift Keying

$$\begin{cases} \mathbf{y} = \sqrt{\rho} \mathbf{H} \mathbf{x} + \mathbf{n} \\ \mathbf{y} \in \mathbb{C}^{N_r \times 1}, \mathbf{x} \in \mathbb{R}^{N_t \times 1}, \mathbf{H} \in \mathbb{C}^{N_r \times N_t}, \mathbf{n} \in \mathbb{C}^{N_r \times 1} \\ \mathbf{x} \text{ is a zero/one vector with } n_t \text{ one entries} \end{cases}$$

- The idea is to leverage the inherent sparsity of SSK modulation: **the number of active antennas is much less than the radiating elements** ( $n_t < N_t$ )
- **x** can be re-constructed with high probability by 1-norm minimization, as follows:

$$\hat{\mathbf{x}} = \arg \min_{\mathbf{y} = \Phi \mathbf{x}} \left\{ \|\mathbf{x}\|_1 \right\}$$

# Receiver Design – Demodulation (6/12)

## Compressed Sensing (CS) Generalized Space Shift Keying

□ where:

- $\Phi$  is an  $N_r \times N_t$  that satisfies the Restricted Isometric Property (RIP). CS theory says that, with high probability, matrix  $\Phi$  can be obtained by generating its elements from a Normal distribution with zero mean and variance  $1/N_r$ . The RIP ensures that pairs of columns of  $\Phi$  are orthogonal to each other with high probability.
- The number of observations  $N_r$  should be chosen as follows:

$$N_r = O\left(n_t \log_2\left(\frac{N_t}{n_t}\right)\right)$$

- The authors use Orthogonal Matching Pursuit (OMP). The idea is find the non-zero elements of  $\mathbf{x}$  by computing the correlation  $\Phi^T \mathbf{y}$ . If  $\Phi$  satisfies the RIP, then  $\Phi^T \Phi$  is nearly orthonormal and the largest coefficients of  $\Phi^T \mathbf{y}$  correspond to the non-zero coefficients of  $\mathbf{x}$ .

# Receiver Design – Demodulation (7/12)

## Sphere Decoding (SD) Spatial Modulation

- Optimum detector based on the ML principle:

$$\begin{aligned} [\ell_t^{(\text{ML})}, s_t^{(\text{ML})}] &= \arg \min_{\substack{\ell \in \{1, 2, \dots, N_t\} \\ s \in \{s_1, s_2, \dots, s_M\}}} \left\{ \|\mathbf{y} - \mathbf{h}_\ell s\|_F^2 \right\} \\ &= \arg \min_{\substack{\ell \in \{1, 2, \dots, N_t\} \\ s \in \{s_1, s_2, \dots, s_M\}}} \left\{ \sum_{r=1}^{N_r} |y_r - h_{\ell,r} s|^2 \right\} \end{aligned}$$

- Computational complexity of ML (real multiplications):

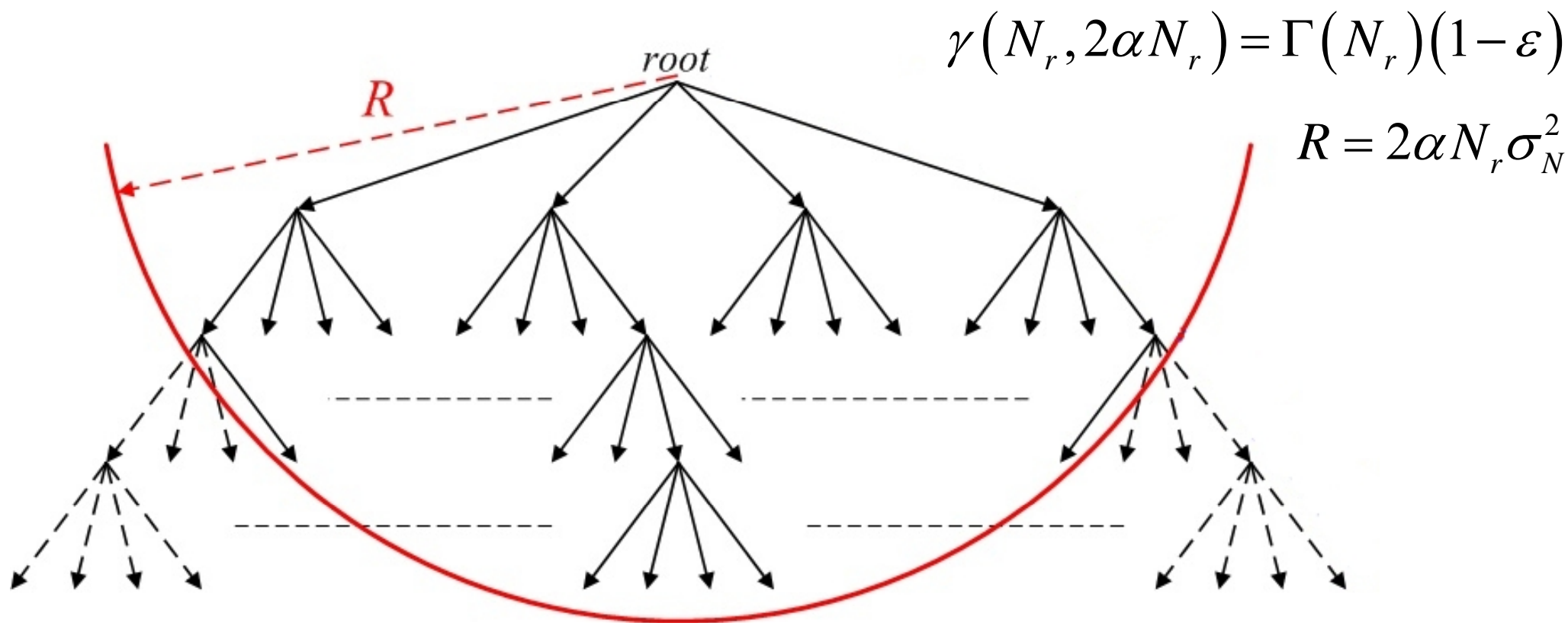
$$C_{\text{ML}} = 8N_r N_t M$$

since evaluating each Euclidean distance requires 8 real multiplications

# Receiver Design – Demodulation (7/12)

## Sphere Decoding (SD) Spatial Modulation

- The SD algorithm avoids an exhaustive search by examining only those points that lie inside a sphere of radius  $R$ :



# Receiver Design – Demodulation (8/12)

## Sphere Decoding (SD) Spatial Modulation

□ Three sphere decoders for SM are proposed and studied:

1. **Rx-SD**, which aims at reducing the receive search space

$$[\ell_t^{(\text{Rx-SD})}, s_t^{(\text{Rx-SD})}] = \arg \min_{\substack{\ell \in \{1, 2, \dots, N_t\} \\ s \in \{s_1, s_2, \dots, s_M\} \\ \tilde{N}_r(\ell, s) = N_r}} \left\{ \sum_{r=1}^{\tilde{N}_r(\ell, s)} |y_r - h_{\ell, r} s|^2 \right\}$$

2. **Tx-SD**, which aims at reducing the transmit search space

$$[\ell_t^{(\text{Tx-SD})}, s_t^{(\text{Tx-SD})}] = \arg \min_{(\ell, s) \in \Theta_R} \left\{ \sum_{r=1}^{N_r} |y_r - h_{\ell, r} s|^2 \right\}$$

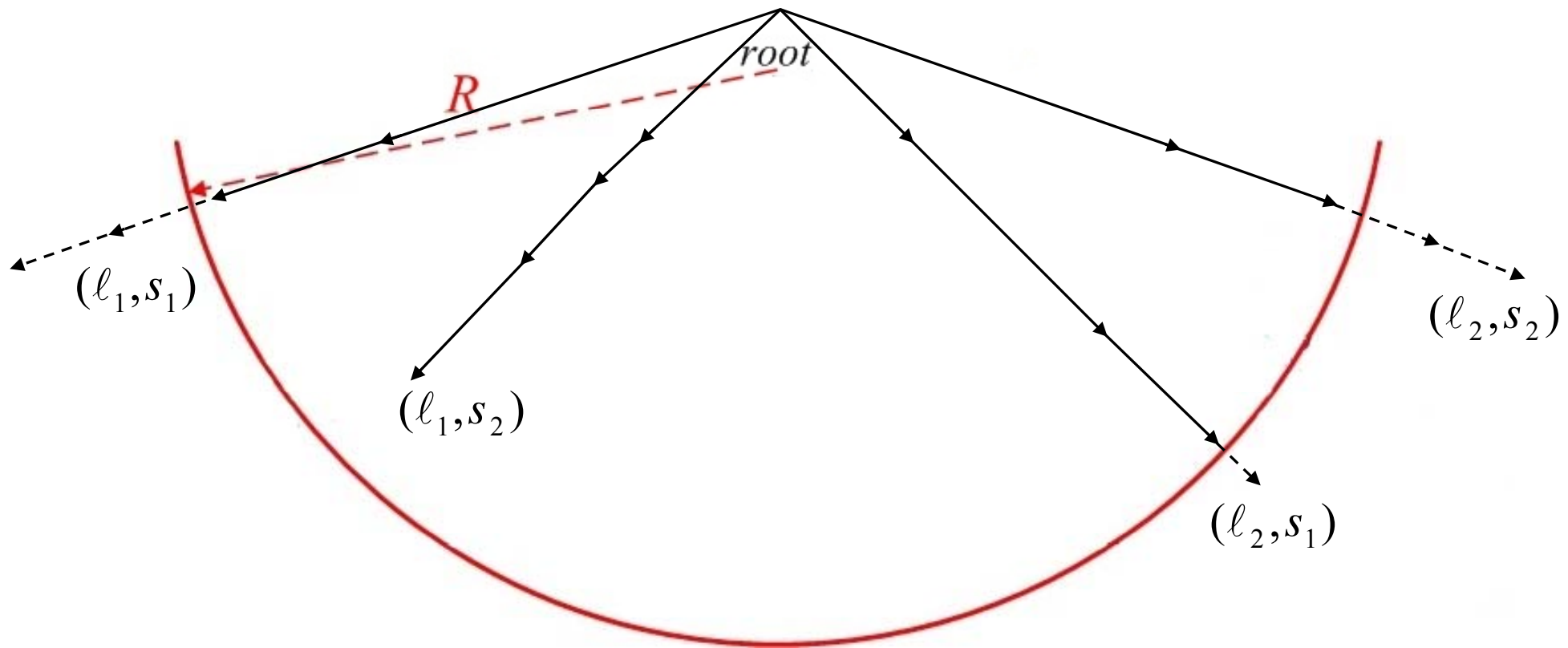
3. **C-SD**, which aims at reducing both transmit and receive search spaces

$$[\ell_t^{(\text{C-SD})}, s_t^{(\text{C-SD})}] = \arg \min_{\substack{(\ell, s) \in \Theta_R \\ \tilde{N}_r(\ell, s) = N_r}} \left\{ \sum_{r=1}^{\tilde{N}_r(\ell, s)} |y_r - h_{\ell, r} s|^2 \right\}$$

# Receiver Design – Demodulation (9/12)

## Sphere Decoding (SD) Spatial Modulation – Rx-SD

- Rx-SD searches the paths leading to each point  $(l, s)$  as long as it is still inside the sphere when adding up the signals at each receive-antenna



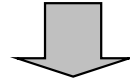


# Receiver Design – Demodulation (10/12)

## Sphere Decoding (SD) Spatial Modulation – Tx-SD

$$[\ell_t^{(\text{Tx-SD})}, s_t^{(\text{Tx-SD})}] = \arg \min_{(\ell, s) \in \Theta_R} \left\{ \sum_{r=1}^{N_r} |y_r - h_{\ell, r} s|^2 \right\}$$

$$\begin{aligned} \Theta_R &= \left\{ (\ell, s) \text{ with } \ell \in \{1, 2, \dots, N_t\} \text{ and } s \in \{s_1, s_2, \dots, s_M\} \mid \|\bar{\mathbf{y}} - \bar{\mathbf{H}}\bar{\mathbf{x}}_{\ell, s}\|_F^2 \leq R^2 \right\} \\ &= \left\{ (\ell, s) \text{ with } \ell \in \{1, 2, \dots, N_t\} \text{ and } s \in \{s_1, s_2, \dots, s_M\} \mid \sum_{i=1}^{2N_t} \left( \bar{z}_i - \sum_{j=i}^{2N_t} \bar{p}_{i,j} \bar{x}_j(\ell, s) \right)^2 \leq R_Q^2 \right\} \end{aligned}$$



$$\begin{aligned} \frac{-R_Q + \bar{z}_i}{\bar{p}_{i,i}} &\leq \bar{x}_i(\ell, s) \leq \frac{R_Q + \bar{z}_i}{\bar{p}_{i,i}} \\ \frac{-R_Q + \bar{z}_{i,i+N_t}}{\bar{p}_{i,i}} &\leq \bar{x}_i(\ell, s) \leq \frac{R_Q + \bar{z}_{i,i+N_t}}{\bar{p}_{i,i}} \end{aligned}$$

# Receiver Design – Demodulation (11/12)

## Sphere Decoding (SD) Spatial Modulation – C-SD

□ The C-SD is a two-step detector that works as follows:

1. First, the Tx-SD algorithm is used to reduce the transmit search space. The subset of points  $\Theta_R$  is computed
2. Second, the Rx-SD algorithm is used to reduce the receive search space. More specifically, Rx-SD is applied only on the subset of points  $\Theta_R$  computed in Step 1

$$[\ell_t^{(\text{C-SD})}, s_t^{(\text{C-SD})}] = \arg \min_{\substack{(\ell, s) \in \Theta_R \\ \tilde{N}_r(\ell, s) = N_r}} \left\{ \sum_{r=1}^{\tilde{N}_r(\ell, s)} |y_r - h_{\ell, r} s|^2 \right\}$$

# Receiver Design – Demodulation (12/12)

## Sphere Decoding (SD) Spatial Modulation – C-SD

□ The complexity of Rx-SD is:

$$C_{Rx-SD} = 8 \sum_{\ell=1}^{N_t} \sum_{s=1}^M \tilde{N}_r(\ell, s)$$

□ The complexity of Tx-SD is:

$$C_{Tx-SD} = C_{\Theta_R} + 8N_r \text{card}\{\Theta_r\}$$

□ The complexity of Cx-SD is:

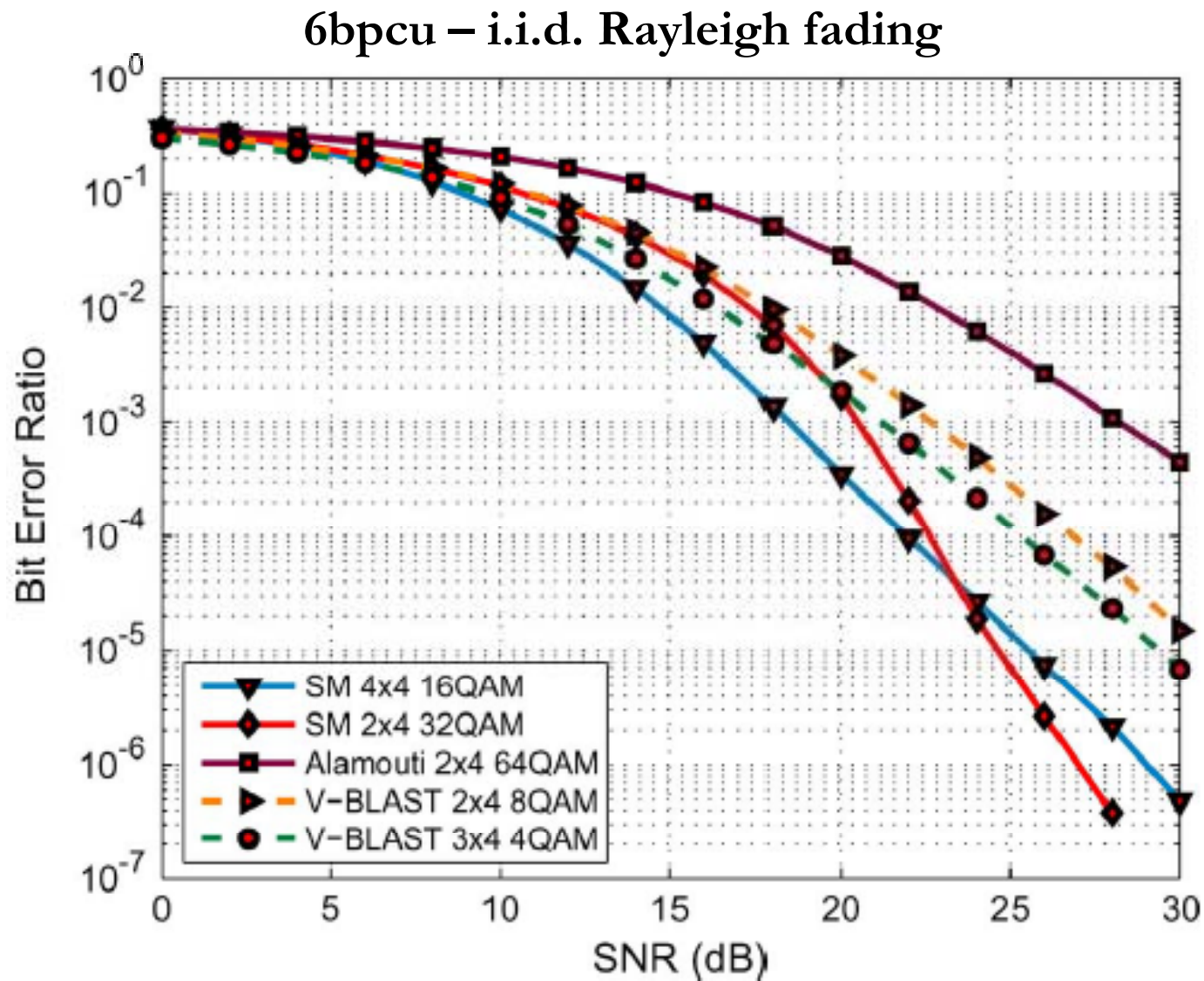
$$C_{C-SD} = C_{\Theta_R} + 8 \sum_{(\ell, s) \in \Theta_R} \tilde{N}_r(\ell, s)$$

# *Outline*

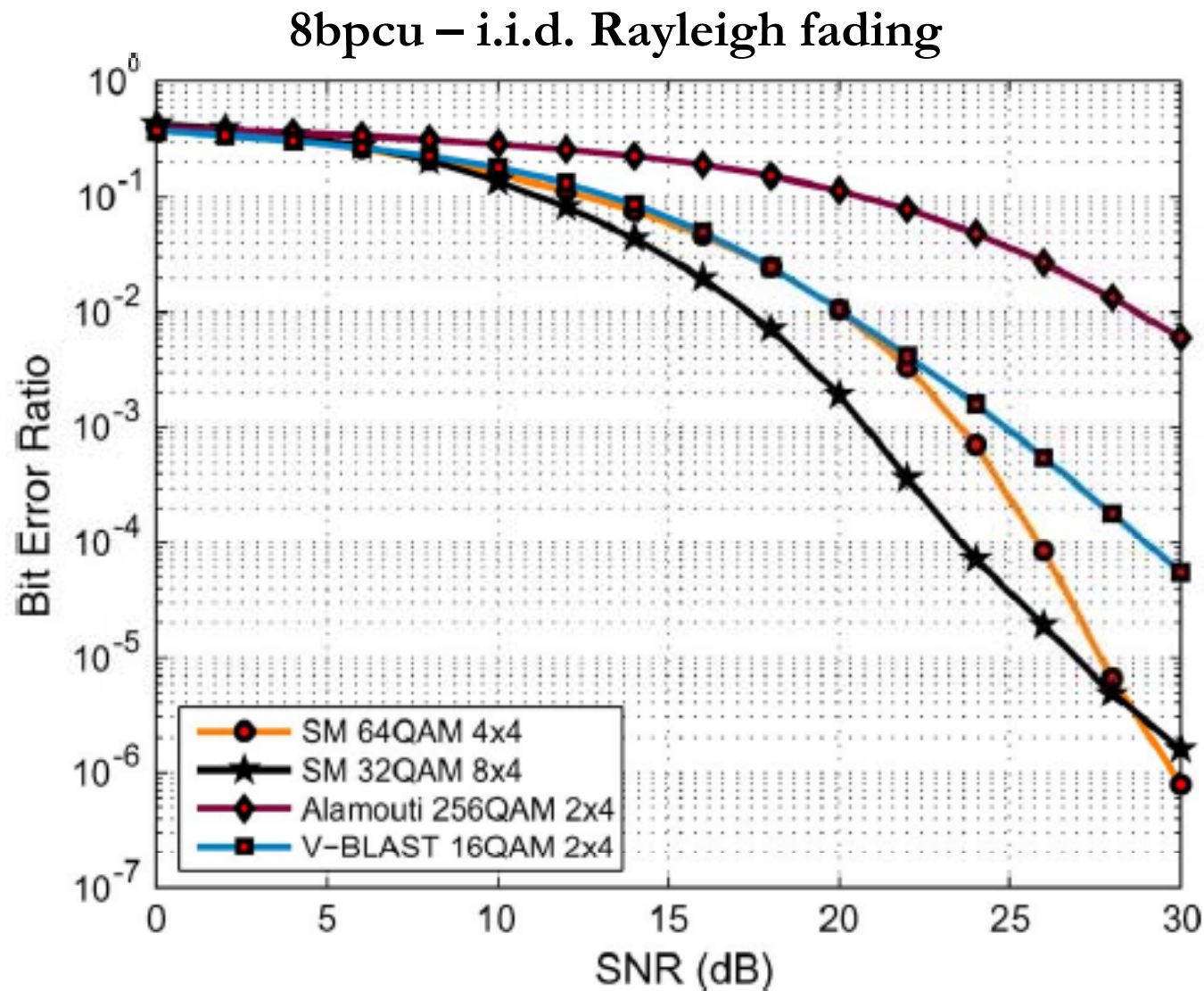
---

1. Introduction and Motivation behind SM-MIMO
2. History of SM Research and Research Groups Working on SM
3. Transmitter Design – Encoding
4. Receiver Design – Demodulation
5. **Error Performance (Numerical Results and Main Trends)**
6. Achievable Capacity
7. Channel State Information at the Transmitter
8. Imperfect Channel State Information at the Receiver
9. Multiple Access Interference
10. Energy Efficiency
11. Transmit-Diversity for SM
12. Spatially-Modulated Space-Time-Coded MIMO
13. Relay-Aided SM
14. SM in Heterogeneous Cellular Networks
15. SM for Visible Light Communications
16. Experimental Evaluation of SM
17. The Road Ahead – Open Research Challenges/Opportunities
18. Implementation Challenges of SM-MIMO

## Error Performance – Numerical Results (1/24)

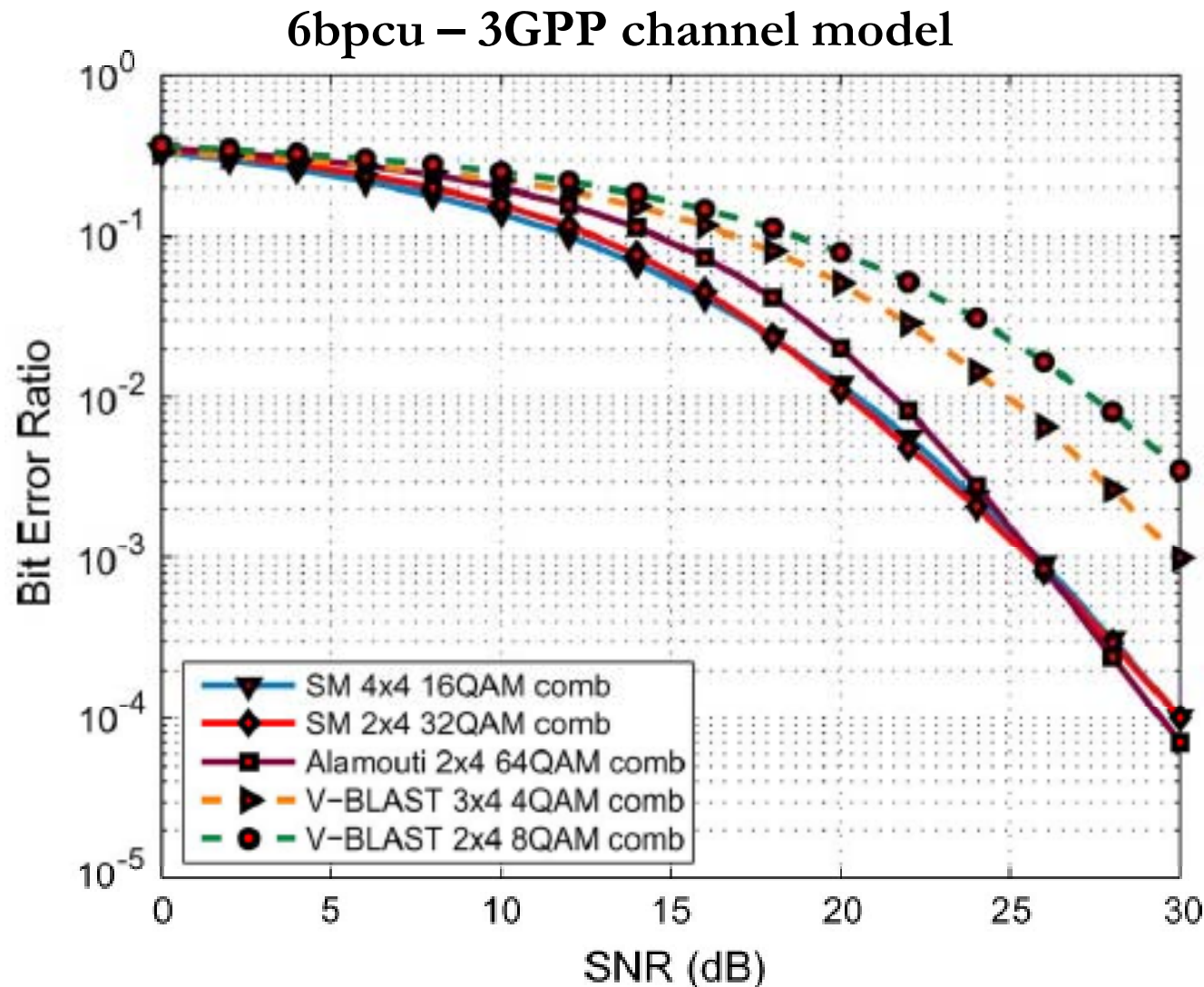


## *Error Performance – Numerical Results (2/24)*

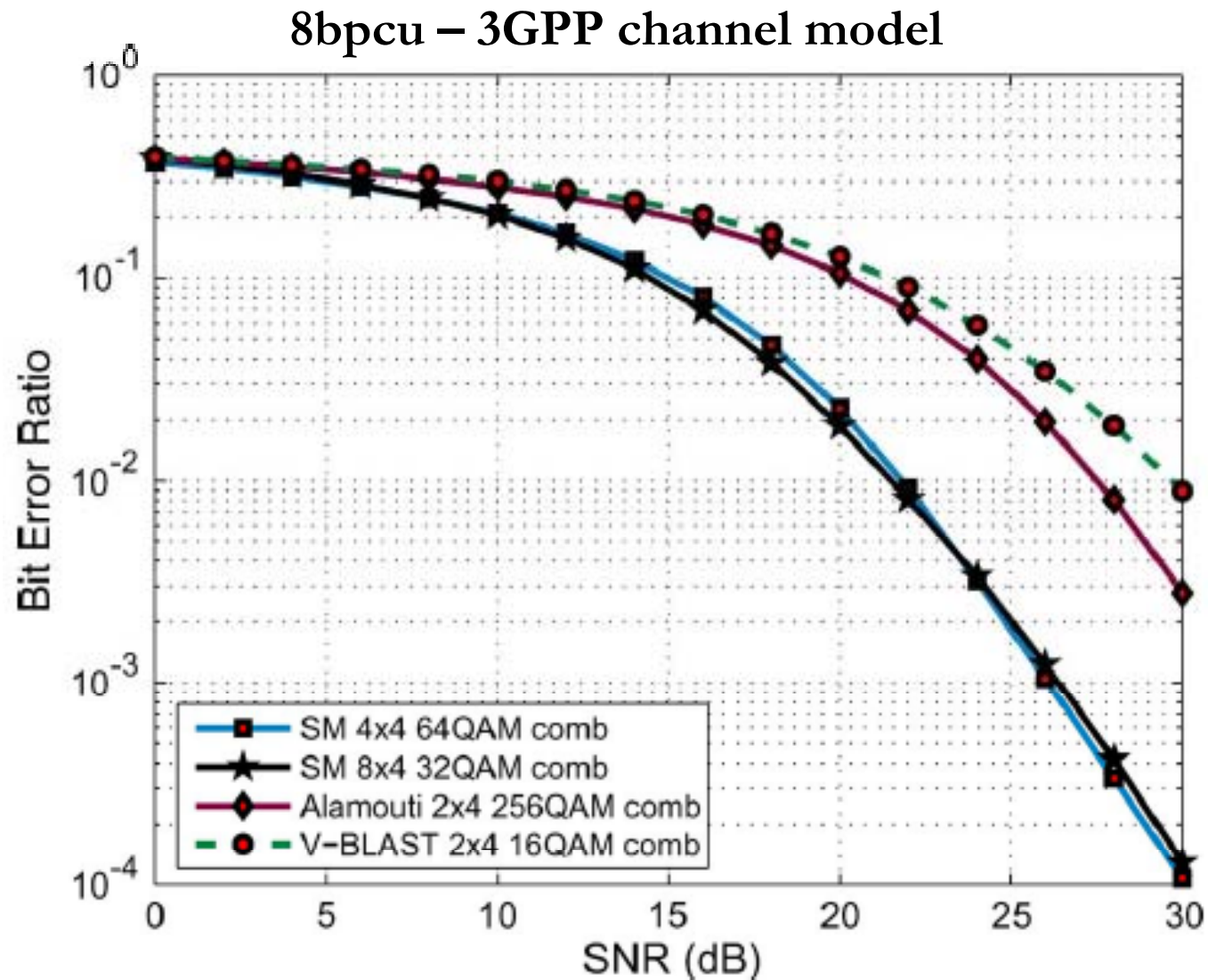




## *Error Performance – Numerical Results (3/24)*



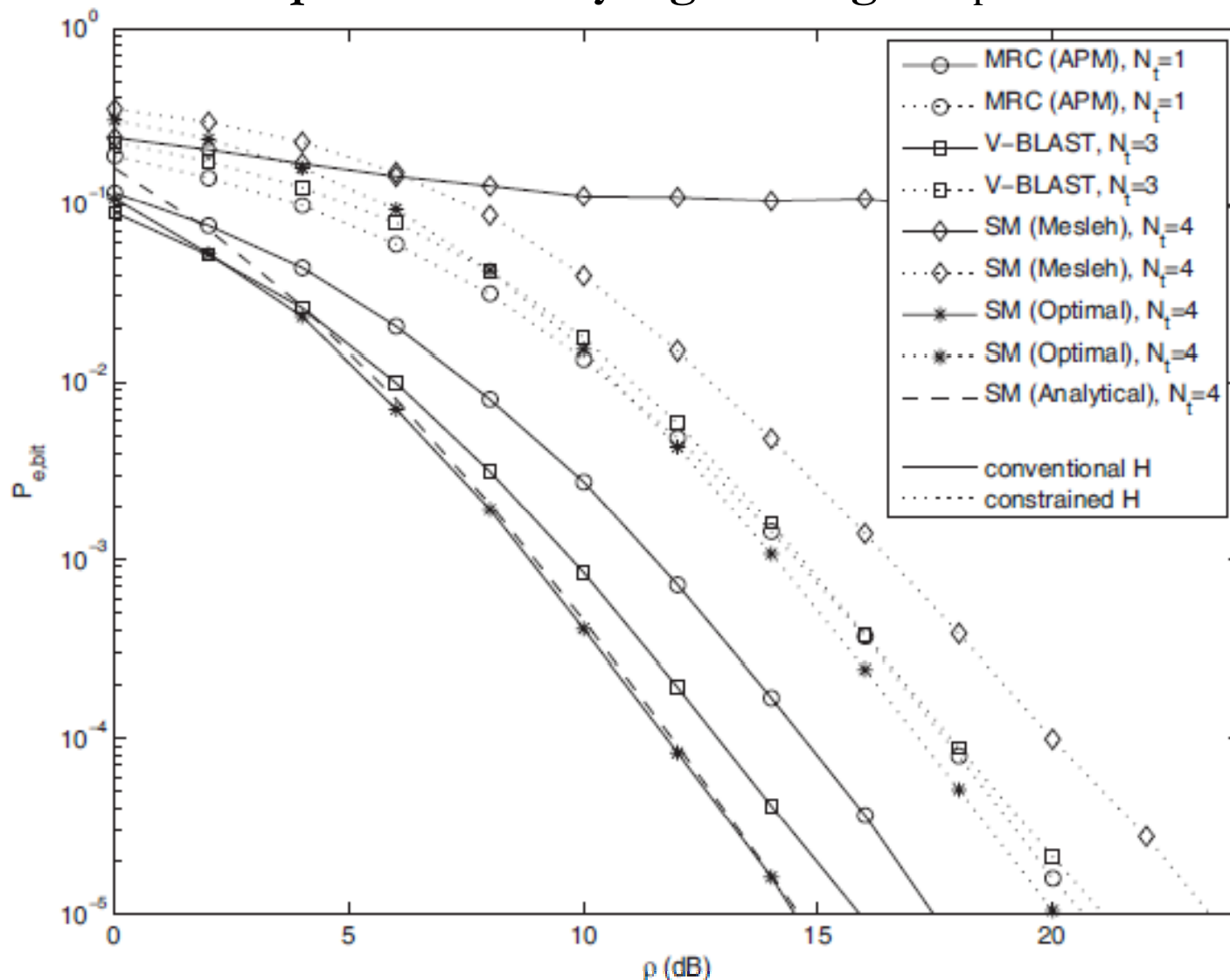
## *Error Performance – Numerical Results (4/24)*



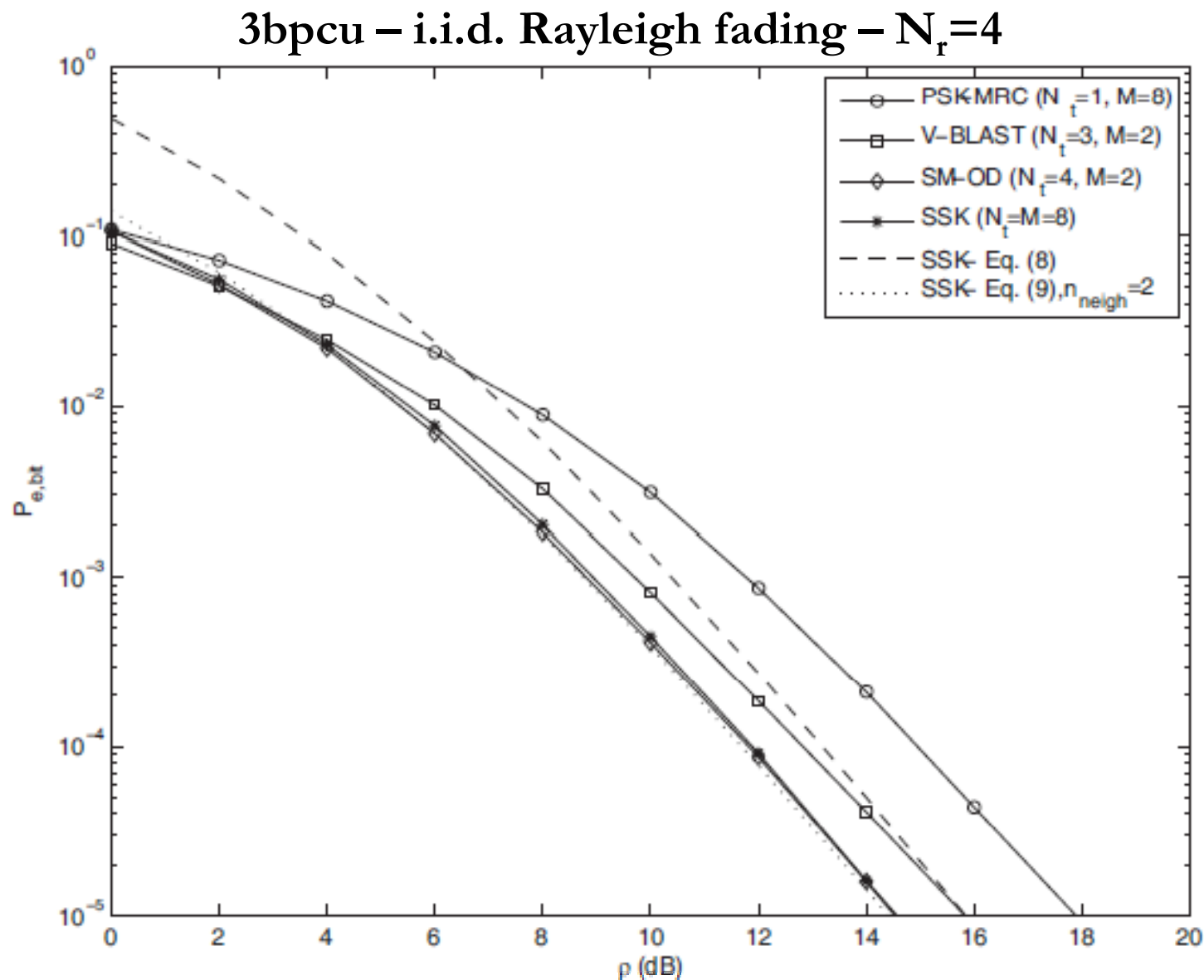


# Error Performance – Numerical Results (5/24)

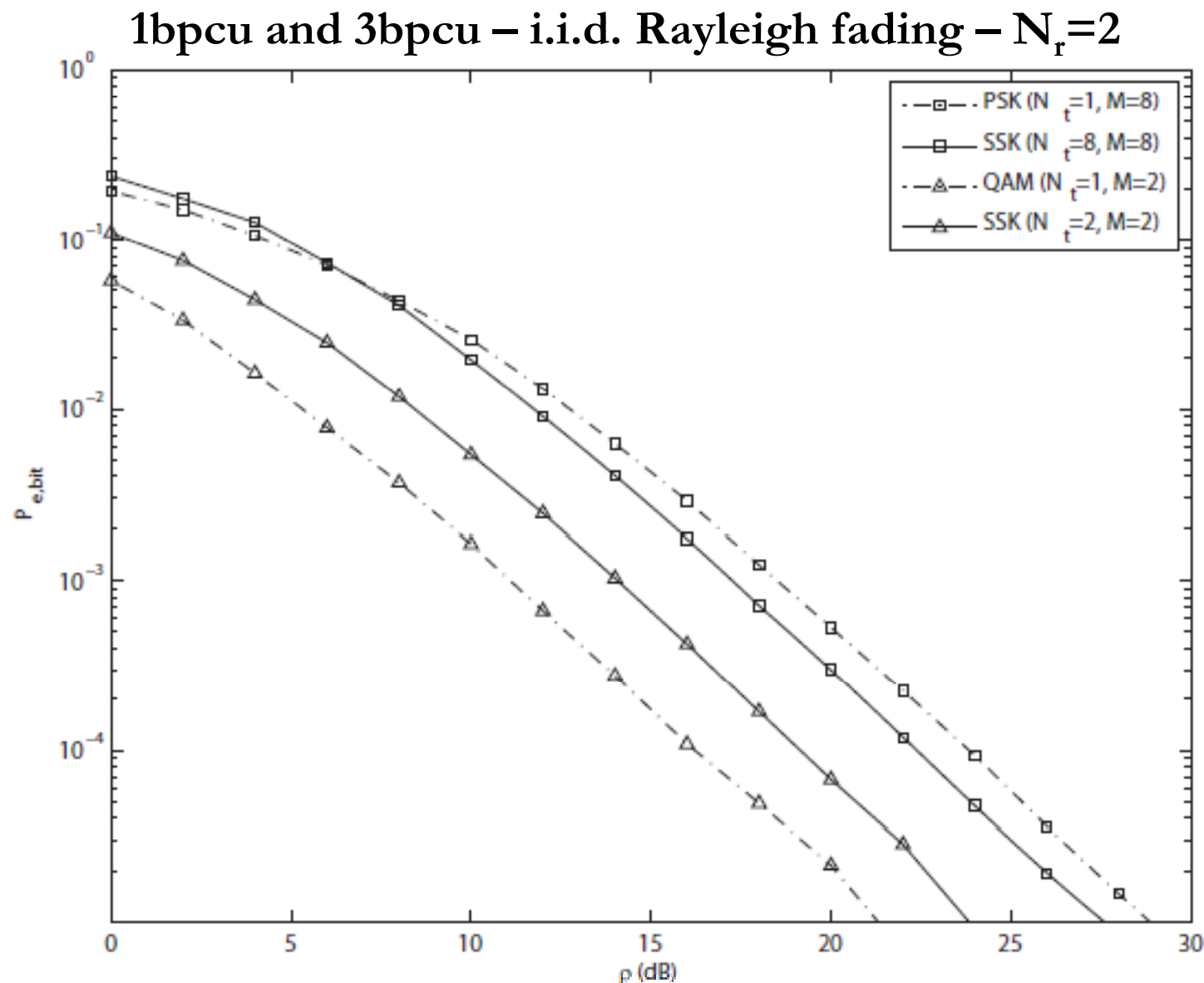
3bpcu – i.i.d. Rayleigh fading –  $N_r=4$



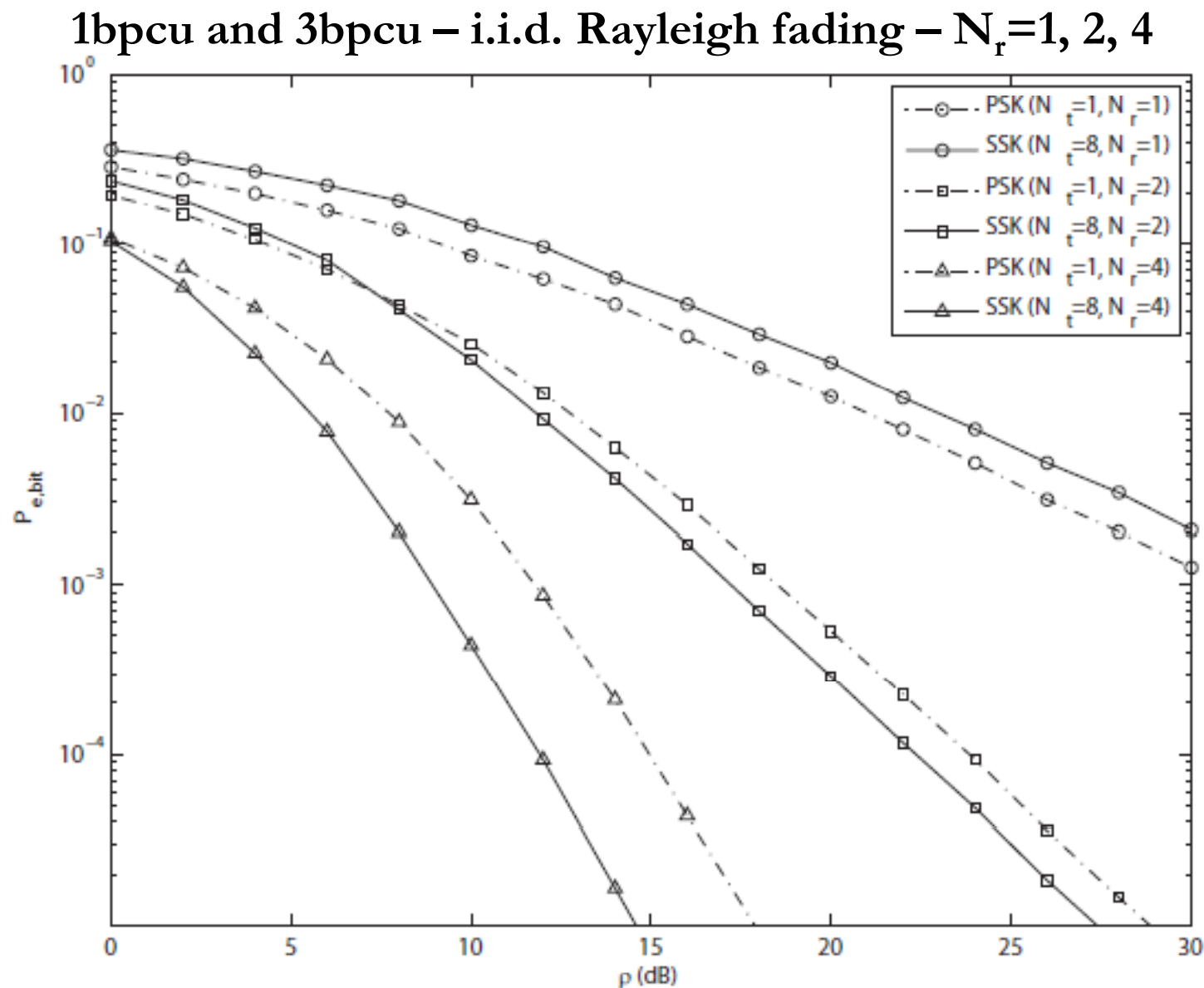
## Error Performance – Numerical Results (6/24)



# Error Performance – Numerical Results (7/24)

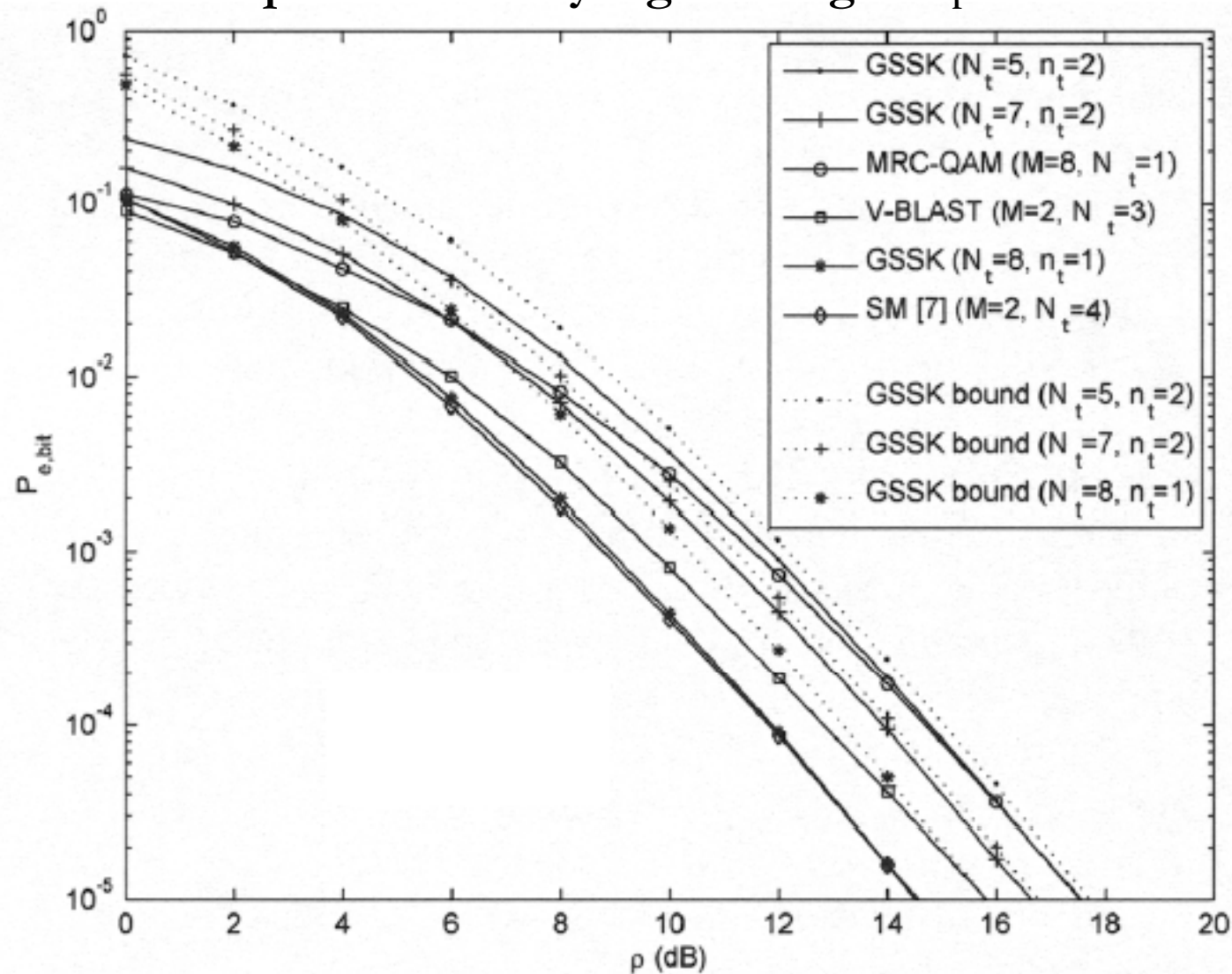


## Error Performance – Numerical Results (8/24)

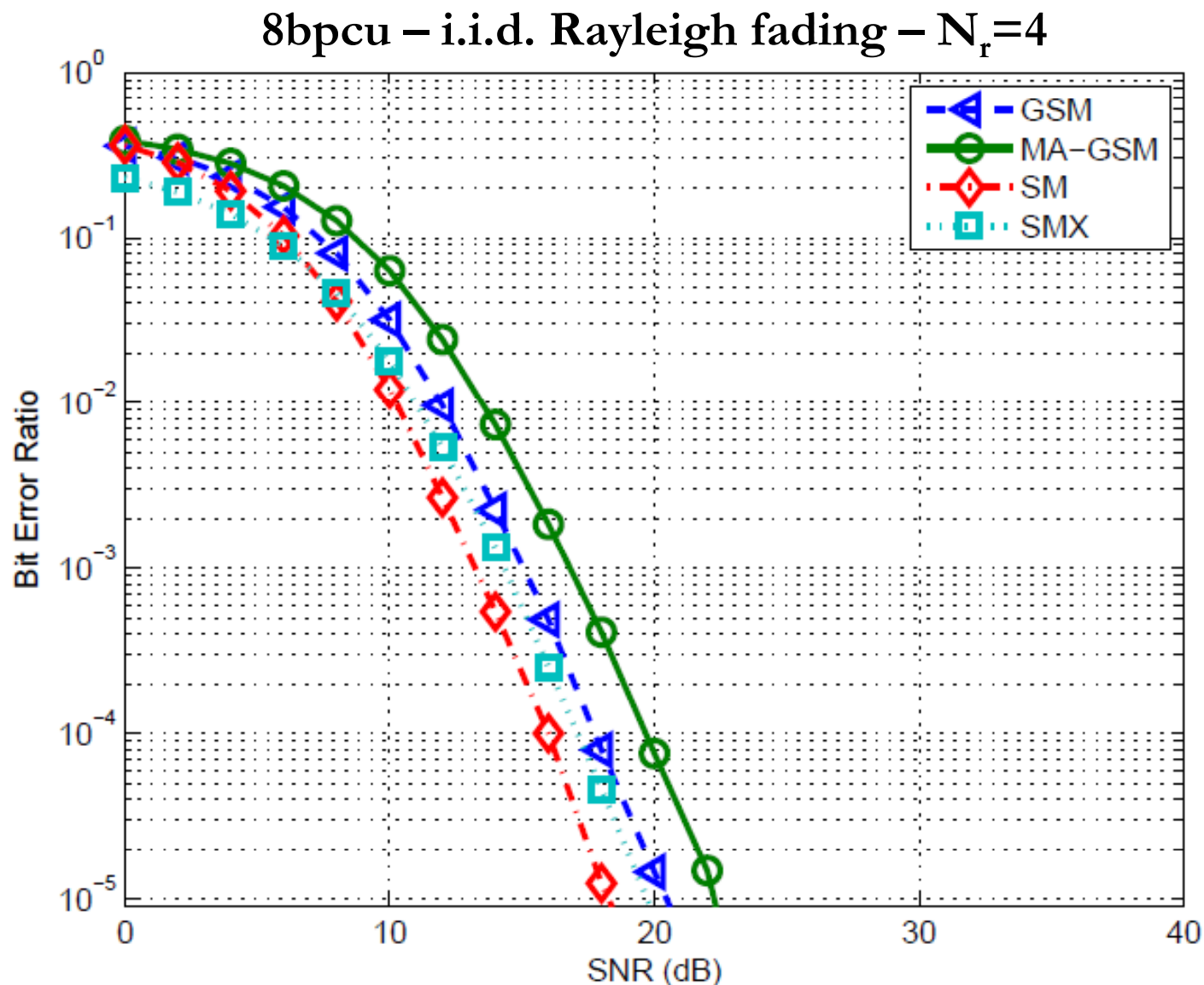


## Error Performance – Numerical Results (9/24)

3bpcu – i.i.d. Rayleigh fading –  $N_r=4$



## Error Performance – Numerical Results (10/24)



GSM:  $N_t = 12$ ,  $n_t = 3$

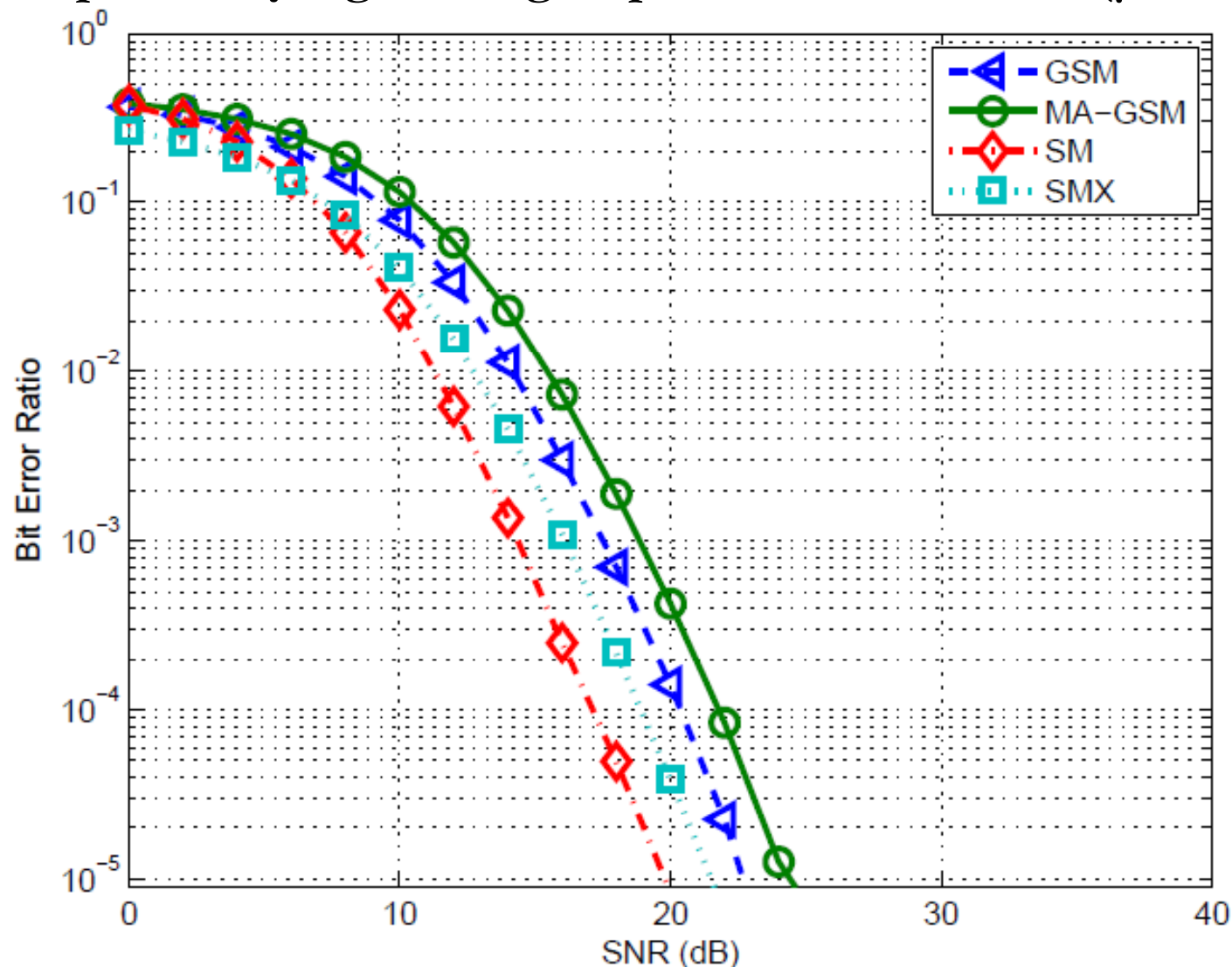
VGSM:  $N_t = 8$ ,  $M = 2$

SM:  $N_t = 128$ ,  $M = 2$

SMX:  $N_t = 8$ ,  $M = 2$

# Error Performance – Numerical Results (11/24)

8bpcu – Rayleigh fading, exponential correlation ( $\beta=0.6$ ) –  $N_r=4$



GSM:  $N_t = 12$ ,  $n_t = 3$

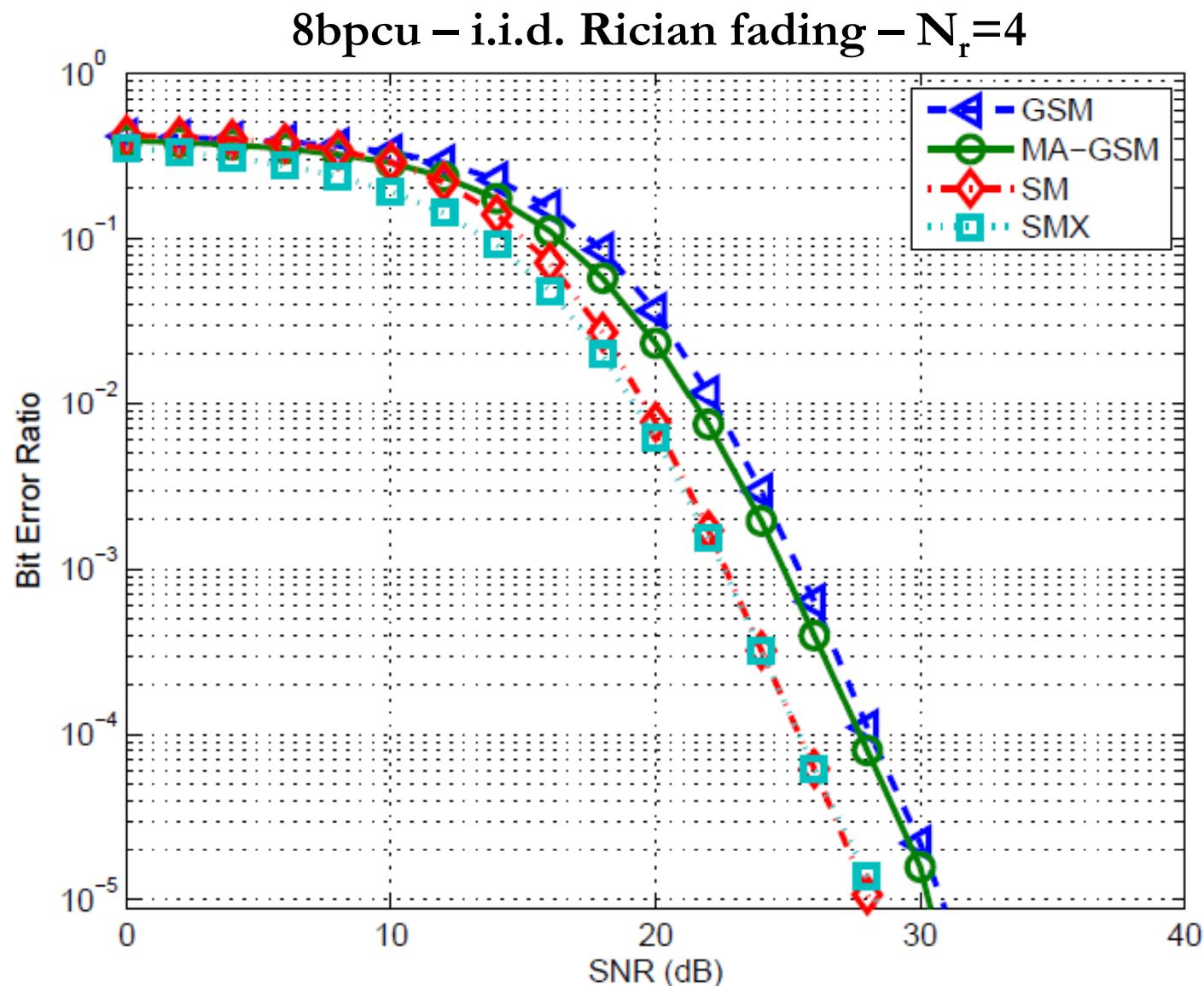
VGSM:  $N_t = 8$ ,  $M = 2$

SM:  $N_t = 128$ ,  $M = 2$

SMX:  $N_t = 8$ ,  $M = 2$



# Error Performance – Numerical Results (12/24)

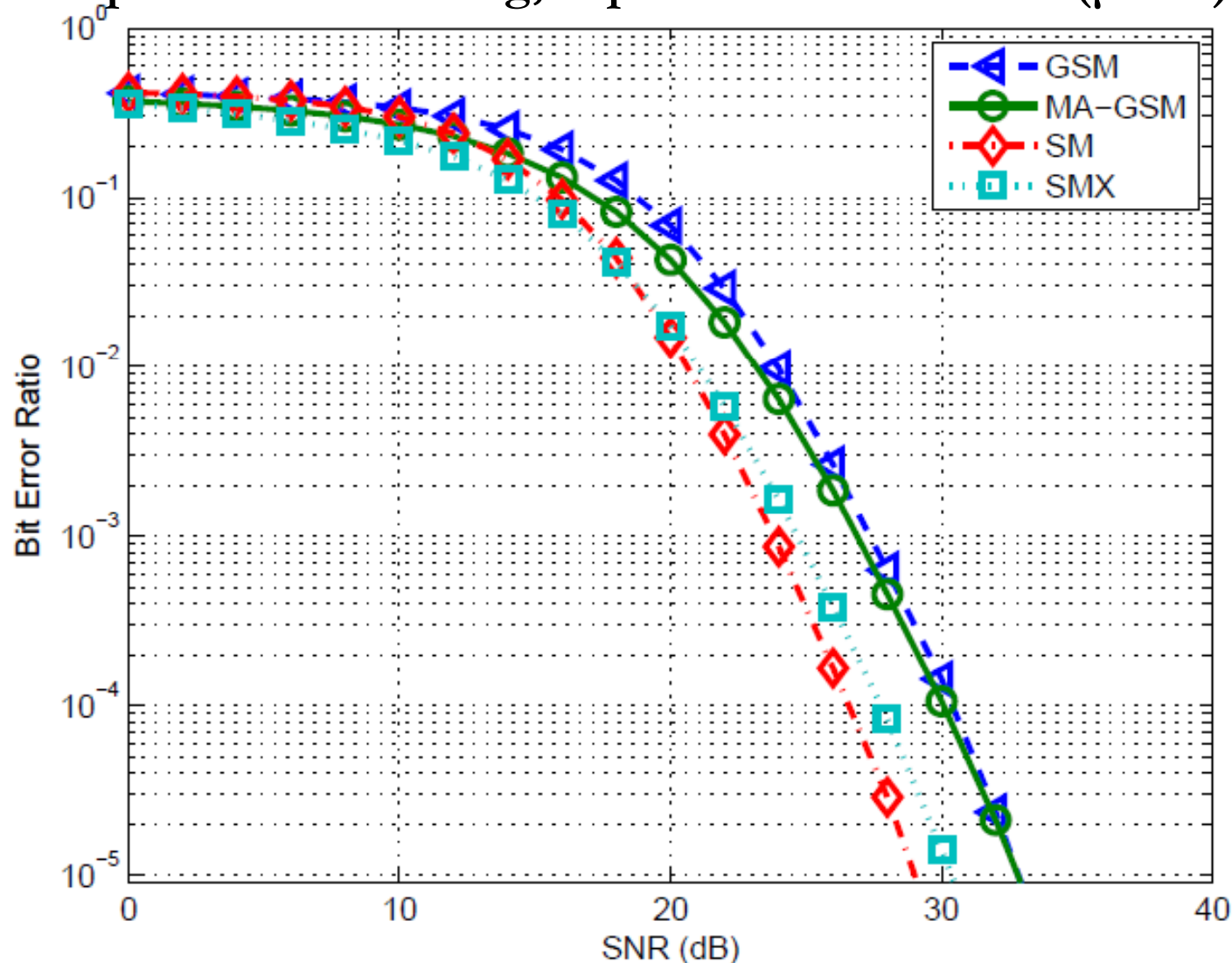


GSM:  $N_t = 12, n_t = 3$   
VGSM:  $N_t = 8, M = 2$   
SM:  $N_t = 128, M = 2$   
SMX:  $N_t = 8, M = 2$



## Error Performance – Numerical Results (13/24)

8bpcu – Rician fading, exponential correlation ( $\beta=0.6$ ) –  $N_r=4$



GSM:  $N_t = 12$ ,  $n_t = 3$

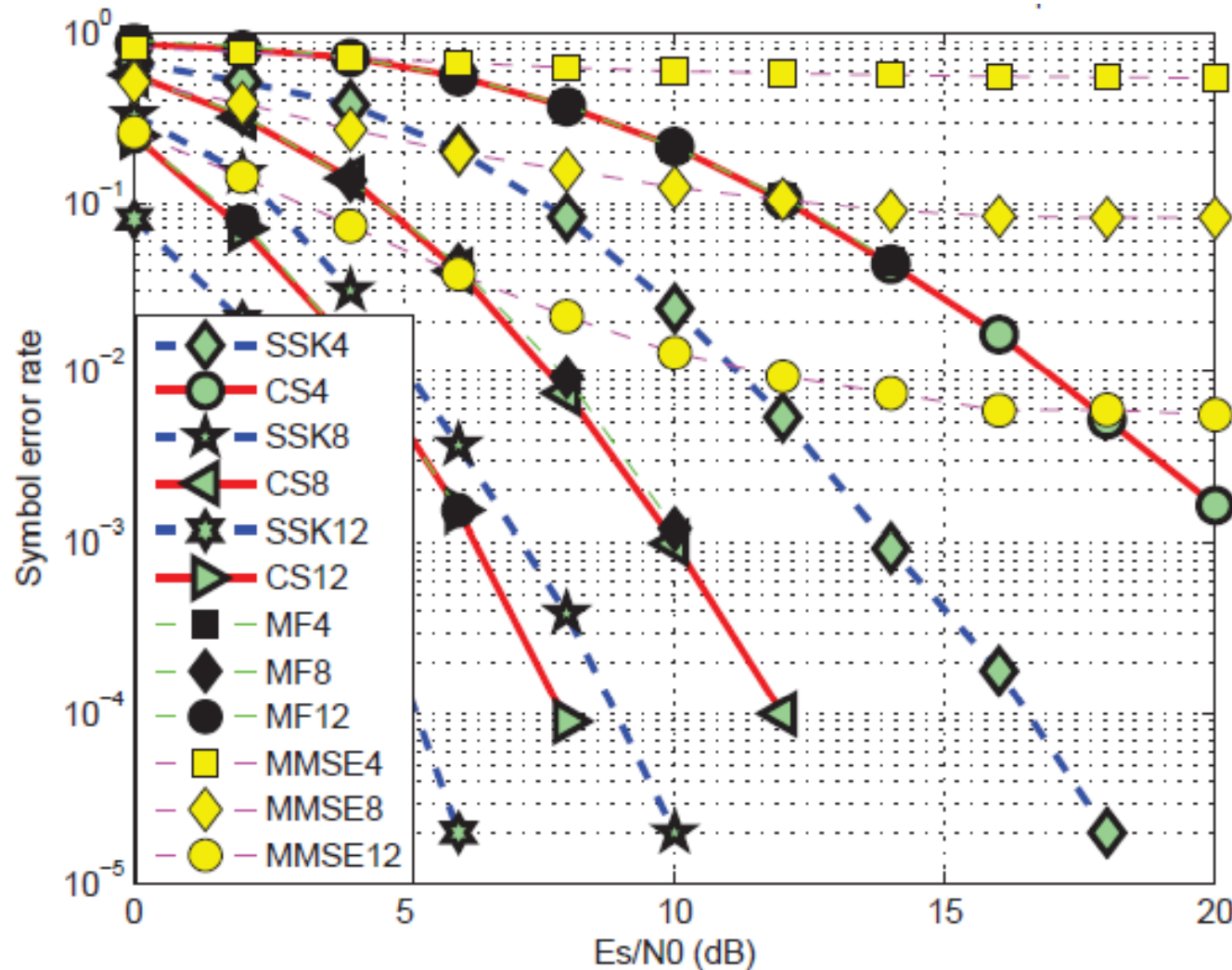
VGSM:  $N_t = 8$ ,  $M = 2$

SM:  $N_t = 128$ ,  $M = 2$

SMX:  $N_t = 8$ ,  $M = 2$

# Error Performance – Numerical Results (14/24)

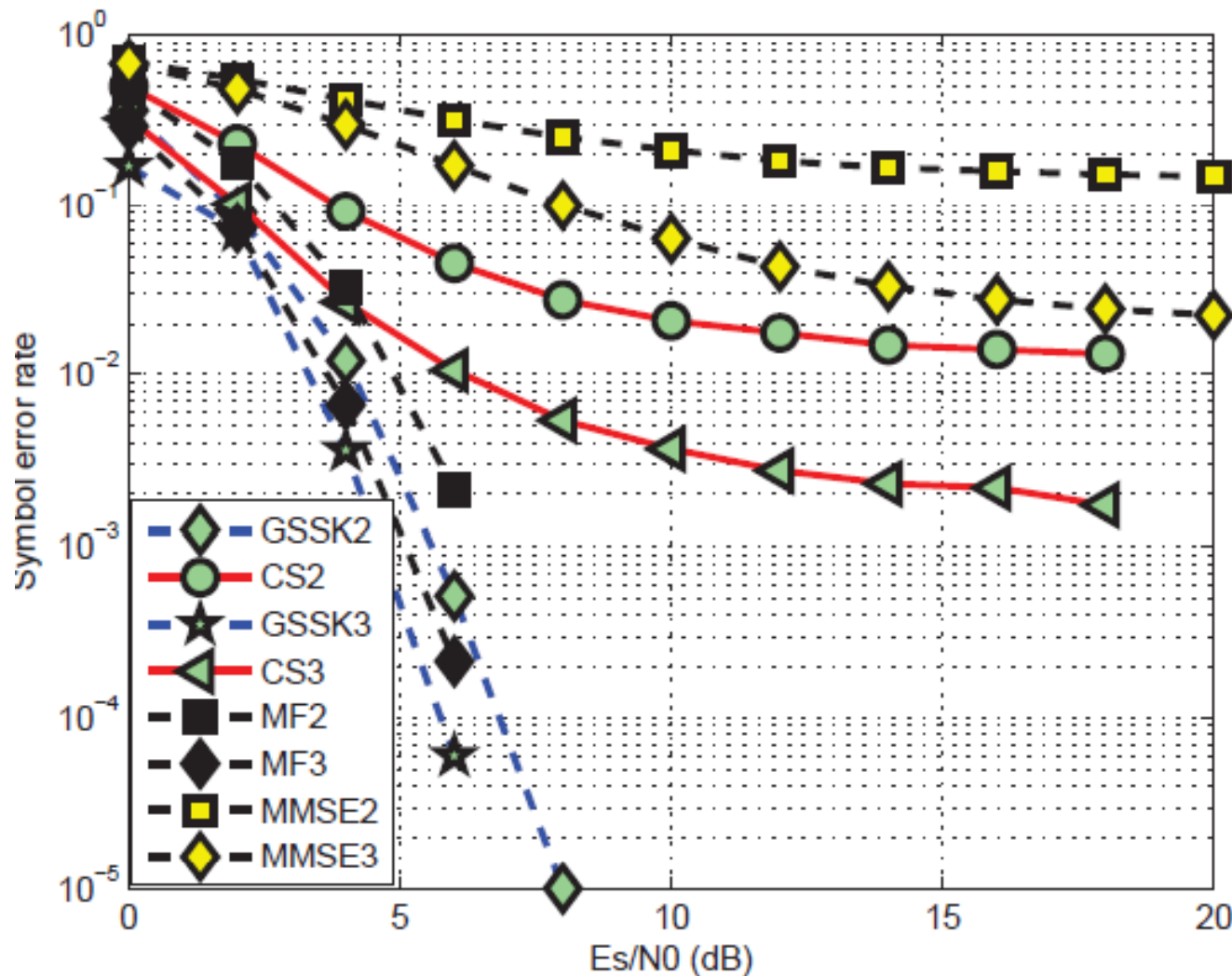
i.i.d. Rayleigh fading



$N_t = 256$   
 $n_t = 1$   
 Varying  $N_r$

# Error Performance – Numerical Results (15/24)

i.i.d. Rayleigh fading



Setup “2”:

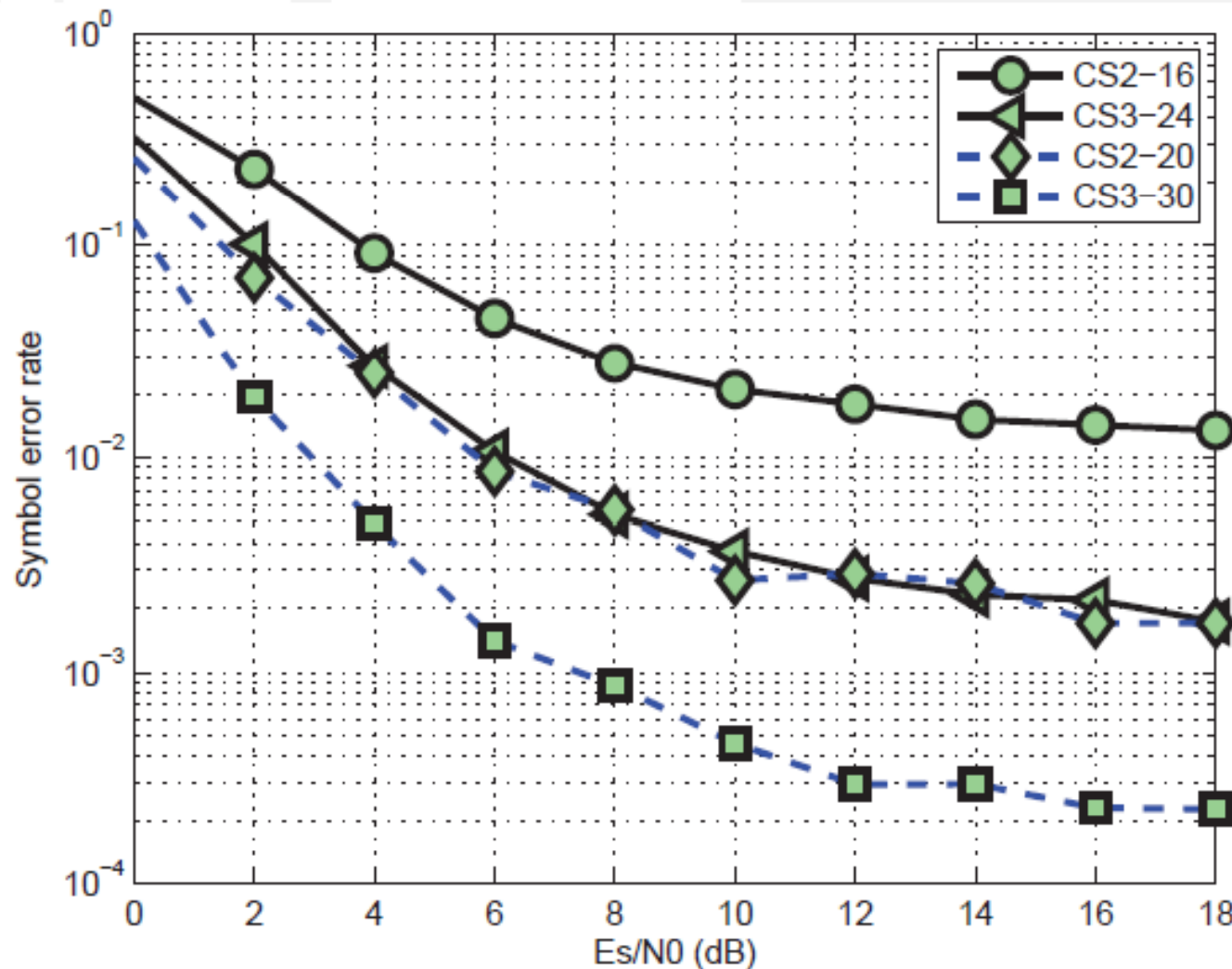
$$N_t = 256, n_t = 2, N_r = 16$$

Setup “3”:

$$N_t = 64, n_t = 3, N_r = 24$$

# Error Performance – Numerical Results (16/24)

i.i.d. Rayleigh fading



Setup “CS2-16”:

$N_t = 256, n_t = 2, N_r = 16$

Setup “CS2-20”:

$N_t = 256, n_t = 2, N_r = 20$

Setup “CS3-24”:

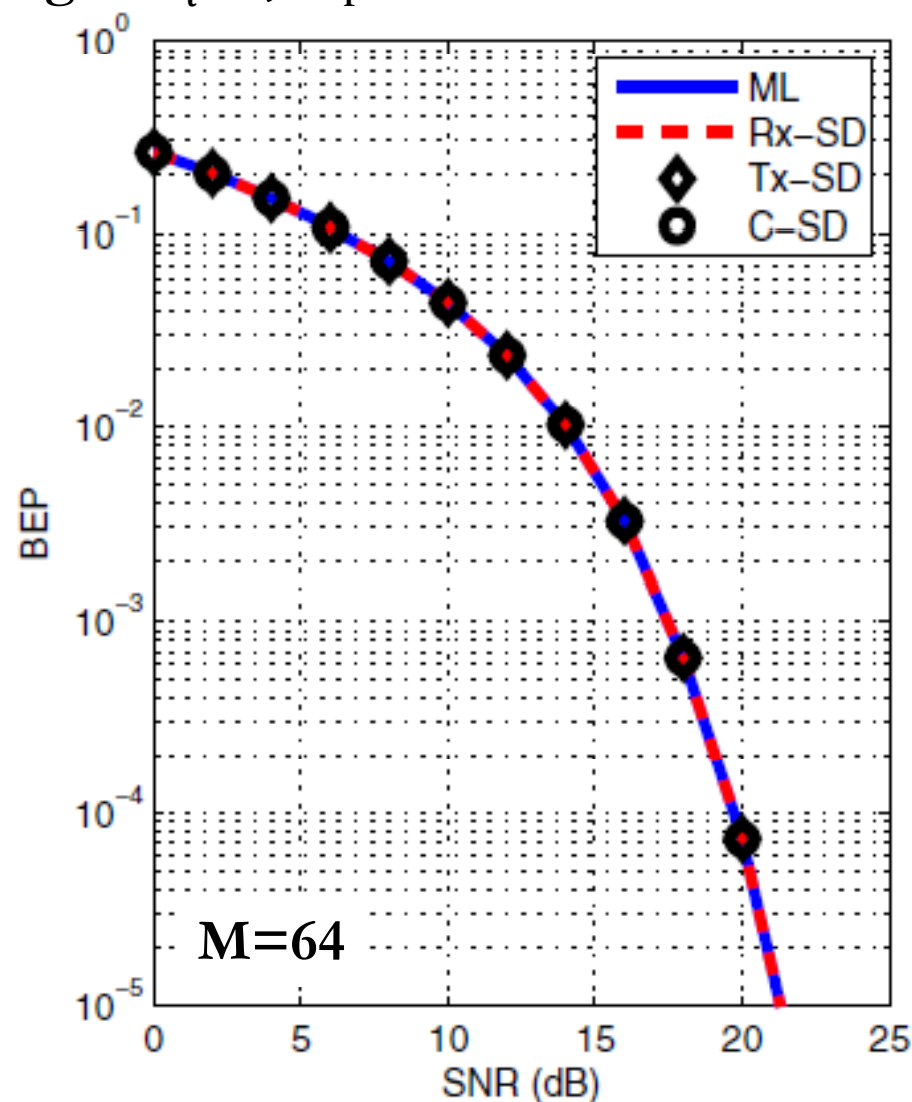
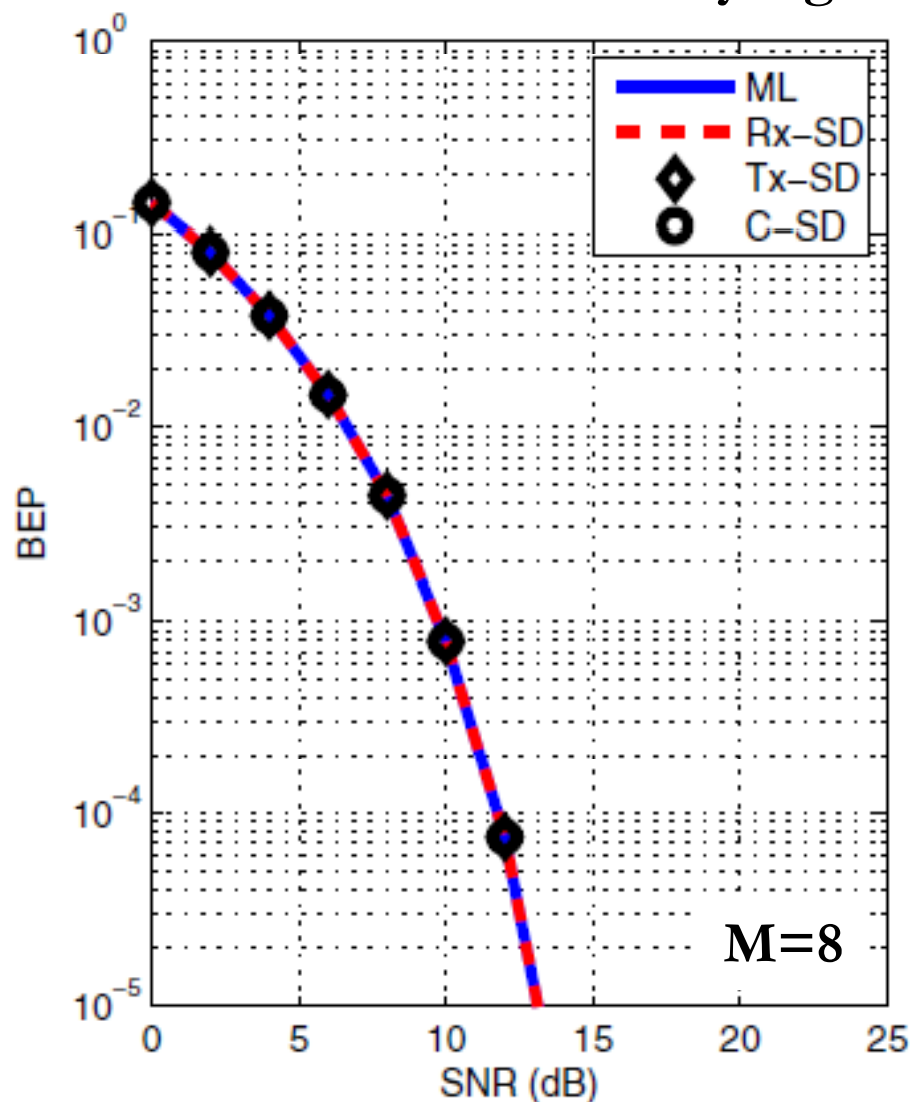
$N_t = 64, n_t = 3, N_r = 24$

Setup “CS3-30”:

$N_t = 64, n_t = 3, N_r = 30$

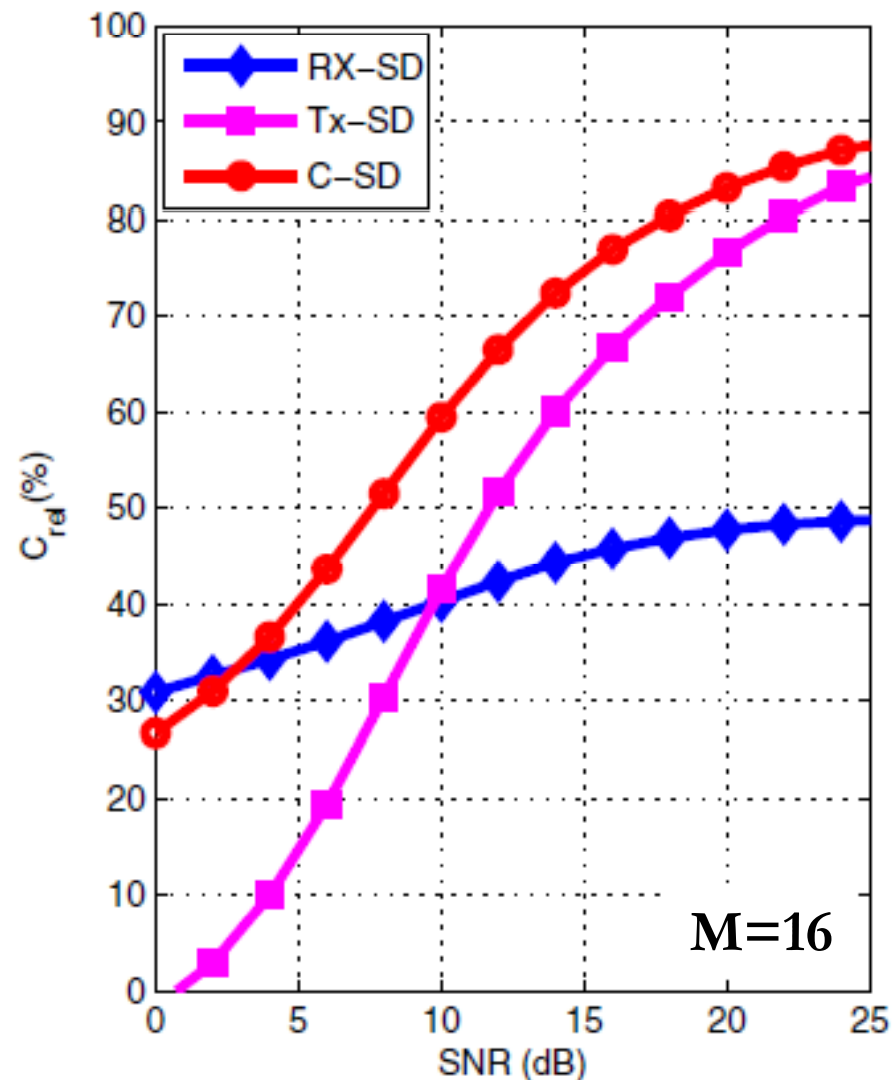
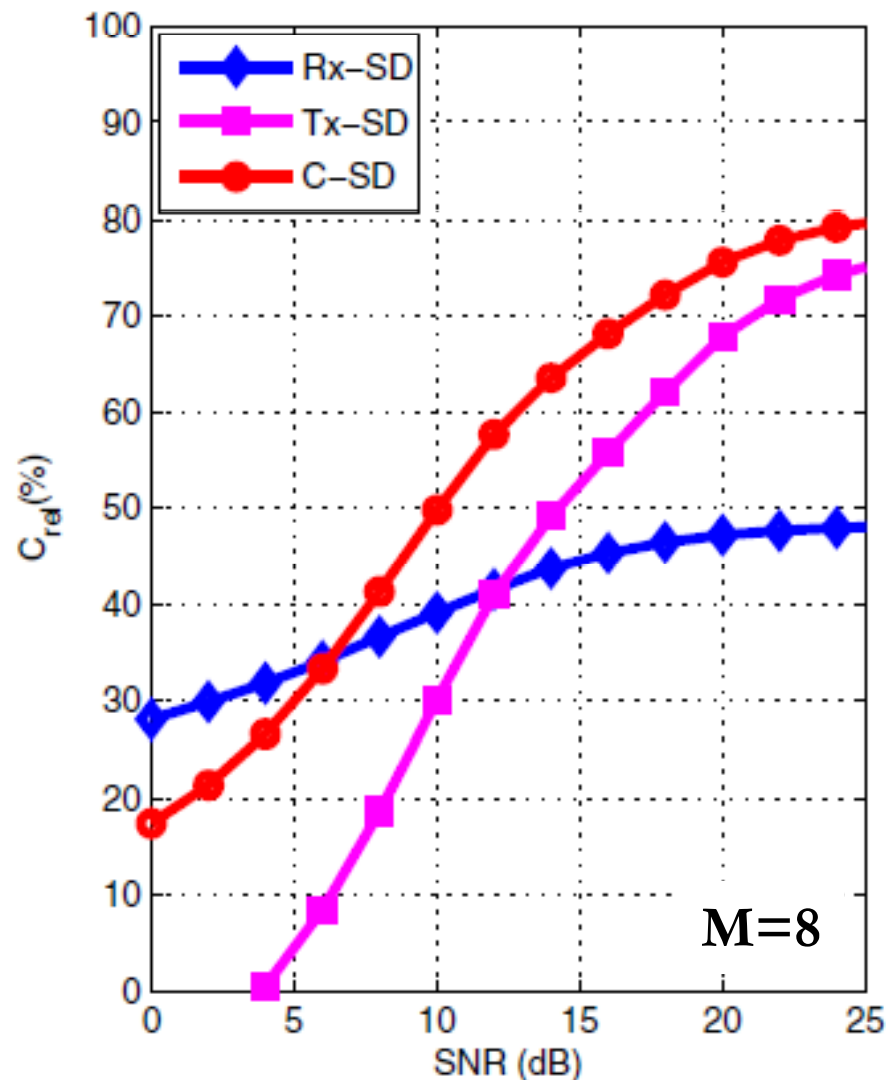
## Error Performance – Numerical Results (17/24)

i.i.d. Rayleigh fading –  $N_t=4$ ,  $N_r=4$



## Error Performance – Numerical Results (18/24)

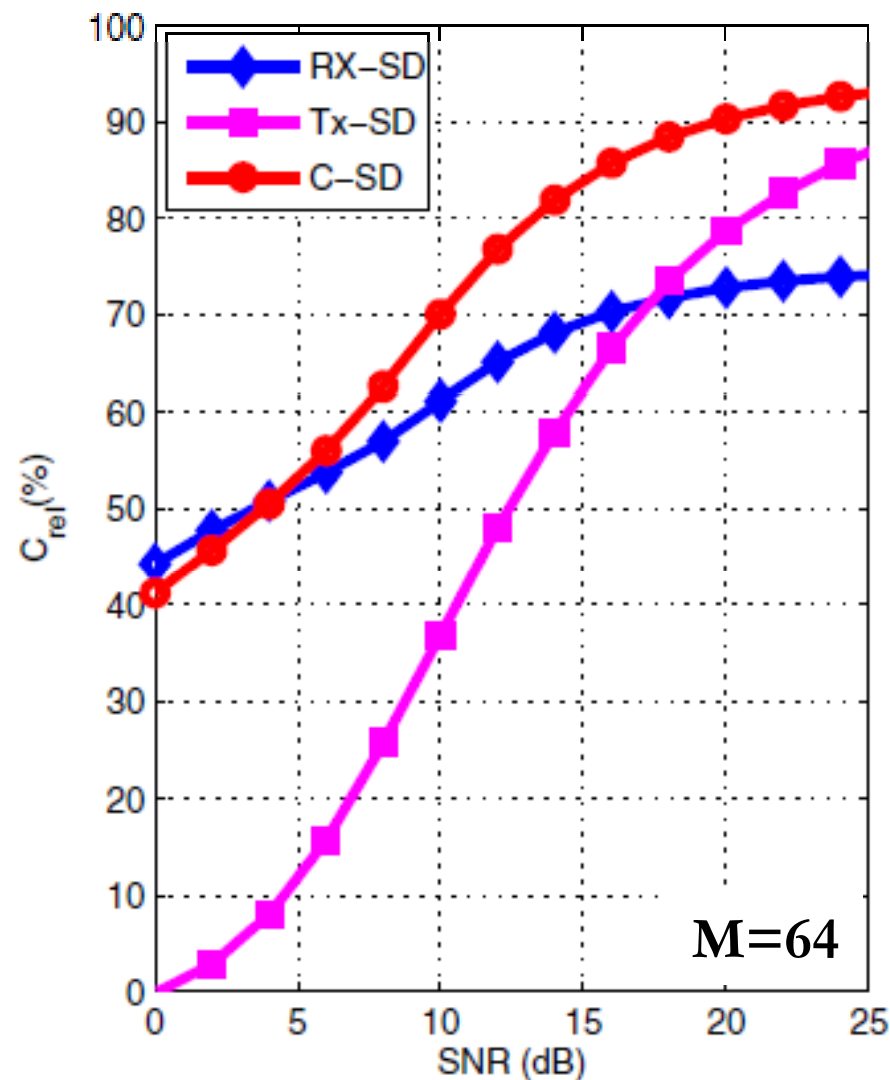
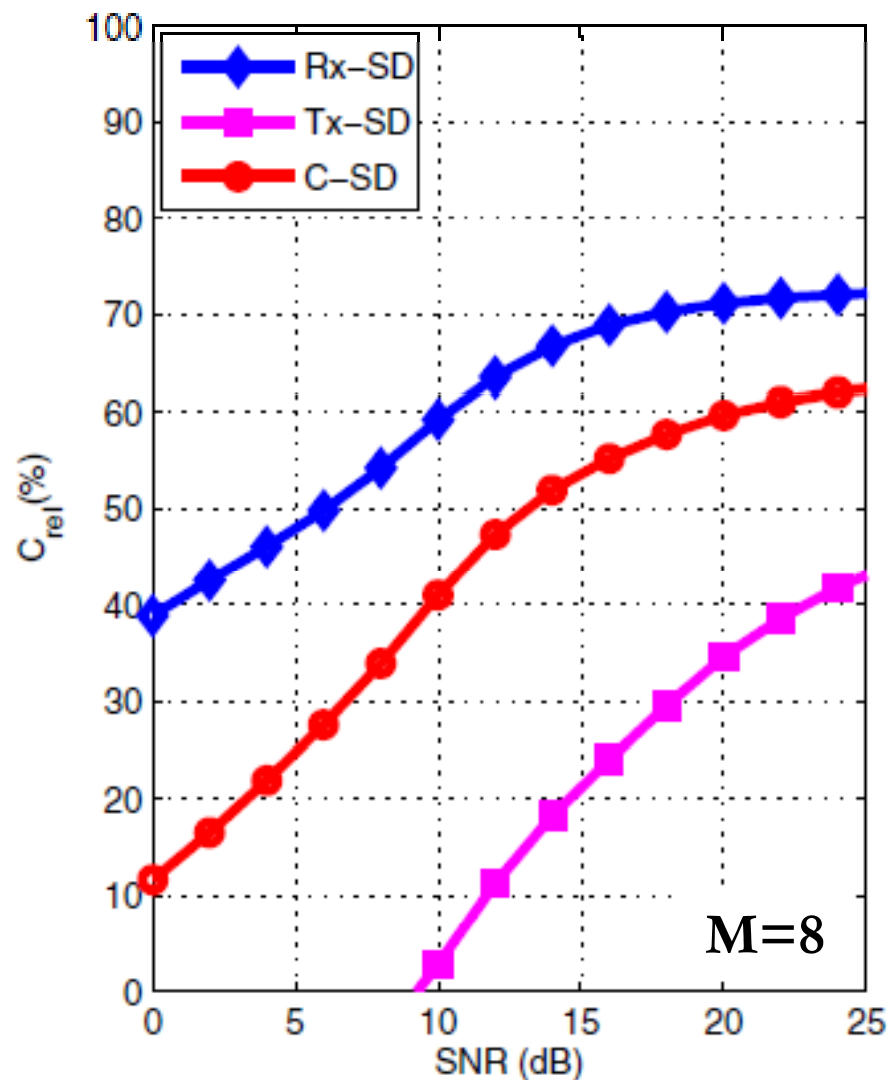
i.i.d. Rayleigh fading –  $N_t=2$ ,  $N_r=2$





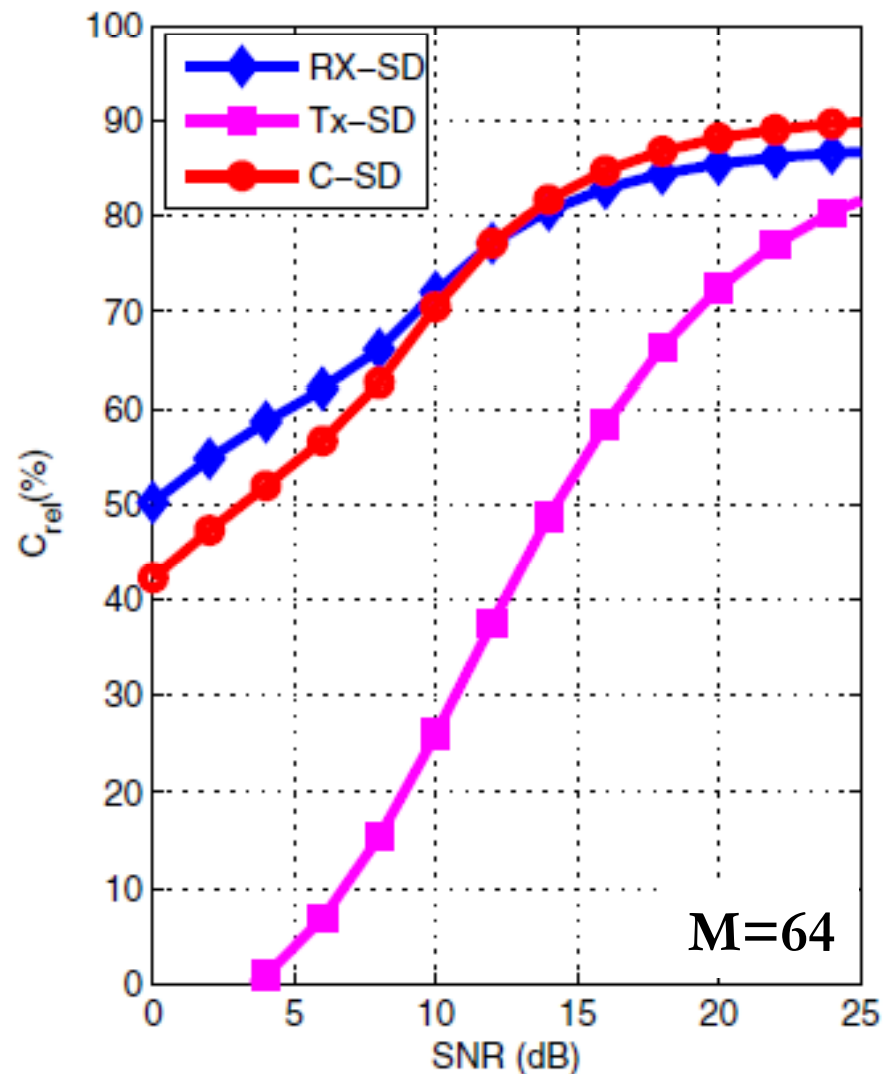
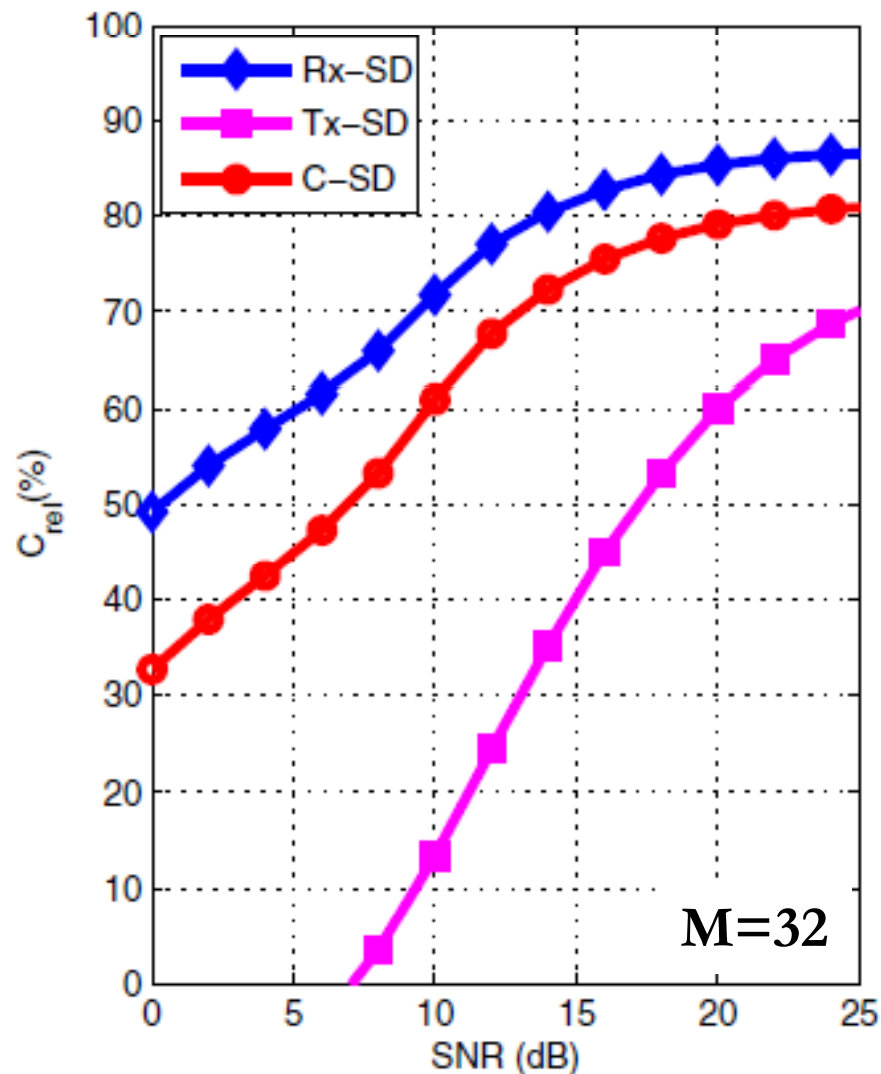
# Error Performance – Numerical Results (19/24)

i.i.d. Rayleigh fading –  $N_t=4$ ,  $N_r=4$



# Error Performance – Numerical Results (20/24)

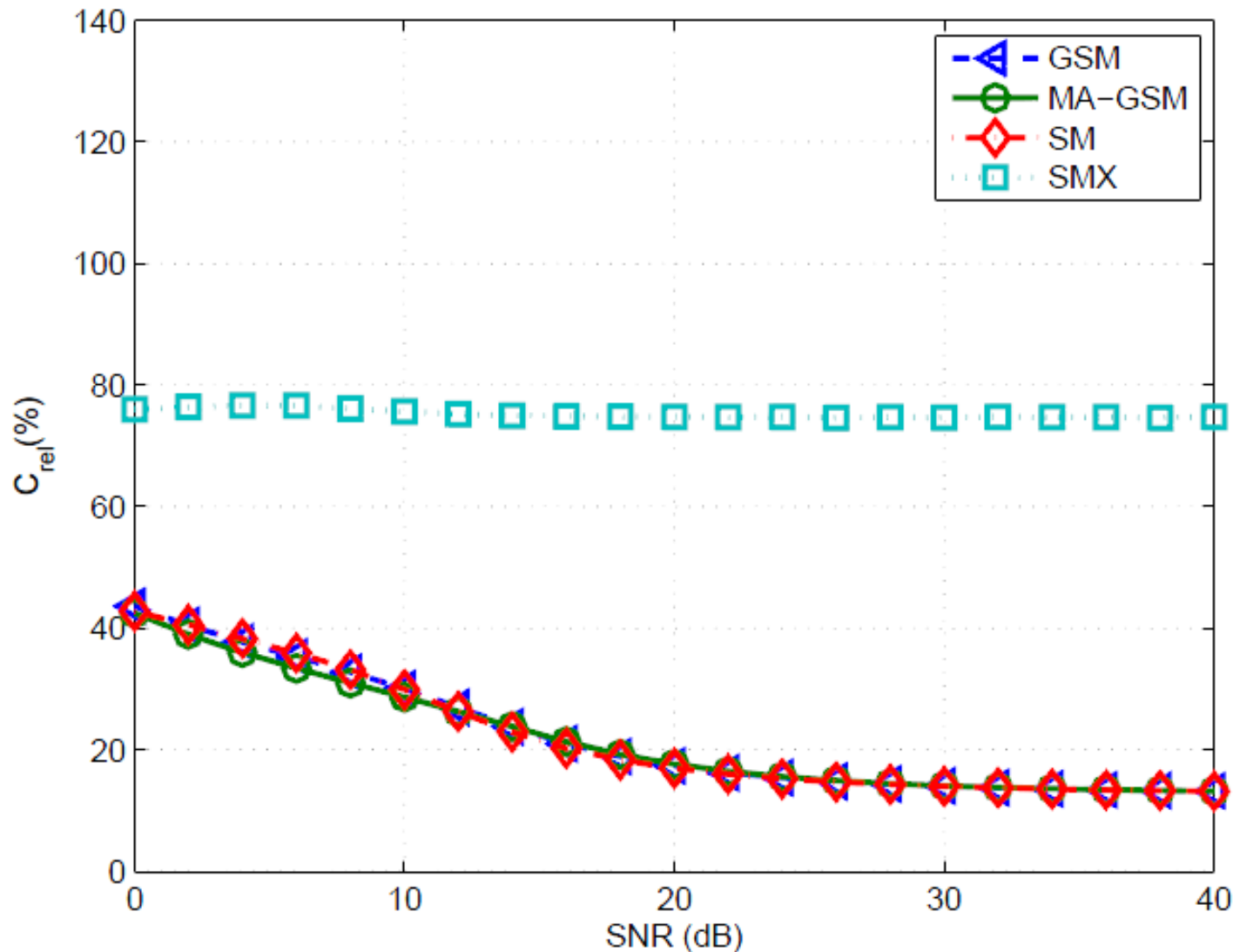
i.i.d. Rayleigh fading –  $N_t=8$ ,  $N_r=8$





## Error Performance – Numerical Results (21/24)

8bpcu – i.i.d. Rayleigh fading –  $N_r=4$



GSM:  $N_t = 12, n_t = 3$

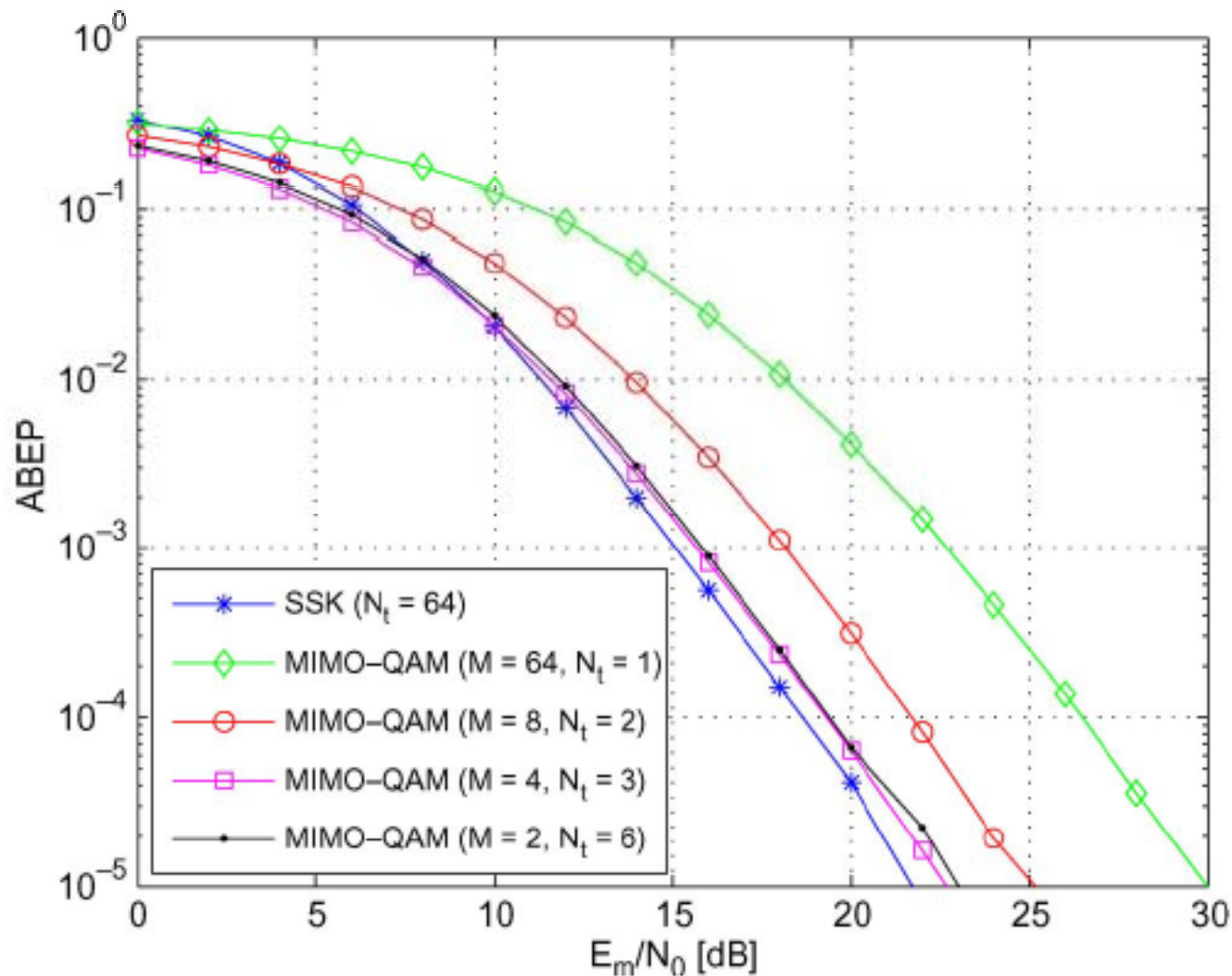
VGSM:  $N_t = 8, M = 2$

SM:  $N_t = 128, M = 2$

SMX:  $N_t = 8, M = 2$

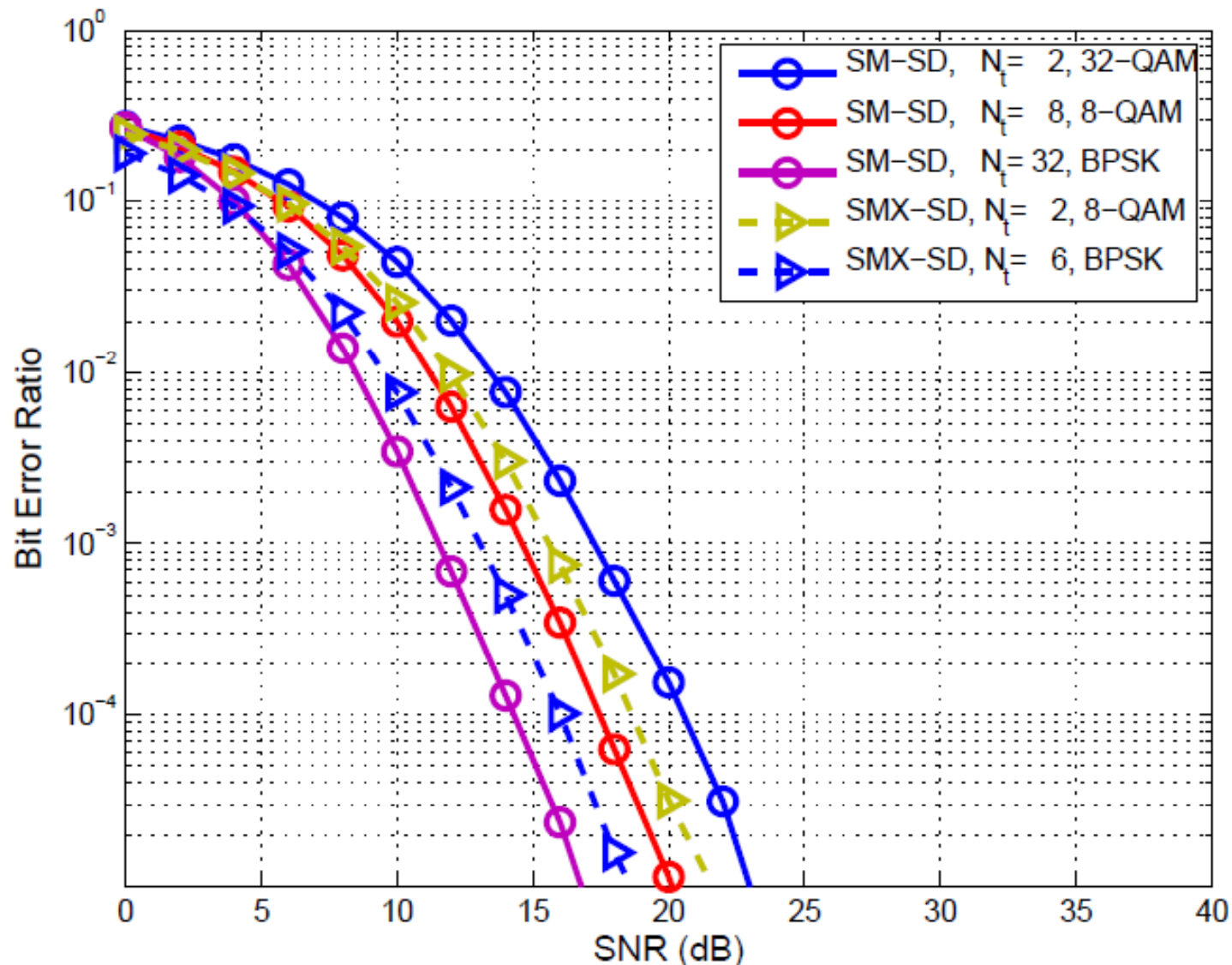
# Error Performance – Numerical Results (22/24)

## Single-RF vs. Multi-RF (SSK vs. Spatial-Multiplexing MIMO)



# Error Performance – Numerical Results (23/24)

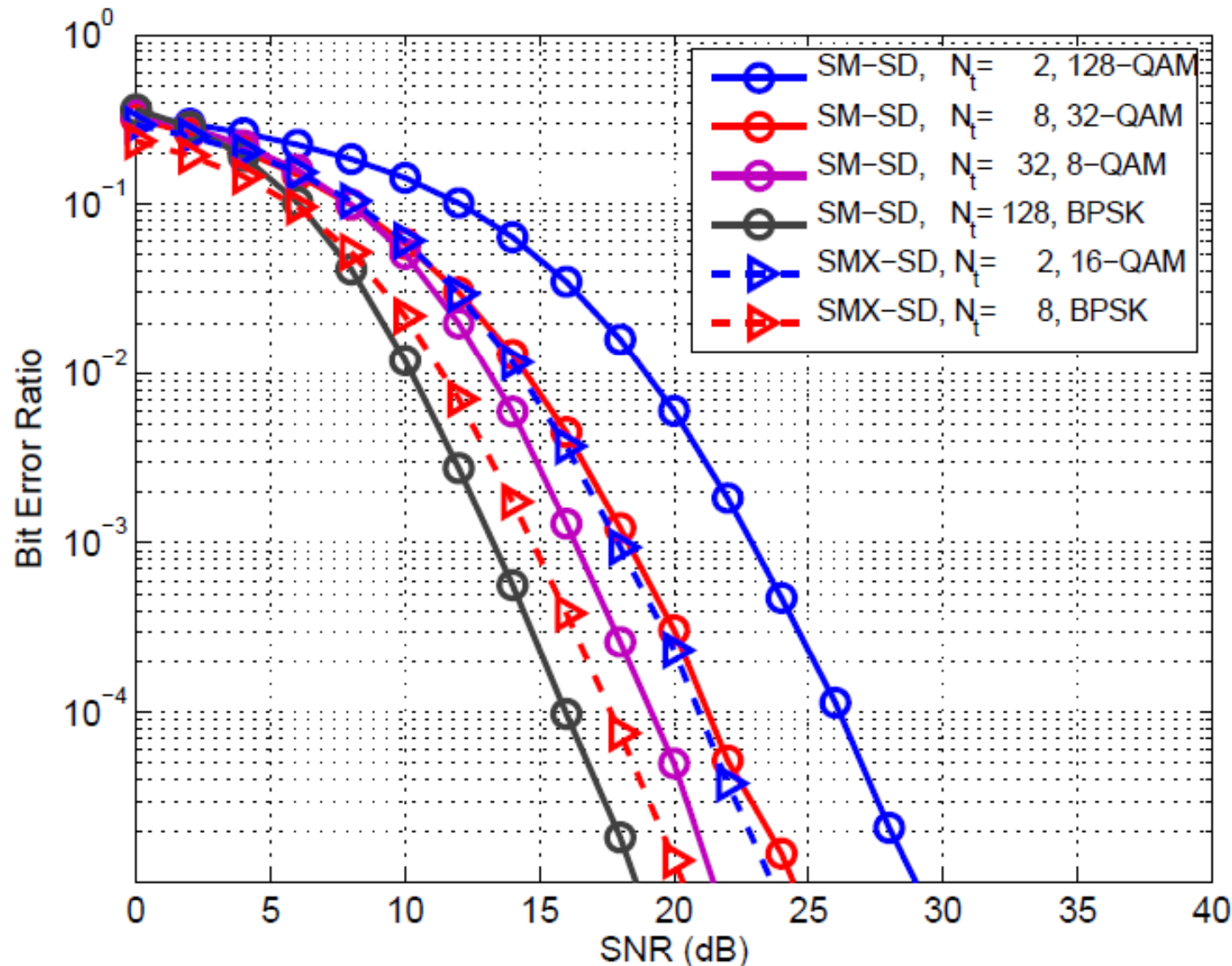
## Single-RF vs. Multi-RF (SM vs. Spatial-Multiplexing MIMO)



i.i.d. Rayleigh fading  
6 bpcu  
 $N_r = 4$

# Error Performance – Numerical Results (24/24)

## Single-RF vs. Multi-RF (SM vs. Spatial-Multiplexing MIMO)



i.i.d. Rayleigh fading  
8 bpcu  
 $N_r = 4$

## Error Performance – Main Trends (1/38)

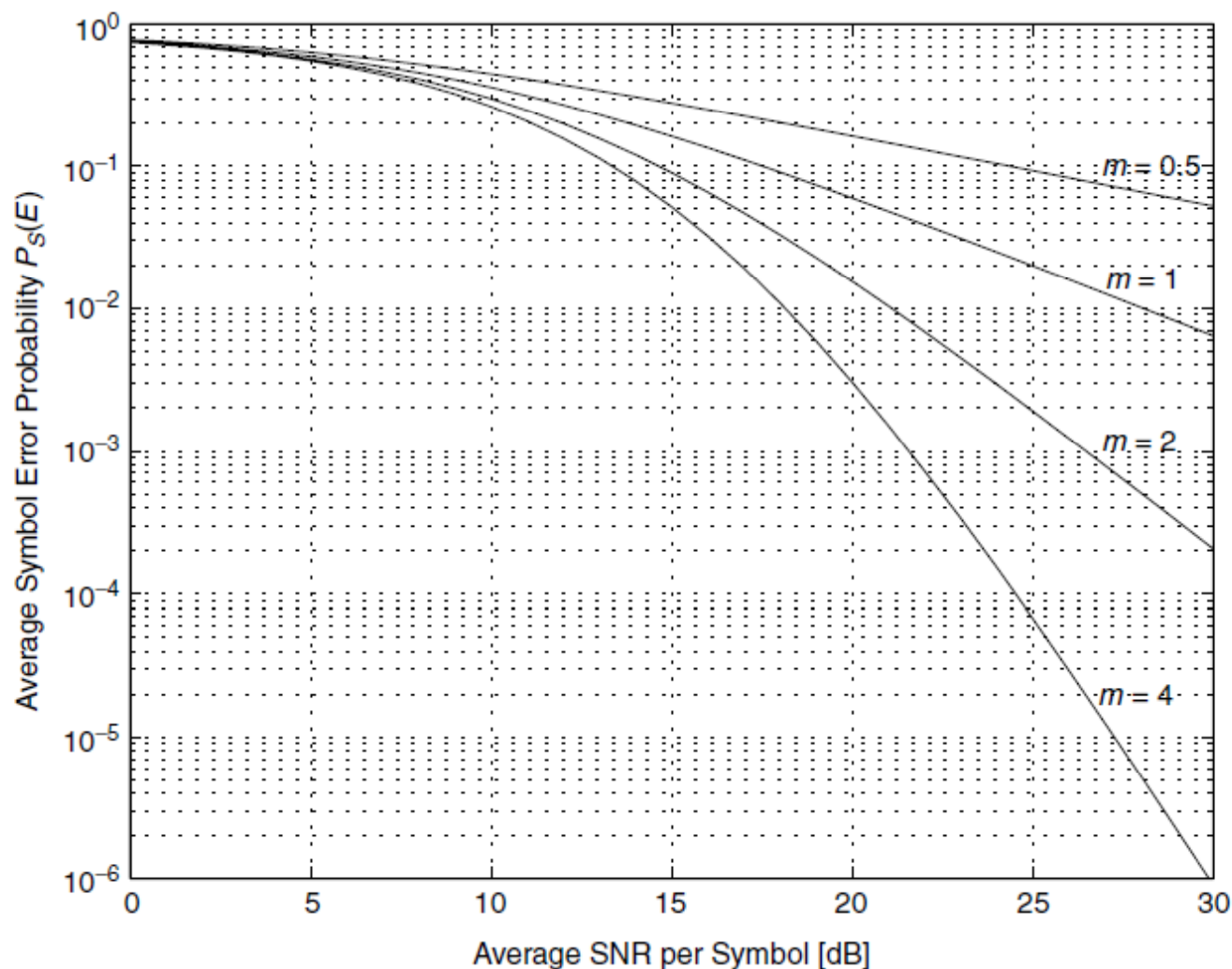


Figure 8.3 Average SEP of 16-QAM over a Nakagami- $m$  channel versus the average SNR per symbol.

## *Error Performance – Main Trends (2/38)*

$$\text{ABEP} \leq \text{ABEP}^{\text{CUB}} = \frac{2}{N_t \log_2(N_t)} \sum_{i_1=1}^{N_t} \sum_{i_2=i_1+1}^{N_t} N(i_1, i_2) \text{APEP}(\text{TX}_{i_2} \rightarrow \text{TX}_{i_1})$$

$$\text{APEP}(\text{TX}_{i_2} \rightarrow \text{TX}_{i_1}) = \frac{1}{\pi} \int_0^{\pi/2} M_{\gamma_{1,2}} \left( \frac{E_u/4N_0}{2 \sin^2(\theta)} \right) d\theta$$

$$\left\{ \begin{array}{l} M_{\gamma_{1,2}}(s) = \sum_{k=0}^{+\infty} \left[ \frac{A C^{m+2k-1}}{2^{m-1} 4^k (k!) \Gamma(k+m)} \Psi_k(s) \right] \\ \Psi_k(s) = \frac{A}{4} (s+B_1)^{-(m+k)} (s+B_2)^{-(m+k)} G_{2,2}^{1,2} \left( -\frac{s^2}{(s+B_1)(s+B_2)} \middle| \begin{matrix} 1-m-k & 1-m-k \\ 0 & 0 \end{matrix} \right) \\ A = \frac{4m^{m+1}}{\Gamma(m) \Omega_1 \Omega_2 (1-\rho_{\beta_1^2 \beta_2^2}) \left( \sqrt{\Omega_1 \Omega_2 \rho_{\beta_1^2 \beta_2^2}} \right)^{m-1}}; \{B_i\}_{i=1}^2 = \frac{m}{\Omega_i (1-\rho_{\beta_1^2 \beta_2^2})}; C = \frac{2m \sqrt{\rho_{\beta_1^2 \beta_2^2}}}{\sqrt{\Omega_1 \Omega_2} (1-\rho_{\beta_1^2 \beta_2^2})} \end{array} \right.$$

## Error Performance – Main Trends (3/38)

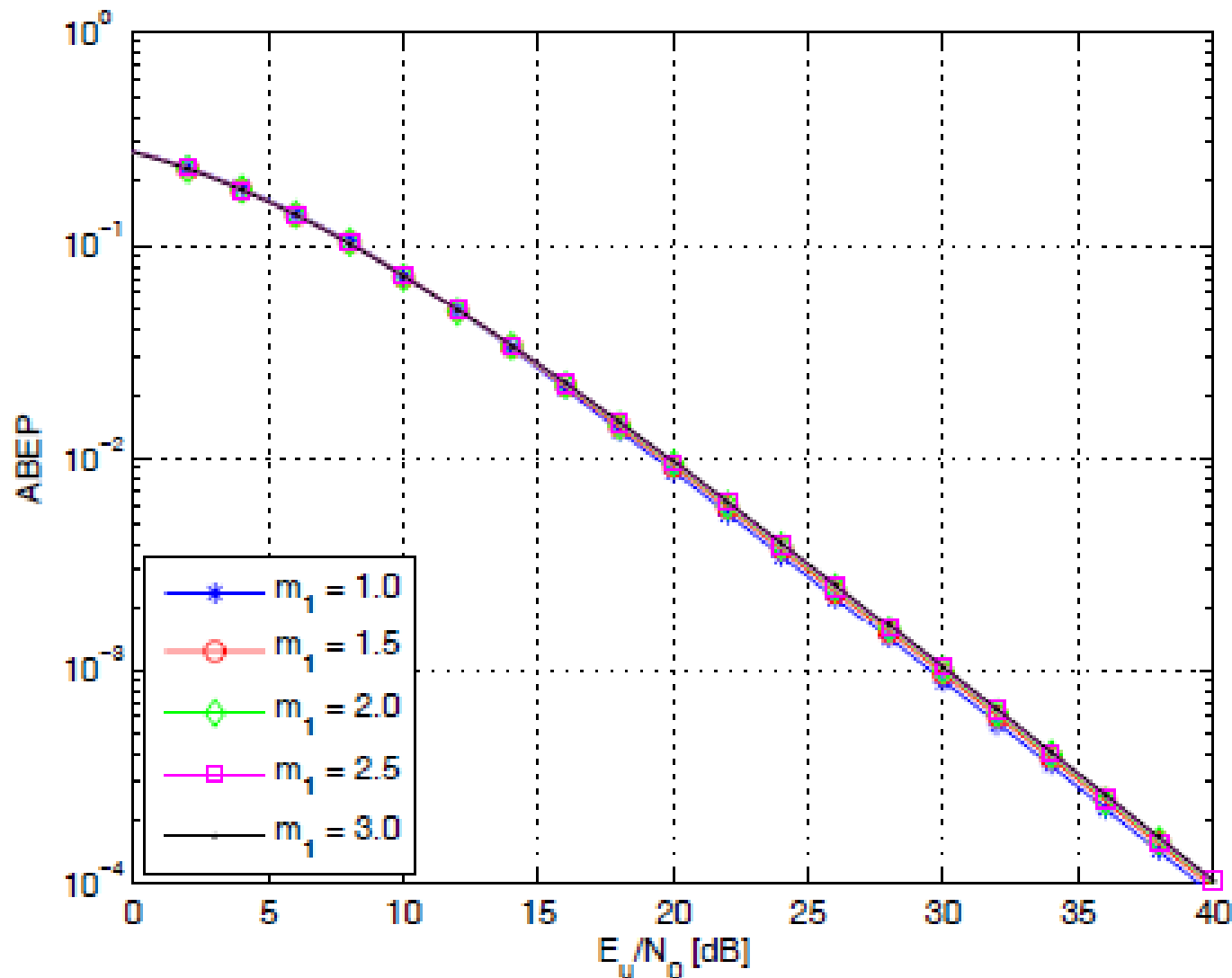


Fig. 1. Comparison between Monte Carlo simulation (markers) and analytical model (solid lines).  $2 \times 1$  MISO system. Uncorrelated fading model in (16) (i.e.,  $\rho_{\beta_1^2 \beta_2^2} = 0$ ) with balanced power (i.e.,  $\Omega_1 = \Omega_2 = 1$ ), and  $m_2 = 2$ .

## Error Performance – Main Trends (4/38)

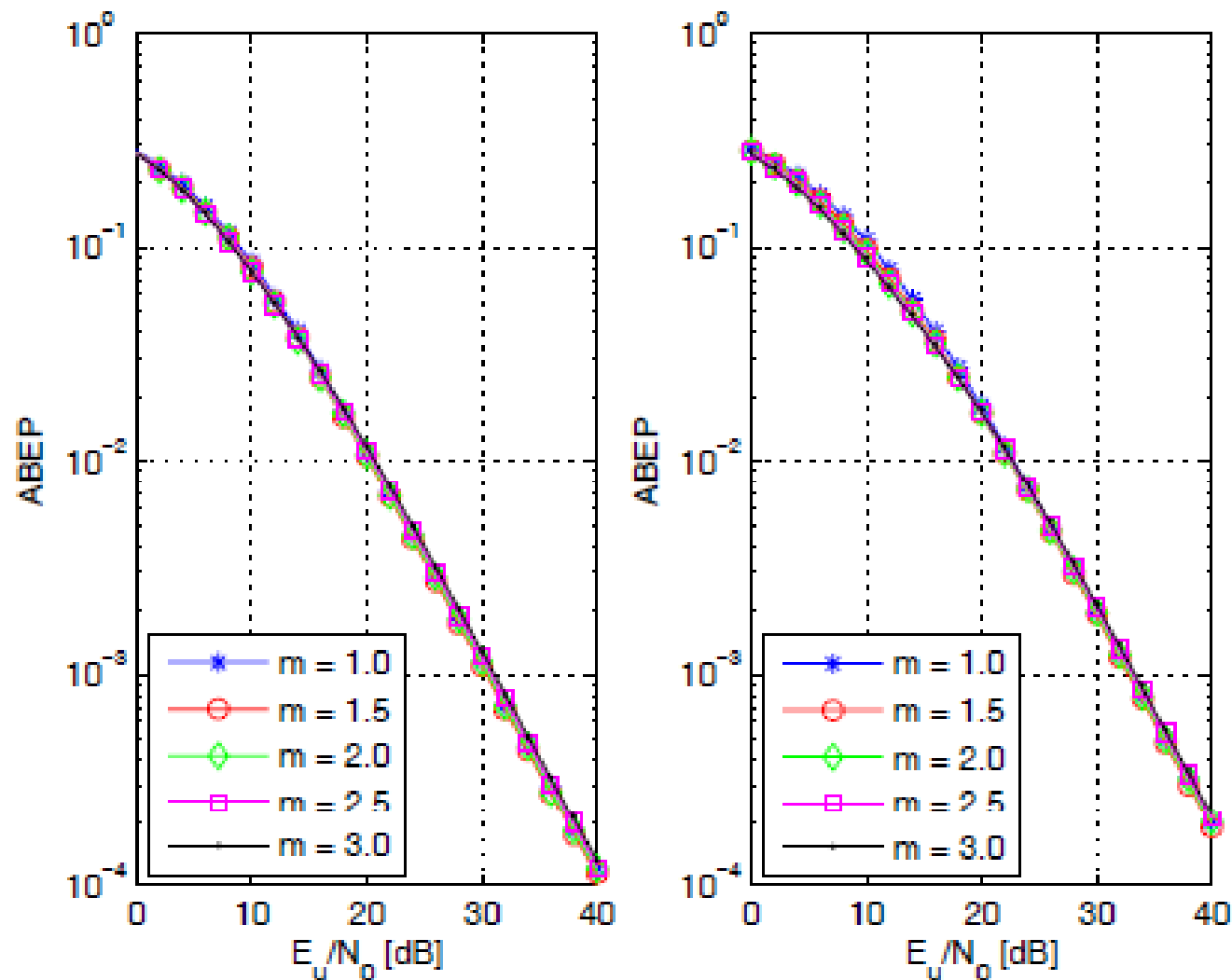


Fig. 3. Comparison between Monte Carlo simulation (markers) and analytical model (solid lines).  $2 \times 1$  MISO system. Correlated fading model in (21) (*i.e.*,  $\rho_{\beta_1^2 \beta_2^2} = 0.25$  on the left and  $\rho_{\beta_1^2 \beta_2^2} = 0.75$  on the right) with balanced power (*i.e.*,  $\Omega_1 = \Omega_2 = 1$ ).



## Error Performance – Main Trends (5/38)

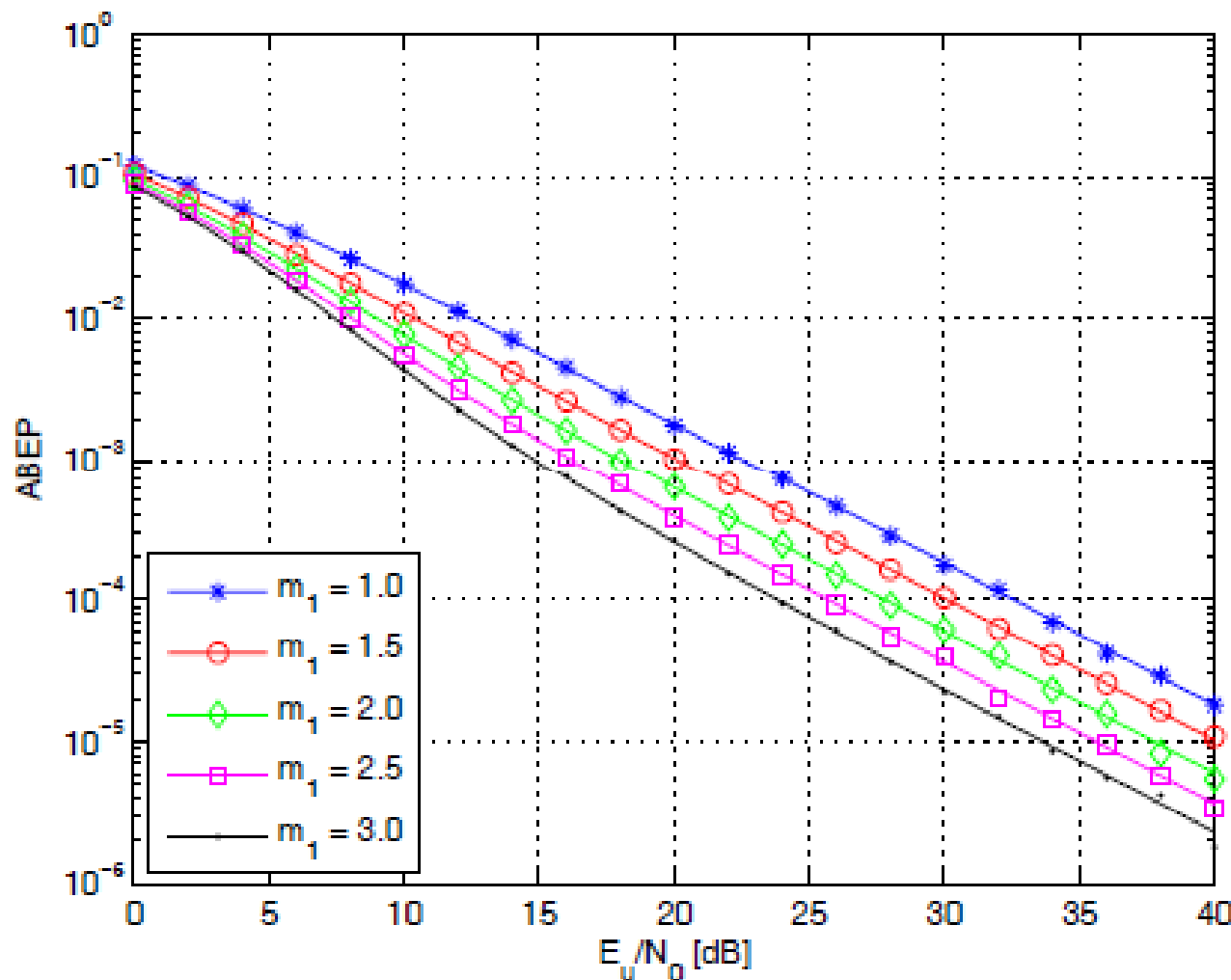


Fig. 2. Comparison between Monte Carlo simulation (markers) and analytical model (solid lines).  $2 \times 1$  MISO system. Uncorrelated fading model in (16) (i.e.,  $\rho_{\beta_1^2 \beta_2^2} = 0$ ) with unbalanced power (i.e.,  $\Omega_1 = 10\Omega_2$ ), and  $m_2 = 2$ ,  $\Omega_2 = 1$ .

## Error Performance – Main Trends (6/38)

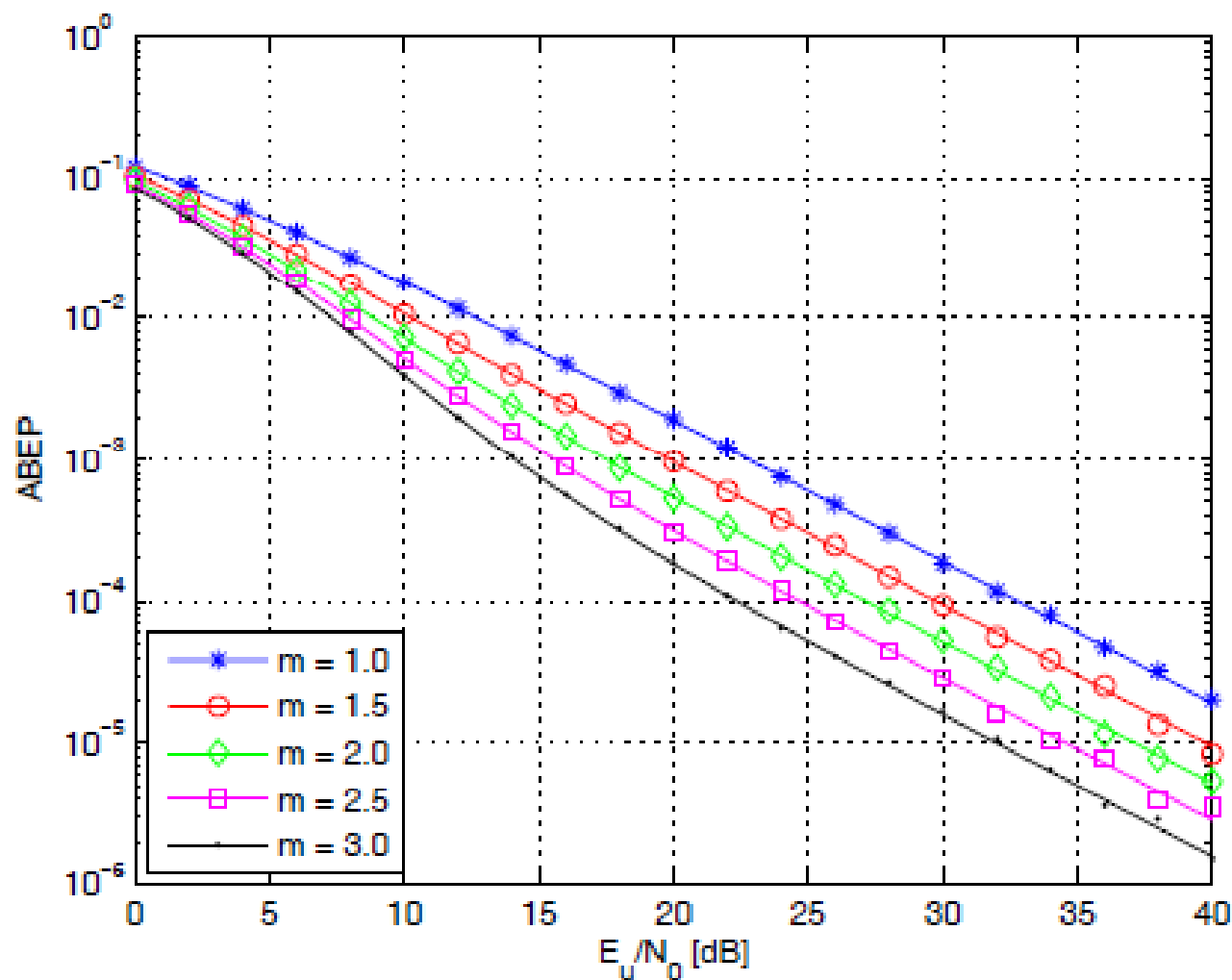


Fig. 4. Comparison between Monte Carlo simulation (markers) and analytical model (solid lines).  $2 \times 1$  MISO system. Correlated fading model in (21) (i.e.,  $\rho_{\beta_1^2 \beta_2^2} = 0.25$ ) with unbalanced power (i.e.,  $\Omega_1 = 10\Omega_2$ ), and  $\Omega_2 = 1$ .

## Error Performance – Main Trends (7/38)

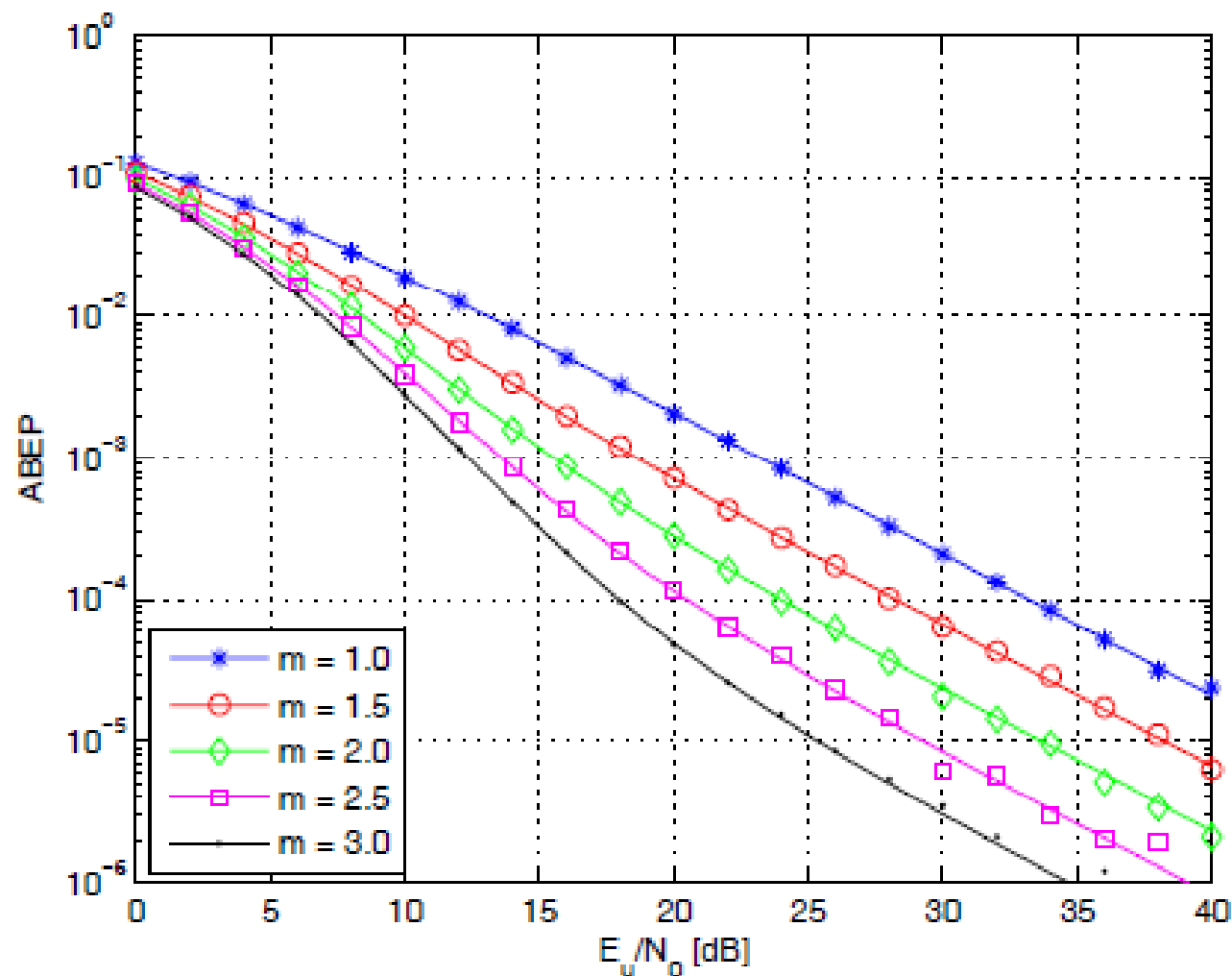


Fig. 5. Comparison between Monte Carlo simulation (markers) and analytical model (solid lines).  $2 \times 1$  MISO system. Correlated fading model in (21) (i.e.,  $\rho_{\beta_1^2 \beta_2^2} = 0.75$ ) with unbalanced power (i.e.,  $\Omega_1 = 10\Omega_2$ ), and  $\Omega_2 = 1$ .

## Error Performance – Main Trends (8/38)

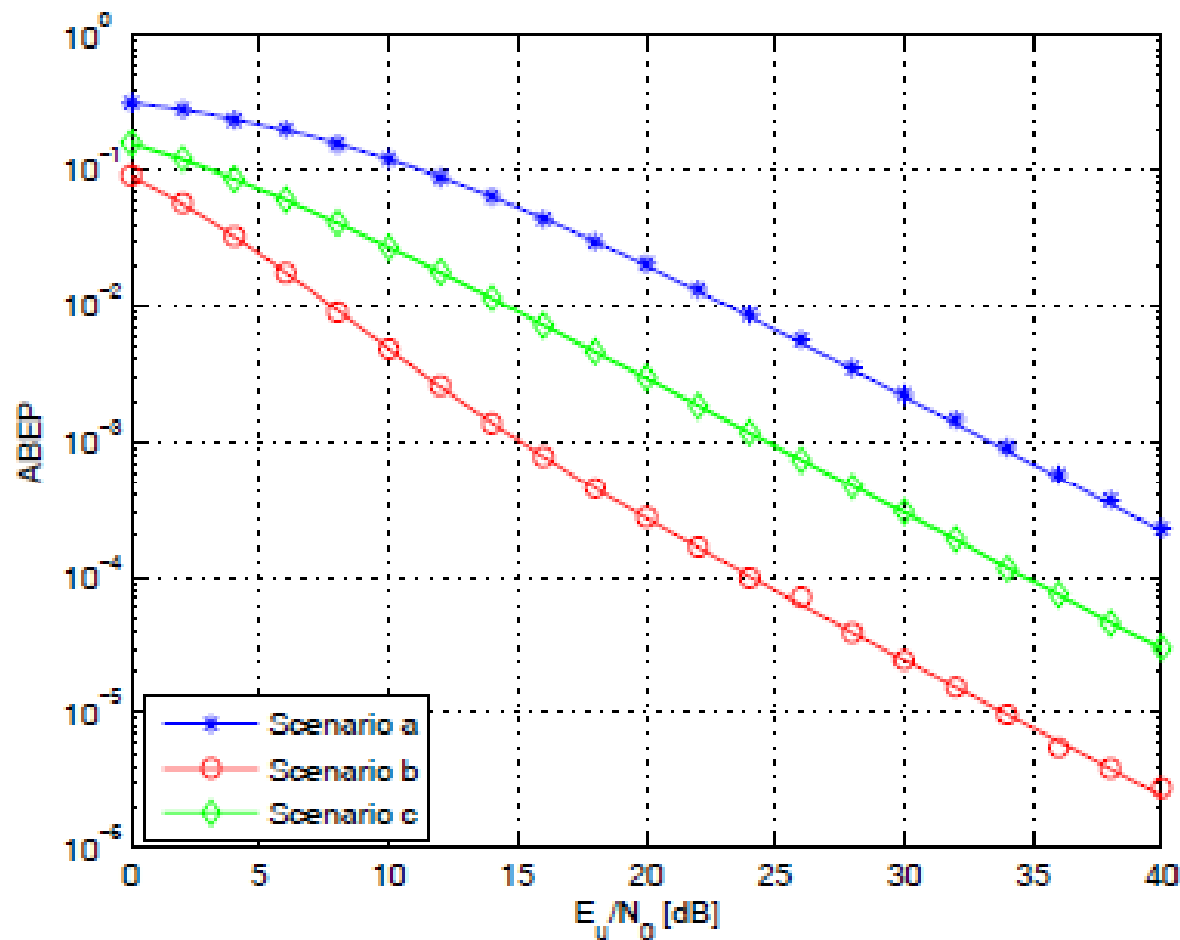


Fig. 6. Comparison between Monte Carlo simulation (markers) and analytical model (solid lines).  $2 \times 1$  MISO system. Correlated fading model in (28). Scenario a:  $m_1 = m_2 = 1$ ,  $\Omega_1 = \Omega_2 = 2/3$ ,  $\delta_1 = 0.50$ ,  $\delta_2 = \delta_3 = \delta_4 = 0.45$ . Scenario b:  $m_1 = 1$ ,  $m_2 = 2.5$ ,  $\Omega_1 = 1$ ,  $\Omega_2 = 10$ ,  $\delta_1 = \delta_2 = \delta_3 = 0.45$ ,  $\delta_4 = -0.45$ . Scenario c:  $m_1 = m_2 = 1$ ,  $\Omega_1 = 2/3$ ,  $\Omega_2 = 20/3$ ,  $\delta_1 = 0.50$ ,  $\delta_2 = \delta_3 = \delta_4 = 0.45$ .

## Error Performance – Main Trends (9/38)

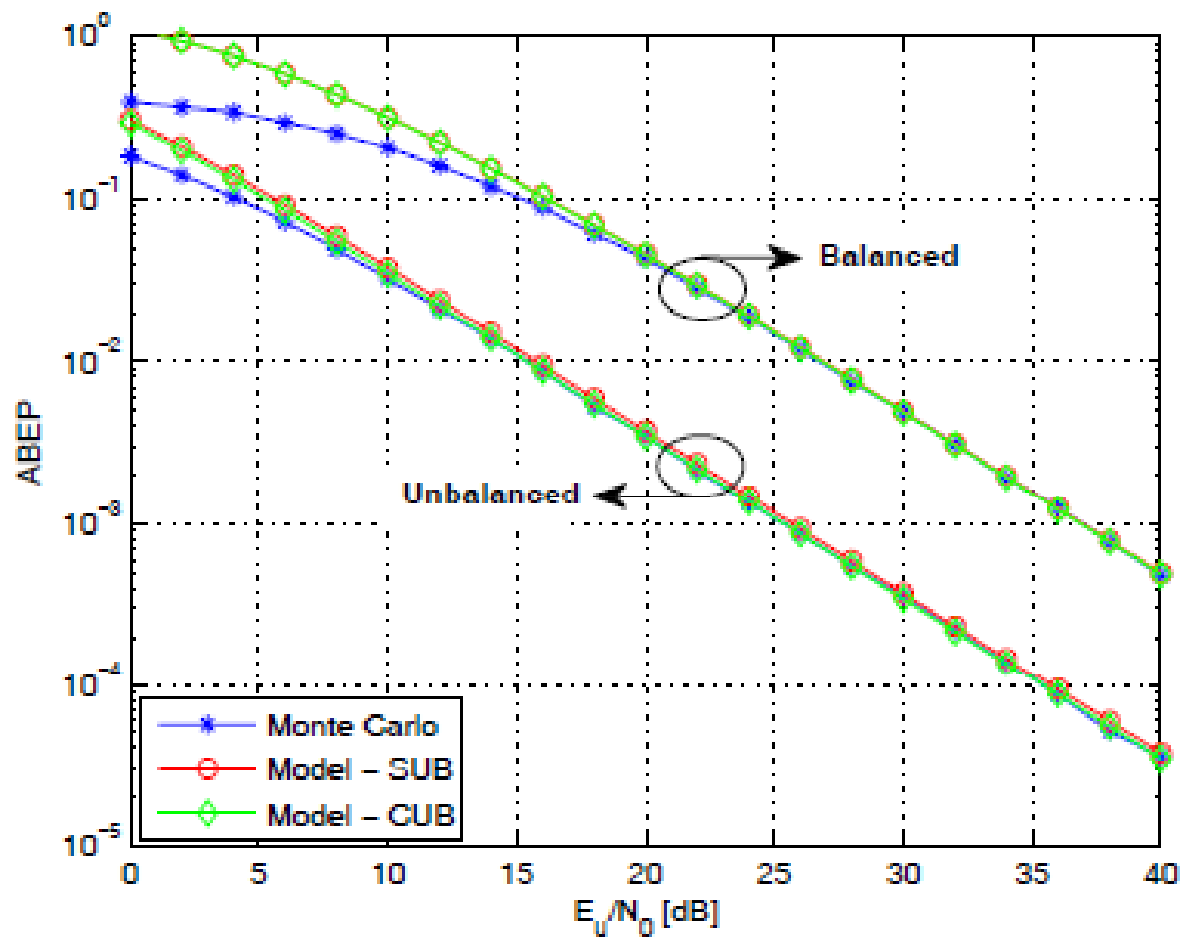


Fig. 11. Comparison between Monte Carlo simulation and analytical model.  $8 \times 1$  MISO system. Correlated fading model in (21) (i.e.,  $\left\{ \rho \beta_i^2 \beta_j^2 \right\}_{i,j=1}^8 \cong \left\{ \rho \beta_i \beta_j \right\}_{i,j=1}^8 = \exp(-0.5|i-j|)$ ) with balanced (i.e.,  $\{\Omega_i\}_{i=1}^8 = 1$ ) and unbalanced (i.e.,  $\Omega_1 = 1, \{\Omega_i\}_{i=2}^8 = 3(i-1)$ ) power, and  $\{m_i\}_{i=1}^8 = 2$ .

## Error Performance – Main Trends (10/38)

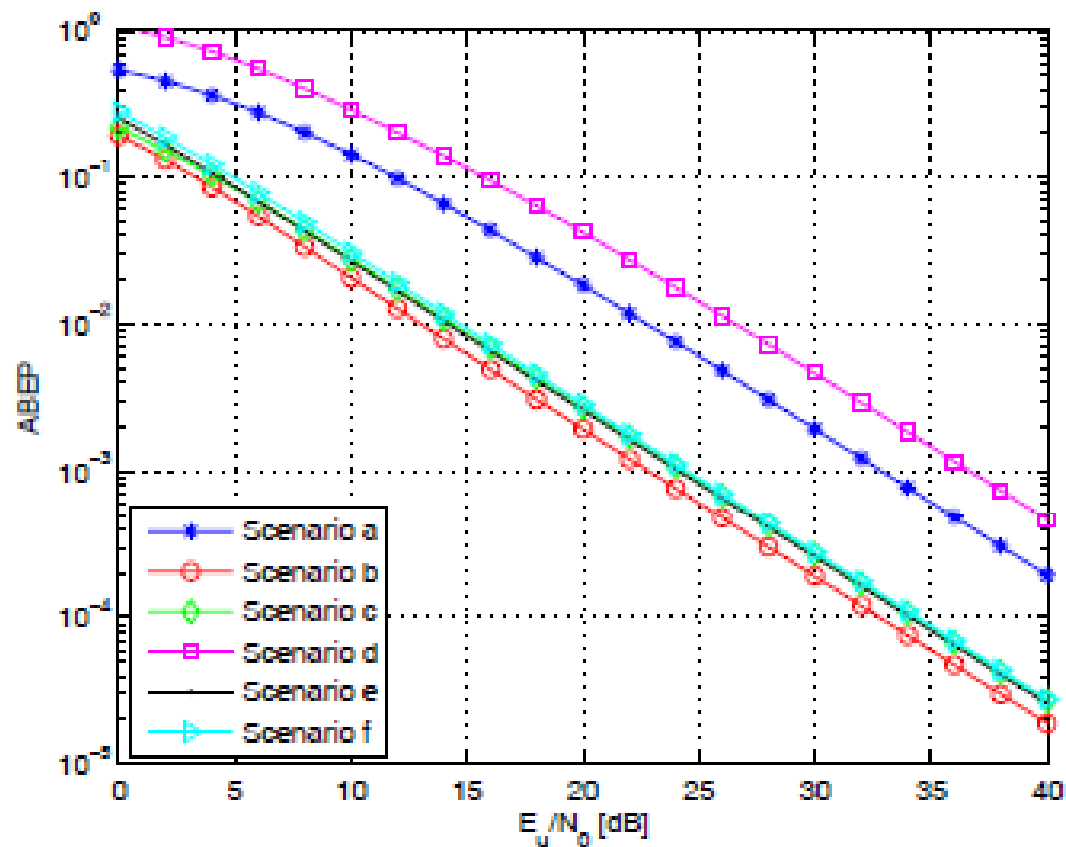
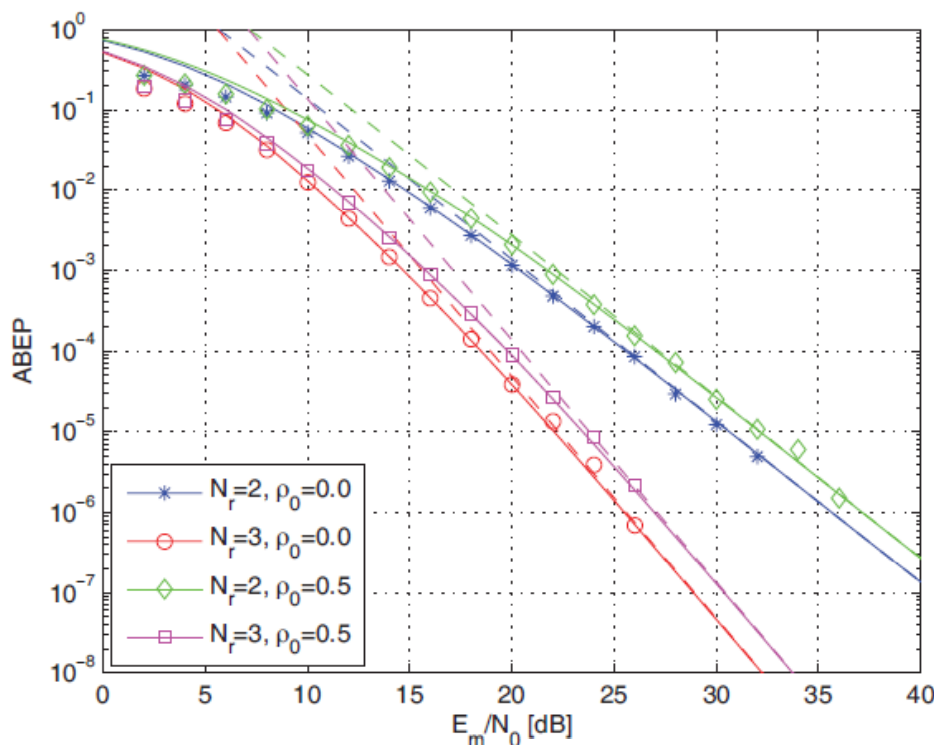


Fig. 9. Performance comparison (analytical model only) between  $4 \times 1$  and  $8 \times 1$  MISO systems for various fading scenarios. Uncorrelated fading model in (16) (i.e.,  $\left\{ \rho_{\beta_i^2 \beta_j^2} \right\}_{i \neq j=1}^8 = 0$ ). Scenario a:  $N_t = 4$ ,  $\{m_i\}_{i=1}^{N_t} = i$ ,  $\{\Omega_i\}_{i=1}^{N_t} = 1$ . Scenario b:  $N_t = 4$ ,  $\{m_i\}_{i=1}^{N_t} = i$ ,  $\Omega_1 = 1$ ,  $\{\Omega_i\}_{i=2}^{N_t} = 4(i-1)$ . Scenario c:  $N_t = 4$ ,  $\{m_i\}_{i=1}^{N_t} = 5-i$ ,  $\Omega_1 = 1$ ,  $\{\Omega_i\}_{i=2}^{N_t} = 4(i-1)$ . Scenario d:  $N_t = 8$ ,  $\{m_i\}_{i=1}^{N_t} = i$ ,  $\{\Omega_i\}_{i=1}^{N_t} = 1$ . Scenario e:  $N_t = 8$ ,  $\{m_i\}_{i=1}^{N_t} = i$ ,  $\Omega_1 = 1$ ,  $\{\Omega_i\}_{i=2}^{N_t} = 3(i-1)$ . Scenario f:  $N_t = 8$ ,  $\{m_i\}_{i=1}^{N_t} = 9-i$ ,  $\Omega_1 = 1$ ,  $\{\Omega_i\}_{i=2}^{N_t} = 3(i-1)$ .

# Error Performance – Main Trends (11/38)

$$\text{PEP}(t_1 \rightarrow t_2) = \frac{2^{N_r-1} \left[ \prod_{r=1}^{N_r} \frac{\Omega_{t_1,r}^{m_{t_1,r}} \Omega_{t_2,r}^{m_{t_2,r}}}{\Omega_{t_1,r}^{m_{t_1,r}} \Omega_{t_2,r}^{m_{t_2,r}} \Gamma(m_{t_1,r}) \Gamma(m_{t_2,r})} \left( \frac{m_{t_1,r}}{\Omega_{t_1,r}} + \frac{m_{t_2,r}}{\Omega_{t_2,r}} \right)^{-(m_{t_1,r}+m_{t_2,r}-1)} \Gamma(m_{t_1,r} + m_{t_2,r} - 1) \right] \Gamma(N_r + 1/2)}{\sqrt{\pi} \Gamma(N_r + 1)} \left( \frac{E_m}{4N_0} \right)^{-N_r}$$

$$\text{PEP}(t_1 \rightarrow t_2) = \frac{2^{N_r-1} \left[ \left( \sum_{k_1=0}^{+\infty} \frac{C_{t_1,t_2,r}^{m_r+2k_1-1} b_{k_1}}{2^{m_r-1} 4^{k_1} (k_1!) \Gamma(k_1+m_r)} \right) \cdots \left( \sum_{k_{N_r}=0}^{+\infty} \frac{C_{t_1,t_2,r}^{m_r+2k_{N_r}-1} b_{k_{N_r}}}{2^{m_r-1} 4^{k_{N_r}} (k_{N_r}!) \Gamma(k_{N_r}+m_r)} \right) \right] \Gamma(N_r + 1/2)}{\sqrt{\pi} \Gamma(N_r + 1)} \left( \frac{E_m}{4N_0} \right)^{-N_r}$$



$$\begin{aligned} N_t &= 8 \\ m &= 2.5 \\ \Omega &= 1 \end{aligned}$$

## Error Performance – Main Trends (12/38)

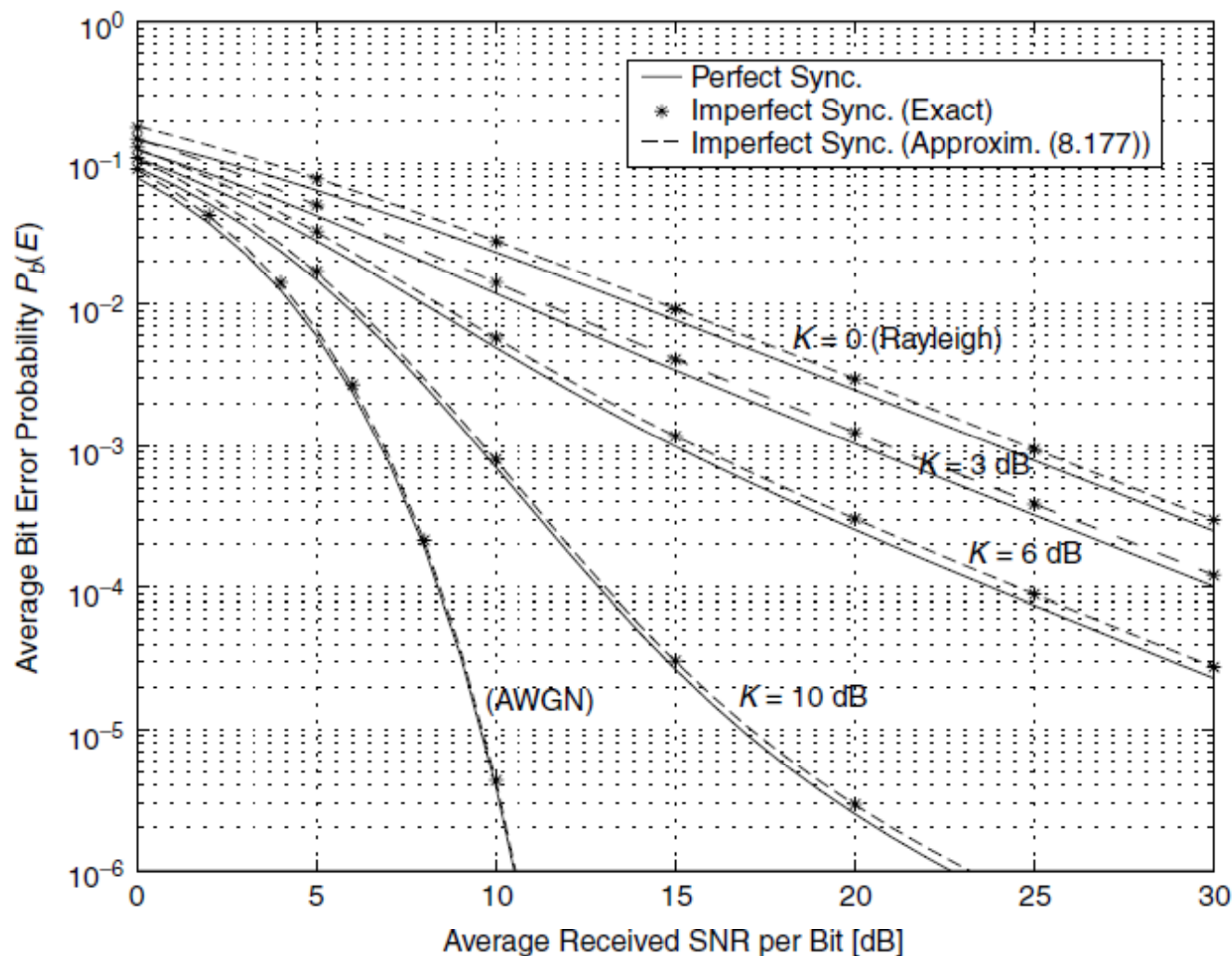


Figure 8.8 Combined effect of Nakagami- $n$  (Rice) fading and imperfect synchronization on the average bit error probability of BPSK.



## Error Performance – Main Trends (13/38)

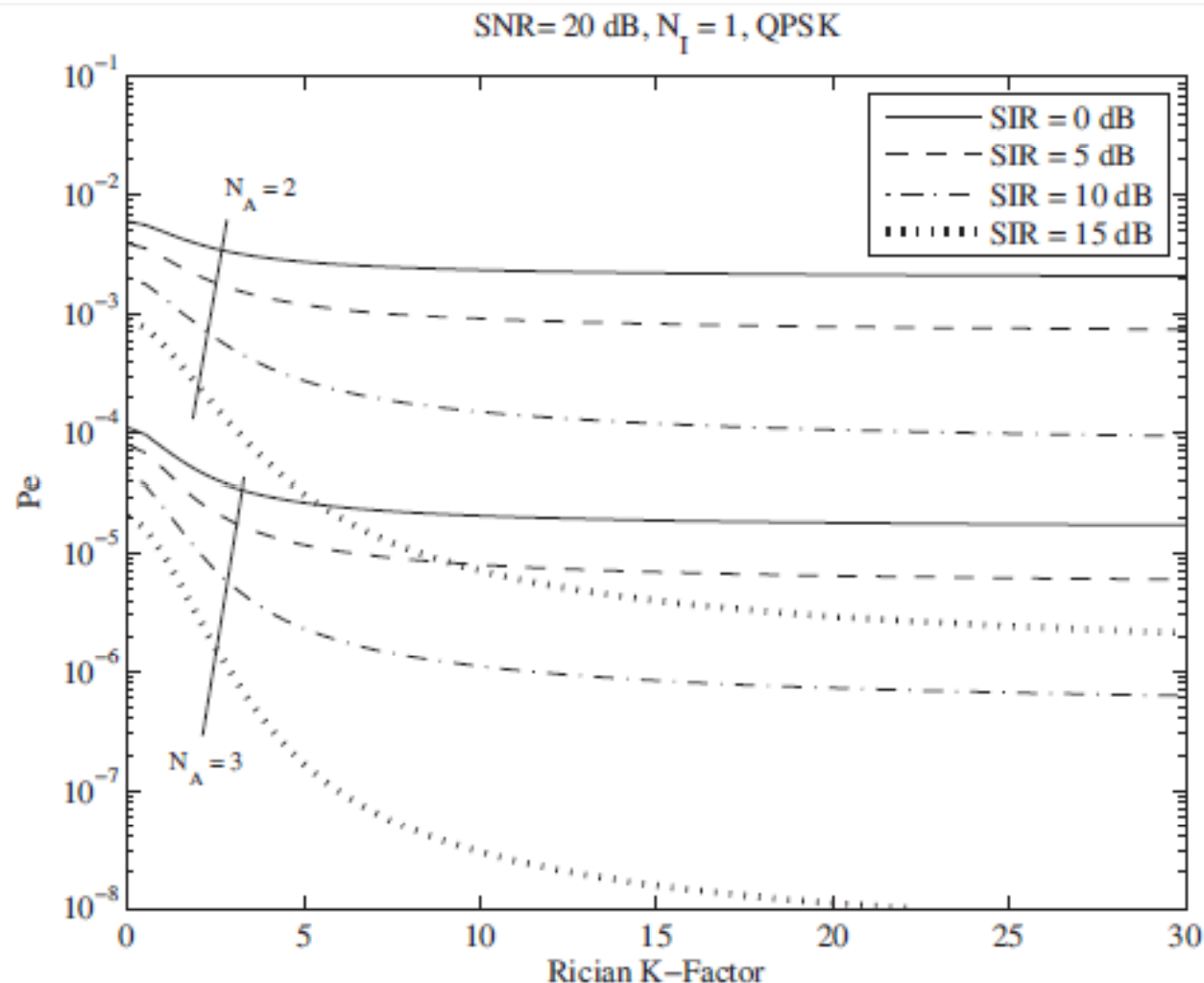


Fig. 3. SEP of Rician-Rayleigh OC as a function of  $K$  for  $N_I = 1$ , SNR = 20 dB, and QPSK; analytical results for different SIRs and different  $N_A$ .

## Error Performance – Main Trends (14/38)

$$L = 2N_r$$

$$\begin{aligned} \text{ABEP}_{2,1} &= \int_0^{+\infty} Q\left(\sqrt{\bar{\gamma}\zeta}\right) f_{\gamma_{2,1}}(\zeta) d\zeta \\ &= \frac{\Psi_{2,1}}{2\sqrt{\pi}} \sum_{k=0}^{+\infty} \left[ \frac{\vartheta_k^{(2,1)}}{\Gamma(v^{(2,1)} + k)} G_{2,2}^{2,1} \left( \frac{\bar{\gamma}\chi_1^{(2,1)}}{2} \middle| \begin{matrix} 1 - v^{(2,1)} - k & 1 \\ 0 & 1/2 \end{matrix} \right) \right] \end{aligned}$$

$$\begin{cases} \Psi_{2,1} = \prod_{h=1}^L \left[ \frac{\chi_1^{(2,1)}}{\chi_h^{(2,1)}} \exp\left(-\frac{\kappa_h^{(2,1)}}{\chi_h^{(2,1)}}\right) \right] \\ \vartheta_k^{(2,1)} = \frac{1}{k} \sum_{r=1}^k \left\{ \sum_{b=1}^L \left[ v_r^{(2,1)} \left(1 - \frac{\chi_1^{(2,1)}}{\chi_b^{(2,1)}}\right)^r + \frac{r\chi_1^{(2,1)}\kappa_r^{(2,1)}}{(\chi_b^{(2,1)})^2} \left(1 - \frac{\chi_1^{(2,1)}}{\chi_b^{(2,1)}}\right)^{r-1} \right] \vartheta_{k-r}^{(2,1)} \right\} \quad k \geq 1 \end{cases}$$

$$\text{ABEP}_{2,1} = \frac{1}{\pi} \int_0^{\pi/2} M_{\gamma_{2,1}} \left( \frac{\bar{\gamma}}{2 \sin^2(\theta)} \right) d\theta$$

$$M_{\gamma_{2,1}}(s) = \prod_{h=1}^L \left[ \left(1 + \chi_h^{(2,1)} s\right)^{-v_h^{(2,1)}} \exp\left(-\frac{\kappa_h^{(2,1)} s}{1 + \chi_h^{(2,1)} s}\right) \right]$$

## Error Performance – Main Trends (15/38)

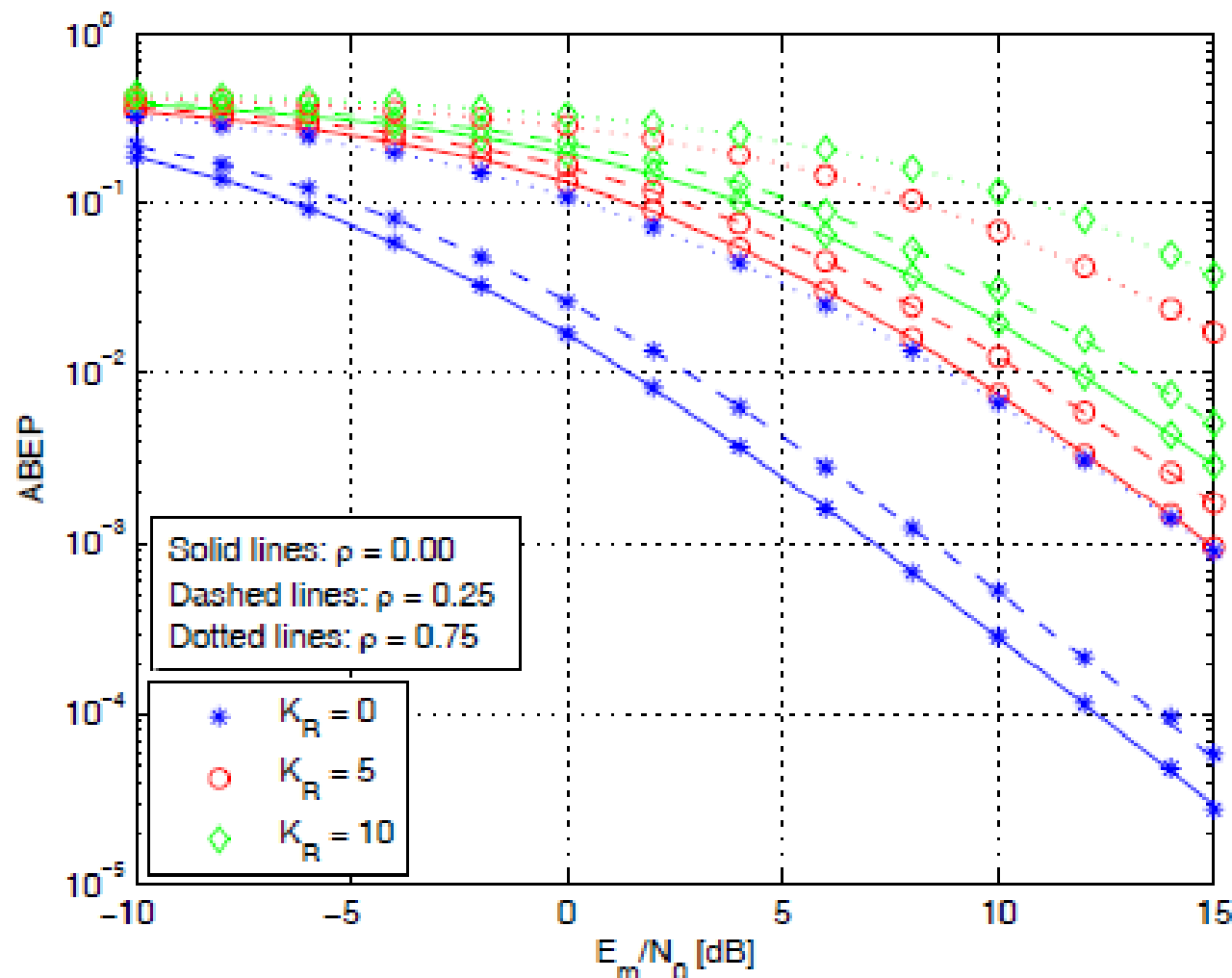


Fig. 1. SSK modulation: ABEP against  $E_m/N_0$ . Solid, dashed, and dotted lines denote the analytical model in Section III and markers Monte Carlo simulations. Setup: i)  $N_t = 2$ , ii)  $N_r = 2$ , iii)  $\Omega_{i,l} = 10\text{dB}$  and  $K_R^{(i,l)} = K_R$  for  $i = 1, 2, \dots, N_t$  and  $l = 1, 2, \dots, N_r$ , and iv)  $\rho = 0.00$  (solid lines),  $\rho = 0.25$  (dashed lines),  $\rho = 0.75$  (dotted lines).

## Error Performance – Main Trends (16/38)

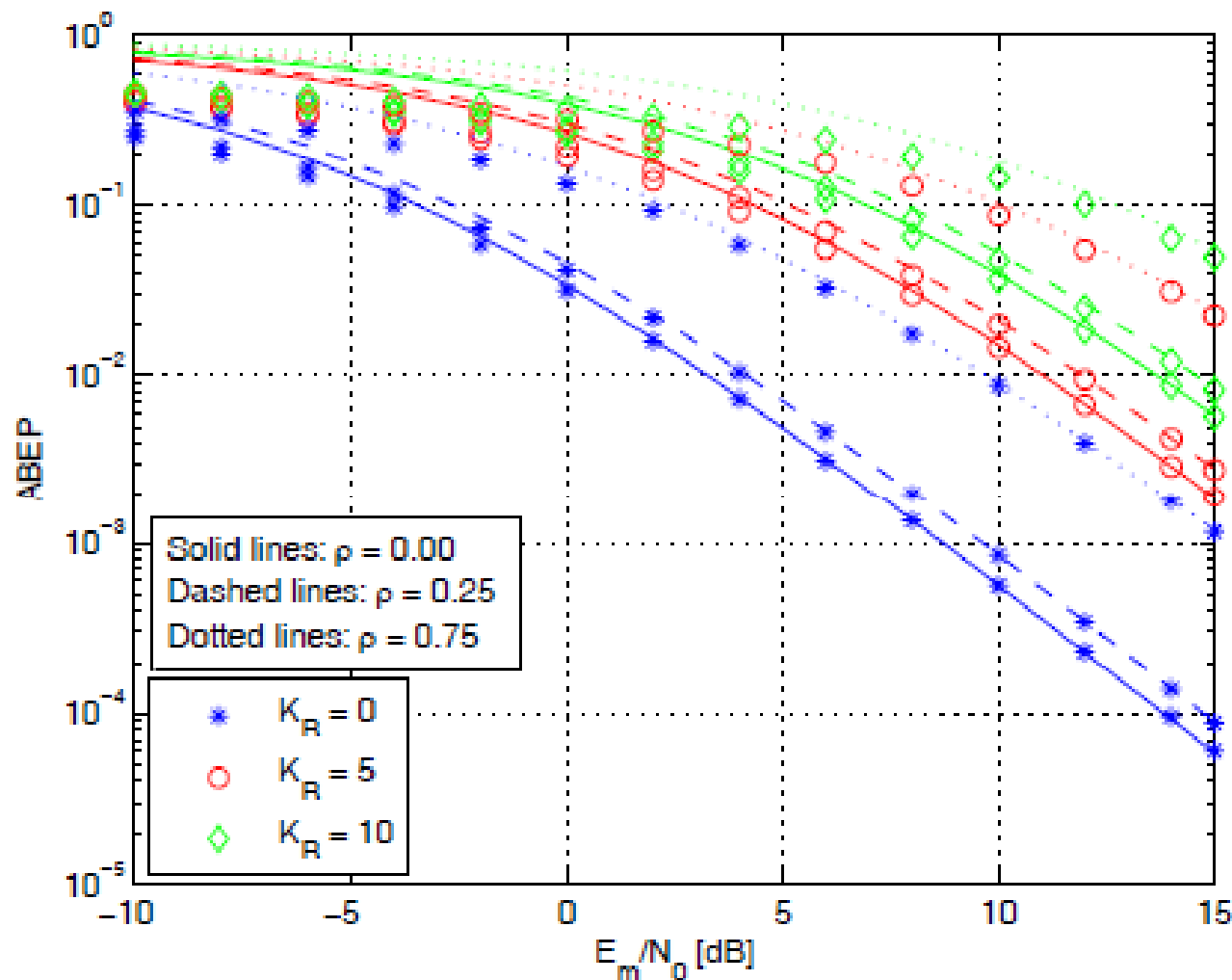


Fig. 3. SSK modulation: ABEP against  $E_m/N_0$ . Solid, dashed, and dotted lines denote the analytical model in Section III and markers Monte Carlo simulations. Setup: i)  $N_t = 4$ , ii)  $N_r = 2$ , iii)  $\Omega_{i,l} = 10\text{dB}$  and  $K_R^{(i,l)} = K_R$  for  $i = 1, 2, \dots, N_t$  and  $l = 1, 2, \dots, N_r$ , and iv)  $\rho = 0.00$  (solid lines),  $\rho = 0.25$  (dashed lines),  $\rho = 0.75$  (dotted lines).

## Error Performance – Main Trends (17/38)

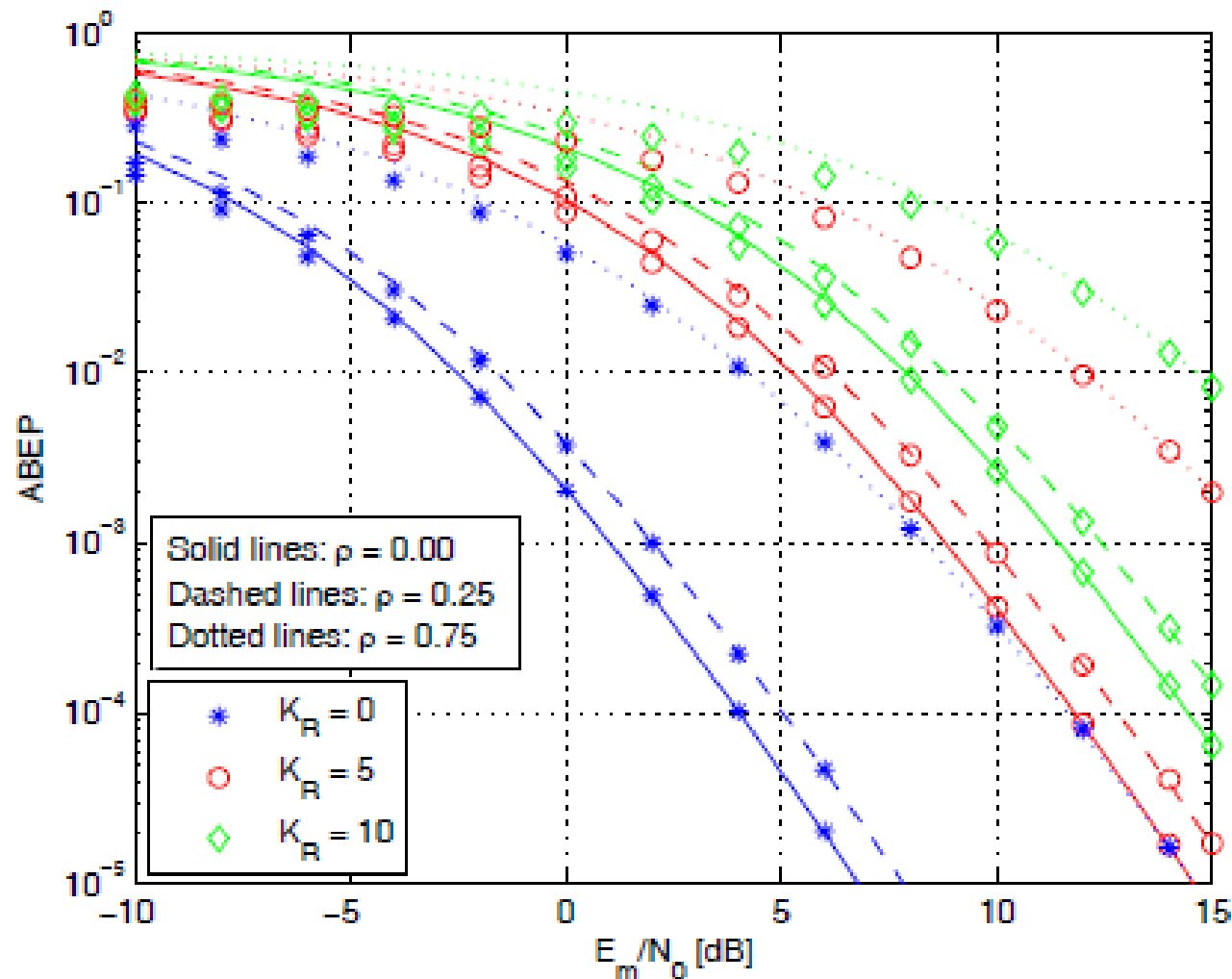


Fig. 4. SSK modulation: ABEP against  $E_m/N_0$ . Solid, dashed, and dotted lines denote the analytical model in Section III and markers Monte Carlo simulations. Setup: i)  $N_t = 4$ , ii)  $N_r = 4$ , iii)  $\Omega_{i,l} = 10\text{dB}$  and  $K_R^{(i,l)} = K_R$  for  $i = 1, 2, \dots, N_t$  and  $l = 1, 2, \dots, N_r$ , and iv)  $\rho = 0.00$  (solid lines),  $\rho = 0.25$  (dashed lines),  $\rho = 0.75$  (dotted lines).

## *Error Performance – Main Trends (18/38)*

*Proposition 1:* The ABEP in (3) can be tightly upper bounded as follows:

$$\text{ABEP} \leq \text{ABEP}_{\text{signal}} + \text{ABEP}_{\text{spatial}} + \text{ABEP}_{\text{joint}}$$

where  $\text{ABEP}_{\text{signal}}$ ,  $\text{ABEP}_{\text{spatial}}$ , and  $\text{ABEP}_{\text{joint}}$  are defined as

$$\left\{ \begin{array}{l} \text{ABEP}_{\text{signal}} = \frac{1}{N_t} \frac{\log_2(M)}{\log_2(N_t M)} \sum_{n_t=1}^{N_t} \text{ABEP}_{\text{MOD}}(n_t) \\ \text{ABEP}_{\text{spatial}} = \frac{1}{M} \frac{\log_2(N_t)}{\log_2(N_t M)} \sum_{l=1}^M \text{ABEP}_{\text{SSK}}(l) \\ \text{ABEP}_{\text{joint}} = \frac{1}{N_t M} \frac{1}{\log_2(N_t M)} \sum_{n_t=1}^{N_t} \sum_{l=1}^M \sum_{\tilde{n}_t \neq n_t=1}^{N_t} \sum_{\tilde{l} \neq l=1}^M \\ \quad \times \{ [N_H(\tilde{n}_t \rightarrow n_t) + N_H(\chi_{\tilde{l}} \rightarrow \chi_l)] \Upsilon(n_t, \chi_l, \tilde{n}_t, \chi_{\tilde{l}}) \} \end{array} \right.$$

## *Error Performance – Main Trends (19/38)*

$$\left\{ \begin{array}{l} \text{ABEP}_{\text{MOD}}(n_t) = \frac{1}{M} \frac{1}{\log_2(M)} \sum_{l=1}^M \sum_{\tilde{l}=1}^M \\ \quad \times [N_H(\chi_{\tilde{l}} \rightarrow \chi_l) E_{\alpha(n_t)} \{ \Pr \{ \chi_{\tilde{l}} = \chi_l | \chi_{\tilde{l}} \} \}] \\ \text{ABEP}_{\text{SSK}}(l) = \frac{1}{N_t} \frac{1}{\log_2(N_t)} \sum_{n_t=1}^{N_t} \sum_{\tilde{n}_t=1}^{N_t} \\ \quad \times [N_H(\tilde{n}_t \rightarrow n_t) \Psi_l(n_t, \tilde{n}_t)] \end{array} \right.$$

$$\Psi_l(n_t, \tilde{n}_t) = (1/\pi) \int_0^{\pi/2} \mathcal{M}_{\gamma(n_t, \tilde{n}_t)}(\bar{\gamma} \kappa_l^2 / 2 \sin^2(\theta)) d\theta;$$

$$\Upsilon(n_t, \chi_l, \tilde{n}_t, \chi_{\tilde{l}}) = (1/\pi) \int_0^{\pi/2} \mathcal{M}_{\gamma(n_t, \chi_l, \tilde{n}_t, \chi_{\tilde{l}})}(\bar{\gamma}/2 \times \sin^2(\theta)) d\theta.$$

# Error Performance – Main Trends (20/38)

## Diversity Analysis of Spatial Modulation

- The diversity order over **Nakagami-m fading** channels is:

$$\text{Div}_{\text{SM}} = \min \{ N_r, m_{\text{Nak}} N_r \}$$

- If  $m_{\text{Nak}} > 1$ ,  $\text{Div}_{\text{SM}} = N_r$ , the ABEP is dominated by the spatial-constellation diagram
- If  $m_{\text{Nak}} < 1$ ,  $\text{Div}_{\text{SM}} = m_{\text{Nak}} N_r$ , the ABEP is dominated by the signal-constellation diagram
- $\text{Div}_{\text{SIMO}} = m_{\text{Nak}} N_r$  for every  $m_{\text{Nak}}$

- The diversity order over **Rician fading** channels is:

$$\text{Div}_{\text{SM}} = N_r$$



# Error Performance – Main Trends (21/38)

## i.i.d. Rayleigh Fading

$$\begin{cases} \text{ABEP}_{\text{signal}} = \frac{\log_2(M)}{\log_2(N_t M)} \text{ABEP}_{\text{MOD}}^{\text{Rayleigh}} \\ \text{ABEP}_{\text{spatial}} = \frac{1}{M} \frac{\log_2(N_t)}{\log_2(N_t M)} \frac{N_t}{2} \sum_{l=1}^M \mathcal{R}(4\sigma_0^2 \bar{\gamma} \kappa_l^2) \\ \text{ABEP}_{\text{joint}} = \frac{1}{M} \frac{1}{\log_2(N_t M)} \sum_{l=1}^M \sum_{\tilde{l} \neq l=1}^M \left[ \left( \frac{N_t \log_2(N_t)}{2} + (N_t - 1) N_H(\chi_{\tilde{l}} \rightarrow \chi_l) \right) \mathcal{R} \left( 2\sigma_0^2 \bar{\gamma} (\kappa_l^2 + \kappa_{\tilde{l}}^2) \right) \right] \end{cases}$$

$$\mathcal{R}(\xi) = \left[ \frac{1}{2} \left( 1 - \sqrt{\frac{\xi}{2+\xi}} \right) \right]^{N_r} \sum_{n_r=0}^{N_r-1} \left\{ \binom{N_r+1-n_r}{n_r} \left[ \frac{1}{2} \left( 1 + \sqrt{\frac{\xi}{2+\xi}} \right) \right]^{n_r} \right\}$$

High-SNR

$$\begin{cases} \text{ABEP}_{\text{spatial}} \stackrel{\bar{\gamma} \gg 1}{\approx} \left[ \frac{N_t}{2} \frac{1}{M} \frac{\log_2(N_t)}{\log_2(N_t M)} 2^{-N_r} \binom{2N_r-1}{N_r} \Theta_{\text{spatial}}^{(M, N_r)} \right] (4\sigma_0^2 \bar{\gamma})^{-N_r} \\ \text{ABEP}_{\text{joint}} \stackrel{\bar{\gamma} \gg 1}{\approx} \left[ \frac{N_t}{2} \frac{1}{M} \frac{\log_2(N_t)}{\log_2(N_t M)} \binom{2N_r-1}{N_r} \Theta_{\text{joint}}^{(M, N_r)} + \frac{N_t-1}{M} \frac{1}{\log_2(N_t M)} \binom{2N_r-1}{N_r} \Theta_{\text{joint}}^{(M, N_r, H)} \right] (4\sigma_0^2 \bar{\gamma})^{-N_r} \end{cases}$$

# Error Performance – Main Trends (22/38)

## i.i.d. Rayleigh Fading

$\Delta_{\text{SNR}}^{(X/Y)}$  : SNR gain of Y compared to X

$$\Delta_{\text{SNR}}^{(X/Y)} = 10 \log_{10} (\text{SNR}_X / \text{SNR}_Y) = - (10/N_r) \log_{10} (\Pi_{\text{SNR}}^{(X/Y)})$$

$$\Pi_{\text{SNR}}^{(\text{PSK}/\text{SM}-\text{PSK})} = \frac{\left[ \frac{N_t M}{2} \frac{\log_2(N_t)}{\log_2(N_t M)} + 2^{-N_r} \frac{\log_2(M)}{\log_2(N_t M)} G_{\text{MOD}}^{\text{PSK}}(M^{\text{PSK}}) + \frac{(N_t-1)M}{2} \frac{\log_2(M)}{\log_2(N_t M)} \right]}{2^{-N_r} G_{\text{MOD}}^{\text{PSK}}(M^{\text{PSK}})}$$

$$\Pi_{\text{SNR}}^{(\text{QAM}/\text{SM}-\text{QAM})} = \frac{\frac{1}{M} \left[ \frac{N_t}{2} \log_2(N_t) \Theta_{\text{spatial}}^{(M, N_r)} + \frac{N_t}{2} 2^{N_r} \log_2(N_t) \Theta_{\text{joint}}^{(M, N_r)} + (N_t-1) 2^{N_r} \Theta_{\text{joint}}^{(M, N_r, H)} \right] + \log_2(M) [G_{\text{MOD}}^{\text{QAM}}(I_M) + G_{\text{MOD}}^{\text{QAM}}(J_M)]}{\log_2(M^{\text{QAM}}) [G_{\text{MOD}}^{\text{QAM}}(I_M^{\text{QAM}}) + G_{\text{MOD}}^{\text{QAM}}(J_M^{\text{QAM}})]}$$

$$\Pi_{\text{SNR}}^{(\text{SSK}/\text{SM}-\text{QAM})} = \frac{\frac{1}{M} \left[ \frac{N_t}{2} \log_2(N_t) \Theta_{\text{spatial}}^{(M, N_r)} + \frac{N_t}{2} 2^{N_r} \log_2(N_t) \Theta_{\text{joint}}^{(M, N_r)} + (N_t-1) 2^{N_r} \Theta_{\text{joint}}^{(M, N_r, H)} \right] + \log_2(M) [G_{\text{MOD}}^{\text{QAM}}(I_M) + G_{\text{MOD}}^{\text{QAM}}(J_M)]}{\frac{N_t^{\text{SSK}}}{2} \log_2(N_t^{\text{SSK}})}$$

$$\Pi_{\text{SNR}}^{(\text{SSK}/\text{QAM})} = \frac{G_{\text{MOD}}^{\text{QAM}}(I_M^{\text{QAM}}) + G_{\text{MOD}}^{\text{QAM}}(J_M^{\text{QAM}})}{\frac{N_t^{\text{SSK}}}{2} \log_2(N_t^{\text{SSK}})}$$

$$\Pi_{\text{SNR}}^{(\text{SSK}/\text{PSK})} = \frac{2^{-N_r} G_{\text{MOD}}^{\text{PSK}}(M^{\text{PSK}})}{\frac{N_t^{\text{SSK}}}{2}}$$

# Error Performance – Main Trends (23/38)

## i.i.d. Rayleigh Fading

$N_r = 1$					
Rate ( $R$ ) / $\Delta_{\text{SNR}}^{(X/Y)}$	2 bpcu	3 bpcu	4 bpcu	5 bpcu	6 bpcu
(PSK, SM-PSK)	−2.4304	−0.9691	0.5799	2.0412	3.2906
	N.A.	−1.5761	0.2803	2.2640	4.2597
	N.A.	N.A.	0.0684	2.1512	4.3511
(QAM, SM-QAM)	−2.4304	−1.0939	−3.3199	−2.2055	−4.1422
	N.A.	−1.7009	−2.7542	−3.3406	−4.3064
	N.A.	N.A.	−2.9661	−2.3416	−4.9156
(SSK, SM-QAM)	0.5799	0.7918	−0.2854	0.2460	−0.3481
	N.A.	0.1848	0.2803	−0.8890	−0.5123
	N.A.	N.A.	0.0684	0.1100	−1.1215

# Error Performance – Main Trends (24/38)

## i.i.d. Rayleigh Fading

$N_r = 2$					
Rate / $\Delta_{\text{SNR}}^{(X/Y)}$	2 bpcu	3 bpcu	4 bpcu	5 bpcu	6 bpcu
(PSK, SM-PSK)	−1.0543	1.9011	4.5154	5.6931	5.9642
	N.A.	1.6453	5.3471	8.8845	11.1650
	N.A.	N.A.	5.2585	9.2429	13.1632
(QAM, SM-QAM)	−1.0543	1.7709	0.1040	2.3751	0.9242
	N.A.	1.5152	2.0064	2.2836	2.6976
	N.A.	N.A.	1.9177	4.2581	2.5484
(SSK, SM-QAM)	0.4509	0.3959	−1.7622	−1.8280	−3.6242
	N.A.	0.1401	0.1401	−1.9196	−1.8508
	N.A.	N.A.	0.0515	0.0550	−2.0000

# Error Performance – Main Trends (25/38)

## i.i.d. Rayleigh Fading

$N_r = 3$					
Rate / $\Delta_{\text{SNR}}^{(X/Y)}$	2 bpcu	3 bpcu	4 bpcu	5 bpcu	6 bpcu
(PSK, SM-PSK)	−0.6461	3.0103	5.5248	5.9627	6.0094
	N.A.	2.8560	7.2677	10.9352	11.9378
	N.A.	N.A.	7.2144	11.8624	16.1295
(QAM, SM-QAM)	−0.6461	2.7651	0.9978	3.3520	1.6807
	N.A.	2.6108	3.6577	3.8842	4.4339
	N.A.	N.A.	3.6044	6.5402	4.7666
(SSK, SM-QAM)	0.3574	0.2639	−2.5664	−3.1516	−5.7457
	N.A.	0.1096	0.0934	−2.6194	−2.9926
	N.A.	N.A.	0.0401	0.0367	−2.6598

## Error Performance – Main Trends (26/38)

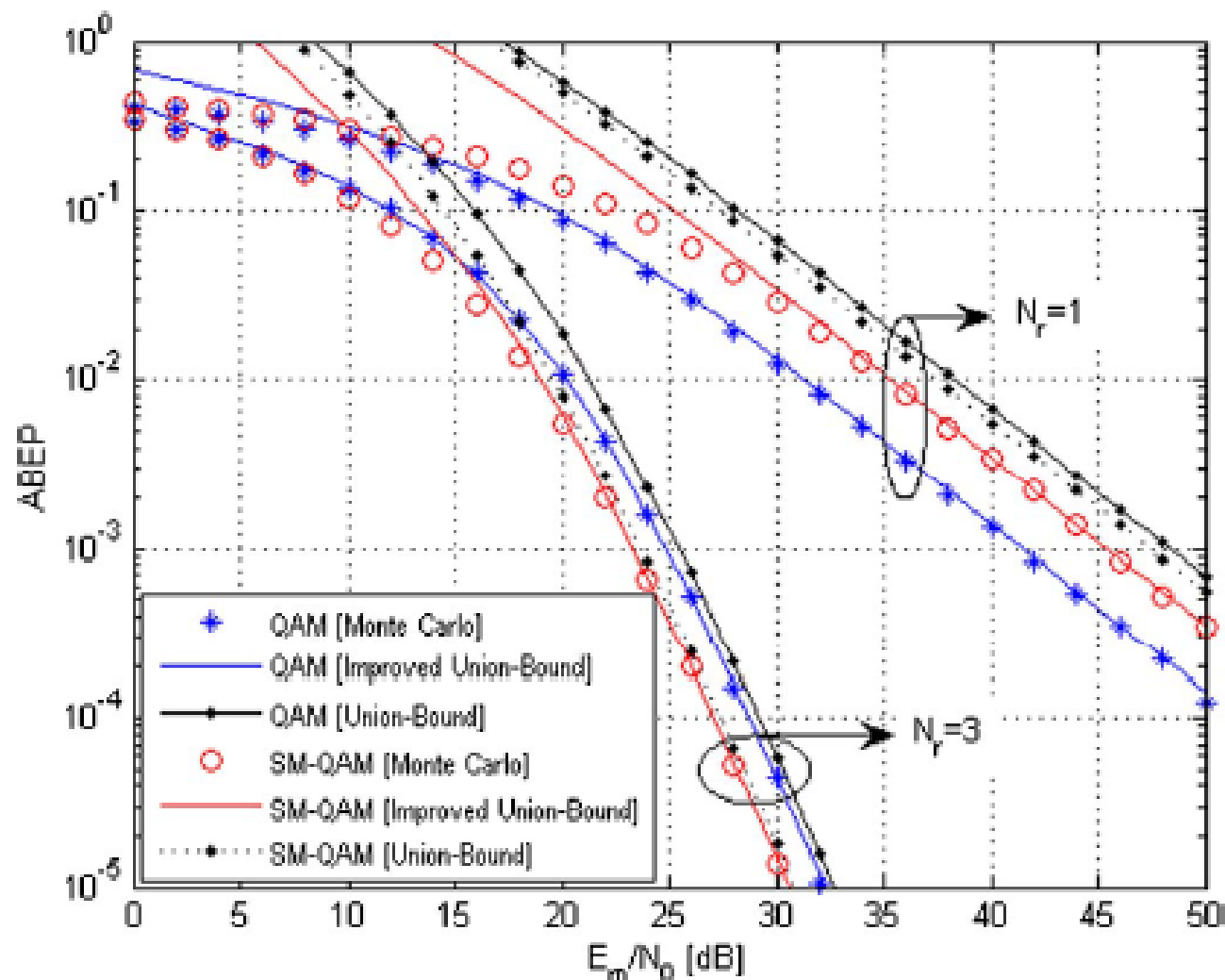


Fig. 2. ABEP of QAM ( $M^{\text{QAM}} = 64$ ) and SM-QAM ( $M = 32, N_t = 2$ ) against  $E_m/N_0$ . Accuracy of proposed analytical framework (denoted by “improved union-bound” in the legend) and conventional union bound (denoted by “union-bound” in the legend) for unit-power ( $\sigma_0^2 = 1$ ) i.i.d. Rayleigh fading (the rate is  $R = 6$  bpcu).

## Error Performance – Main Trends (27/38)

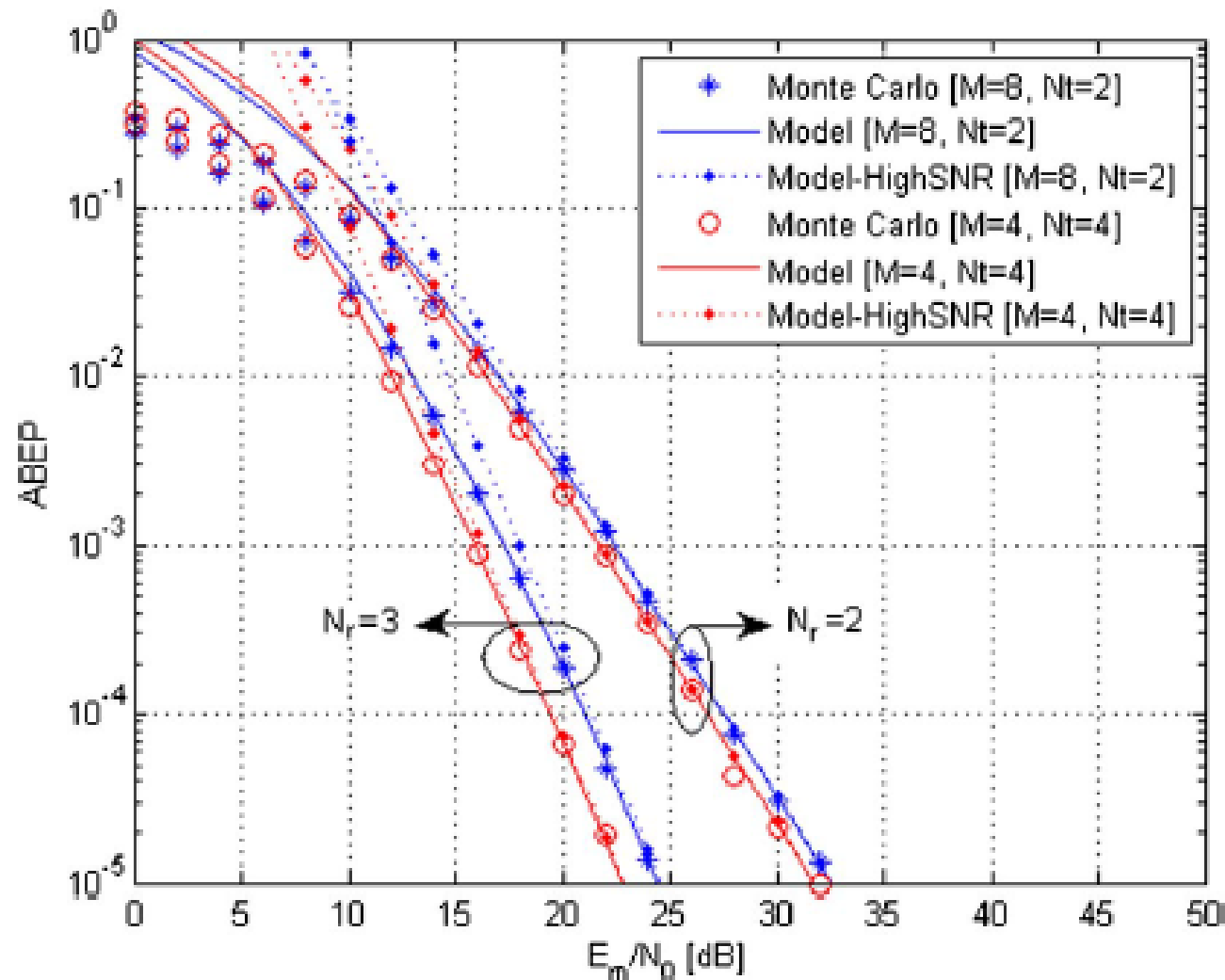


Fig. 3. ABEP of SM-PSK against  $E_m/N_0$ . Performance comparison for various sizes of signal and spatial constellation diagrams. Accuracy of proposed analytical frameworks for unit-power ( $\sigma_0^2 = 1$ ) i.i.d. Rayleigh fading (the rate is  $R = 4$  bpcu). The setup ( $M = 2, N_t = 8$ ) is not shown as it overlaps with the setup ( $M = 4, N_t = 4$ ).

## Error Performance – Main Trends (28/38)

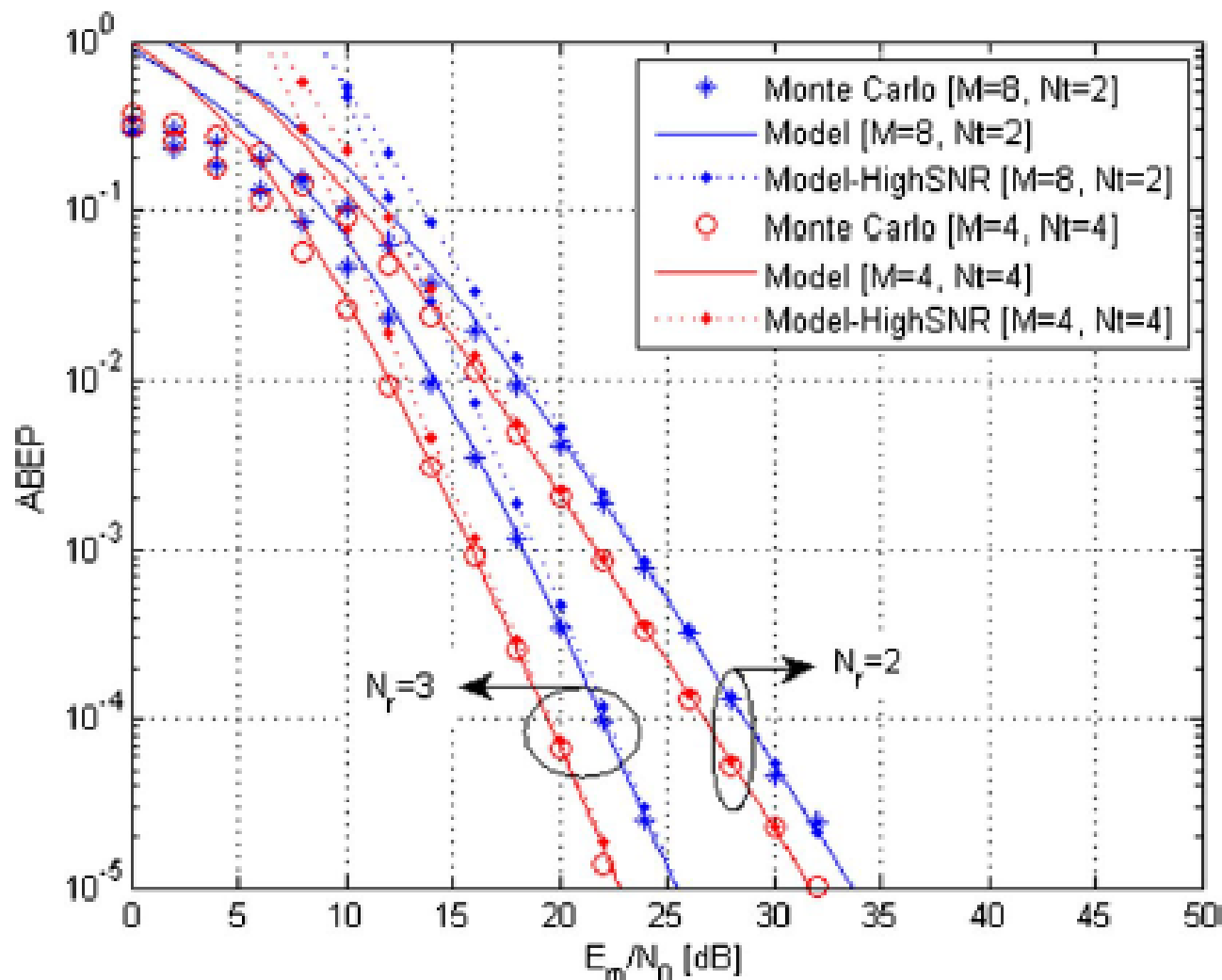


Fig. 4. ABEP of SM-QAM against  $E_m/N_0$ . Performance comparison for various sizes of signal and spatial constellation diagrams. Accuracy of proposed analytical frameworks for unit-power ( $\sigma_0^2 = 1$ ) i.i.d. Rayleigh fading (the rate is  $R = 4$  bpcu). The setup ( $M = 2, N_t = 8$ ) is not shown as it overlaps with the setup ( $M = 4, N_t = 4$ ).



## Error Performance – Main Trends (29/38)

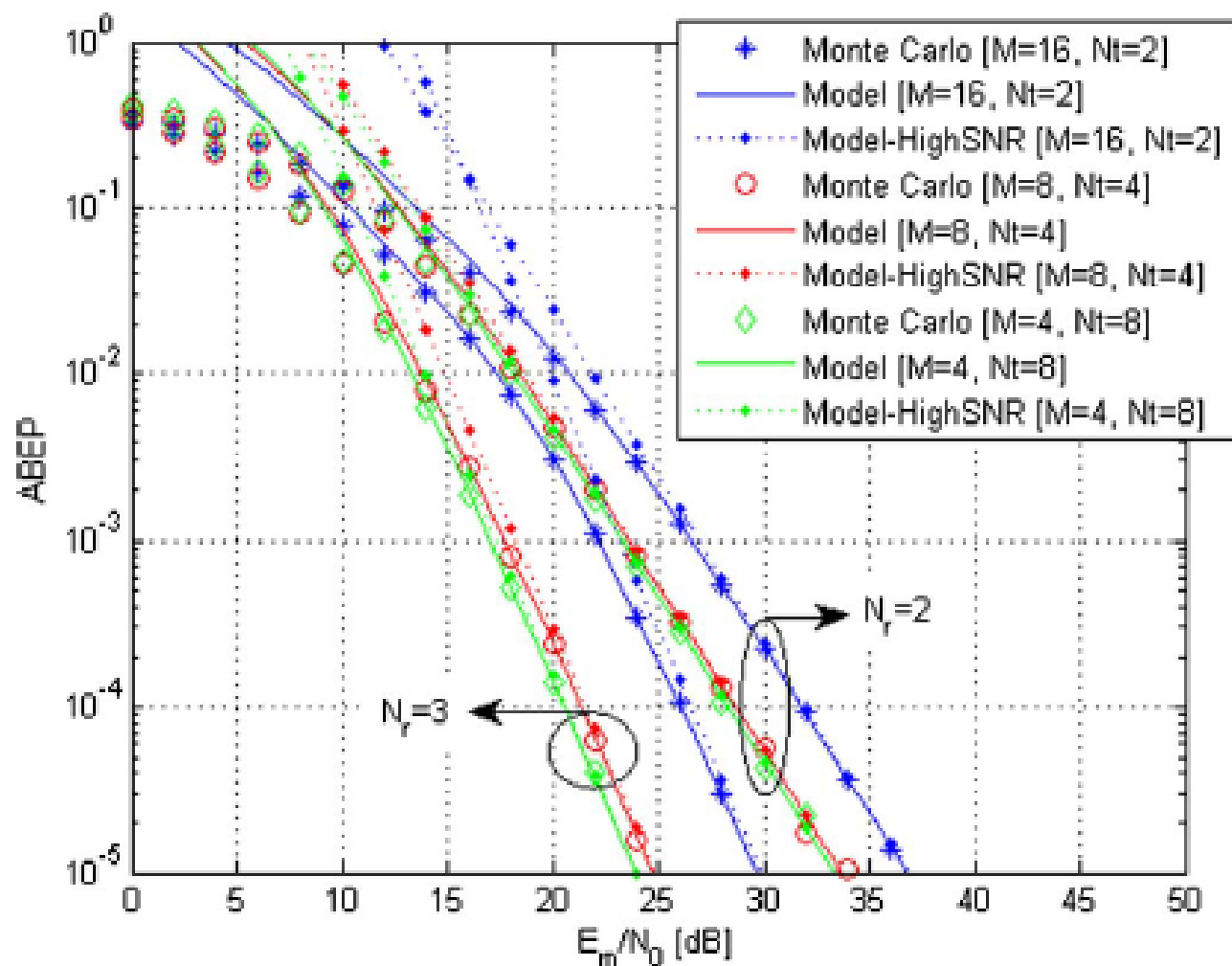


Fig. 5. ABEP of SM-PSK against  $E_m/N_0$ . Performance comparison for various sizes of signal and spatial constellation diagrams. Accuracy of proposed analytical frameworks for unit-power ( $\sigma_0^2 = 1$ ) i.i.d. Rayleigh fading (the rate is  $R = 5$  bpcu). The setup ( $M = 2, N_t = 16$ ) is not shown as it overlaps with the setup ( $M = 4, N_t = 8$ ).

## Error Performance – Main Trends (30/38)

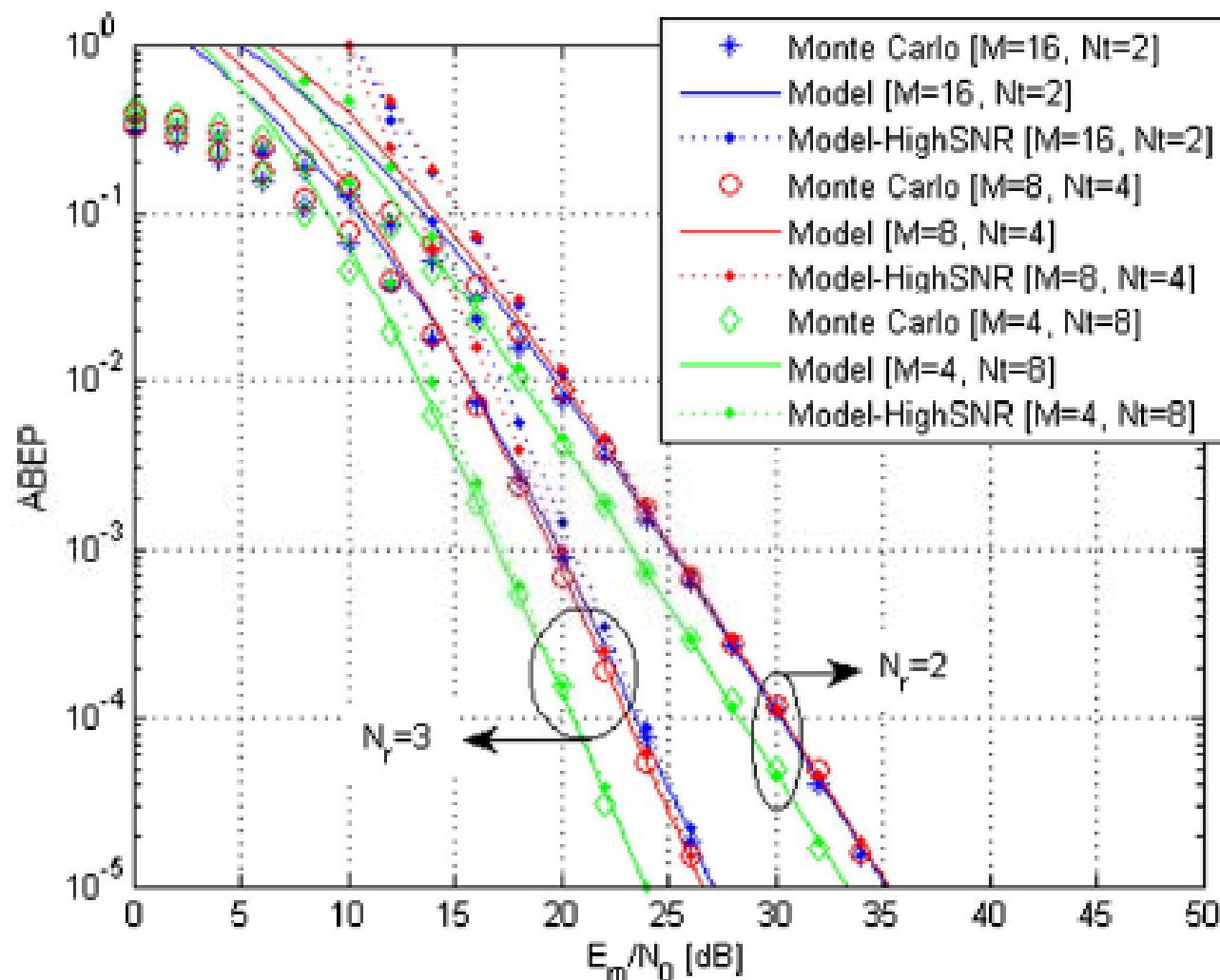


Fig. 6. ABEP of SM-QAM against  $E_m/N_0$ . Performance comparison for various sizes of signal and spatial constellation diagrams. Accuracy of proposed analytical frameworks for unit-power ( $\sigma_0^2 = 1$ ) i.i.d. Rayleigh fading (the rate is  $R = 5$  bpcu). The setup ( $M = 2, N_t = 16$ ) is not shown as it overlaps with the setup ( $M = 4, N_t = 8$ ).

## Error Performance – Main Trends (31/38)

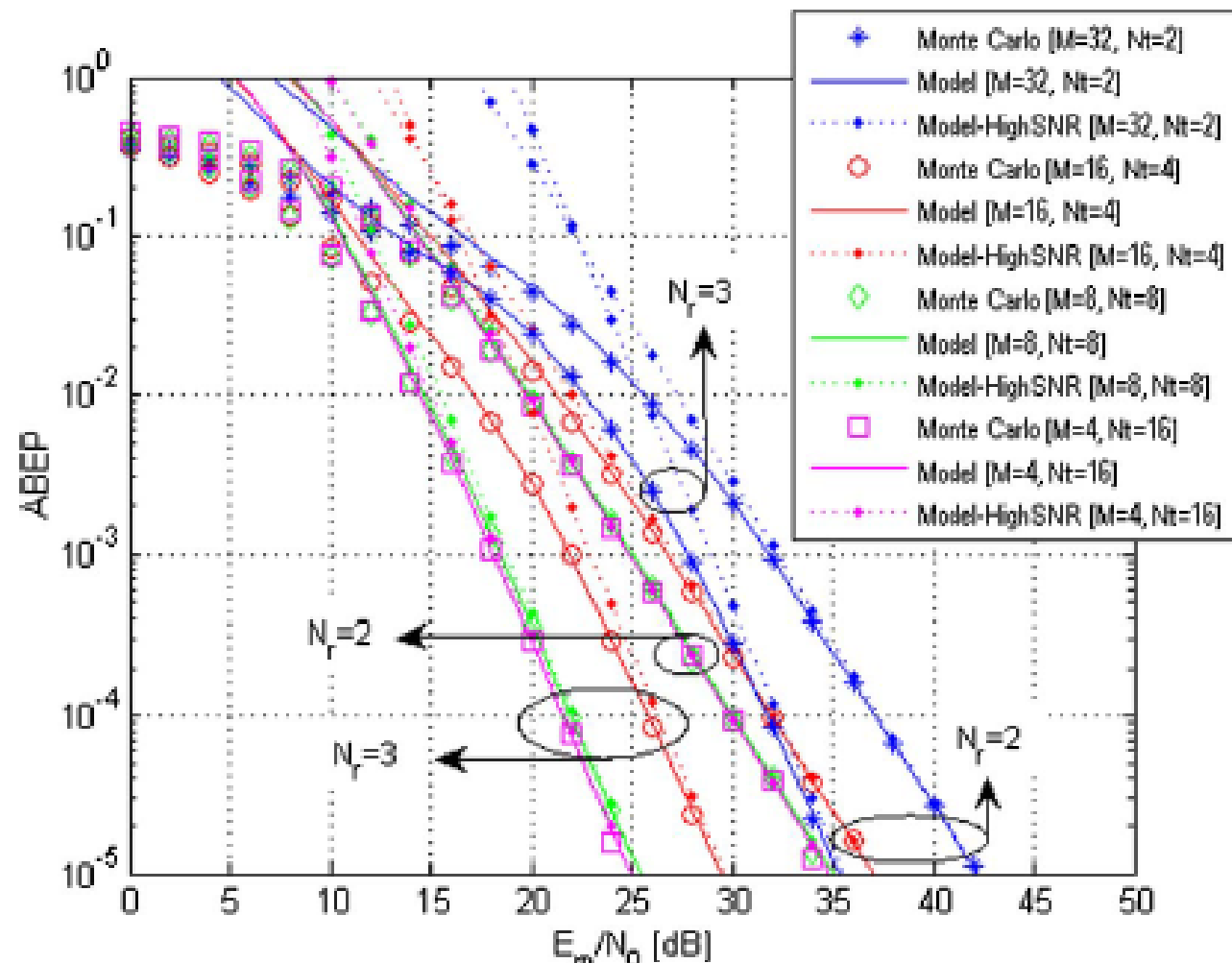


Fig. 7. ABEP of SM-PSK against  $E_m/N_0$ . Performance comparison for various sizes of signal and spatial constellation diagrams. Accuracy of proposed analytical frameworks for unit-power ( $\sigma_0^2 = 1$ ) i.i.d. Rayleigh fading (the rate is  $R = 6$  bpcu). The setup ( $M = 2, N_t = 32$ ) is not shown as it overlaps with the setup ( $M = 4, N_t = 16$ ).

## Error Performance – Main Trends (32/38)

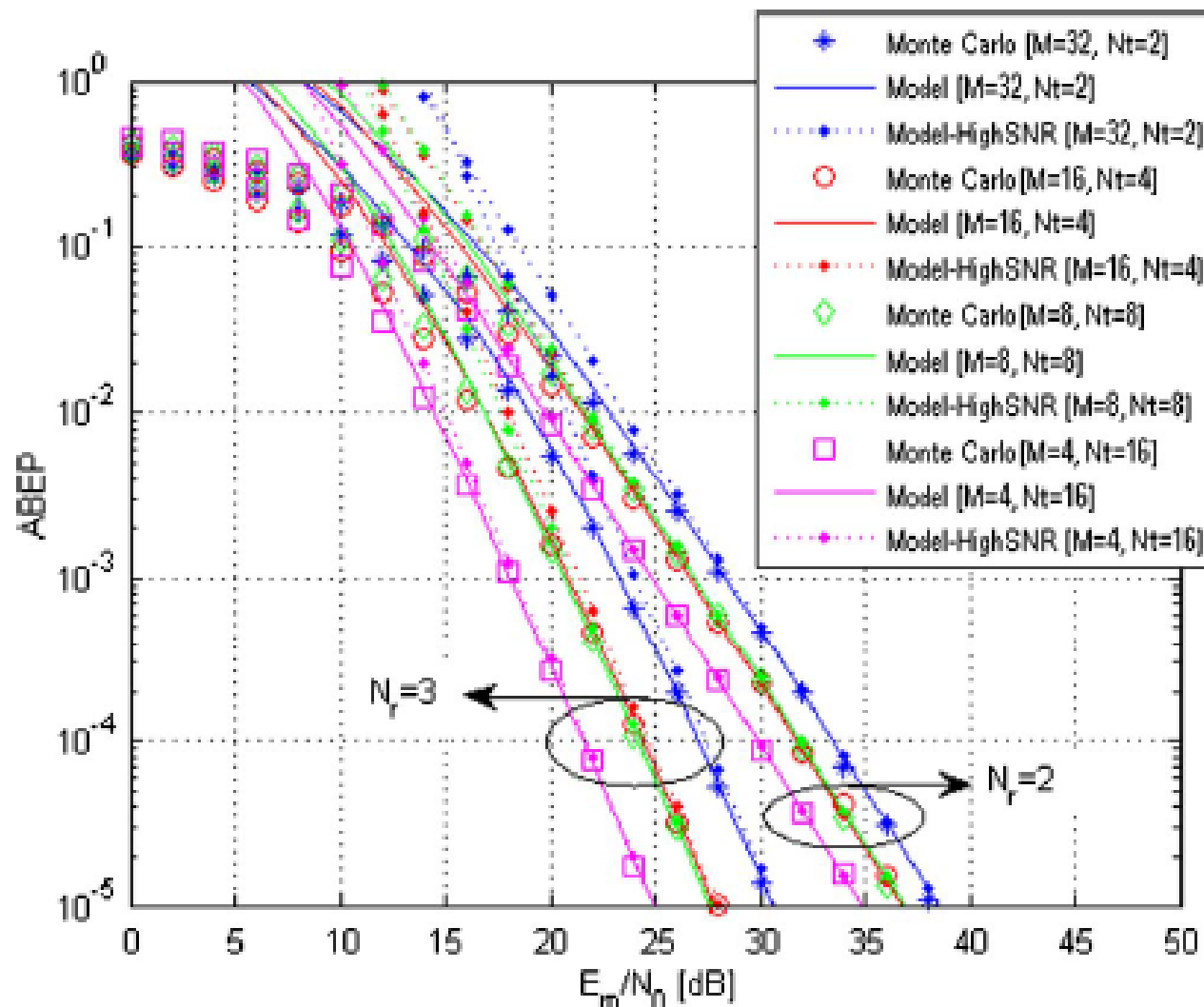


Fig. 8. ABEP of SM-QAM against  $E_m/N_0$ . Performance comparison for various sizes of signal and spatial constellation diagrams. Accuracy of proposed analytical frameworks for unit-power ( $\sigma_0^2 = 1$ ) i.i.d. Rayleigh fading (the rate is  $R = 6$  bpcu). The setup ( $M = 2, N_t = 32$ ) is not shown as it overlaps with the setup ( $M = 4, N_t = 16$ ).

## Error Performance – Main Trends (33/38)

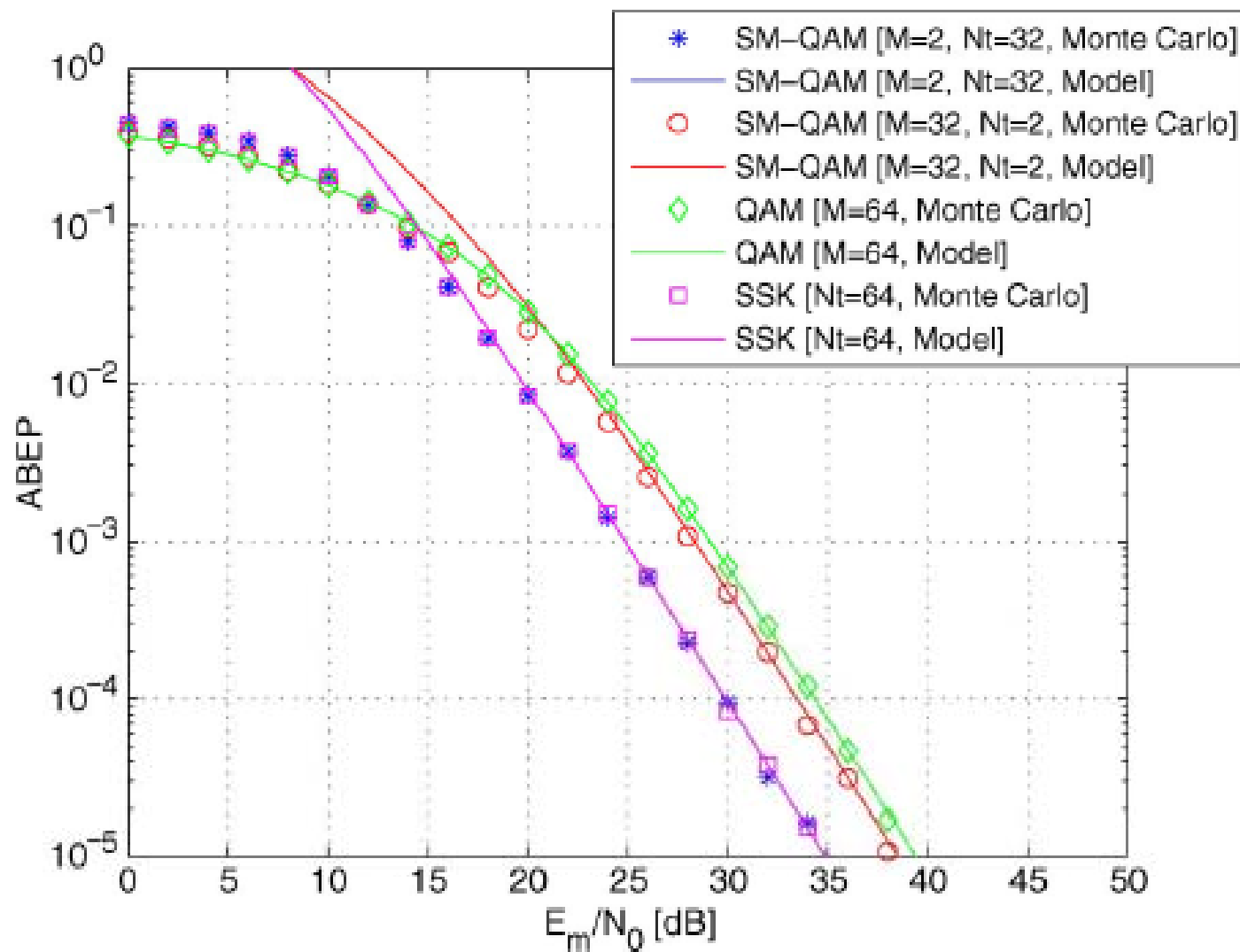


Fig. 9. ABEP against  $E_m/N_0$  over i.i.d. Nakagami- $m$  fading ( $m_{\text{Nak}} = 1.0$ , i.e., Rayleigh,  $N_r = 2$ , and rate  $R = 6$  bpcu). Performance comparison and accuracy of the analytical framework for SM-QAM, QAM, and SSK.

## Error Performance – Main Trends (34/38)

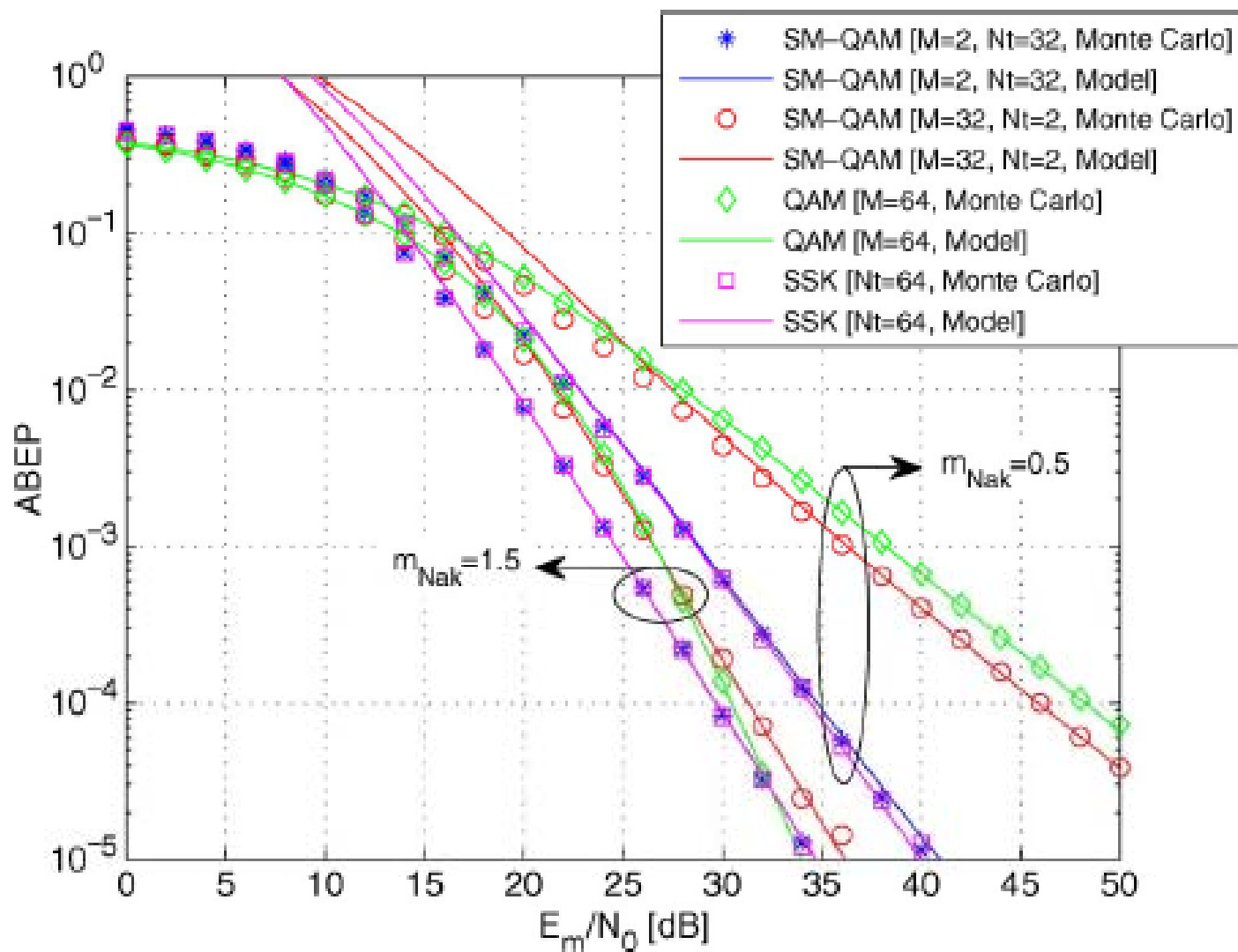


Fig. 10. ABEP against  $E_m/N_0$  over i.i.d. Nakagami- $m$  fading ( $m_{\text{Nak}} = 0.5$  and  $m_{\text{Nak}} = 1.5$ ,  $N_r = 2$ , and rate  $R = 6$  bpcu). Performance comparison and accuracy of the analytical framework for SM-QAM, QAM, and SSK.

## Error Performance – Main Trends (35/38)

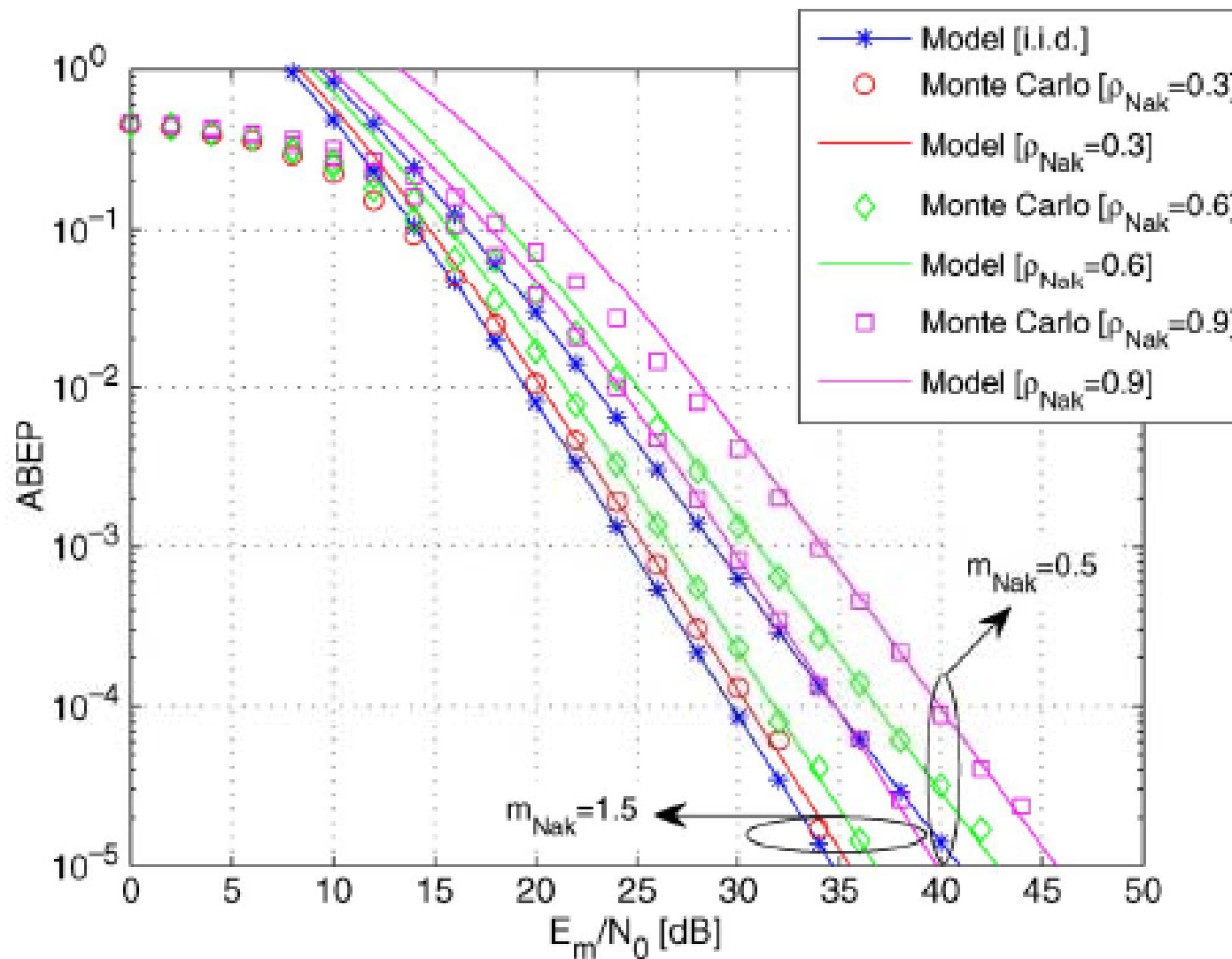


Fig. 11. ABEP of SM-QAM against  $E_m/N_0$  over correlated (at the transmitter) and identically distributed Nakagami- $m$  fading ( $m_{\text{Nak}} = 0.5$  and  $m_{\text{Nak}} = 1.5$ ,  $N_r = 2$ , and rate  $R = 6$  bpcu). Performance comparison and accuracy of the analytical framework for  $M = 2$  and  $N_t = 32$ .

## Error Performance – Main Trends (36/38)

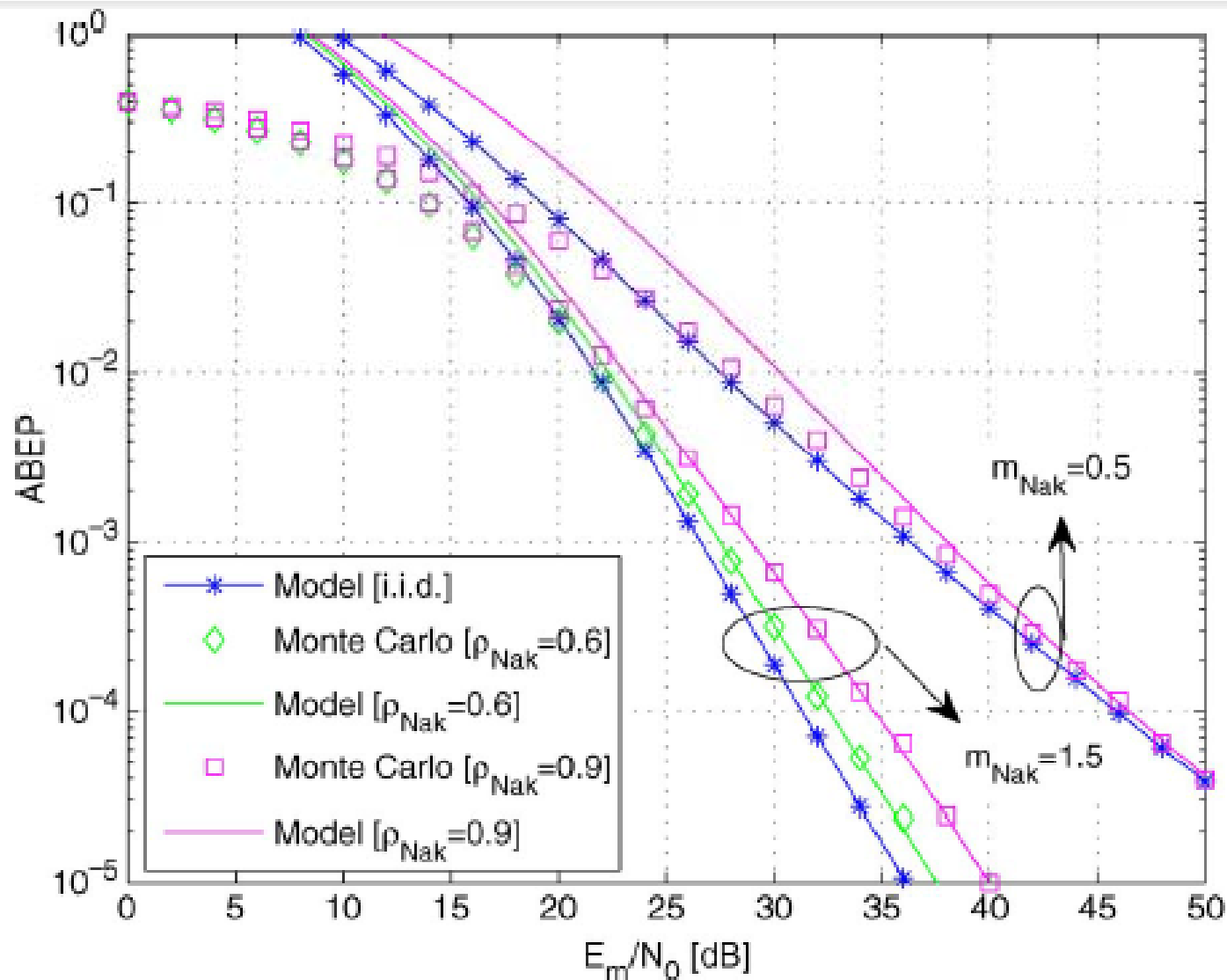


Fig. 12. ABEP of SM-QAM against  $E_m/N_0$  over correlated (at the transmitter) and identically distributed Nakagami- $m$  fading ( $m_{\text{Nak}} = 0.5$  and  $m_{\text{Nak}} = 1.5$ ,  $N_r = 2$ , and rate  $R = 6$  bpcu). Performance comparison and accuracy of the analytical framework for  $M = 32$  and  $N_t = 2$ .



## Error Performance – Main Trends (37/38)

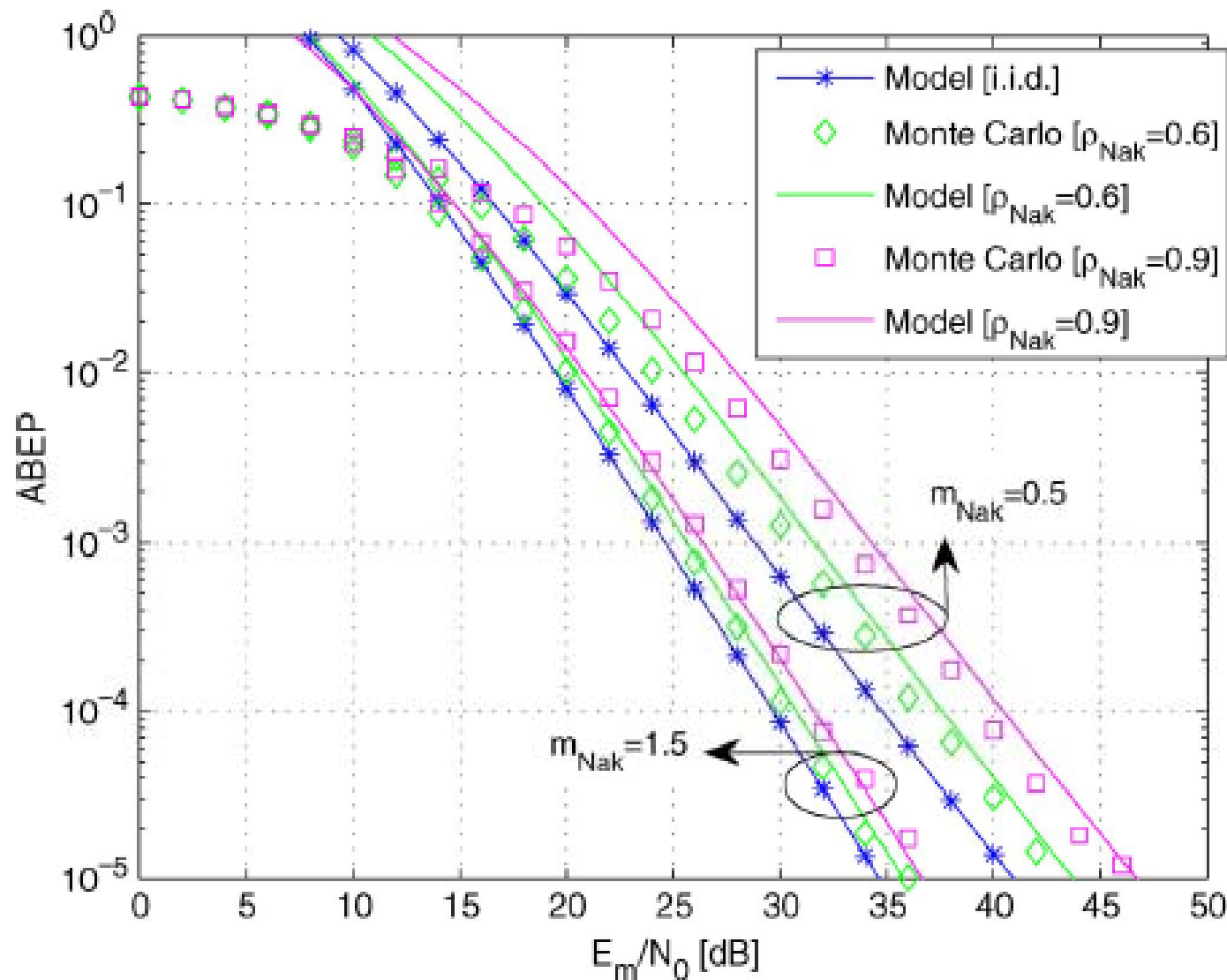


Fig. 13. ABEP of SM-QAM against  $E_m/N_0$  over correlated (at the receiver) and identically distributed Nakagami- $m$  fading ( $m_{\text{Nak}} = 0.5$  and  $m_{\text{Nak}} = 1.5$ ,  $N_r = 2$ , and rate  $R = 6$  bpcu). Performance comparison and accuracy of the analytical framework for  $M = 2$  and  $N_t = 32$ .

## Error Performance – Main Trends (38/38)

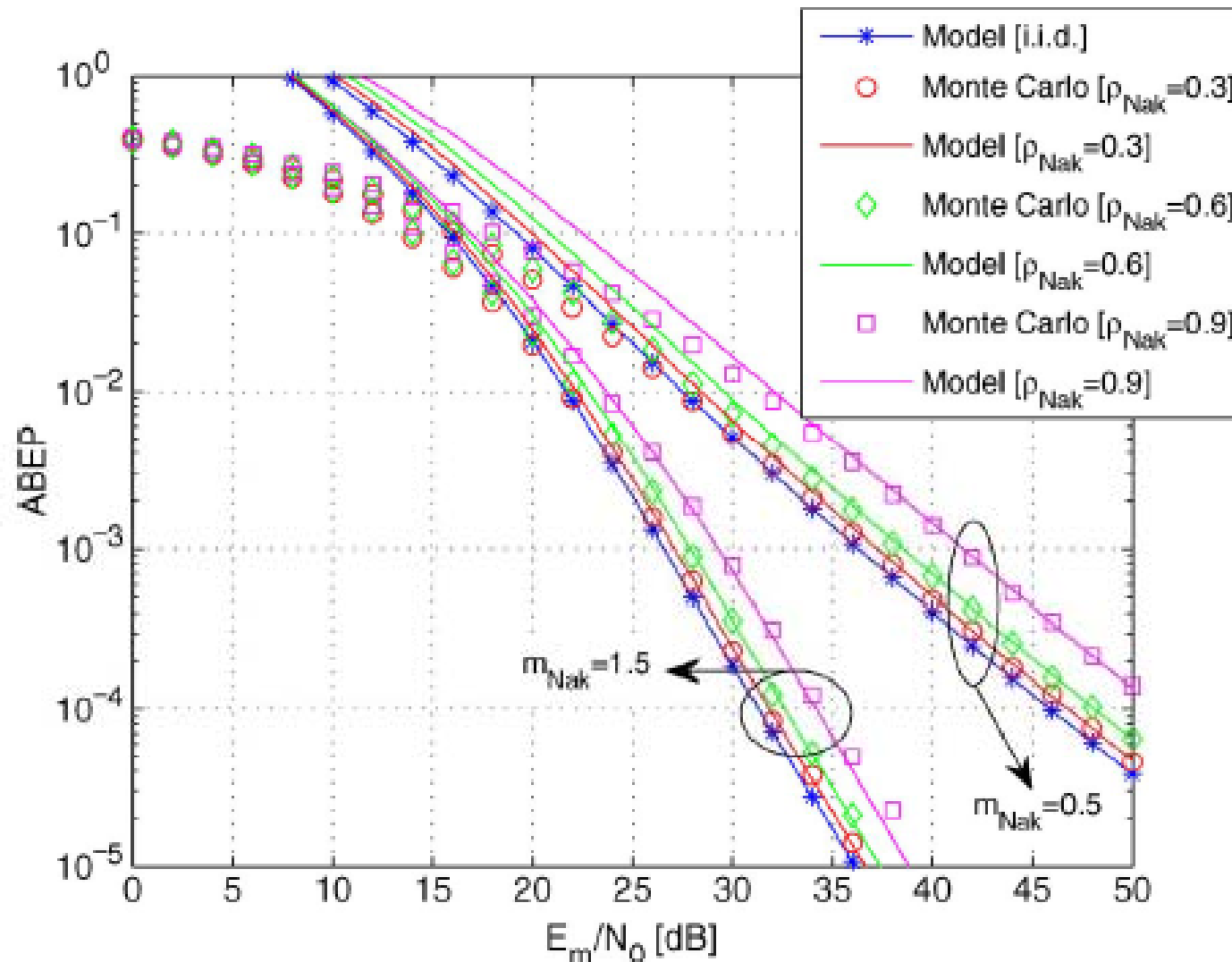


Fig. 14. ABEP of SM-QAM against  $E_m/N_0$  over correlated (at the receiver) and identically distributed Nakagami- $m$  fading ( $m_{\text{Nak}} = 0.5$  and  $m_{\text{Nak}} = 1.5$ ,  $N_r = 2$ , and rate  $R = 6$  bpcu). Performance comparison and accuracy of the analytical framework for  $M = 32$  and  $N_t = 2$ .

# *Outline*

---

1. Introduction and Motivation behind SM-MIMO
2. History of SM Research and Research Groups Working on SM
3. Transmitter Design – Encoding
4. Receiver Design – Demodulation
5. Error Performance (Numerical Results and Main Trends)
6. **Achievable Capacity**
7. Channel State Information at the Transmitter
8. Imperfect Channel State Information at the Receiver
9. Multiple Access Interference
10. Energy Efficiency
11. Transmit-Diversity for SM
12. Spatially-Modulated Space-Time-Coded MIMO
13. Relay-Aided SM
14. SM in Heterogeneous Cellular Networks
15. SM for Visible Light Communications
16. Experimental Evaluation of SM
17. The Road Ahead – Open Research Challenges/Opportunities
18. Implementation Challenges of SM-MIMO

## *Achievable Capacity (1/5)*

---

- ❑ Receiver Diversity case:  $n_t = 1, n_r = n$

$$C = \log_2[1 + \rho \chi_{2n}^2]$$

- ❑ Transmit Diversity case:  $n_t = n, n_r = 1$

$$C = \log_2[1 + (\rho / n_T) \chi_{2n}^2]$$

- ❑ Combined Transmit and Receiver Diversity:  $n_t \geq n_r$

$$C > \sum_{k=n_T-(n_R-1)}^{n_T} \log_2[1 + (\rho / n_T) \chi_{2k}^2]$$

- ❑ Cycling using one transmitted at a time:

$$C = (1 / n_T) \sum_{i=1}^{n_T} \log_2[1 + \rho \chi_{2n_R i}^2]$$

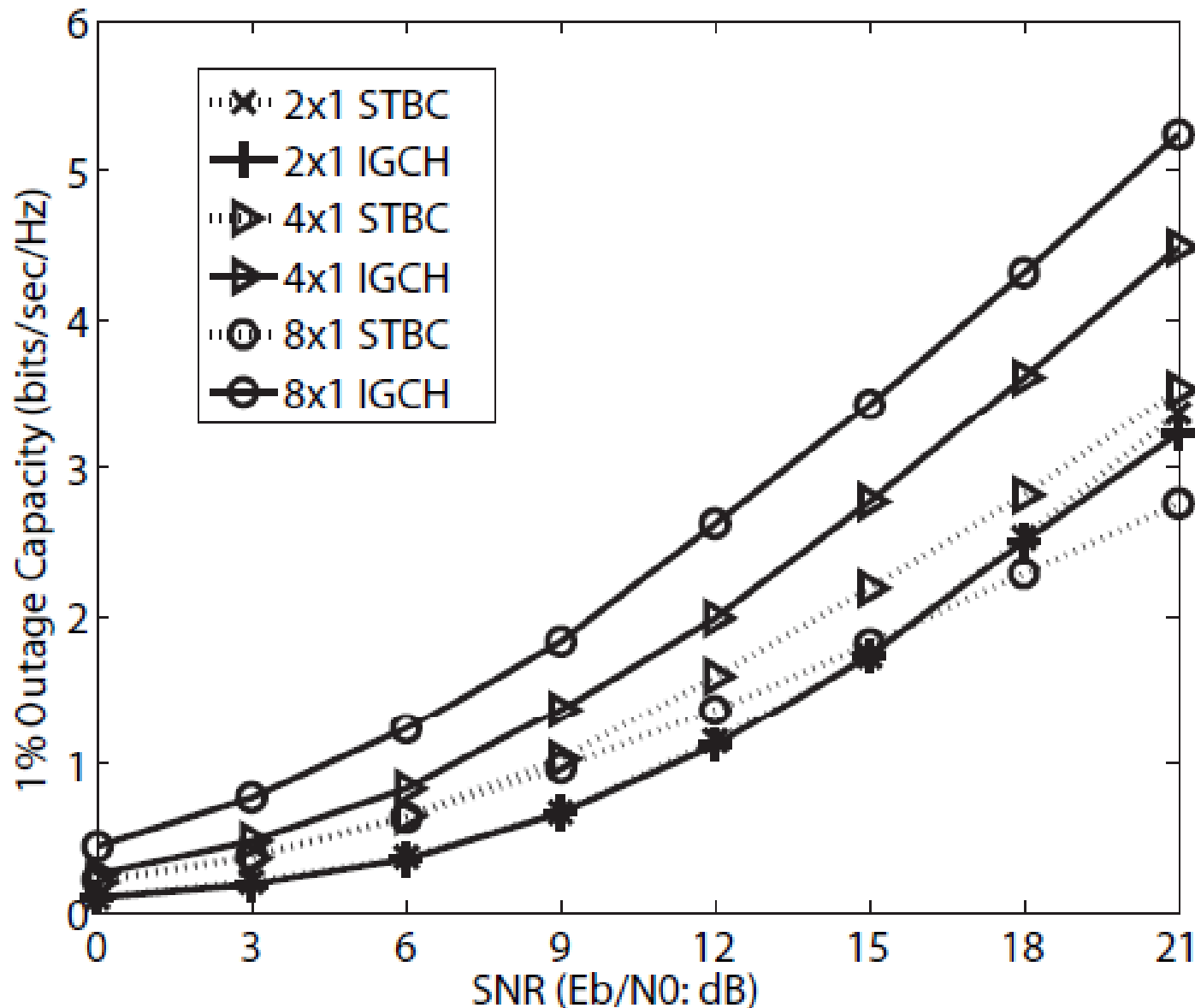
## *Achievable Capacity (2/5)*

$$C_{\text{SM}} (N_t \times 1) = C_1 + C_2 \approx C_1$$

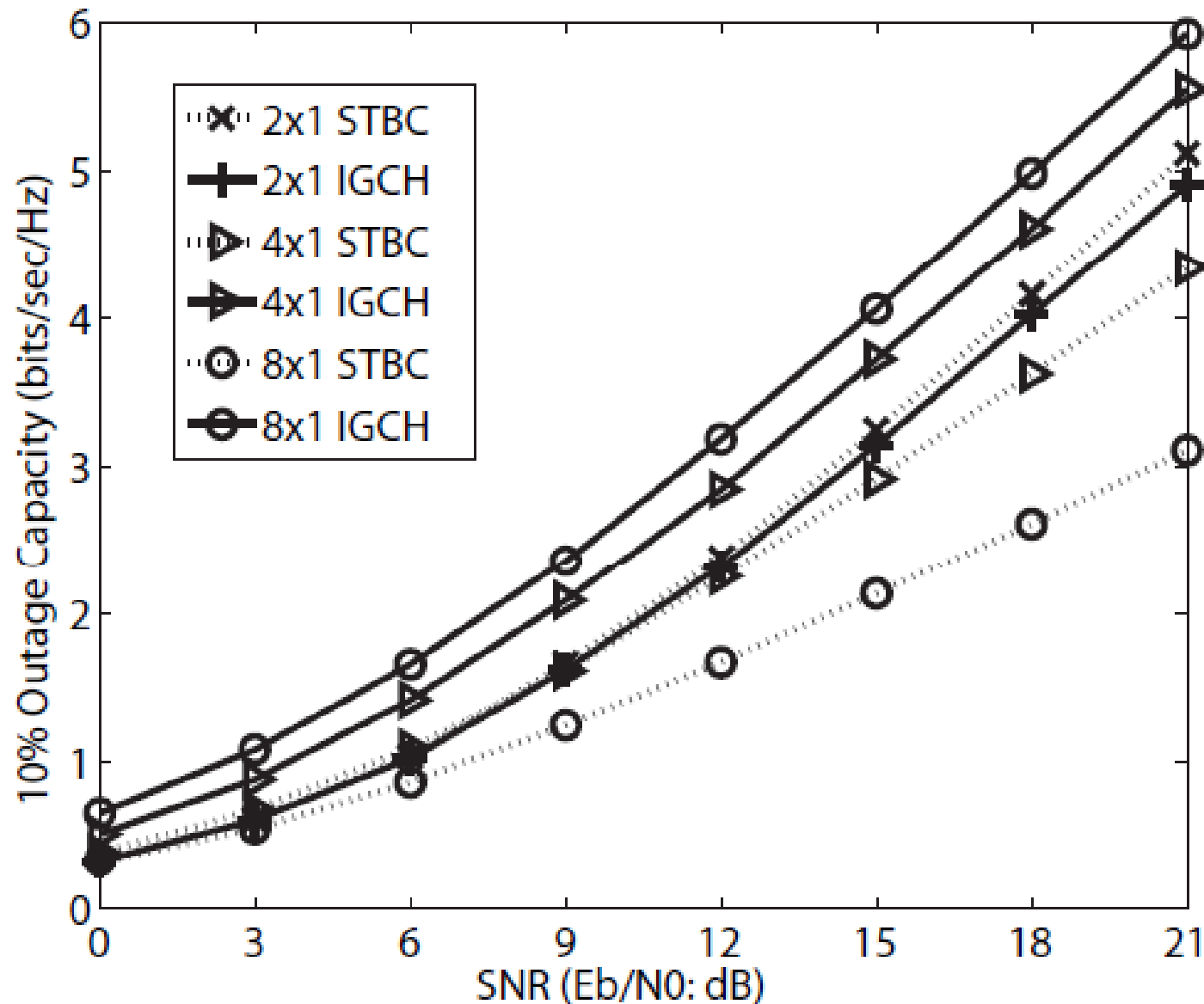
$$C_1 = \frac{1}{N_t} \sum_{m=1}^{N_t} \log_2 \left( 1 + \rho |h_m|^2 \right)$$

$$\left\{ \begin{array}{l} C_2 = \frac{1}{N_t} \sum_{m=1}^{N_t} \left[ \int_y f(y|h_m) \log_2 \left( \frac{f(y|h_m)}{f(y)} \right) dy \right] \\ f(y) = \frac{1}{N_t} \sum_{m=1}^{N_t} \left[ \underbrace{\frac{1}{\pi (|h_m|^2 \sigma_X^2 + \sigma_N^2)}}_{f(y|h_m)} \exp \left( -\frac{|y|^2}{|h_m|^2 \sigma_X^2 + \sigma_N^2} \right) \right] \end{array} \right.$$

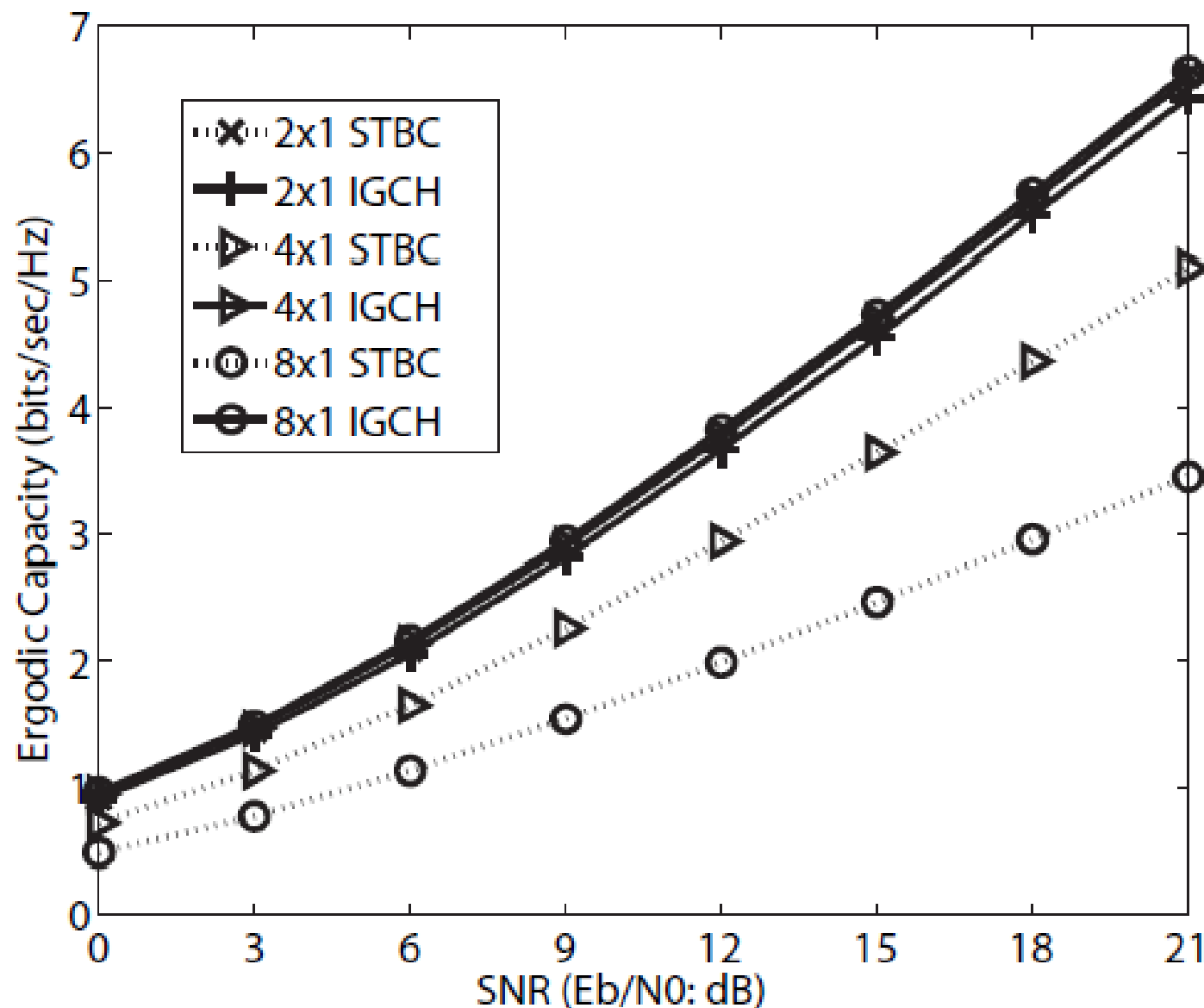
## Achievable Capacity (3/5)



## Achievable Capacity (4/5)



## Achievable Capacity (5/5)





# *Outline*

---

1. Introduction and Motivation behind SM-MIMO
2. History of SM Research and Research Groups Working on SM
3. Transmitter Design – Encoding
4. Receiver Design – Demodulation
5. Error Performance (Numerical Results and Main Trends)
6. Achievable Capacity
7. **Channel State Information at the Transmitter**
8. Imperfect Channel State Information at the Receiver
9. Multiple Access Interference
10. Energy Efficiency
11. Transmit-Diversity for SM
12. Spatially-Modulated Space-Time-Coded MIMO
13. Relay-Aided SM
14. SM in Heterogeneous Cellular Networks
15. SM for Visible Light Communications
16. Experimental Evaluation of SM
17. The Road Ahead – Open Research Challenges/Opportunities
18. Implementation Challenges of SM-MIMO

# Channel State Information at the Transmitter (1/22)

- ❑ The performance of SSK/SM modulation significantly depends on the wireless channel statistics, and power imbalance may improve the performance
- ❑ Can power imbalance be created via opportunistic power allocation?

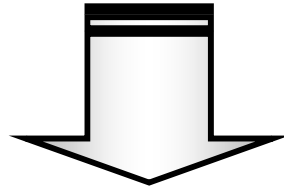
## ❑ Assumptions:

- $N_t = 2$
- Correlated Rayleigh fading channel
- $E_1 \neq E_2$

$$\begin{cases} \text{ABEP}(E_1, E_2) = \frac{1}{2} - \frac{1}{2} \sqrt{\frac{\bar{\sigma}^2 \bar{\gamma}}{1 + \bar{\sigma}^2 \bar{\gamma}}} \\ \bar{\sigma}^2 = E_1 \sigma_1^2 + E_2 \sigma_2^2 - 2\rho \sqrt{E_1} \sqrt{E_2} \sigma_1 \sigma_2 \quad \text{and} \quad \bar{\gamma} = 1/(4N_0) \end{cases}$$

## Channel State Information at the Transmitter (2/22)

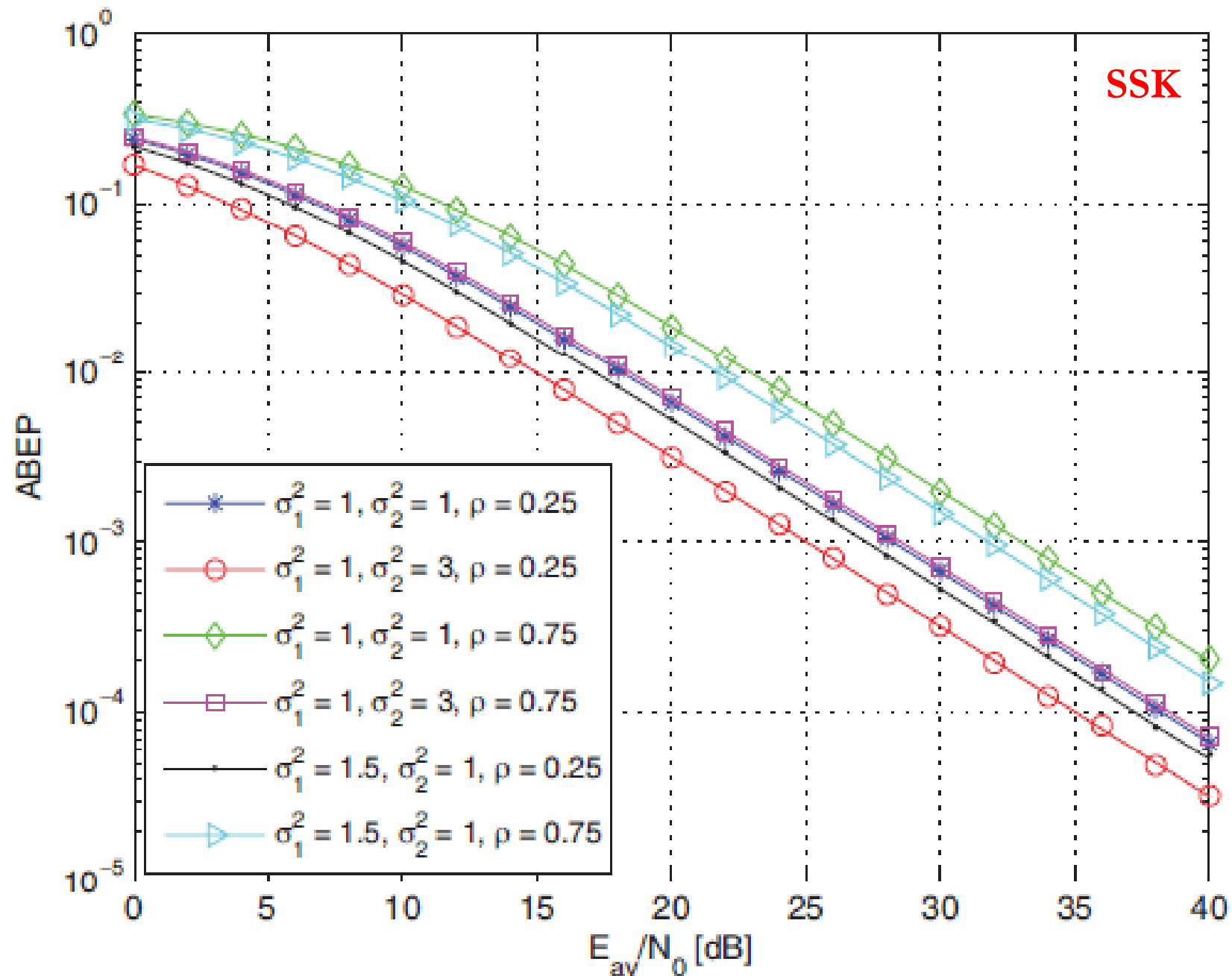
$$\begin{cases} (E_1^*, E_2^*) = \arg \min_{(E_1, E_2)} \{ \text{ABEP}(E_1, E_2) \} \\ \text{subject to: } \frac{E_1}{2} + \frac{E_2}{2} = E_{\text{av}} \end{cases}$$



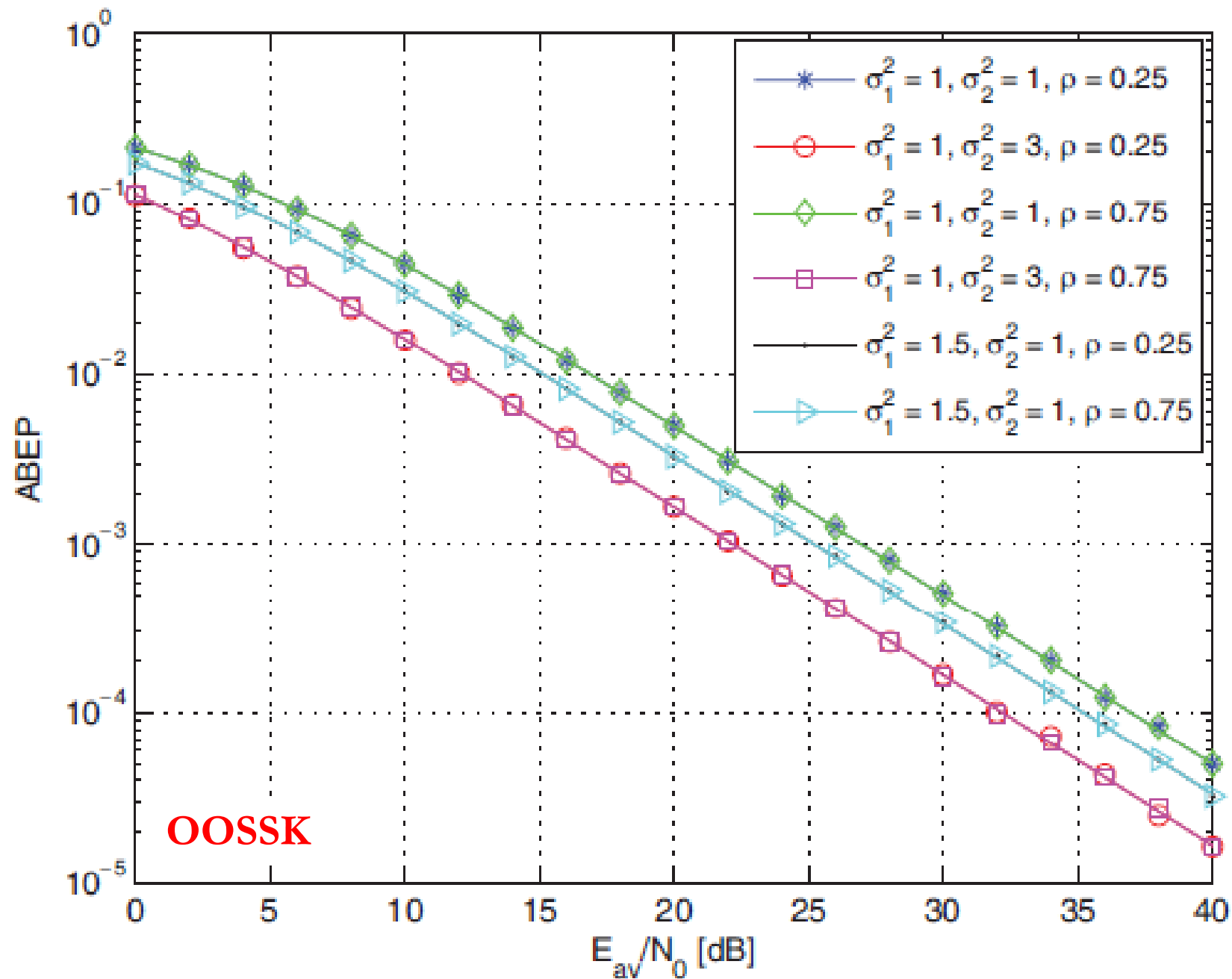
- If  $\sigma_1^2 > \sigma_2^2 \rightarrow (E_1^*, E_2^*) = (2E_{\text{av}}, 0)$  and  $\sigma_M^2 = \sigma_1^2$
- If  $\sigma_2^2 > \sigma_1^2 \rightarrow (E_1^*, E_2^*) = (0, 2E_{\text{av}})$  and  $\sigma_M^2 = \sigma_2^2$

$$\text{SNR}_{\text{gain}} \cong \left. \frac{\text{SNR}_{\text{SSK}}^{\infty}}{\text{SNR}_{\text{OOSSK}}^{\infty}} \right|_{\text{dB}} \cong 10 \log_{10} \left[ \frac{2\sigma_M^2}{\sigma_1^2 + \sigma_2^2 - 2\rho\sigma_1\sigma_2} \right] \geq 0$$

## Channel State Information at the Transmitter (3/22)



## Channel State Information at the Transmitter (4/22)



## *Channel State Information at the Transmitter (5/22)*

---

- ❑ The symbol error rate (SER) performance highly depends on the Euclidean distance between pairs of these vectors
- ❑ **Optimization problem:** how to design the transmit vectors using CSIT such that the distance between pairs of constellation vectors at the receiver is larger
- ❑ Two methods are proposed:
  - In the first method, no constraint on the structure of the transmit vectors is imposed (**Multi-Antenna Space Modulation: MSMod**)
  - In the second method, the transmit vectors have only one non-zero entry (**Modified Space Shift Keying: MSSK**)

# Channel State Information at the Transmitter (6/22)

## MSMod with Full-CSIT

$$\begin{aligned} P_M | \mathbf{H} &\leq \frac{1}{N_t} \sum_{\substack{k=1 \\ l=1 \\ k \neq l}}^{N_t} Q \left( \sqrt{\frac{\rho}{2}} \|\mathbf{H}\mathbf{p}_l - \mathbf{H}\mathbf{p}_k\| \right) \\ &\leq \frac{1}{2N_t} \sum_{\substack{k=1 \\ l=1 \\ k \neq l}}^{N_t} \exp \left( -\gamma \|\mathbf{H}\mathbf{p}_l - \mathbf{H}\mathbf{p}_k\|^2 \right) = A_P \end{aligned}$$



$$\left\{ \begin{array}{l} (\mathbf{p}_1^*, \mathbf{p}_2^*, \dots, \mathbf{p}_{N_t}^*) = \arg \min_{(\mathbf{p}_1, \mathbf{p}_2, \dots, \mathbf{p}_{N_t})} \{A_P\} \\ s.t. \quad \sum_{l=1}^{N_t} \|\mathbf{p}_l\|^2 = N_t \end{array} \right.$$

# Channel State Information at the Transmitter (7/22)

## MSMod with Full-CSIT: Optimal Solution

$$\mathbf{p}_k^* = \theta_k \mathbf{v}_1$$
$$\sum_{k=1, k \neq l}^{N_t} \left(1 - \frac{\theta_k}{\theta_l}\right) \exp\left(-\gamma \varepsilon_1^2 |\theta_l - \theta_k|^2\right) = \frac{\lambda'}{\varepsilon_1^2}$$
$$\sum_{k=1}^{N_t} |\theta_k|^2 = N_t$$

- ❑  $\mathbf{v}_1$  is the right singular vector related to the largest singular value of  $\mathbf{H}$
- ❑  $\varepsilon_1$  is the largest singular value of  $\mathbf{H}$
- ❑  $\lambda'$  is a constant
- ❑ Bottom line:  $\theta_k$  can be chosen from conventional PSK/QAM constellations
- ❑ Similar results apply to the imperfect CSIT case ( $\mathbf{H}_{\text{error}} = \mathbf{H} + \mathbf{N}$ )



# Channel State Information at the Transmitter (8/22)

## MSSK with Full-CSIT

$$\begin{aligned} P_M | \mathbf{H} &\leq \frac{1}{N_t} \sum_{\substack{l=1, \\ l \neq k}}^{N_t} Q \left( \sqrt{\frac{\rho}{2}} \|p_l \mathbf{h}_l - p_k \mathbf{h}_k\| \right) \\ &\leq \frac{1}{2N_t} \sum_{\substack{l=1, \\ l \neq k}}^{N_t} \exp \left( -\gamma \|p_l \mathbf{h}_l - p_k \mathbf{h}_k\|^2 \right) = A_P \end{aligned}$$



$$\left\{ \begin{array}{l} (p_1^*, p_2^*, \dots, p_{N_t}^*) = \arg \min_{(p_1, p_2, \dots, p_{N_t})} \{A_P\} \\ s.t. \quad \sum_{l=1}^{N_t} |p_l|^2 = N_t \end{array} \right.$$

# Channel State Information at the Transmitter (9/22)

## MSSK with Full-CSIT: Optimal Solution

□ Find

$$p_i = r_i \exp(j\varphi_i)$$

□ Such that the following function is MINIMIZED:

$$\sum_{\substack{k=1, l=1 \\ k \neq l}}^{N_t} \exp \left\{ -\gamma \left( r_l^2 \|\mathbf{h}_l\|^2 + r_k^2 \|\mathbf{h}_k\|^2 - 2r_l r_k \omega_{l,k} \right) \right\}$$

$$\text{where } \omega_{l,k} = \Re \left\{ e^{j(\varphi_k - \varphi_l)} \mathbf{h}_l^H \mathbf{h}_k \right\}$$

# Channel State Information at the Transmitter (10/22)

## MSSK with Full-CSIT: Optimal Solution

□ If  $N_t = 2$ :

$$\begin{cases} p_1 = \sqrt{1 + \frac{\|\mathbf{h}_1\|^2 - \|\mathbf{h}_2\|^2}{\sqrt{4\mu^2 + (\|\mathbf{h}_1\|^2 - \|\mathbf{h}_2\|^2)^2}}} \cdot \exp(j(\pi + \varphi_2 - \phi)) \\ p_2 = \sqrt{1 + \frac{\|\mathbf{h}_2\|^2 - \|\mathbf{h}_1\|^2}{\sqrt{4\mu^2 + (\|\mathbf{h}_1\|^2 - \|\mathbf{h}_2\|^2)^2}}} \cdot \exp(j\varphi_2) \end{cases}$$

➤ with

$$\mathbf{h}_2^H \mathbf{h}_1 = \mu \exp(j\phi)$$

$$\varphi_1 - \varphi_2 = \pi - \phi$$

# Channel State Information at the Transmitter (11/22)

## MSSK with Full-CSIT: Optimal Solution

□ If  $N_t > 2$ , a sub-optimal iterative approach is proposed:

- In each iteration, the pair of vectors with s-th minimum distance is considered and the optimal solution for  $N_t = 2$  is computed
- To guarantee that the error performance does not increase with the iterations, an error function is introduced

$$\text{err}(x, l) \triangleq \sum_{i=1, i \neq l}^{N_t} Q\left(\sqrt{\frac{\rho}{2}} \|x\mathbf{h}_l - p_i\mathbf{h}_i\|\right)$$

- **Iteration over s:** s-th minimum distance over pairs of transmission vectors

---

**Algorithm 1** MSSK signal design algorithm with full CSIT ( $N_t > 2$ )

---

1.  $p_1 = p_2 = \dots = p_{N_t} = 1, \quad s = 1$
  2.  $\mathbf{G} = \mathbf{H} \cdot \text{diag}\{p_1, p_2, \dots, p_{N_t}\}$
  3.  $(l^*, k^*) = \arg \min_{l, k} \{\|\mathbf{g}_l - \mathbf{g}_k\|, s\}$
  4.  $m_{l^*, k^*} = \sqrt{\frac{\|\mathbf{p}_{l^*}\|^2 + \|\mathbf{p}_{k^*}\|^2}{2}}$
  5. Calculate  $q_{l^*}$  and  $q_{k^*}$  using (36) with  $\varphi^* = 0$
  6.  $\varphi^* = \arg \min_{\varphi} \{\text{err}(q_{l^*} \cdot \exp(j\varphi), l^*) + \text{err}(q_{k^*} \cdot \exp(j\varphi), k^*)\}$
  7.  $q_{l^*} = q_{l^*} \cdot \exp(j\varphi^*), \quad q_{k^*} = q_{k^*} \cdot \exp(j\varphi^*)$
  8.  

*If*  $\text{err}(q_{l^*}, l^*) + \text{err}(q_{k^*}, k^*) \leq \text{err}(p_{l^*}, l^*) + \text{err}(p_{k^*}, k^*)$ 
    - $s = 1$
    - $p_{l^*} = q_{l^*}$
    - $p_{k^*} = q_{k^*}$*else*
    - $s = s + 1$*endif*
  9. Go to step 2
-

## Channel State Information at the Transmitter (12/22)

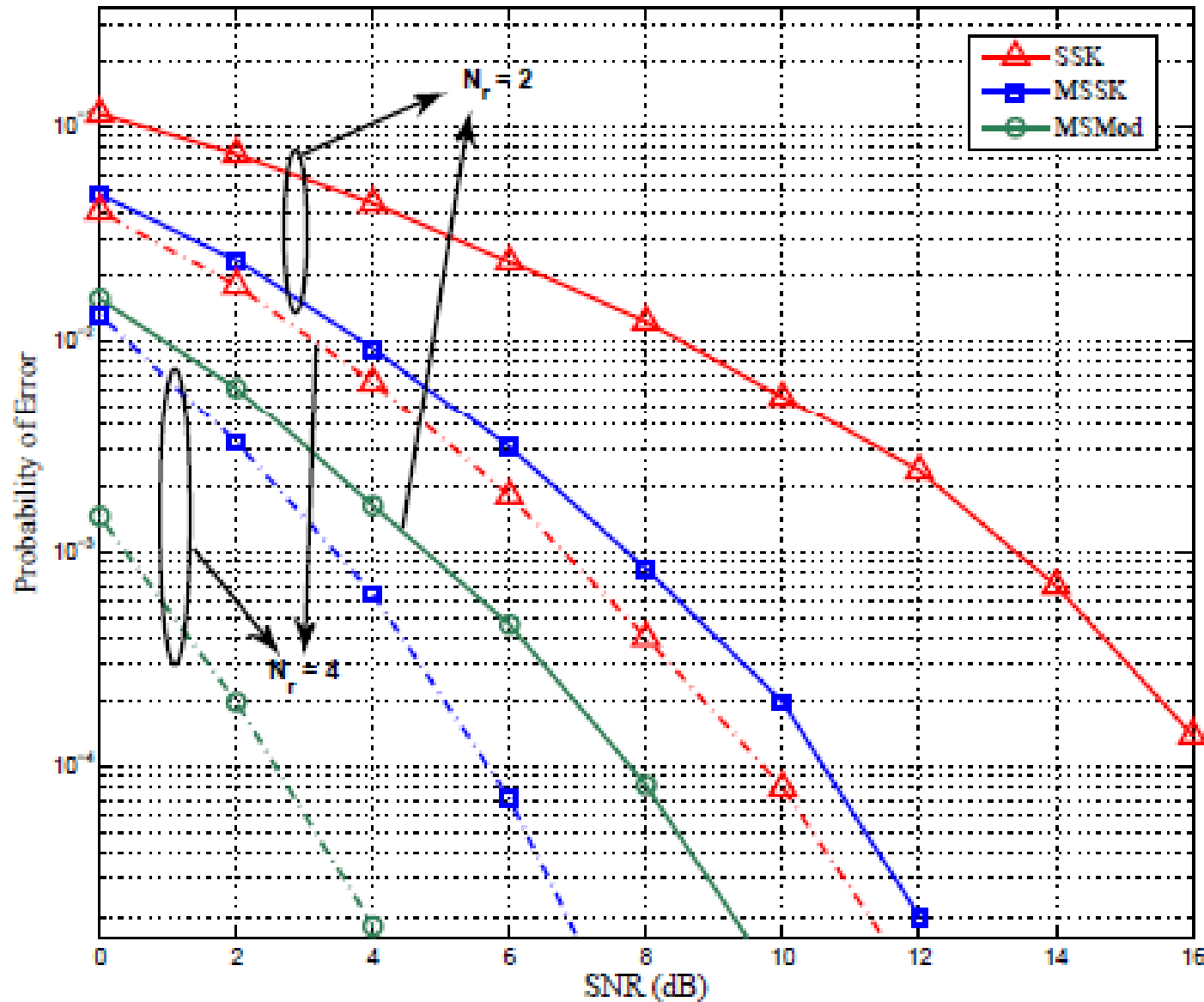


Fig. 2. SER for SSK, MSSK, and MSMod schemes with full CSIT ( $N_t = 2$ ,  $N_r = 2, 4$ )

## Channel State Information at the Transmitter (13/22)

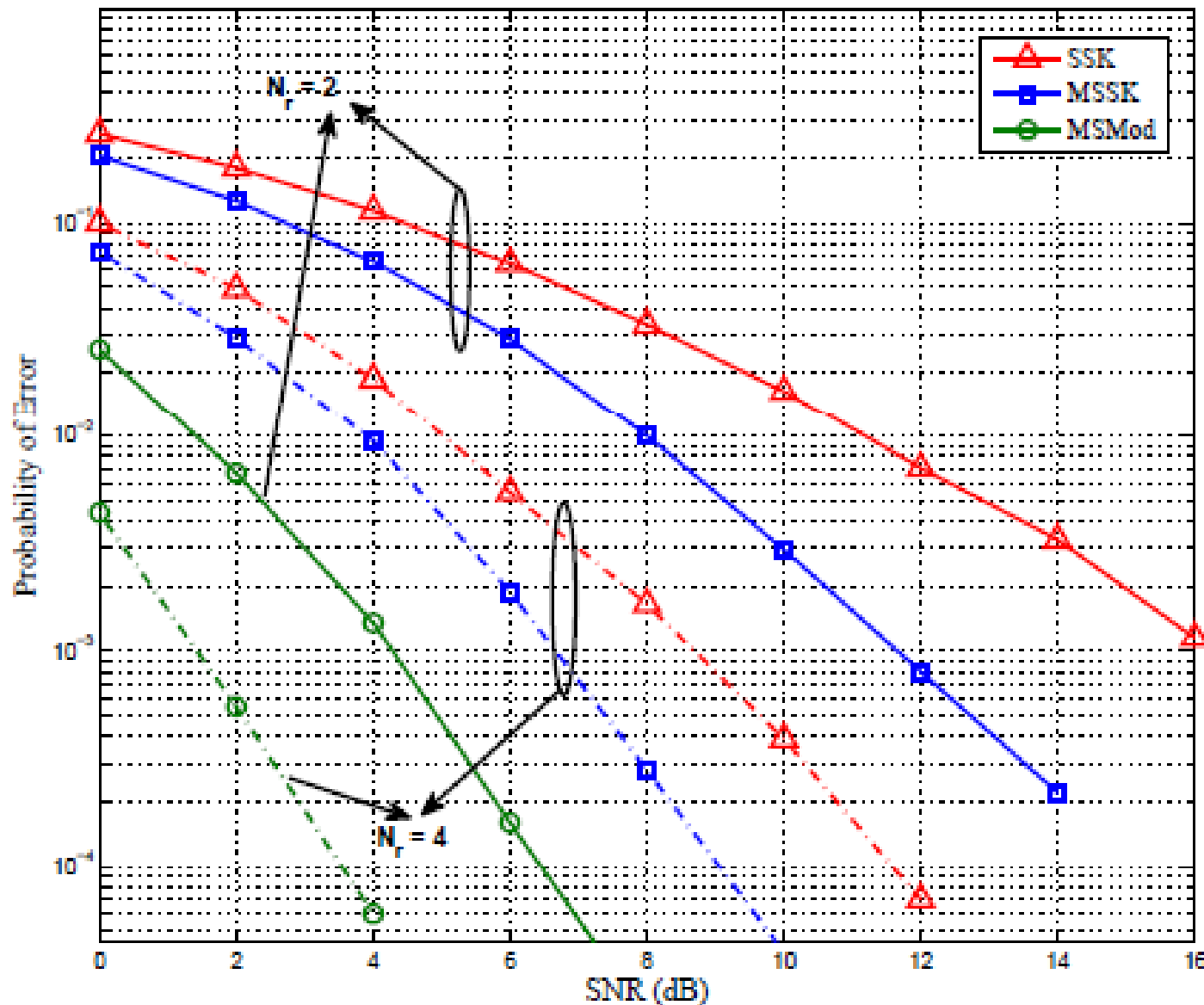


Fig. 3. SER for SSK, MSSK, and MSMod schemes with full CSIT ( $N_t = 4$ ,  $N_r = 2, 4$ )

## Channel State Information at the Transmitter (14/22)

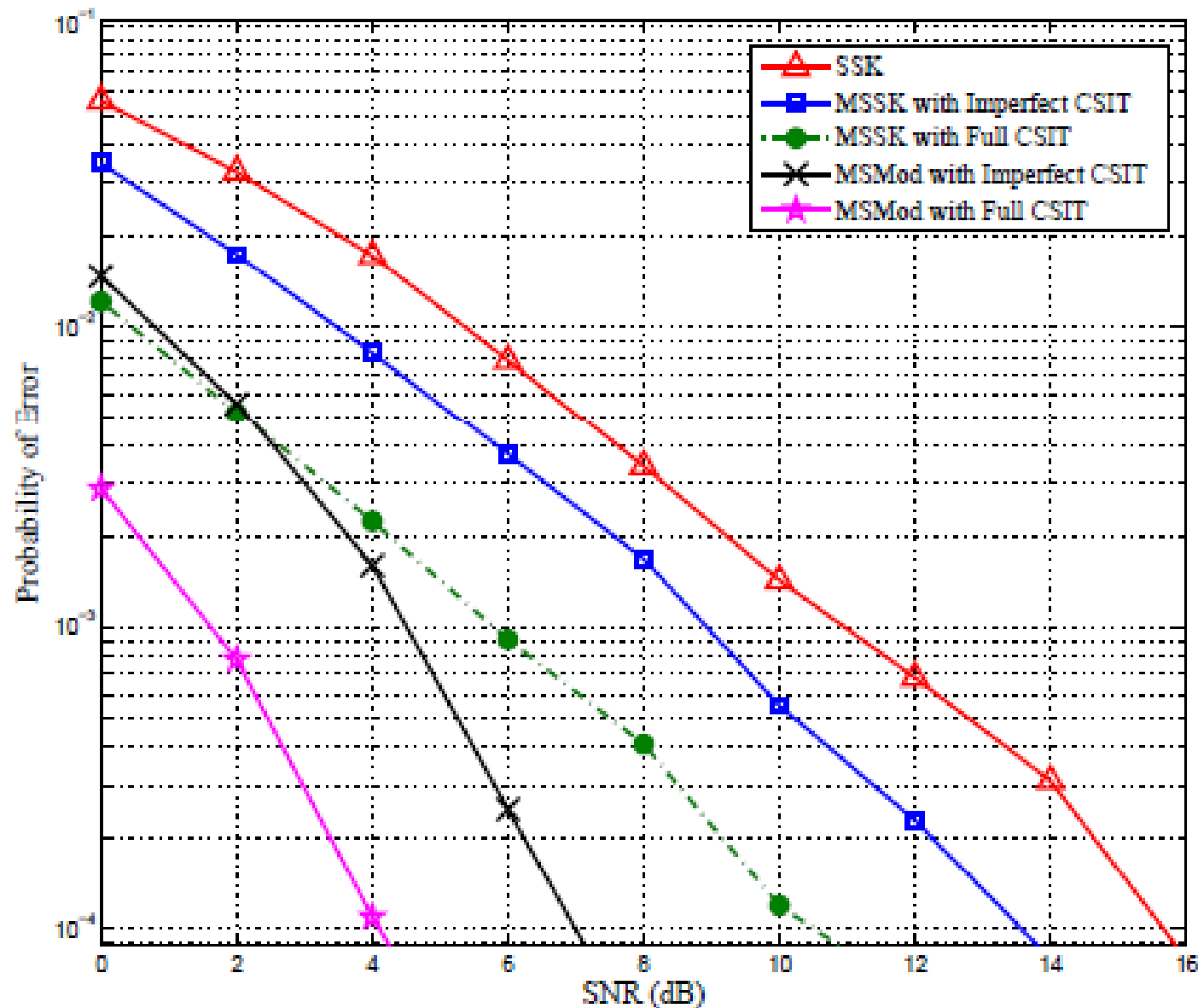


Fig. 4. SER for SSK, MSSK, and MSMod schemes with imperfect CSIT ( $N_t = 2$ ,  $N_r = 2$ ,  $\sigma_N^2 = 1$ )

## Channel State Information at the Transmitter (15/22)

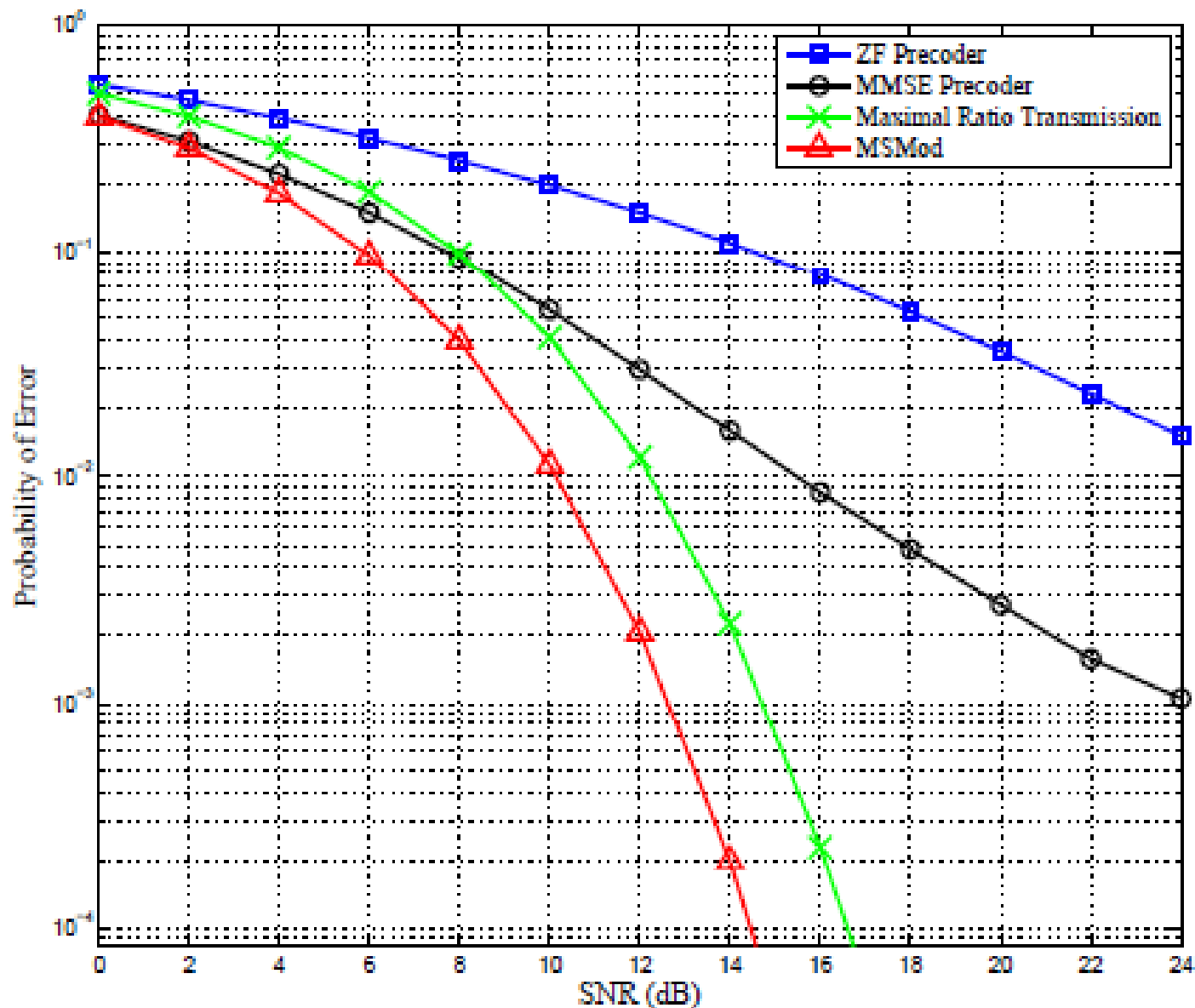


Fig. 5. Performance comparison of MSMod with other MIMO transmission schemes with CSIT ( $N_t = 4$ ,  $N_r = 4$ )



## Channel State Information at the Transmitter (16/22)

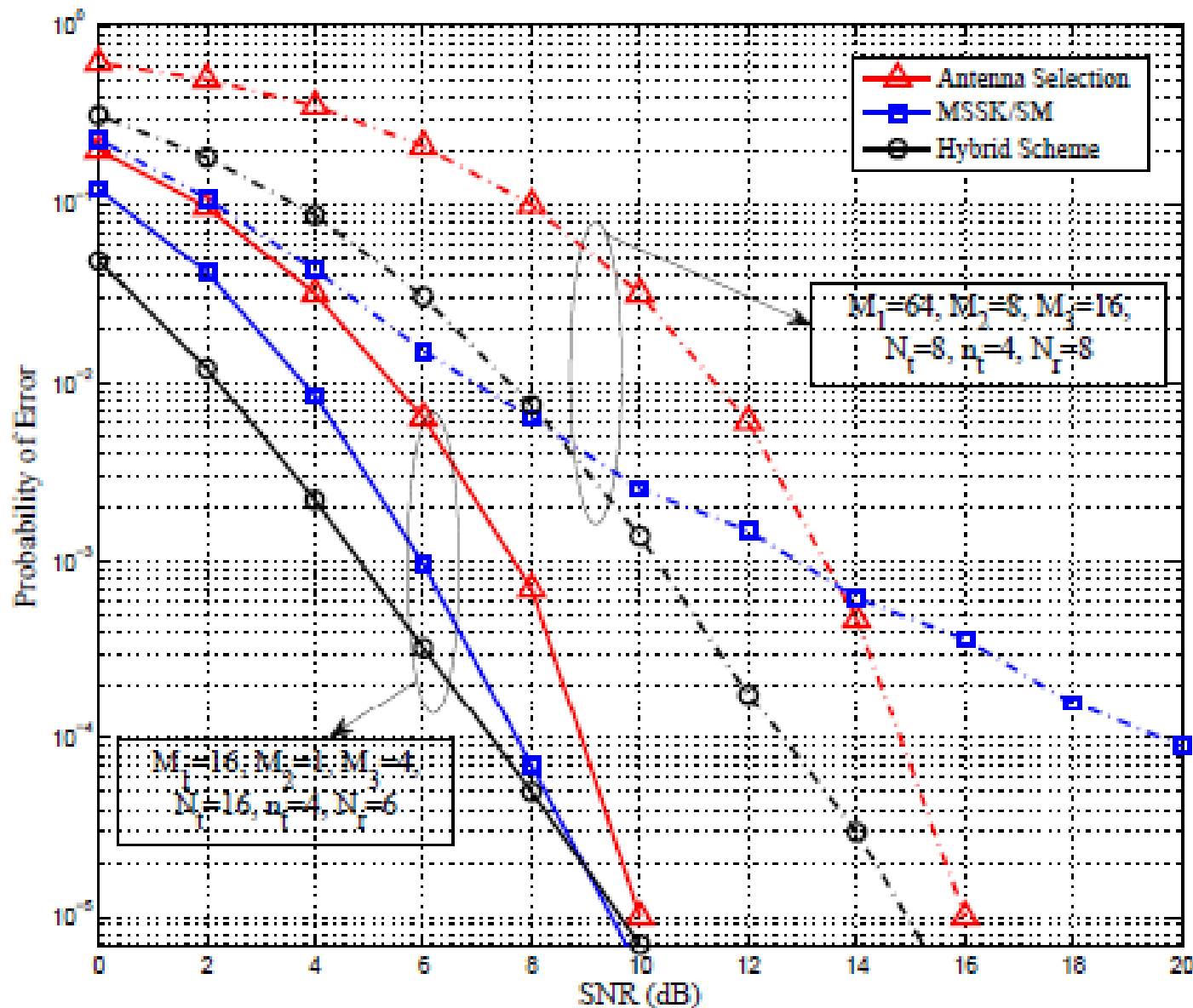
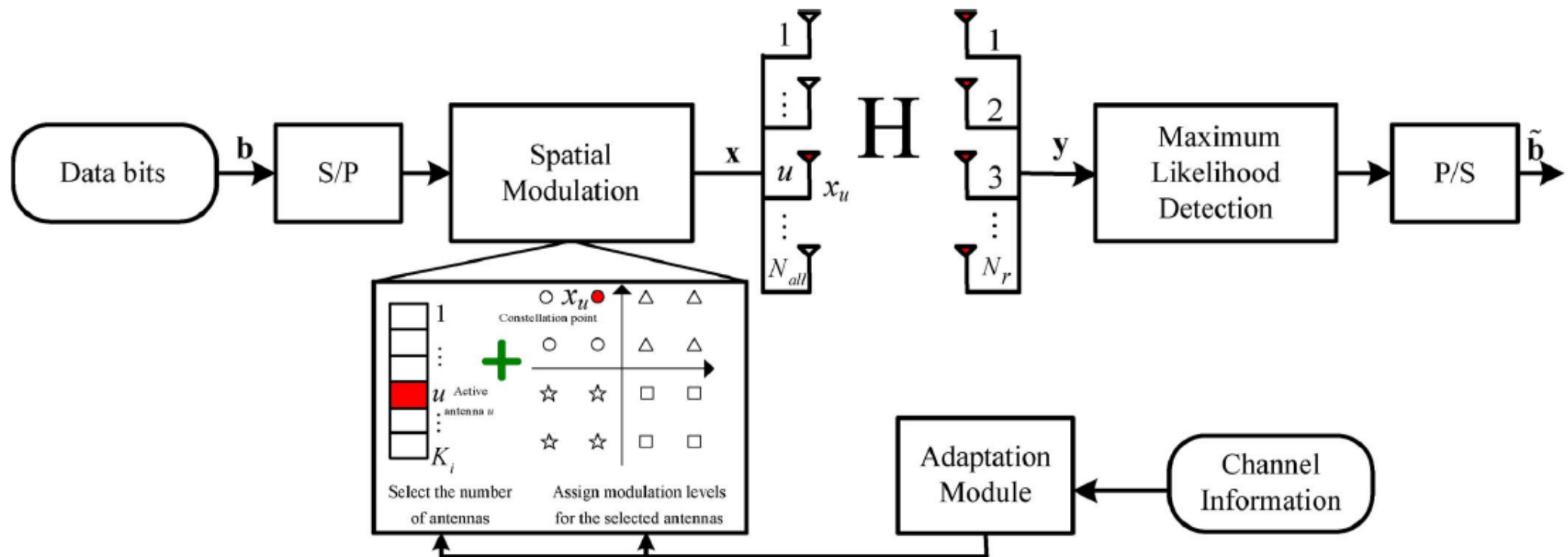


Fig. 6. Performance comparison of modified SSK/SM with antenna selection

# Channel State Information at the Transmitter (17/22)



# *Channel State Information at the Transmitter (18/22)*

## The Approach

$$P(\mathbf{x}_i \rightarrow \mathbf{x}_j | \mathbf{H}) \approx \lambda \cdot Q \left( \sqrt{\frac{1}{2N_0} d_{\min}^2(\mathbf{H})} \right)$$



$$d_{\min}(\mathbf{H}) = \max_{\substack{\mathbf{x}_i, \mathbf{x}_j \in \Lambda \\ \mathbf{x}_i \neq \mathbf{x}_j}} \|\mathbf{H}(\mathbf{x}_i - \mathbf{x}_j)\|_F$$

# Channel State Information at the Transmitter (19/22)

## The Proposed Adaptive Transmission Schemes

$$[\tilde{\mathbf{q}}, \tilde{\mathbf{d}}] = \underset{\substack{\mathbf{q}_i = \{K_i, d_i\} \\ \mathbf{d}_j = \{d_j^1, \dots, d_j^K\}}}{\arg \max} d_{\min}(\mathbf{q}_i, \mathbf{d}_j)$$

subject to

$$\left\{ \begin{array}{ll} \left\{ \mathbf{q}_i, \mathbf{d}_j \mid \log(d_i \cdot K_i) = m, \text{ and } d_j^k = d_i \right\} & \text{for AMS-SM} \\ \left\{ \mathbf{q}_i, \mathbf{d}_j \mid \log(K) + \frac{1}{K} \log \left( \prod_{k=1}^K d_j^k \right) = m, \text{ and } K \in \{K_1, \dots, K_L\} \right\} & \text{for ASM} \\ \left\{ \mathbf{q}_i, \mathbf{d}_j \mid \log(K_i) + \frac{1}{K_i} \log \left( \prod_{k=1}^{K_i} d_j^k \right) = m, \text{ and } i = 1, \dots, L \right\} & \text{for OH-SM} \\ \left\{ \mathbf{q}_i, \mathbf{d}_j \mid \log(K_{\text{AMS}}) + \frac{1}{K_{\text{AMS}}} \log \left( \prod_{k=1}^{K_{\text{AMS}}} d_j^k \right) = m, \text{ and } \tilde{\mathbf{q}}_i = \mathbf{q}_{\text{AMS}} \right\} & \text{for C-SM} \end{array} \right.$$

- ❑ **AMS-SM:** Adaptive Modulation Scheme Spatial Modulation
- ❑ **ASM:** Adaptive Spatial Modulation
- ❑ **OH-SM:** Optimal Hybrid Spatial Modulation
- ❑ **C-SM:** Concatenated Spatial Modulation

## Channel State Information at the Transmitter (20/22)

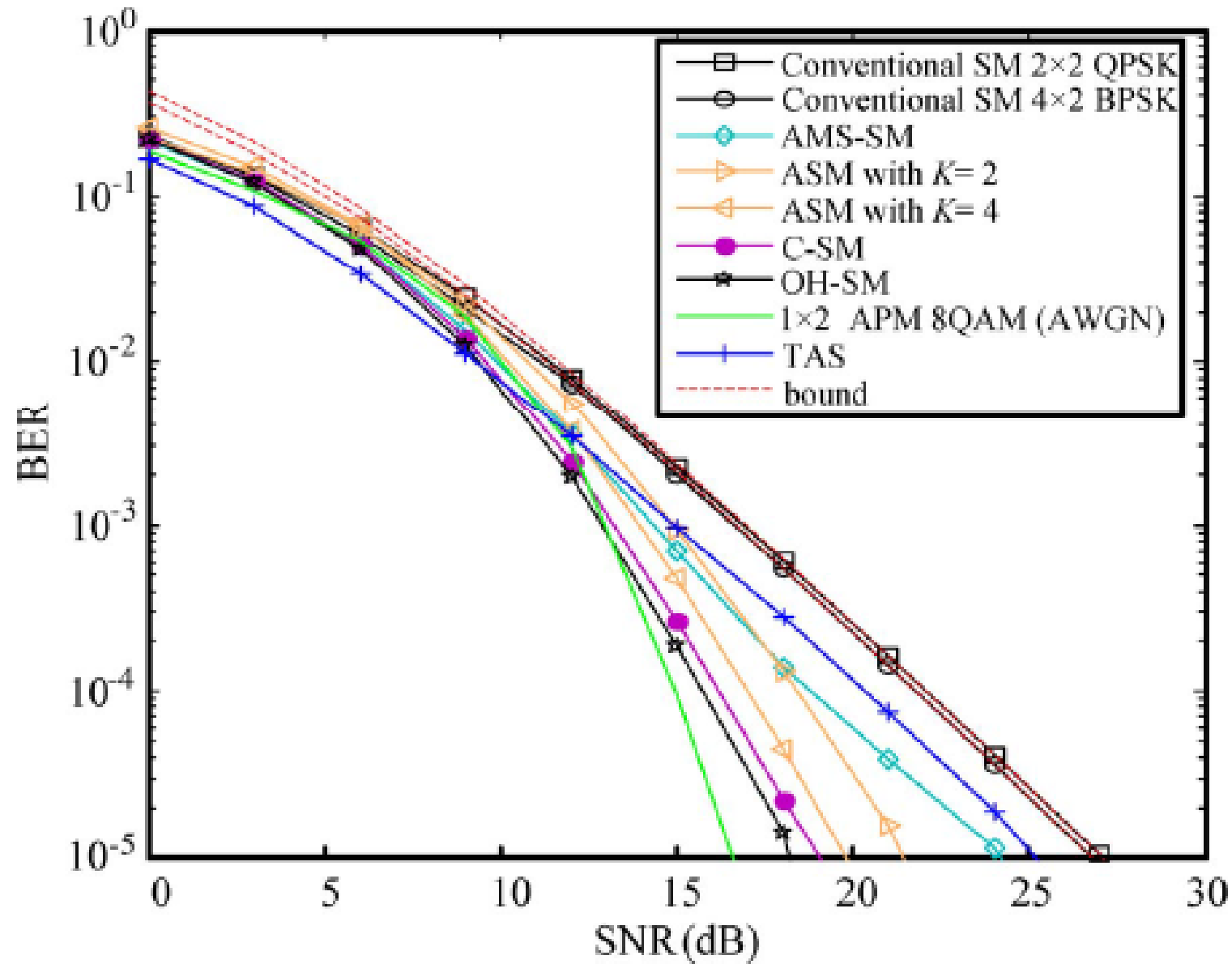


Fig. 2. BER performance at 3 bits/s/Hz for link-adaptation and conventional SM schemes under uncorrelated channel conditions.

## Channel State Information at the Transmitter (21/22)

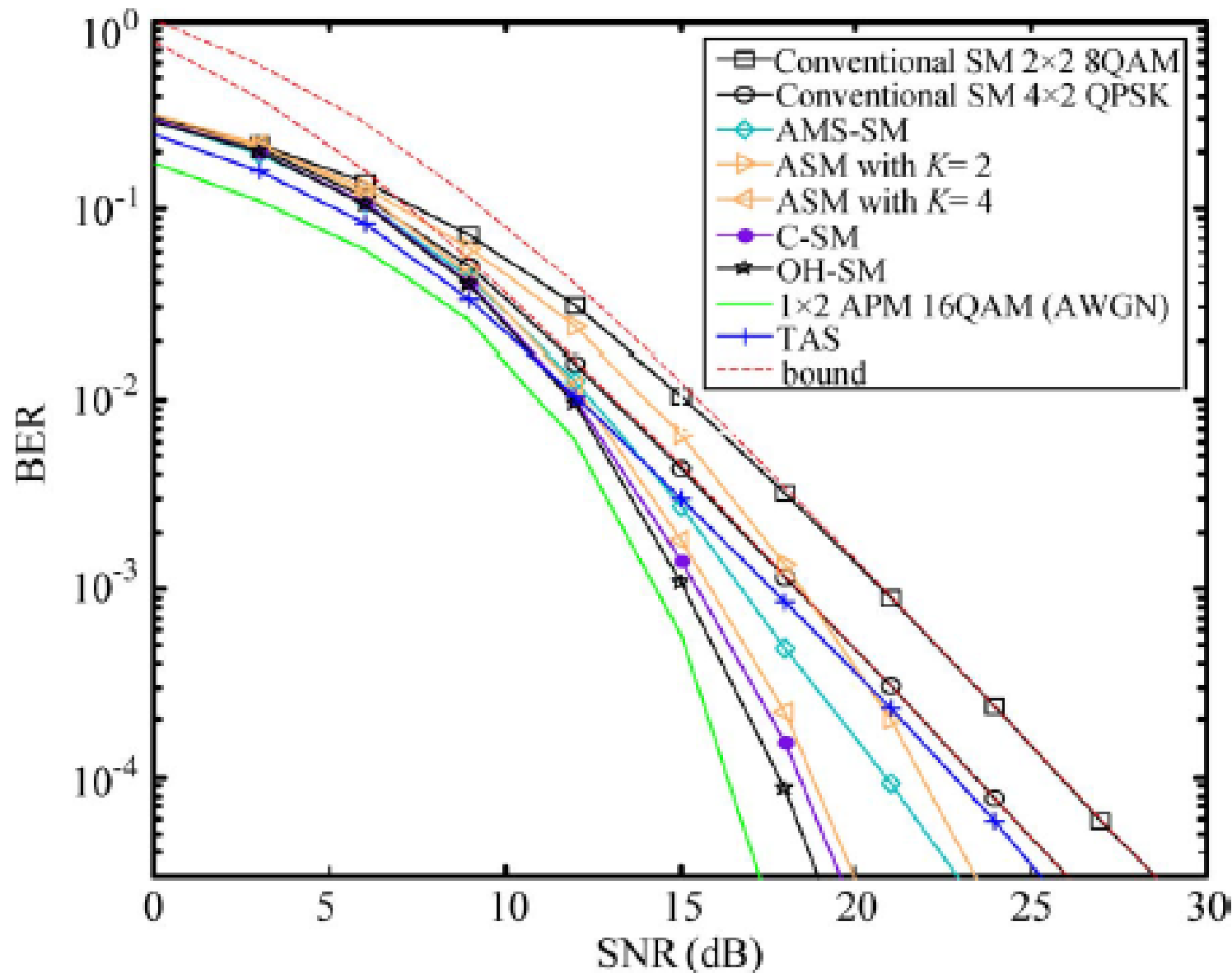


Fig. 3. BER performance at 4 bits/s/Hz for link-adaptation and conventional SM schemes under uncorrelated channel conditions.

## Channel State Information at the Transmitter (22/22)

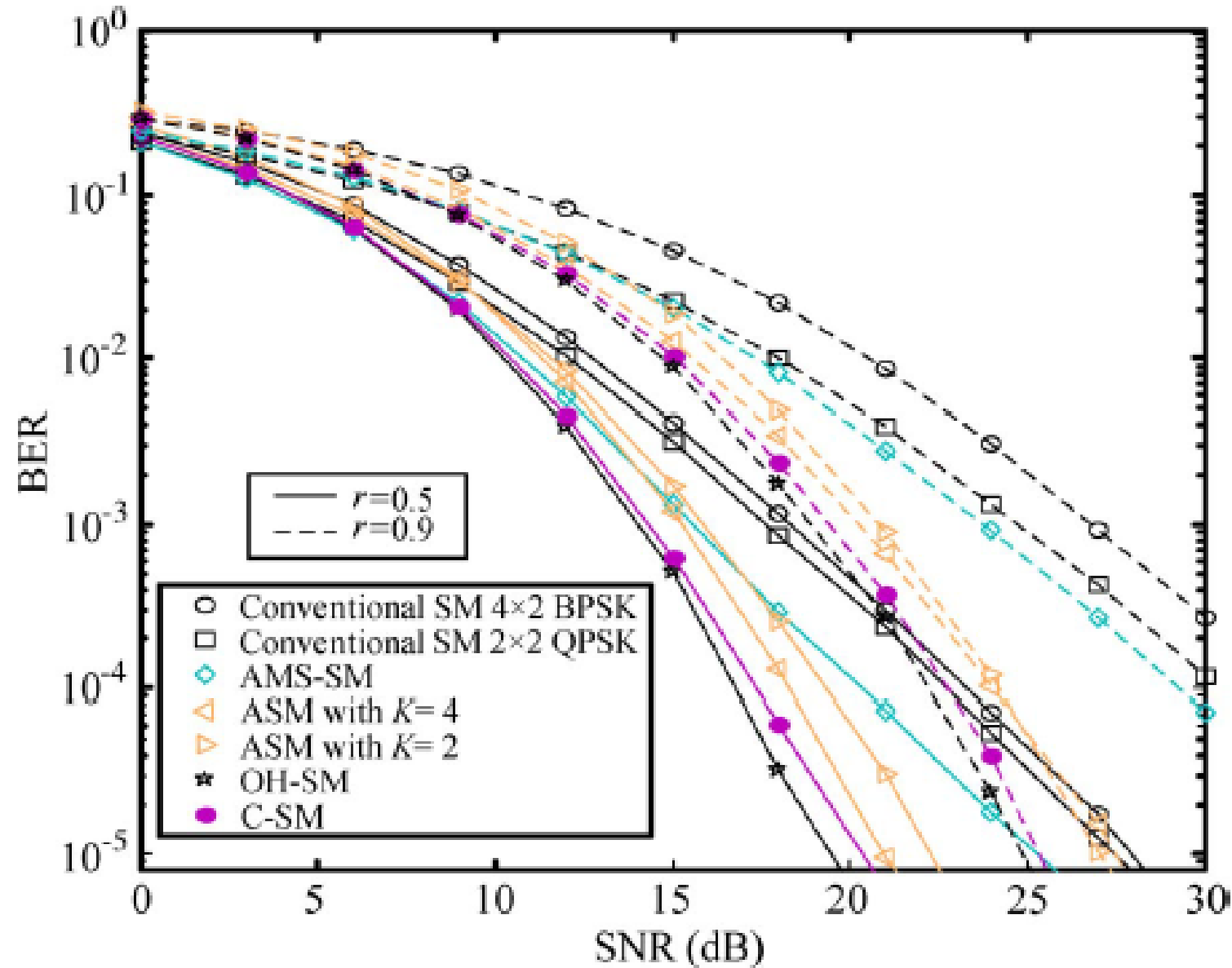


Fig. 5. BER performance at 3 bits/s/Hz for link-adaptation and conventional SM schemes under correlated channel conditions with  $r = 0.5$  and  $0.9$ .

# *Outline*

---

1. Introduction and Motivation behind SM-MIMO
2. History of SM Research and Research Groups Working on SM
3. Transmitter Design – Encoding
4. Receiver Design – Demodulation
5. Error Performance (Numerical Results and Main Trends)
6. Achievable Capacity
7. Channel State Information at the Transmitter
8. **Imperfect Channel State Information at the Receiver**
9. Multiple Access Interference
10. Energy Efficiency
11. Transmit-Diversity for SM
12. Spatially-Modulated Space-Time-Coded MIMO
13. Relay-Aided SM
14. SM in Heterogeneous Cellular Networks
15. SM for Visible Light Communications
16. Experimental Evaluation of SM
17. The Road Ahead – Open Research Challenges/Opportunities
18. Implementation Challenges of SM-MIMO



## *Imperfect Channel State Information at the Receiver (1/23)*

The working principle of SM/SSK is based on the following facts:

1. The wireless environment **naturally** modulates the transmitted signal
2. Each transmit-receive wireless link has a **different** channel
3. The receiver employs the **a priori** channel knowledge to detect the transmitted signal
4. Thus, part of the information is conveyed by the Channel Impulse Response (CIR), i.e., the channel/spatial signature

**How Much Important is  
Channel State Information for SSK/SM Modulation?**

## *Imperfect Channel State Information at the Receiver (2/23)*

### □ Perfect CSI (channel gains and phases): F–CSI (SSK)

$$\hat{m} = \arg \max_{\{m_i\}_{i=1}^{N_t}} \{D_i\} \quad D_i = \operatorname{Re} \left\{ \int_{T_m} r(t) \bar{s}_i^*(t) dt \right\} - \frac{1}{2} \int_{T_m} \bar{s}_i(t) \bar{s}_i^*(t) dt$$

### □ Partial CSI (channel gains): P–CSI (SSK)

$$\hat{m} = \arg \max_{\{m_i\}_{i=1}^{N_t}} \{ \ln [D_i] \} \quad \bar{D}_i = \ln [D_i] = \begin{cases} \ln \left[ I_0 \left( \frac{\sqrt{E_m} \beta_i}{N_0} |\bar{r}| \right) \right] - \frac{E_m \beta_i^2}{2N_0} \\ \sqrt{E_m} \beta_i |\bar{r}| - \frac{E_m \beta_i^2}{2} \end{cases}$$

## *Imperfect Channel State Information at the Receiver (3/23)*

$$\left\{ \begin{array}{l} r(t) = \sqrt{E_m} \beta_l \exp(j\varphi_l) w(t) + n(t) \\ \bar{r} = \int_{T_m} r(t) w^*(t) dt \end{array} \right\} \left\{ \begin{array}{l} \hat{m} = \arg \max_{\{m_i\}_{i=1}^{N_t}} \{ \ln [D_i] \} \\ \bar{D}_i = \ln [D_i] = \sqrt{E_m} \beta_i |\bar{r}| - \frac{E_m \beta_i^2}{2} \end{array} \right.$$



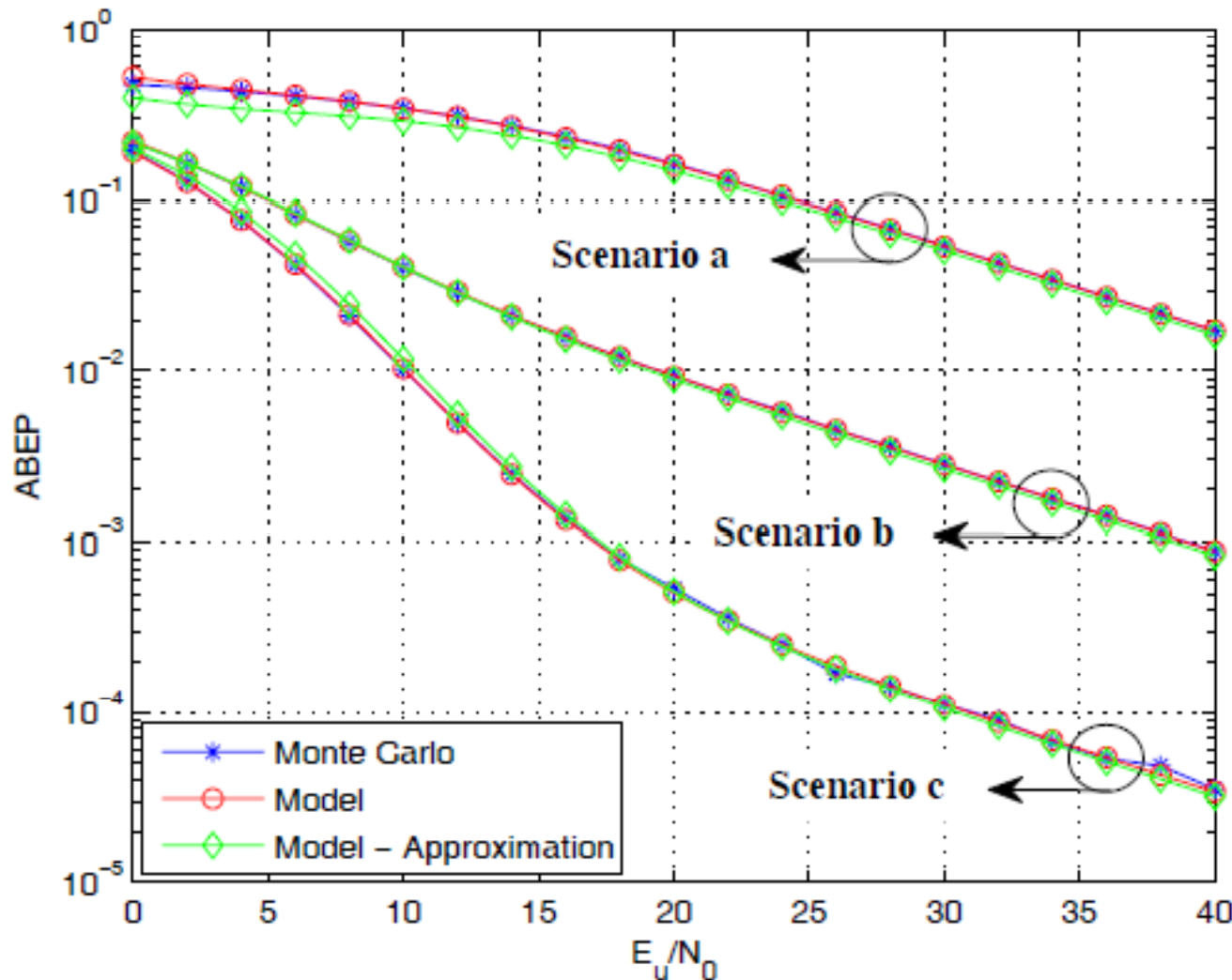
$$\left\{ \begin{array}{l} \text{ABEP} \leq \frac{2}{N_t \log_2(N_t)} \sum_{i_1=1}^{N_t} \sum_{i_2=i_1+1}^{N_t} N(i_1, i_2) \text{APEP}(\text{TX}_{i_2} \rightarrow \text{TX}_{i_1}) \\ \text{APEP} = \mathbb{E}_{h_{i_1}, h_{i_2}} \{ P_E(1, 2) \} \end{array} \right.$$



$$\begin{aligned} P_E(1, 2) = & \left[ \frac{1}{2} - \frac{1}{2} Q \left( \frac{\sqrt{E_m} \beta_1}{\sqrt{N_0}}, \frac{\sqrt{E_m} (\beta_1 + \beta_2)}{2\sqrt{N_0}} \right) + \frac{1}{2} Q \left( \frac{\sqrt{E_m} \beta_2}{\sqrt{N_0}}, \frac{\sqrt{E_m} (\beta_1 + \beta_2)}{2\sqrt{N_0}} \right) \right] \cdot \Pr \{ \beta_1 \geq \beta_2 \} \\ & + \left[ \frac{1}{2} - \frac{1}{2} Q \left( \frac{\sqrt{E_m} \beta_2}{\sqrt{N_0}}, \frac{\sqrt{E_m} (\beta_1 + \beta_2)}{2\sqrt{N_0}} \right) + \frac{1}{2} Q \left( \frac{\sqrt{E_m} \beta_1}{\sqrt{N_0}}, \frac{\sqrt{E_m} (\beta_1 + \beta_2)}{2\sqrt{N_0}} \right) \right] \cdot \Pr \{ \beta_1 < \beta_2 \} \end{aligned}$$

# Imperfect Channel State Information at the Receiver (4/23)

## 2x1 MIMO, Correlated ( $\rho=0.64$ ) Nakagami-m Fading



Scenario a:

$$\Omega_1=1, \Omega_2=1, m_1=2, m_2=5$$

Scenario b:

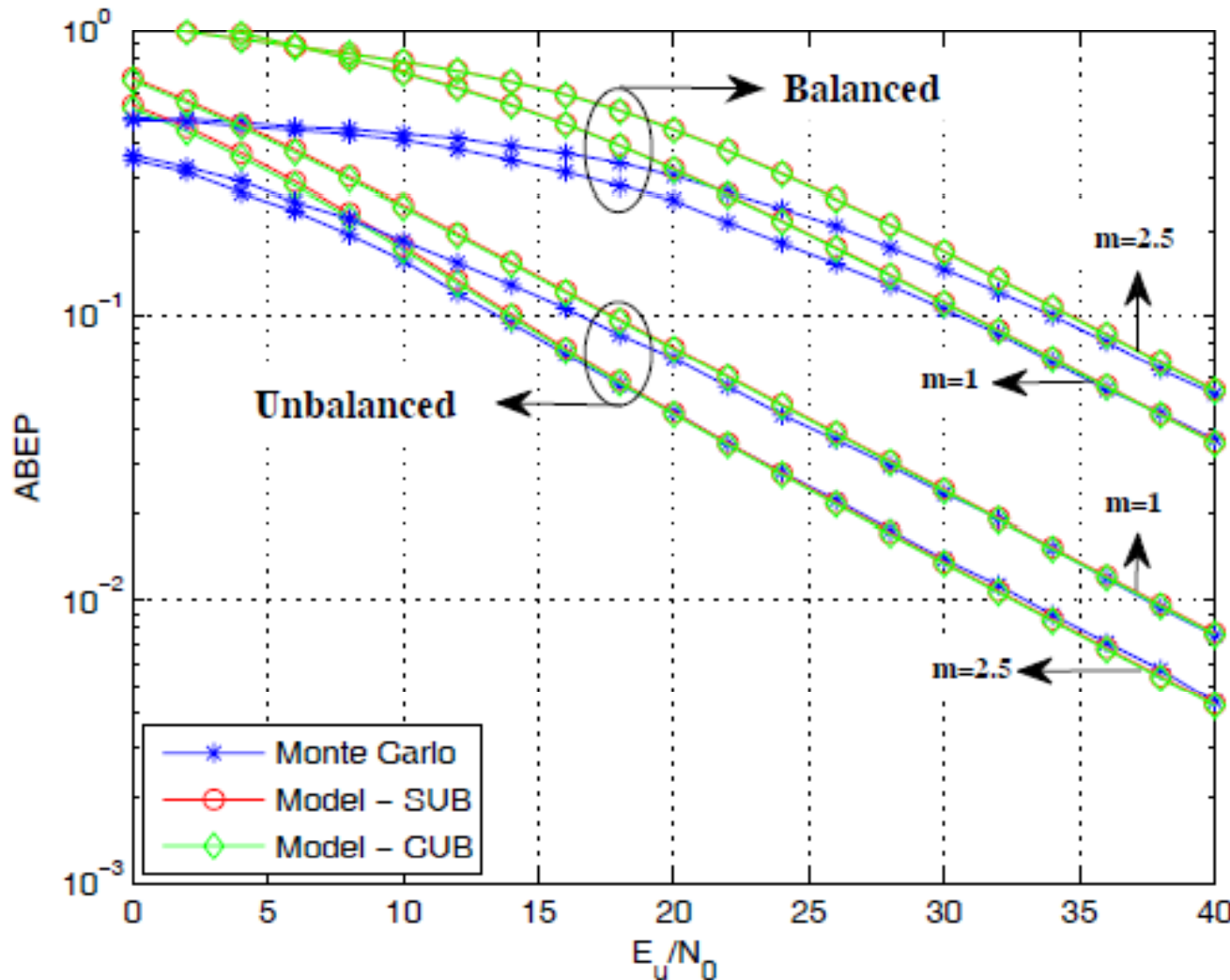
$$\Omega_1=10, \Omega_2=1, m_1=2, m_2=5$$

Scenario c:

$$\Omega_1=10, \Omega_2=1, m_1=5, m_2=2$$

# Imperfect Channel State Information at the Receiver (5/23)

## 4x1 MIMO, Correlated (exponential) Nakagami-m Fading



Balanced:

$$\{\Omega_i\}_{i=1,\dots,4} = 1$$

Unbalanced:

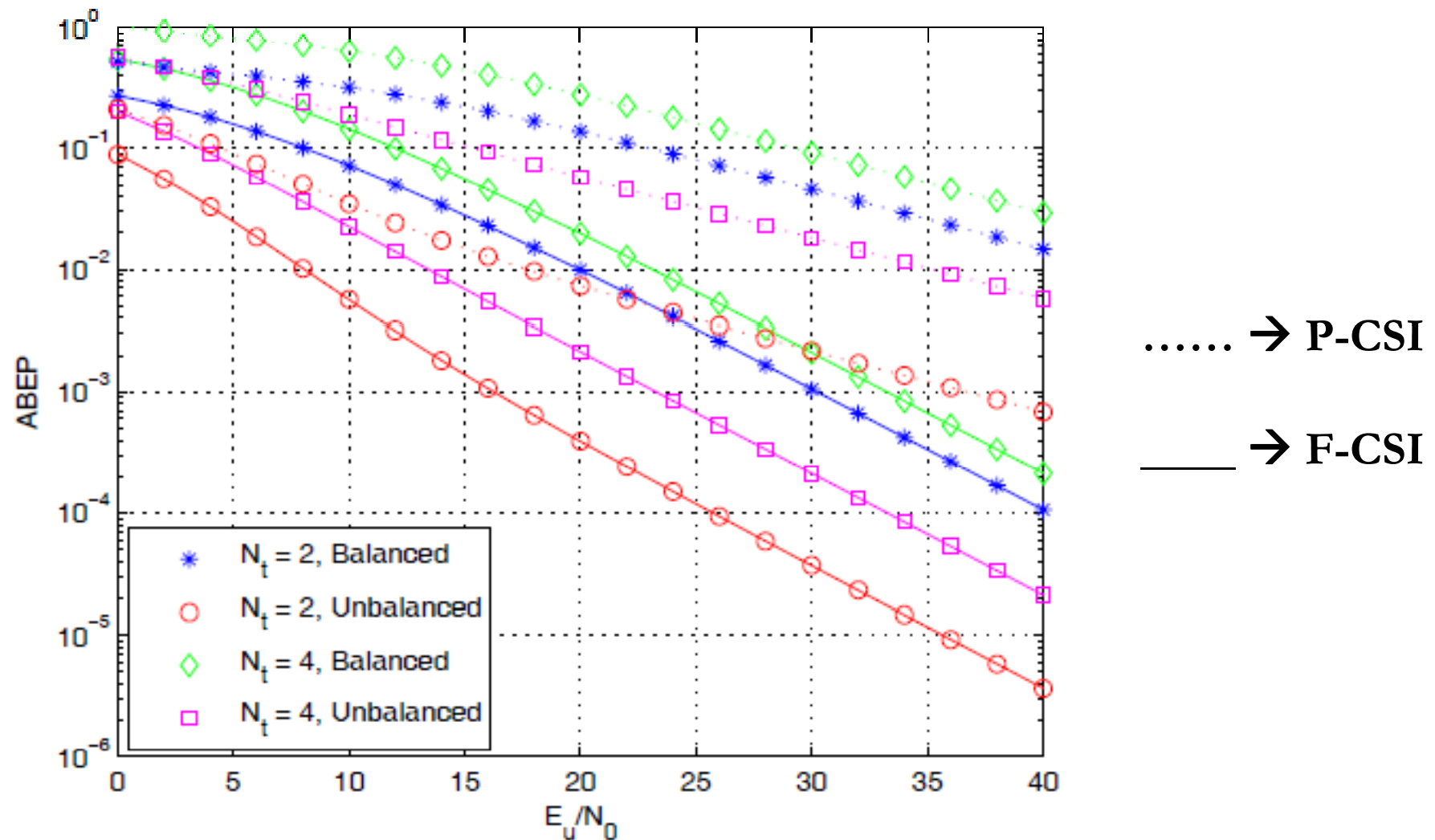
$$\Omega_1 = 1, \{\Omega_i\}_{i=2,\dots,4} = 4i-4$$

Correlation:

$$\rho_{i,j} = \exp(-d_0 |i-j|)$$
$$d_0 = 0.22$$

# *Imperfect Channel State Information at the Receiver (6/23)*

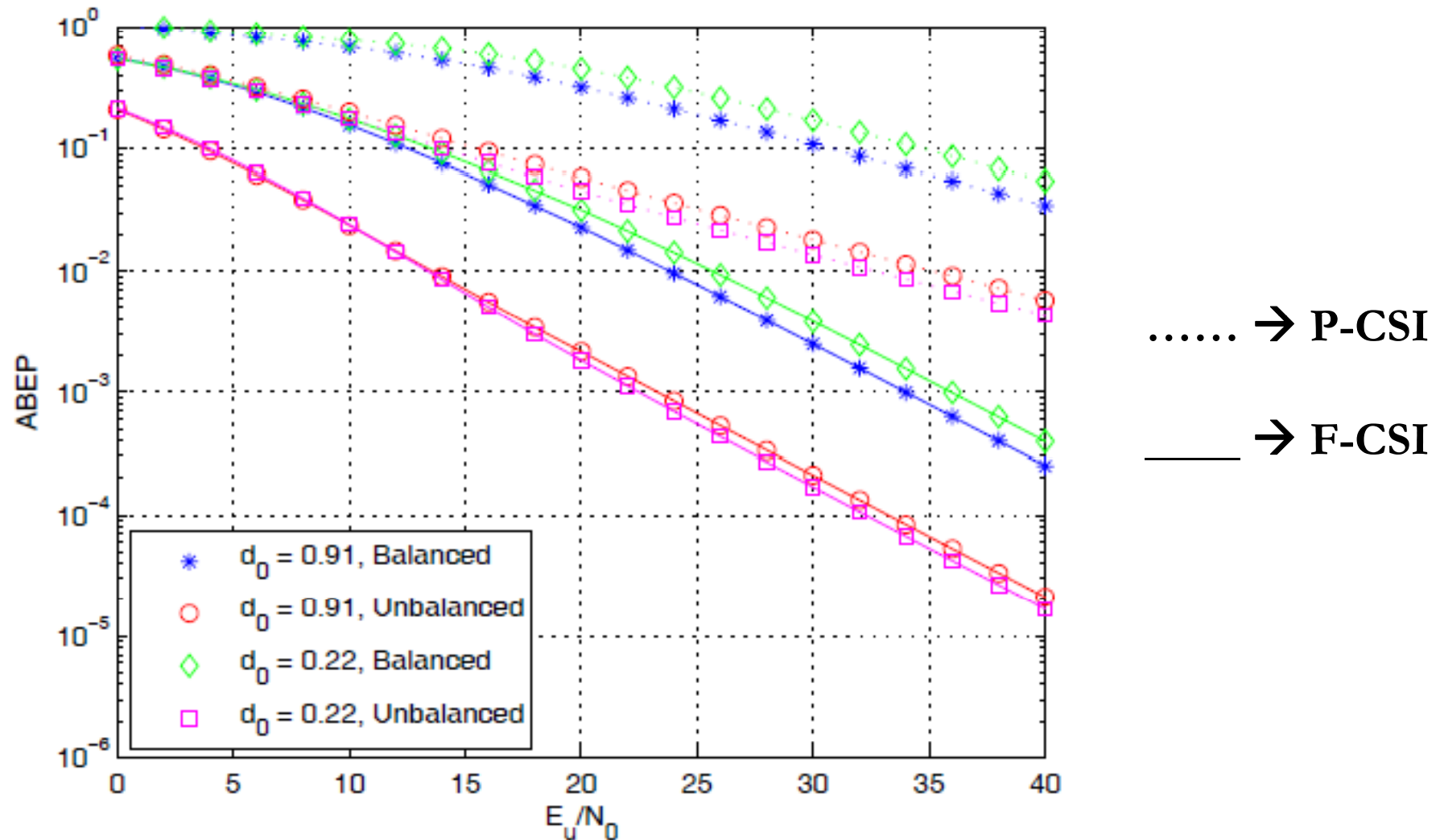
## 2x1 MIMO, Uncorrelated Nakagami-m Fading



M. Di Renzo and H. Haas, “Space Shift Keying (SSK) Modulation With Partial Channel State Information: Optimal Detector and Performance Analysis Over Fading Channels”, *IEEE Trans. Commun.*, Vol. 58, No. 11, pp. 3196-3210, Nov. 2010.

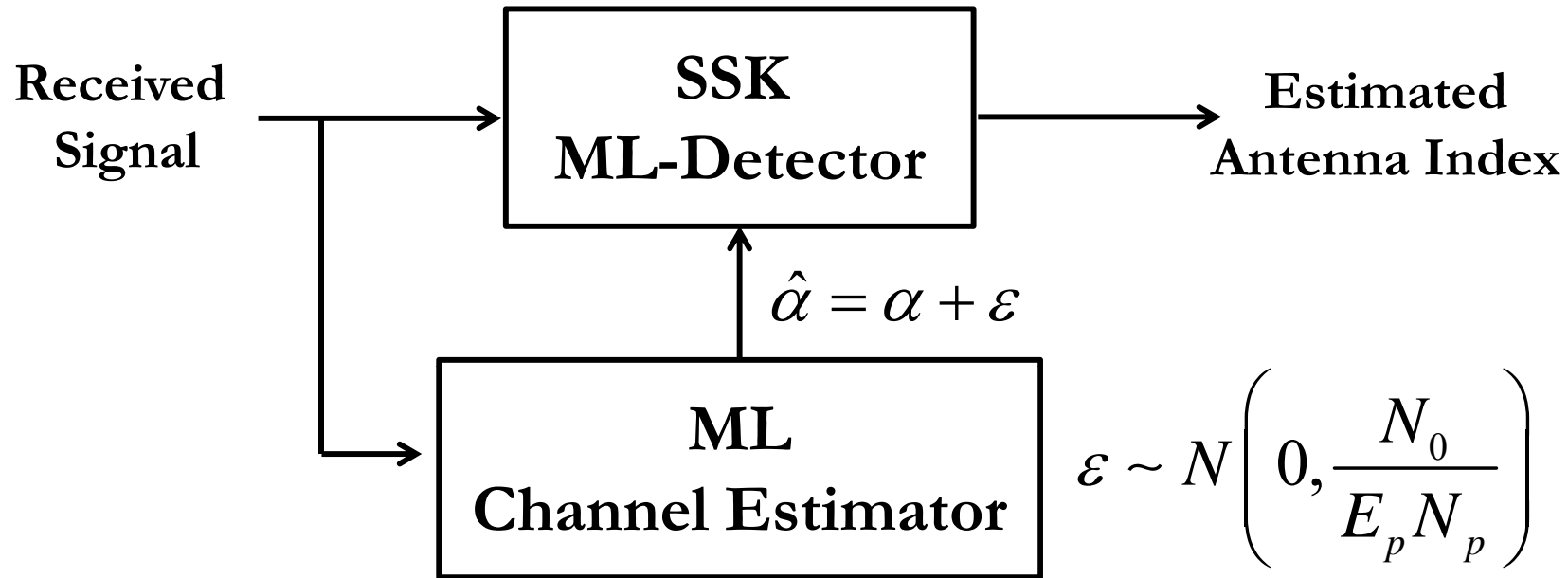
# *Imperfect Channel State Information at the Receiver (7/23)*

## 4x1 MIMO, Correlated (exponential) Nakagami-m Fading



# Imperfect Channel State Information at the Receiver (8/23)

## SSK with Mismatched Decoder



$$\hat{m} = \arg \min_{m_t \text{ for } t=1,2,\dots,N_t} \left\{ \hat{D}_{m_q} (m_t) \right\}$$

$$= \arg \min_{m_t \text{ for } t=1,2,\dots,N_t} \left\{ \sum_{r=1}^{N_r} \left\{ \left| \frac{\tilde{\eta}_{0,r}}{\sqrt{N_0}} - \left[ \sqrt{\frac{E_m}{N_0}} (\alpha_{t,r} - \alpha_{q,r}) + \sqrt{\frac{E_m}{N_0}} \varepsilon_{t,r} \right] \right|^2 \right\} \right\}$$



# *Imperfect Channel State Information at the Receiver (9/23)*

## **ABEP**

$$\text{ABEP} \leq \frac{1}{N_t \log_2(N_t)} \sum_{q=1}^{N_t} \sum_{t=1}^{N_t} \left[ N_H(t, q) \left( \frac{1}{2} - \frac{1}{\pi} \int_0^{+\infty} \left[ \frac{\text{Im} \{ \Upsilon(\nu) M_{\gamma_{t,q}}(\Delta(\nu)) \}}{\nu} \right] d\nu \right) \right]$$

$$M_{\gamma_{t,q}}(s) = \mathbb{E} \left\{ \exp(-s \gamma_{t,q}) \right\} \quad \gamma_{t,q} = \gamma(\mathbf{a}) = \sum_{r=1}^{N_r} |\alpha_{q,r} - \alpha_{t,r}|^2$$

## **Methodology for computation:**

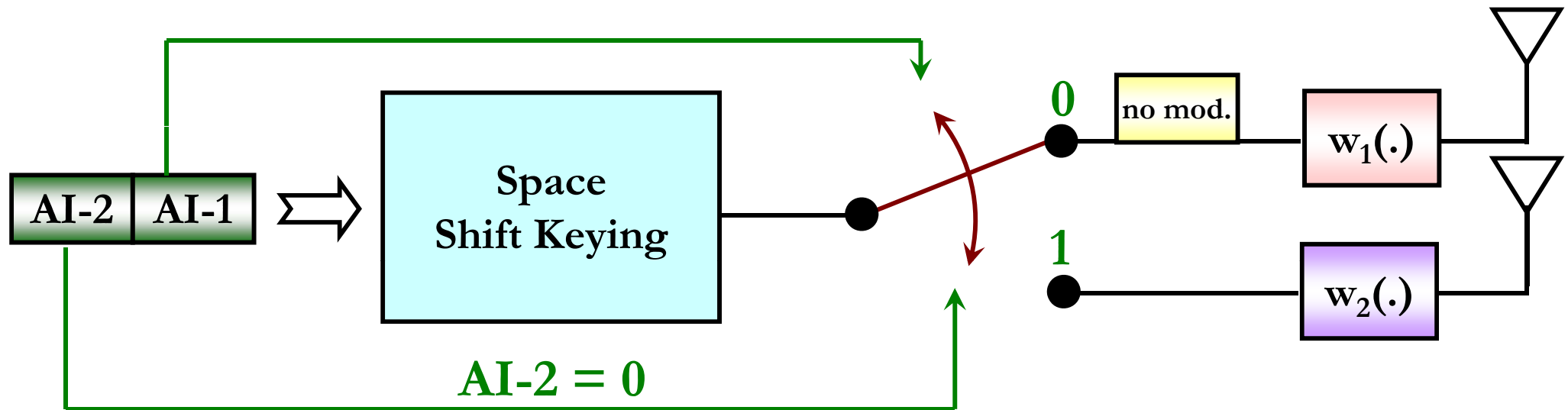
1. Union bound: the ABEP can be obtained from the APEP

$$\text{APEP}(m_q \rightarrow m_t) = \mathbb{E} \left\{ \Pr \left\{ \hat{D}_{m_q}(m_t) < \hat{D}_{m_q}(m_q) \right\} \right\} = \Pr \left\{ \hat{D}_{m_q}(m_t) - \hat{D}_{m_q}(m_q) < 0 \right\}$$

2. The (difference) decision variable is a quadratic-form in complex Gaussian RVs (when conditioning upon fading channel statistics)
3. The PEP is obtained by using the Gil-Pelaez inversion theorem

# Imperfect Channel State Information at the Receiver (10/23)

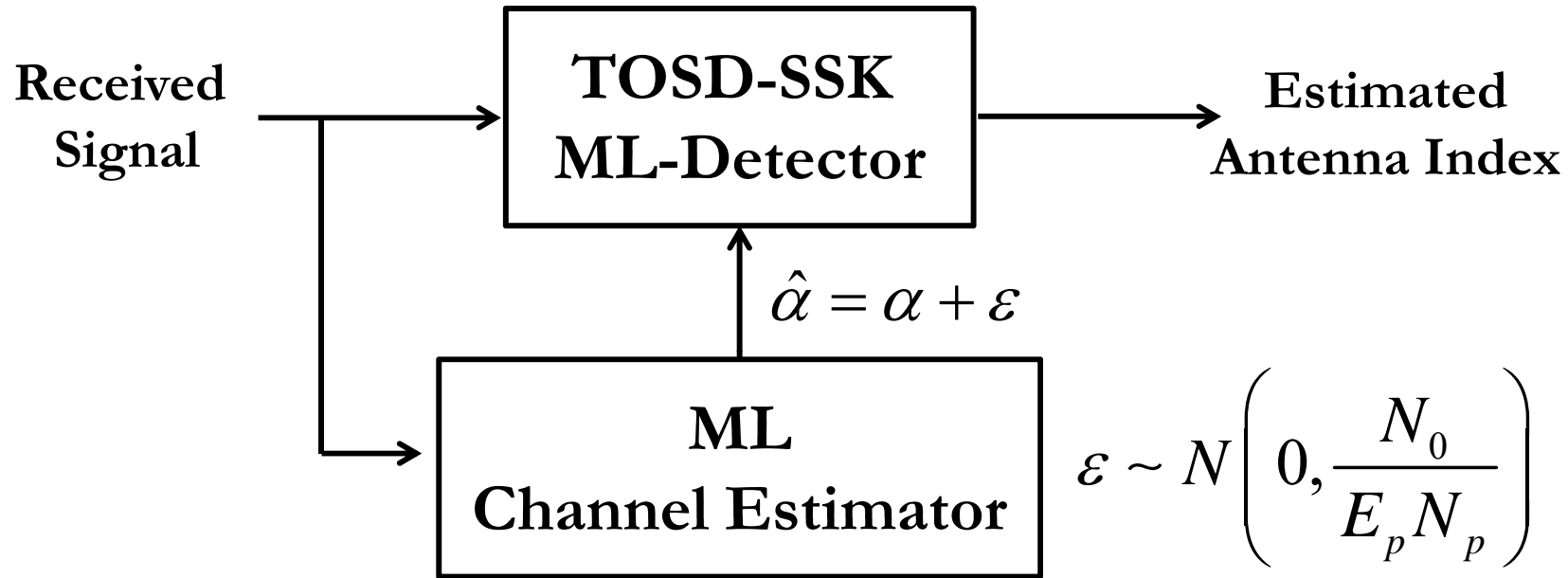
## Time-Orthogonal Signal Design assisted SSK (TOSD-SSK)



- ◆ If  $w_1(t) = w_2(t) \rightarrow \text{Diversity} = N_r$  (conventional SSK)
- ◆ If  $w_1(t)$  is “time-orthogonal” to  $w_2(t) \rightarrow \text{Diversity} = 2N_r$  (**TOSD-SSK**)
- ◆ This is true for any  $N_t$  with no bandwidth expansion and with a single active transmit-antenna at any time-instance

# Imperfect Channel State Information at the Receiver (11/23)

## TOSD-SSK with Mismatched Decoder



$$\begin{aligned}\hat{m} &= \arg \min_{m_t \text{ for } t=1,2,\dots,N_t} \left\{ \hat{D}_{m_q}(m_t) \right\} \\ &= \arg \min_{m_t \text{ for } t=1,2,\dots,N_t} \left\{ \sum_{r=1}^{N_r} \text{Re} \left\{ \alpha_{q,r} \hat{\alpha}_{t,r}^* E_m \delta_{t,q} + \hat{\alpha}_{t,r}^* \sqrt{E_m} \tilde{\eta}_{t,r} \right\} - \frac{E_m}{2} \sum_{r=1}^{N_r} |\hat{\alpha}_{t,r}|^2 \right\}\end{aligned}$$

# Imperfect Channel State Information at the Receiver (12/23)

## ABEP

$$\text{ABEP} \leq \frac{1}{N_t \log_2(N_t)} \sum_{q=1}^{N_t} \sum_{t=1}^{N_t} \left[ N_H(t, q) \left( \frac{1}{2} - \frac{1}{\pi} \int_0^{+\infty} \left[ \frac{\text{Im} \left\{ \Upsilon_q(\nu) \Upsilon_t(-\nu) M_{\gamma_{t,q}^{(\Delta)}(\nu)}(1) \right\}}{\nu} \right] d\nu \right) \right]$$

$$M_{\gamma_{t,q}^{(\Delta)}(\nu)}(s) = \mathbb{E} \left\{ \exp \left( -s \gamma_{t,q}^{(\Delta)}(\nu) \right) \right\} \quad \gamma_{t,q}^{(\Delta)}(\nu) = \Delta_q(\nu) \sum_{r=1}^{N_r} |\alpha_{q,r}|^2 + \Delta_t(-\nu) \sum_{r=1}^{N_r} |\alpha_{t,r}|^2$$

## Methodology for computation:

1. Union bound: the ABEP can be obtained from the APEP

$$\text{APEP}(m_q \rightarrow m_t) = \mathbb{E} \left\{ \Pr \left\{ \hat{D}_{m_q}(m_t) < \hat{D}_{m_q}(m_q) \right\} \right\} = \Pr \left\{ \hat{D}_{m_q}(m_t) - \hat{D}_{m_q}(m_q) < 0 \right\}$$

2. The (difference) decision variable is the **difference of two independent** quadratic-forms in complex Gaussian RVs (when conditioning upon fading channel statistics)
3. The PEP is obtained by using the Gil-Pelaez inversion theorem

# *Imperfect Channel State Information at the Receiver (13/23)*

## **Diversity Analysis (i.i.d. Rayleigh Fading)**

### **SSK**

$$\text{ABEP} \leq \frac{N_t}{4} - \frac{N_t}{2\pi} \int_0^{+\infty} \left[ \text{Im} \left\{ \frac{\Upsilon(\nu)}{\nu} \frac{1}{(1 - 2\Omega_0 \Delta(\nu))^{N_r}} \right\} \right] d\nu$$

### **TOSD-SSK**

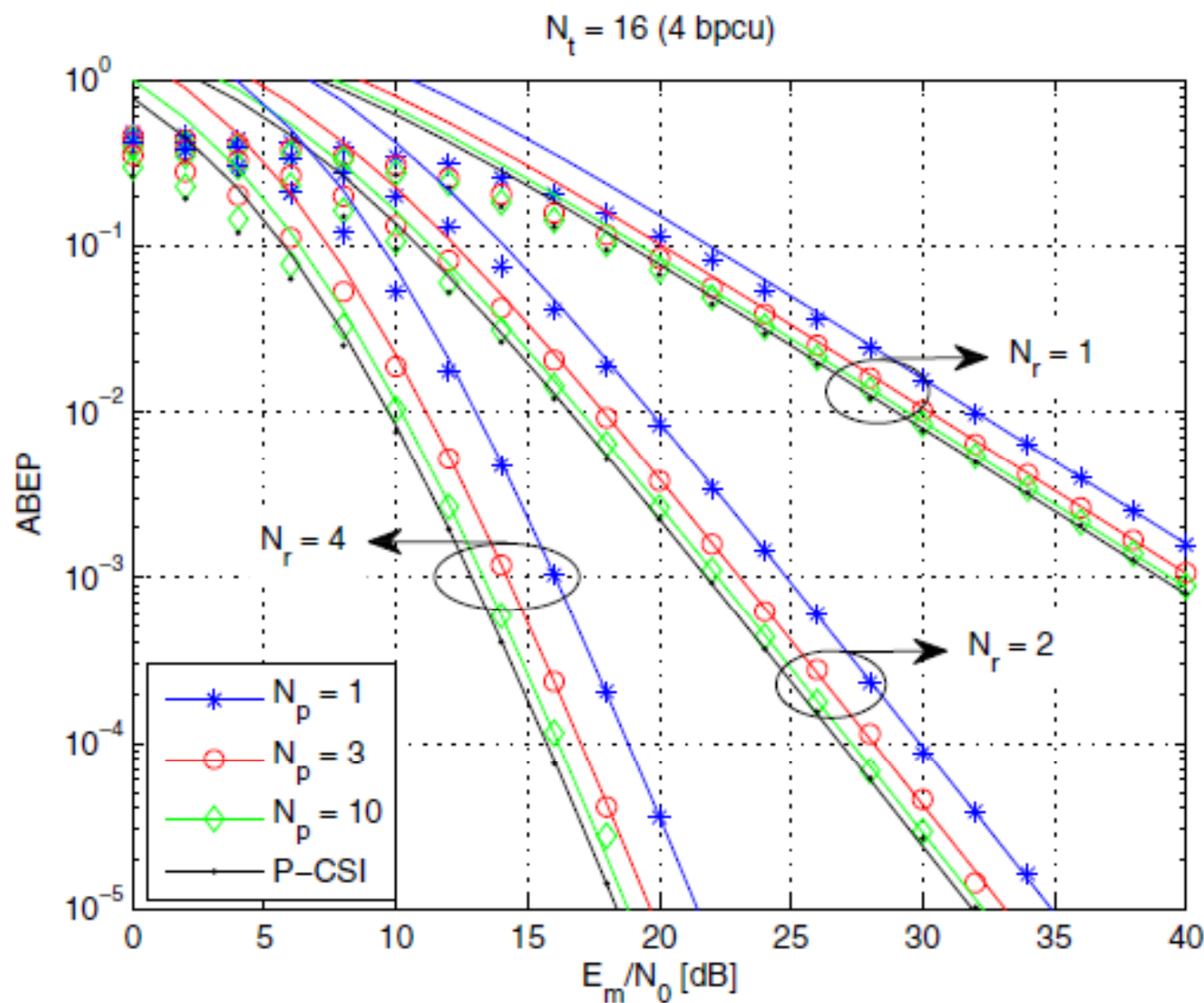
$$\text{ABEP} \leq \frac{N_t}{4} - \frac{N_t}{2\pi} \int_0^{+\infty} \left[ \text{Im} \left\{ \frac{\Upsilon_q(\nu) \Upsilon_t(-\nu)}{\nu} \frac{1}{(1 - \Omega_0 \Delta_q(\nu))^{N_r} (1 - \Omega_0 \Delta_t(-\nu))^{N_r}} \right\} \right] d\nu$$

### **With channel estimation errors:**

1. Diversity order of SSK is:  $N_r$
2. Diversity order of TOSD-SSK is:  $2N_r$

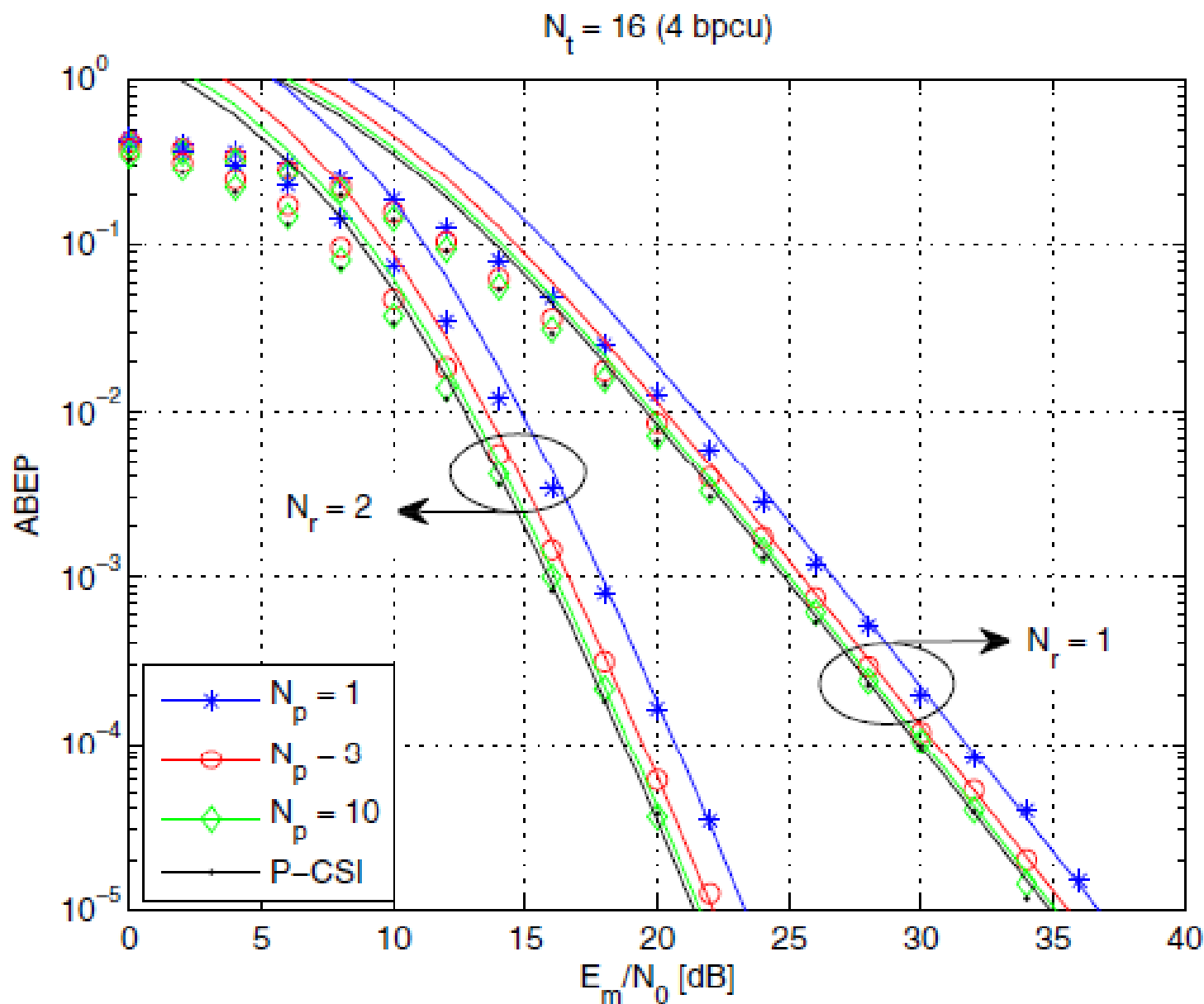
# *Imperfect Channel State Information at the Receiver (14/23)*

## Numerical Results (SSK)



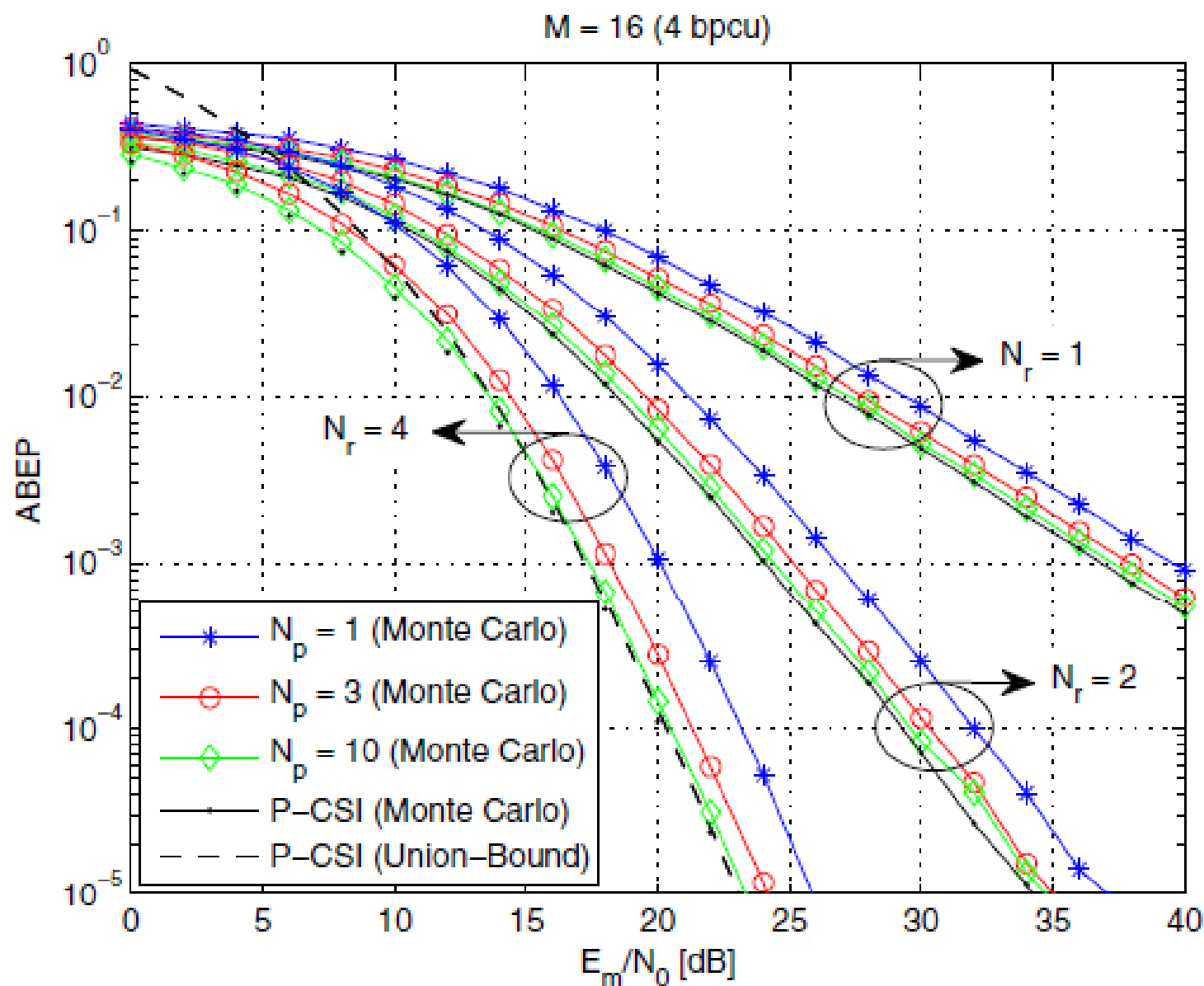
# Imperfect Channel State Information at the Receiver (15/23)

## Numerical Results (TOSD-SSK)



# Imperfect Channel State Information at the Receiver (16/23)

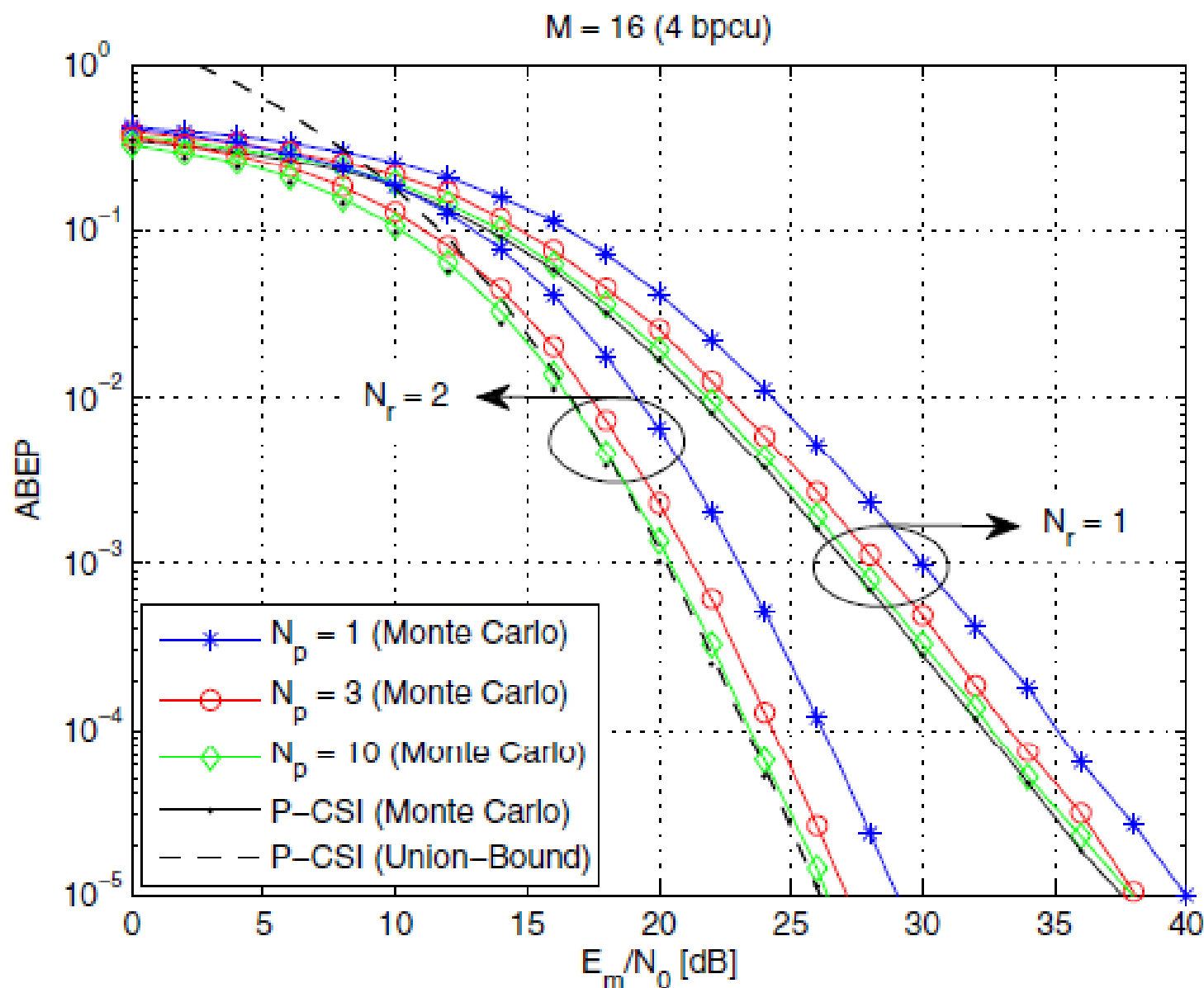
## Single-Antenna MQAM





# Imperfect Channel State Information at the Receiver (17/23)

## Alamouti MQAM



## Imperfect Channel State Information at the Receiver (18/23)

### SSK vs. Single-Antenna MQAM ( $N_r=1$ / $N_r=2$ / $N_r=4$ )

SSK				
Rate	$N_p = 1$	$N_p = 3$	$N_p = 10$	P – CSI
1 bpcu	22.9 / 25.3 / 16.2	21.1 / 23.5 / 14.5	20.3 / 22.7 / 13.6	19.9 / 22.3 / 13.2
2 bpcu	26 / 26.8 / 17	24.2 / 25.1 / 15.4	23.4 / 24.3 / 14.5	23 / 23.8 / 14
3 bpcu	29 / 28.4 / 17.9	27.3 / 26.6 / 16.2	26.4 / 25.8 / 15.3	26 / 25.4 / 14.9
4 bpcu	32 / 29.9 / 18.7	30.3 / 28.1 / 17	29.5 / 27.3 / 16.2	29 / 26.9 / 15.7
Single-Antenna QAM				
Rate	$N_p = 1$	$N_p = 3$	$N_p = 10$	P – CSI
1 bpcu	19.8 / 22.3 / 13.1	18.2 / 20.6 / 11.5	17.2 / 19.7 / 10.6	16.8 / 19.3 / 10.1
2 bpcu	22.7 / 25.2 / 16.2	21.1 / 23.5 / 14.5	20.3 / 22.7 / 13.6	19.9 / 22.2 / 13.2
3 bpcu	27.5 / 29.9 / 21.1	25.6 / 28 / 19.1	24.9 / 27.4 / 18.2	24.6 / 27 / 18.1
4 bpcu	29.6 / 32 / 23.3	27.8 / 30.1 / 21.3	27.1 / 29.6 / 20.5	26.8 / 29.1 / 20.3

#### Take Away Message:

- SSK is better than single-antenna MQAM if Rate > 2bpcu and  $N_r > 1$
- The robustness to channel estimation errors is the same

## Imperfect Channel State Information at the Receiver (19/23)

### TOSD-SSK vs. Alamouti MQAM ( $N_r=1$ / $N_r=2$ )

TOSD-SSK				
Rate	$N_p = 1$	$N_p = 3$	$N_p = 10$	P – CSI
1 bpcu	27.2 / 18.2	26 / 16.9	25.5 / 16.4	25.3 / 16.2
2 bpcu	28.7 / 19	27.5 / 17.8	27 / 17.3	26.8 / 17
3 bpcu	30.2 / 19.8	29 / 18.6	28.5 / 18.2	28.4 / 17.8
4 bpcu	31.9 / 20.7	30.5 / 19.4	30.1 / 18.9	29.9 / 18.7

Alamouti QAM				
Rate	$N_p = 1$	$N_p = 3$	$N_p = 10$	P – CSI
1 bpcu	25.3 / 16.2	23.5 / 14.5	22.8 / 13.5	22.3 / 13.2
2 bpcu	28.4 / 19.3	26.5 / 17.5	25.7 / 16.6	25.4 / 16.3
3 bpcu	32.9 / 24	31.4 / 22.2	30.4 / 21.3	30 / 21
4 bpcu	35.2 / 26.2	33.3 / 24.3	32.6 / 23.5	32.3 / 23.3

#### Take Away Message:

- TOSD-SSK is better than Alamouti MQAM if Rate > 2bpcu
- TOSD-SSK is more robust to channel estimation errors

# *Imperfect Channel State Information at the Receiver (20/23)*

## SM with Imperfect CSIR

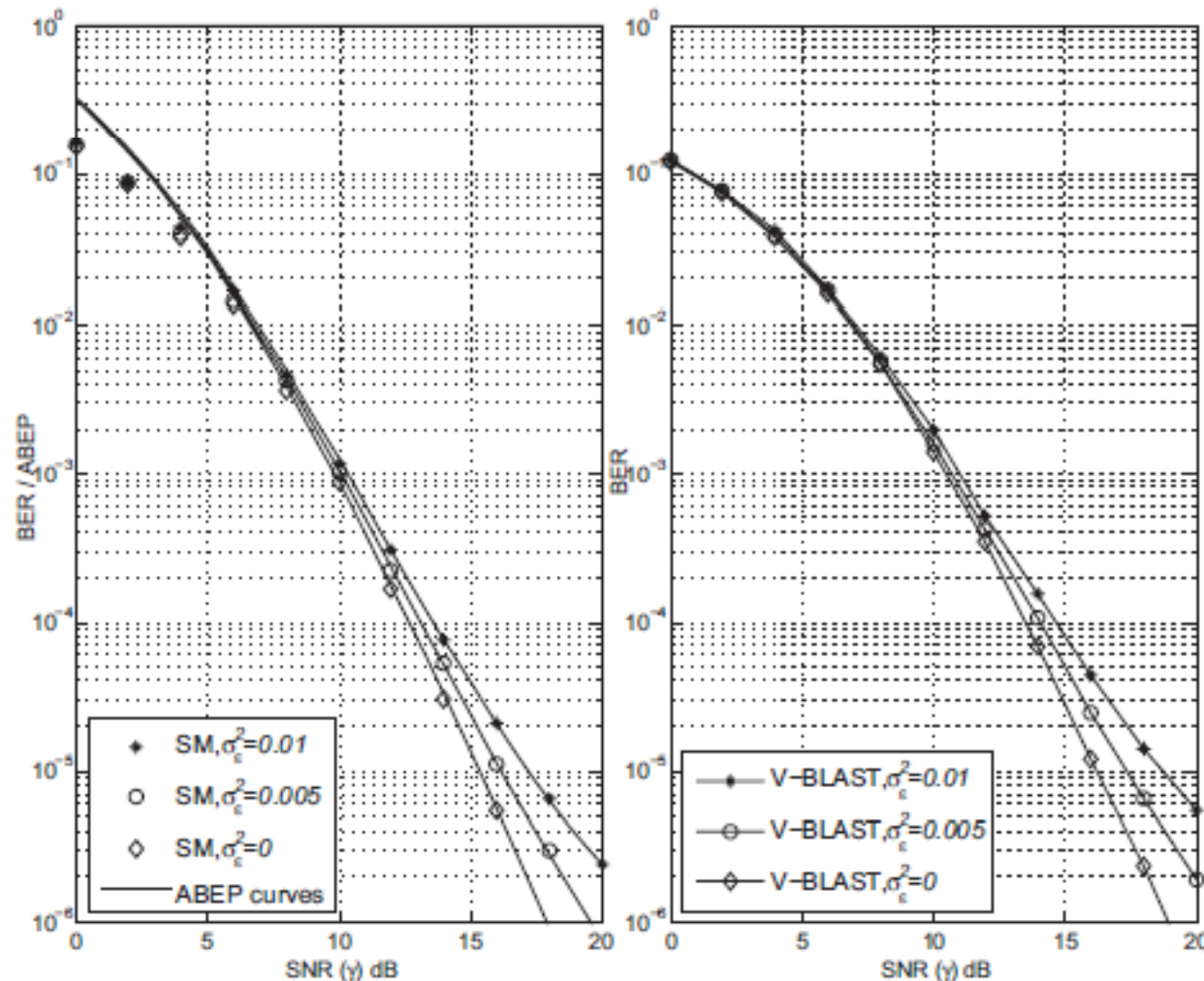
□ Channel estimation model:

$$\begin{cases} \beta = \alpha + \varepsilon & \text{with } \rho(\alpha, \beta) = 1/\sqrt{1 + \sigma_\varepsilon^2} \\ \sigma_\varepsilon^2 = \text{const} & \text{and } \sigma_\varepsilon^2 = 1/(\gamma N) \end{cases}$$

□ SM with MPSK modulation:  $(\hat{j}, \hat{s}) = \arg \min_{j,s} \left\{ \sum_{r=1}^{N_r} |y_r - \rho^2 \beta_{j,r} s|^2 \right\}$

□ SM with MQAM modulation:  $(\hat{j}, \hat{s}) = \arg \min_{j,s} \left\{ \sum_{r=1}^{N_r} |y_r - \beta_{j,r} s|^2 \right\}$

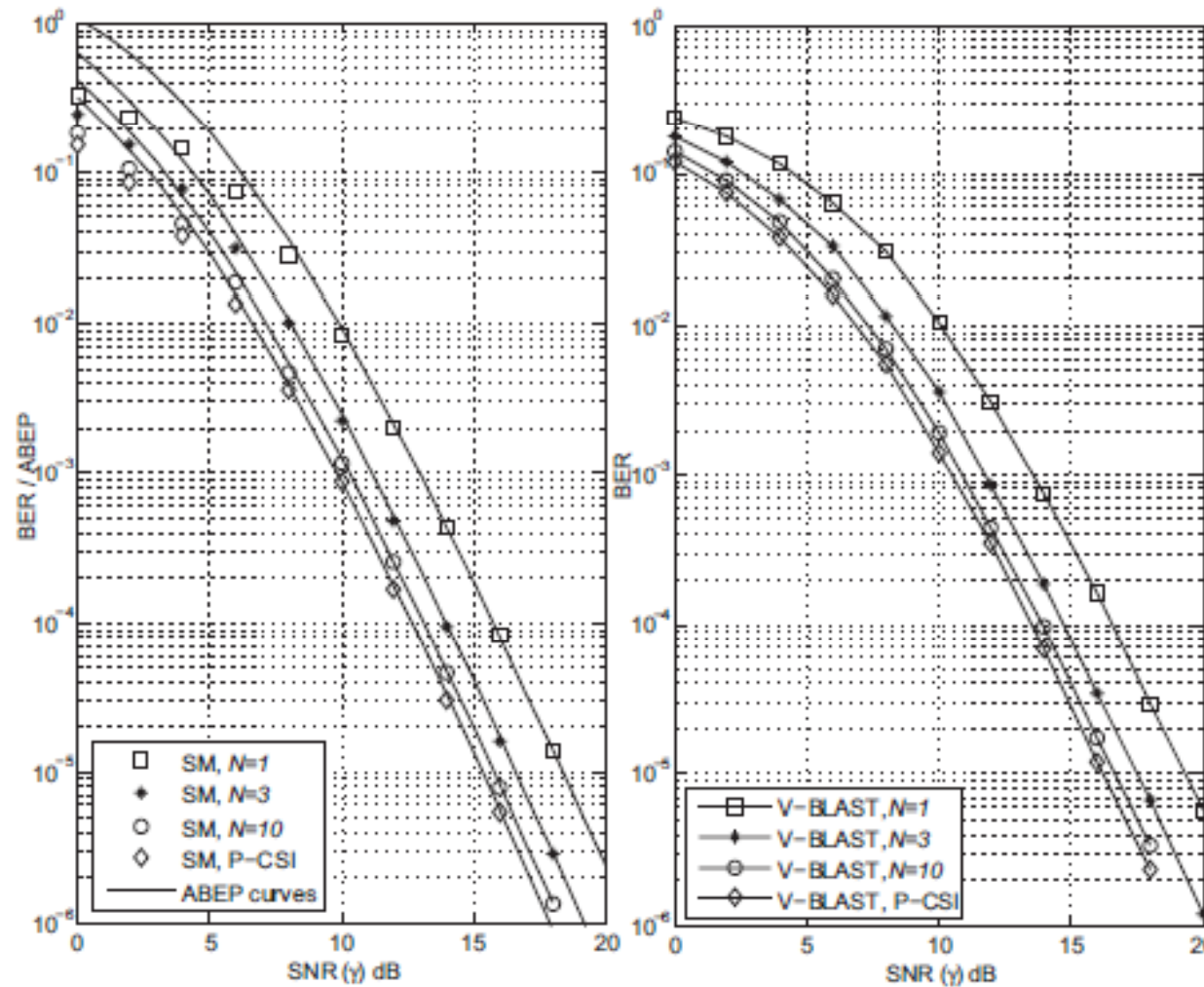
# Imperfect Channel State Information at the Receiver (21/23)



$$N_r = 4$$

Fig. 1. BER performance of SM with  $n_T = 4$ , QPSK and V-BLAST with  $n_T = 4$ , BPSK (4 bits/s/Hz) with optimal receivers (fixed  $\sigma_\epsilon^2$ ).

# Imperfect Channel State Information at the Receiver (22/23)

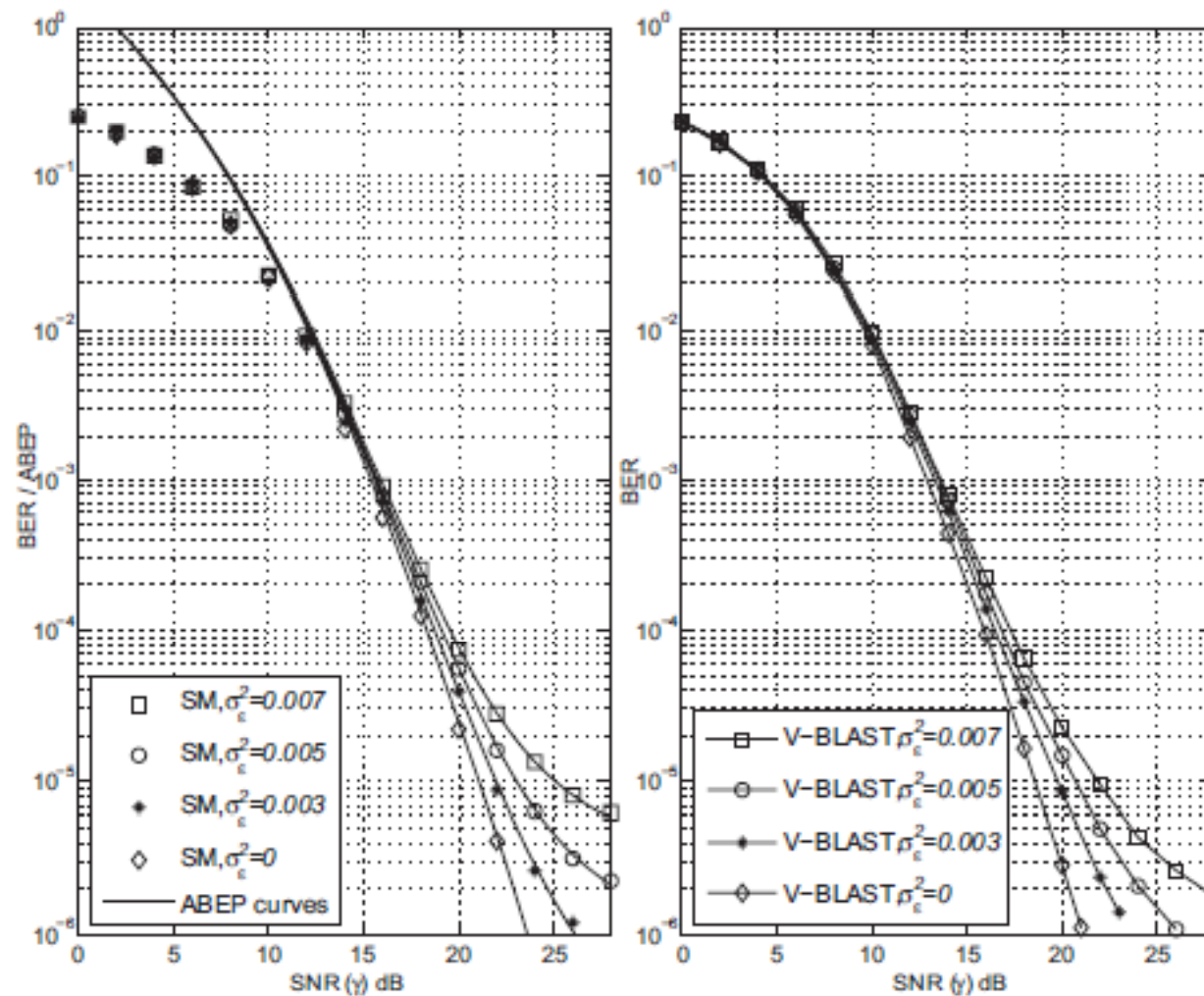


$$N_r = 4$$

Fig. 2. BER performance of SM with  $n_T = 4$ , QPSK and V-BLAST with  $n_T = 4$ , BPSK (4 bits/s/Hz) with optimal receivers (variable  $\sigma_\epsilon^2$ ).



# Imperfect Channel State Information at the Receiver (23/23)



$$N_r = 4$$

Fig. 3. BER performance of SM with  $n_T = 4$ , 16-QAM and V-BLAST with  $n_T = 3$ , QPSK (6 bits/s/Hz) with mismatched receivers (fixed  $\sigma_\epsilon^2$ ).

# *Outline*

---

1. Introduction and Motivation behind SM-MIMO
2. History of SM Research and Research Groups Working on SM
3. Transmitter Design – Encoding
4. Receiver Design – Demodulation
5. Error Performance (Numerical Results and Main Trends)
6. Achievable Capacity
7. Channel State Information at the Transmitter
8. Imperfect Channel State Information at the Receiver
9. **Multiple Access Interference**
10. Energy Efficiency
11. Transmit-Diversity for SM
12. Spatially-Modulated Space-Time-Coded MIMO
13. Relay-Aided SM
14. SM in Heterogeneous Cellular Networks
15. SM for Visible Light Communications
16. Experimental Evaluation of SM
17. The Road Ahead – Open Research Challenges/Opportunities
18. Implementation Challenges of SM-MIMO



# *Multiple Access Interference (1/22)*

---

The working principle of SM/SSK is based on the following facts:

1. The wireless environment **naturally** modulates the transmitted signal
2. Each transmit-receive wireless link has a **different** channel
3. The receiver employs the **a priori** channel knowledge to detect the transmitted signal
4. Thus, part of the information is conveyed by the Channel Impulse Response (CIR), i.e., the channel/spatial signature

**Can the randomness of the fading channel be used for Multiple-Access too rather than just for Modulation?**

# Multiple Access Interference (2/22)

## Signal Model

$$z^{(r)}(t) = \underbrace{\sqrt{E_\xi} h_\xi^{(x_\xi, r)} w(t)}_{\text{probe link}} + \underbrace{\sum_{\substack{u=1 \\ u \neq \xi}}^{N_u} \left[ \sqrt{E_u} h_u^{(x_u, r)} w(t) \right]}_{\text{interference}} + \underbrace{n^{(r)}(t)}_{\text{AWGN}}$$

## Single-User Detector

$$\hat{x}_\xi = \arg \min_{y_\xi=1,2,\dots,N_t} \left\{ D_\xi^{(y_\xi)} \right\} = \arg \min_{y_\xi=1,2,\dots,N_t} \left\{ \sum_{r=1}^{N_r} \int_{T_s} \left| z^{(r)}(t) - \sqrt{E_\xi} h_\xi^{(y_\xi, r)} w(t) \right|^2 dt \right\}$$

## Multi-User Detector

$$\hat{\mathbf{x}} = \arg \min_{\substack{\mathbf{y}=[y_1, y_2, \dots, y_{N_u}] \\ \text{for } y_u=1,2,\dots,N_t}} \left\{ D(\mathbf{y}) \right\} = \arg \min_{\substack{\mathbf{y}=[y_1, y_2, \dots, y_{N_u}] \\ \text{for } y_u=1,2,\dots,N_t}} \left\{ \sum_{r=1}^{N_r} \int_{T_s} \left| z^{(r)}(t) - \sum_{u=1}^{N_u} \left[ \sqrt{E_u} h_u^{(y_u, r)} w(t) \right] \right|^2 dt \right\}$$

## *Multiple Access Interference (3/22)*

### **SSK with Single-User Detector (i.i.d. Rayleigh)**

$$\text{ABEP}_{\xi} \leq \frac{N_t}{2} \left[ \frac{1}{2} \left( 1 - \sqrt{\frac{\text{SINR}}{2 + \text{SINR}}} \right) \right]^{N_r} \sum_{r=1}^{N_r} \left\{ \binom{N_r - 1 + r}{r} \left[ \frac{1}{2} \left( 1 + \sqrt{\frac{\text{SINR}}{2 + \text{SINR}}} \right) \right]^r \right\}$$
$$\begin{cases} \text{SINR} = \text{SNR}_{\xi} / (1 + \text{INR}_{\setminus \xi}) \\ \text{SNR}_{\xi} = (E_{\xi} \sigma_{\xi}^2) / N_0 \quad \text{and} \quad \text{INR}_{\setminus \xi} = \sum_{u \neq \xi=1}^{N_u} \left[ (E_u \sigma_u^2) / N_0 \right] \end{cases}$$

□  $E_u = 0$  (no interference): framework reduces to single-user case

□  $\text{SNR}_{\xi} \gg 1$  and  $\text{INR}_{\setminus \xi} \ll 1$  (noise limited):

$$\text{ABEP}_{\xi} \rightarrow 2^{-(N_r+1)} \binom{2N_r-1}{N_r} N_t \text{SNR}_{\xi}^{-N_r}$$

# *Multiple Access Interference (4/22)*

## SSK with Single-User Detector (i.i.d. Rayleigh)

□  $\text{INR}_{\setminus\xi} \gg 1$  and  $\text{SIR} = \text{SNR}_{\xi} / \text{INR}_{\setminus\xi} \gg 1$  (interference limited):

$$\text{ABEP}_{\xi} \rightarrow 2^{-(N_r+1)} \binom{2N_r-1}{N_r} N_t \text{SIR}^{-N_r} \text{ with } \text{SIR} = E_{\xi} \sigma_{\xi}^2 / \sum_{u \neq \xi=1}^{N_u} (E_u \sigma_u^2)$$

□  $N_r \gg 1$ :

$$\text{ABEP}_{\xi} \rightarrow (N_t/2) Q\left(\sqrt{N_r \text{SIR}}\right)$$

$$\begin{cases} \text{SIR} = \text{SNR}_{\xi} / (1 + \text{INR}_{\setminus\xi}) \\ \text{SNR}_{\xi} = (E_{\xi} \sigma_{\xi}^2) / N_0 \quad \text{and} \quad \text{INR}_{\setminus\xi} = \sum_{u \neq \xi=1}^{N_u} \left[ (E_u \sigma_u^2) / N_0 \right] \end{cases}$$

# *Multiple Access Interference (5/22)*

## SSK vs. MPSK/MQAM (Single-User Detector, i.i.d. Rayleigh)

$$M = N_t \text{ (same bpcu)}$$

$$\frac{\text{ABEP}_{\xi}^{\text{PSK}}}{\text{ABEP}_{\xi}^{\text{SSK}}} \rightarrow \frac{2}{N_t^2 \log_2(N_t)} \sum_{x_{\xi}=1}^{N_t} \sum_{y_{\xi}=1}^{N_t} \left\{ N_H \left( s_{\xi}^{(x_{\xi})}, s_{\xi}^{(y_{\xi})} \right) \left[ 2 / \underbrace{\left| s_{\xi}^{(y_{\xi})} - s_{\xi}^{(x_{\xi})} \right|^2}_Q \right]^{N_r} \right\}$$

- ❑ SSK will never be better than MPSK/MQAM if  $Q \geq 2$ . This occurs if  $M = N_t = 2$  and  $M = N_t = 4$ . If  $M = N_t > 4$  a crossing point exists
- ❑ If  $Q < 2$ , the performance gain of SSK exponentially increases with  $N_r$

# Multiple Access Interference (6/22)

## GSSK with Single-User Detector (i.i.d. Rayleigh)

$$\text{SINR} = \frac{1}{2} \frac{\text{SNR}_\xi}{1 + \text{INR}_{\setminus \xi}} \frac{N_{\text{ta}}^\neq(\mathbf{x}_\xi, \mathbf{y}_\xi)}{N_{\text{ta}}}$$

- $N_{\text{ta}}$  is the number of active antennas
- $N_{\text{ta}}^\neq$  is the number of different antenna indexes:  $2 \leq N_{\text{ta}}^\neq \leq 2N_{\text{ta}}$
- Asymptotic performance:

$$\begin{cases} \text{APEP}(\mathbf{x}_\xi \rightarrow \mathbf{y}_\xi) \rightarrow \left[ N_{\text{ta}} / N_{\text{ta}}^\neq(\mathbf{x}_\xi, \mathbf{y}_\xi) \right]^{N_r} \binom{2N_r - 1}{N_r} \Upsilon^{-N_r} \\ \Upsilon = \text{SNR}_\xi \text{ (noise limited) or } \Upsilon = \text{SIR} \text{ (interference limited)} \end{cases}$$

# Multiple Access Interference (7/22)

## SSK vs. GSSK (Single-User Detector, i.i.d. Rayleigh)

$$\frac{\text{APEP}^{\text{GSSK}}(\mathbf{x}_\xi \rightarrow \mathbf{y}_\xi)}{\text{APEP}_\xi^{\text{SSK}}} \rightarrow \left[ \frac{2N_{\text{ta}}}{N_{\text{ta}}^\neq(\mathbf{x}_\xi, \mathbf{y}_\xi)} \right]^{N_r}$$

- Since  $2 \leq N_{\text{ta}}^\neq \leq 2N_{\text{ta}}$ , GSSK is worse than SSK regardless of the choice of the spatial-constellation diagram
- The SNR gap is:

$$0 \leq \Delta_\gamma \leq 10 \log_{10}(N_{\text{ta}})$$

thus, the larger  $N_{\text{ta}}$ , the worse GSSK compared to SSK

# Multiple Access Interference (8/22)

## SSK and GSSK with Multi-User Detector (i.i.d. Rayleigh)

$$\text{APEP}(\mathbf{x} \rightarrow \mathbf{y}) = \left[ \frac{1}{2} \left( 1 - \sqrt{\frac{\text{AggrSNR}}{2 + \text{AggrSNR}}} \right) \right]^{N_r} \sum_{r=1}^{N_r} \left\{ \binom{N_r - 1 + r}{r} \left[ \frac{1}{2} \left( 1 + \sqrt{\frac{\text{AggrSNR}}{2 + \text{AggrSNR}}} \right) \right]^r \right\}$$

□ **SSK**       $\text{AggrSNR} = \sum_{u=1}^{N_u} \left[ \frac{E_u \sigma_u^2 (1 - \delta_{x_u, y_u})}{N_0} \right]$

□ **GSSK**       $\text{AggrSNR} = \sum_{u=1}^{N_u} \left[ \frac{E_u \sigma_u^2}{2N_0} \frac{N_{\text{ta}}^\#(x_u, y_u)}{N_{\text{ta}}} (1 - \delta_{x_u, y_u}) \right]$

□ Unlike the single-user detector,  $\text{APEP} \rightarrow 0$  if  $N_0 \rightarrow 0$



# Multiple Access Interference (9/22)

## SSK with Multi-User Detector (i.i.d. Rayleigh) – Asymptotic Analysis

□ AggSNR  $\gg 1$

$$\text{ABEP}_\xi \rightarrow \left[ N_t^{N_u} \log_2(N_t) \right]^{-1} \binom{2N_r - 1}{N_r} 2^{-N_r} \sum_{\mathbf{x}} \sum_{\mathbf{y}} \left[ \left( 1 - \delta_{x_\xi, y_\xi} \right) N_H(x_\xi, y_\xi) \text{AggrSNR}^{-N_r} \right]$$

□ Single-user lower bound ( $N_u = 1$ )

$$\text{ABEP}_\xi^{\text{SULB}} \rightarrow 2^{-(N_r+1)} \binom{2N_r - 1}{N_r} N_t \text{SNR}_\xi^{-N_r}$$

□ SNR gap due to multiple-access interference

$$\Delta_{\text{SNR}} = \frac{10}{N_r} \log_{10} \left( \frac{\text{ABEP}_\xi}{\text{ABEP}_\xi^{\text{SULB}}} \right) \rightarrow \frac{10}{N_r} \log_{10} \left( \frac{1}{N_t^{(N_u+1)} \log_2(N_t)} \sum_{\mathbf{x}} \sum_{\mathbf{y}} \left[ \frac{\left( 1 - \delta_{x_\xi, y_\xi} \right) N_H(x_\xi, y_\xi) E_\xi \sigma_\xi^2}{2 \sum_{u=1}^{N_u} \left[ E_u \sigma_u^2 \left( 1 - \delta_{x_u, y_u} \right) \right]} \right] \right)$$

# *Multiple Access Interference (10/22)*

## **SSK with Multi-User Detector (i.i.d. Rayleigh) – Asymptotic Analysis**

□ Strong interference case ( $E_w \sigma_w^2 \ll E_u \sigma_u^2$ , for every  $u$ )

$$\text{ABEP}_w \rightarrow 2^{-(N_r+1)} N_t \binom{2N_r-1}{N_r} (E_w \sigma_w^2 / N_0)^{-N_r} = \text{ABEP}_w^{\text{SULB}}$$

□ Weak interference case ( $E_b \sigma_b^2 \gg E_u \sigma_u^2$ , for every  $u$ )

$$\text{ABEP}_b \rightarrow 2^{-(N_r+1)} N_t^{N_u} \binom{2N_r-1}{N_r} [E_b \sigma_b^2 / N_0]^{-N_r}$$

$$\Delta_{\text{SNR}_b} = (10/N_r) \log_{10} (\text{ABEP}_b / \text{ABEP}_b^{\text{SULB}}) = 10 [(N_u - 1)/N_r] \log_{10} (N_t)$$

# *Multiple Access Interference (11/22)*

## SSK with Multi-User Detector (i.i.d. Rayleigh) – Asymptotic Analysis

### □ Generic user

$$\text{ABEP}_u^L \leq \text{ABEP}_u \leq \text{ABEP}_u^U$$

$$\left\{ \begin{array}{l} \text{ABEP}_u^L = 2^{-(N_r+1)} N_t \binom{2N_r-1}{N_r} \left( \frac{E_u \sigma_u^2}{N_0} \right)^{-N_r} \\ \text{ABEP}_u^U = 2^{-(N_r+1)} N_t^{N_u} \binom{2N_r-1}{N_r} \left[ \frac{E_u \sigma_u^2}{N_0} \right]^{-N_r} \end{array} \right.$$

$$\Delta_{\text{SNR}_u} = (10/N_r) \log_{10} \left( \text{ABEP}_u^U / \text{ABEP}_u^L \right) = 10 \left[ (N_u - 1)/N_r \right] \log_{10} (N_t)$$

# Multiple Access Interference (12/22)

## GSSK with Multi-User Detector (i.i.d. Rayleigh) – Asymptotic Analysis

$$\left\{ \begin{array}{l} \text{ABEP}_u^L \mapsto \text{SULB} \quad \text{and} \quad \text{ABEP}_u^U \mapsto \text{weak interference case} \\ \text{ABEP}_u^L \leq \text{ABEP}_u \leq \text{ABEP}_u^U \\ \underbrace{2^{-(N_r+1)} N_t \binom{2N_r-1}{N_r} \left( \frac{E_u \sigma_u^2}{N_0} \right)^{-N_r}}_{\text{ABEP}_u^{LL}} \leq \text{ABEP}_u^L \leq 2^{-(N_r+1)} 2^{\left\lfloor \log_2 \left( \frac{N_t}{N_{\text{ta}}} \right) \right\rfloor} N_{\text{ta}}^{N_r} \binom{2N_r-1}{N_r} \left( \frac{E_u \sigma_u^2}{N_0} \right)^{-N_r} \\ 2^{-(N_r+1)} 2^{N_u \left\lfloor \log_2 \left( \frac{N_t}{N_{\text{ta}}} \right) \right\rfloor} \binom{2N_r-1}{N_r} \left( \frac{E_u \sigma_u^2}{N_0} \right)^{-N_r} \leq \text{ABEP}_u^U \leq 2^{-(N_r+1)} \underbrace{2^{N_u \left\lfloor \log_2 \left( \frac{N_t}{N_{\text{ta}}} \right) \right\rfloor} N_{\text{ta}}^{N_r} \binom{2N_r-1}{N_r} \left( \frac{E_u \sigma_u^2}{N_0} \right)^{-N_r}}_{\text{ABEP}_u^{UU}} \end{array} \right.$$



$$\begin{aligned} \Delta_{\text{SNR}_u} &= (10/N_r) \log_{10} \left( \text{ABEP}_u^{UU} / \text{ABEP}_u^{LL} \right) \\ &= 10 \log_{10} (N_t) + (10/N_r) \log_{10} \left( 2^{N_u \left\lfloor \log_2 \left( \frac{N_t}{N_{\text{ta}}} \right) \right\rfloor} / N_t \right) \end{aligned}$$

# Multiple Access Interference (13/22)

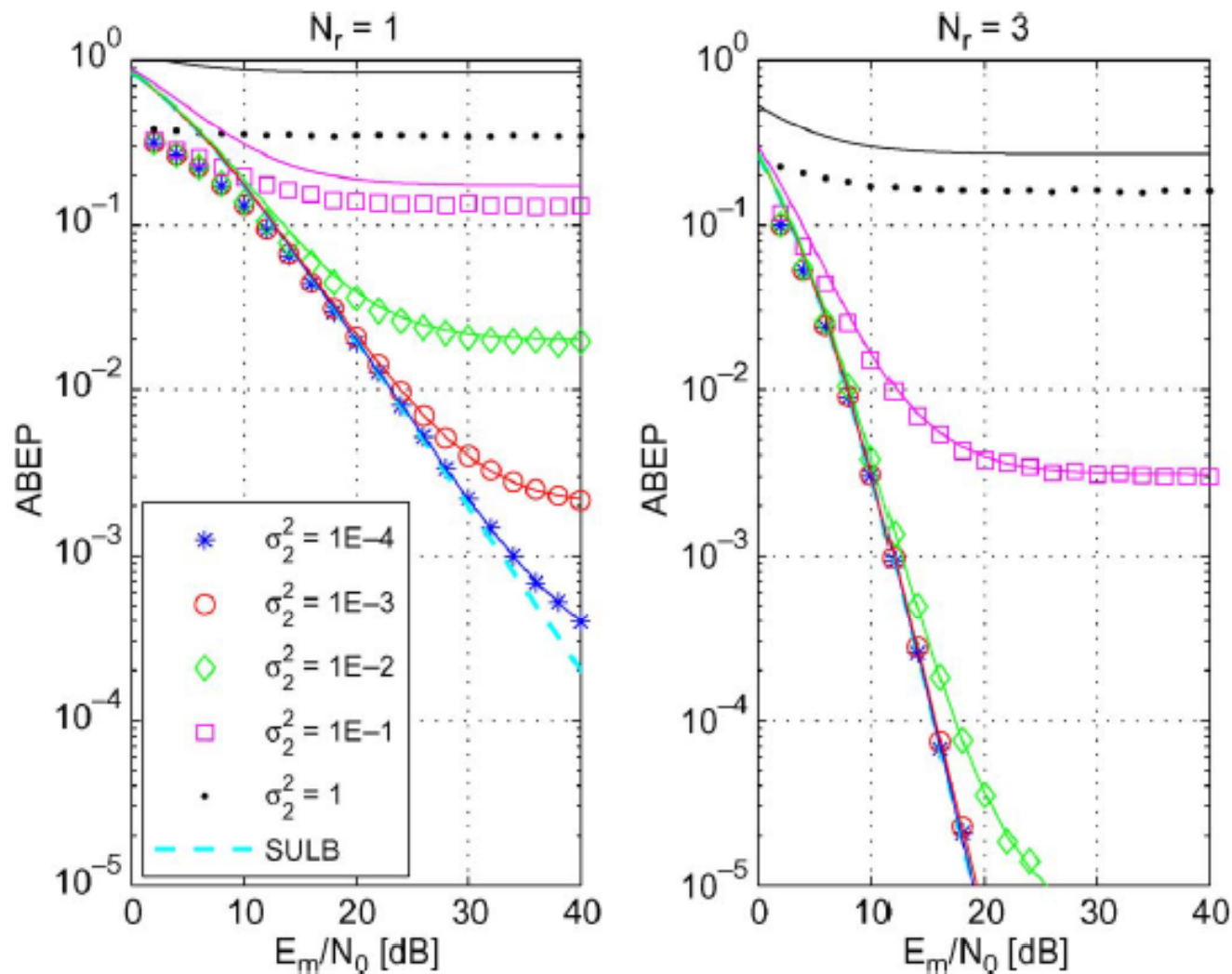


Fig. 1. ABEP of SSK modulation with single-user detection. Setup:  $N_t = 8$ ;  $N_u = 2$ ;  $\sigma_1^2 = 1$ ; and (left)  $N_r = 1$  and (right)  $N_r = 3$ . Markers show Monte Carlo simulations, and solid lines show the analytical model [i.e., (8) and (9)]. The ABEP of user 1 (probe/intended link) is shown. SULB stands for SULB, i.e., it represents the scenario with no multiple-access interference.

# Multiple Access Interference (14/22)

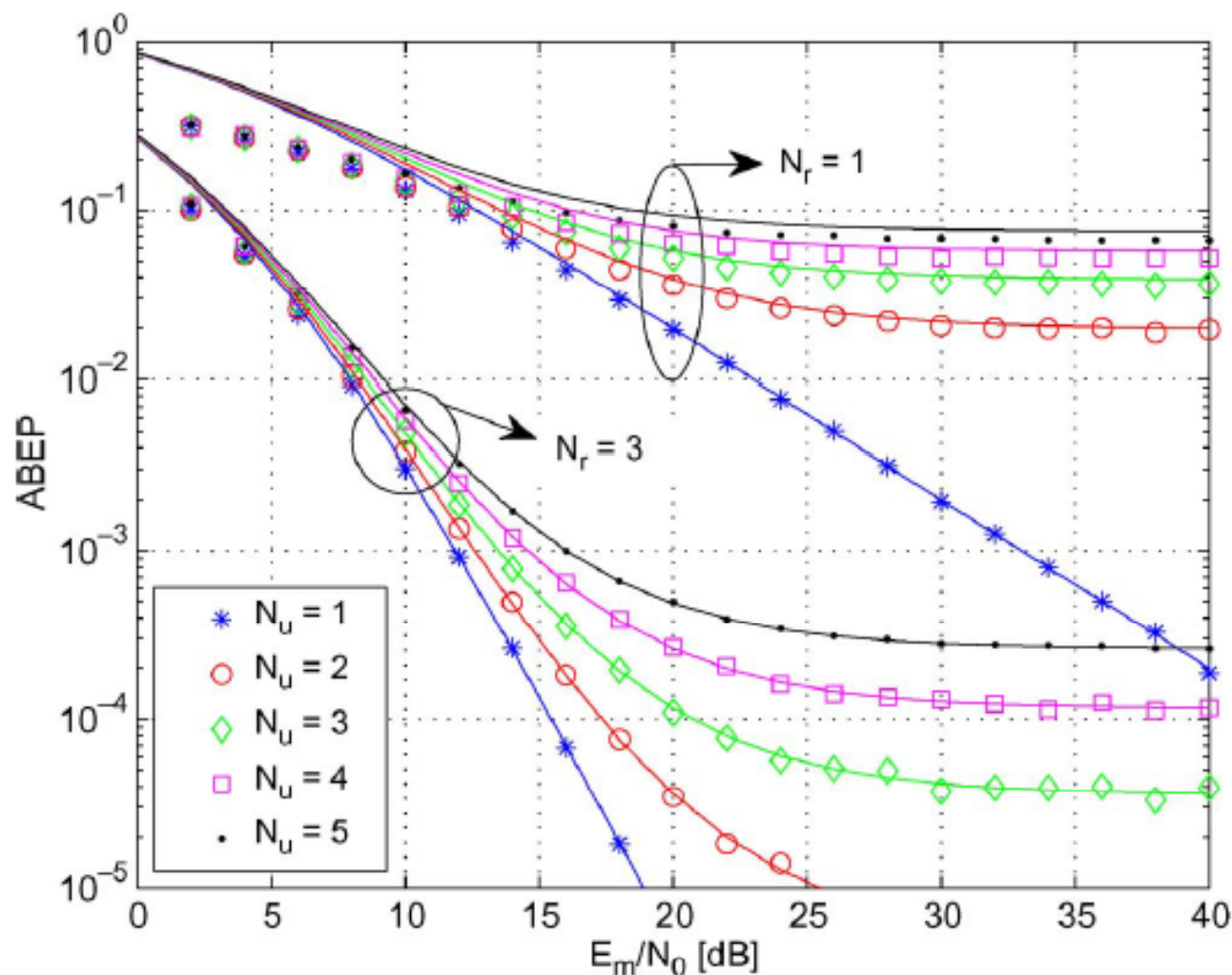


Fig. 2. ABEP of SSK modulation with single-user detection. Setup:  $N_t = 8$ ;  $\sigma_1^2 = 1$ ;  $\sigma_i^2 = 10^{-2}$  for  $i = 2, 3, \dots, N_u$ ;  $N_r = 1$ ; and  $N_r = 3$ . Markers show Monte Carlo simulations, and solid lines show the analytical model [i.e., (8) and (9)]. The ABEP of user 1 (probe/intended link) is shown.



# Multiple Access Interference (15/22)

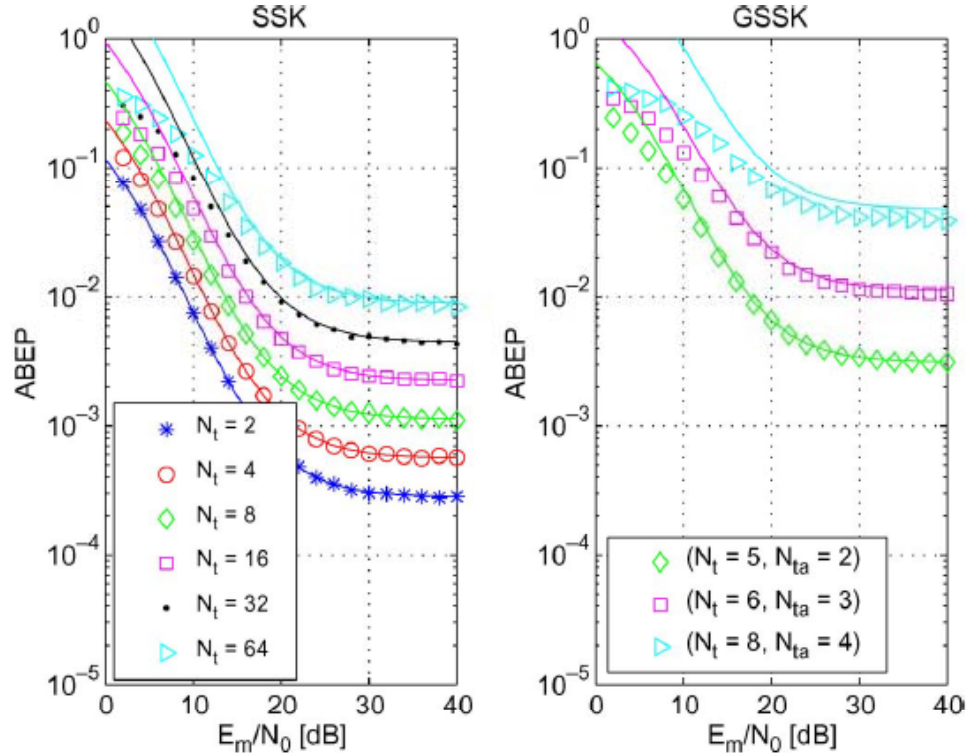


Fig. 3. ABEP of (left) SSK and (right) GSSK modulations with single-user detection. Setup:  $N_u = 3$ ;  $\sigma_1^2 = 1$ ;  $\sigma_i^2 = 10^{-2}$  for  $i = 2, 3, \dots, N_u$ ; and  $N_r = 2$ . Markers show Monte Carlo simulations, and solid lines show the analytical model (i.e., (8) and (9) for SSK modulation and (13) for GSSK modulation). The ABEP of user 1 (probe/intended link) is shown.

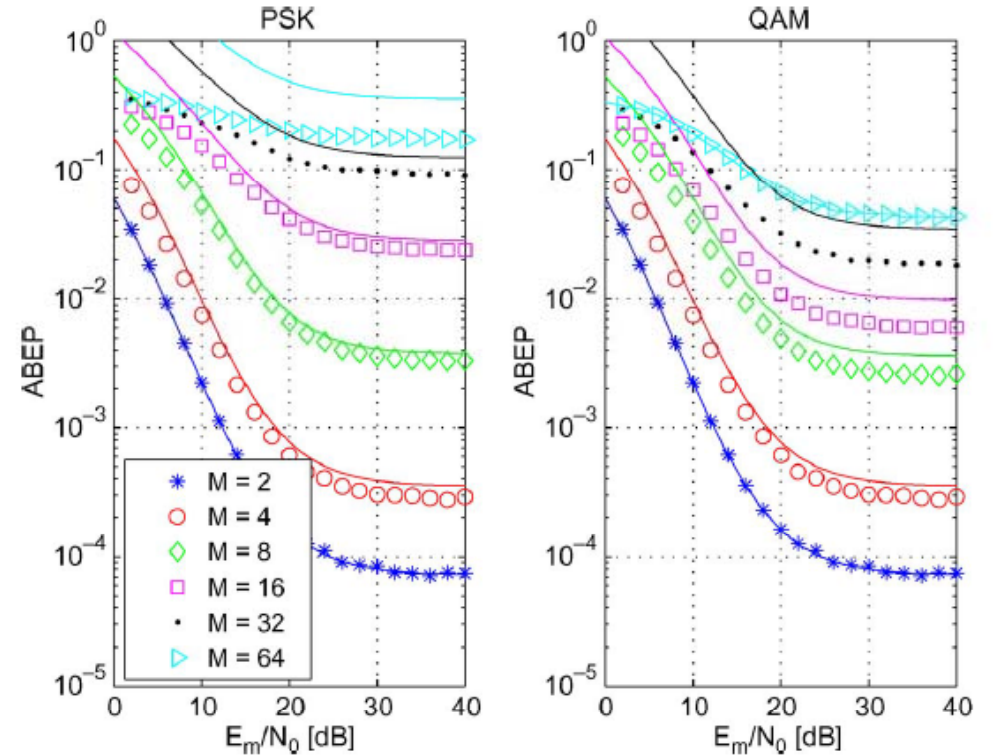


Fig. 4. ABEP of (left) PSK and (right) QAM modulations with single-user detection. Setup:  $N_u = 3$ ;  $\sigma_1^2 = 1$ ;  $\sigma_i^2 = 10^{-2}$  for  $i = 2, 3, \dots, N_u$ ; and  $N_r = 2$ . Markers show Monte Carlo simulations, and solid lines show the analytical model (i.e., the union bound in the first and second rows of Table I). The ABEP of user 1 (probe/intended link) is shown.

# Multiple Access Interference (16/22)

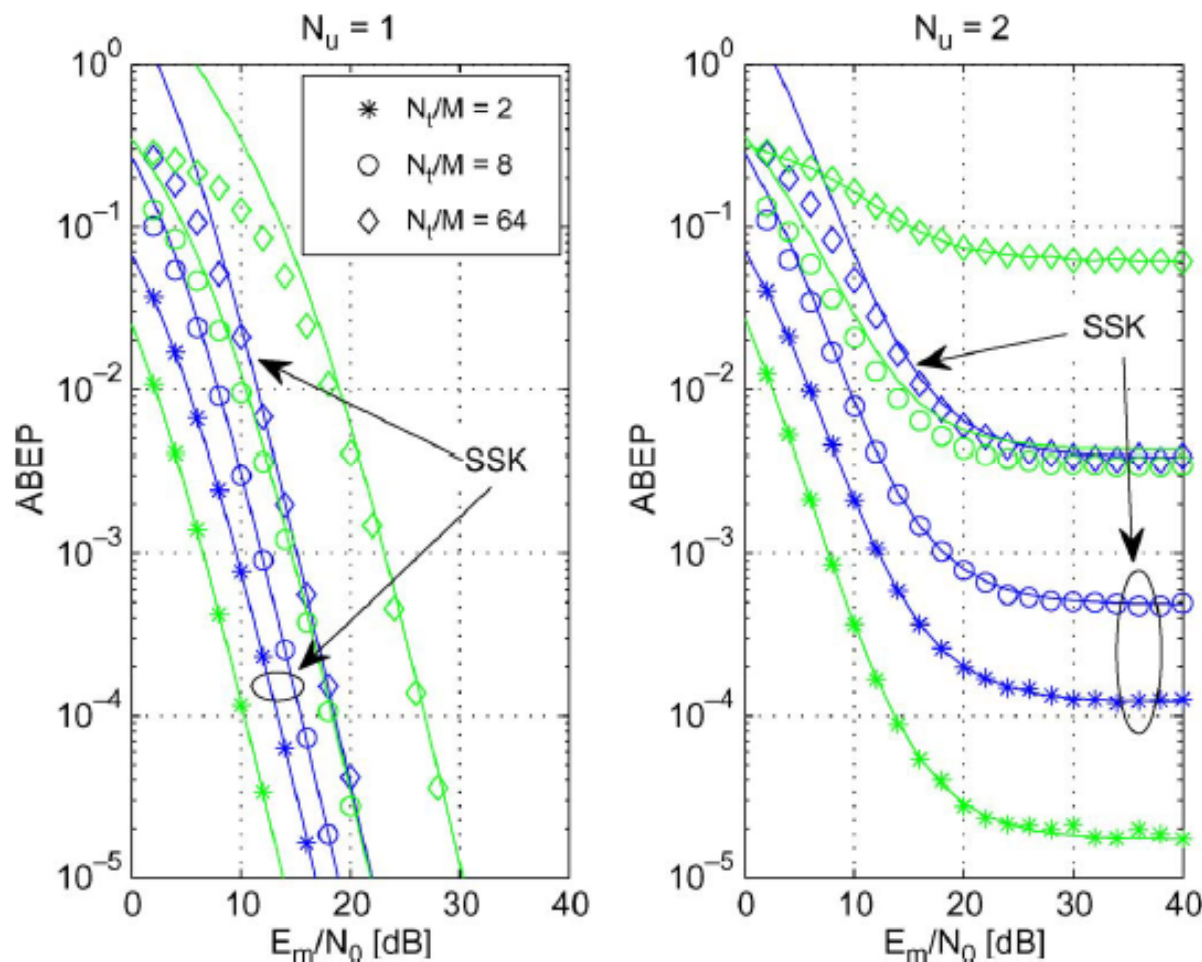


Fig. 5. ABEP of (blue curves) SSK and (green curves) QAM modulations with single-user detection. Setup: (left)  $N_u = 1$  and (right)  $N_u = 2$ ;  $\sigma_1^2 = 1$  and  $\sigma_2^2 = 5 \times 10^{-2}$ ; and  $N_r = 3$ . Markers show Monte Carlo simulations, and solid lines show the analytical model (i.e., (8) and (9) for SSK modulation and the union bound in the second row of Table I). The ABEP of user 1 (probe/intended link) is shown.



# Multiple Access Interference (17/22)

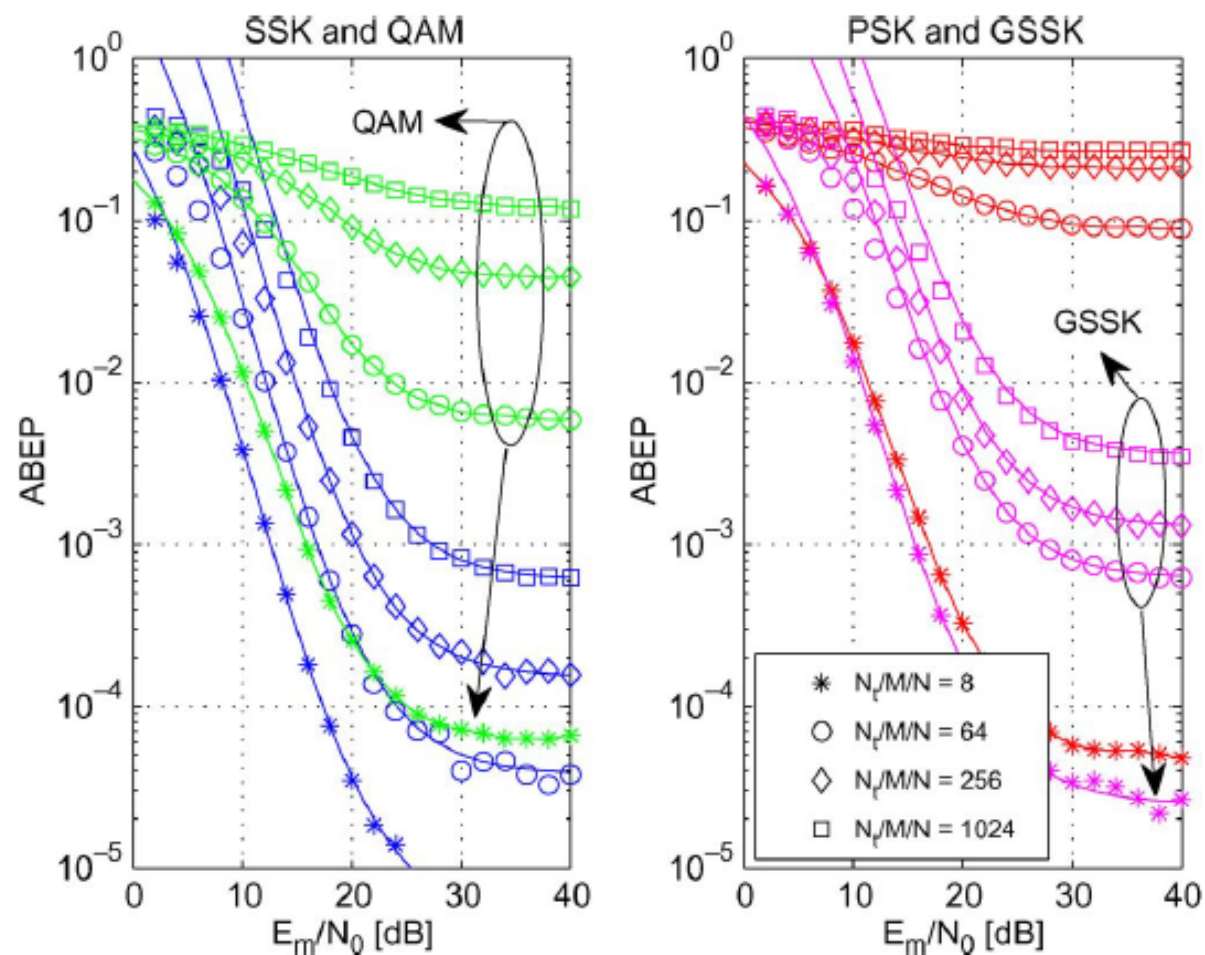


Fig. 7. ABEP of, on the left, (blue curves) SSK and (green curves) QAM, and, on the right, (red curves) PSK and (magenta curves) GSSK modulations with single-user detection. Setup:  $N_u = 2$ ;  $\sigma_1^2 = 1$  and  $\sigma_2^2 = 10^{-2}$ ; and  $N_r = 3$ . For GSSK modulation, we have  $(N_t, N_{ta}) = (5, 2)$  if  $N = 8$ ;  $(N_t, N_{ta}) = (8, 4)$  if  $N = 64$ ;  $(N_t, N_{ta}) = (11, 4)$  if  $N = 256$ ; and  $(N_t, N_{ta}) = (12, 5)$  if  $N = 1024$ . For SSK and GSSK modulations, markers show Monte Carlo

## Multiple Access Interference (18/22)

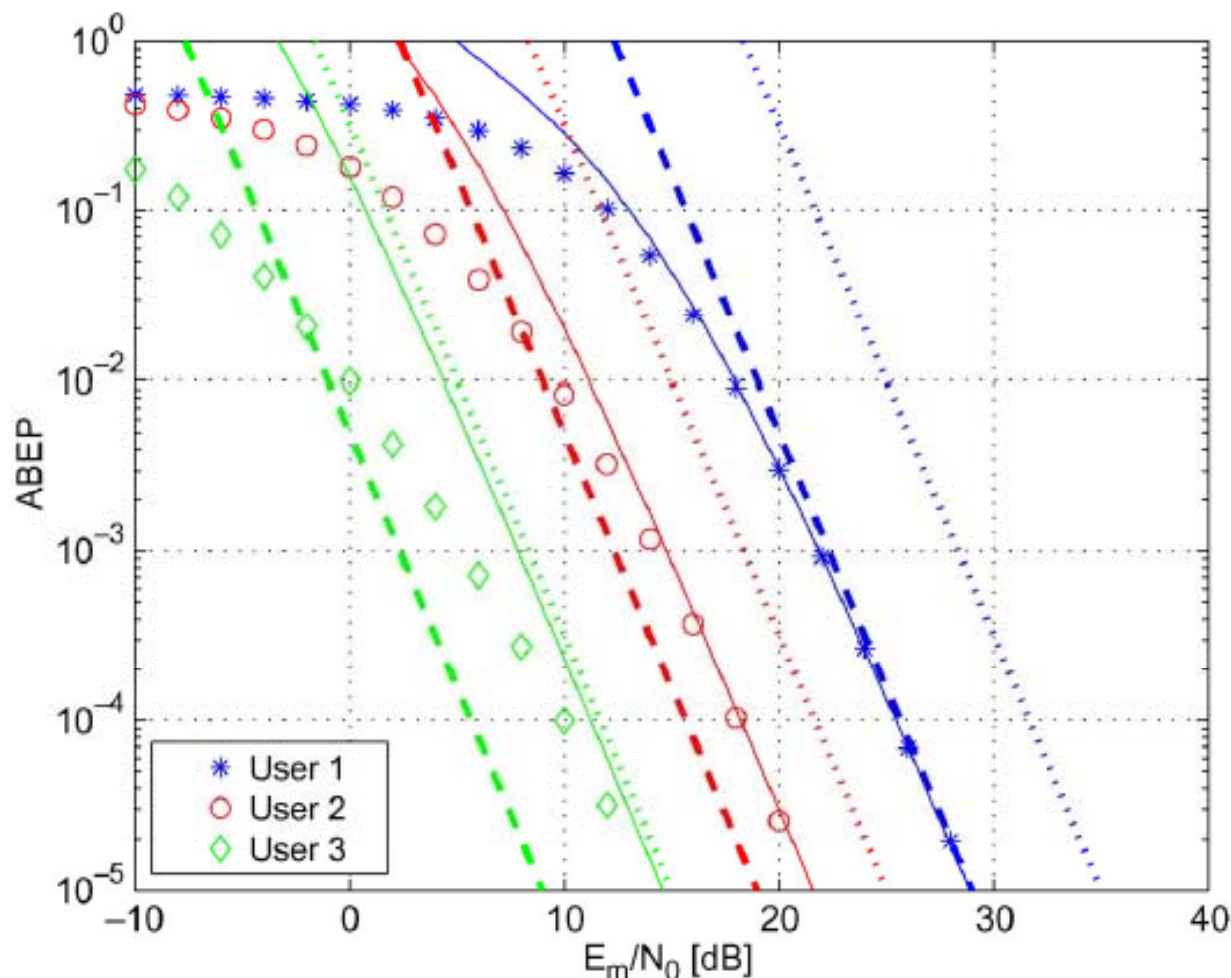


Fig. 10. ABEP of SSK modulation with multiuser detection. Setup:  $N_t = 8$ ;  $N_u = 3$ ;  $\sigma_1^2 = 0.1$ ,  $\sigma_2^2 = 1$ ,  $\sigma_3^2 = 10$ ; and  $N_r = 3$ . Markers show Monte Carlo simulations, and solid lines show the analytical model [i.e., (16) and (18)]. Furthermore, dashed lines show the estimated lower bound [i.e.,  $\text{ABEP}_u^L$  in (22)], which corresponds to the SULB when no multiple-access interference is present; and dotted lines show the estimated upper bound [i.e.,  $\text{ABEP}_u^U$  in (22)]. The ABEP of all the users is shown.

# Multiple Access Interference (19/22)

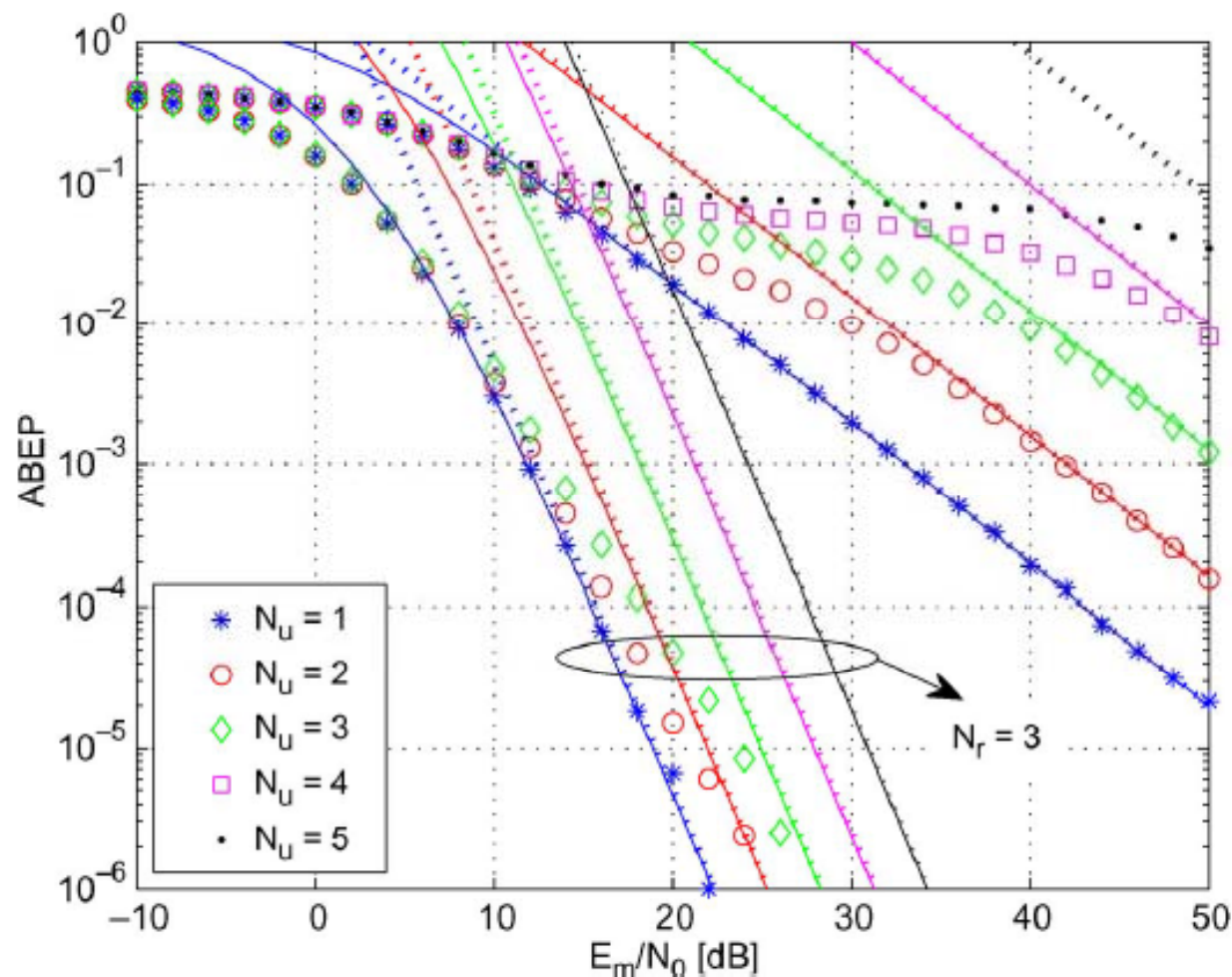


Fig. 11. ABEP of SSK modulation with multiuser detection. Setup:  $N_t = 8$ ;  $\sigma_1^2 = 1$  and  $\sigma_i^2 = 10^{-2}$  for  $i = 2, 3, \dots, N_u$ ;  $N_r = 1$ ; and  $N_r = 3$ . Markers show Monte Carlo simulations, and solid lines show the analytical model [i.e., (16) and (18)]. Furthermore, dotted lines show the estimated upper bound [i.e.,  $\text{ABEP}_u^U$  in (22)]. The ABEP of user 1 (probe/intended link) is shown. It is worth mentioning that some simulation results (markers) are not shown due to the long simulation time for medium/high values of  $E_m/N_0$ .



# Multiple Access Interference (20/22)

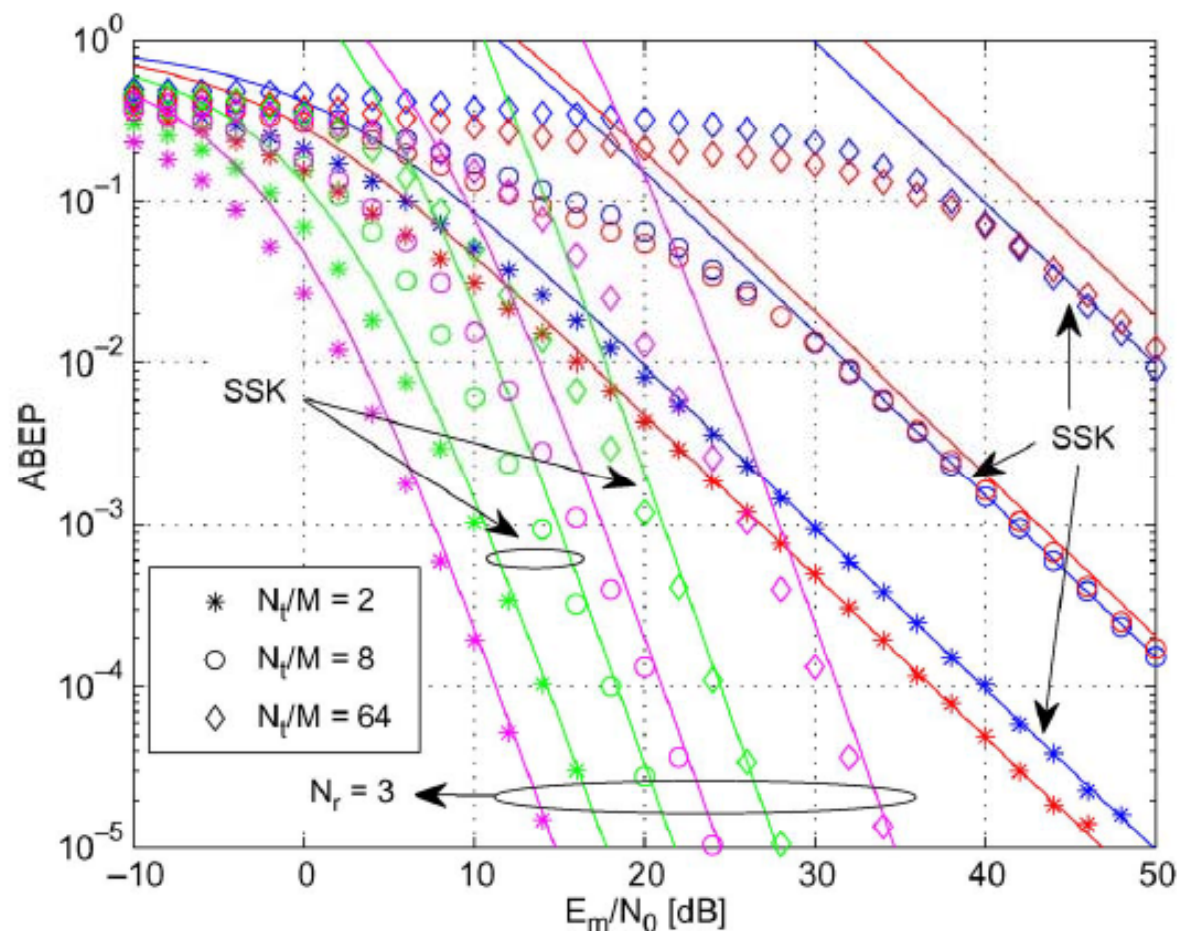


Fig. 16. ABEP of SSK (blue and green lines for  $N_r = 1$  and  $N_r = 3$ , respectively) and QAM (red and magenta lines for  $N_r = 1$  and  $N_r = 3$ , respectively) modulations with multiuser detection. Setup:  $N_u = 2$ ;  $\sigma_1^2 = 1$ ; and  $\sigma_2^2 = 5 \times 10^{-2}$ . Markers show Monte Carlo simulations, and solid lines show the analytical model (i.e., (16) and (18) for SSK modulation and the formula in the first row of Table II for QAM). The ABEP of user 1 (probe/intended link) is shown.

# Multiple Access Interference (21/22)

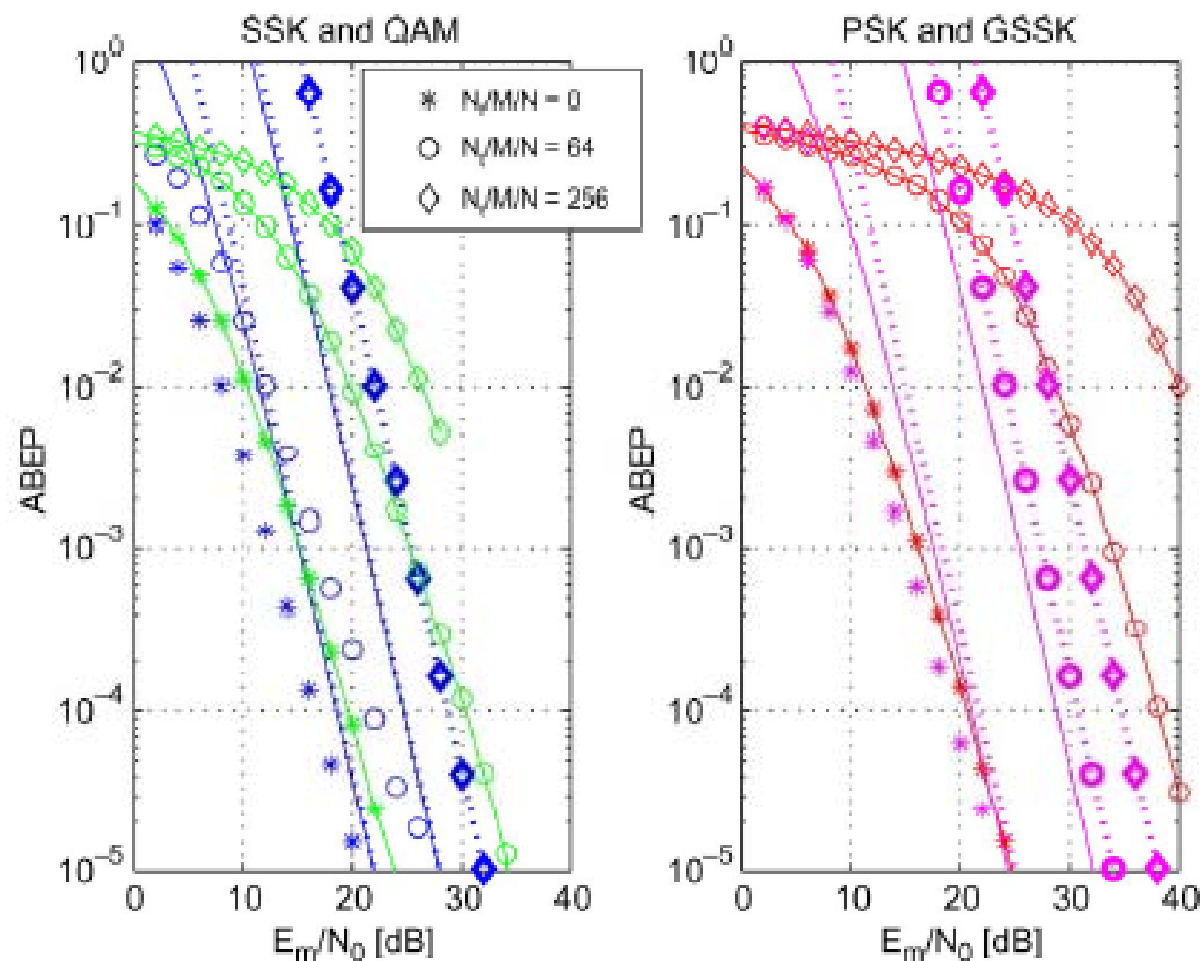
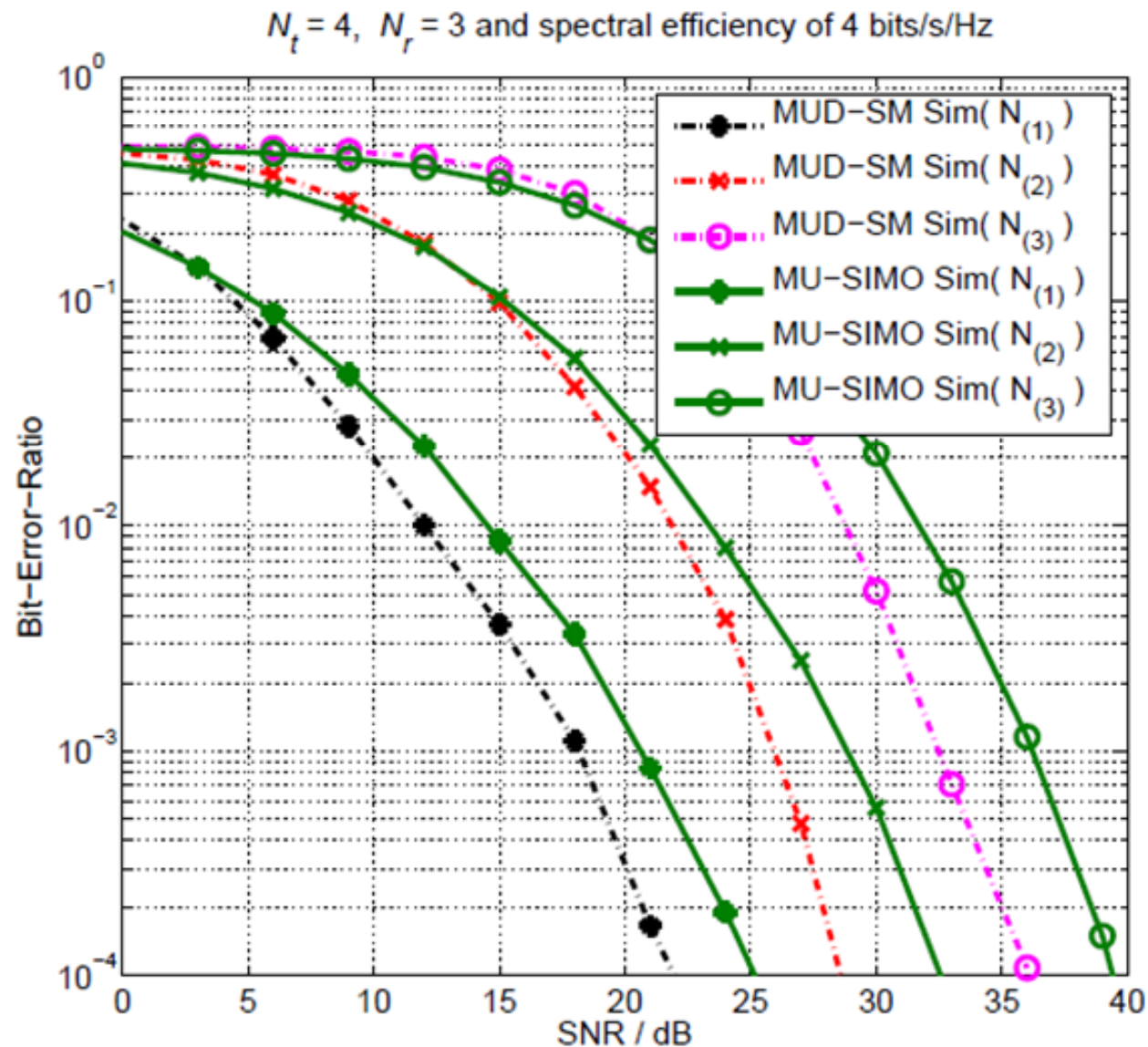


Fig. 17. ABEP of, on the left, (blue curves) SSK and (green curves) QAM, and, on the right, (red curves) PSK and (magenta curves) GSSK modulations with multiuser detection. Setup:  $N_u = 2$ ;  $\sigma_1^2 = 1$  and  $\sigma_2^2 = 10^{-2}$ ; and  $N_r = 3$ . For GSSK modulation, we have  $(N_t, N_{ta}) = (5, 2)$  if  $N = 8$ ;  $(N_t, N_{ta}) = (8, 4)$  if  $N = 64$ ; and  $(N_t, N_{ta}) = (11, 4)$  if  $N = 256$ .

# Multiple Access Interference (22/22)



3-user scenario  
The ABEP of each  
user is shown

# *Outline*

---

1. Introduction and Motivation behind SM-MIMO
2. History of SM Research and Research Groups Working on SM
3. Transmitter Design – Encoding
4. Receiver Design – Demodulation
5. Error Performance (Numerical Results and Main Trends)
6. Achievable Capacity
7. Channel State Information at the Transmitter
8. Imperfect Channel State Information at the Receiver
9. Multiple Access Interference
10. **Energy Efficiency**
11. Transmit-Diversity for SM
12. Spatially-Modulated Space-Time-Coded MIMO
13. Relay-Aided SM
14. SM in Heterogeneous Cellular Networks
15. SM for Visible Light Communications
16. Experimental Evaluation of SM
17. The Road Ahead – Open Research Challenges/Opportunities
18. Implementation Challenges of SM-MIMO

## Energy Efficiency (1/26)

- The EARTH power model is a very simple and elegant model that relates the **transmitted power** of a BS to **the total power consumed**
  - G. Auer et al., “Cellular Energy Evaluation Framework,” IEEE VTC-Spring, May 2011

$$P_{\text{supply}} = \begin{cases} N_{\text{RF}}P_0 + mN_{\text{RF}}P_t, & 0 < P_t \leq P_{\text{max}} \\ P_{\text{sleep}}, & P_t = 0. \end{cases}$$

- $P_{\text{supply}}$  is the total power supplied to the BS
- $N_{\text{RF}}$  is the number of RF chains at the BS
- $P_0$  is the power consumption per RF chain at the least transmission power
- $m$  is the slope of the load-depended power consumption
- $P_t$  is the RF transmit-power per antenna
- $P_{\text{max}}$  is the maximum transmit-power per antenna



## Energy Efficiency (2/26)

### POWER MODEL PARAMETERS FOR DIFFERENT BS (SOTA 2010)

BS type	$P_0$ (W)	$m$	$P_{\max}$ (W)	$P_{\text{sleep}}$ (W)
Macro	118.7	2.66	40.0	63
Micro	53.0	3.1	6.3	-
Pico	6.8	4.0	0.13	-
Femto	4.8	7.5	0.05	-

Simulation Parameters	Values
BS Type	Macro, Micro, Pico, Femto
Power Model Parameters	SOTA 2010
Carrier Frequency	2 GHz
Path Loss Model	3GPP NLOS [14]
Iterations (Number of Channels)	100000
Bandwidth	10 MHz
Operating Temperature	Outdoor:290 K, Indoor: 293.5 K

BS type	$d_{\min}$ (m)	$d_{\max}$ (m)
Macro	10	5000
Micro	10	1000
Pico	10	150
Femto	5	50

## *Energy Efficiency (3/26)*

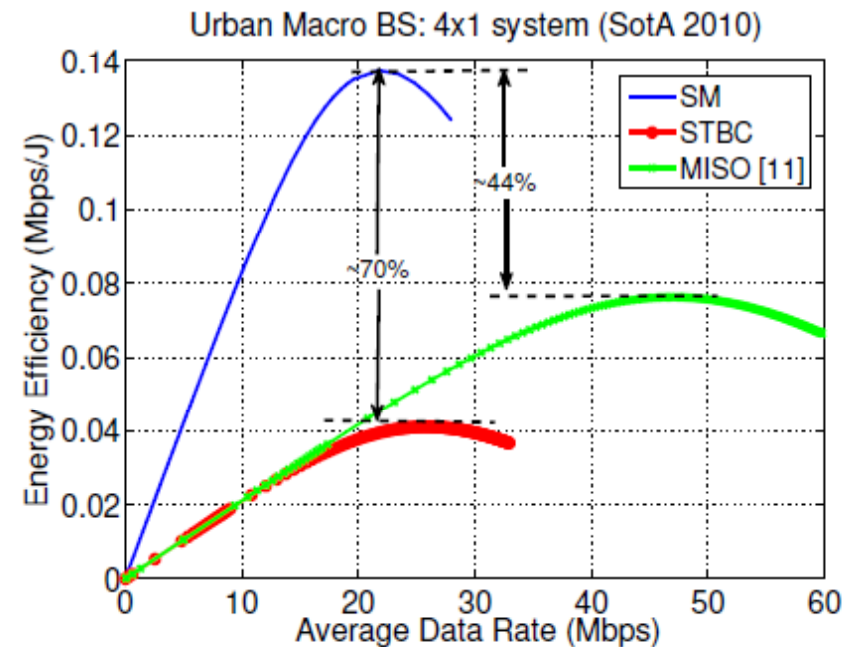
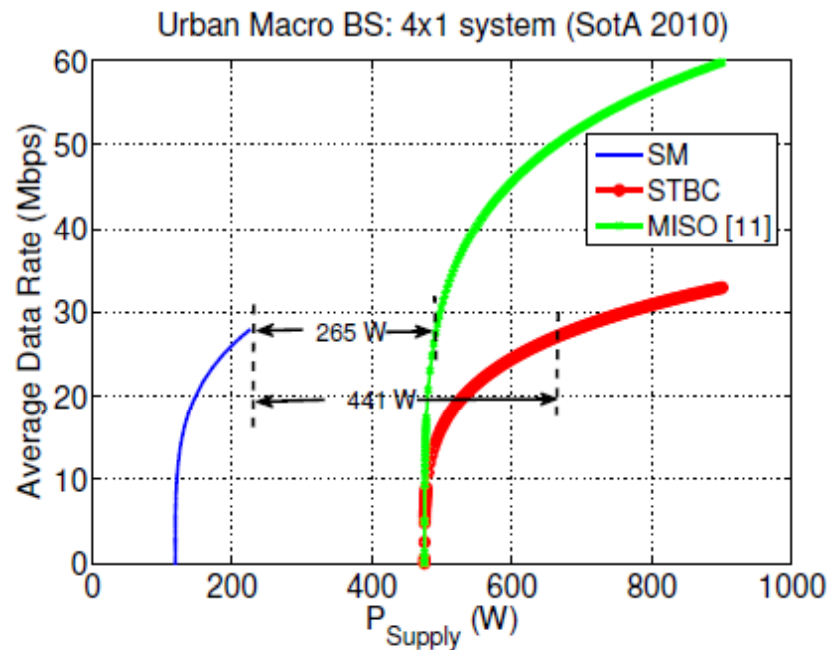
$$C_{\text{SM}} = C_1 + C_2 \approx C_1 = \frac{W}{N_t} \sum_{m=1}^{N_t} \log_2 \left( 1 + \frac{P}{N_0} \|\mathbf{h}_m\|_2^2 \right)$$

$$C_{\text{STBC}} = WR_{\text{STBC}} \log_2 \left( 1 + \frac{P}{N_0 N_t} \sum_{m=1}^{N_t} \|\mathbf{h}_m\|_2^2 \right)$$

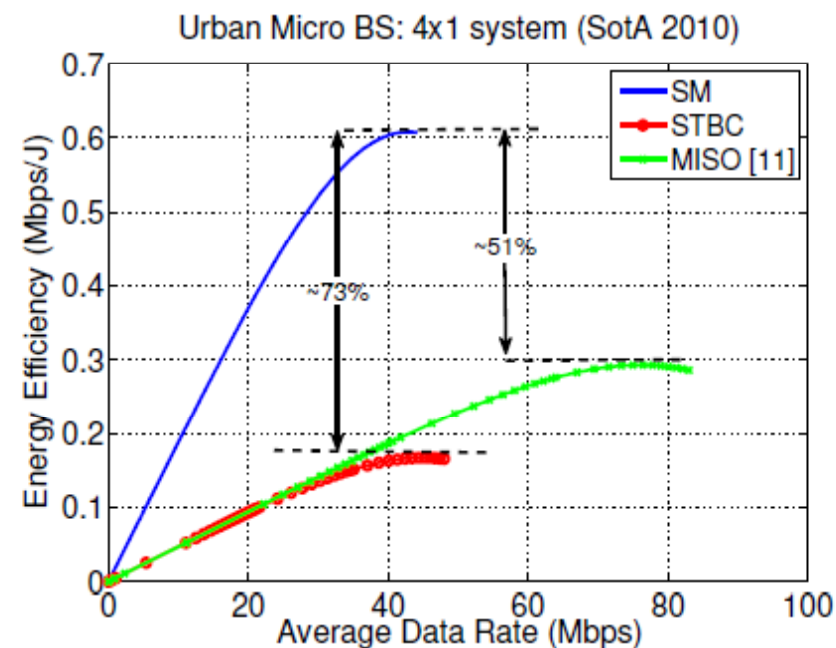
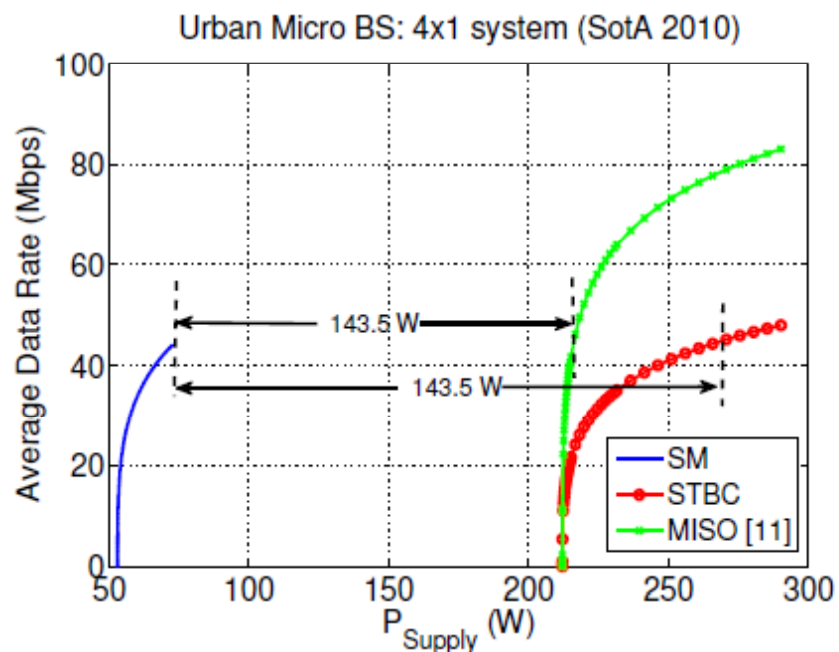
$$C_{\text{MISO}} (\text{CSIT}) = W \log_2 \left( 1 + \frac{P}{N_0} \|\mathbf{h}\|_2^2 \right)$$

$$\text{EE} = \frac{\text{Capacity}}{P_{\text{supply}}}$$

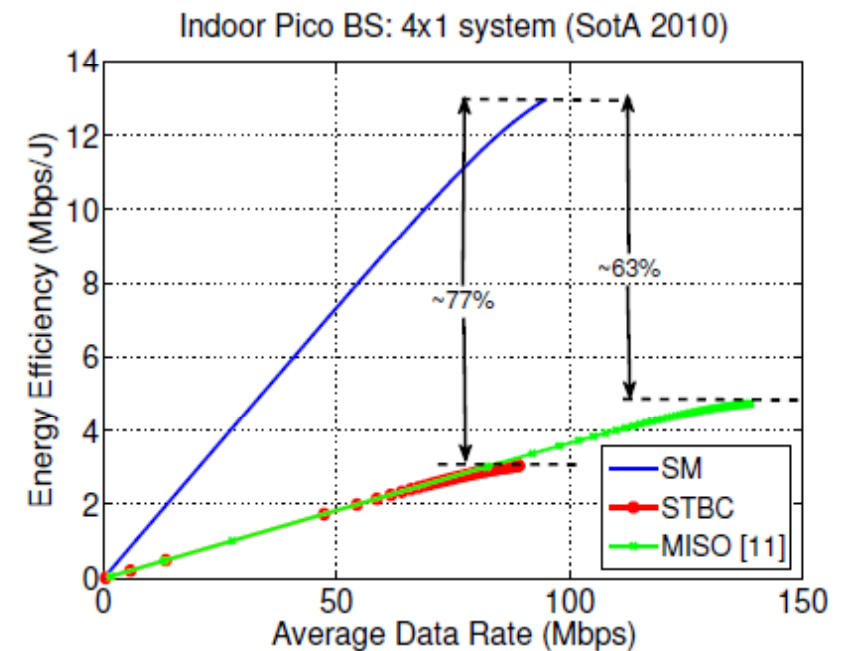
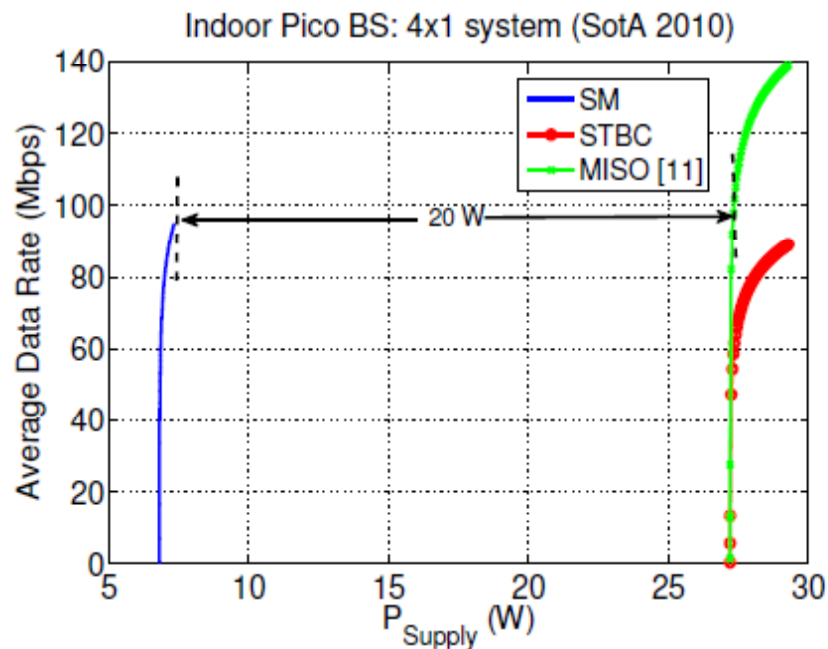
# Energy Efficiency (4/26)



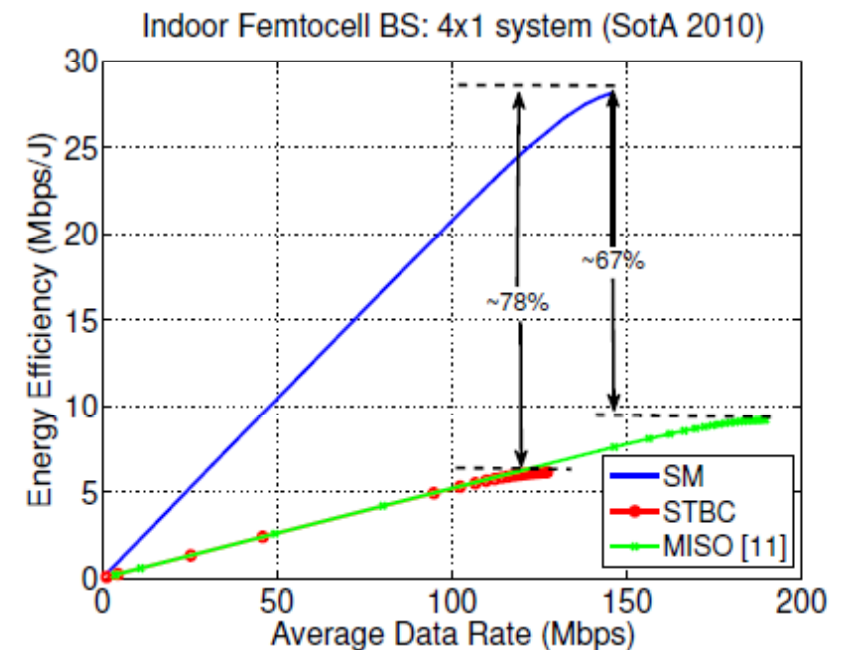
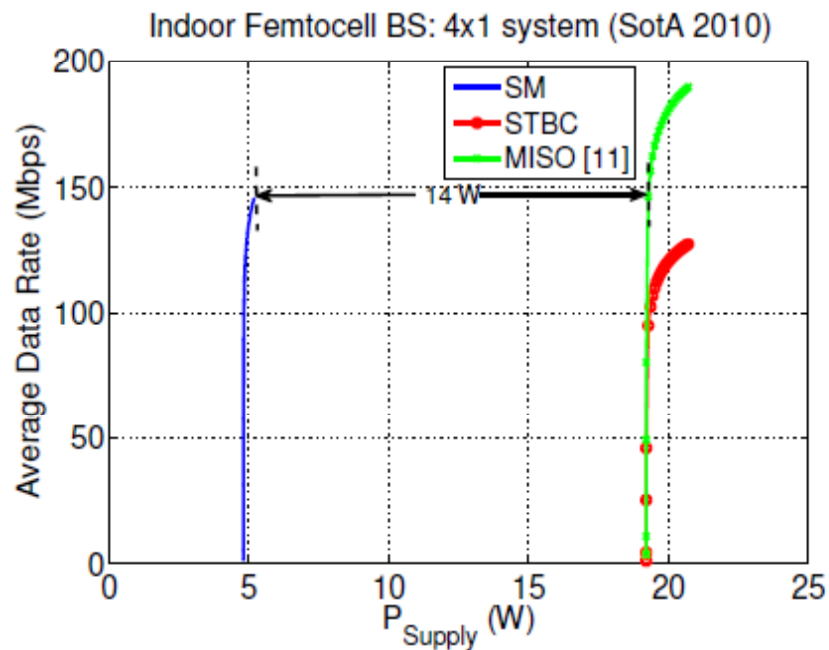
# Energy Efficiency (5/26)



# Energy Efficiency (6/26)



# Energy Efficiency (7/26)



## Energy Efficiency (8/26)

□ The following energy-model is considered:

- S. Cui, A. J. Goldsmith, and A. Bahai, “Energy-efficiency of MIMO and cooperative MIMO techniques in sensor networks”, IEEE JSAC, vol. 22, no. 6, pp. 1089–1098, Aug. 2004

$$E_{tot} = \xi E_b \times \frac{(4\pi d)^2}{\eta G_t G_r \lambda^2} M_l N_f + \frac{P_{circuit}}{R_b}$$

- $E_b$  is the bit energy
- $d$  is the transmission distance
- $G_t$  and  $G_r$  are transmit and receive antenna gains
- $N_f$  is the noise figure
- $\eta$  is the drain efficiency of the power amplifier
- $\xi$  is the peak-to-average-power-ratio (PAPR)
- $P_{circuit} = P_{DAC} + P_{mixer} + P_{filters} + P_{freqSynt}$
- $R_b$  is the bit rate
- $M_l$  is the link margin
- $\lambda$  is the wavelength

# Energy Efficiency (9/26)

□ The following energy-model is considered:

- $E_b$  is the bit energy  $R_b$  is the bit rate
- $d$  is the transmission distance  $M_l$  is the link margin
- $G_t$  and  $G_r$  are transmit and receive antenna gains
- $N_f$  is the noise figure  $\lambda$  is the wavelength
- $\eta$  is the drain efficiency of the power amplifier
- $\xi$  is the peak-to-average-power-ratio (PAPR)
- $P_{\text{circuit}} = P_{\text{DAC}} + P_{\text{mixer}} + P_{\text{filters}} + P_{\text{freqSynt}}$

$f_c = 2.5 \text{ GHz}$	$\eta = 0.35$
$d = 750 \text{ m}$	Symbol Rate = 15 ksymbols/sec
$G_t G_r = 5 \text{ dBi}$	$N_0 = -174 \text{ dBm/Hz}$
$P_{mix} = 30.3 \text{ mW}$	$M_l = 40 \text{ dB}$
Target ABEP = $10^{-5}$	$N_f = 10 \text{ dB}$
$P_{filt} = 2.5 \text{ mW}$	$P_{syn} = 50 \text{ mW}$



# Energy Efficiency (10/26)

## SM vs. Single-RF QAM – 4 bpcu

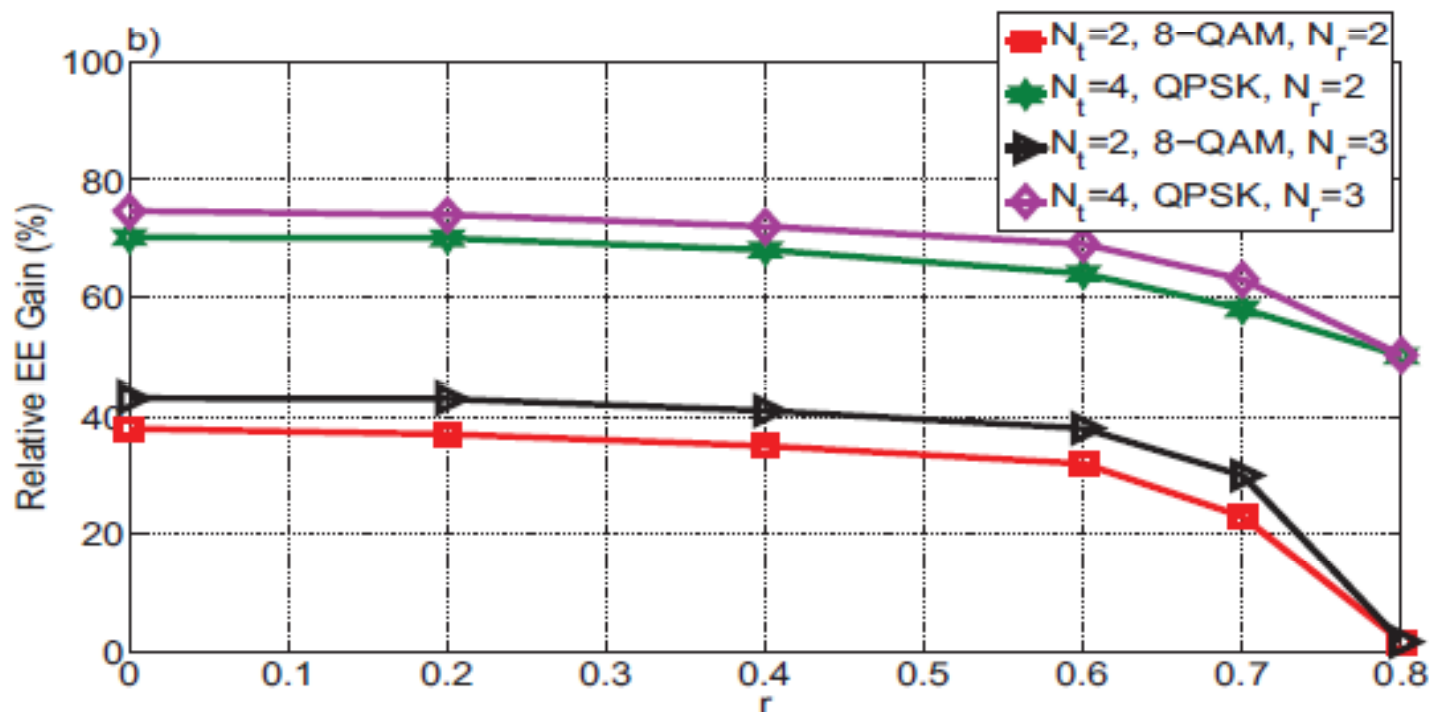


Fig. 2. SM and single antenna/MRC comparison in Rayleigh channels in terms of: a) ABEP vs.  $E_s/N_0$  and b) Relative energy gain vs. correlation factor.

# Energy Efficiency (11/26)

## SM vs. Single-RF QAM – 4 bpcu

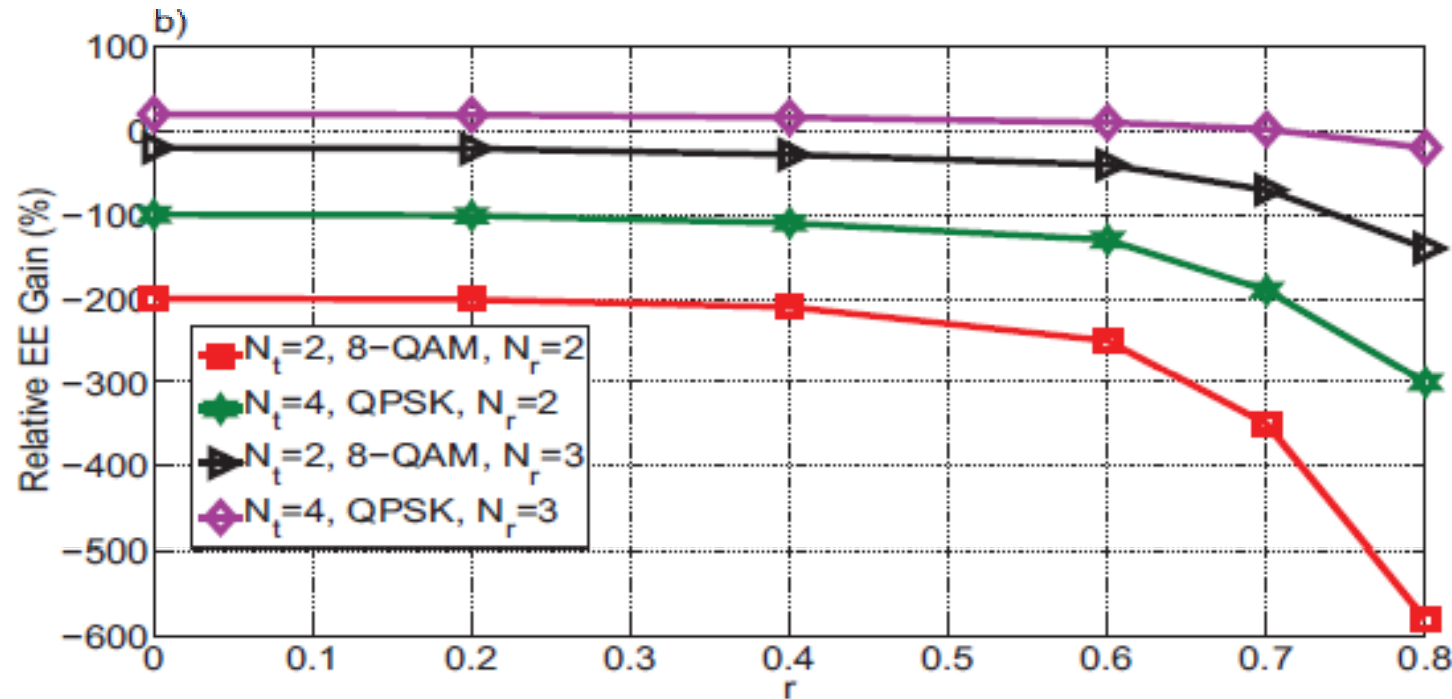


Fig. 3. SM and single antenna/MRC comparison in Nakagami- $m$  channels with  $m = 2$  in terms of: a) ABEP vs.  $E_s/N_0$  and b) Relative energy gain vs. correlation factor.

## Energy Efficiency (12/26)

### SM vs. Single-RF QAM – 4 bpcu

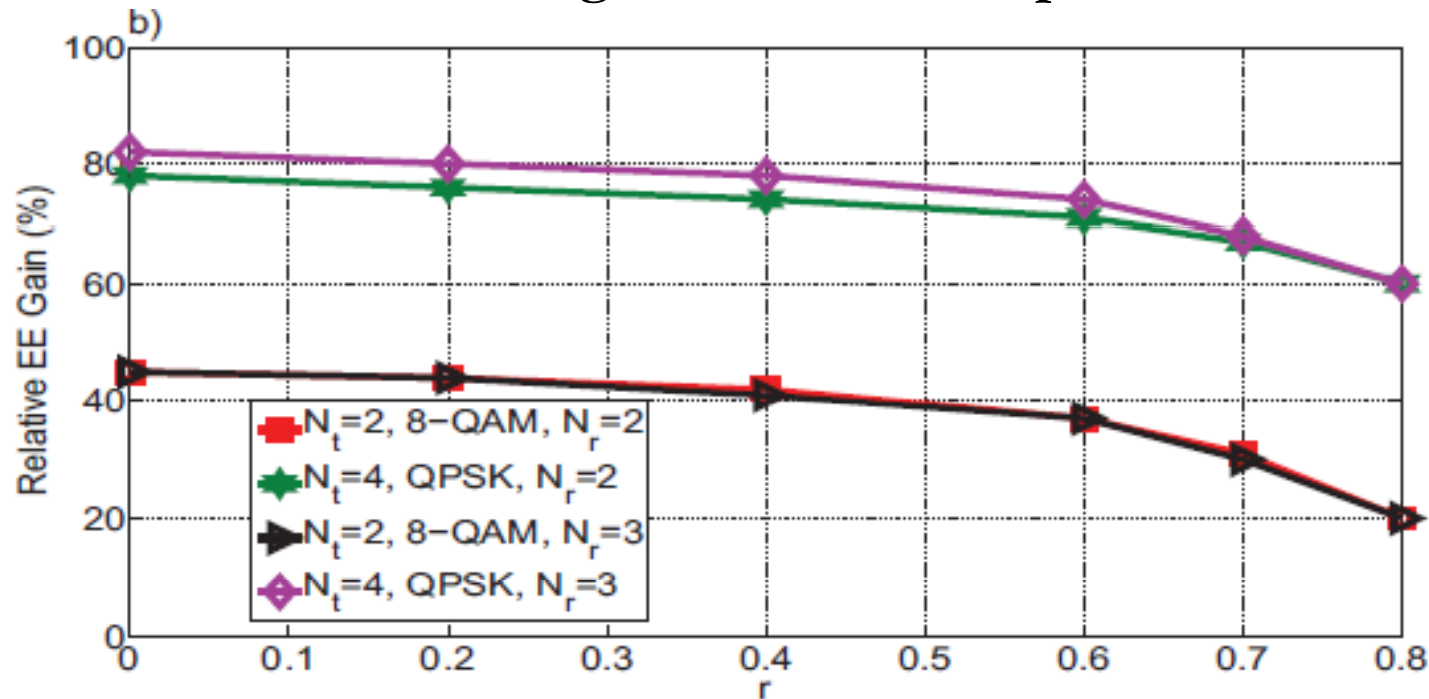


Fig. 4. SM and single antenna/MRC comparison in Nakagami- $m$  channels with  $m = 0.7$  in terms of: a) ABEP vs.  $E_s/N_0$  and b) Relative energy gain vs. correlation factor.

## Energy Efficiency (13/26)

### SM vs. Single-RF QAM – 4 bpcu

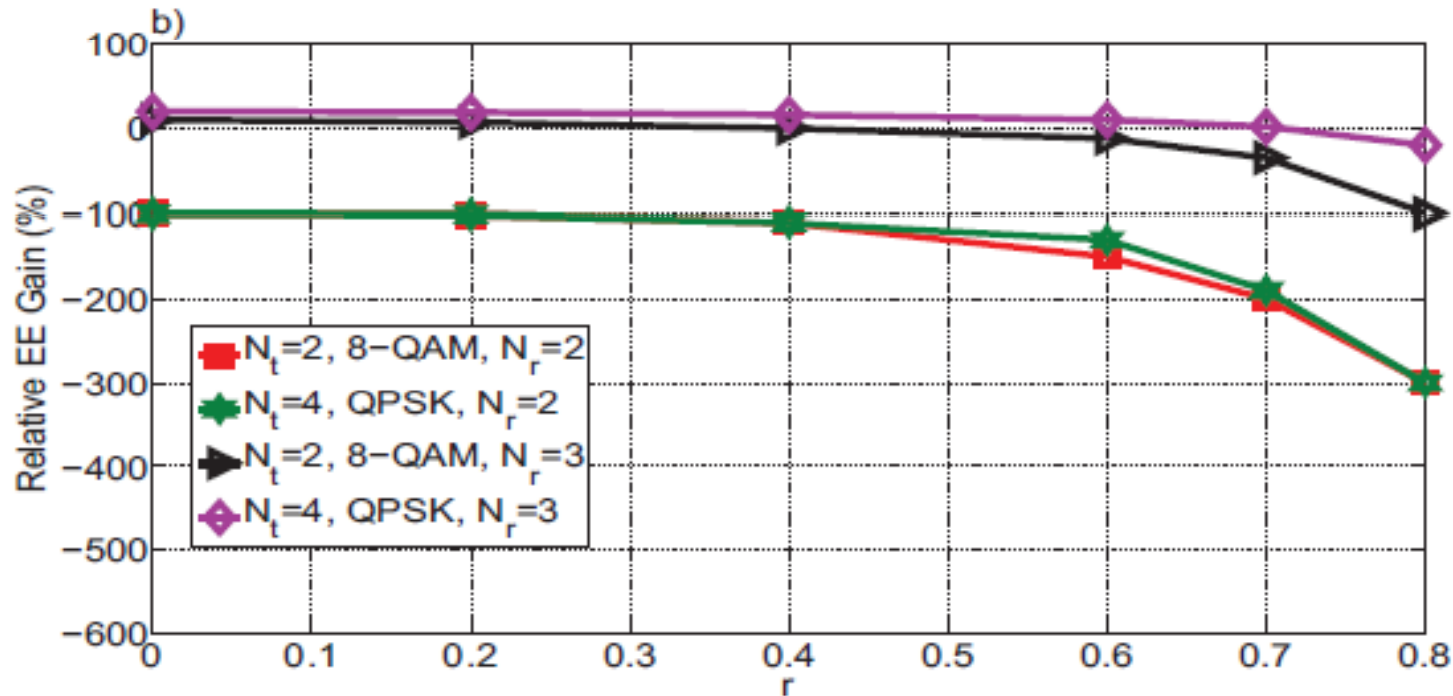


Fig. 5. SM and single antenna/MRC comparison in Weibull channels with  $b = 3$  in terms of: a) ABEP vs.  $E_s/N_0$  and b) Relative energy gain vs. correlation factor.

# Energy Efficiency (14/26)

## SM vs. Single-RF QAM – 4 bpcu

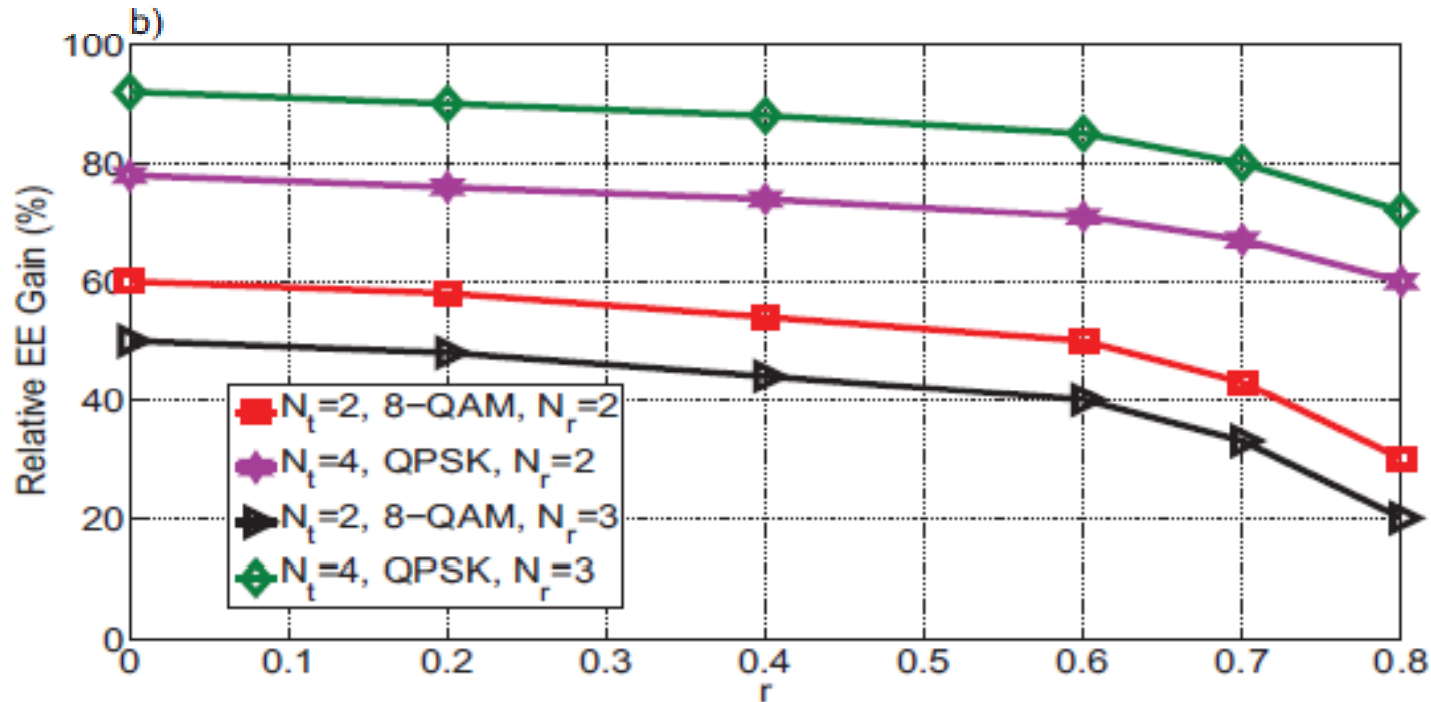


Fig. 6. SM and single antenna/MRC comparison in Weibull channels with  $b = 1.5$  in terms of: a) ABEP vs.  $E_s/N_0$  and b) Relative energy gain vs. correlation factor.

## *Energy Efficiency (15/26)*

---

- ❑ Energy efficiency is achieved by **non-equiprobable signaling** where less power-consuming modulation symbols are used more frequently to transmit a given amount of information
- ❑ The **energy efficient modulation design is formulated as a convex optimization problem**, where minimum achievable average symbol power consumption is derived with rate, performance, and hardware constraints



- ❑ **Energy-Efficient Hamming Code-Aided (EE-HSSK) modulation**



# Energy Efficiency (16/26)

## From GSSK ...

EXAMPLE OF GSSK ( $n_t = 2$ ) MODULATION ALPHABET AND BIT MAPPING FOR 3 BITS/S/Hz TRANSMISSION IN A SYSTEM WITH  $N_T = 5$

Source bits	GSSK symbols $\in \mathcal{A}^{(\text{GSSK})}$
000	$[0, 0, 0, 1, 1]^T$
001	$[0, 0, 1, 0, 1]^T$
010	$[0, 1, 0, 0, 1]^T$
011	$[1, 0, 0, 0, 1]^T$
100	$[0, 0, 1, 1, 0]^T$
101	$[0, 1, 0, 1, 0]^T$
110	$[1, 0, 0, 1, 0]^T$
111	$[0, 1, 1, 0, 0]^T$

### □ Limitations of GSSK:

- Transmission rate
- Selection of the spatial-constellation diagram
- System performance ( $d_{\min} = 2$ )

# Energy Efficiency (17/26)

## ... to (EE)-HSSK

EXAMPLE OF HSSK MODULATION ALPHABET AND BIT MAPPING FOR 4 BITS/S/Hz TRANSMISSION IN A SYSTEM WITH  $N_T = 5$

Source bits	HSSK symbols $\in \mathcal{A}^{(\text{HSSK})}$
0000	$[0, 0, 0, 0, 1]^T$
0001	$[0, 0, 0, 1, 0]^T$
0010	$[0, 0, 1, 0, 0]^T$
0011	$[0, 1, 0, 0, 0]^T$
0100	$[1, 0, 0, 0, 0]^T$
0101	$[0, 0, 1, 1, 1]^T$
0110	$[0, 1, 0, 1, 1]^T$
0111	$[1, 0, 0, 1, 1]^T$
1000	$[0, 1, 1, 0, 1]^T$
1001	$[1, 0, 1, 0, 1]^T$
1010	$[1, 1, 0, 0, 1]^T$
1011	$[0, 1, 1, 1, 0]^T$
1100	$[1, 0, 1, 1, 0]^T$
1101	$[1, 1, 0, 1, 0]^T$
1110	$[1, 1, 1, 0, 0]^T$
1111	$[1, 1, 1, 1, 1]^T$

### □ In HSSK:

- The set of antenna indices is fully utilized
- It employs a different number of 1's in each modulation symbol based on the Hamming code (in general, binary linear block code) construction technique
- Increased number of RF chains



# Energy Efficiency (18/26)

## Problem Formulation

- ❑ The objective of EE-HSSK modulation is to **design an alphabet and the symbol a priori probabilities** so that **minimum average symbol power per transmission is achieved**, while the target transmission rate (**spectral-efficiency** constraint), the minimum Hamming distance property (**performance** constraint), and the maximum required number of RF chains (**hardware** constraint) are met
- ❑ Given a code  $C = \{C_i\}$  with the specified minimum distance property
- ❑ Given that each element in  $C_i$  requires  $i$  RF chains at the transmitter
- ❑ Given that each element in  $C_i$  consumes power equal to  $i$
- ❑ Given that the maximum number of RF chains is restricted to  $i \leq M$
- ❑ Then...

# Energy Efficiency (19/27)

## Problem Formulation

□ ... the design problem is mathematically formulated as:

$$\begin{aligned} \min_{P_i} \quad & \sum_{\substack{i: \mathcal{C}_i \subseteq \mathcal{C} \\ i \leq \bar{M}}} i |\mathcal{C}_i| P_i \\ \text{s.t.} \quad & \sum_{\substack{i: \mathcal{C}_i \subseteq \mathcal{C} \\ i \leq \bar{M}}} |\mathcal{C}_i| P_i = 1 \\ & \sum_{\substack{i: \mathcal{C}_i \subseteq \mathcal{C} \\ i \leq \bar{M}}} |\mathcal{C}_i| r(P_i) \geq m \end{aligned} \quad (9)$$

The a priori probabilities of all symbols in the alphabet sum to one, and  $P_i = 0$  if  $i > M$

The target information rate of  $m$  bits is met, as described by Shannon's entropy formula

where  $P_i$  is the *a priori* probability of each symbol in  $\mathcal{C}_i$ , i.e.,  $P_i \triangleq P(\mathbf{x}), \mathbf{x} \in \mathcal{C}_i$ , and

$$r(P_i) = \begin{cases} -P_i \log_2 P_i, & \text{if } P_i > 0 \\ 0, & \text{if } P_i = 0 \\ -\infty, & \text{otherwise} \end{cases} \quad (10)$$

### Optimal Solution

- The optimization problem has a linear objective function subject to an affine equality and convex inequality constraints. Therefore, it is convex with a globally optimal solution, which can be found using the Lagrange multiplier method
- The optimal a priori transmission probabilities  $\mathbf{P}_i$  associated to the Lagrange multipliers  $\lambda_1$  and  $\lambda_2$  can be computed as follows:

$$i|C_i| + \lambda_1^*|C_i| + \lambda_2^*|C_i|\left(\log_2 P_i^* + \frac{1}{\log 2}\right) = 0. \quad (14)$$

Arranging the terms yields  $P_i^* = \alpha\beta^i$ , where  $\alpha = (1/e)2^{-\lambda_1^*/\lambda_2^*}$  and  $\beta = 2^{-1/\lambda_2^*}$ . Normalizing  $P_i^*$ 's according to the equality constraint of Problem (9), we obtain

$$P_i^* = \frac{\beta^i}{\sum_{i: C_i \subseteq C, i \leq M} |C_i| \beta^i}, \quad 0 < \beta \leq 1. \quad (15)$$

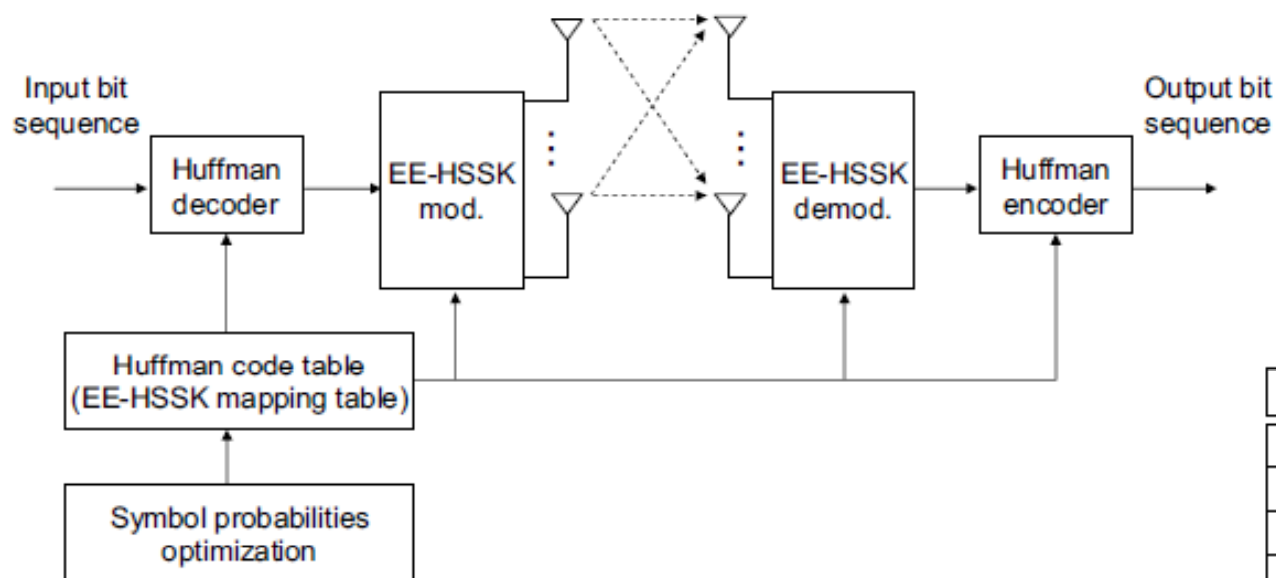
# Energy Efficiency (21/26)

## Optimal Solution

- ❑ The value of  $\beta$  determines the optimal a priori probabilities for the alphabet:
  - If  $\beta = 1$ , all codewords in  $C$  are included in the alphabet equiprobably to achieve the highest information rate. The cost is to have the largest average symbol power consumption
  - If  $\beta = 0^+$ , only the least power-consuming codewords in  $C$  are included in the alphabet equiprobably
- ❑ The solution provides the optimal symbol a priori probabilities. However, no information is given for accomplishing the bit mapping. Variable-length coding is proposed for creating an efficient bit-string representation of symbols with unequal a priori probabilities: **Huffman coding**
  - The length of the bit strings is roughly reversely proportional to the symbol power. Since longer bit strings appear less frequently in a random input sequence, symbols more power-consuming are used less frequently to achieve energy efficiency

# Energy Efficiency (22/26)

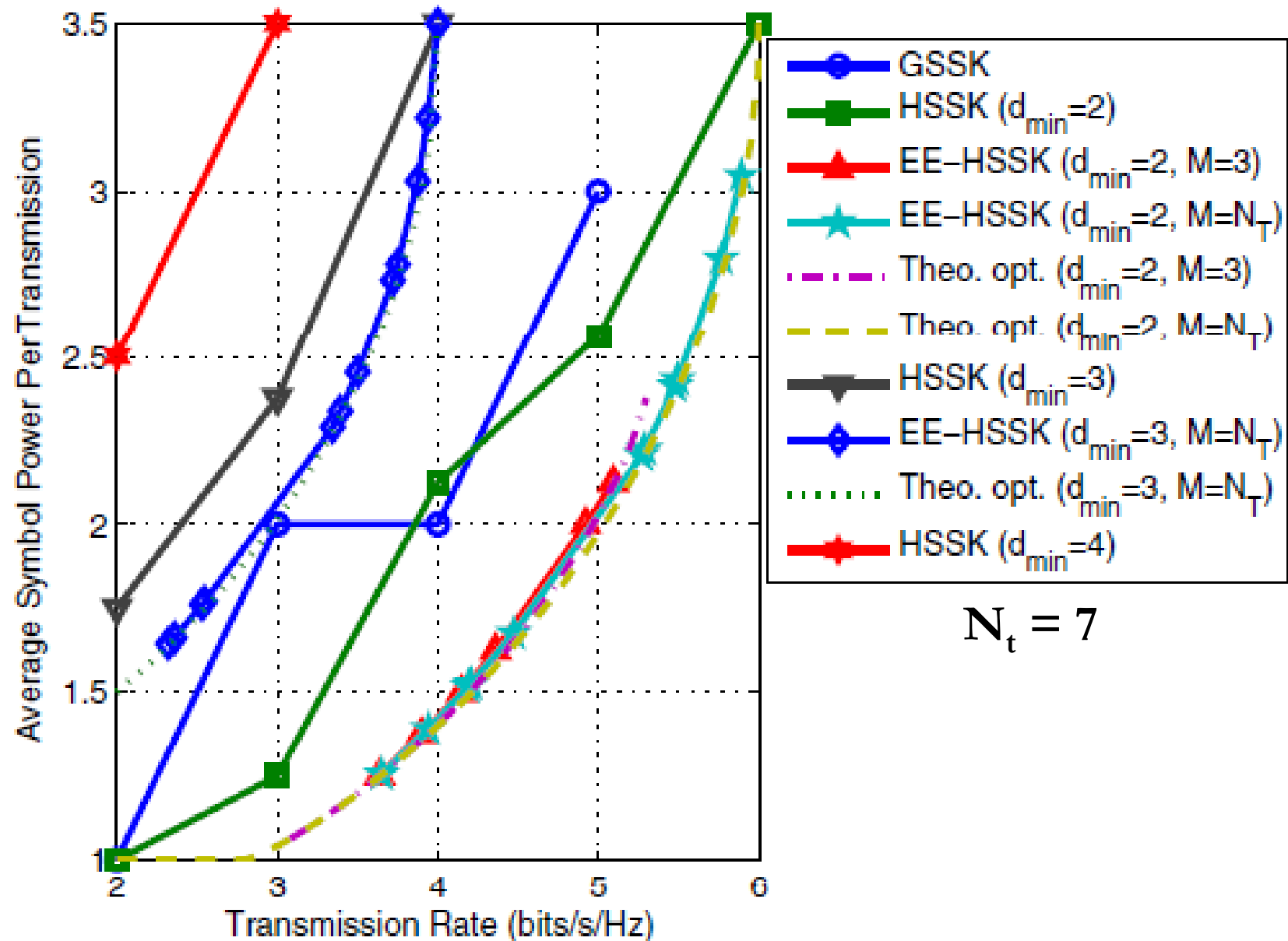
## Implementation



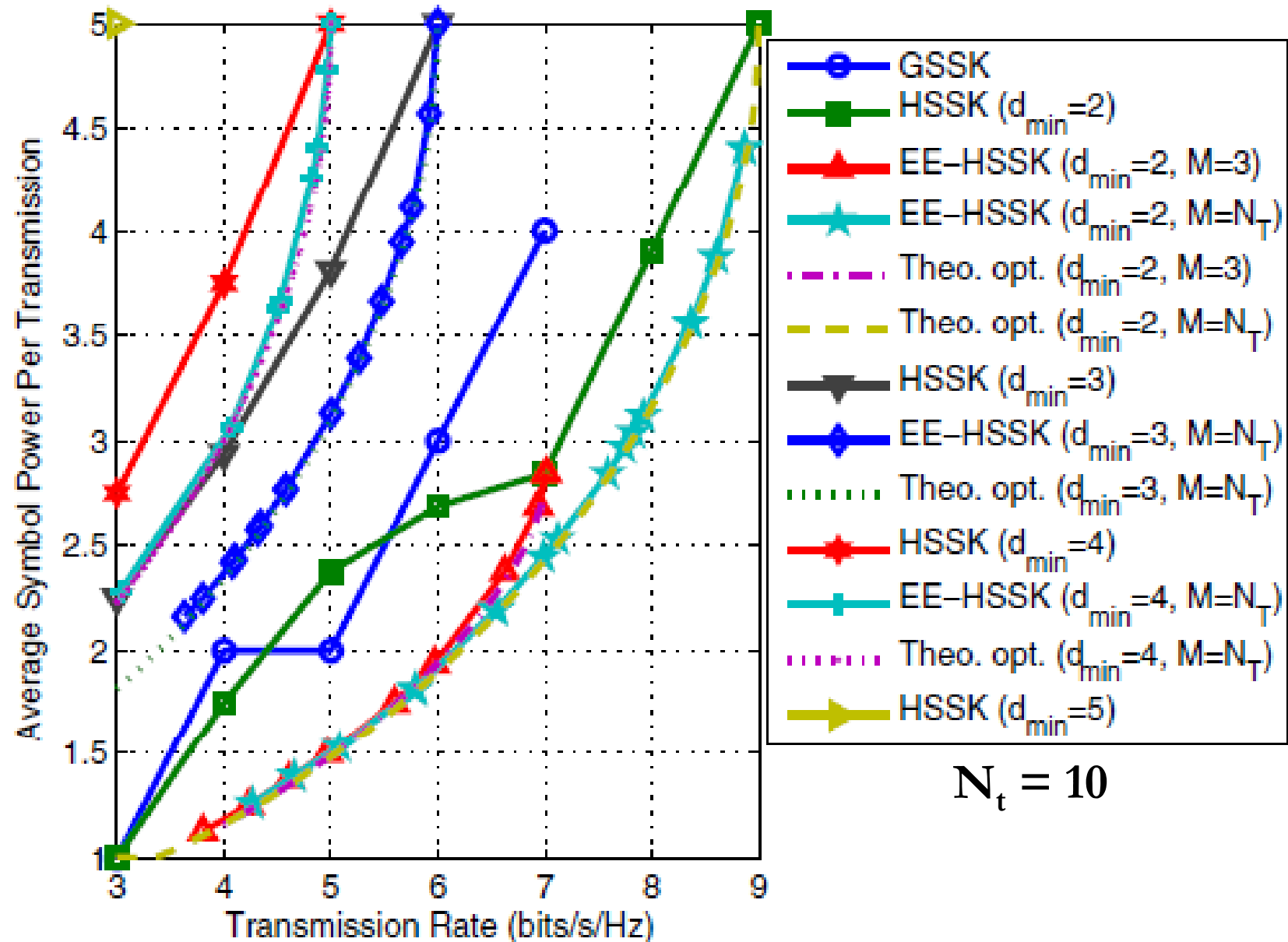
EXAMPLE OF EE-HSSK ( $M = 3$ ) MODULATION ALPHABET AND BIT MAPPING FOR APPROXIMATELY 3 BITS/S/Hz TRANSMISSION IN A SYSTEM WITH  $N_T = 5$

Source bits	EE-HSSK symbols $\in \mathcal{A}^{(\text{EE-HSSK})}$
00	$[0, 0, 0, 0, 1]^T$
01	$[0, 0, 0, 1, 0]^T$
100	$[0, 0, 1, 0, 0]^T$
101	$[0, 1, 0, 0, 0]^T$
110	$[1, 0, 0, 0, 0]^T$
111000	$[0, 0, 1, 1, 1]^T$
111001	$[0, 1, 0, 1, 1]^T$
111010	$[1, 0, 0, 1, 1]^T$
111011	$[0, 1, 1, 0, 1]^T$
111100	$[1, 0, 1, 0, 1]^T$
111101	$[1, 1, 0, 0, 1]^T$
1111100	$[0, 1, 1, 1, 0]^T$
1111101	$[1, 0, 1, 1, 0]^T$
1111110	$[1, 1, 0, 1, 0]^T$
1111111	$[1, 1, 1, 0, 0]^T$

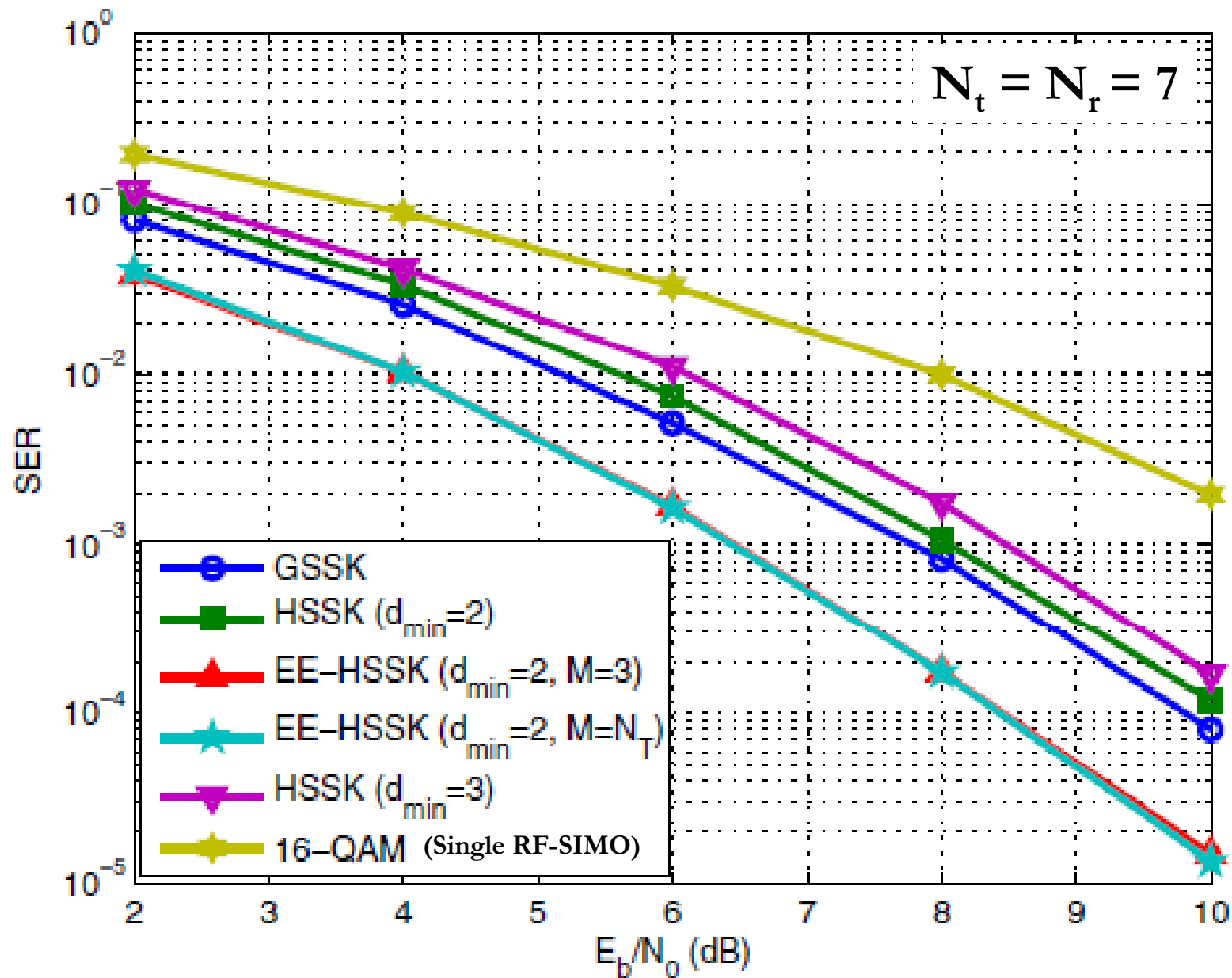
## Energy Efficiency (23/26)



# Energy Efficiency (24/26)

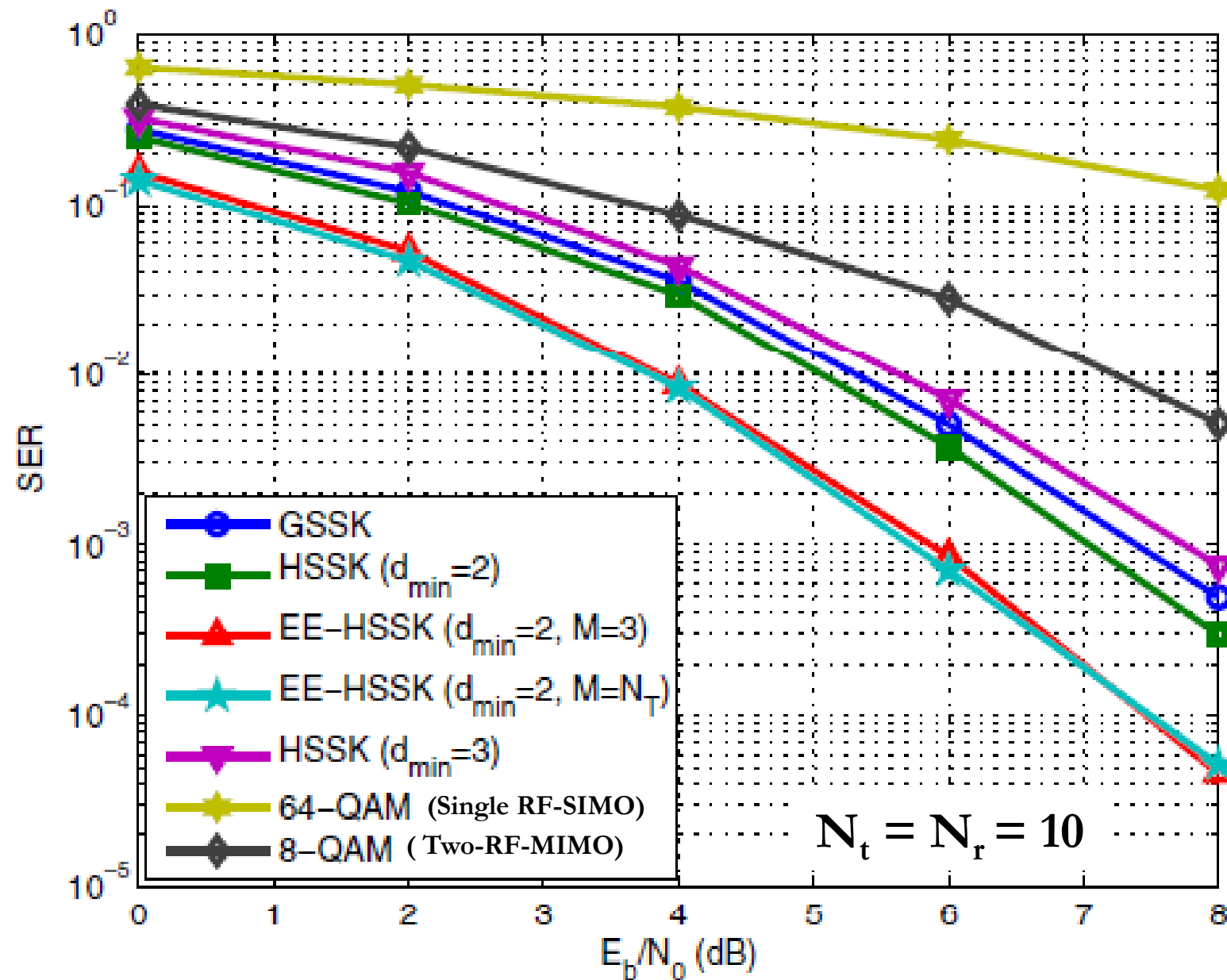


## Energy Efficiency (25/26)





## Energy Efficiency (26/26)



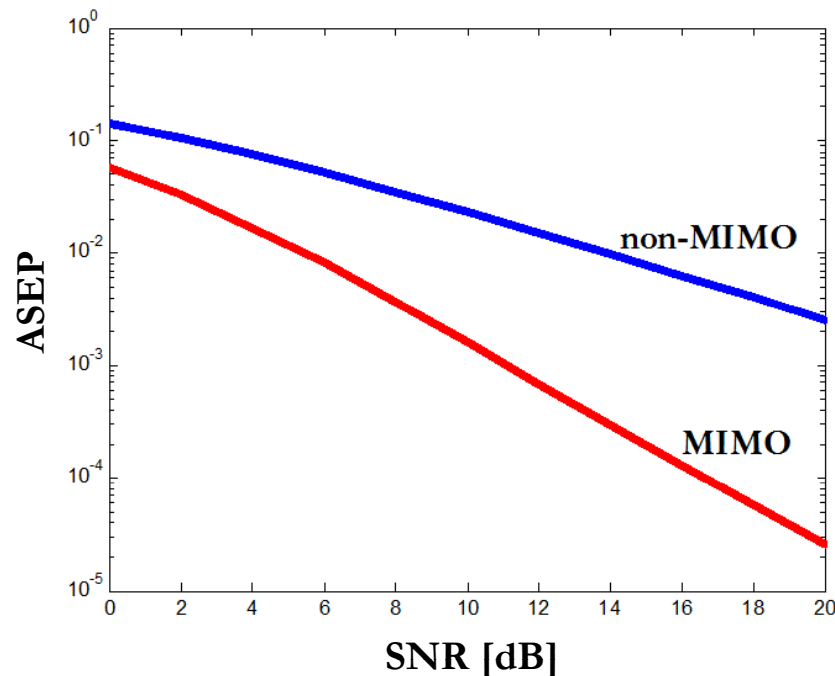
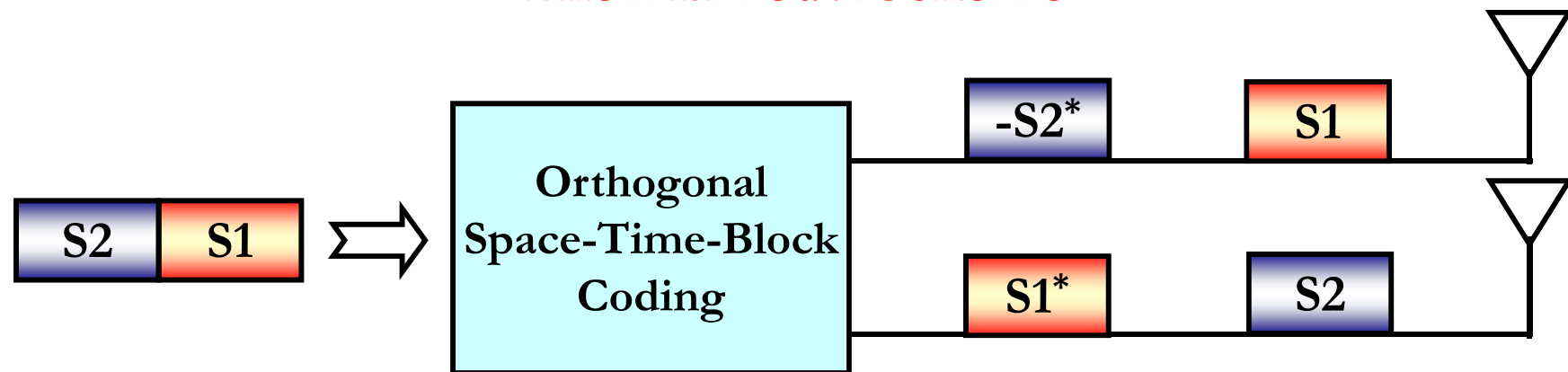
# *Outline*

---

1. Introduction and Motivation behind SM-MIMO
2. History of SM Research and Research Groups Working on SM
3. Transmitter Design – Encoding
4. Receiver Design – Demodulation
5. Error Performance (Numerical Results and Main Trends)
6. Achievable Capacity
7. Channel State Information at the Transmitter
8. Imperfect Channel State Information at the Receiver
9. Multiple Access Interference
10. Energy Efficiency
11. **Transmit-Diversity for SM**
12. Spatially-Modulated Space-Time-Coded MIMO
13. Relay-Aided SM
14. SM in Heterogeneous Cellular Networks
15. SM for Visible Light Communications
16. Experimental Evaluation of SM
17. The Road Ahead – Open Research Challenges/Opportunities
18. Implementation Challenges of SM-MIMO

# Transmit-Diversity for SM (1/61)

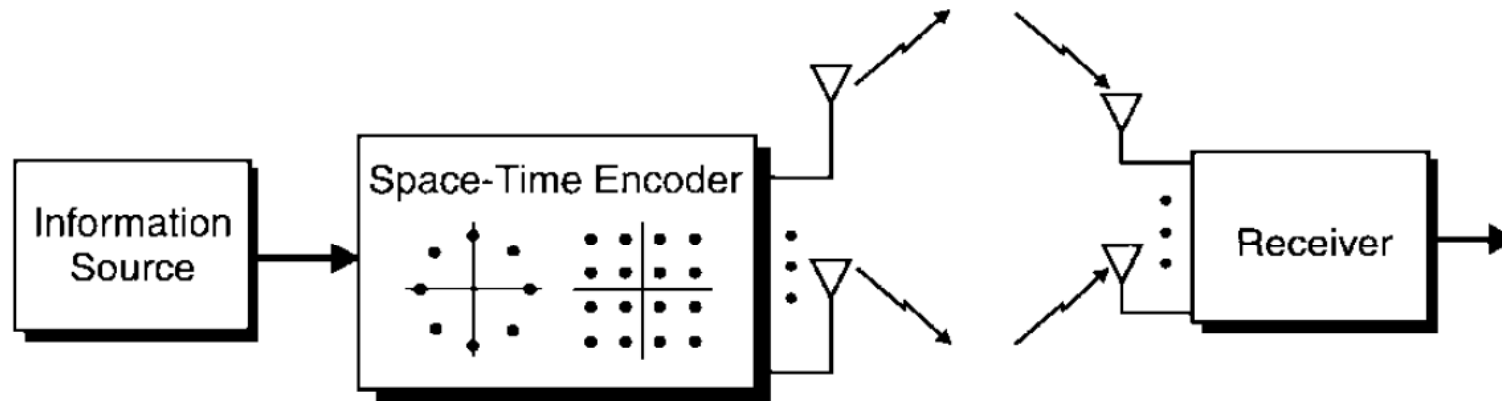
## The Alamouti Scheme



$$\mathcal{G}_2 = \begin{pmatrix} x_1 & x_2 \\ -x_2^* & x_1^* \end{pmatrix}$$

# Transmit-Diversity for SM (2/61)

## Orthogonal Space-Time Block Codes (OSTBCs)

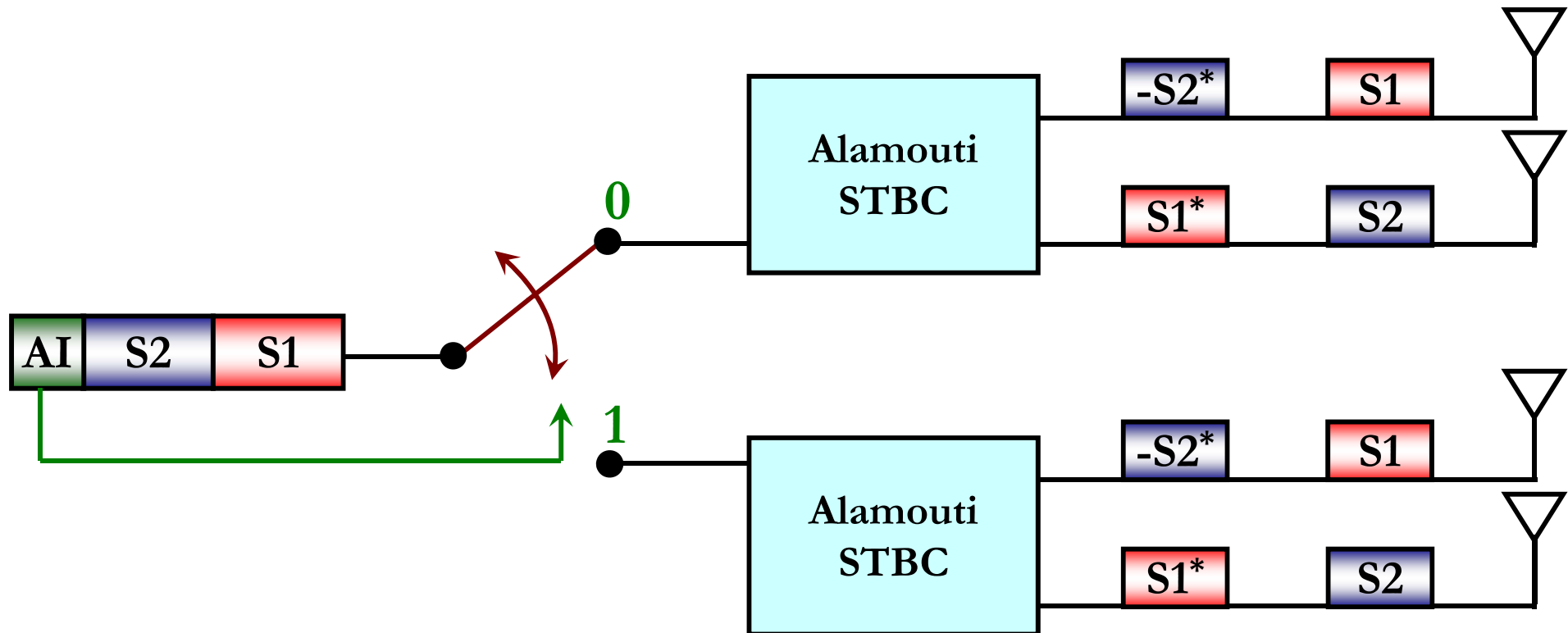


$$\mathcal{H}_3 = \begin{pmatrix} x_1 & x_2 & \frac{x_3}{\sqrt{2}} \\ -x_2^* & x_1^* & \frac{x_3}{\sqrt{2}} \\ \frac{x_3^*}{\sqrt{2}} & \frac{x_3^*}{\sqrt{2}} & \frac{(-x_1 - x_1^* + x_2 - x_2^*)}{2} \\ \frac{x_3^*}{\sqrt{2}} & -\frac{x_3^*}{\sqrt{2}} & \frac{(x_2 + x_2^* + x_1 - x_1^*)}{2} \end{pmatrix}$$

$$\mathcal{H}_4 = \begin{pmatrix} x_1 & x_2 & \frac{x_3}{\sqrt{2}} & \frac{x_3}{\sqrt{2}} \\ -x_2^* & x_1^* & \frac{x_3}{\sqrt{2}} & -\frac{x_3}{\sqrt{2}} \\ \frac{x_3^*}{\sqrt{2}} & \frac{x_3^*}{\sqrt{2}} & \frac{(-x_1 - x_1^* + x_2 - x_2^*)}{2} & \frac{(-x_2 - x_2^* + x_1 - x_1^*)}{2} \\ \frac{x_3^*}{\sqrt{2}} & -\frac{x_3^*}{\sqrt{2}} & \frac{(x_2 + x_2^* + x_1 - x_1^*)}{2} & -\frac{(x_1 + x_1^* + x_2 - x_2^*)}{2} \end{pmatrix}$$

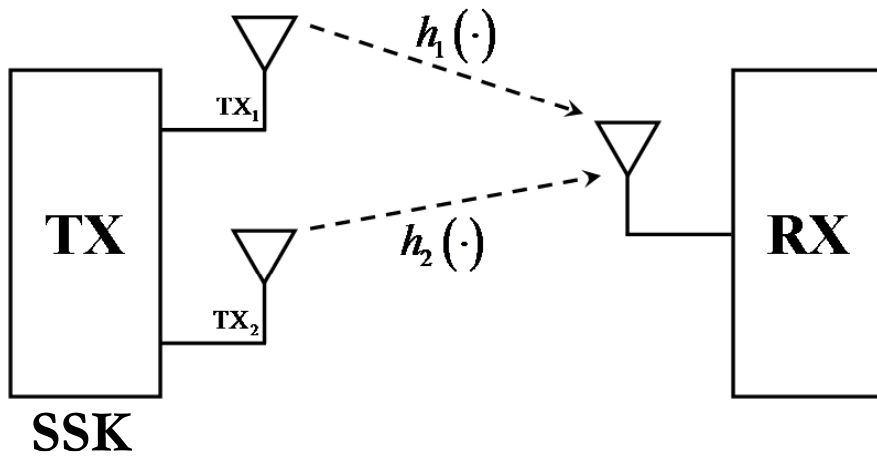
# Transmit-Diversity for SM (3/61)

## Opportunities and Challenges for SM



- ❑ Opportunity: Transmit-diversity with rate greater than one
- ❑ Challenge: Transmit-diversity with rate greater than one and single-stream decoding complexity

# Transmit-Diversity for SM (4/61)



$$\begin{cases} h_1(t) = \beta_1 \exp(j\varphi_1) \delta(t - \tau_0) \\ h_2(t) = \beta_2 \exp(j\varphi_2) \delta(t - \tau_0) \end{cases}$$

$$\begin{cases} \tilde{s}_1(t | \{m_n\}_{n=1}^2) = \sqrt{E_m} \beta_1 \exp(j\varphi_1) s_1(t | \{m_n\}_{n=1}^2) \\ \tilde{s}_2(t | \{m_n\}_{n=1}^2) = \sqrt{E_m} \beta_2 \exp(j\varphi_2) s_2(t | \{m_n\}_{n=1}^2) \end{cases}$$

$$\begin{cases} r(t | m_1) = \tilde{s}_1(t | m_1) + \tilde{s}_2(t | m_1) + n(t) = \bar{s}_1(t) + n(t) \\ r(t | m_2) = \tilde{s}_1(t | m_2) + \tilde{s}_2(t | m_2) + n(t) = \bar{s}_2(t) + n(t) \end{cases}$$

$$\hat{m} = \begin{cases} m_1 & \text{if } D_1 \geq D_2 \\ m_2 & \text{if } D_2 < D_1 \end{cases}$$

$$\begin{cases} D_1 = \text{Re} \left\{ \int_{T_m} r(t) \bar{s}_1^*(t) dt \right\} - \frac{1}{2} \int_{T_m} \bar{s}_1(t) \bar{s}_1^*(t) dt \\ D_2 = \text{Re} \left\{ \int_{T_m} r(t) \bar{s}_2^*(t) dt \right\} - \frac{1}{2} \int_{T_m} \bar{s}_2(t) \bar{s}_2^*(t) dt \end{cases}$$

# Transmit-Diversity for SM (5/61)

## Transmitted Signal:

- If  $\mathbf{m}_1$  needs to be transmitted:  $\text{TX}_1$  is active and  $\text{TX}_2$  radiates no power
- If  $\mathbf{m}_2$  needs to be transmitted:  $\text{TX}_1$  and  $\text{TX}_2$  are both active

$$\begin{cases} s_1(t|m_1) = s_1(t|m_2) = s_2(t|m_2) = 1 \\ s_2(t|m_1) = 0 \end{cases}$$

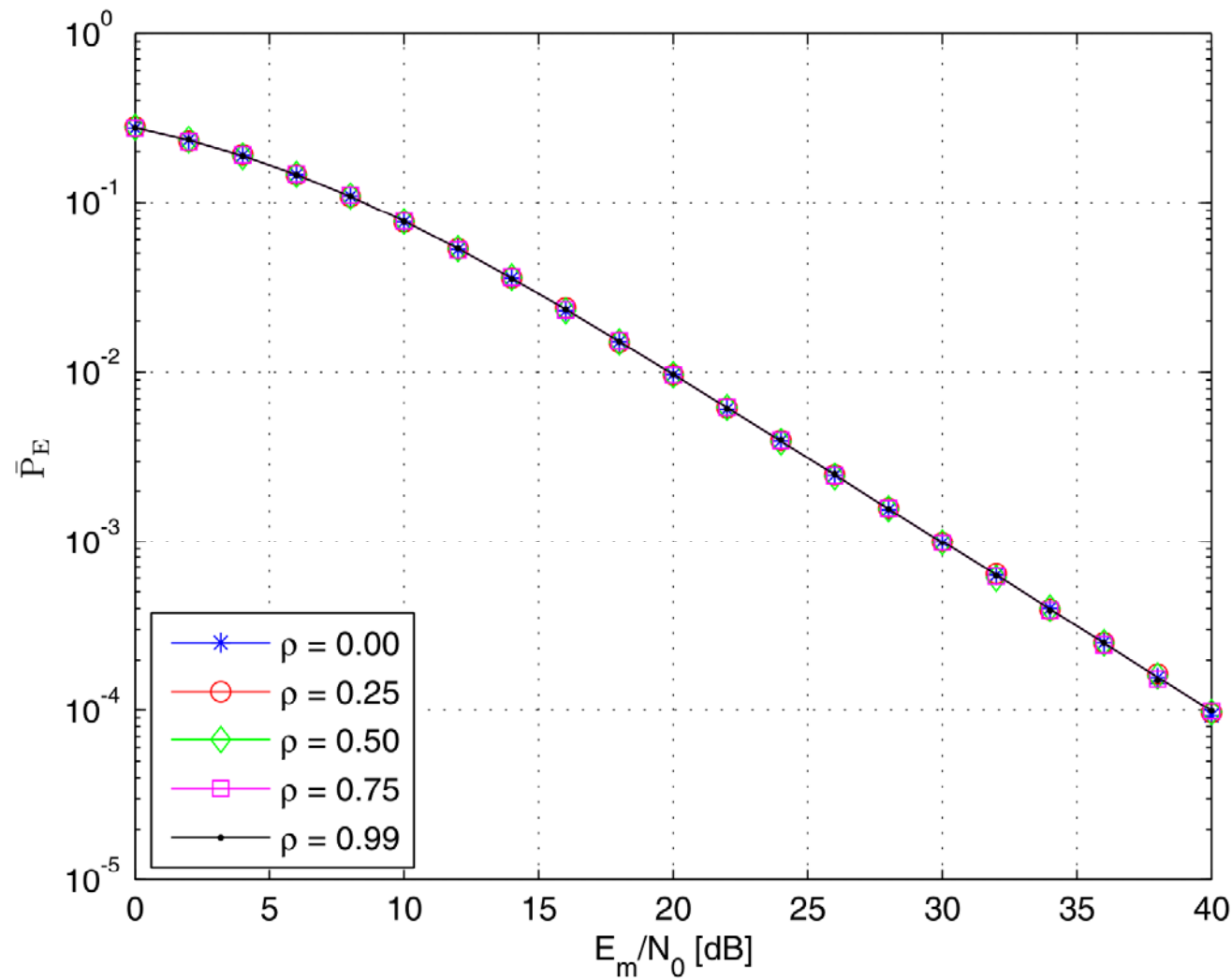
## Received Signal:

$$\begin{cases} r(t|m_1) = \sqrt{E_m} \beta_1 \exp(j\varphi_1) + n(t) \\ r(t|m_2) = \sqrt{E_m} \beta_1 \exp(j\varphi_1) + \sqrt{E_m} \beta_2 \exp(j\varphi_2) + n(t) \end{cases}$$

## Error Probability:

$$\text{BEP} = Q\left(\sqrt{\frac{E_m}{4N_0}} \beta_2\right) \Rightarrow \text{ABEP} = \frac{1}{2} - \frac{1}{2} \sqrt{\frac{\sigma_2^2(E_m/4N_0)}{1 + \sigma_2^2(E_m/4N_0)}}$$

## Transmit-Diversity for SM (6/61)





# Transmit-Diversity for SM (7/61)

## Transmitted Signal:

- If  $\mathbf{m}_1$  needs to be transmitted:  $\text{TX}_1$  is active and  $\text{TX}_2$  radiates no power
- If  $\mathbf{m}_2$  needs to be transmitted:  $\text{TX}_1$  radiates no power and  $\text{TX}_2$  is active

$$\begin{cases} s_1(t|m_1) = s_2(t|m_2) = 1 \\ s_1(t|m_2) = s_2(t|m_1) = 0 \end{cases}$$

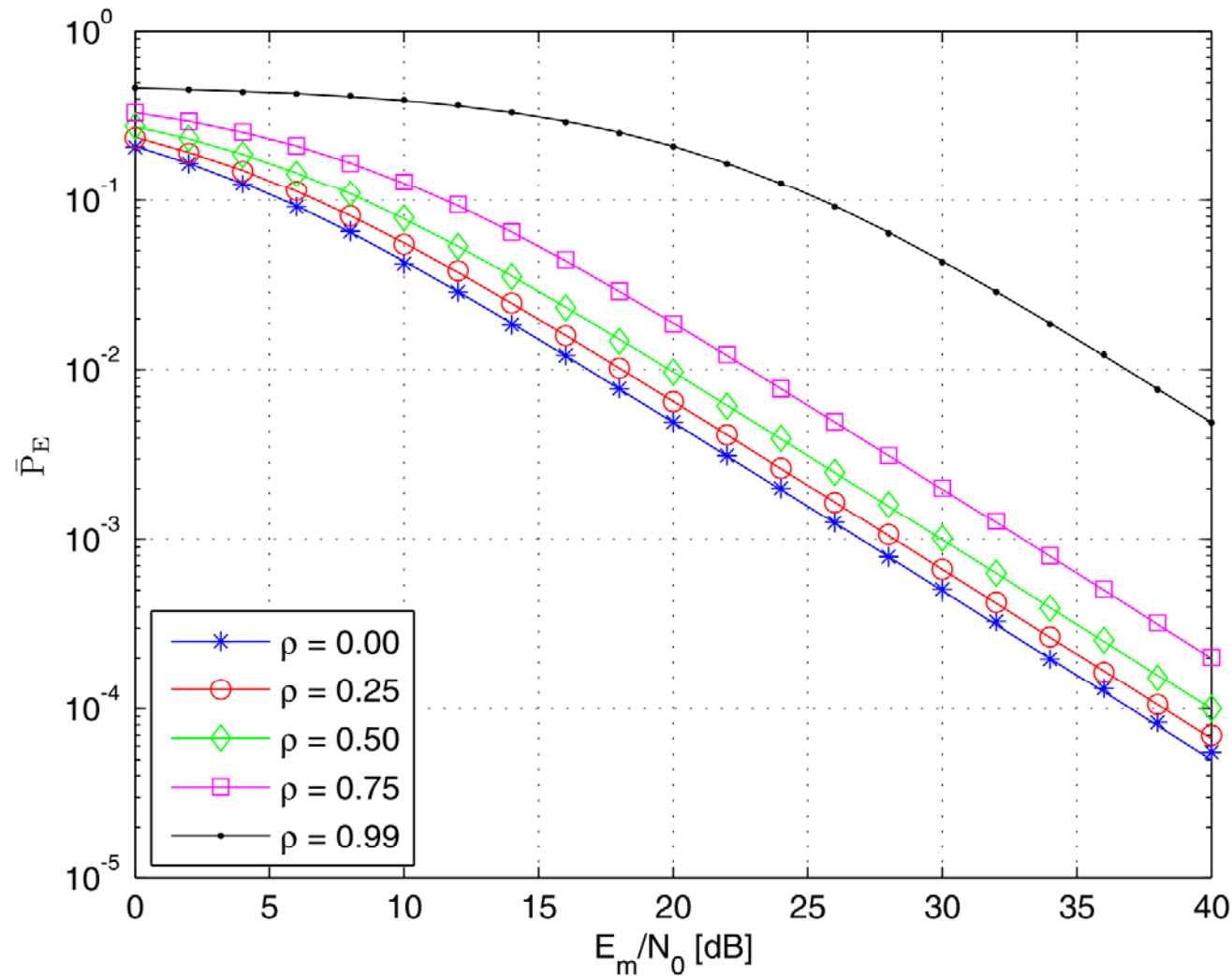
## Received Signal:

$$\begin{cases} r(t|m_1) = \sqrt{E_m} \beta_1 \exp(j\varphi_1) + n(t) \\ r(t|m_2) = \sqrt{E_m} \beta_2 \exp(j\varphi_2) + n(t) \end{cases}$$

## Error Probability:

$$\text{BEP} = Q\left(\sqrt{\frac{E_m}{4N_0}} |\beta_2 \exp(j\varphi_2) - \beta_1 \exp(j\varphi_1)|^2\right) \Rightarrow \begin{cases} \text{ABEP} = \frac{1}{2} - \frac{1}{2} \sqrt{\frac{\bar{\sigma}^2 (E_m/4N_0)}{1 + \bar{\sigma}^2 (E_m/4N_0)}} \\ \bar{\sigma}^2 = \sigma_1^2 + \sigma_2^2 - 2\rho\sigma_1\sigma_2 \end{cases}$$

# Transmit-Diversity for SM (8/61)



# Transmit-Diversity for SM (9/61)

## Transmitted Signal (TOSD-SSK):

- If  $\mathbf{m}_1$  needs to be transmitted: TX<sub>1</sub> is active and TX<sub>2</sub> radiates no power
- If  $\mathbf{m}_2$  needs to be transmitted: TX<sub>1</sub> radiates no power and TX<sub>2</sub> is active

$$\begin{cases} s_1(t|m_1) = w_1(t) \\ s_2(t|m_2) = w_2(t) \\ s_1(t|m_2) = s_2(t|m_1) = 0 \end{cases} \quad \text{and} \quad \int_{-\infty}^{+\infty} w_1(t-\tau_1) w_2(t-\tau_2) dt = 0$$

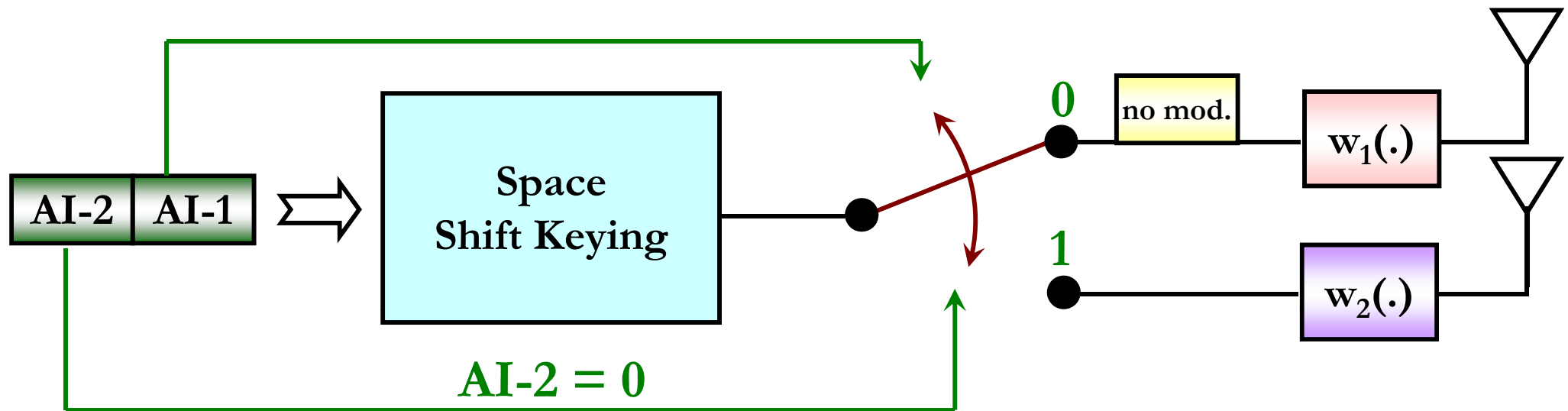
## Received Signal:

$$\begin{cases} r(t|m_1) = \sqrt{E_m} \beta_1 \exp(j\varphi_1) w_1(t) + n(t) \\ r(t|m_2) = \sqrt{E_m} \beta_2 \exp(j\varphi_2) w_2(t) + n(t) \end{cases}$$

## Error Probability:

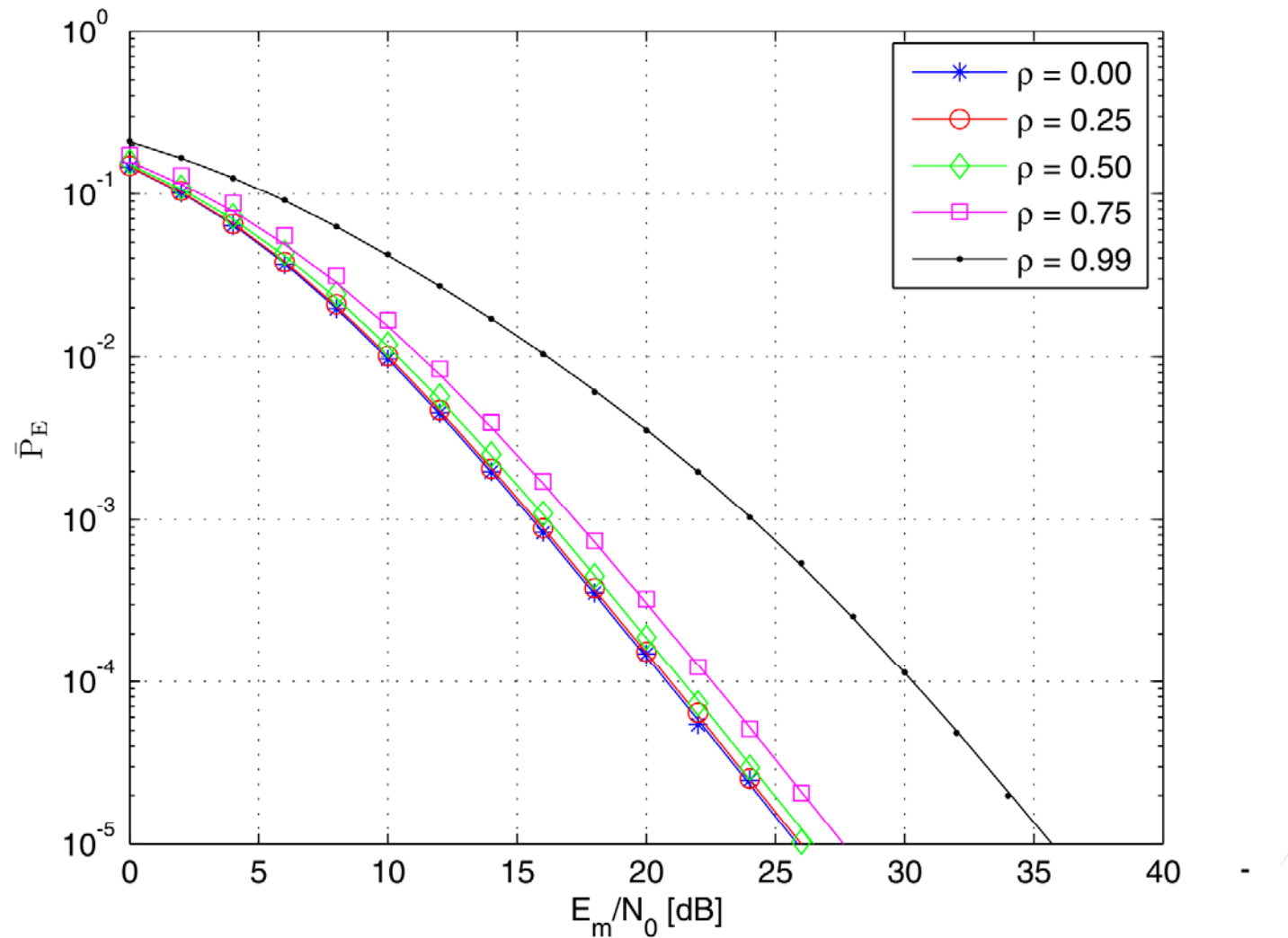
$$\text{BEP} = Q\left(\sqrt{\frac{E_m}{4N_0}(\beta_1^2 + \beta_2^2)}\right) \Rightarrow \begin{cases} \text{ABEP} = \frac{1}{\pi} \int_0^{\pi/2} M\left(\frac{E_m/4N_0}{2\sin^2(\theta)}\right) d\theta \\ M(s) = \left[1 + 2(\sigma_1^2 + \sigma_2^2)s + 4(1-\rho^2)\sigma_1^2\sigma_2^2s^2\right]^{-1} \end{cases} \quad 239$$

# Transmit-Diversity for SM (10/61)

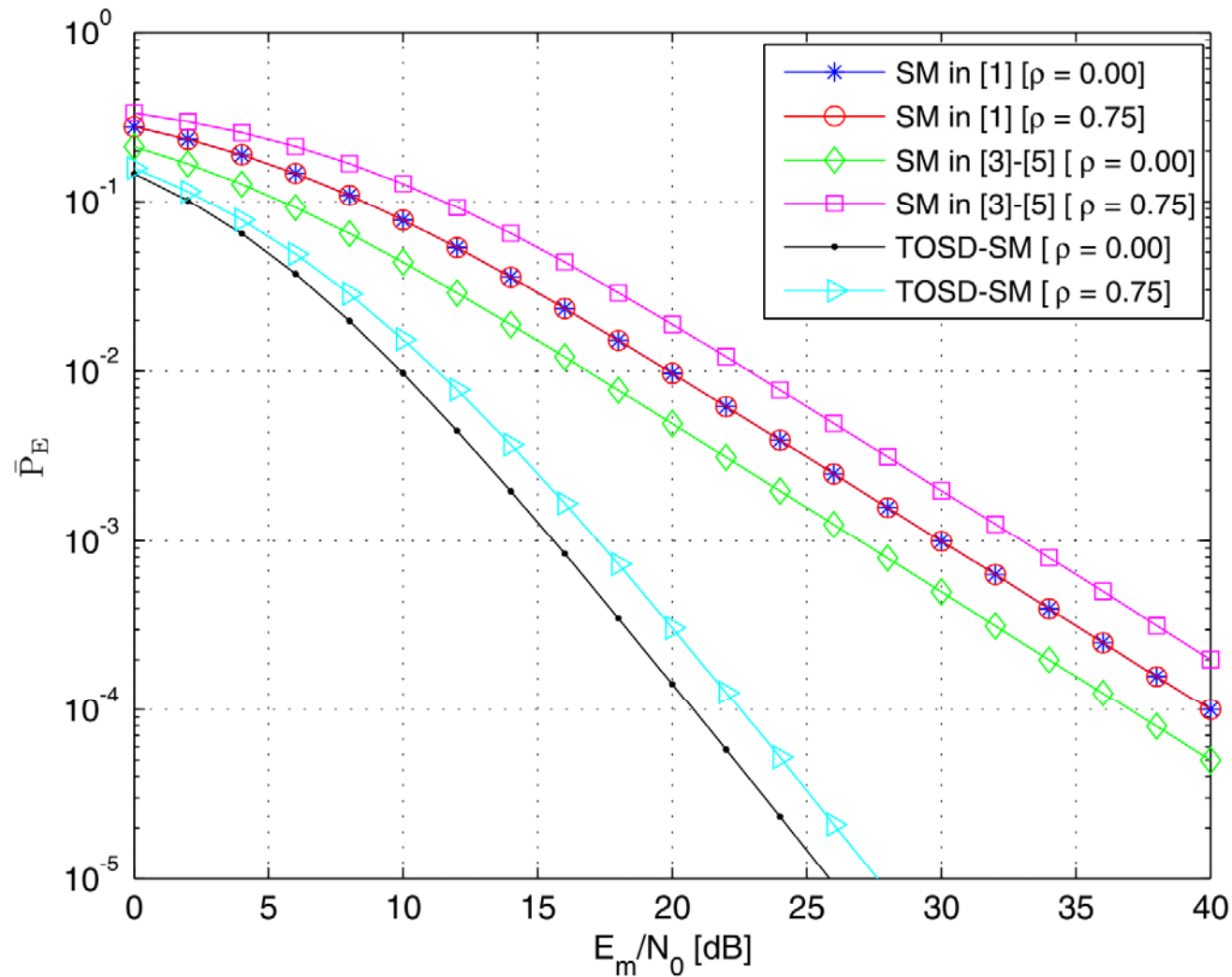


- If  $w_1(t) = w_2(t) \rightarrow$  Diversity = 1 (conventional SSK)
- If  $w_1(t)$  is “time-orthogonal” to  $w_2(t) \rightarrow$  Diversity = 2 (**TOSD-SSK**)

# Transmit-Diversity for SM (11/61)



# Transmit-Diversity for SM (12/61)



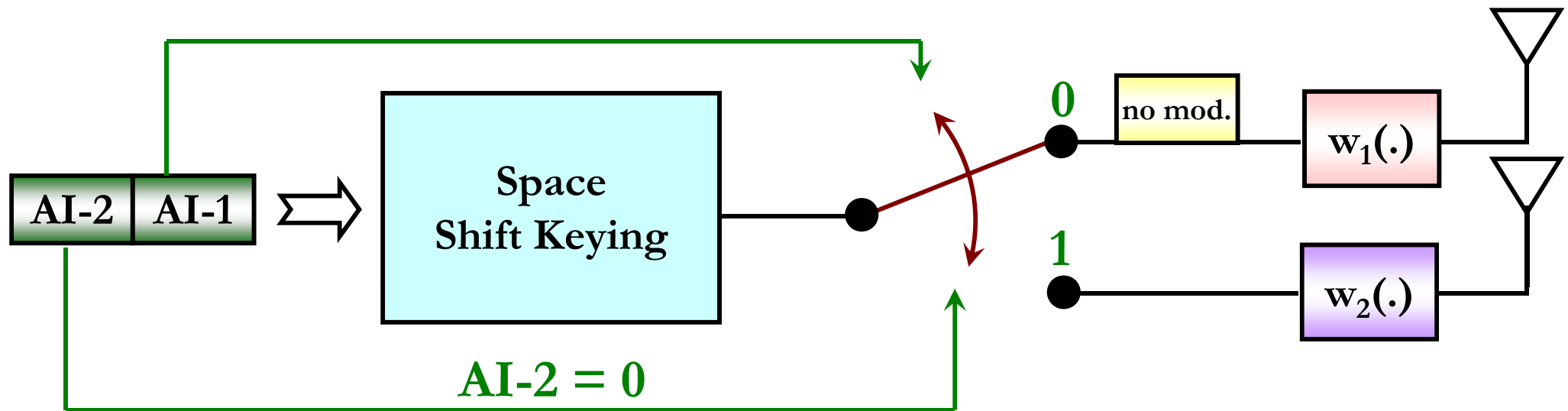
[1] Chau and Yu

[3]-[5]: Mesleh et al.  
and Jeganathan et al.

TOSD-SM: Time-  
Orthogonal Signal  
Design assisted SM

# Transmit-Diversity for SM (13/61)

Generalization to Rician Fading,  $N_t > 2$ , and  $N_r > 1$



- ❑ If  $w_i(t) = w_j(t) \rightarrow \text{Diversity} = N_r$  (conventional SSK)
- ❑ If  $w_i(t)$  is “time-orthogonal” to  $w_j(t) \rightarrow \text{Diversity} = 2N_r$  (**TOSD-SSK**)
- ❑ This is true for any  $N_t$  with no bandwidth expansion and with a single active transmit-antenna at any time-instance

# Transmit-Diversity for SM (14/61)

## Orthogonal Waveforms Design with Bandwidth Constraint

$$\begin{cases} p_1(\xi) = \left( \frac{1}{\sqrt{\sqrt{\pi}}} \right) \exp \left[ -\frac{1}{2} \left( \frac{\xi}{t_0} \right)^2 \right] \\ p_2(\xi) = \left( \frac{2\xi}{\sqrt{2}\sqrt{\pi}} \right) \exp \left[ -\frac{1}{2} \left( \frac{\xi}{t_0} \right)^2 \right] \\ p_3(\xi) = \left( \frac{4\xi^2 - 2}{\sqrt{8}\sqrt{\pi}} \right) \exp \left[ -\frac{1}{2} \left( \frac{\xi}{t_0} \right)^2 \right] \\ p_4(\xi) = \left( \frac{8\xi^3 - 12\xi}{\sqrt{48}\sqrt{\pi}} \right) \exp \left[ -\frac{1}{2} \left( \frac{\xi}{t_0} \right)^2 \right] \\ p_5(\xi) = \left( \frac{16\xi^4 - 48\xi^2 + 12}{\sqrt{384}\sqrt{\pi}} \right) \exp \left[ -\frac{1}{2} \left( \frac{\xi}{t_0} \right)^2 \right] \end{cases}$$

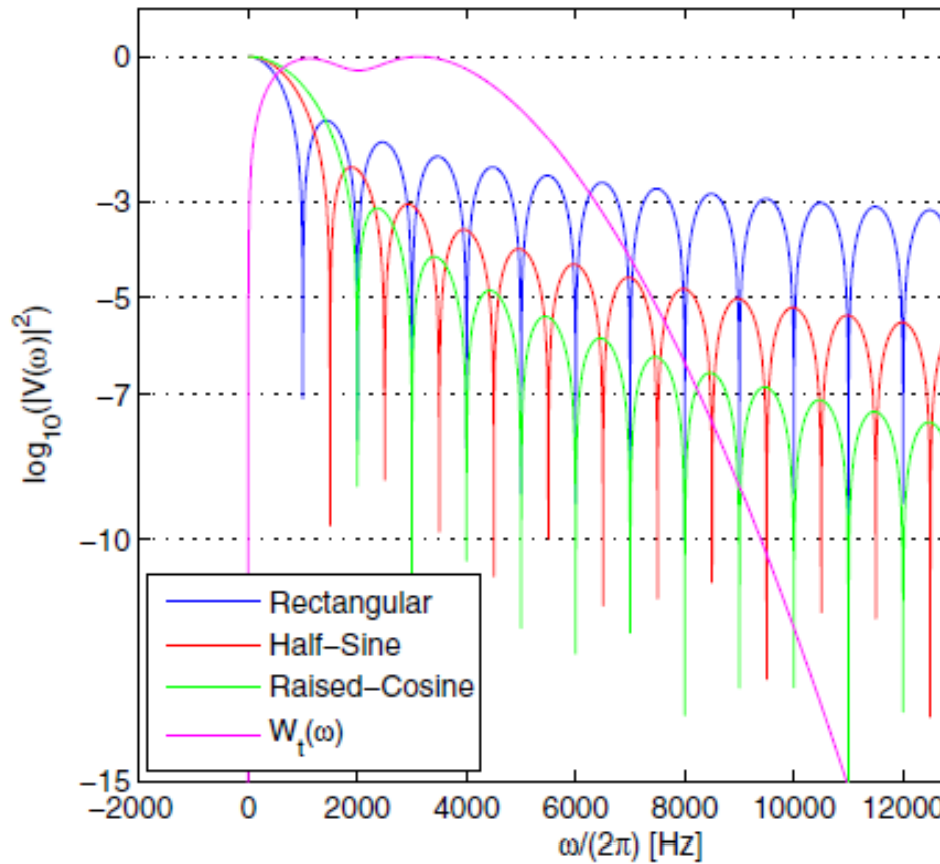
$$\begin{cases} w_{t_1}(\xi) = \left( -\frac{4}{\sqrt{165}} \right) p_1(\xi) + \left( \frac{\sqrt{4-2\sqrt{2}}}{4} \right) p_2(\xi) + \left( \sqrt{\frac{11}{30}} \right) p_3(\xi) + \left( -\frac{\sqrt{4+2\sqrt{2}}}{4} \right) p_4(\xi) + \left( -\frac{2}{\sqrt{110}} \right) p_5(\xi) \\ w_{t_2}(\xi) = \left( -\frac{4}{\sqrt{165}} \right) p_1(\xi) + \left( -\frac{\sqrt{4-2\sqrt{2}}}{4} \right) p_2(\xi) + \left( \sqrt{\frac{11}{30}} \right) p_3(\xi) + \left( \frac{\sqrt{4+2\sqrt{2}}}{4} \right) p_4(\xi) + \left( -\frac{2}{\sqrt{110}} \right) p_5(\xi) \\ w_{t_3}(\xi) = \left( \sqrt{\frac{3}{22}} \right) p_1(\xi) + \left( -\frac{\sqrt{4+2\sqrt{2}}}{4} \right) p_2(\xi) + (0) p_3(\xi) + \left( \frac{\sqrt{4-2\sqrt{2}}}{4} \right) p_4(\xi) + \left( -\frac{2}{\sqrt{11}} \right) p_5(\xi) \\ w_{t_4}(\xi) = \left( \sqrt{\frac{3}{22}} \right) p_1(\xi) + \left( \frac{\sqrt{4+2\sqrt{2}}}{4} \right) p_2(\xi) + (0) p_3(\xi) + \left( -\frac{\sqrt{4-2\sqrt{2}}}{4} \right) p_4(\xi) + \left( -\frac{2}{\sqrt{11}} \right) p_5(\xi) \end{cases}$$

M. Di Renzo, D. De Leonardis, F. Graziosi, and H. Haas, “Space Shift Keying (SSK-) MIMO with Practical Channel Estimates”, **IEEE Trans. Commun.**, Vol. 60, No. 4, pp. 998-1112, Apr. 2012.

J. A. Ney da Silva and M. L. R. de Campos, “Spectrally efficient UWB pulse shaping with application in orthogonal PSM,” **IEEE Trans. Commun.**, vol. 55, no. 2, pp. 313–322, Feb. 2007.



# Transmit-Diversity for SM (15/61)



Fractional Power Containment Bandwidth ( $B/(2\pi)$ kHz)				
$X_{\%}$	Rectangular	Half-Sine	Raised-Cosine	$w_t(\cdot)$
99%	7.61	1.18	1.41	4.97
99.995%	>30	6.98	3.29	6.46
99.9999%	>30	22.14	6.64	7.31
99.99999%	>30	29.96	10.57	7.76

Bounded Power Spectral Density Bandwidth ( $B/(2\pi)$ kHz)				
$TH_{dB}$	Rectangular	Half-Sine	Raised-Cosine	$w_t(\cdot)$
3dB	9.59	2.28	1.85	6.35
5dB	>30	8.18	4.62	7.40
6dB	>30	15.13	6.64	7.85
7dB	>30	28.03	9.65	8.27
10dB	>30	>30	>30	9.39

$$FPCB_{X_{\%}} = \min_{B \in [0, +\infty)} \left\{ B \left| \frac{\int_0^B |P(\omega)|^2 d\omega}{\int_0^{+\infty} |P(\omega)|^2 d\omega} > X_{\%} \right. \right\}$$

$$BPSDB_{TH_{dB}} = \min_{B \in [0, +\infty)} \left\{ B \left| \log_{10} \left( |P(\omega)|^2 \right) < \log_{10} \left( |P(\omega_{peak})|^2 \right) - TH_{dB}, \forall \omega > B \right. \right\}$$

# Transmit-Diversity for SM (16/61)

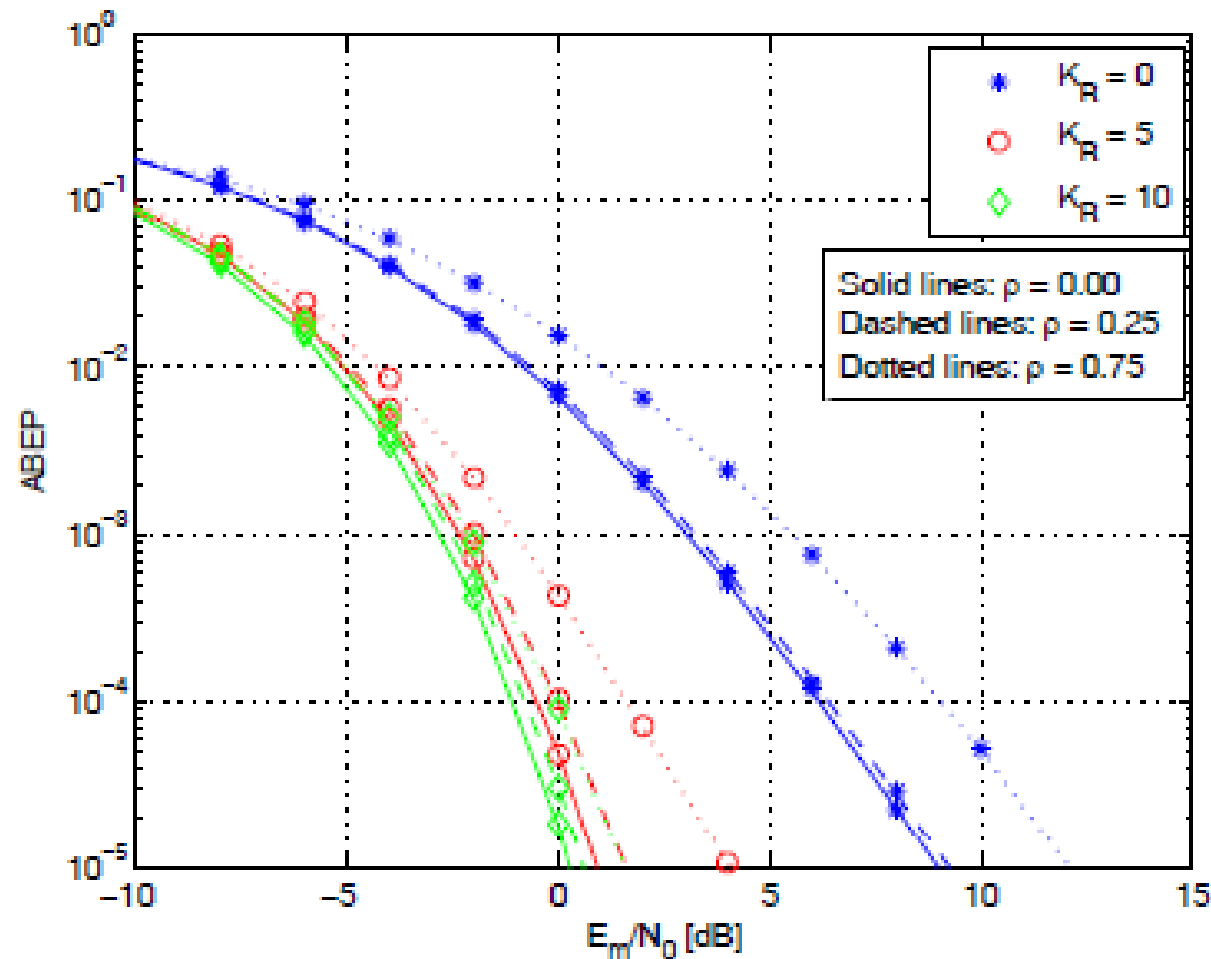


Fig. 5. TOSD-SSK modulation: ABEP against  $E_m/N_0$ . Solid, dashed, and dotted lines denote the analytical model in Section IV and markers Monte Carlo simulations. Setup: i)  $N_t = 2$ , ii)  $N_r = 2$ , iii)  $\Omega_{i,l} = 10\text{dB}$  and  $K_R^{(i,l)} = K_R$  for  $i = 1, 2, \dots, N_t$  and  $l = 1, 2, \dots, N_r$ , and iv)  $\rho = 0.00$  (solid lines),  $\rho = 0.25$  (dashed lines),  $\rho = 0.75$  (dotted lines).

## Transmit-Diversity for SM (17/61)

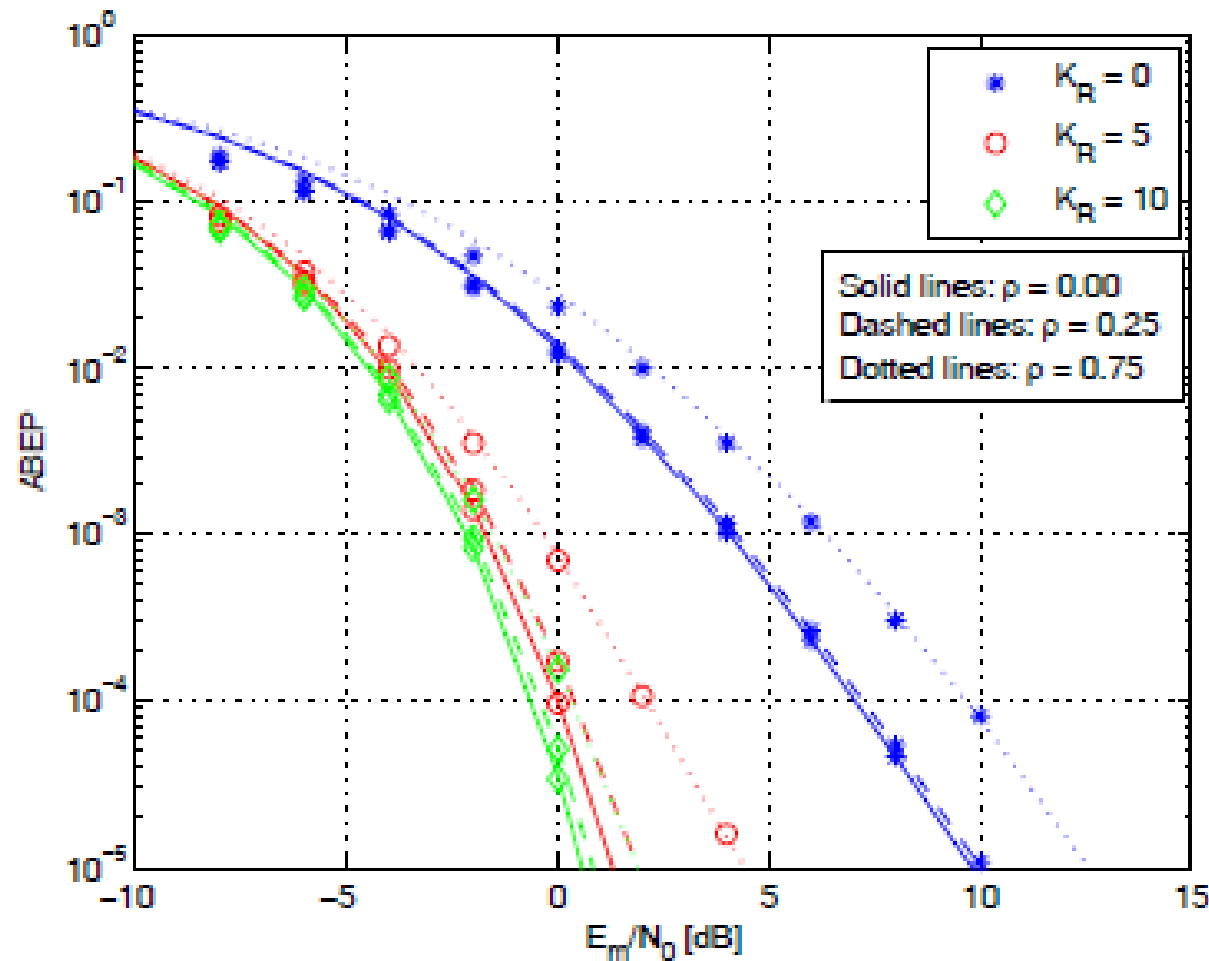


Fig. 7. TOSD-SSK modulation: ABEP against  $E_m/N_0$ . Solid, dashed, and dotted lines denote the analytical model in Section IV and markers Monte Carlo simulations. Setup: i)  $N_t = 4$ , ii)  $N_r = 2$ , iii)  $\Omega_{i,l} = 10\text{dB}$  and  $K_R^{(i,l)} = K_R$  for  $i = 1, 2, \dots, N_t$  and  $l = 1, 2, \dots, N_r$ , and iv)  $\rho = 0.00$  (solid lines),  $\rho = 0.25$  (dashed lines),  $\rho = 0.75$  (dotted lines).

## Transmit-Diversity for SM (18/61)

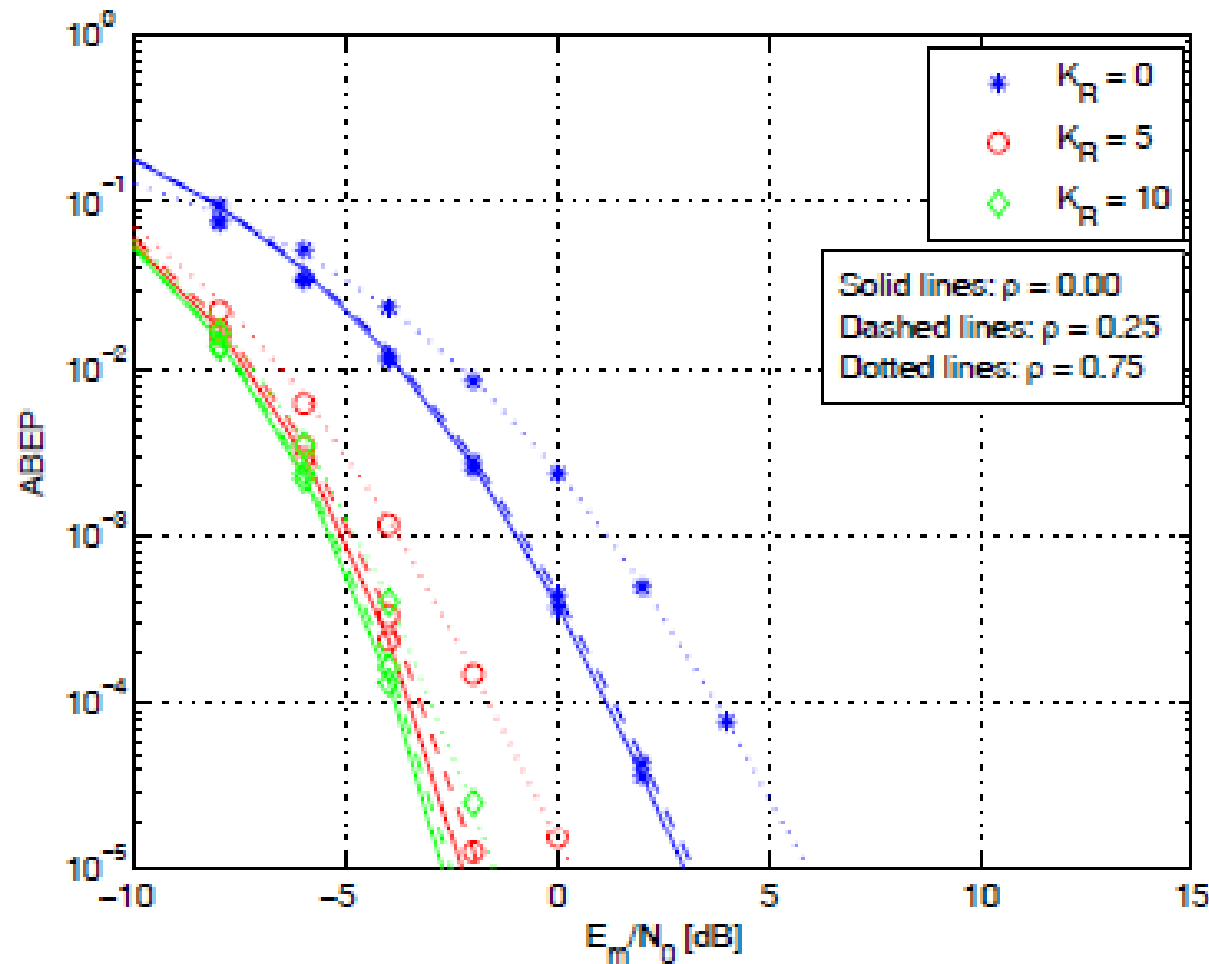


Fig. 8. TOSD-SSK modulation: ABEP against  $E_m/N_0$ . Solid, dashed, and dotted lines denote the analytical model in Section IV and markers Monte Carlo simulations. Setup: i)  $N_t = 4$ , ii)  $N_r = 4$ , iii)  $\Omega_{i,l} = 10\text{dB}$  and  $K_R^{(i,l)} = K_R$  for  $i = 1, 2, \dots, N_t$  and  $l = 1, 2, \dots, N_r$ , and iv)  $\rho = 0.00$  (solid lines),  $\rho = 0.25$  (dashed lines),  $\rho = 0.75$  (dotted lines).

# Transmit-Diversity for SM (19/61)

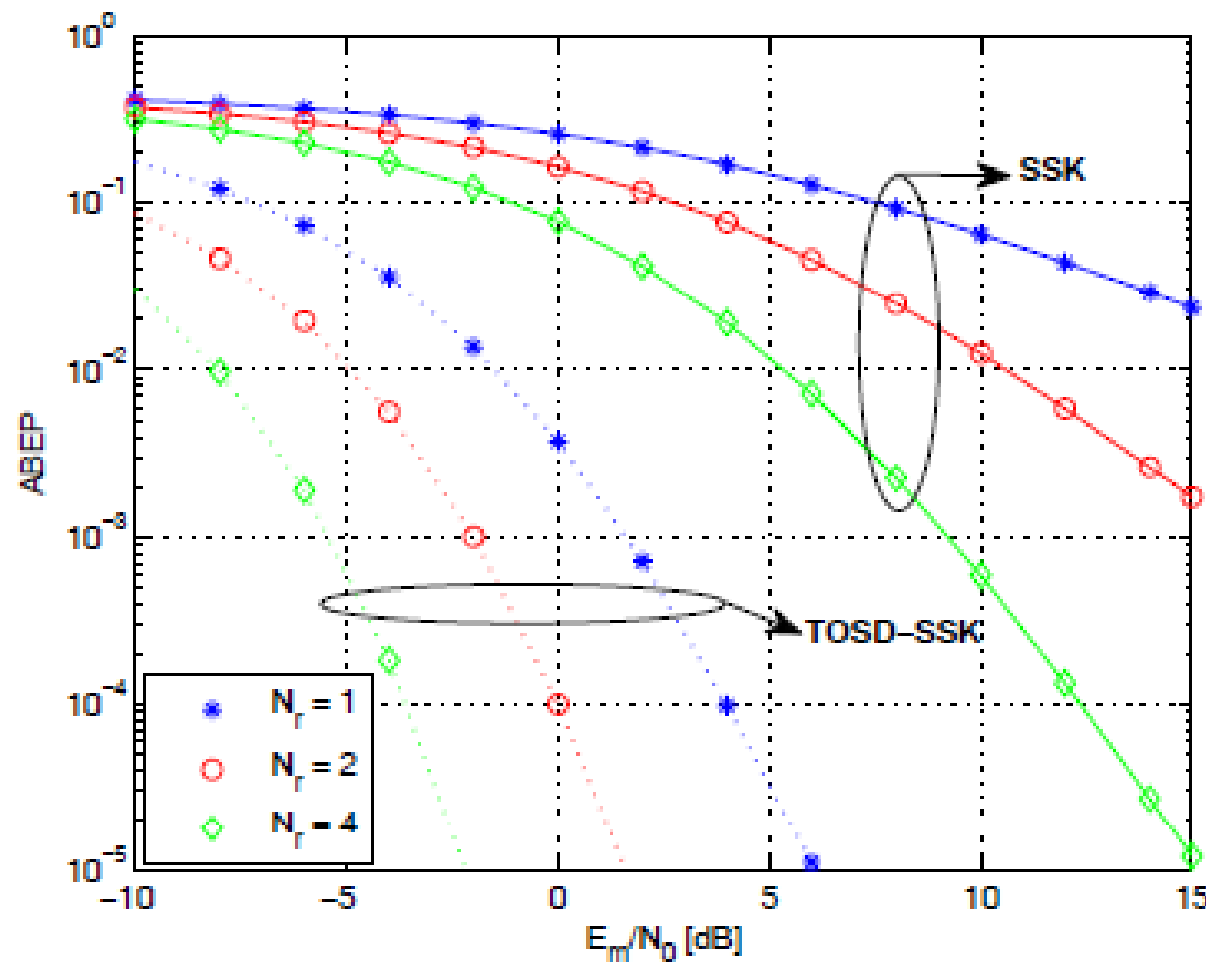


Fig. 11. Comparison between SSK and TOSD-SSK modulation: ABEP against  $E_m/N_0$ . Markers with solid lines denote the analytical model in Section III and markers with dotted lines the analytical model in Section IV. Setup: i)  $N_t = 2$ , ii)  $\Omega_{i,l} = 10\text{dB}$  and  $K_R^{(i,l)} = 5\text{dB}$  for  $i = 1, 2, \dots, N_t$  and  $l = 1, 2, \dots, N_r$ , and iii)  $\rho = 0.25$ .

## Transmit-Diversity for SM (20/61)

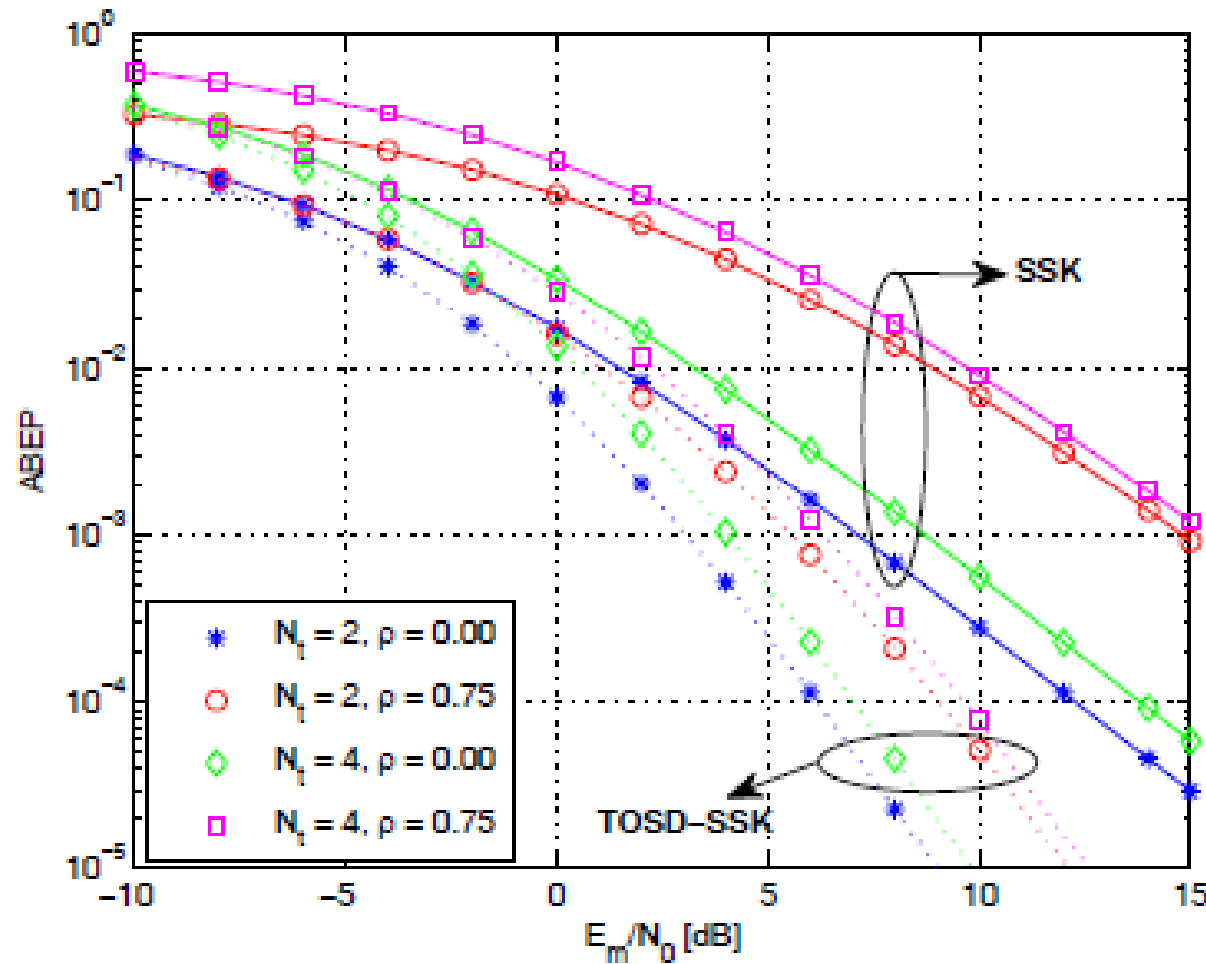


Fig. 12. Comparison between SSK and TOSD-SSK modulation: ABEP against  $E_m/N_0$ . Markers with solid lines denote the analytical model in Section III and markers with dotted lines the analytical model in Section IV. Setup: i)  $N_r = 2$ , and ii)  $\Omega_{i,l} = 10\text{dB}$  and  $K_R^{(i,l)} = 0\text{dB}$  for  $i = 1, 2, \dots, N_t$  and  $l = 1, 2, \dots, N_r$ .

# *Transmit-Diversity for SM (21/61)*

---

## □ In summary:

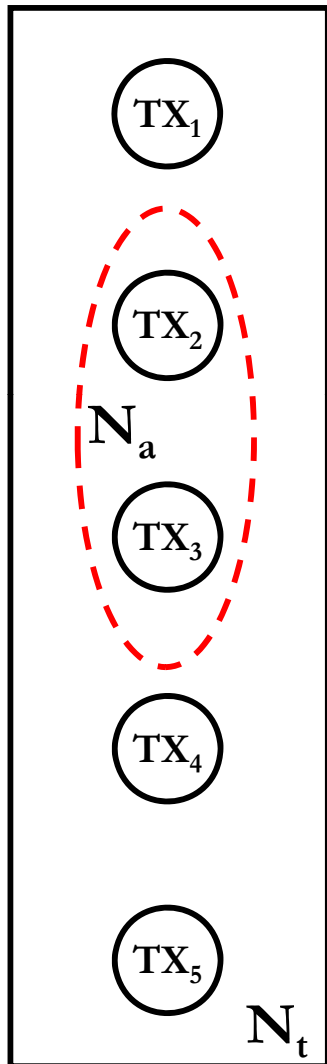
- TOSD-SSK achieves transmit-diversity with just 1 active antenna at the transmitter
- However, TOSD-SSK achieves transmit-diversity only equal to 2 → **Full transmit-diversity is possible only if  $N_t=2$**
- Furthermore, the data rate of SSK is only  $\text{Rate}=\log_2(N_t)$  → **This is too low for high data rate applications**

## □ Questions:

- Can we achieve a transmit-diversity gain greater than 2?
- At the same time, can we increase the rate?
- Given a pair (rate, diversity), how to design a SSK scheme achieving it?

# Transmit-Diversity for SM (22/61)

## Increasing the Rate via GSSK



- Size of the spatial-constellation diagram ( $N_H > N_t$ )

$$N_H = 2^{\left\lfloor \log_2 \left( \frac{N_t}{N_a} \right) \right\rfloor}$$

- Rate =  $\log_2(N_H) > \log_2(N_t)$

- Spatial-constellation diagram:

- $N_a=1$  (i.e., SSK)  $\rightarrow D=\{1; 2; 3; 4; 5\}$
- $N_a=2 \rightarrow D=\{(1,2); (1,3); (1,4); (1,5); (2,3); (2,4); \dots\}$
- $N_a=3 \rightarrow D=\{(1,2,3); (1,2,4); (1,2,5); (1,3,4); \dots\}$



# Transmit-Diversity for SM (23/61)

## □ Problem statement

- Let  $N_t$  be the transmit-antennas and  $N_a$  be the active transmit-antennas
- Then, the largest possible size of the spatial-constellation diagram is:

$$\tilde{N}_H = 2^{\left\lfloor \log_2 \left( \frac{N_t}{N_a} \right) \right\rfloor}$$

## □ Objectives

- Find the actual spatial constellation diagram of size  $N_H \leq \tilde{N}_H$  such that transmit-diversity is Div
- Understand the role played by the TOSD principle for transmit-diversity

## □ Methodology

- We have computed the PEP (Pairwise Error Probability) of any pair of points in the spatial-constellation diagram and have analyzed the transmit-diversity order of each of them

# *Transmit-Diversity for SM (24/61)*

---

## **Main Result: Transmit-Diversity 1 and 2**

### **□ Result 1 (Div=1)**

- The system achieves transmit-diversity  $\text{Div}=1$  and rate  $R=\log_2(N_H)$  if the  $N_t$  transmit-antennas have the same shaping filter
- This scheme is called GSSK and reduces to SSK if  $N_a=1$

### **□ Result 2 (Div=2)**

- The system achieves transmit-diversity  $\text{Div}=2$  and rate  $R=\log_2(N_H)$  if the  $N_t$  transmit-antennas have orthogonal shaping filters
- This scheme is called TOSD-GSSK and reduces to TOSD-SSK if  $N_a=1$

# Transmit-Diversity for SM (25/61)

## Main Result: Transmit-Diversity $> 2$

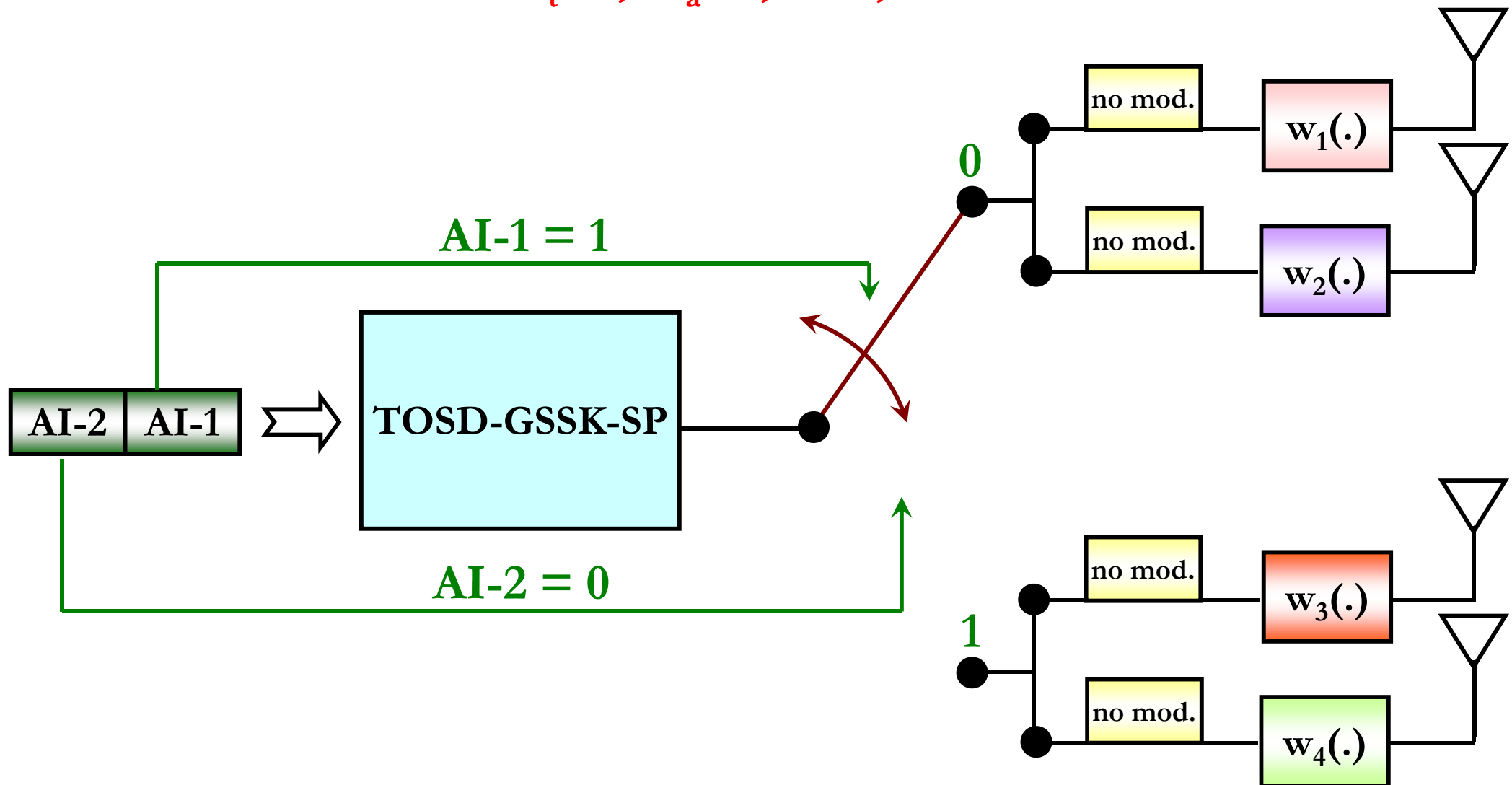
### □ Result 3 (Div $>2$ )

- Let  $N_H^\perp$  be the size of the partition of the set of  $N_t$  transmit-antennas such that  $N_t = N_H^\perp \cdot N_a \rightarrow$  each subset of the partition has  $N_a$  distinct antenna-elements and the subsets are pairwise disjoint
- Then, the system achieves transmit-diversity  $\text{Div} = 2 \cdot N_a$  and rate  $R = \log_2(N_H^\perp)$  if the  $N_t$  transmit-antennas have orthogonal shaping filters
- This scheme is called TOSD-GSSK with mapping by pairwise disjoint set partitioning (TOSD-GSSK-SP)

$$R = \log_2 \left( \frac{N_t}{N_a} \right) \stackrel{\text{tradeoff}}{\Leftrightarrow} \text{Div} = 2N_a$$

# Transmit-Diversity for SM (26/61)

$$N_t=4, N_a=2, R=1, \text{Div}=4$$



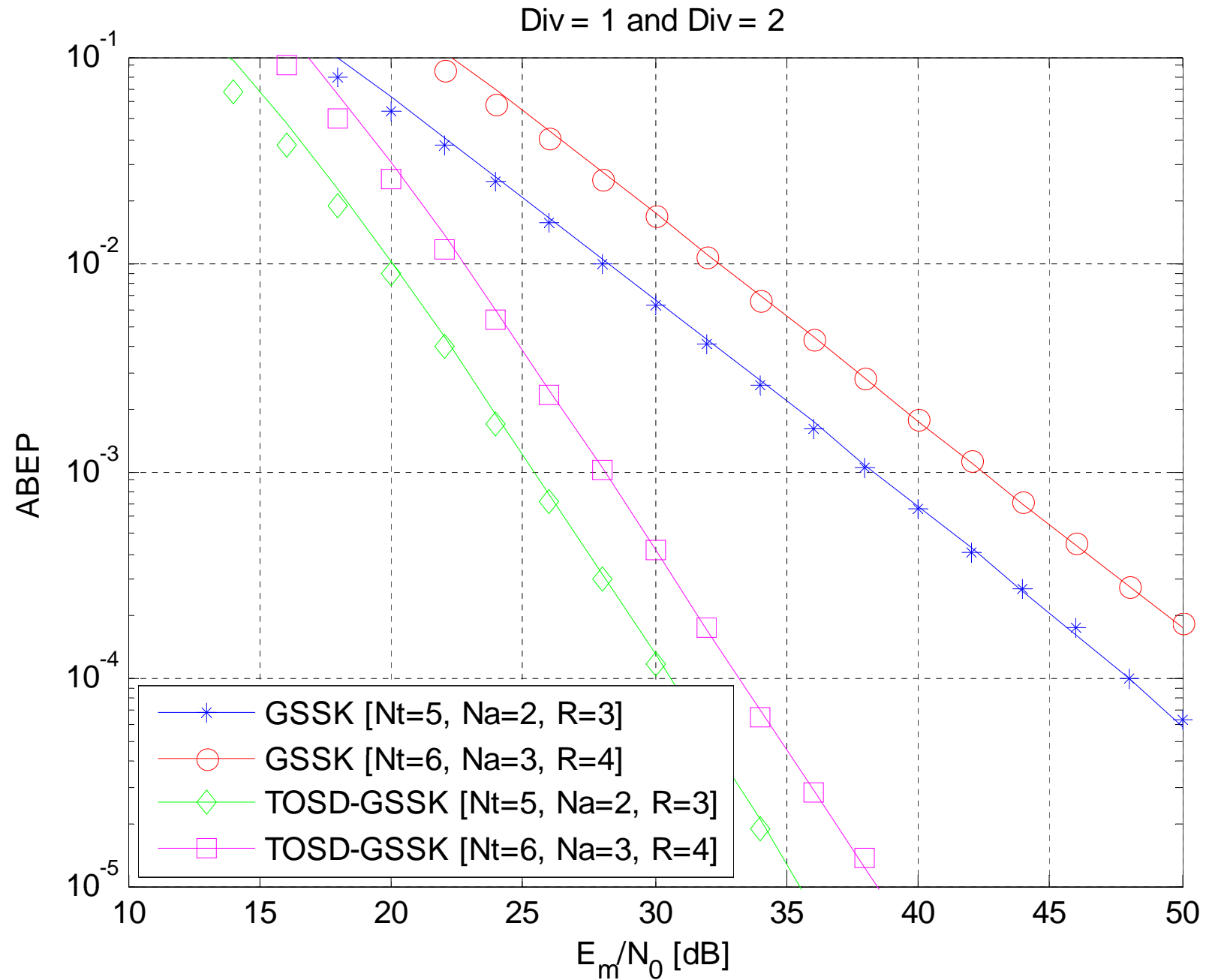
## *Transmit-Diversity for SM (27/61)*

---

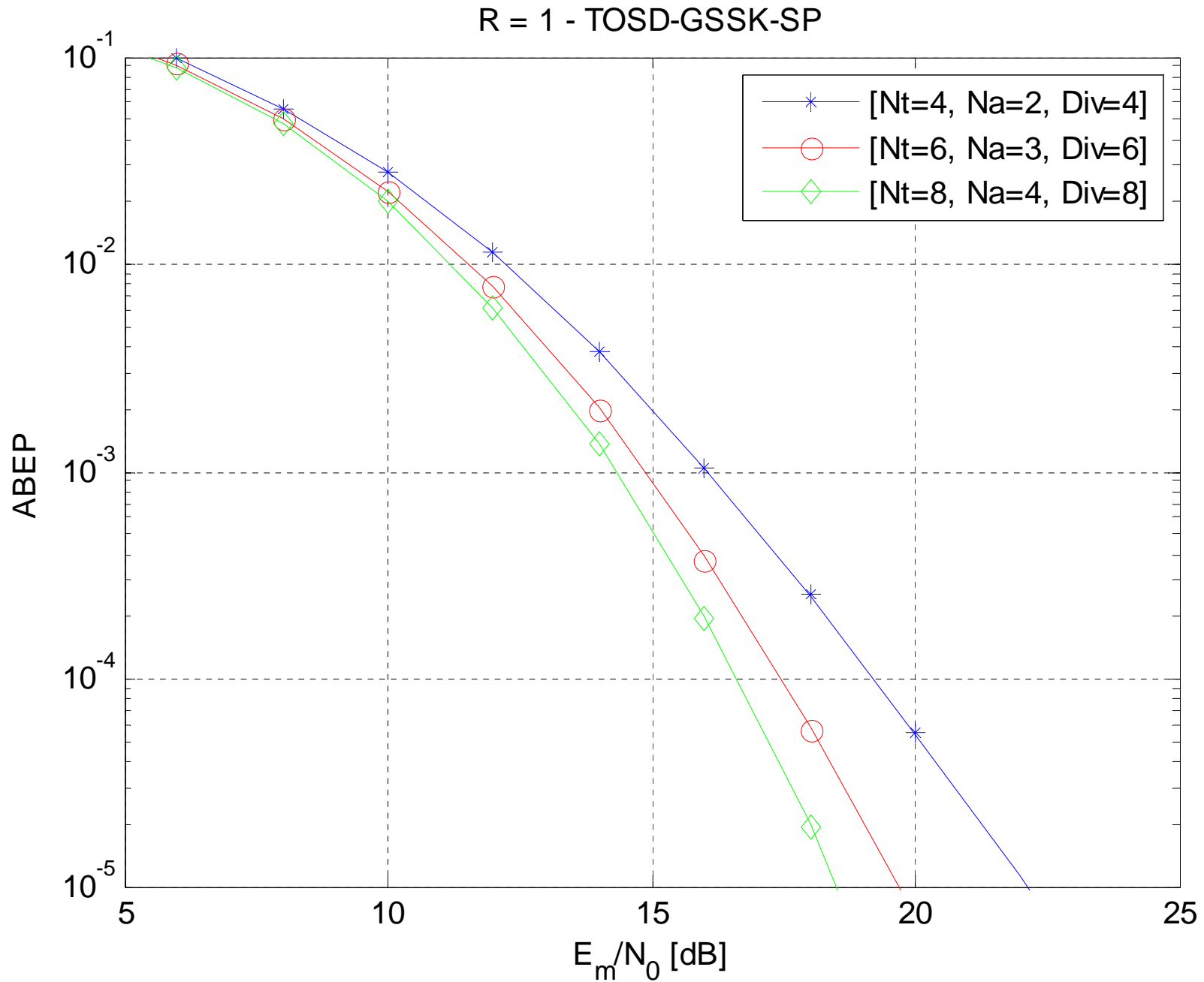
### □ Five schemes are studied:

- **SSK:**  $N_a=1$ ,  $w_0(.)=w_i(.)$ ,  $\text{Div}=1$
- **GSSK:**  $N_a>1$ ,  $w_0(.)=w_i(.)$ ,  $\text{Div}=1$
- **TOSD-SSK:**  $N_a=1$ ,  $N_t$  orthogonal  $w_i(.)$ ,  $\text{Div}=2$
- **TOSD-GSSK:**  $N_a>1$ ,  $N_t$  orthogonal  $w_i(.)$ ,  $\text{Div}=2$
- **TOSD-GSSK-SP:**  $N_a>1$ ,  $N_t$  orthogonal  $w_i(.)$ , the spatial-constellation diagram is a partition of  $N_t$ ,  $\text{Div}=2 \cdot N_a$

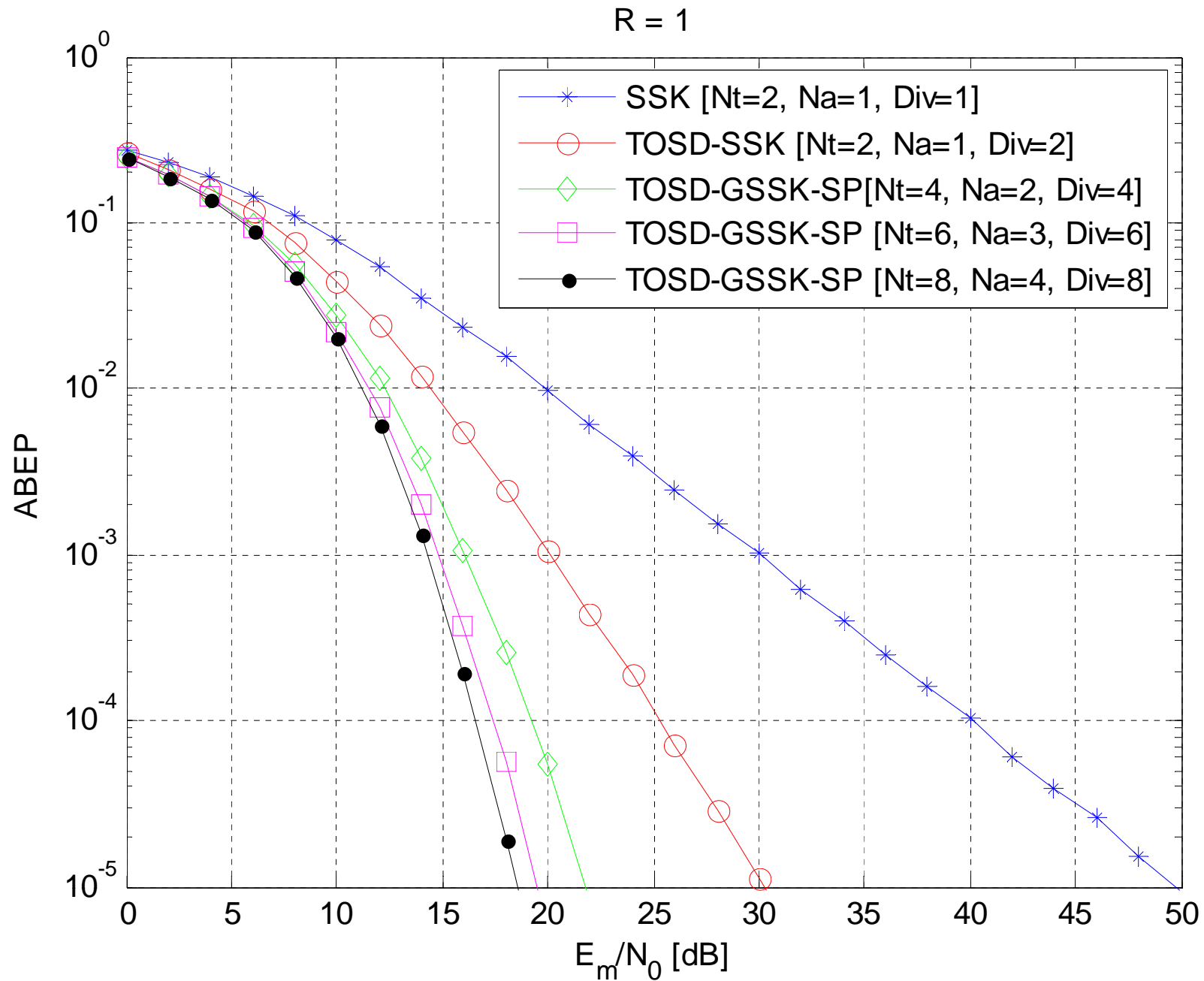
# Transmit-Diversity for SM (28/61)



# *Transmit-Diversity for SM (29/61)*

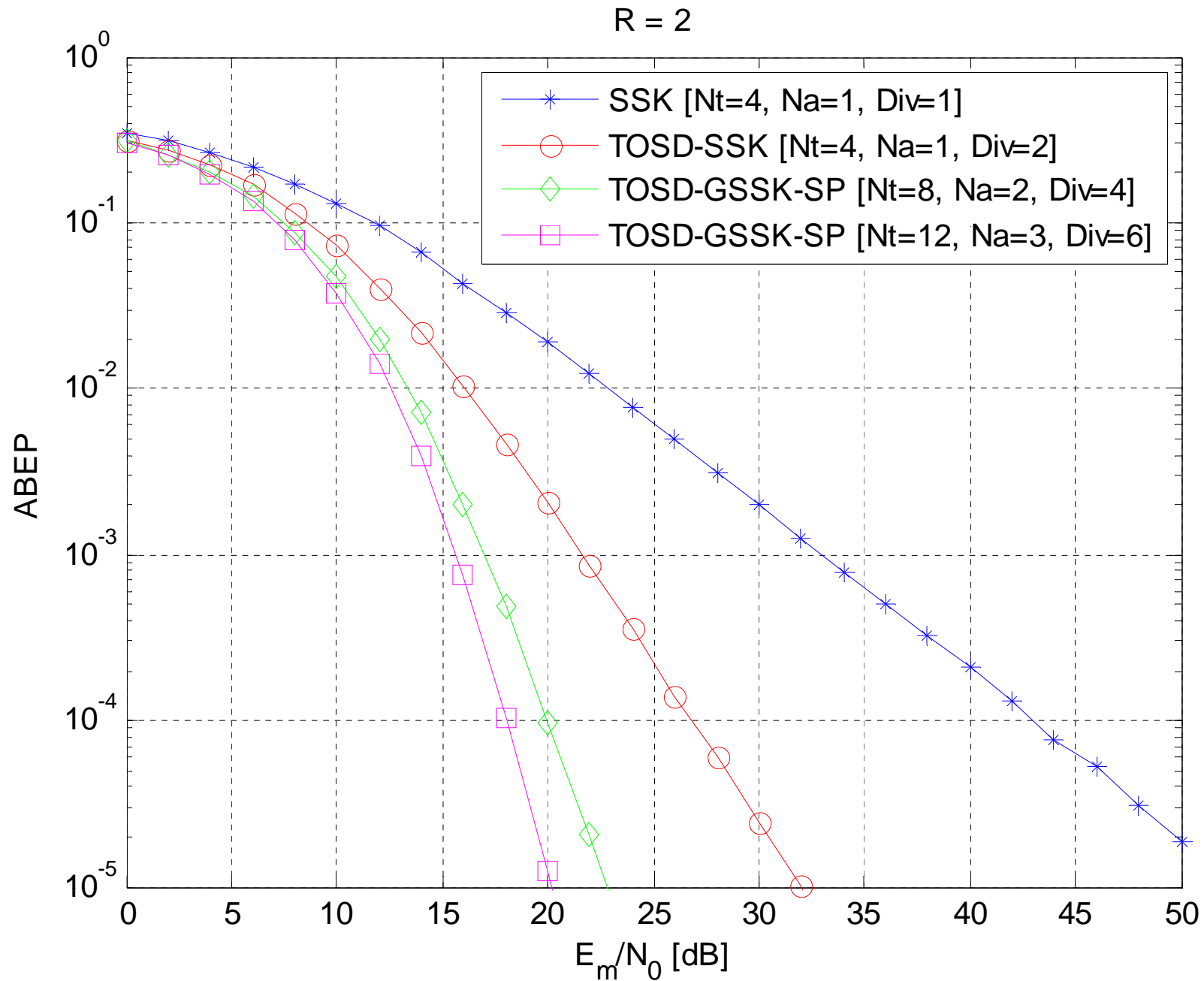


# Transmit-Diversity for SM (30/61)

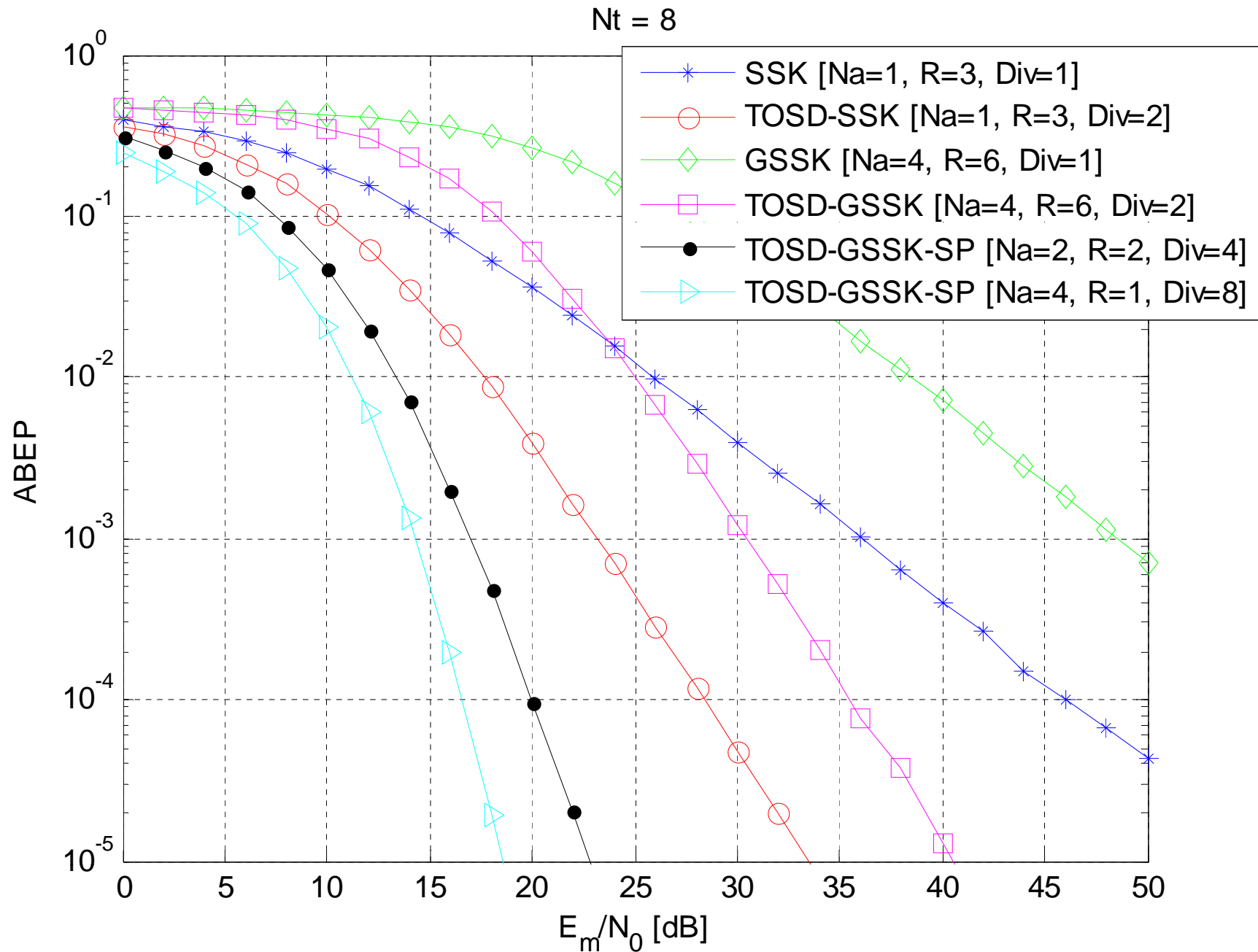




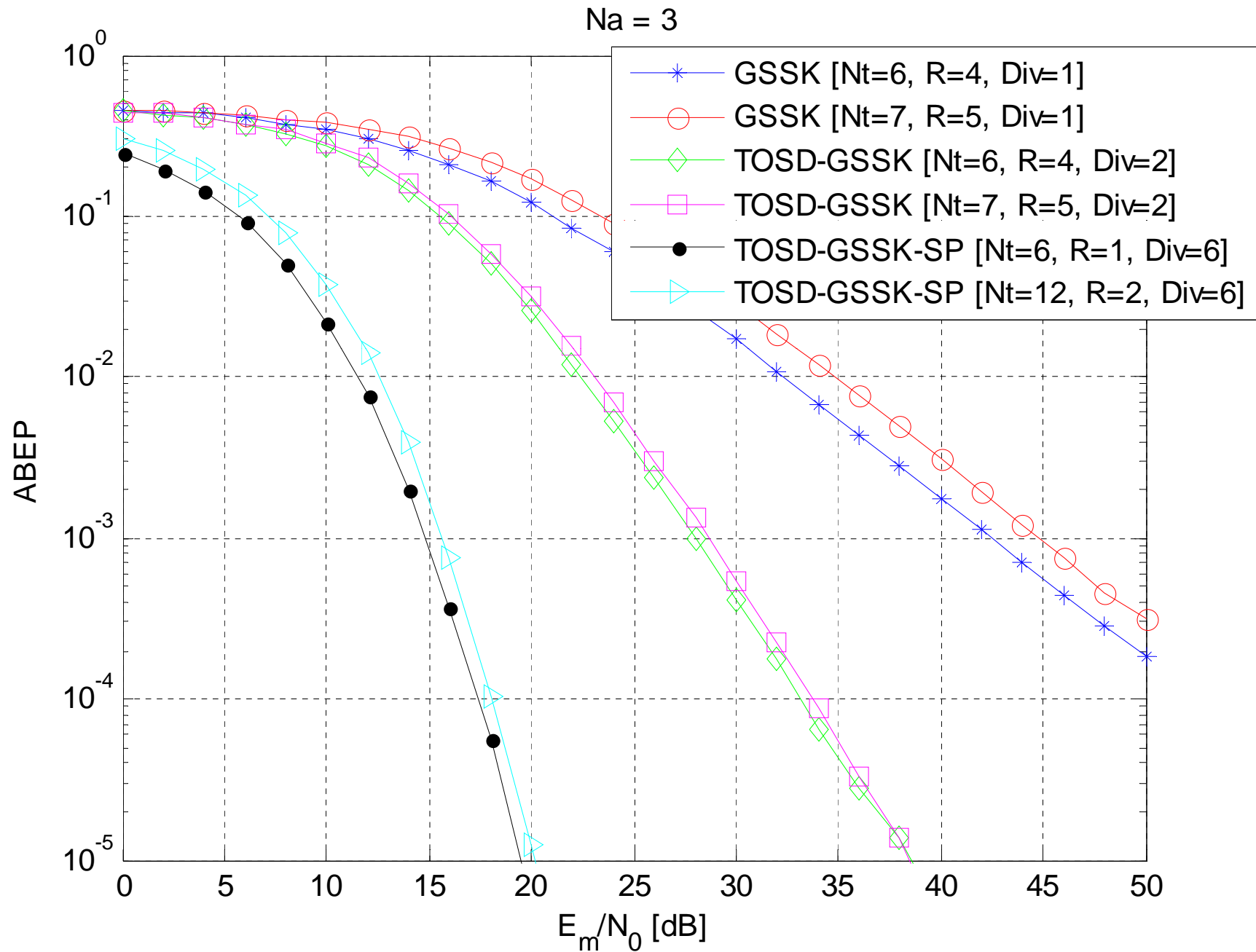
# Transmit-Diversity for SM (31/61)



# Transmit-Diversity for SM (32/61)



# Transmit-Diversity for SM (33/61)

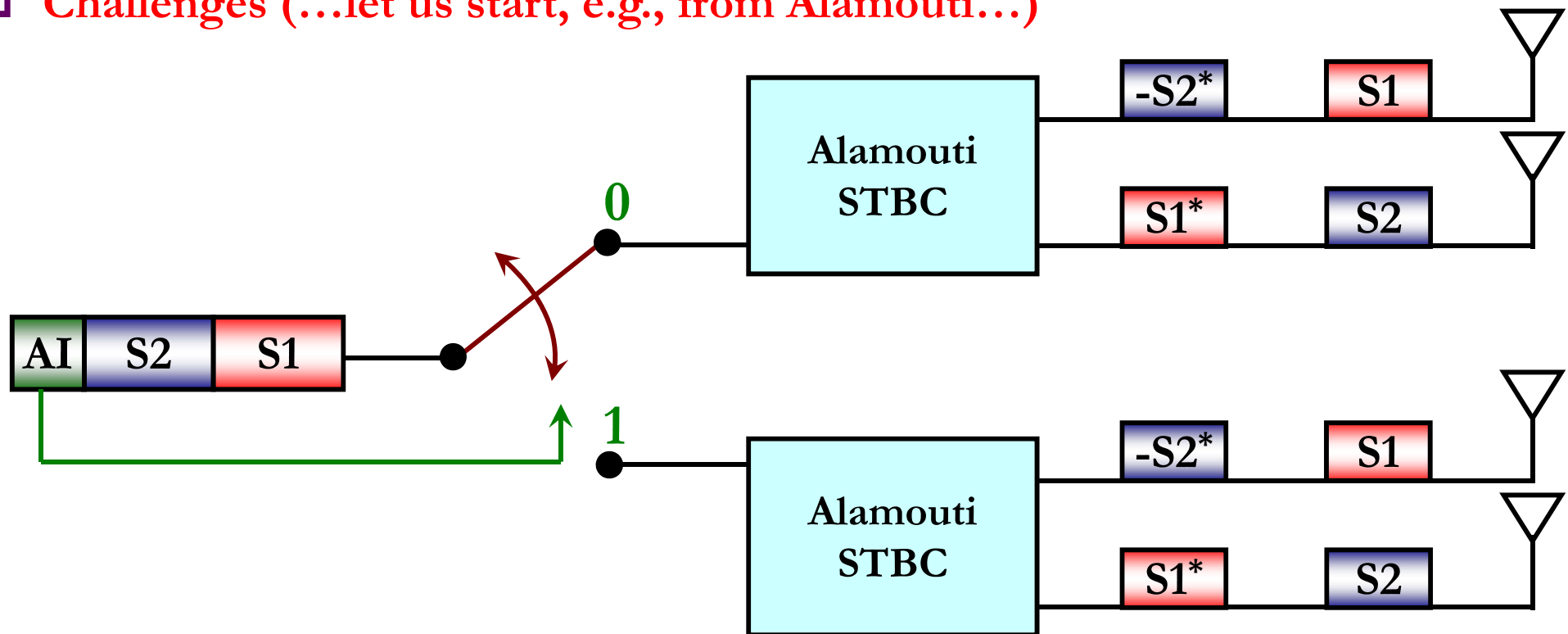


# Transmit-Diversity for SM (34/61)

## ❑ From SSK to SM

- Understanding the design challenges of transmit-diversity for SM
- Generalizing the TOSD approach to SM (TOSD-SM)
- Interested in transmit-diversity equal to 2 (extension of Alamouti code)

## ❑ Challenges (...let us start, e.g., from Alamouti...)



# Transmit-Diversity for SM (35/61)

## □ Problem statement

- Let  $N_t$  be the transmit-antennas and  $N_a$  be the active transmit-antennas
- Then, the largest possible size of the spatial-constellation diagram is:

$$N_H = 2^{\left\lfloor \log_2 \left( \frac{N_t}{N_a} \right) \right\rfloor}$$

- Objective. Find the actual spatial constellation diagram of size  $N_h \leq N_H$  such that:
  - ✓ Transmit-diversity is 2 for  $N_a=2$
  - ✓ Transmit-diversity can be achieved with single-stream decoding complexity

## □ Methodology

- We have computed the PEP (Pairwise Error Probability) of any pair of (antenna-index, modulated-symbol) and have analyzed transmit-diversity and single-stream decoding optimality of each of them

# *Transmit-Diversity for SM (36/61)*

---

## **Main Result: Same Shaping Filters at Tx**

### □ **Result 1 (receiver complexity)**

- Whatever the spatial-constellation diagram is, if the shaping filters at the transmitter are all the same, adding the SSK component on top of the Alamouti code destroys its inherent orthogonality. So, no single-stream decoder can be used and the receiver complexity is of the order of  $N_h \cdot M^{N_a}$  correlations

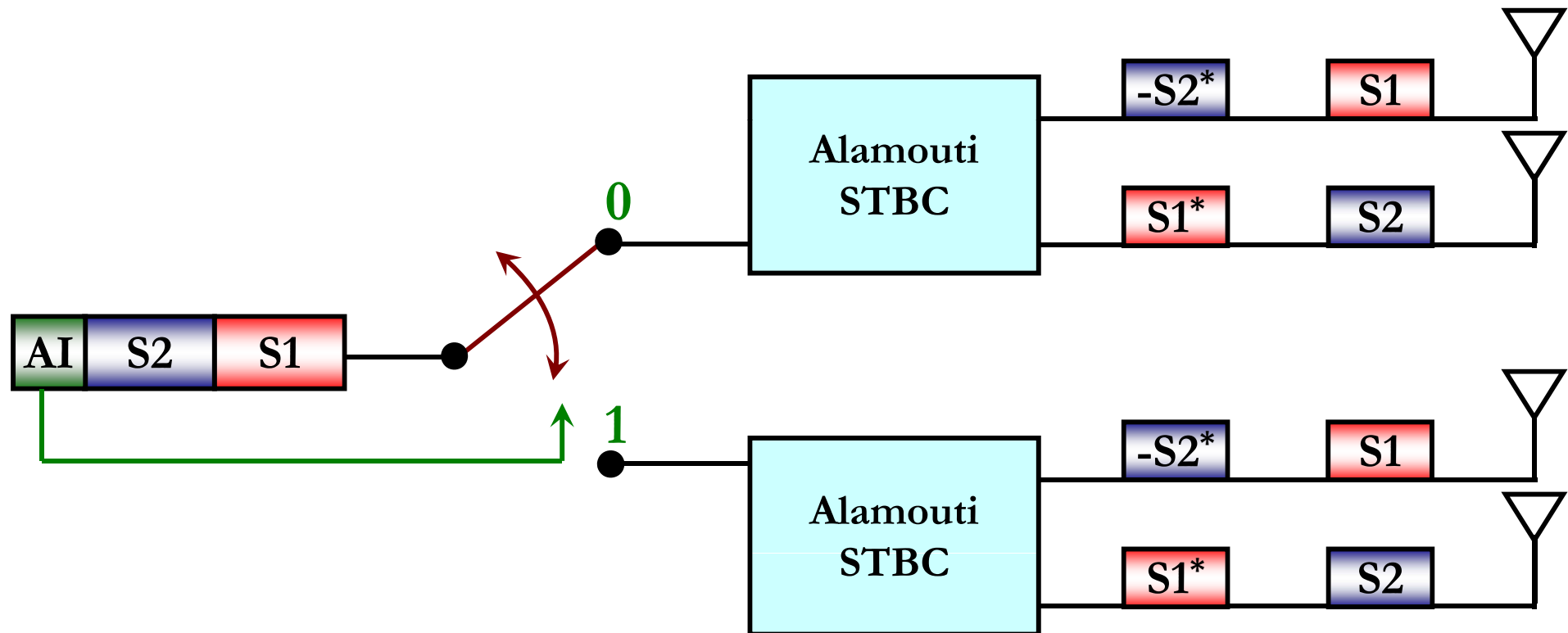
### □ **Result 2 (transmit-diversity)**

- If the shaping filters at the transmitter are all the same, transmit-diversity equal to 2 can be guaranteed by partitioning the spatial-constellation diagram into non-overlapping sets of antennas. However, a multi-stream receiver is needed at the destination for ML-optimum decoding

# Transmit-Diversity for SM (37/61)

## Same Shaping Filters at Tx – Example

- From Result 1 and Result 2, it follows that this scheme achieves transmit-diversity equal to 2 but multi-stream decoding is needed



# *Transmit-Diversity for SM (38/61)*

---

## **Main Result: Time-Orthogonal Shaping Filters at Tx**

### **□ Result 3 (receiver complexity)**

- ML-optimum low-complexity single-stream decoding can be guaranteed via an adequate choice of the (precoding) shaping filters at the transmitter. In particular, some pairs of filters should have zero cross-correlation function

### **□ Result 4 (transmit-diversity)**

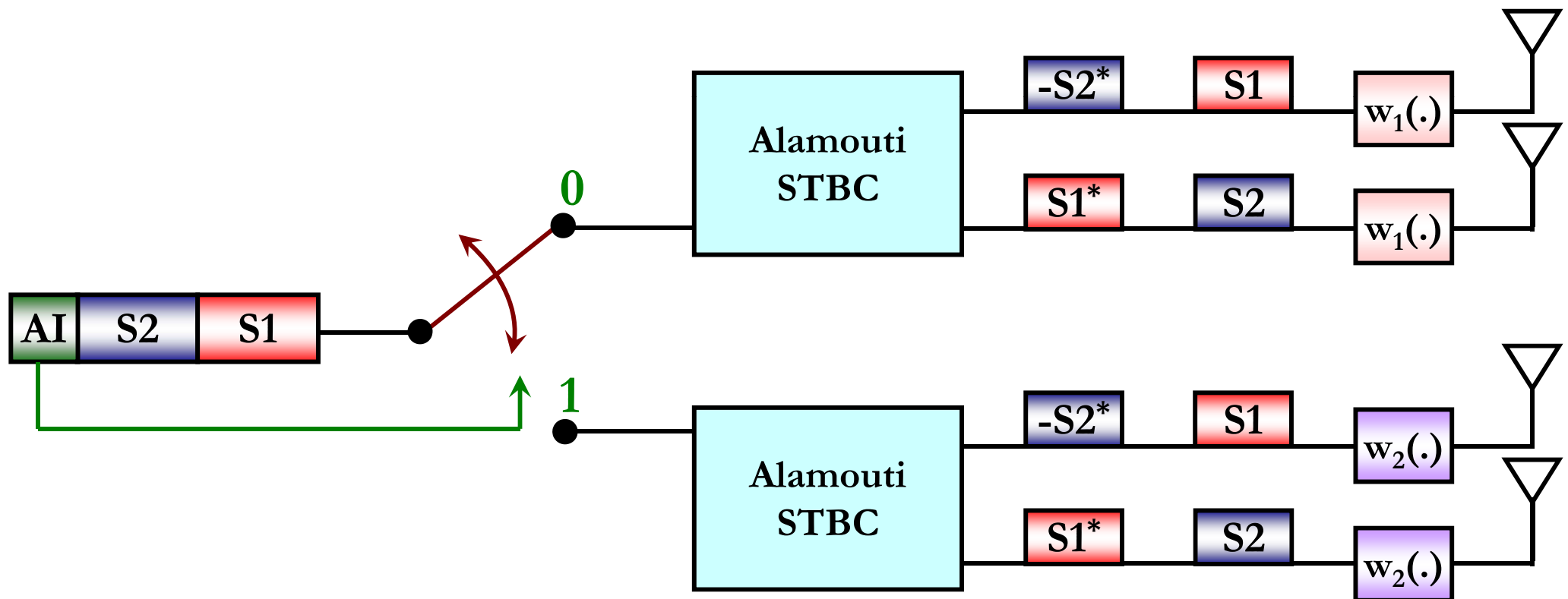
- ML-optimum low-complexity single-stream decoding with transmit-diversity of 2 can be guaranteed via an adequate choice of both the precoding shaping filters and the spatial-constellation diagram at the transmitter. In particular, some pairs of filters must have zero cross-correlation function, and the **spatial-constellation diagram should be a partition of the transmit-antenna array**



# Transmit-Diversity for SM (39/61)

## Time-Orthogonal Shaping Filters at Tx – Example

- From Result 3 and Result 4, it follows that this scheme achieves transmit-diversity equal to 2 with single-stream decoding



# *Transmit-Diversity for SM (40/61)*

---

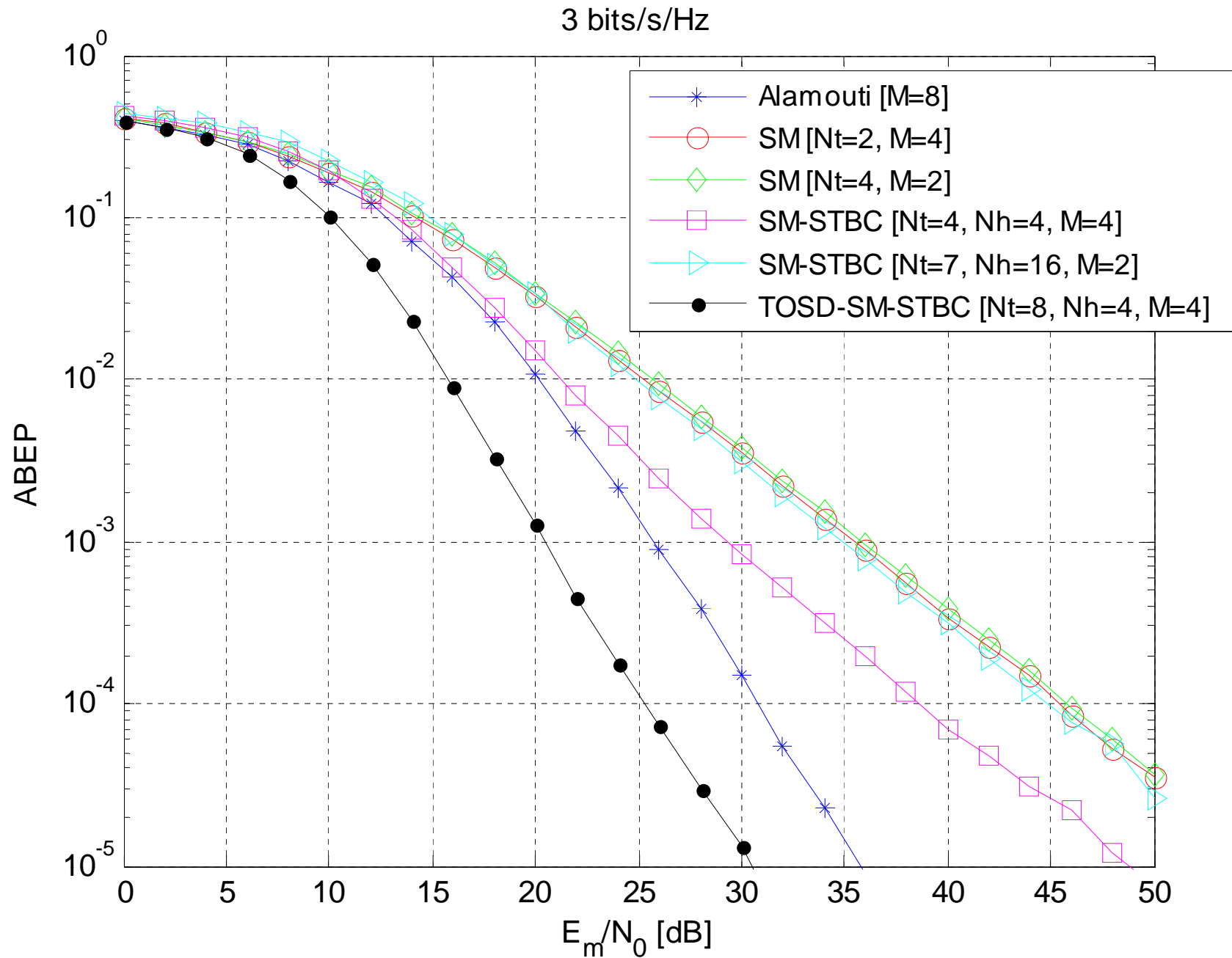
## □ Case studies

- **Worst-case setup**, which achieves transmit-diversity equal to 1 and needs a multi-stream decoder at the destination. It is obtained by using the same shaping filters in all the antennas at the transmitter along with a spatial-constellation diagram with overlapping sets of points (**SM-STBC**)
- **Best-case setup**, which achieves transmit-diversity equal to 2 and needs a single-stream decoder at the destination. This is obtained by using different and time-orthogonal shaping filters at the transmitter along with a spatial-constellation diagram composed by non-overlapping sets of points (**TOSD-SM-STBC**)

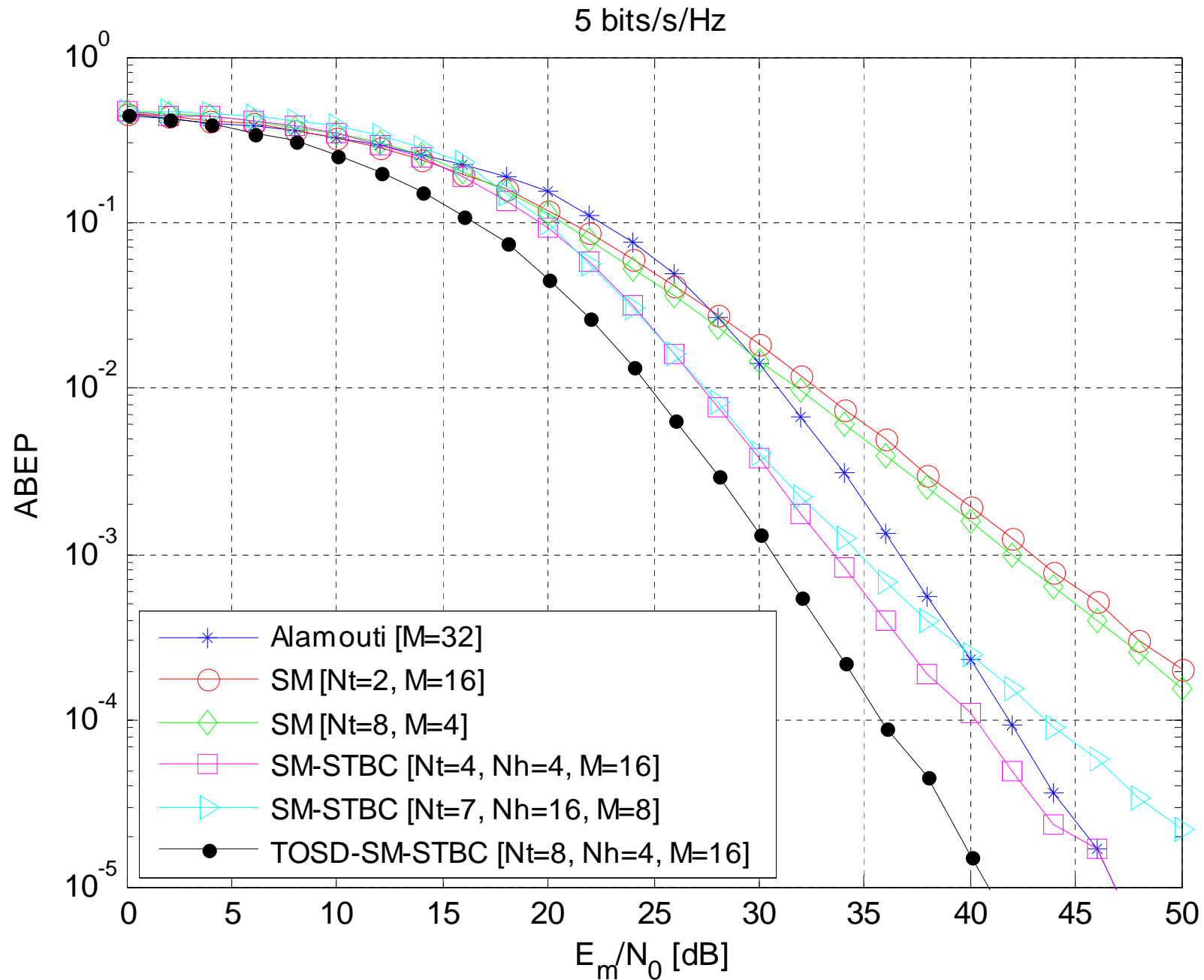
## □ Baseline schemes

- SM
- Alamouti code (rate=1)
- H3 and H4 OSTBCs (rate=3/4)

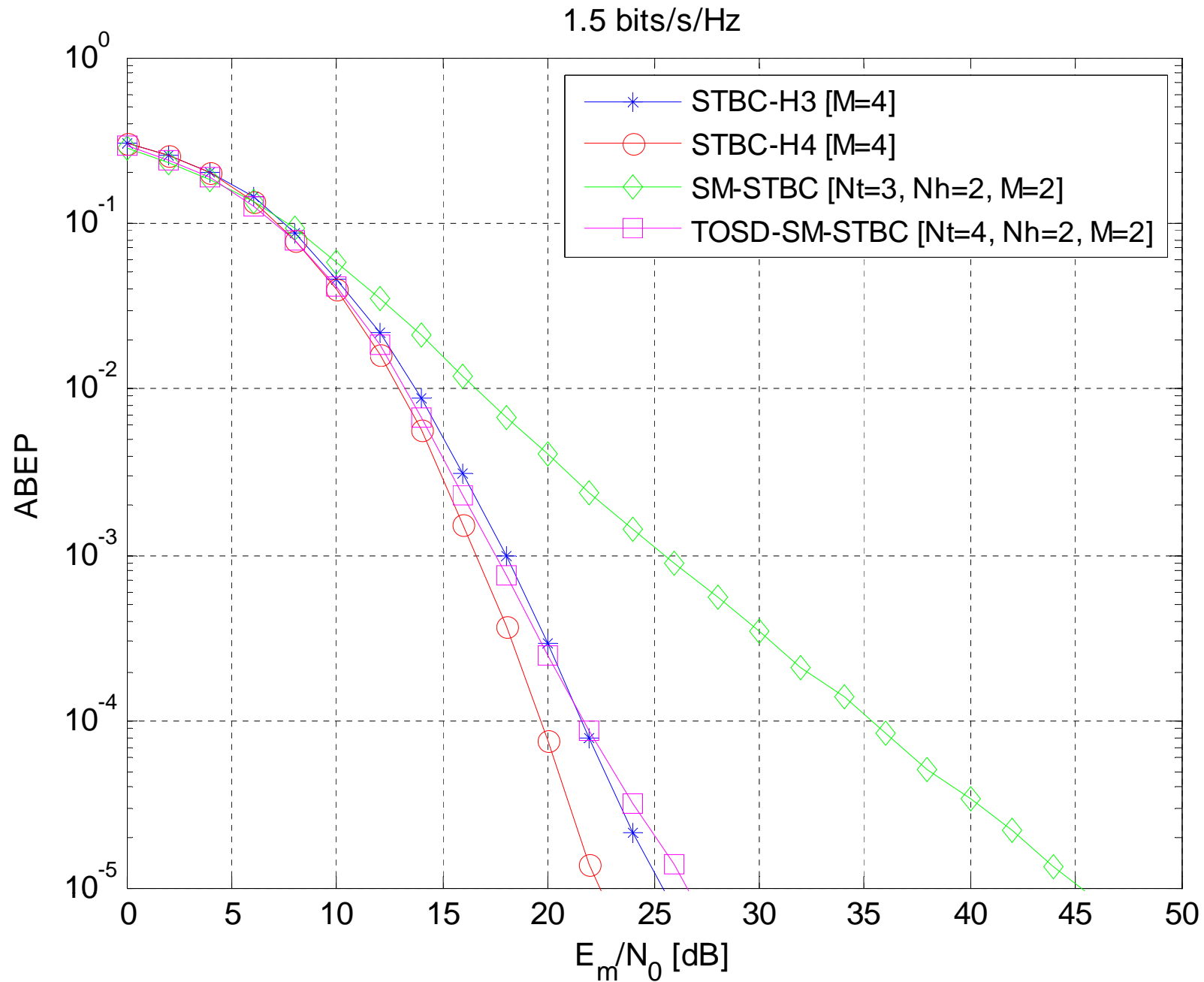
# Transmit-Diversity for SM (41/61)



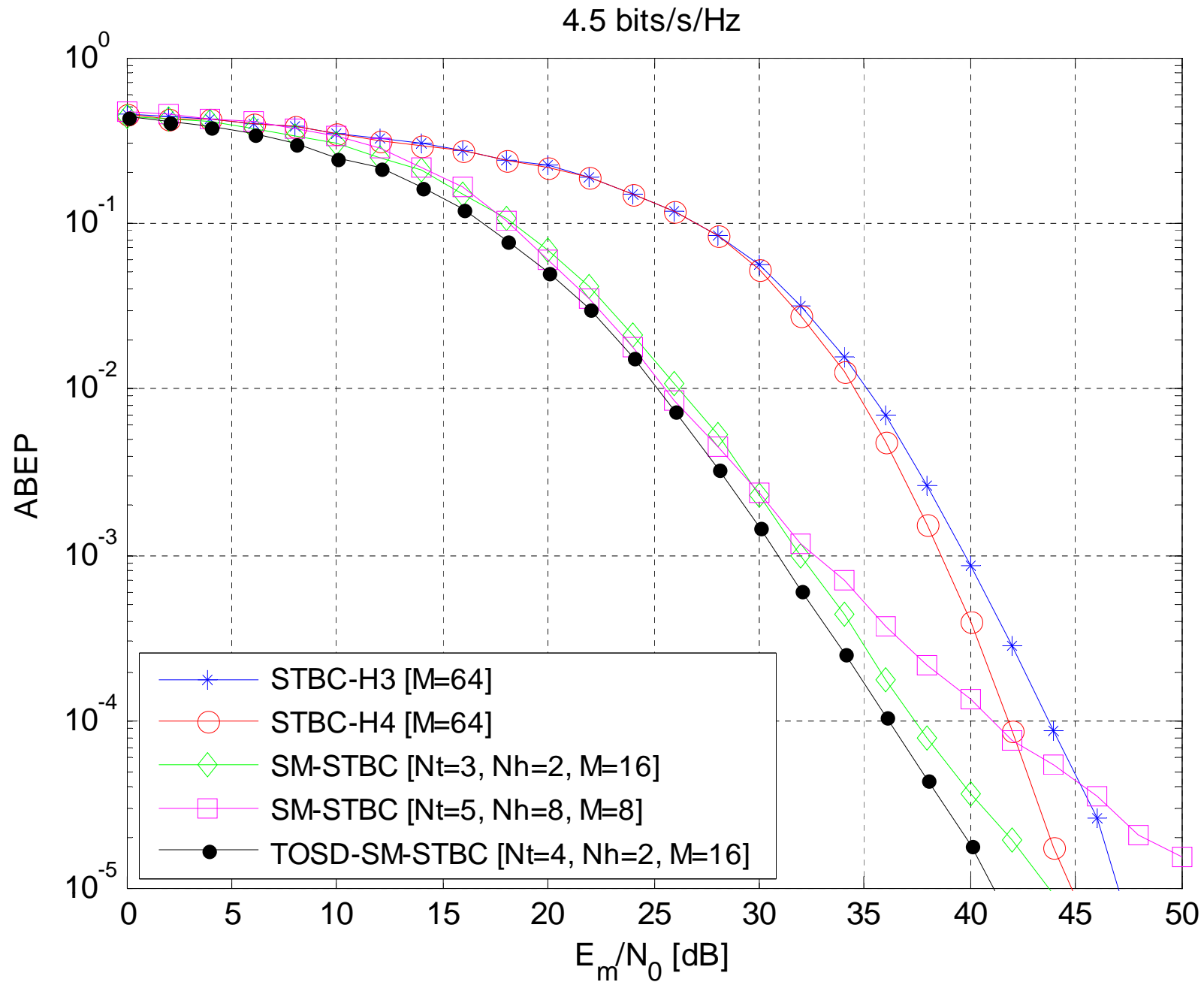
# Transmit-Diversity for SM (42/61)



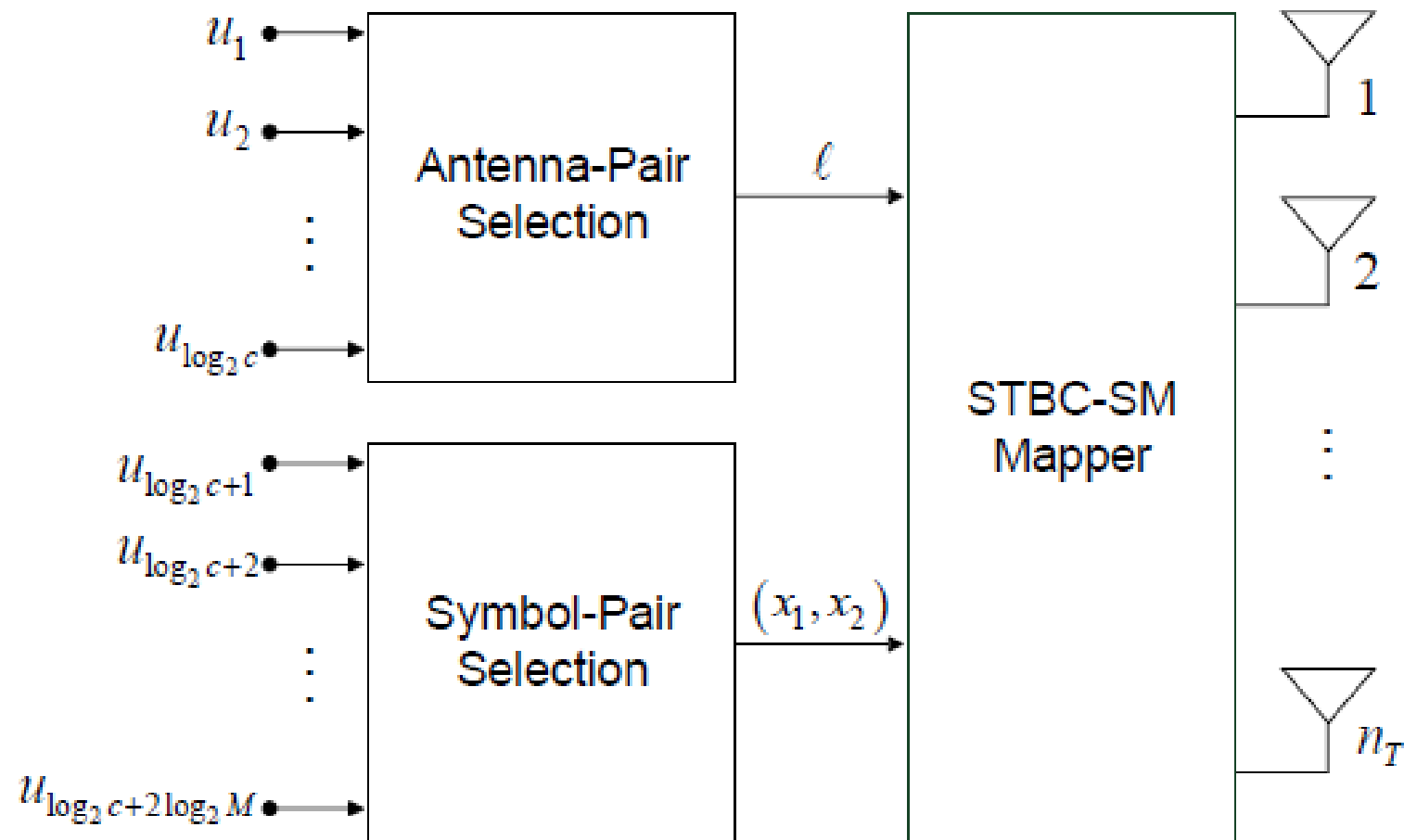
# Transmit-Diversity for SM (43/61)



# Transmit-Diversity for SM (44/61)



# Transmit-Diversity for SM (45/61)



$$m = \frac{1}{2} \log_2 c + \log_2 M \quad [\text{bits/s/Hz}]$$

# Transmit-Diversity for SM (46/61)

Example:

- $N_t = 4$
- BPSK Alamouti
- $R = 2$  bpcu

TABLE I  
STBC-SM MAPPING RULE FOR 2 BITS/s/Hz TRANSMISSION USING  
BPSK, FOUR TRANSMIT ANTENNAS AND ALAMOUTI'S STBC

		Input Bits	Transmission Matrices			Input Bits	Transmission Matrices
$\chi_1$	$\ell = 0$	0000	$\begin{pmatrix} 1 & 1 & 0 & 0 \\ -1 & 1 & 0 & 0 \end{pmatrix}$	$\chi_2$	$\ell = 2$	1000	$\begin{pmatrix} 0 & 1 & 1 & 0 \\ 0 & -1 & 1 & 0 \end{pmatrix} e^{j\theta}$
		0001	$\begin{pmatrix} 1 & -1 & 0 & 0 \\ 1 & 1 & 0 & 0 \end{pmatrix}$			1001	$\begin{pmatrix} 0 & 1 & -1 & 0 \\ 0 & 1 & 1 & 0 \end{pmatrix} e^{j\theta}$
		0010	$\begin{pmatrix} -1 & 1 & 0 & 0 \\ -1 & -1 & 0 & 0 \end{pmatrix}$			1010	$\begin{pmatrix} 0 & -1 & 1 & 0 \\ 0 & -1 & -1 & 0 \end{pmatrix} e^{j\theta}$
		0011	$\begin{pmatrix} -1 & -1 & 0 & 0 \\ 1 & -1 & 0 & 0 \end{pmatrix}$			1011	$\begin{pmatrix} 0 & -1 & -1 & 0 \\ 0 & 1 & -1 & 0 \end{pmatrix} e^{j\theta}$
	$\ell = 1$	0100	$\begin{pmatrix} 0 & 0 & 1 & 1 \\ 0 & 0 & -1 & 1 \end{pmatrix}$		$\ell = 3$	1100	$\begin{pmatrix} 1 & 0 & 0 & 1 \\ 1 & 0 & 0 & -1 \end{pmatrix} e^{j\theta}$
		0101	$\begin{pmatrix} 0 & 0 & 1 & -1 \\ 0 & 0 & 1 & 1 \end{pmatrix}$			1101	$\begin{pmatrix} -1 & 0 & 0 & 1 \\ 1 & 0 & 0 & 1 \end{pmatrix} e^{j\theta}$
		0110	$\begin{pmatrix} 0 & 0 & -1 & 1 \\ 0 & 0 & -1 & -1 \end{pmatrix}$			1110	$\begin{pmatrix} 1 & 0 & 0 & -1 \\ -1 & 0 & 0 & -1 \end{pmatrix} e^{j\theta}$
		0111	$\begin{pmatrix} 0 & 0 & -1 & -1 \\ 0 & 0 & 1 & -1 \end{pmatrix}$			1111	$\begin{pmatrix} -1 & 0 & 0 & -1 \\ -1 & 0 & 0 & 1 \end{pmatrix} e^{j\theta}$

$$\chi_1 = \left\{ \begin{pmatrix} x_1 & x_2 & 0 & 0 \\ -x_2^* & x_1^* & 0 & 0 \end{pmatrix}, \begin{pmatrix} 0 & 0 & x_1 & x_2 \\ 0 & 0 & -x_2^* & x_1^* \end{pmatrix} \right\}$$

$$\chi_2 = \left\{ \begin{pmatrix} 0 & x_1 & x_2 & 0 \\ 0 & -x_2^* & x_1^* & 0 \end{pmatrix}, \begin{pmatrix} x_2 & 0 & 0 & x_1 \\ x_1^* & 0 & 0 & -x_2^* \end{pmatrix} \right\} e^{j\theta}$$



## Transmit-Diversity for SM (47/61)

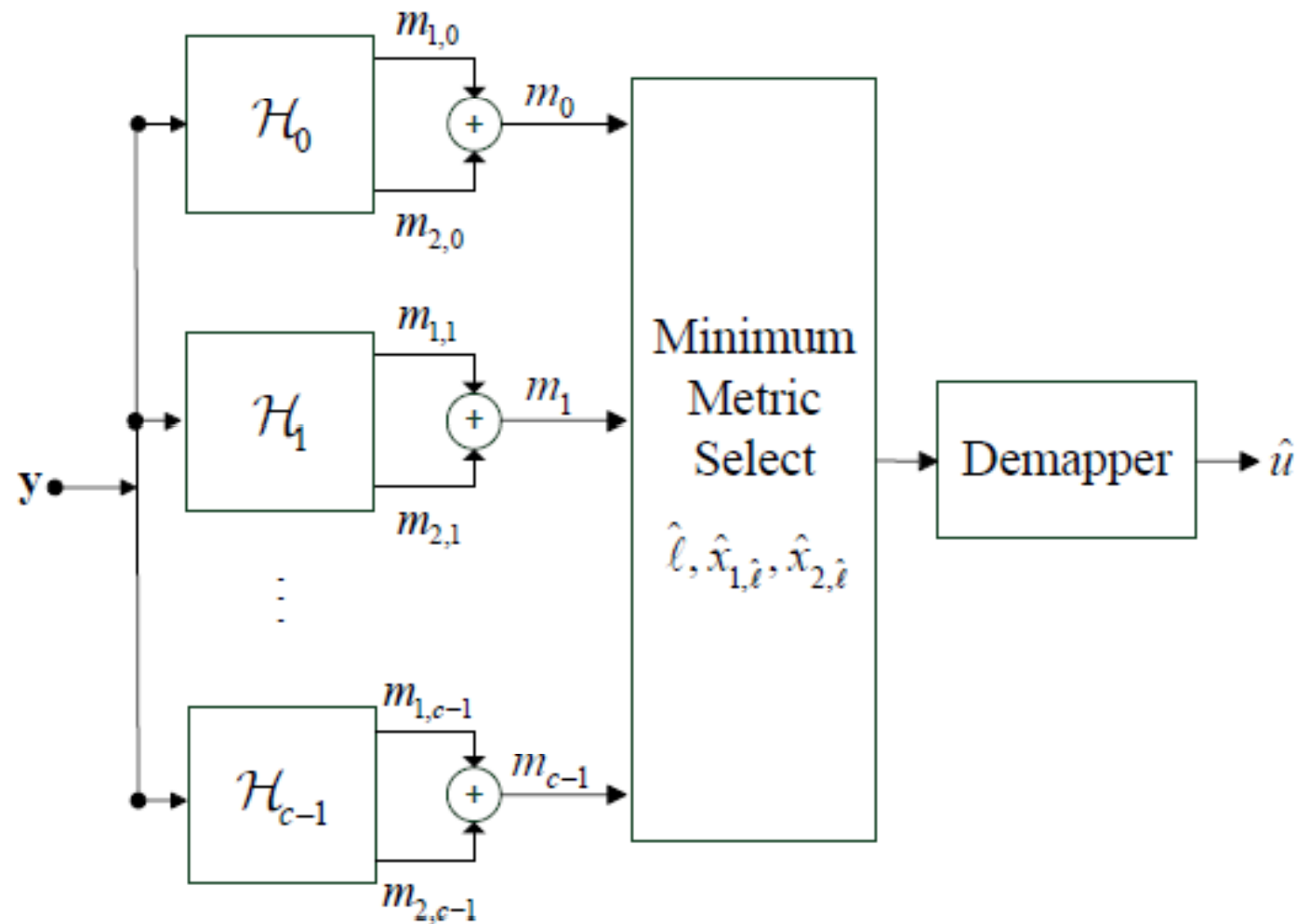


Fig. 3. Block diagram of the STBC-SM ML receiver.

## *Transmit-Diversity for SM (48/61)*

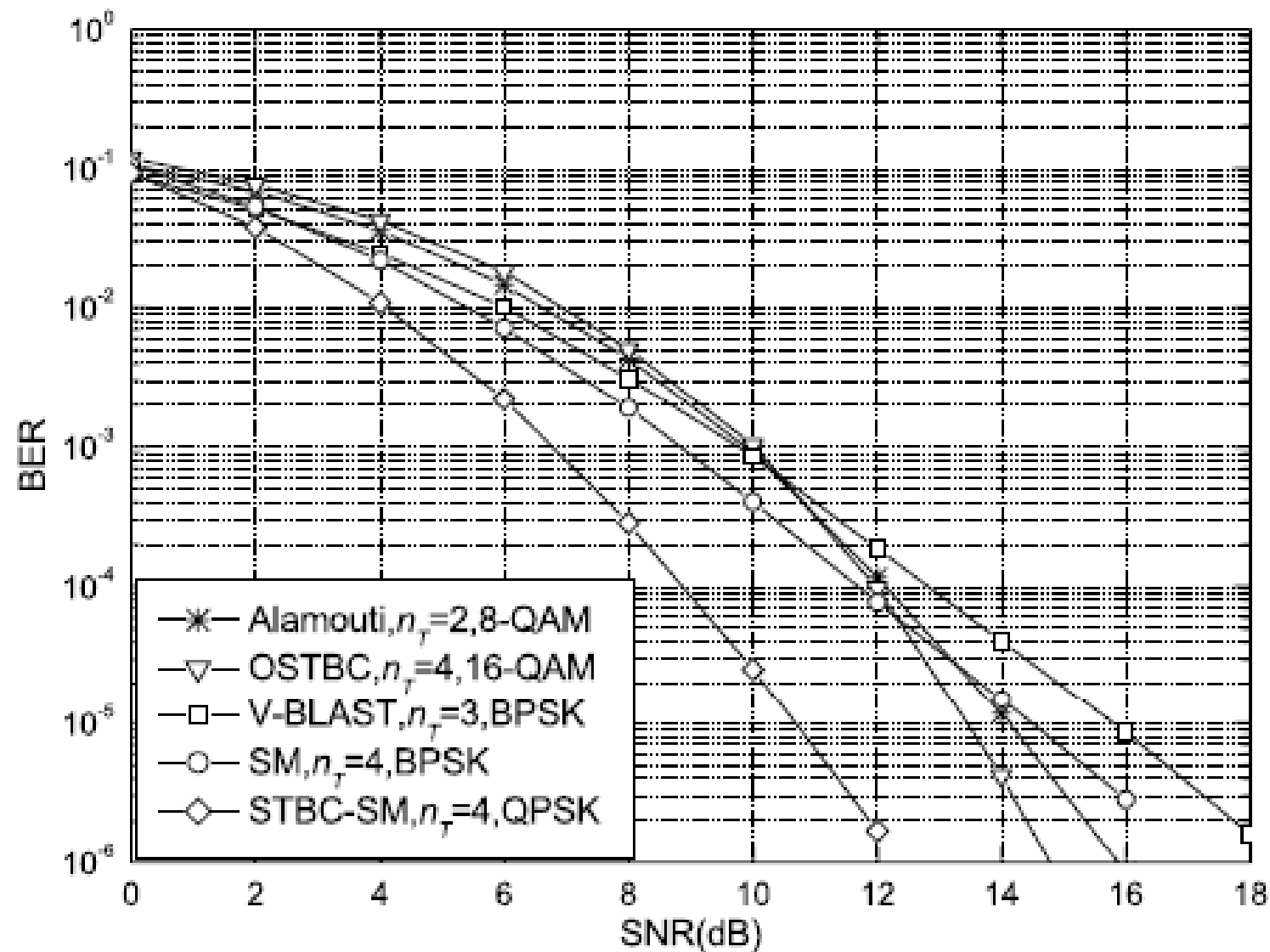


Fig. 5. BER performance at 3 bits/s/Hz for STBC-SM, SM, V-BLAST, OSTBC and Alamouti's STBC schemes.

## Transmit-Diversity for SM (49/61)

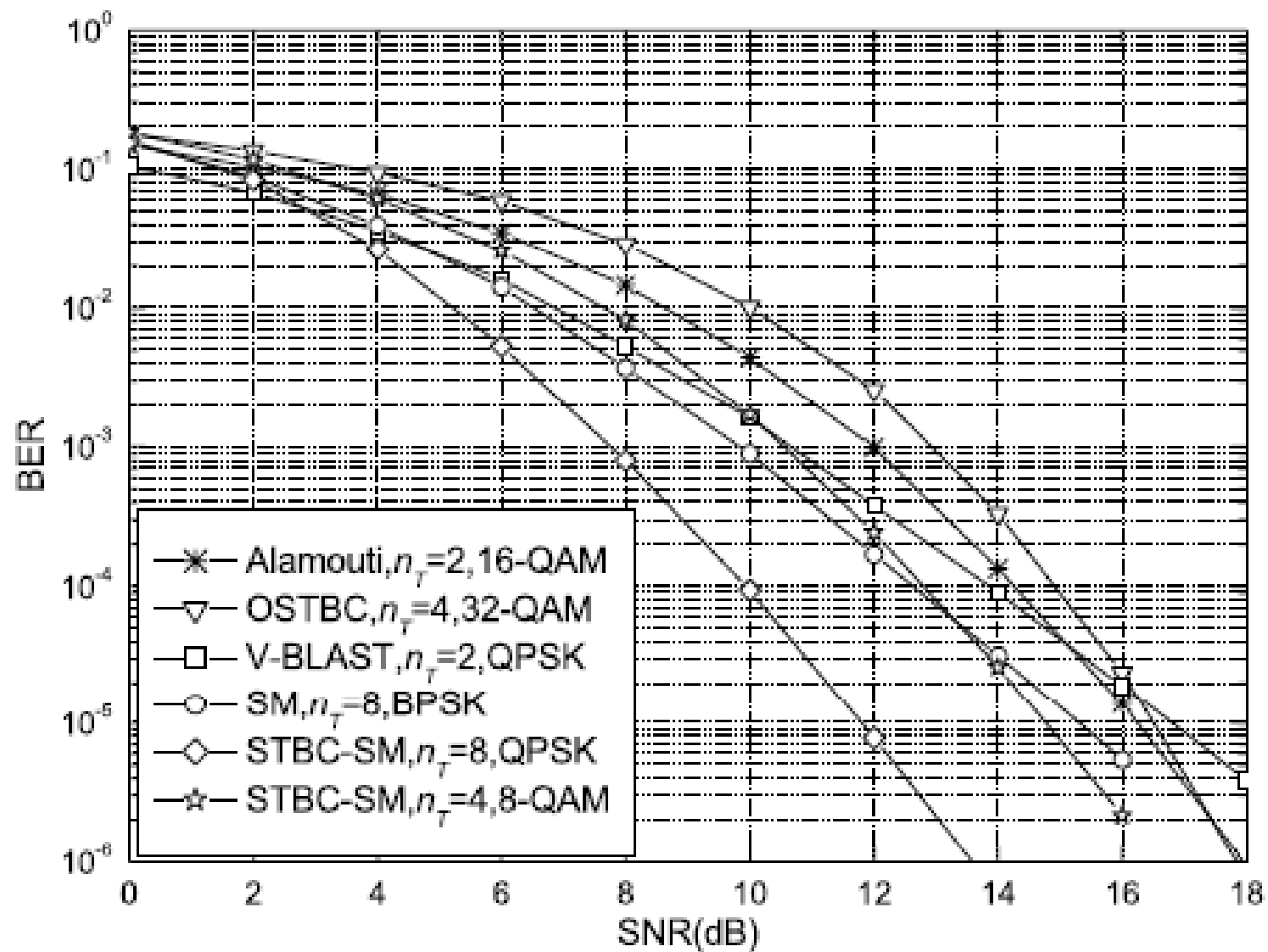


Fig. 6. BER performance at 4 bits/s/Hz for STBC-SM, SM, V-BLAST, OSTBC and Alamouti's STBC schemes.

## *Transmit-Diversity for SM (50/61)*

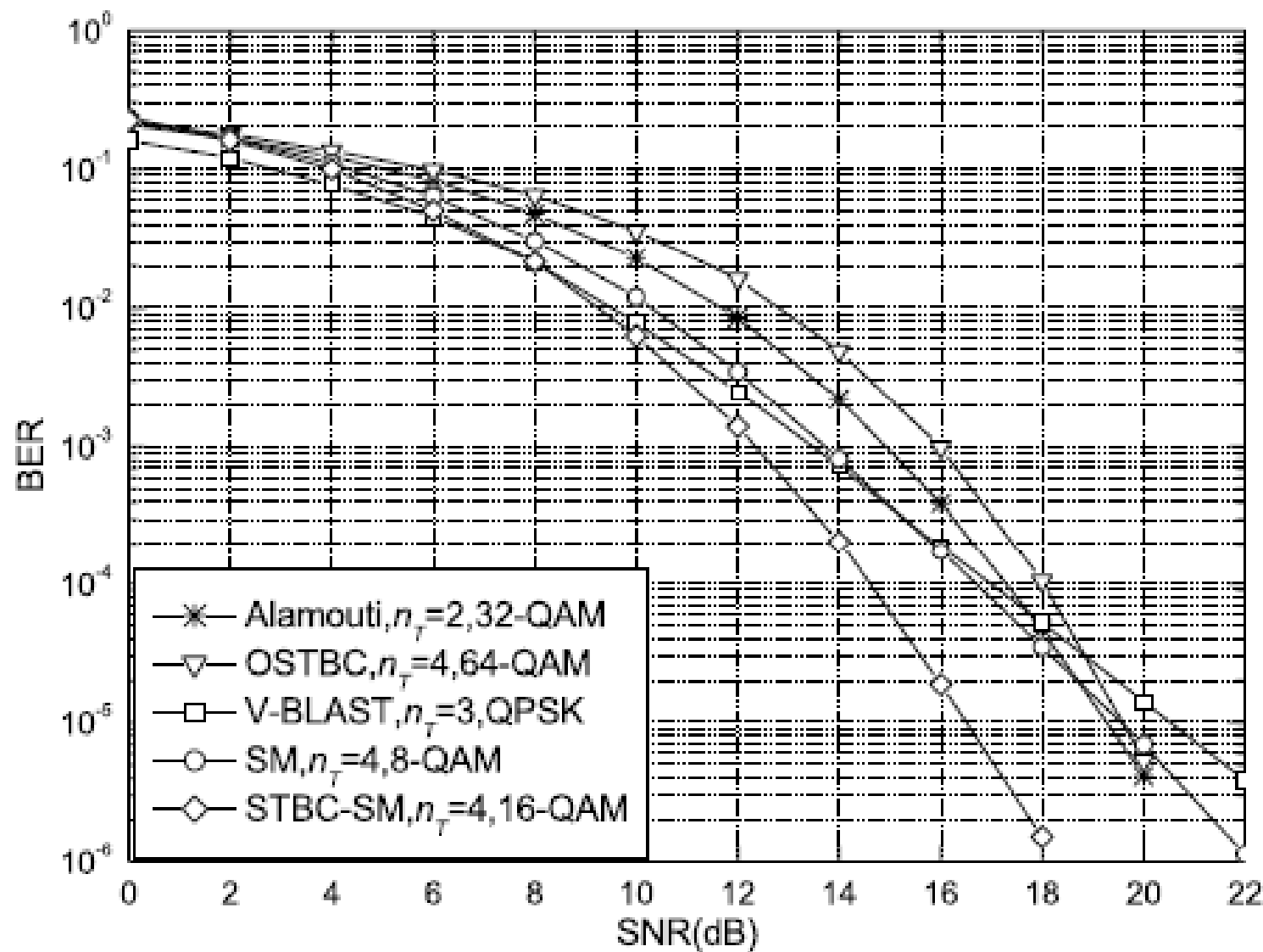


Fig. 7. BER performance at 5 bits/s/Hz for STBC-SM, SM, V-BLAST, OSTBC and Alamouti's STBC schemes.

## Transmit-Diversity for SM (51/61)

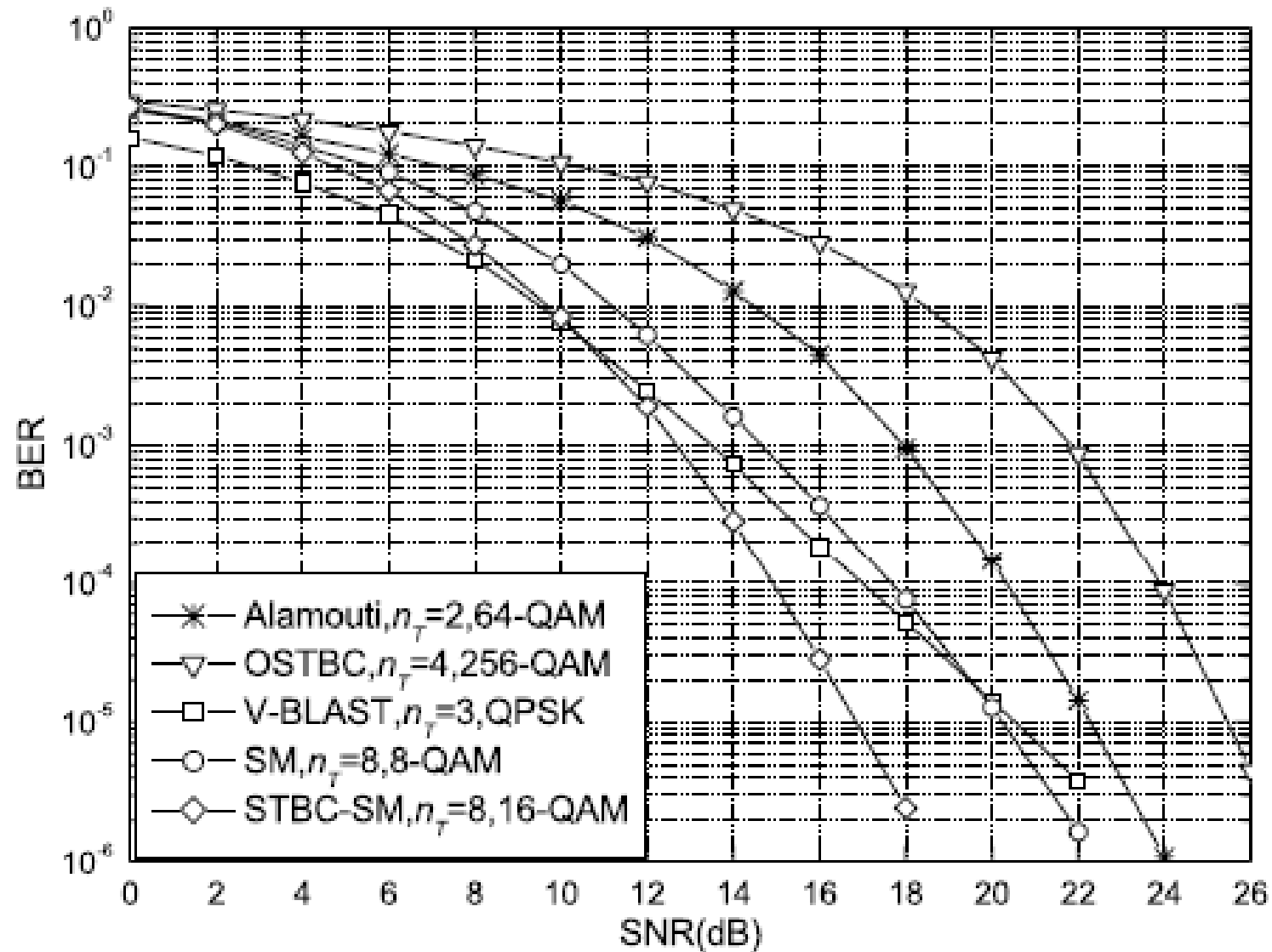


Fig. 8. BER performance at 6 bits/s/Hz for STBC-SM, SM, V-BLAST, OSTBC and Alamouti's STBC schemes.

# *Transmit-Diversity for SM (52/61)*

## The Golden Code

The codewords  $\mathbf{X}$  of the Golden Code are 2x2 complex matrices of the following form :

$$\mathbf{X} = 1/\sqrt{5} * \begin{array}{|c|c|} \hline \alpha [\mathbf{a}+\mathbf{b}\theta] & \alpha [\mathbf{c}+\mathbf{d}\theta] \\ \hline i \sigma(\alpha) [\mathbf{c}+\mathbf{d}\sigma(\theta)] & \sigma(\alpha) [\mathbf{a}+\mathbf{b}\sigma(\theta)] \\ \hline \end{array}$$

where

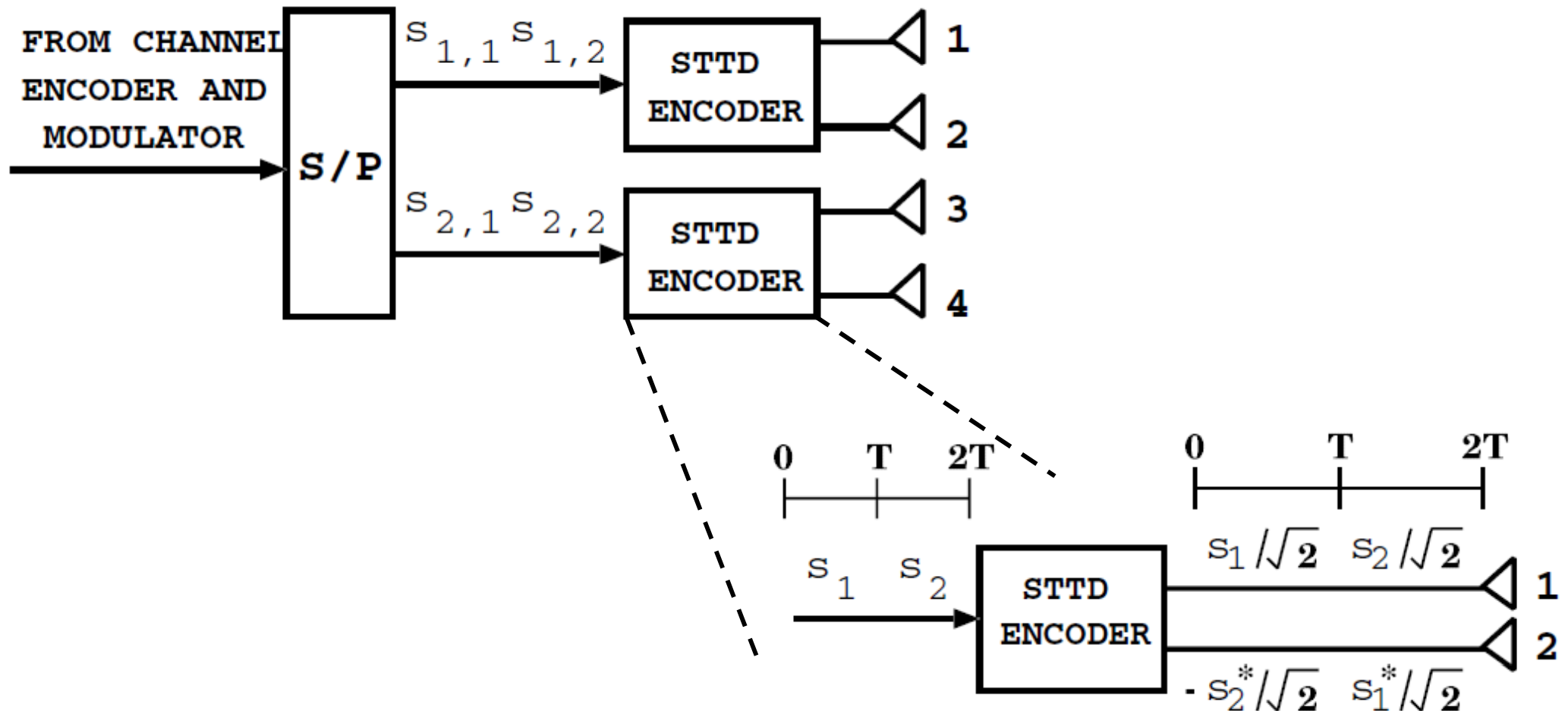
- $\mathbf{a}, \mathbf{b}, \mathbf{c}, \mathbf{d}$  are the information symbols which can be taken from any M-QAM constellation carved from  $\mathbb{Z}[i]$
- $i = \sqrt{-1}$
- $\theta = (1+\sqrt{5})/2 = 1.618\dots$  (*Golden number*)
- $\sigma(\theta) = (1-\sqrt{5})/2 = 1-\theta$
- $\alpha = 1 + i - i \theta = 1 + i \sigma(\theta)$
- $\sigma(\alpha) = 1 + i - i \sigma(\theta) = 1 + i \theta$

J.-C. Belfiore, G. Rekaya, and E. Viterbo, “The golden code: A  $2 \times 2$  full-rate space-time code with nonvanishing determinants”, *IEEE Trans. Inform. Theory*, vol. 51, no. 4, pp. 1432–1436, Apr. 2005.

[http://www.ecse.monash.edu.au/staff/eviterbo/perfect\\_codes/Golden\\_Code.html](http://www.ecse.monash.edu.au/staff/eviterbo/perfect_codes/Golden_Code.html)

# Transmit-Diversity for SM (53/61)

## Double Space-Time Transmit Diversity (DSTTD)



## *Transmit-Diversity for SM (54/61)*

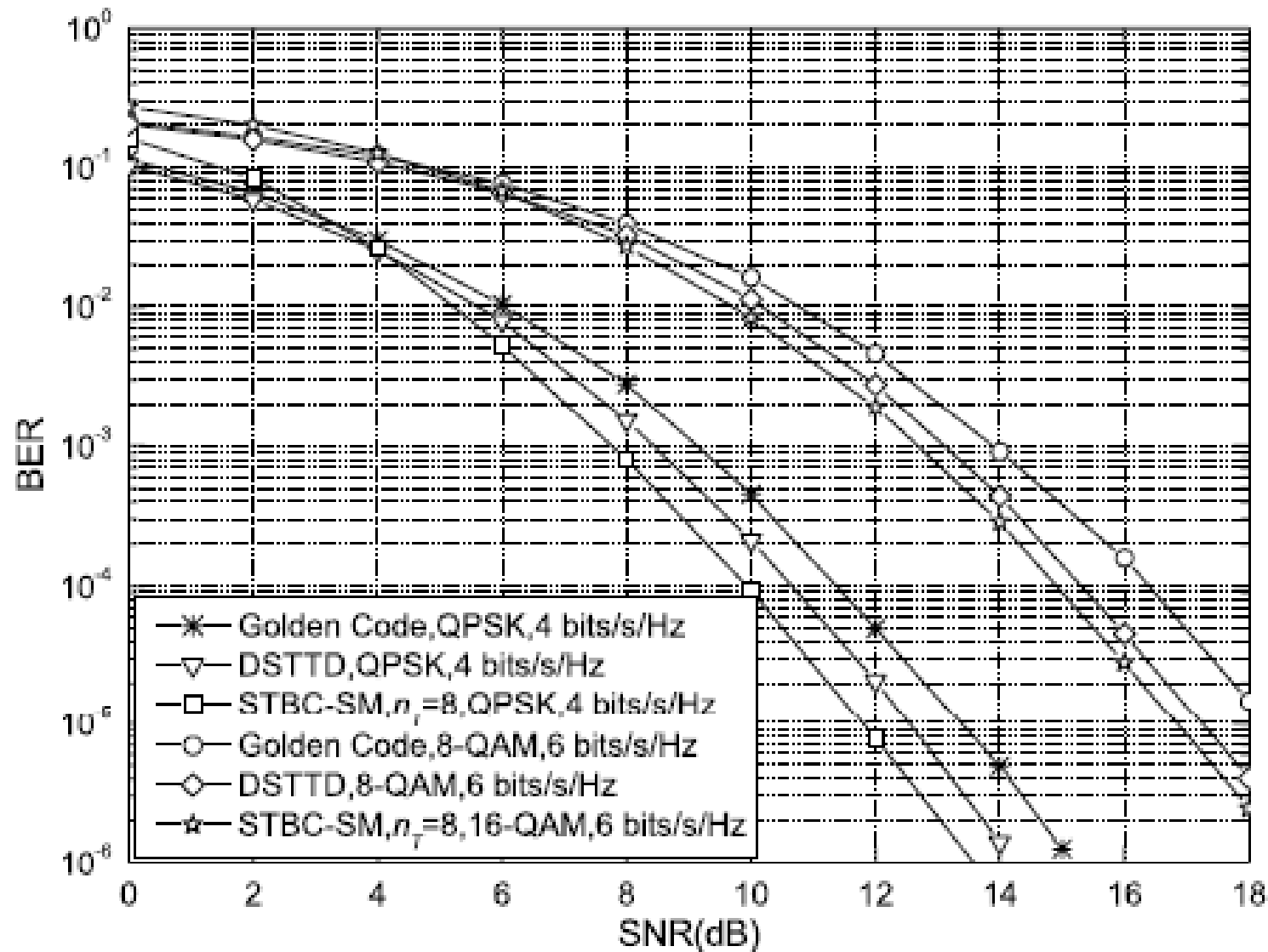


Fig. 9. BER performance for STBC-SM, the Golden code and DSTTD schemes at 4 and 6 bits/s/Hz spectral efficiencies.



## Transmit-Diversity for SM (55/61)

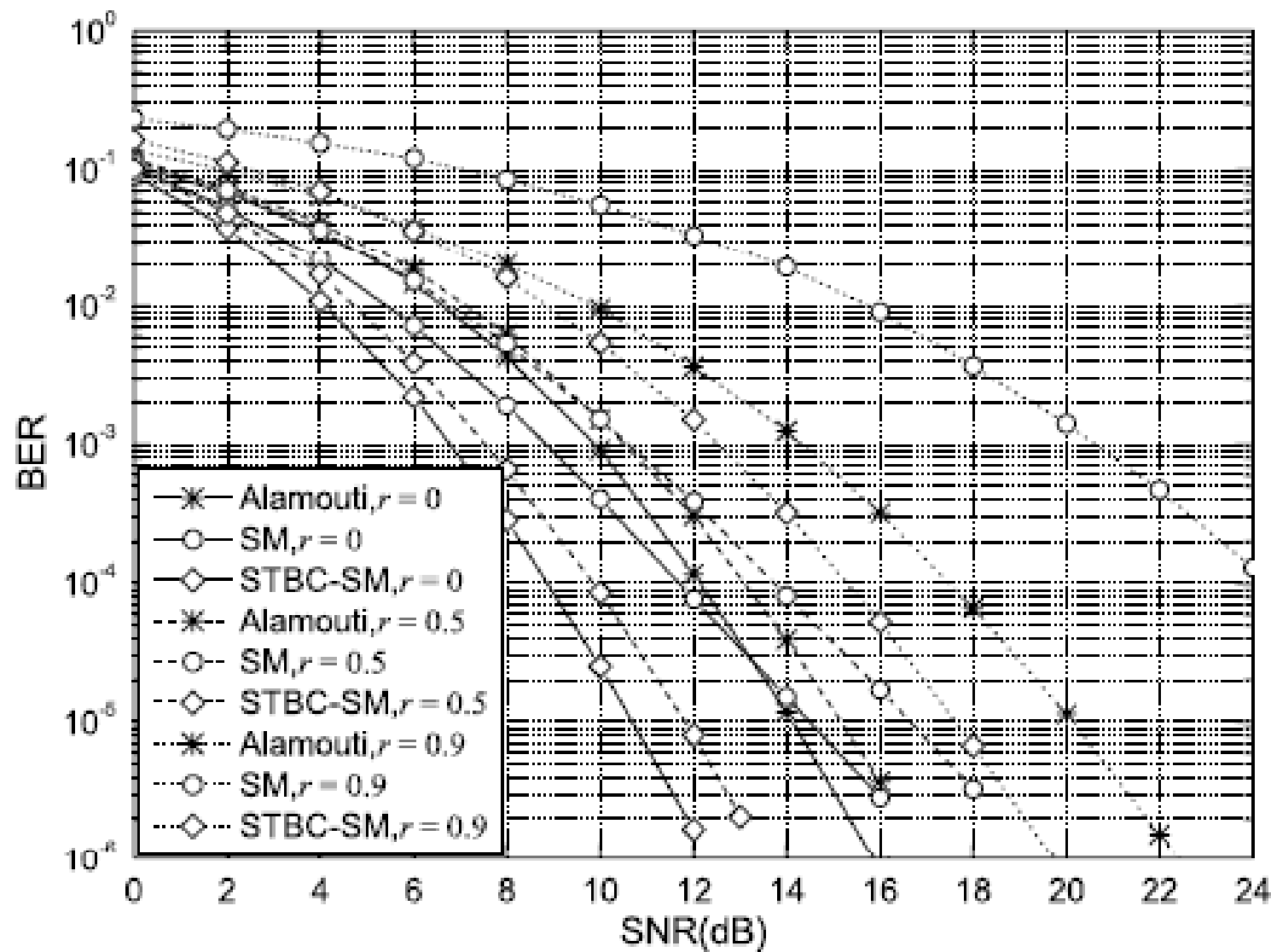



Fig. 10. BER performance at 3 bits/s/Hz for STBC-SM, SM, and Alamouti's STBC schemes for SC channel with  $r = 0, 0.5$  and  $0.9$ .

## *Transmit-Diversity for SM (56/61)*

### SM-CIOD: Transmit-Diversity with a Single-RF Chain

antennas  $\left\{ \underbrace{\begin{bmatrix} \tilde{s}_1 & 0 \\ 0 & \tilde{s}_2 \end{bmatrix}}_{\text{channel uses}} \right.$

$$s = \exp\left(j \frac{\arctan(2)}{2}\right) x_{\text{QAM}}$$


$$\begin{cases} \tilde{s}_1 = s_{1,I} + js_{2,Q} \\ \tilde{s}_2 = s_{2,I} + js_{1,Q} \end{cases}$$

# Transmit-Diversity for SM (57/61)

## SM-CIOD: Transmit-Diversity with a Single-RF Chain

$$\left\{ \underbrace{\begin{bmatrix} \tilde{s}_1 & 0 \\ 0 & \tilde{s}_2 \\ 0 & 0 \\ \vdots & \vdots \\ 0 & 0 \\ 0 & 0 \end{bmatrix}}_{CB_1}, \underbrace{\begin{bmatrix} 0 & 0 \\ \tilde{s}_1 & 0 \\ 0 & \tilde{s}_2 \\ \vdots & \vdots \\ 0 & 0 \\ 0 & 0 \end{bmatrix}}_{CB_2}, \underbrace{\begin{bmatrix} 0 & 0 \\ 0 & 0 \\ \tilde{s}_1 & 0 \\ 0 & \tilde{s}_2 \\ \vdots & \vdots \\ 0 & 0 \end{bmatrix}}_{CB_3}, \dots, \underbrace{\begin{bmatrix} 0 & 0 \\ 0 & 0 \\ 0 & 0 \\ \vdots & \vdots \\ \tilde{s}_1 & 0 \\ 0 & \tilde{s}_2 \end{bmatrix}}_{CB_{N_t-1}}, \underbrace{\begin{bmatrix} 0 & \tilde{s}_2 \\ 0 & 0 \\ 0 & 0 \\ \vdots & \vdots \\ 0 & 0 \\ \tilde{s}_1 & 0 \end{bmatrix}}_{CB_{N_t}} \right\}$$

$$\frac{\log_2 N_t + \log_2 M^2}{2} \text{ bpcu.}$$

- First channel use: antenna **1** is used
- Second channel use: antenna **(l+1) mod N<sub>t</sub>** is used

# Transmit-Diversity for SM (58/61)

## SM-CIOD: Transmit-Diversity with a Single-RF Chain

$$\begin{aligned}
 CBS_1 &= \left\{ \begin{bmatrix} \tilde{s}_1 & * \\ 0 & \tilde{s}_2 \\ 0 & 0 \\ \bullet & 0 \end{bmatrix}, \begin{bmatrix} 0 & 0 \\ \tilde{s}_1 & * \\ 0 & \tilde{s}_2 \\ \bullet & 0 \end{bmatrix}, \begin{bmatrix} 0 & 0 \\ 0 & 0 \\ \tilde{s}_1 & * \\ 0 & \tilde{s}_2 \end{bmatrix}, \begin{bmatrix} 0 & 0 \\ 0 & 0 \\ \tilde{s}_1 & * \\ \bullet & \tilde{s}_2 \end{bmatrix} \right\} \\
 CBS_2 &= \left\{ \begin{bmatrix} \tilde{s}_1 & * \\ 0 & 0 \\ 0 & \tilde{s}_2 \\ \bullet & 0 \end{bmatrix}, \begin{bmatrix} 0 & 0 \\ \tilde{s}_1 & * \\ 0 & 0 \\ \bullet & \tilde{s}_2 \end{bmatrix}, \begin{bmatrix} 0 & 0 \\ 0 & 0 \\ \tilde{s}_1 & * \\ 0 & 0 \end{bmatrix}, \begin{bmatrix} 0 & \tilde{s}_2 \\ 0 & 0 \\ \tilde{s}_1 & * \\ \bullet & 0 \end{bmatrix} \right\} \\
 CBS_3 &= \left\{ \begin{bmatrix} \tilde{s}_1 & * \\ 0 & 0 \\ 0 & 0 \\ \bullet & \tilde{s}_2 \end{bmatrix}, \begin{bmatrix} 0 & 0 \\ \tilde{s}_1 & * \\ 0 & 0 \\ \bullet & \tilde{s}_2 \end{bmatrix}, \begin{bmatrix} 0 & \tilde{s}_2 \\ 0 & 0 \\ \tilde{s}_1 & * \\ \bullet & 0 \end{bmatrix}, \begin{bmatrix} 0 & 0 \\ 0 & \tilde{s}_2 \\ 0 & 0 \\ \tilde{s}_1 & * \end{bmatrix} \right\} \\
 CBS_4 &= \left\{ \begin{bmatrix} \tilde{s}_1 & * \\ 0 & 0 \\ 0 & 0 \\ \bullet & \tilde{s}_2 \end{bmatrix}, \begin{bmatrix} 0 & \tilde{s}_2 \\ \tilde{s}_1 & * \\ 0 & 0 \\ \bullet & 0 \end{bmatrix}, \begin{bmatrix} 0 & 0 \\ 0 & \tilde{s}_2 \\ \tilde{s}_1 & * \\ \bullet & 0 \end{bmatrix}, \begin{bmatrix} 0 & 0 \\ 0 & 0 \\ 0 & \tilde{s}_2 \\ \tilde{s}_1 & * \end{bmatrix} \right\} \\
 CBS_i &= \{e^{j\theta_i} CB_{i,j} \mid 1 \leq j \leq N_t\} \text{ for } 1 \leq i \leq N_t,
 \end{aligned}$$

$$\frac{\log_2 N_t^2 + \log_2 M^2}{2} = \log_2 (N_t M) \text{ bpcu.}$$

- $N_t + 1$  antennas
- $N_t^2$  CBS

# *Transmit-Diversity for SM (59/61)*

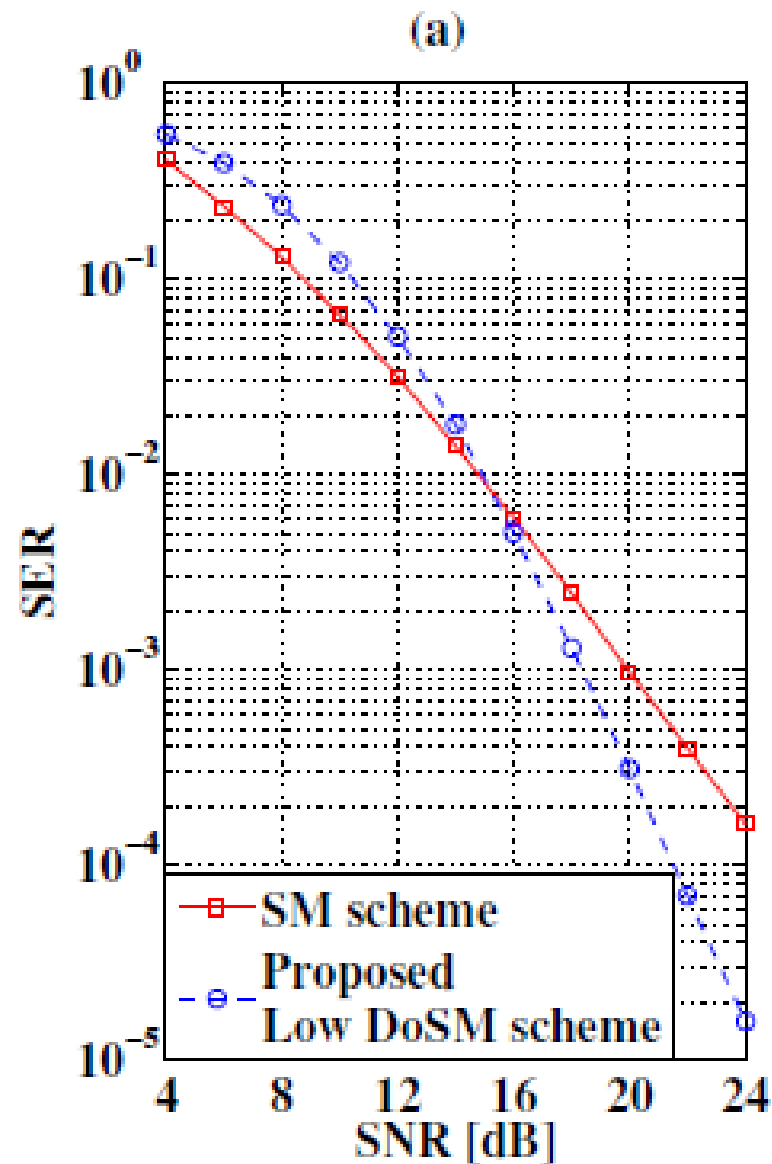
## Phase Rotations

TABLE III  
CODING GAIN OPTIMIZED EXPONENTIALS FOR THE PROPOSED SCHEME WITH HIGH DoSM.

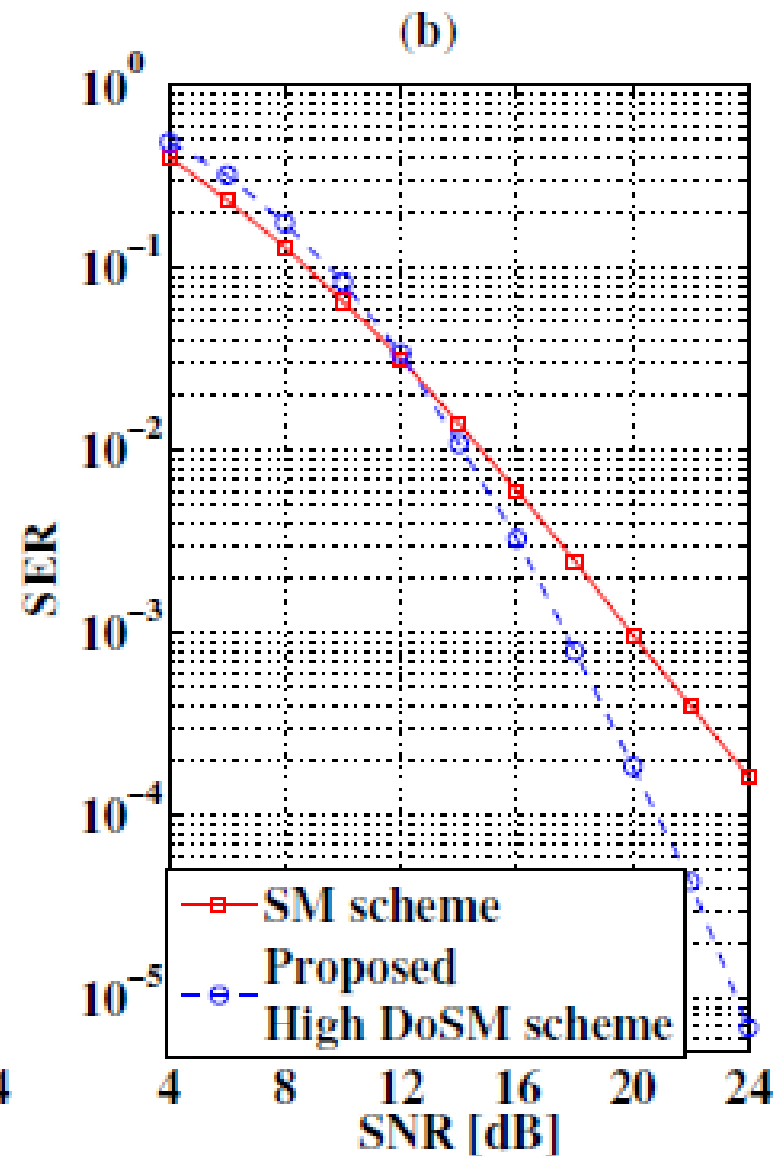
	$e^{j\theta_1}$	$e^{j\theta_2}$	$e^{j\theta_3}$	$e^{j\theta_4}$
4-QAM	$-0.9239 + 0.3827j$	$1.0000j$	$0.7071 + 0.7071j$	$0.9239 + 0.3827j$
8-QAM	1	$0.8090 - 0.5878j$	$-0.3090 + 0.951j$	$0.3090 + 0.951j$

## Transmit-Diversity for SM (60/61)

Low DoSM scheme with  $N_t=4$ ,  
 $N_r=2$ , 8-QAM ( $R=4$  bpcu)

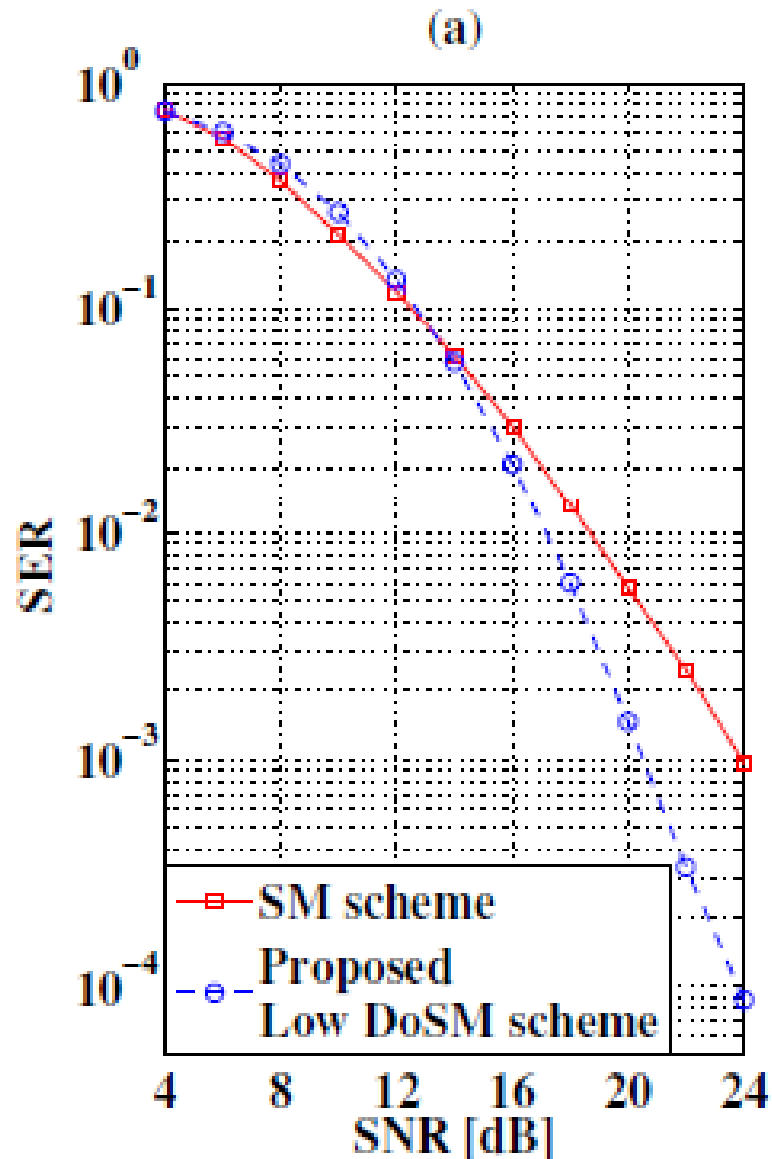


High DoSM scheme with  $N_t=5$ ,  
 $N_r=2$ , 4-QAM ( $R=4$  bpcu)

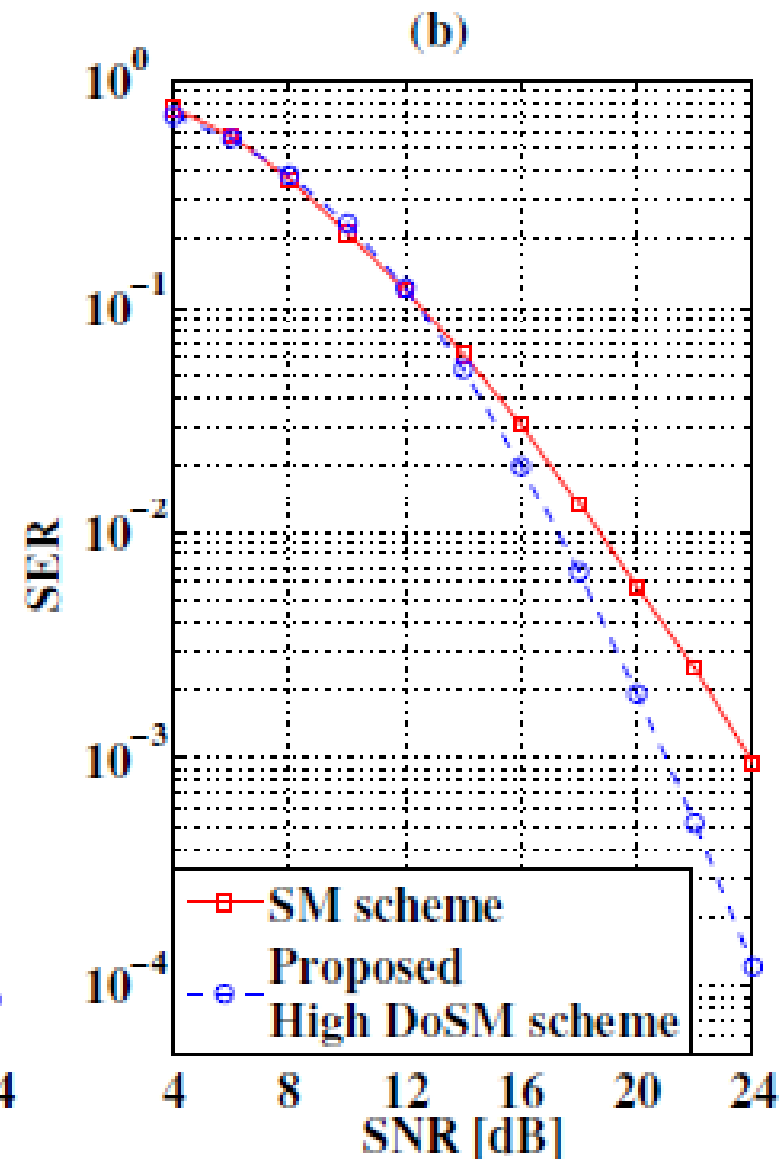


## Transmit-Diversity for SM (61/61)

Low DoSM scheme with  $N_t=4$ ,  
 $N_r=2$ , 16-QAM ( $R=5$  bpcu)



High DoSM scheme with  $N_t=5$ ,  
 $N_r=2$ , 8-QAM ( $R=5$  bpcu)



# *Outline*

---

1. Introduction and Motivation behind SM-MIMO
2. History of SM Research and Research Groups Working on SM
3. Transmitter Design – Encoding
4. Receiver Design – Demodulation
5. Error Performance (Numerical Results and Main Trends)
6. Achievable Capacity
7. Channel State Information at the Transmitter
8. Imperfect Channel State Information at the Receiver
9. Multiple Access Interference
10. Energy Efficiency
11. Transmit-Diversity for SM
- 12. Spatially-Modulated Space-Time-Coded MIMO**
13. Relay-Aided SM
14. SM in Heterogeneous Cellular Networks
15. SM for Visible Light Communications
16. Experimental Evaluation of SM
17. The Road Ahead – Open Research Challenges/Opportunities
18. Implementation Challenges of SM-MIMO



## *Spatially-Modulated Space-Time-Coded MIMO (1/23)*

The signal received at the  $r$ -th receive-antenna and at the  $s$ -th time-slot is  $((s-1)T_s \leq \xi < sT_s)$ :

$$z_{s,r}(\xi) = \sqrt{\frac{E_S}{\|\mathbf{a}^{(\alpha)}\|_{\tilde{\mathbf{F}}}^2}} \sum_{t=1}^{N_t} \left[ \mathbf{X}_{s,t}^{(\alpha)}(\mu) \mathbf{H}_{r,t} w_t(\xi) \right] + n_{s,r}(\xi)$$

where we have defined:

$$\begin{aligned} \mathbf{X}_{s,t}^{(\alpha)}(\mu) &= \mathbf{a}_t^{(\alpha)} \mathbf{M}_{s,t \circ N_\alpha}(\mu) \\ &= \begin{cases} 0 & \text{if } \mathbf{a}_t^{(\alpha)} = 0 \\ \mathbf{M}_{s,t \circ N_\alpha}(\mu) & \text{if } \mathbf{a}_t^{(\alpha)} = 1 \end{cases} \end{aligned}$$

□  $N_t$  transmit-antennas

$N_\alpha$  active transmit-antennas

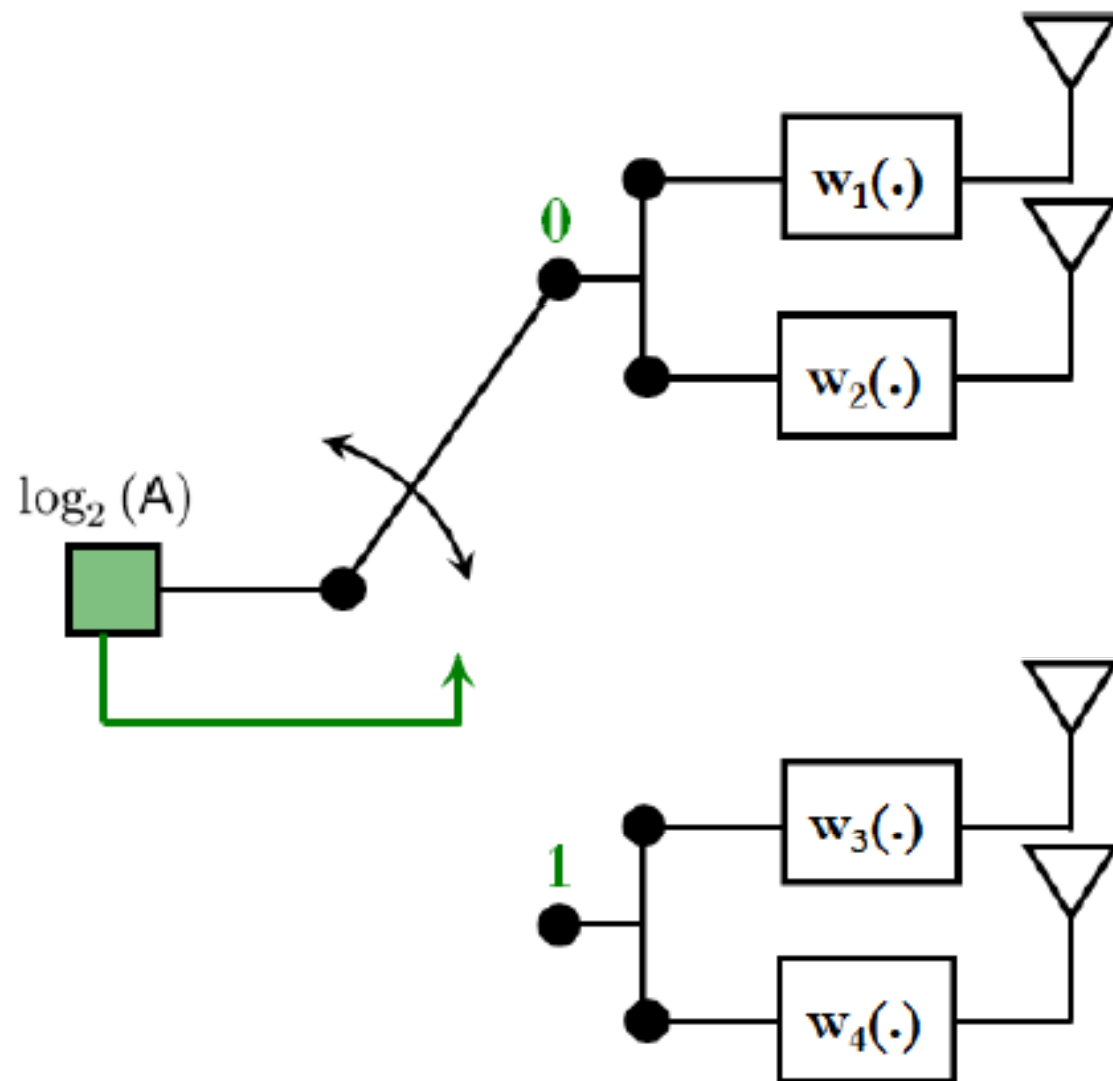
□  $N_r$  receive-antennas

$N_s$  time-slots

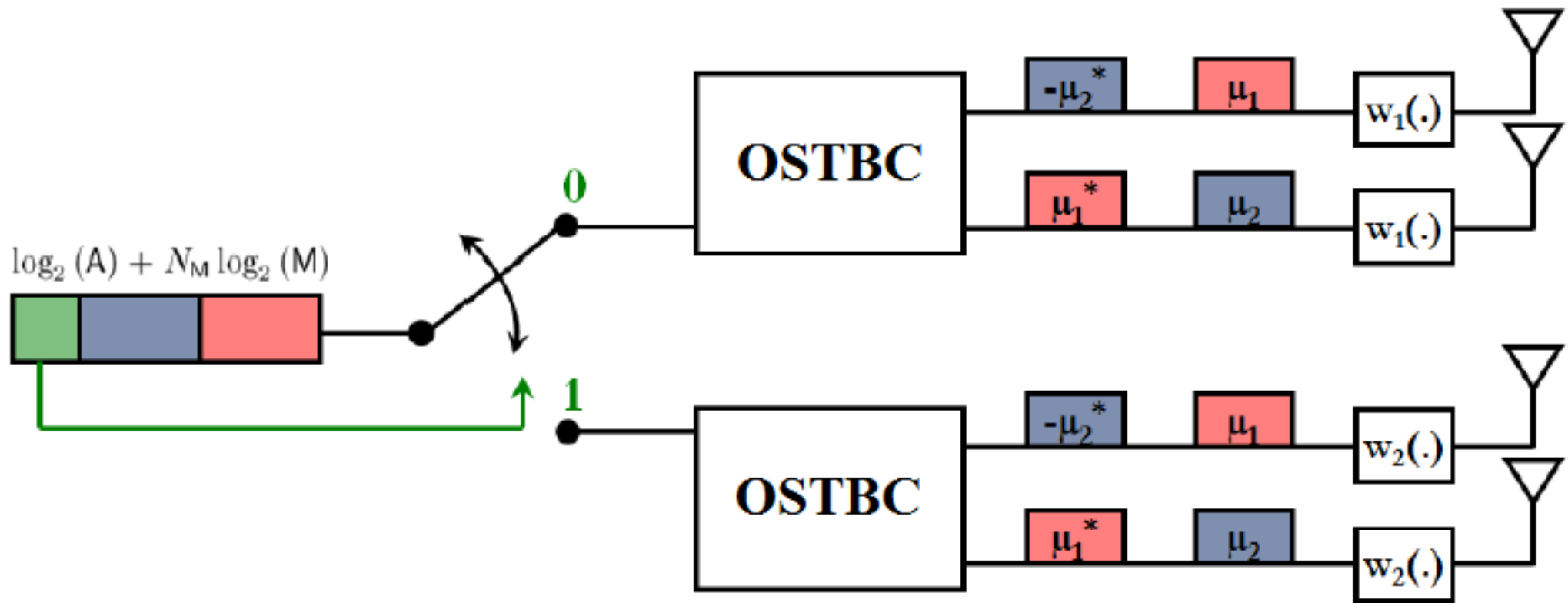
M. Di Renzo and H. Haas, “On Transmit-Diversity for Spatial Modulation MIMO: Impact of Spatial-Constellation Diagram and Shaping Filters at the Transmitter”, *IEEE Transactions on Vehicular Technology*, Vol. 62, No. 6, pp. 2507–2531, July 2013. – See “Correction Paper” too:

[http://hal.archives-ouvertes.fr/docs/00/84/75/74/PDF/Correction\\_TransmitDiversitySM.pdf](http://hal.archives-ouvertes.fr/docs/00/84/75/74/PDF/Correction_TransmitDiversitySM.pdf)

## *Spatially-Modulated Space-Time-Coded MIMO (2/23)*



# *Spatially-Modulated Space-Time-Coded MIMO (3/23)*



# Spatially-Modulated Space-Time-Coded MIMO (4/23)

$$(\hat{\alpha}, \hat{\mu}) = \arg \min_{\mathbf{a}^{(\hat{\alpha})} \in \mathcal{A}, \tilde{\mu} = [\tilde{\mu}_1 \in \mathcal{M}, \tilde{\mu}_2 \in \mathcal{M}, \dots, \tilde{\mu}_{N_M} \in \mathcal{M}]^T} \underbrace{\left\{ \sum_{s=1}^{N_s} \sum_{r=1}^{N_r} \int_{(s-1)T_s}^{sT_s} \left| z_{s,r}(\xi) - \sqrt{\frac{E_S}{\|\mathbf{a}^{(\hat{\alpha})}\|_{\tilde{\mathbf{F}}}^2}} \sum_{t=1}^{N_t} [\mathbf{X}_{s,t}^{(\hat{\alpha})}(\tilde{\mu}) \mathbf{H}_{r,t} w_t(\xi - (s-1)T_s)] \right|^2 d\xi \right\}}_{\Lambda(\tilde{\alpha}, \tilde{\mu})}$$



$$\text{ABEP} \leq \sum_{\chi} \frac{1}{A M^{N_M}} \sum_{\tilde{\chi} \neq \chi} \frac{\mathcal{H}_d(\chi, \tilde{\chi}) \text{APEP}(\chi \rightarrow \tilde{\chi})}{\log_2(A) + N_M \log_2(M)}$$



$$\gamma_{\chi \rightarrow \tilde{\chi}}(\mathbf{H}) = \sum_{s=1}^{N_s} \sum_{r=1}^{N_r} \left\{ \sum_{t_1=1}^{N_t} \sum_{t_2=1}^{N_t} \left[ \left( \frac{\mathbf{X}_{s,t_1}^{(\tilde{\alpha})}(\tilde{\mu})}{\|\mathbf{a}^{(\tilde{\alpha})}\|_{\tilde{\mathbf{F}}}^2} - \frac{\mathbf{X}_{s,t_1}^{(\alpha)}(\mu)}{\|\mathbf{a}^{(\alpha)}\|_{\tilde{\mathbf{F}}}^2} \right) \left( \frac{\mathbf{X}_{s,t_2}^{(\tilde{\alpha})}(\tilde{\mu})}{\|\mathbf{a}^{(\tilde{\alpha})}\|_{\tilde{\mathbf{F}}}^2} - \frac{\mathbf{X}_{s,t_2}^{(\alpha)}(\mu)}{\|\mathbf{a}^{(\alpha)}\|_{\tilde{\mathbf{F}}}^2} \right)^* \mathbf{H}_{r,t_1} \mathbf{H}_{r,t_2}^* \int_0^{T_s} w_{t_1}(\xi) w_{t_2}(\xi) d\xi \right] \right\}$$

$$\gamma_{\chi \rightarrow \tilde{\chi}}(\mathbf{H}) = \eta(\mathbf{H})^H \Psi(\chi, \tilde{\chi}) \eta(\mathbf{H})$$

## *Spatially-Modulated Space-Time-Coded MIMO (5/23)*

$$\begin{aligned}
 \text{APEP}(\chi \rightarrow \tilde{\chi}) &= \mathbb{E}_{\mathbf{H}} \left\{ \mathcal{Q} \left( \sqrt{\frac{E_S}{4N_0}} \gamma_{\chi \rightarrow \tilde{\chi}}(\mathbf{H}) \right) \right\} \\
 &\stackrel{(1)}{=} \frac{1}{\pi} \int_0^{\pi/2} \mathbb{E}_{\mathbf{H}} \left\{ \exp \left( -\frac{E_S}{8N_0 \sin^2(\theta)} \gamma_{\chi \rightarrow \tilde{\chi}}(\mathbf{H}) \right) \right\} d\theta \\
 &\stackrel{(2)}{=} \frac{1}{\pi} \int_0^{\pi/2} \mathcal{L}_{\gamma_{\chi \rightarrow \tilde{\chi}}} \left( \frac{E_S}{8N_0 \sin^2(\theta)} \right) d\theta
 \end{aligned}$$



$$\begin{aligned}
 \text{APEP}(\chi \rightarrow \tilde{\chi}) &= \frac{1}{\pi} \int_0^{\pi/2} \prod_{\bar{\lambda}_q \in \mathcal{K}(\mathbf{R}_\eta \Psi(\chi, \tilde{\chi}))} \left( 1 + \frac{E_S}{8N_0 \sin^2(\theta)} \bar{\lambda}_q \right)^{-1} d\theta \\
 &\xrightarrow{E_S/N_0 \gg 1} \left( G_c(\chi, \tilde{\chi}) \frac{E_S}{4N_0} \right)^{-G_d(\chi, \tilde{\chi})}
 \end{aligned}$$

## *Spatially-Modulated Space-Time-Coded MIMO (6/23)*

$$G_c(\chi, \tilde{\chi}) = \left( \tilde{G}_c(\chi, \tilde{\chi}) \prod_{\bar{\lambda}_q \in \mathcal{K}(\mathbf{R}_\eta \Psi(\chi, \tilde{\chi}))} \bar{\lambda}_q^{-1} \right)^{-1/G_d(\chi, \tilde{\chi})}$$
$$G_d(\chi, \tilde{\chi}) = \text{card} \{ \mathcal{K}(\mathbf{R}_\eta \Psi(\chi, \tilde{\chi})) \}$$



$$\begin{aligned} \mathbb{D} &= \min_{(\chi, \tilde{\chi})} \{ G_d(\chi, \tilde{\chi}) \} \\ &= \min_{(\chi, \tilde{\chi})} \{ \text{card} \{ \mathcal{K}(\mathbf{R}_\eta \Psi(\chi, \tilde{\chi})) \} \} \end{aligned}$$

# Spatially-Modulated Space-Time-Coded MIMO (7/23)

## Description of Transmission Modes

**GSSK (Generalized Space Shift Keying)** – The spatial-constellation diagram is chosen such that its symbols  $\mathbf{a}^{(\alpha)} \in \mathcal{A}$  have  $N_\alpha = N_{\bar{\alpha}}$  for  $\alpha = 1, 2, \dots, A$  and  $A = 2^{\lfloor \log_2 \binom{N_t}{N_{\bar{\alpha}}} \rfloor}$ . This implies  $\mathcal{A} \subseteq \mathcal{U}$ .

**MRSSK (Max-Rate Space Shift Keying)** – The spatial-constellation diagram is chosen such that it contains the largest number of symbols  $\mathbf{a}^{(\alpha)} \in \mathcal{A}$  with  $N_\alpha$  assuming all possible values in  $[0, N_t]$  for  $\alpha = 1, 2, \dots, A$  and  $A = 2^{N_t}$ . This implies  $\mathcal{A} = \mathcal{U}$ .

**MRSSK<sub>\setminus 0</sub> (Max-Rate Space Shift Keying “without the all-zero symbol”)** – The spatial-constellation diagram is chosen such that it contains the largest number of symbols  $\mathbf{a}^{(\alpha)} \in \mathcal{A}$  with  $N_\alpha$  except  $\mathbf{a}^{(\alpha)} = \mathbf{0}_{N_t}$  with  $N_\alpha$  assuming all possible values in  $(0, N_t]$  for  $\alpha = 1, 2, \dots, A$  and  $A = 2^{N_t-1}$ . This implies  $\mathcal{A} \subseteq \mathcal{U}_{\setminus 0}$ .

**SMSTT (Spatially-Modulated Space-Time-Transmission)** – The spatial-constellation diagram is chosen such that its symbols  $\mathbf{a}^{(\alpha)} \in \mathcal{A}$  have  $N_\alpha = N_{\bar{\alpha}}$  for  $\alpha = 1, 2, \dots, A$  and  $A = 2^{\lfloor \log_2 \binom{N_t}{N_{\bar{\alpha}}} \rfloor}$ . This implies  $\mathcal{A} \subseteq \mathcal{U}$ . The mother space-time code  $\mathbf{M}(\cdot)$  is transmitted from the active antennas in  $\mathbf{a}^{(\alpha)} \in \mathcal{A}$  over  $N_s$  time-slots.

**Rand (Random)** – The symbols of the spatial-constellation diagram  $\mathbf{a}^{(\alpha)} \in \mathcal{A} \subseteq \mathcal{U}$  are randomly chosen but kept fixed for the whole communication.

**SetPart (Set Partitioning) and NuSetPart (Non-Uniform Set Partitioning)** – The symbols of the spatial-constellation diagram  $\mathbf{a}^{(\alpha)} \in \mathcal{A} \subseteq \mathcal{U}$  are chosen such that the active antennas in each symbol result in a partition of the antenna-array. Once chosen, the symbols are kept fixed for the whole communication. **SetPart** is obtained if  $N_\alpha = N_{\bar{\alpha}}$  for  $\alpha = 1, 2, \dots, A$ . **NuSetPart** is obtained if  $N_\alpha$  can be different for  $\alpha = 1, 2, \dots, A$ .

**ISF (Identical Shaping Filters)** – The shaping filters are the same for all the antenna-elements, i.e.,  $w_t(\xi) = w_0(\xi)$  for  $t = 1, 2, \dots, N_t$ .

**OSF (Orthogonal Shaping Filters)** – The shaping filters are different and time-orthogonal for all the antenna-elements, i.e.,  $\int_0^{T_s} w_{t_1}(\xi) w_{t_2}(\xi) d\xi = 0$  for  $t_1 \neq t_2 = 1, 2, \dots, N_t$ .

**SWOSF (Symbol-Wise Orthogonal Shaping Filters)** – Let  $\mathbf{a}^{(\alpha_1)} \in \mathcal{A}$  and  $\mathbf{a}^{(\alpha_2)} \in \mathcal{A}$  be two generic symbols of the spatial-constellation diagram for  $\alpha_1 \neq \alpha_2 = 1, 2, \dots, A$ . Let  $w_\alpha(\cdot)$  be the common shaping filter used by all active antennas in  $\mathbf{a}^{(\alpha)}$ . Then the shaping filters are chosen such that  $\int_0^{T_s} w_{\alpha_1}(\xi) w_{\alpha_2}(\xi) d\xi = 0$ . Unlike OSF, the active antennas in  $\mathbf{a}^{(\alpha)}$  have the same shaping filter.

# *Spatially-Modulated Space-Time-Coded MIMO (8/23)*

## Acronym of Transmission Modes, Rate (R), Diversity (D), and Examples (X={ISF, OSF}, Y={ISF, OSF, SWOSF})

- TM1-GSSK-Rand-X( $N_t, N_\alpha$ ):  $R = \left\lfloor \log_2 \left[ \binom{N_t}{N_\alpha} \right] \right\rfloor$  and  $D = N_r$  if X=ISF,  $D = 2N_r$  if X=OSF

Example:  $\mathcal{A} = \left\{ [0, 0, 1, 1]^T, [0, 1, 1, 0]^T, [1, 1, 0, 0]^T, [1, 0, 0, 1]^T \right\}$

- TM1-GSSK-SetPart-Y( $N_t, N_\alpha$ ):  $R = \log_2 (\lfloor N_t / N_\alpha \rfloor)$  and  $D = N_r$  if Y=ISF,  $D = 2N_\alpha N_r$  if Y=OSF,  $D = 2N_r$  if Y=SWOSF

Example:  $\mathcal{A} = \left\{ [0, 0, 1, 1]^T, [1, 1, 0, 0]^T \right\}$

- TM1-NuSetPart-Y( $N_t, N_\alpha$ ):  $R = \log_2 (A)$  and  $D = N_r$  if Y=ISF,  $D = [\min \{N_\alpha\} + \min \{N_\alpha - \{\min \{N_\alpha\}\}]\} N_r$  if Y=OSF,  $D = 2N_r$  if Y=SWOSF

Example:  $\mathcal{A} = \left\{ [1, 1, 1, 0]^T, [0, 0, 0, 1]^T \right\}$  for  $N_\alpha = \{3, 1\}$

- TM1-MRSSK-X( $N_t$ ):  $R = N_t$  and  $D = N_r$

Example:  $\mathcal{A} = \mathcal{U}$

- TM1-MRSSK<sub>0</sub>-Rand-X( $N_t$ ):  $R = N_t - 1$  and  $D = N_r$  if X=ISF,  $D = 2N_r$  if X=OSF

Example:  $\mathcal{A} = \left\{ [0, 0, 0, 1]^T, [0, 0, 1, 1]^T, [0, 1, 1, 0]^T, [0, 1, 1, 1]^T, [1, 0, 0, 0]^T, [1, 1, 0, 0]^T, [1, 1, 0, 1]^T, [1, 1, 1, 0]^T \right\}$

- TM2-SMSTT-Rand-X( $N_t, N_\alpha$ ):  $R = (1/N_s) \left\lfloor \log_2 \left[ \binom{N_t}{N_\alpha} \right] \right\rfloor + (N_M/N_s) \log_2 (M)$  and  $D = N_r$  if X=ISF,  $D \geq N_d N_r$  if X=OSF

Example:  $\mathcal{A} = \left\{ [0, 0, 1, 1]^T, [0, 1, 1, 0]^T, [1, 1, 0, 0]^T, [1, 0, 0, 1]^T \right\}$  and  $M(\cdot) = H_2$

- TM2-SMSTT-SetPart-Y( $N_t, N_\alpha$ ):  $R = (1/N_s) \log_2 (\lfloor N_t / N_\alpha \rfloor) + (N_M/N_s) \log_2 (M)$  and  $D = N_\alpha N_r$

Example:  $\mathcal{A} = \left\{ [0, 0, 1, 1]^T, [1, 1, 0, 0]^T \right\}$  and  $M(\cdot) = H_2$



# Spatially-Modulated Space-Time-Coded MIMO (9/23)

## ML-Optimum Single-Stream Decoding:

### TM2-SMSTT-SetPart-OSF and TM2-SMSTT-SetPart-SWOSF

$$\Lambda(\tilde{\alpha}, \tilde{\mu}) \propto \underbrace{\sum_{r=1}^{N_r} \left[ (E_S/2) |\mathbf{H}_{r,\tilde{t}_1}|^2 |\tilde{\mu}_1|^2 + (E_S/2) |\mathbf{H}_{r,\tilde{t}_2}|^2 |\tilde{\mu}_1|^2 - 2\text{Re} \left\{ \sqrt{E_S/2} \mathbf{H}_{r,\tilde{t}_1}^* \tilde{\mu}_1^* \tilde{z}_{1,r}^{(\tilde{t}_1)} \right\} - 2\text{Re} \left\{ \sqrt{E_S/2} \mathbf{H}_{r,\tilde{t}_2}^* \tilde{\mu}_1 \tilde{z}_{2,r}^{(\tilde{t}_2)} \right\} \right]}_{\Lambda_1(\tilde{\alpha}, \tilde{\mu}_1)} + \underbrace{\sum_{r=1}^{N_r} \left[ (E_S/2) |\mathbf{H}_{r,\tilde{t}_2}|^2 |\tilde{\mu}_2|^2 + (E_S/2) |\mathbf{H}_{r,\tilde{t}_1}|^2 |\tilde{\mu}_2|^2 - 2\text{Re} \left\{ \sqrt{E_S/2} \mathbf{H}_{r,\tilde{t}_2}^* \tilde{\mu}_2^* \tilde{z}_{1,r}^{(\tilde{t}_2)} \right\} + 2\text{Re} \left\{ \sqrt{E_S/2} \mathbf{H}_{r,\tilde{t}_1}^* \tilde{\mu}_2 \tilde{z}_{2,r}^{(\tilde{t}_1)} \right\} \right]}_{\Lambda_2(\tilde{\alpha}, \tilde{\mu}_2)}$$



$$\begin{cases} \Lambda_1(\tilde{\alpha}, \tilde{\mu}_1) = \sum_{r=1}^{N_r} \left[ (E_S/2) |\mathbf{H}_{r,\tilde{t}_1}|^2 |\tilde{\mu}_1|^2 + (E_S/2) |\mathbf{H}_{r,\tilde{t}_2}|^2 |\tilde{\mu}_1|^2 - 2\sqrt{E_S/2} \text{Re} \left\{ \mathbf{H}_{r,\tilde{t}_1}^* \mathbf{H}_{r,\tilde{t}_1} \tilde{\mu}_1^* \mu_1 \rho^{(t_1, \tilde{t}_1)} + \mathbf{H}_{r,\tilde{t}_2}^* \mathbf{H}_{r,\tilde{t}_2} \tilde{\mu}_1 \mu_1^* \rho^{(t_2, \tilde{t}_2)} \right\} \right] - \mathcal{I}_1(\tilde{\alpha}, \tilde{\mu}_1) \\ \Lambda_2(\tilde{\alpha}, \tilde{\mu}_2) = \sum_{r=1}^{N_r} \left[ (E_S/2) |\mathbf{H}_{r,\tilde{t}_1}|^2 |\tilde{\mu}_2|^2 + (E_S/2) |\mathbf{H}_{r,\tilde{t}_2}|^2 |\tilde{\mu}_2|^2 - 2\sqrt{E_S/2} \text{Re} \left\{ \mathbf{H}_{r,\tilde{t}_1}^* \mathbf{H}_{r,\tilde{t}_1} \tilde{\mu}_2 \mu_2^* \rho^{(t_1, \tilde{t}_1)} + \mathbf{H}_{r,\tilde{t}_2}^* \mathbf{H}_{r,\tilde{t}_2} \tilde{\mu}_2^* \mu_2 \rho^{(t_2, \tilde{t}_2)} \right\} \right] - \mathcal{I}_2(\tilde{\alpha}, \tilde{\mu}_2) \end{cases}$$



$$\begin{cases} \mathcal{I}_1(\tilde{\alpha}, \tilde{\mu}_1) = -2\sqrt{E_S/2} \text{Re} \left\{ \mathbf{H}_{r,\tilde{t}_2}^* \mathbf{H}_{r,\tilde{t}_1} \tilde{\mu}_1 \mu_2^* \rho^{(t_1, \tilde{t}_2)} \right\} \\ \quad + 2\sqrt{E_S/2} \text{Re} \left\{ \mathbf{H}_{r,\tilde{t}_1}^* \mathbf{H}_{r,\tilde{t}_2} \tilde{\mu}_1^* \mu_2 \rho^{(t_2, \tilde{t}_1)} \right\} \\ \mathcal{I}_2(\tilde{\alpha}, \tilde{\mu}_2) = 2\sqrt{E_S/2} \text{Re} \left\{ \mathbf{H}_{r,\tilde{t}_2}^* \mathbf{H}_{r,\tilde{t}_1} \tilde{\mu}_2^* \mu_1 \rho^{(t_1, \tilde{t}_2)} \right\} \\ \quad - 2\sqrt{E_S/2} \text{Re} \left\{ \mathbf{H}_{r,\tilde{t}_1}^* \mathbf{H}_{r,\tilde{t}_2} \tilde{\mu}_2 \mu_1^* \rho^{(t_2, \tilde{t}_1)} \right\} \end{cases} \Rightarrow \begin{cases} \mathcal{I}_2(\tilde{\alpha}, \tilde{\mu}_2) = 0 \\ \mathcal{I}_1(\tilde{\alpha}, \tilde{\mu}_1) = 0 \end{cases}$$

# *Spatially-Modulated Space-Time-Coded MIMO (10/23)*

**ML-Optimum Single-Stream Decoding:**  
**TM2-SMSTT-SetPart-OSF and TM2-SMSTT-SetPart-SWOSF**

Alamouti

$$\begin{aligned}(\hat{\alpha}, \hat{\mu}_1, \hat{\mu}_2) &= \arg \min_{\mathbf{a}^{(\tilde{\alpha})} \in \mathcal{A}, \tilde{\mu}_1 \in \mathcal{M}, \tilde{\mu}_2 \in \mathcal{M}} \{ \Lambda_1 (\tilde{\alpha}, \tilde{\mu}_1) + \Lambda_2 (\tilde{\alpha}, \tilde{\mu}_2) \} \\ &\stackrel{(1)}{=} \arg \min_{\mathbf{a}^{(\tilde{\alpha})} \in \mathcal{A}} \left\{ \min_{\tilde{\mu}_1 \in \mathcal{M}, \tilde{\mu}_2 \in \mathcal{M}} \{ \Lambda_1 (\tilde{\alpha}, \tilde{\mu}_1) + \Lambda_2 (\tilde{\alpha}, \tilde{\mu}_2) \} \right\} \\ &\stackrel{(2)}{=} \arg \min_{\mathbf{a}^{(\tilde{\alpha})} \in \mathcal{A}} \left\{ \min_{\tilde{\mu}_1 \in \mathcal{M}} \{ \Lambda_1 (\tilde{\alpha}, \tilde{\mu}_1) \} + \min_{\tilde{\mu}_2 \in \mathcal{M}} \{ \Lambda_2 (\tilde{\alpha}, \tilde{\mu}_2) \} \right\}\end{aligned}$$

# *Spatially-Modulated Space-Time-Coded MIMO (11/23)*

**Step 1:** For every hypothesis  $\mathbf{a}^{(\tilde{\alpha})} \in \mathcal{A}$  of the spatial-constellation diagram, compute:

$$\hat{\mu}_1(\tilde{\alpha}) = \arg \min_{\tilde{\mu}_1 \in \mathcal{M}} \{\Lambda_1(\tilde{\alpha}, \tilde{\mu}_1)\}$$

$$\hat{\mu}_2(\tilde{\alpha}) = \arg \min_{\tilde{\mu}_2 \in \mathcal{M}} \{\Lambda_2(\tilde{\alpha}, \tilde{\mu}_2)\}$$

**Step 2:** Compute the estimate of the symbol belonging to the spatial-constellation diagram as follows:

$$\hat{\alpha} = \arg \min_{\mathbf{a}^{(\tilde{\alpha})} \in \mathcal{A}} \{\Lambda_1(\tilde{\alpha}, \hat{\mu}_1(\tilde{\alpha})) + \Lambda_2(\tilde{\alpha}, \hat{\mu}_2(\tilde{\alpha}))\}$$

**Step 3:** Compute the estimates of the two symbols belonging to the signal-constellation diagram as follows:

$$\hat{\mu}_1 = \hat{\mu}_1(\hat{\alpha}) \quad \text{and} \quad \hat{\mu}_2 = \hat{\mu}_2(\hat{\alpha})$$

# *Spatially-Modulated Space-Time-Coded MIMO (12/23)*

## ML-Optimum Single-Stream Decoding:

### TM2-SMSTT-SetPart-OSF and TM2-SMSTT-SetPart-SWOSF

$$\left\{ \begin{array}{l} \hat{\mu}_m(\tilde{\alpha})|_{m=1,2,\dots,N_M} = \arg \min_{\tilde{\mu}_m \in \mathcal{M}} \left\{ \Lambda_m(\tilde{\alpha}, \tilde{\mu}_m) = \sum_{r=1}^{N_r} \left[ (E_S/2) \left( \sum_{\tau=1}^{N_{\tilde{\alpha}}} |\mathbf{H}_{r,\tilde{t}_\tau}|^2 \right) |\tilde{\mu}_m|^2 - 2\sqrt{E_S/2} \operatorname{Re} \left\{ \Upsilon_m^{(\text{HX})}(\mathbf{t}, \tilde{\mathbf{t}}; r) \tilde{\mu}_m^* \right\} \right] \right\} \\ \hat{\alpha} = \arg \min_{\mathbf{a}(\tilde{\alpha}) \in \mathcal{A}} \left\{ \sum_{m=1}^{N_M} \Lambda_m(\tilde{\alpha}, \hat{\mu}_m(\tilde{\alpha})) \right\} \\ \hat{\mu}_m|_{m=1,2,\dots,N_M} = \hat{\mu}_m(\tilde{\alpha} = \hat{\alpha})|_{m=1,2,\dots,N_M} \end{array} \right.$$

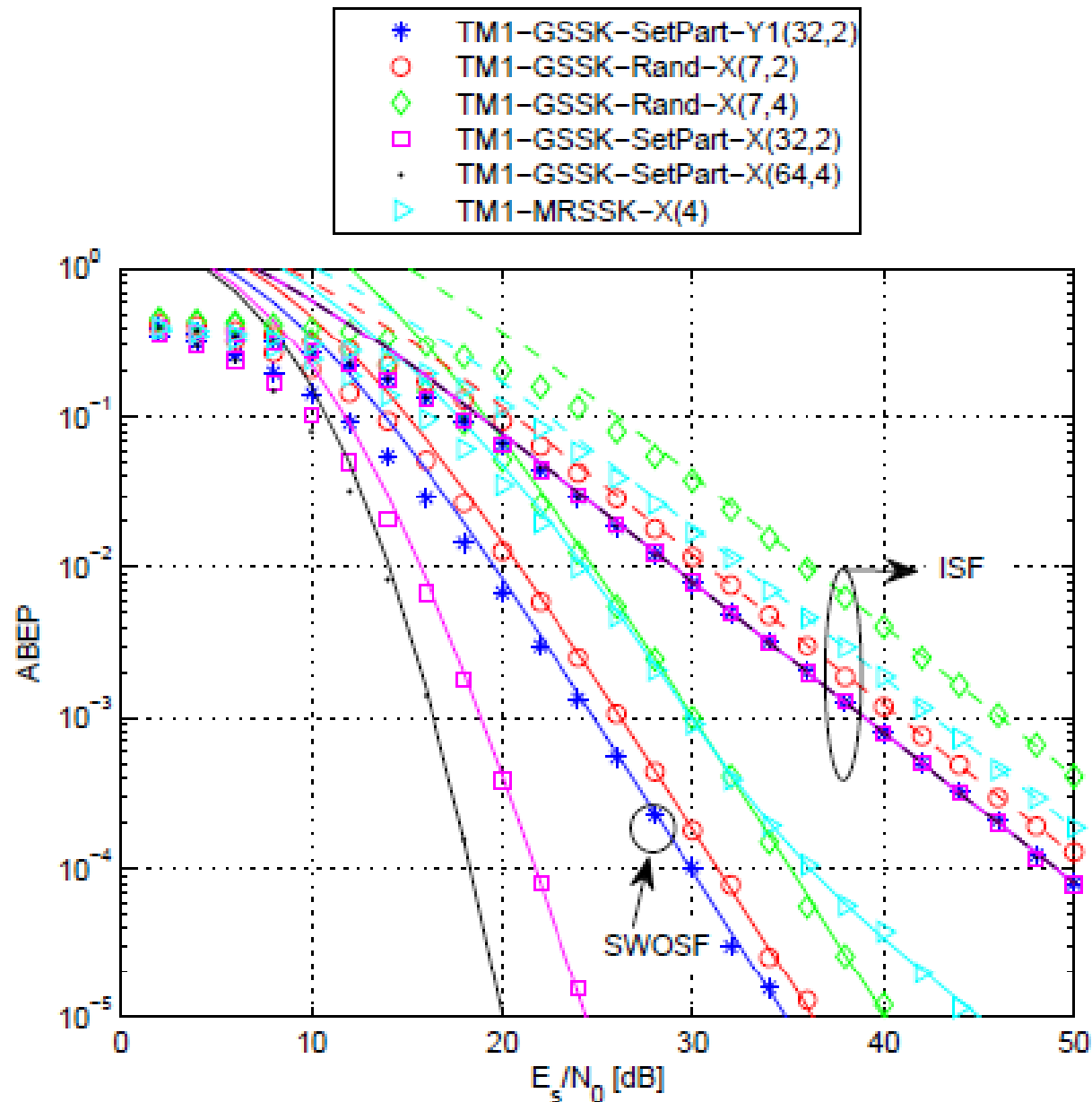
### Example: OSTBC Tarokh-H3

$$\left\{ \begin{array}{l} \Upsilon_1^{(\text{H3})}(\mathbf{t}, \tilde{\mathbf{t}}; r) = \bar{z}_{1,r}^{(\tilde{t}_1)} \mathbf{H}_{r,\tilde{t}_1}^* + \left( \bar{z}_{2,r}^{(\tilde{t}_2)} \right)^* \mathbf{H}_{r,\tilde{t}_2} + (1/2) \left( \bar{z}_{4,r}^{(\tilde{t}_3)} - \bar{z}_{3,r}^{(\tilde{t}_3)} \right) \mathbf{H}_{r,\tilde{t}_3} - (1/2) \left( \bar{z}_{3,r}^{(\tilde{t}_3)} + \bar{z}_{4,r}^{(\tilde{t}_3)} \right)^* \mathbf{H}_{r,\tilde{t}_3} \\ \Upsilon_2^{(\text{H3})}(\mathbf{t}, \tilde{\mathbf{t}}; r) = \bar{z}_{1,r}^{(\tilde{t}_2)} \mathbf{H}_{r,\tilde{t}_2}^* - \left( \bar{z}_{2,r}^{(\tilde{t}_1)} \right)^* \mathbf{H}_{r,\tilde{t}_1} + (1/2) \left( \bar{z}_{3,r}^{(\tilde{t}_3)} + \bar{z}_{4,r}^{(\tilde{t}_3)} \right) \mathbf{H}_{r,\tilde{t}_3} - (1/2) \left( \bar{z}_{4,r}^{(\tilde{t}_3)} - \bar{z}_{3,r}^{(\tilde{t}_3)} \right)^* \mathbf{H}_{r,\tilde{t}_3} \\ \Upsilon_3^{(\text{H3})}(\mathbf{t}, \tilde{\mathbf{t}}; r) = (1/\sqrt{2}) \left( \bar{z}_{1,r}^{(\tilde{t}_3)} + \bar{z}_{2,r}^{(\tilde{t}_3)} \right) \mathbf{H}_{r,\tilde{t}_3}^* + (1/\sqrt{2}) \left( \bar{z}_{3,r}^{(\tilde{t}_1)} \right)^* \mathbf{H}_{r,\tilde{t}_1} + (1/\sqrt{2}) \left( \bar{z}_{3,r}^{(\tilde{t}_2)} \right)^* \mathbf{H}_{r,\tilde{t}_2} \\ \quad + (1/\sqrt{2}) \left( \bar{z}_{4,r}^{(\tilde{t}_1)} \right)^* \mathbf{H}_{r,\tilde{t}_1} - (1/\sqrt{2}) \left( \bar{z}_{4,r}^{(\tilde{t}_2)} \right)^* \mathbf{H}_{r,\tilde{t}_2} \end{array} \right.$$

M. Di Renzo and H. Haas, “On Transmit-Diversity for Spatial Modulation MIMO: Impact of Spatial-Constellation Diagram and Shaping Filters at the Transmitter”, **IEEE Transactions on Vehicular Technology**, Vol. 62, No. 6, pp. 2507–2531, July 2013

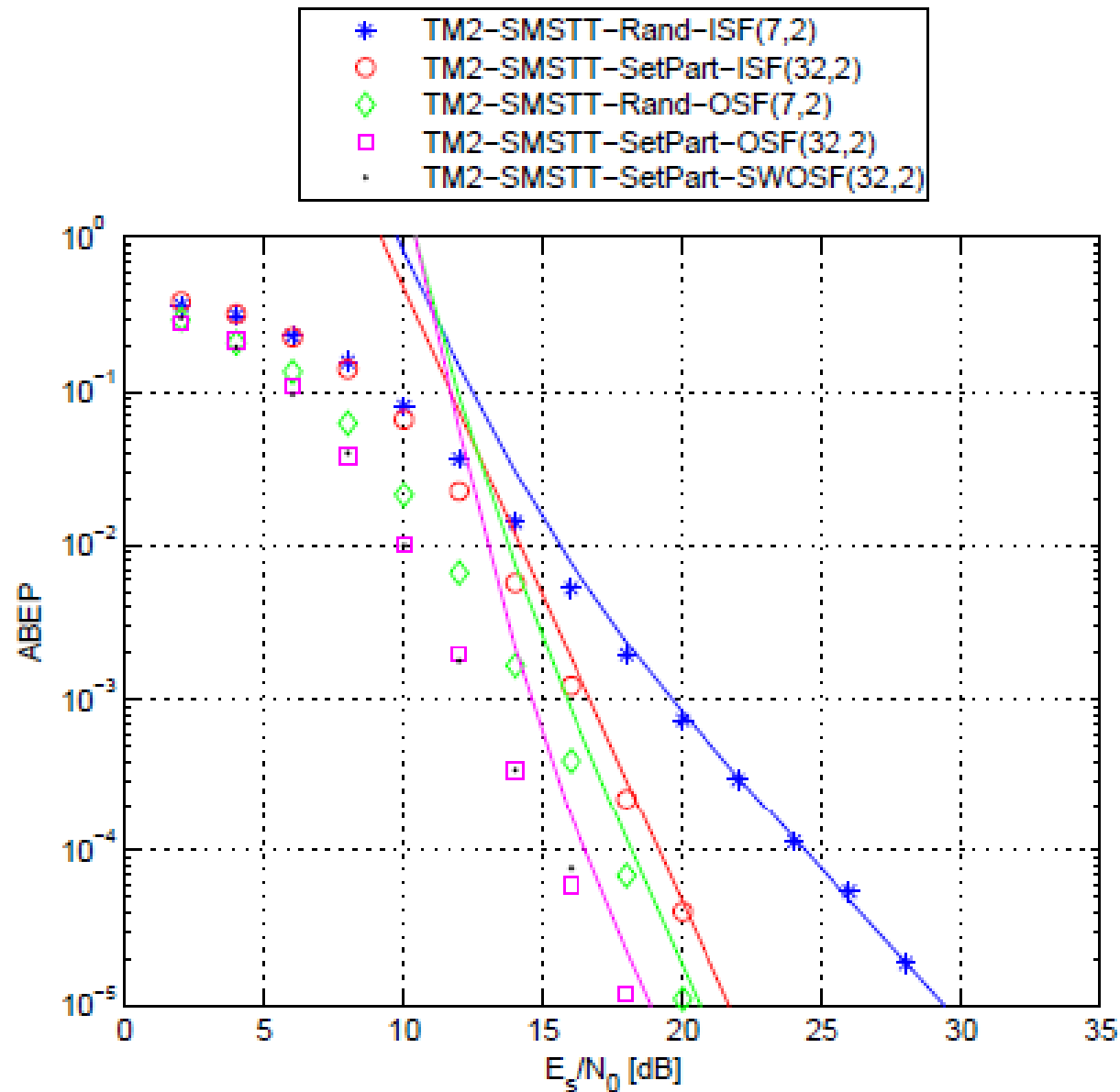
# *Spatially-Modulated Space-Time-Coded MIMO (13/23)*

Diversity Analysis ( $N_r = 1 - R = 4$  bpcu)



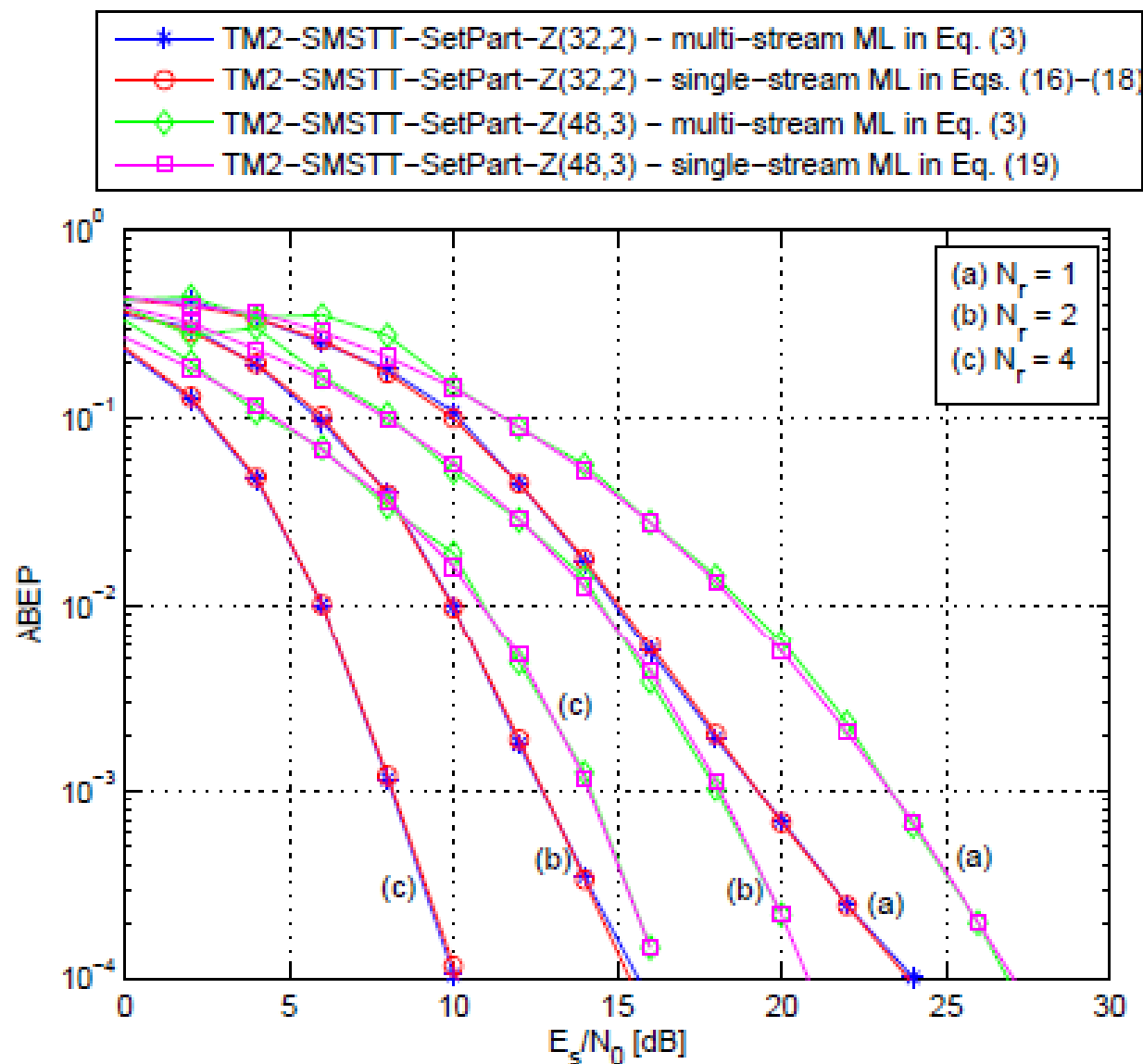
# *Spatially-Modulated Space-Time-Coded MIMO (14/23)*

Diversity Analysis ( $N_r = 2 - R = 4$  bpcu)



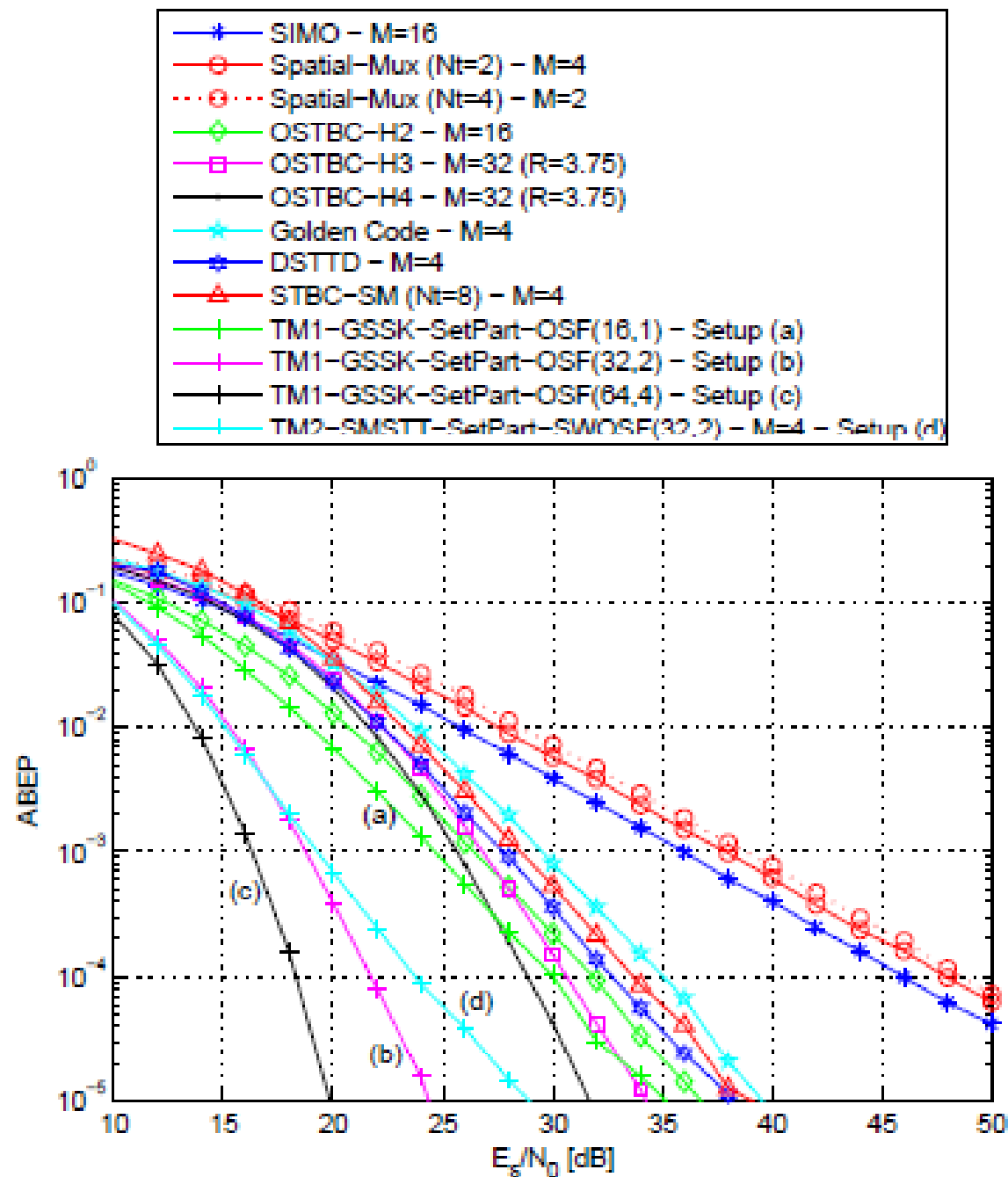
# *Spatially-Modulated Space-Time-Coded MIMO (15/23)*

## Multi vs. Single-Stream Decoding ( $R = 4$ bpcu)



# Spatially-Modulated Space-Time-Coded MIMO (16/23)

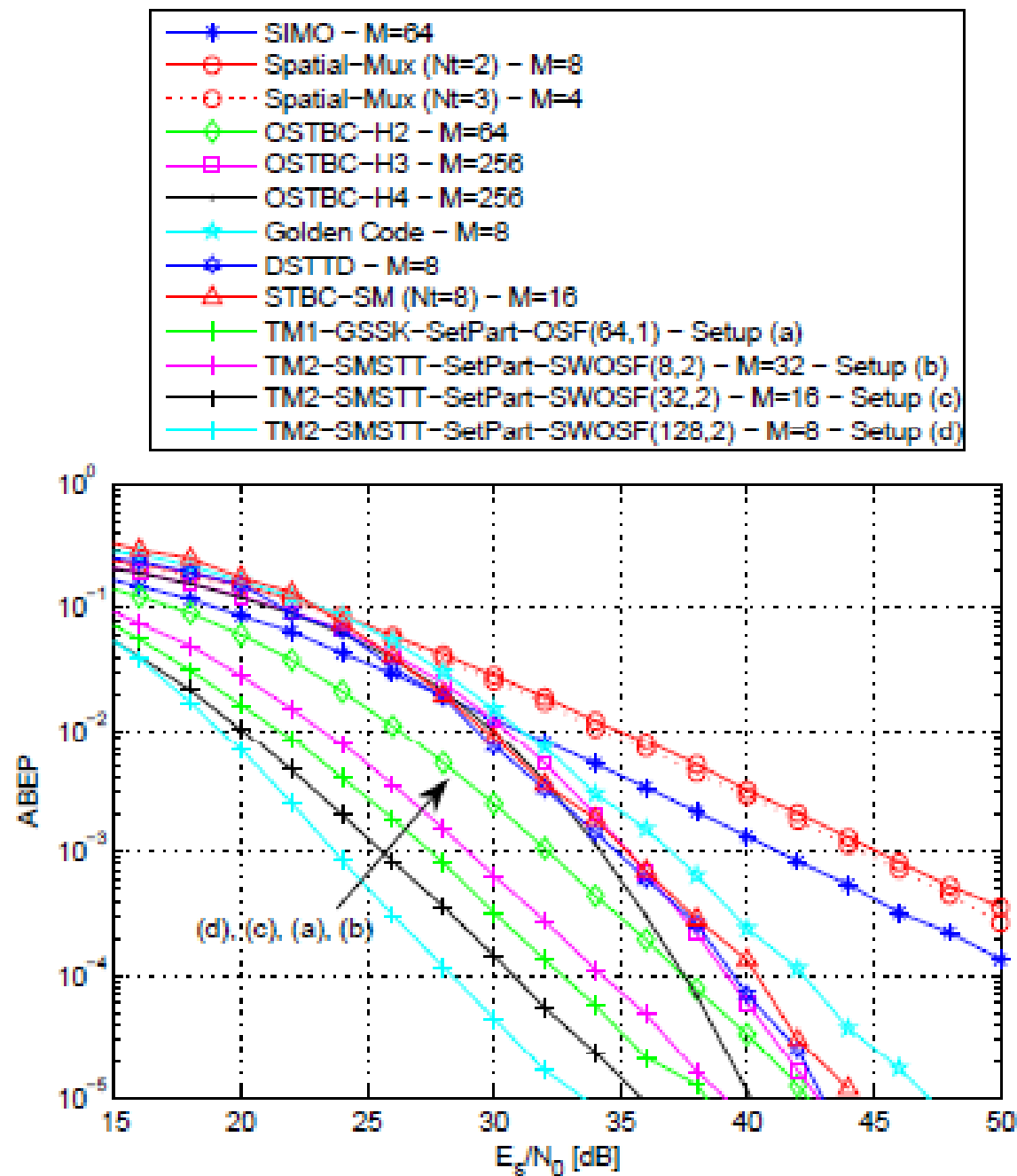
$N_r = 1$   
 $R = 4$  bpcu





# Spatially-Modulated Space-Time-Coded MIMO (17/23)

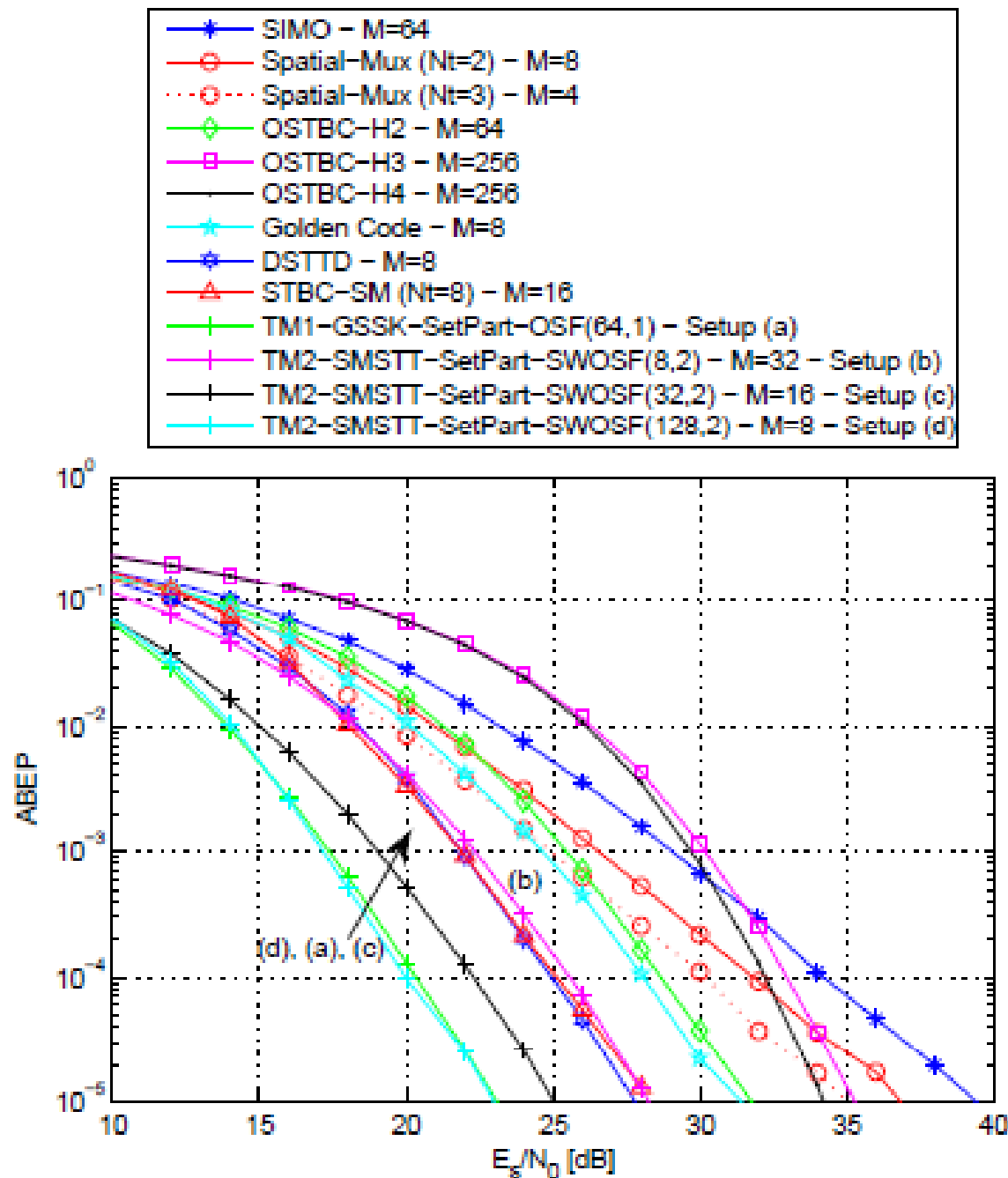
$N_r = 1$   
 $R = 6$  bpcu



# Spatially-Modulated Space-Time-Coded MIMO (18/23)

$$N_r = 2$$

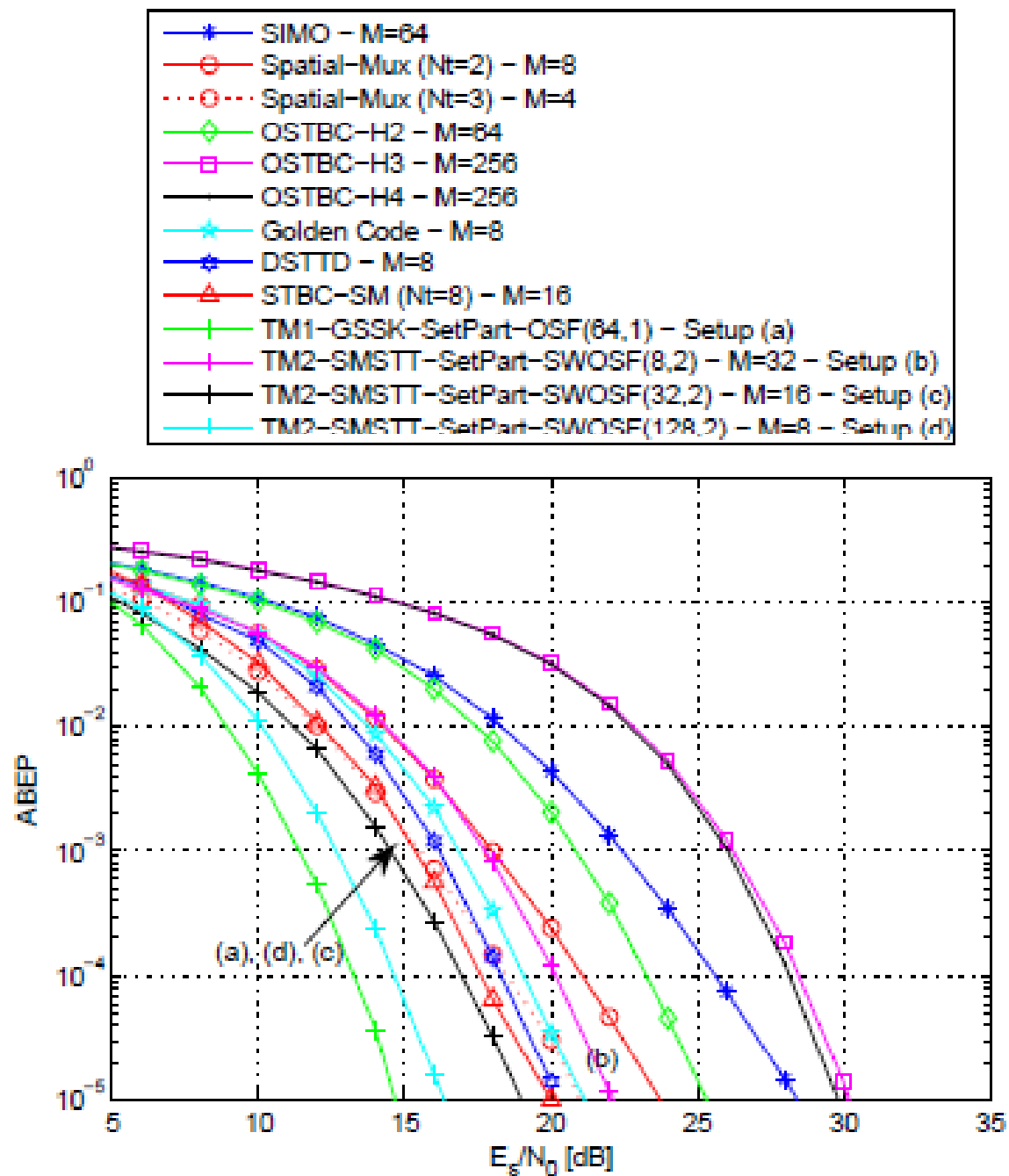
$$R = 6 \text{ bpcu}$$



# Spatially-Modulated Space-Time-Coded MIMO (19/23)

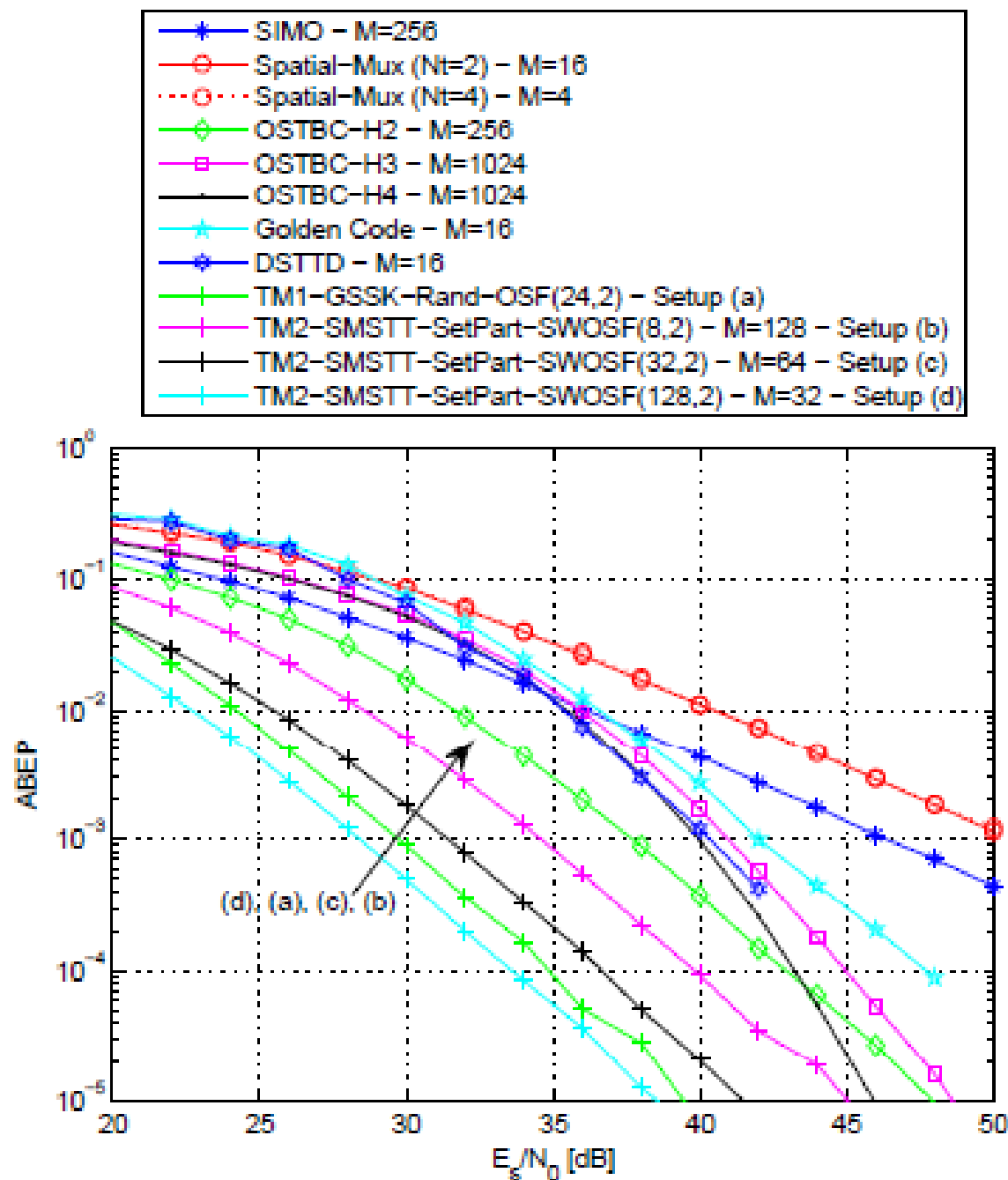
$$N_r = 4$$

$$R = 6 \text{ bpcu}$$



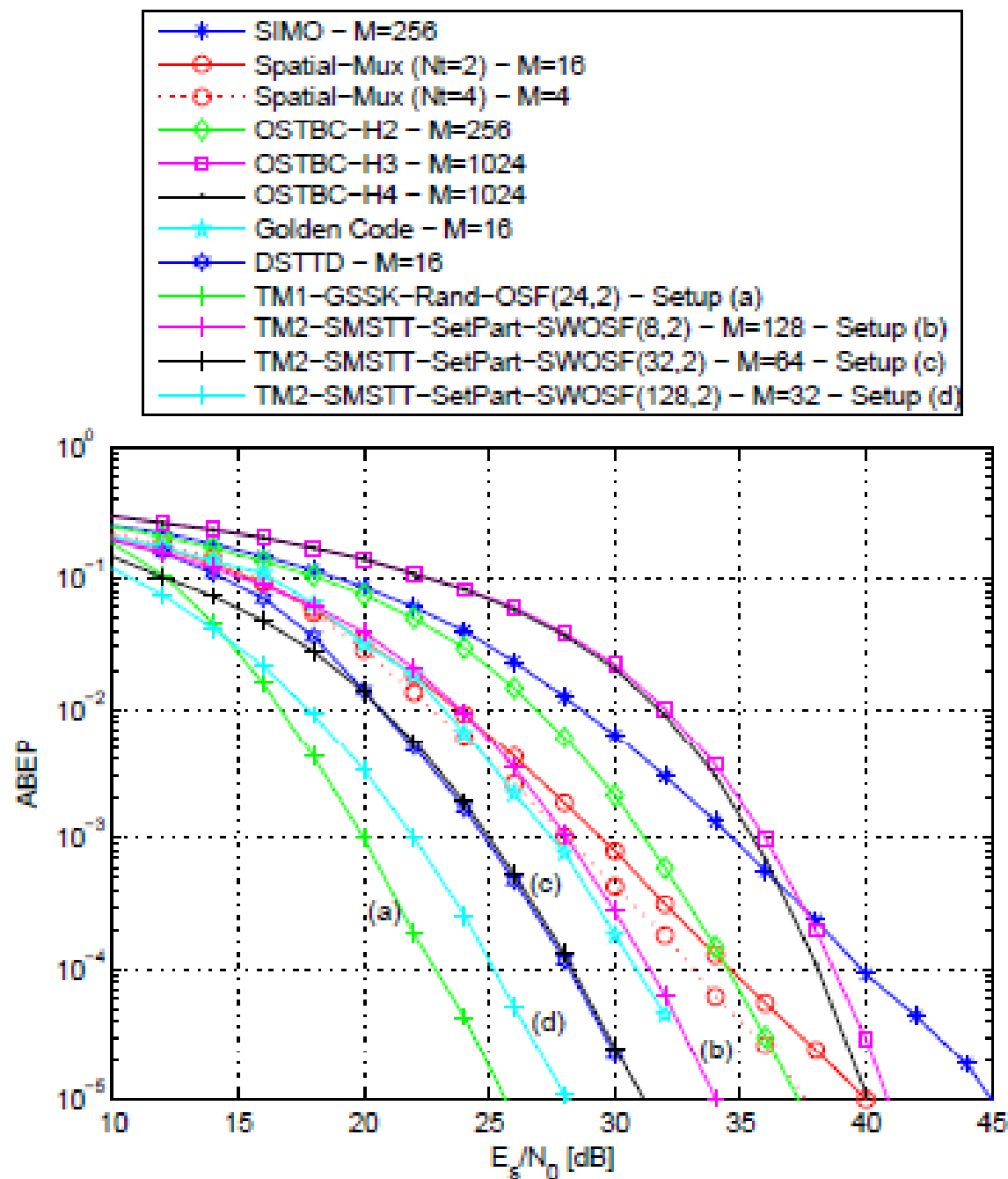
# Spatially-Modulated Space-Time-Coded MIMO (20/23)

$N_r = 1$   
 $R = 8$  bpcu



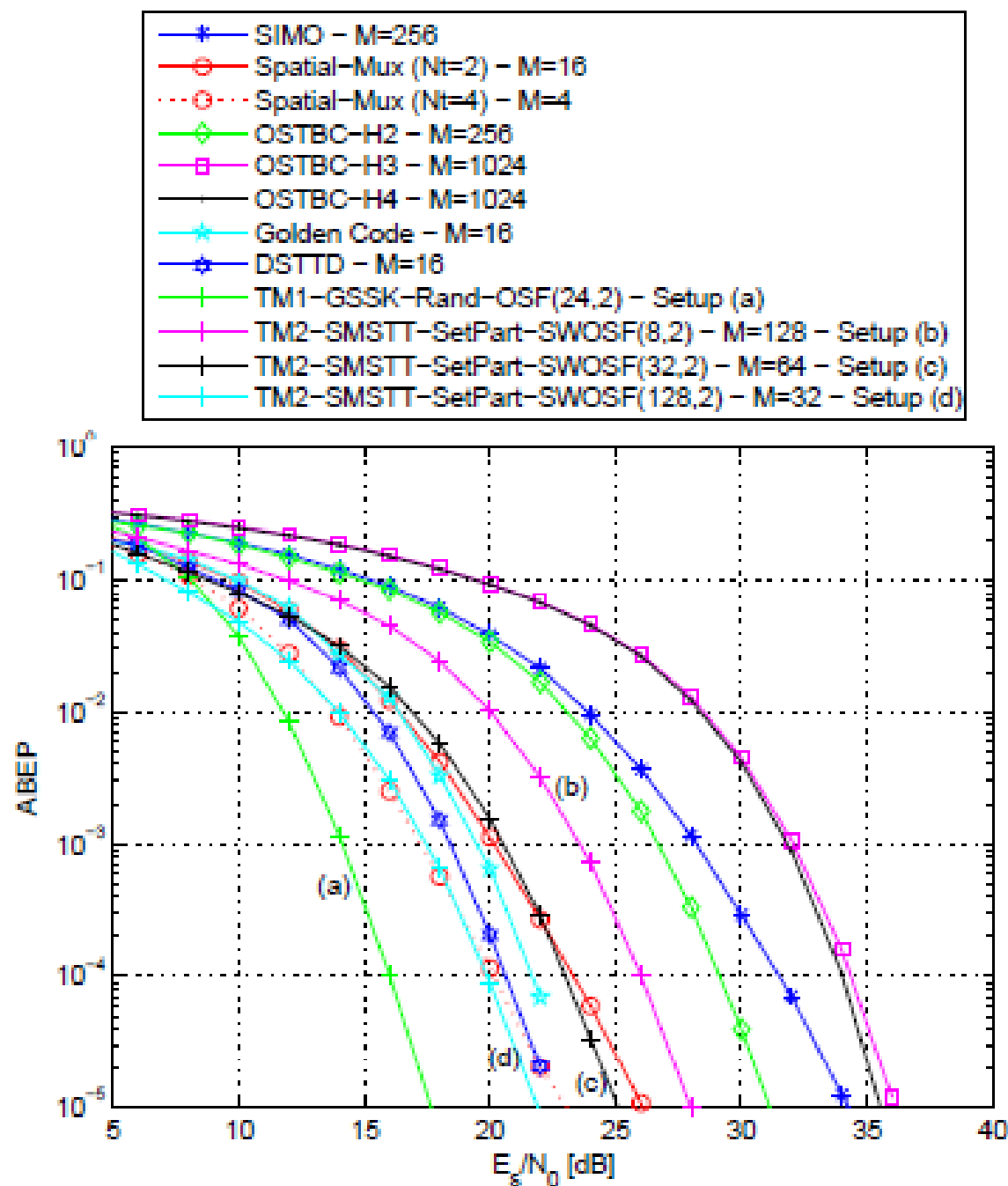
# Spatially-Modulated Space-Time-Coded MIMO (21/23)

$N_r = 2$   
 $R = 8$  bpcu

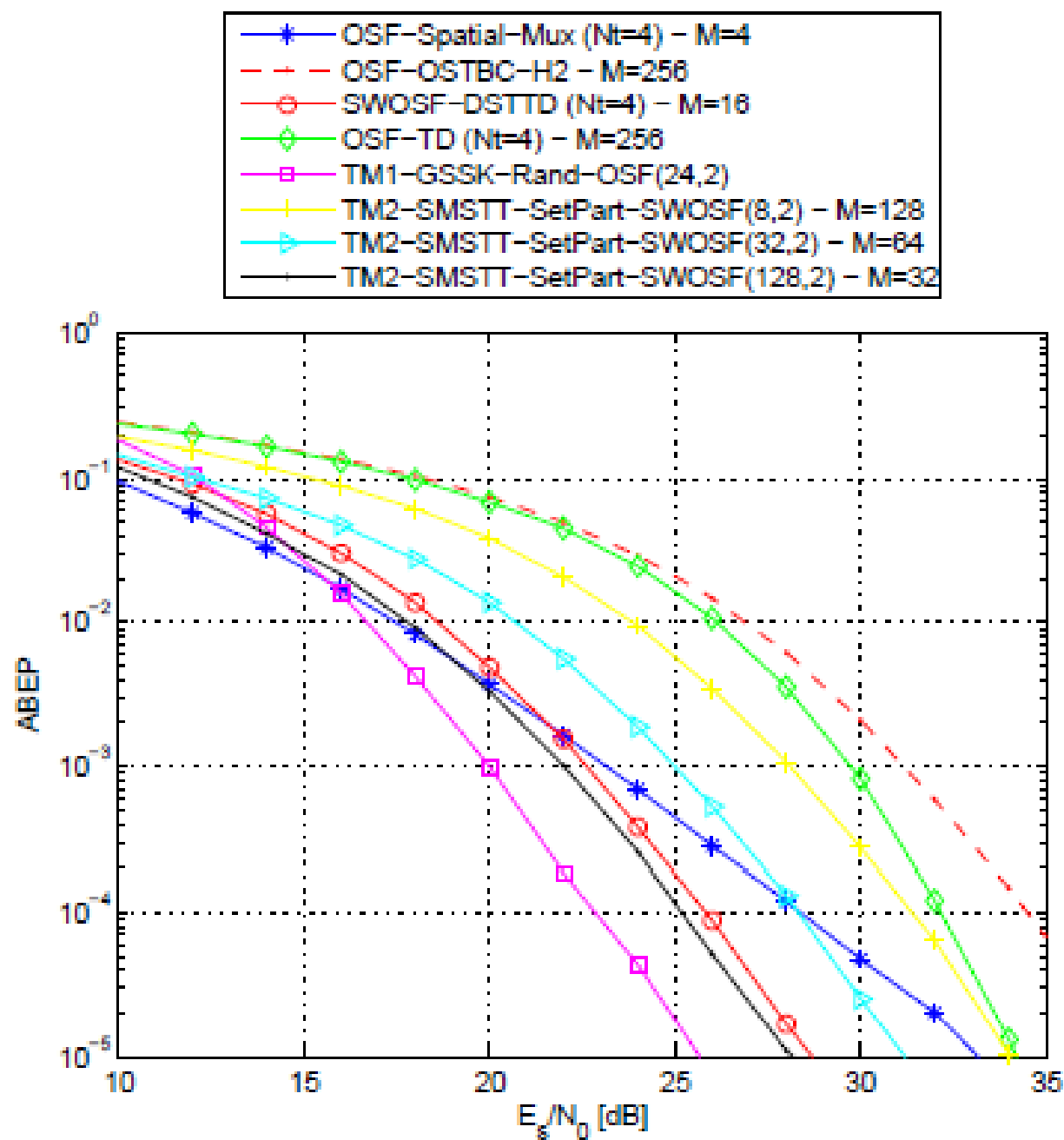


# Spatially-Modulated Space-Time-Coded MIMO (22/23)

$N_r = 4$   
 $R = 8$  bpcu



# *Spatially-Modulated Space-Time-Coded MIMO (23/23)*



OSF-MIMO

$N_r = 2$

$R = 8$  bpcu

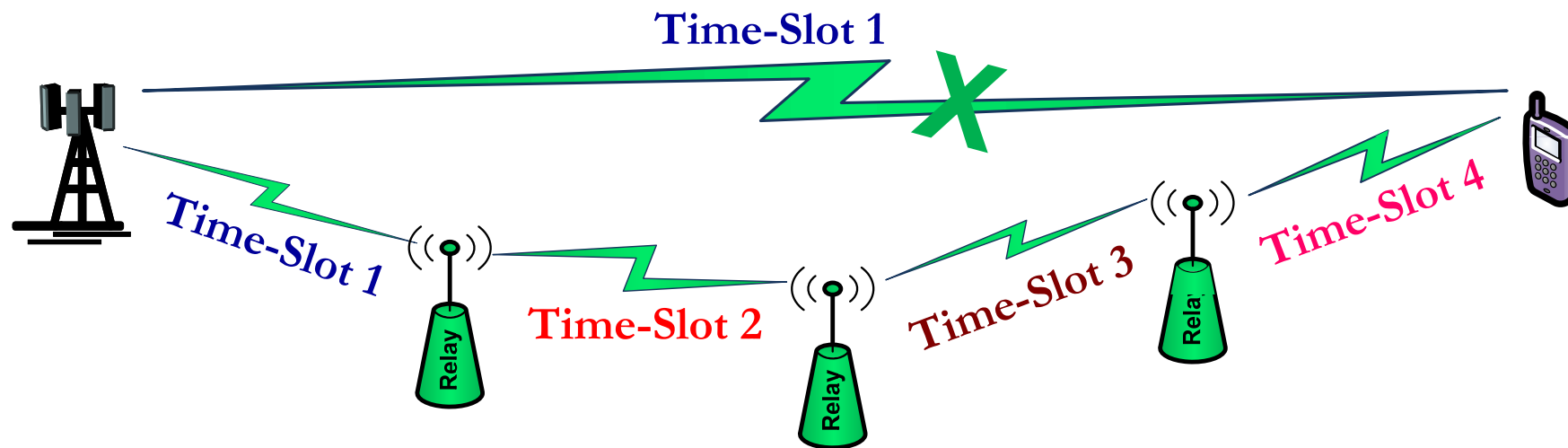
# *Outline*

---

1. Introduction and Motivation behind SM-MIMO
2. History of SM Research and Research Groups Working on SM
3. Transmitter Design – Encoding
4. Receiver Design – Demodulation
5. Error Performance (Numerical Results and Main Trends)
6. Achievable Capacity
7. Channel State Information at the Transmitter
8. Imperfect Channel State Information at the Receiver
9. Multiple Access Interference
10. Energy Efficiency
11. Transmit-Diversity for SM
12. Spatially-Modulated Space-Time-Coded MIMO
13. **Relay-Aided SM**
14. SM in Heterogeneous Cellular Networks
15. SM for Visible Light Communications
16. Experimental Evaluation of SM
17. The Road Ahead – Open Research Challenges/Opportunities
18. Implementation Challenges of SM-MIMO

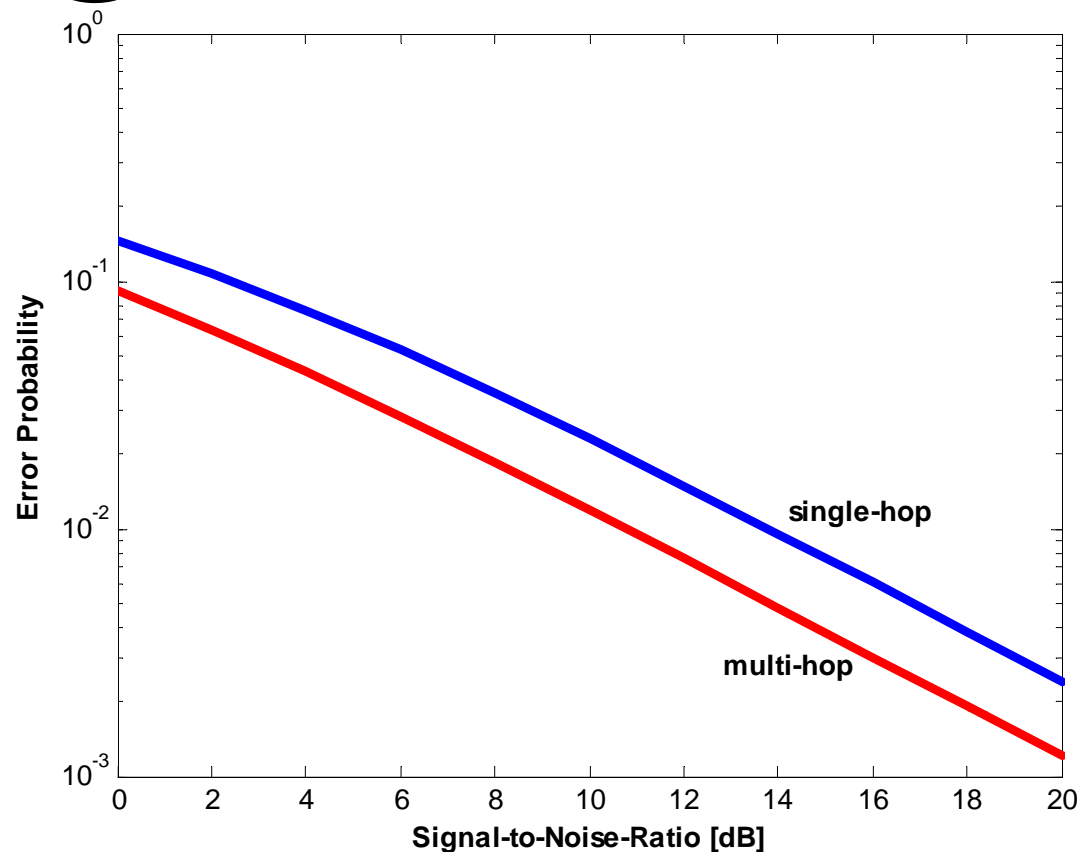


# Relay-Aided SM (1/24)

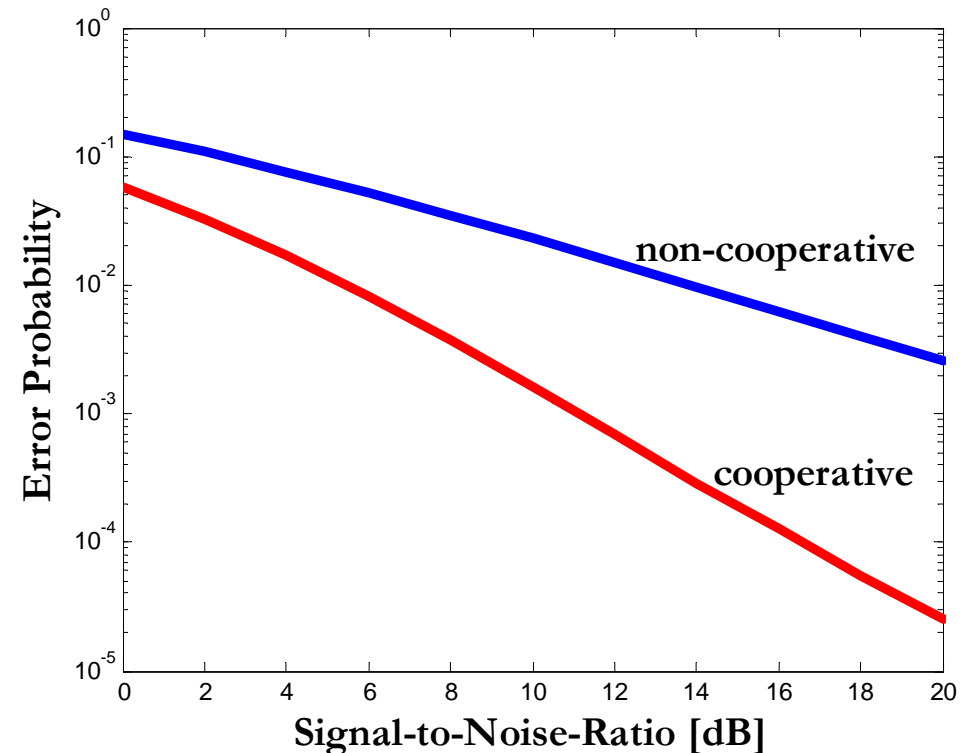
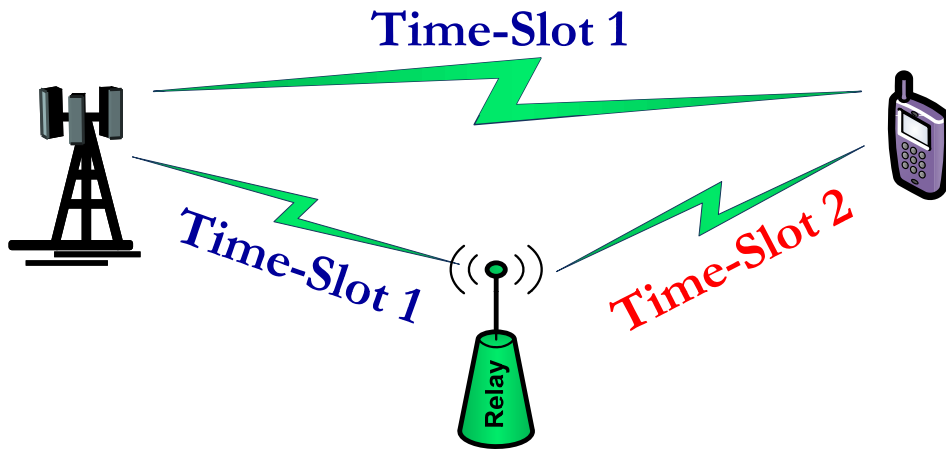


## Multi-Hop Networks:

- ❑ **Advantages:** better performance, extended coverage...
- ❑ **Disadvantages:** additional resources (relays, time-slots, frequencies), capacity reduction, half-duplex constraint...



## Relay-Aided SM (2/24)

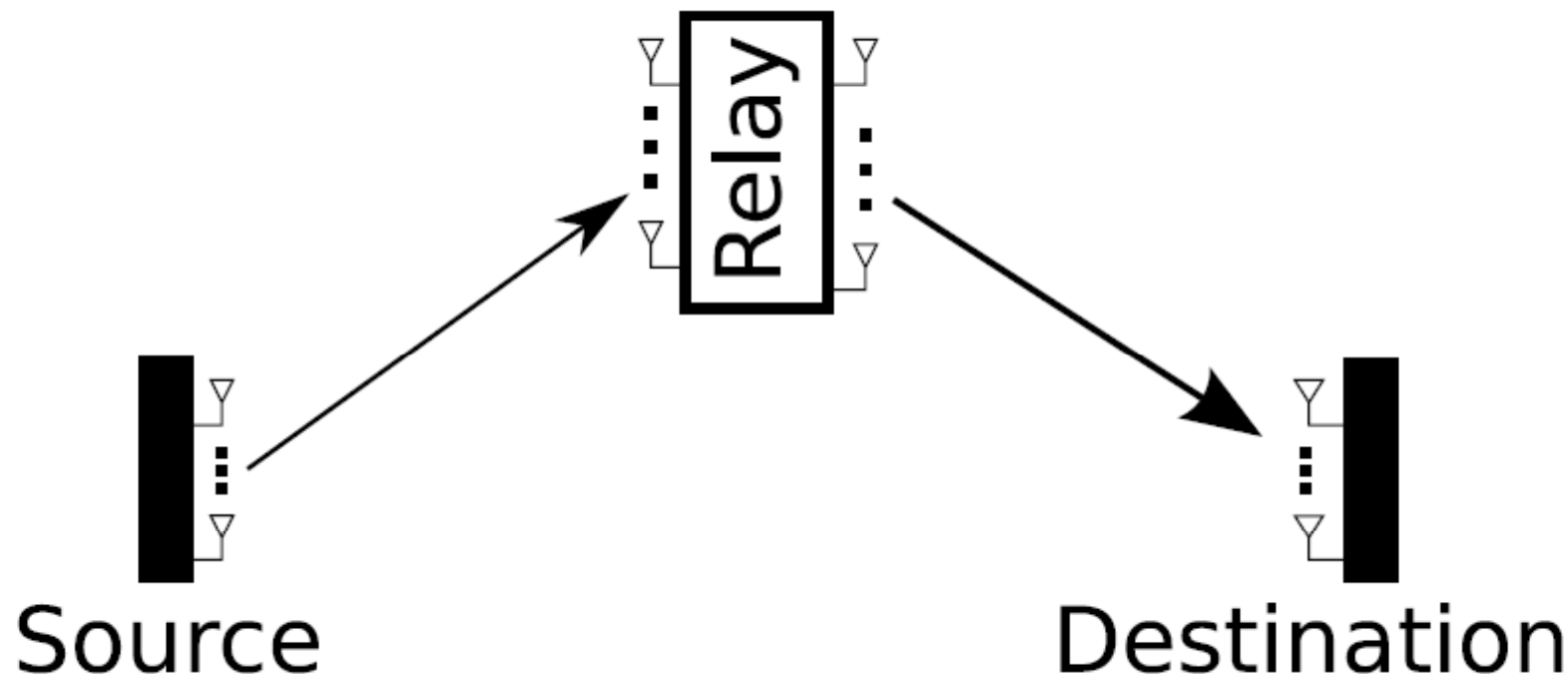


### Cooperative Networks:

- ❑ **Advantages:** better performance, (macro) diversity...
- ❑ **Disadvantages:** additional resources (relays, time-slots, frequencies), capacity reduction, half-duplex constraint...

## *Relay-Aided SM (3/24)*

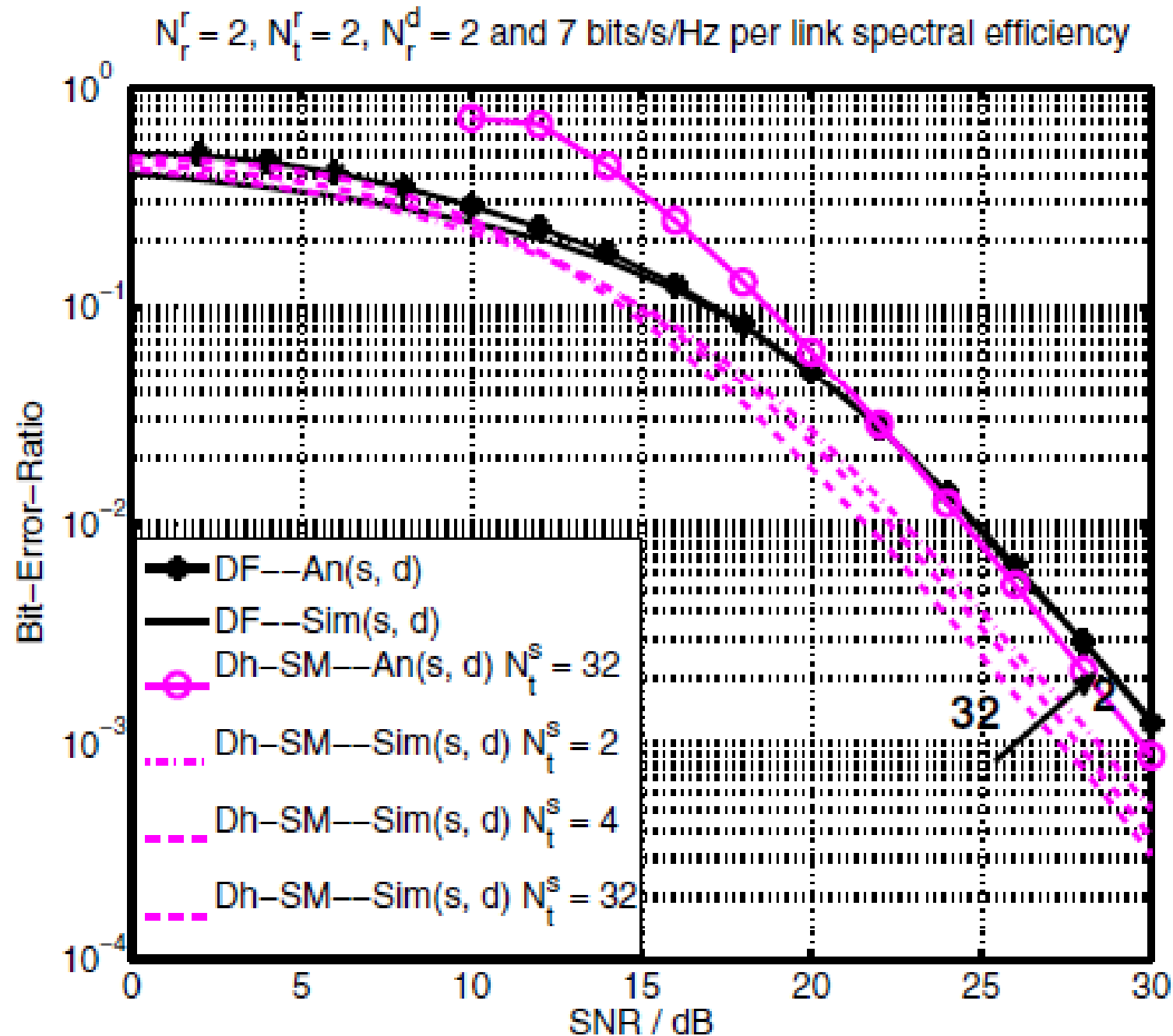
### Dual-Hop Spatial Modulation



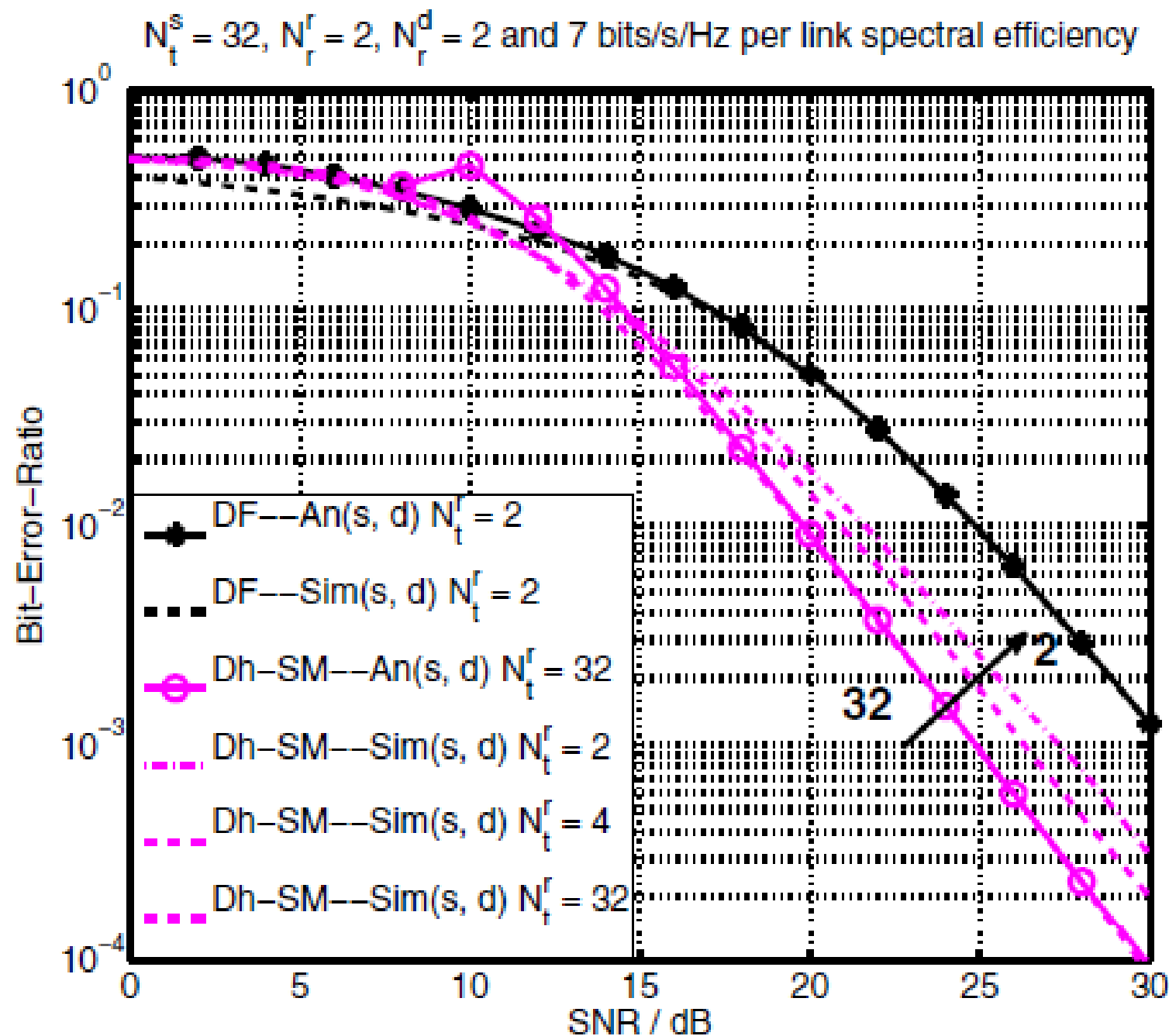
Demodulate-and-Forward (DemF)

$$P_b(\bar{\gamma}_{sd}) = P_b(\bar{\gamma}_{sr}) + P_b(\bar{\gamma}_{rd}) - 2P_b(\bar{\gamma}_{sr})P_b(\bar{\gamma}_{rd})$$

## Relay-Aided SM (4/24)

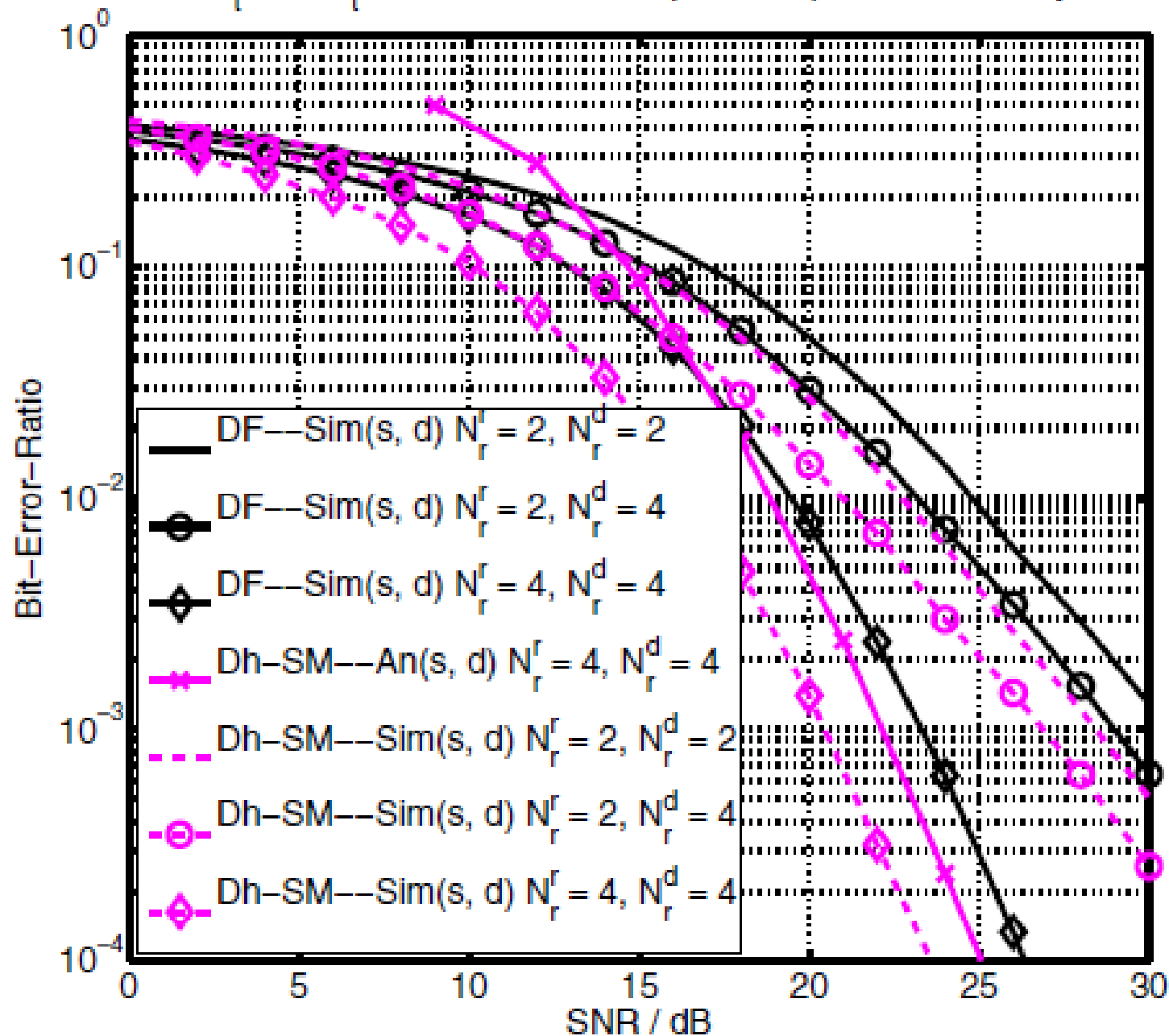


## Relay-Aided SM (5/24)

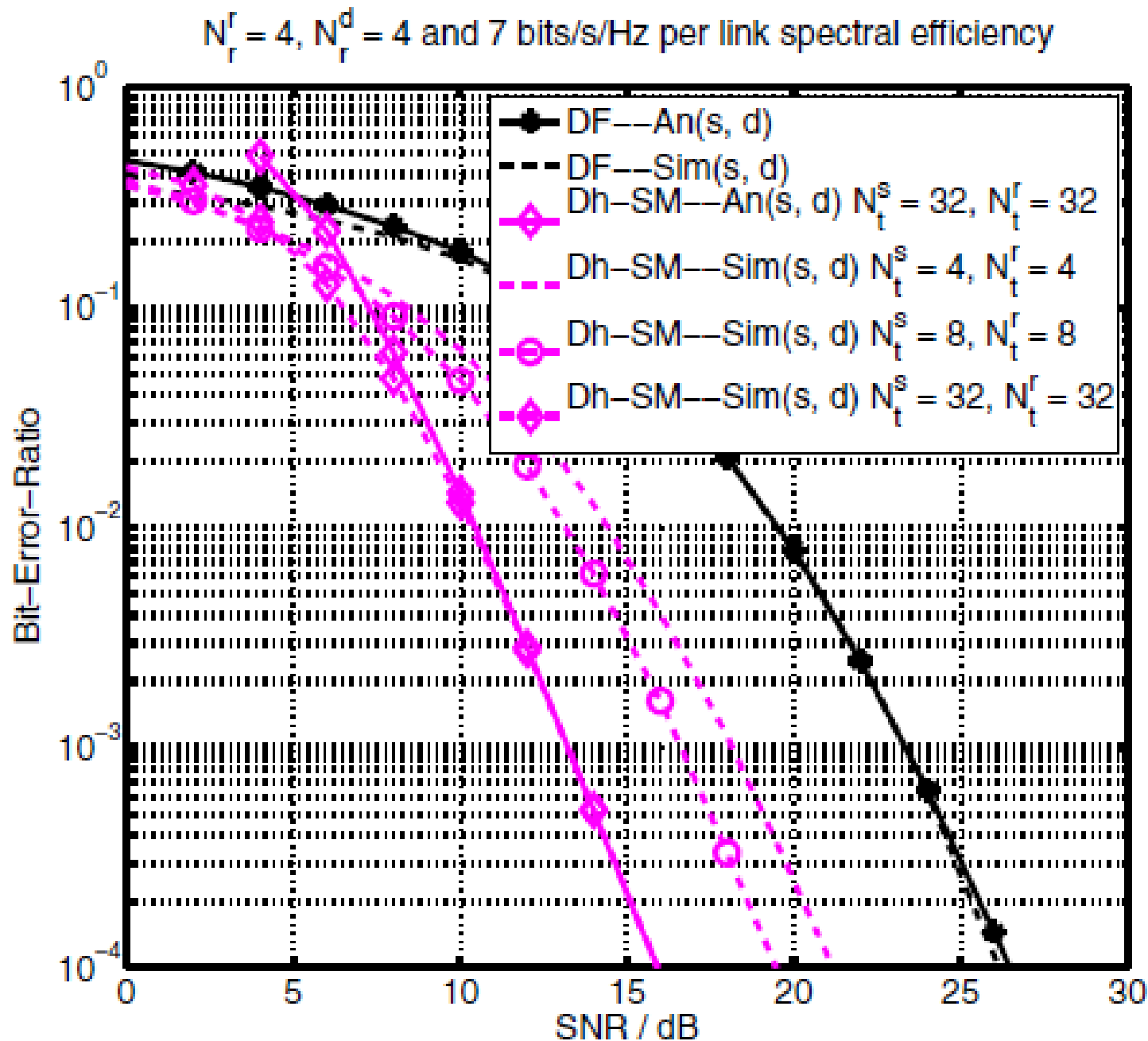


## Relay-Aided SM (6/24)

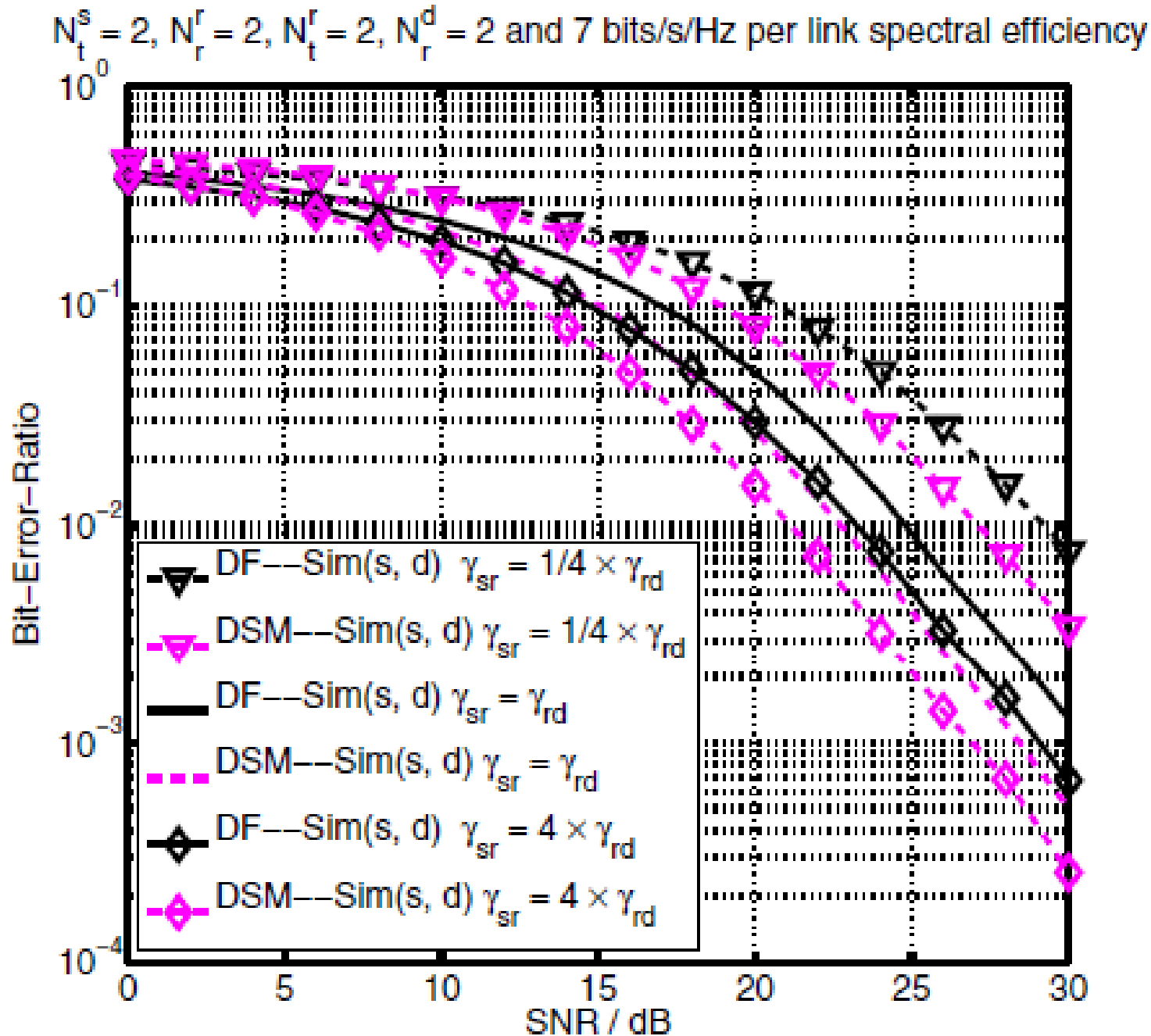
$N_t^s = 2, N_t^r = 2$  and 7 bits/s/Hz per link spectral efficiency



## Relay-Aided SM (7/24)



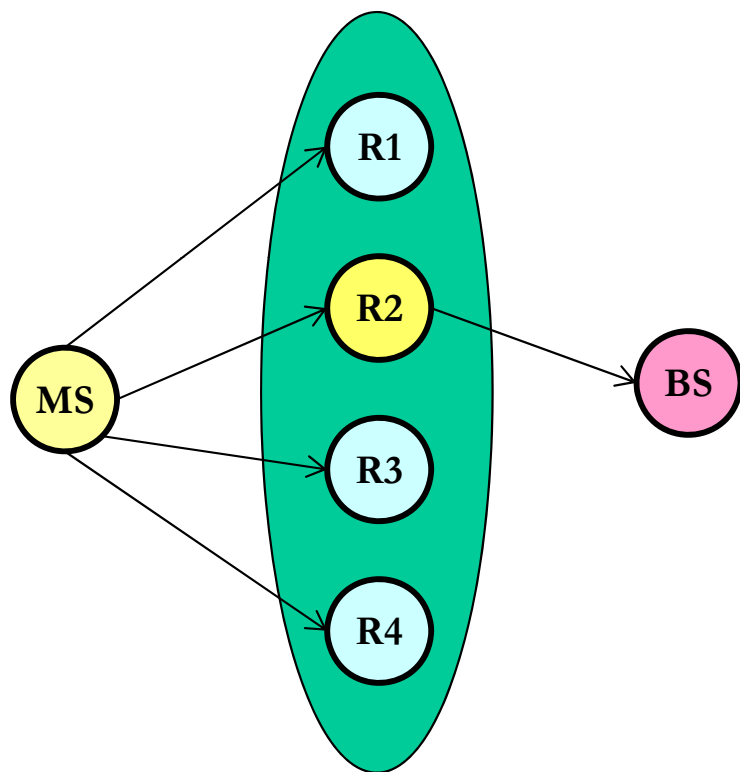
## Relay-Aided SM (8/24)





# Relay-Aided SM (9/24)

## Virtual SM-MIMO for the Uplink

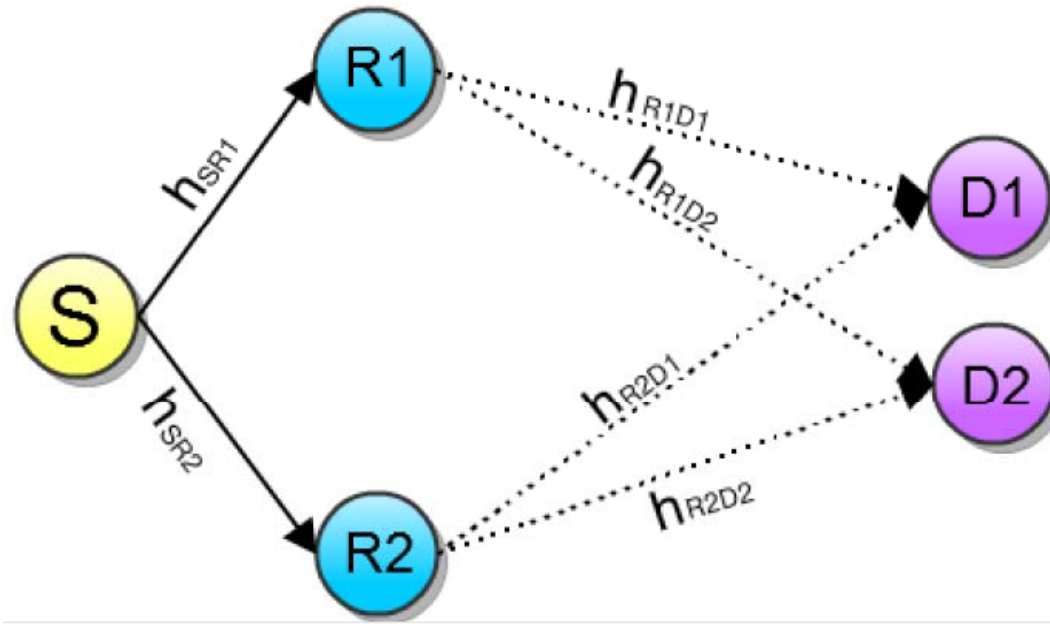


Distributed  
spatial-constellation diagram

- ❑ In TS-1, MS broadcasts its own info symbol to a group of  $N_R$  relays. Each symbol has  $\log_2(N_R)$  bits (QAM or PSK)
- ❑ The relays decode the received symbol without any coordination among them
- ❑ Each relay is assigned an individual ID. If the symbol received from MS coincides with the ID, then the relay is activated for transmission
- ❑ Thus, the relays play the role of a distributed spatial constellation diagram
- ❑ The relay-activation process conveys information
- ❑ Errors may occur, and so multiple or no relays may wake up

# Relay-Aided SM (10/24)

## Virtual SM-MIMO for the Uplink



$$\hat{b}_S^{(D)} = \arg \min_{\substack{(\tilde{b}_S^{(D)}, a_{tx}^{(R_1)}, a_{tx}^{(R_2)}) \\ \in \{(0,1,0), (1,0,1)\}}} \left\{ \sum_{\bar{d}=1}^2 \left| y_{RD_{\bar{d}}} - \mathcal{F} \left( \tilde{b}_S^{(D)}, a_{tx}^{(R_1)}, a_{tx}^{(R_2)} \right) \right|^2 \right\}$$

$$\mathcal{F} \left( \tilde{b}_S^{(D)} = 0, a_{tx}^{(R_1)} = 1, a_{tx}^{(R_2)} = 0 \right) = \sqrt{E_m} h_{R_1 D_{\bar{d}}}$$

$$\mathcal{F} \left( \tilde{b}_S^{(D)} = 1, a_{tx}^{(R_1)} = 0, a_{tx}^{(R_2)} = 1 \right) = \sqrt{E_m} h_{R_2 D_{\bar{d}}}$$

Conventional  
SSK Demodulator

## Relay-Aided SM (11/24)

### Optimal (Error-Aware) Demodulator

$$\begin{cases} y_{SR_1} = h_{SR_1} x_S + n_{SR_1} \\ y_{SR_2} = h_{SR_2} x_S + n_{SR_2} \end{cases}$$



$$\begin{cases} \hat{b}_S^{(R_1)} = \arg \min_{\tilde{b}_S \in \{0,1\}} \left\{ \left| y_{SR_1} - \sqrt{E_m} h_{SR_1} (1 - 2\tilde{b}_S) \right|^2 \right\} \\ \hat{b}_S^{(R_2)} = \arg \min_{\tilde{b}_S \in \{0,1\}} \left\{ \left| y_{SR_2} - \sqrt{E_m} h_{SR_2} (1 - 2\tilde{b}_S) \right|^2 \right\} \end{cases}$$



$$y_{RD_{\bar{d}}} = \sqrt{E_m} h_{R_1 D_{\bar{d}}} \Delta \left( \mathbf{ID}_{R_1}, \hat{b}_S^{(R_1)} \right) + \sqrt{E_m} h_{R_2 D_{\bar{d}}} \Delta \left( \mathbf{ID}_{R_2}, \hat{b}_S^{(R_2)} \right) + n_{RD_{\bar{d}}}$$
$$\Delta \left( \mathbf{ID}_{R_{\bar{r}}}, \hat{b}_S^{(R_{\bar{r}})} \right) = \begin{cases} 1 & \text{if } \mathbf{ID}_{R_{\bar{r}}} = \hat{b}_S^{(R_{\bar{r}})} \\ 0 & \text{if } \mathbf{ID}_{R_{\bar{r}}} \neq \hat{b}_S^{(R_{\bar{r}})} \end{cases}$$

## Relay-Aided SM (12/24)

### Optimal (Error-Aware) Demodulator

$$\hat{b}_S^{(D)} = \arg \max_{\tilde{b}_S^{(D)} \in \{0,1\}} \left\{ \sum_{a_{tx}^{(R_1)}=0}^1 \sum_{a_{tx}^{(R_2)}=0}^1 \left\{ \prod_{\bar{d}=1}^2 \mathcal{P} \left\{ y_{RD_{\bar{d}}} \middle| \mathcal{H} \left( \tilde{b}_S^{(D)}, a_{tx}^{(R_1)}, a_{tx}^{(R_2)} \right) \right\} \right\} \mathcal{P} \left\{ \mathcal{H} \left( \tilde{b}_S^{(D)}, a_{tx}^{(R_1)}, a_{tx}^{(R_2)} \right) \right\} \right\}$$

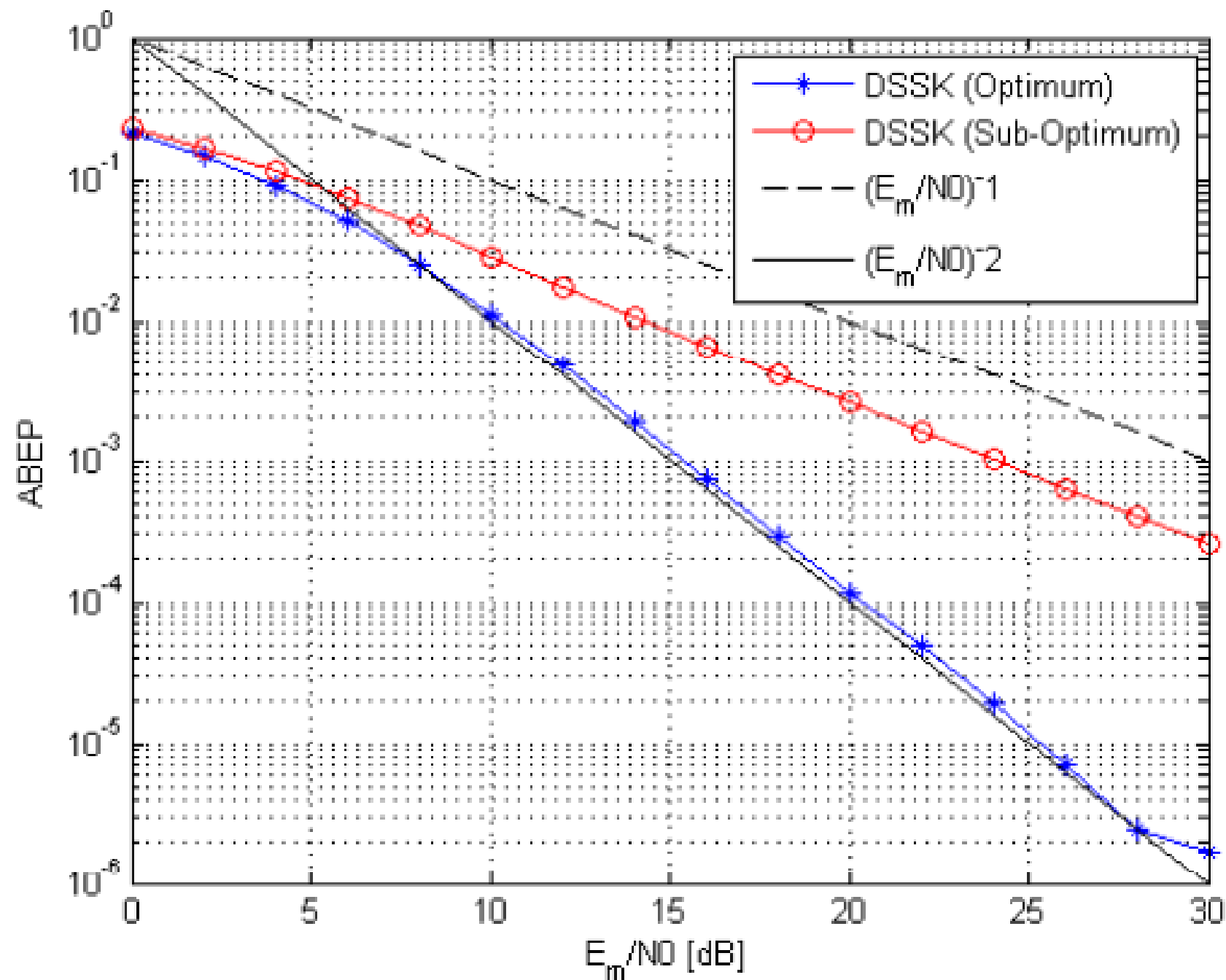


$$\mathcal{P} \left\{ y_{RD_{\bar{d}}} \middle| \mathcal{H} \left( \tilde{b}_S^{(D)}, a_{tx}^{(R_1)}, a_{tx}^{(R_2)} \right) \right\} = \exp \left( - \frac{\left| y_{RD_{\bar{d}}} - \left( \sqrt{E_m} h_{R_1 D_{\bar{d}}} a_{tx}^{(R_1)} + \sqrt{E_m} h_{R_1 D_{\bar{d}}} a_{tx}^{(R_2)} \right) \right|^2}{N_0} \right)$$

$$\mathcal{P} \left\{ \mathcal{H} \left( \tilde{b}_S^{(D)}, a_{tx}^{(R_1)}, a_{tx}^{(R_2)} \right) \right\} = w_{SR_1} \left( \tilde{b}_S^{(D)}, a_{tx}^{(R_1)} \right) w_{SR_2} \left( \tilde{b}_S^{(D)}, a_{tx}^{(R_2)} \right)$$

$$w_{SR_{\bar{r}}} \left( \tilde{b}_S^{(D)}, a_{tx}^{(R_{\bar{r}})} \right) = \begin{cases} 1 - Q \left( \sqrt{2|h_{SR_{\bar{r}}}|^2 (E_m/N_0)} \right) & \text{if } \left( \tilde{b}_S^{(D)} = \bar{r} - 1 \text{ and } a_{tx}^{(R_{\bar{r}})} \neq 0 \right) \text{ or } \left( \tilde{b}_S^{(D)} \neq \bar{r} - 1 \text{ and } a_{tx}^{(R_{\bar{r}})} = 0 \right) \\ Q \left( \sqrt{2|h_{SR_{\bar{r}}}|^2 (E_m/N_0)} \right) & \text{otherwise} \end{cases}$$

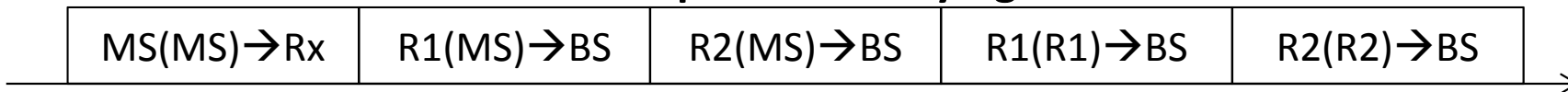
## Relay-Aided SM (13/24)



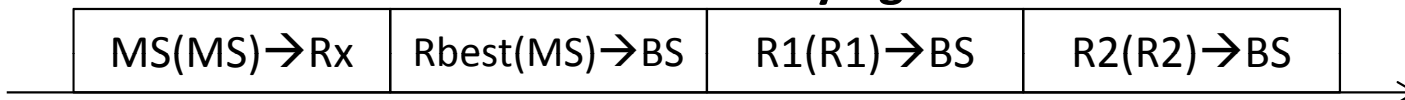
# Relay-Aided SM (14/24)

## Spectral-Efficient Relaying

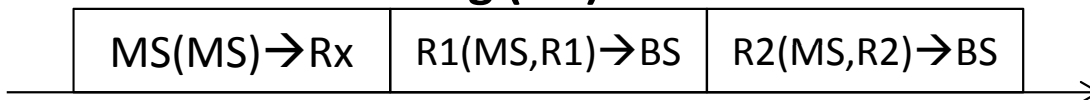
### Repetition Relaying



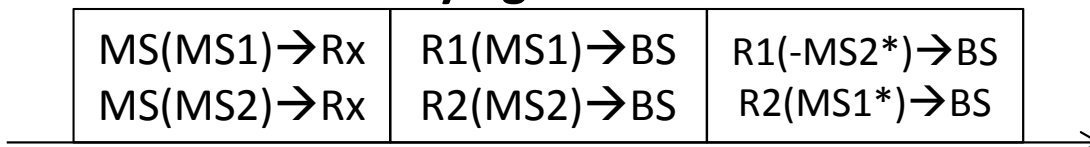
### Selective Relaying



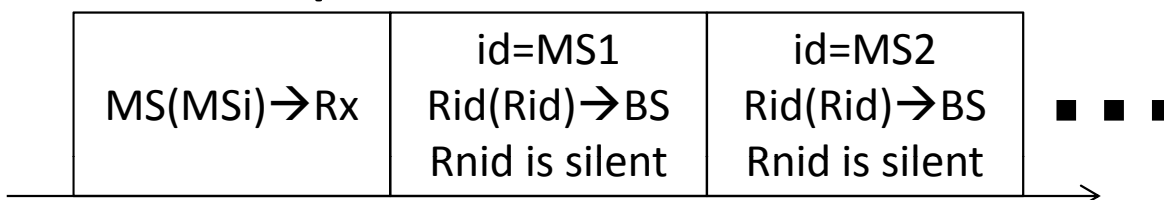
### Network Coding (NC) Based - Phoenix



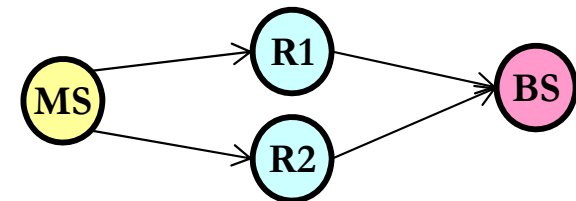
### DSTBC Relaying – Alamouti Based



### Spatial Modulation Based



A new relaying protocol  
based on Spatial Modulation  
(the Relays have data in their buffers)



## Relay-Aided SM (15/24)

### Distributed SM

$$\begin{cases} y_{SR_r} = \sqrt{E_S} h_{SR_r} s_{tx} + n_{SR_r} \\ y_{SD} = \sqrt{E_S} h_{SD} s_{tx} + n_{SD} \end{cases}$$



$$\begin{cases} \hat{s}_{tx}^{(R_r)} = \arg \min_{p_m \in \{p_1, p_2, \dots, p_M\}} \left\{ \left| y_{SR_r} - \sqrt{E_S} h_{SR_r} p_m \right|^2 \right\} \\ \hat{\mathbf{x}}_S^{(R_r)} = \mathfrak{M}_S^{-1} \left( \hat{s}_{tx}^{(R_r)} \right) \end{cases} \quad r_{tx}^{(R_r)} = \begin{cases} \mathfrak{M}_R(\mathbf{x}_{R_r}) & \text{if } \mathbf{ID}_{R_r} = \hat{\mathbf{x}}_S^{(R_r)} \\ 0 & \text{if } \mathbf{ID}_{R_r} \neq \hat{\mathbf{x}}_S^{(R_r)} \end{cases}$$



$$y_{RD} = \sum_{r=1}^M \left( \sqrt{E_{R_r}} h_{R_r D} r_{tx}^{(R_r)} \right) + n_{RD}$$

## Relay-Aided SM (16/24)

### Optimal (Error-Aware) Demodulator

$$\left[ \hat{\mathbf{x}}_S^{(D)}, \hat{\mathbf{x}}_{R_1}^{(D)}, \hat{\mathbf{x}}_{R_2}^{(D)} \right] = \arg \max_{\mathbf{x}_S^{(D)} \in \{0,1\}, \mathbf{x}_{R_1}^{(D)} \in \{0,1,\mathcal{N}\}, \mathbf{x}_{R_2}^{(D)} \in \{0,1,\mathcal{N}\}} \left\{ \mathcal{P} \left\{ [y_{SD}, y_{RD}] | \mathcal{H} \left( \mathbf{x}_S^{(D)}, \mathbf{x}_{R_1}^{(D)}, \mathbf{x}_{R_2}^{(D)} \right) \right\} \mathcal{P} \left\{ \mathcal{H} \left( \mathbf{x}_S^{(D)}, \mathbf{x}_{R_1}^{(D)}, \mathbf{x}_{R_2}^{(D)} \right) \right\} \right\}$$

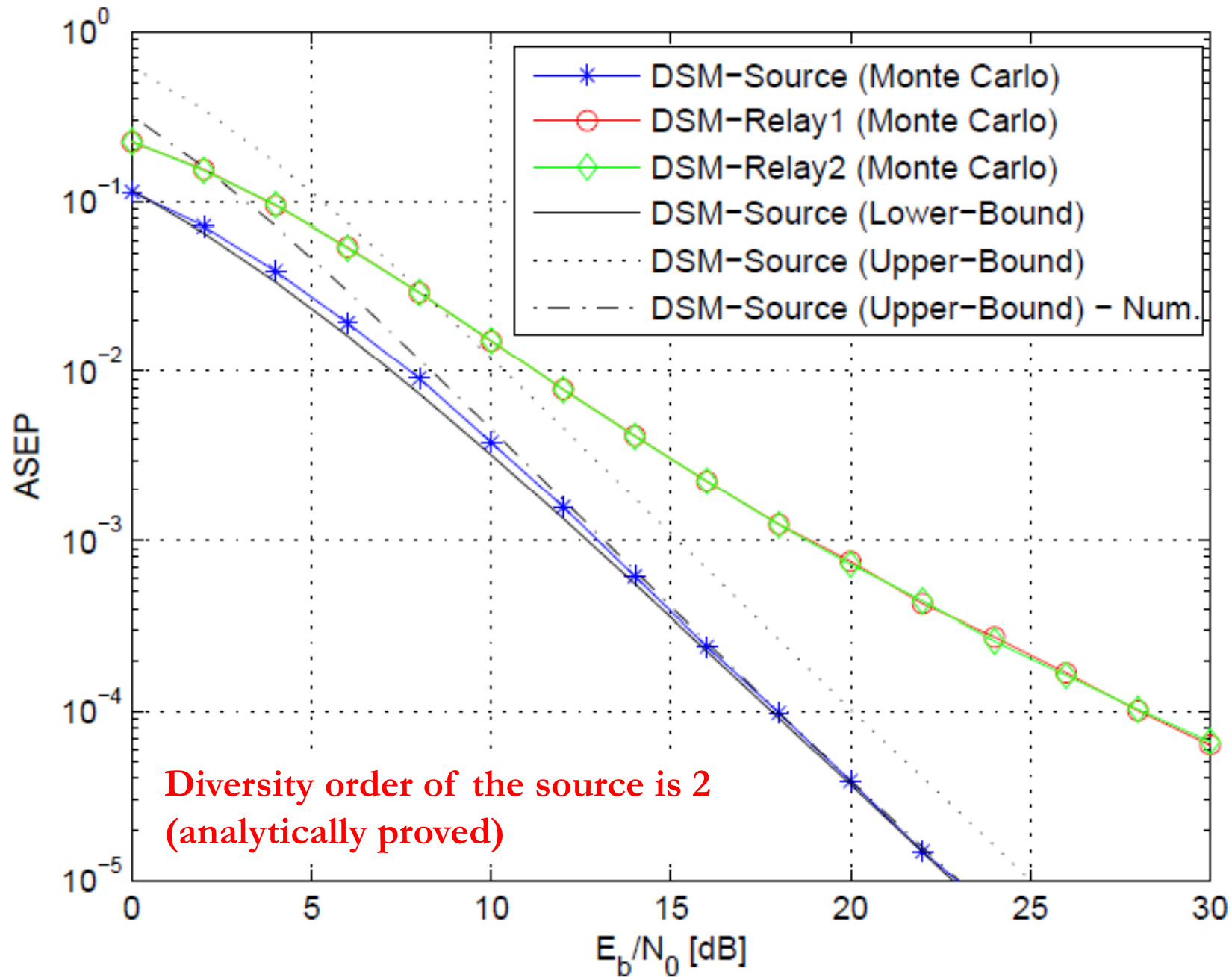


$$\mathcal{P} \left\{ [y_{SD}, y_{RD}] | \mathcal{H} \left( \mathbf{x}_S^{(D)}, \mathbf{x}_{R_1}^{(D)}, \mathbf{x}_{R_2}^{(D)} \right) \right\} = \exp \left( - \frac{\left| y_{SD} - \sqrt{E_S} h_{SD} \mathfrak{M}_S \left( \mathbf{x}_S^{(D)} \right) \right|^2}{N_0} \right) \\ \times \exp \left( - \frac{\left| y_{RD} - \left( \sqrt{E_{R_1}} h_{R_1 D} \widetilde{\mathfrak{M}}_R \left( \mathbf{x}_{R_1}^{(D)} \right) + \sqrt{E_{R_2}} h_{R_2 D} \widetilde{\mathfrak{M}}_R \left( \mathbf{x}_{R_2}^{(D)} \right) \right) \right|^2}{N_0} \right)$$

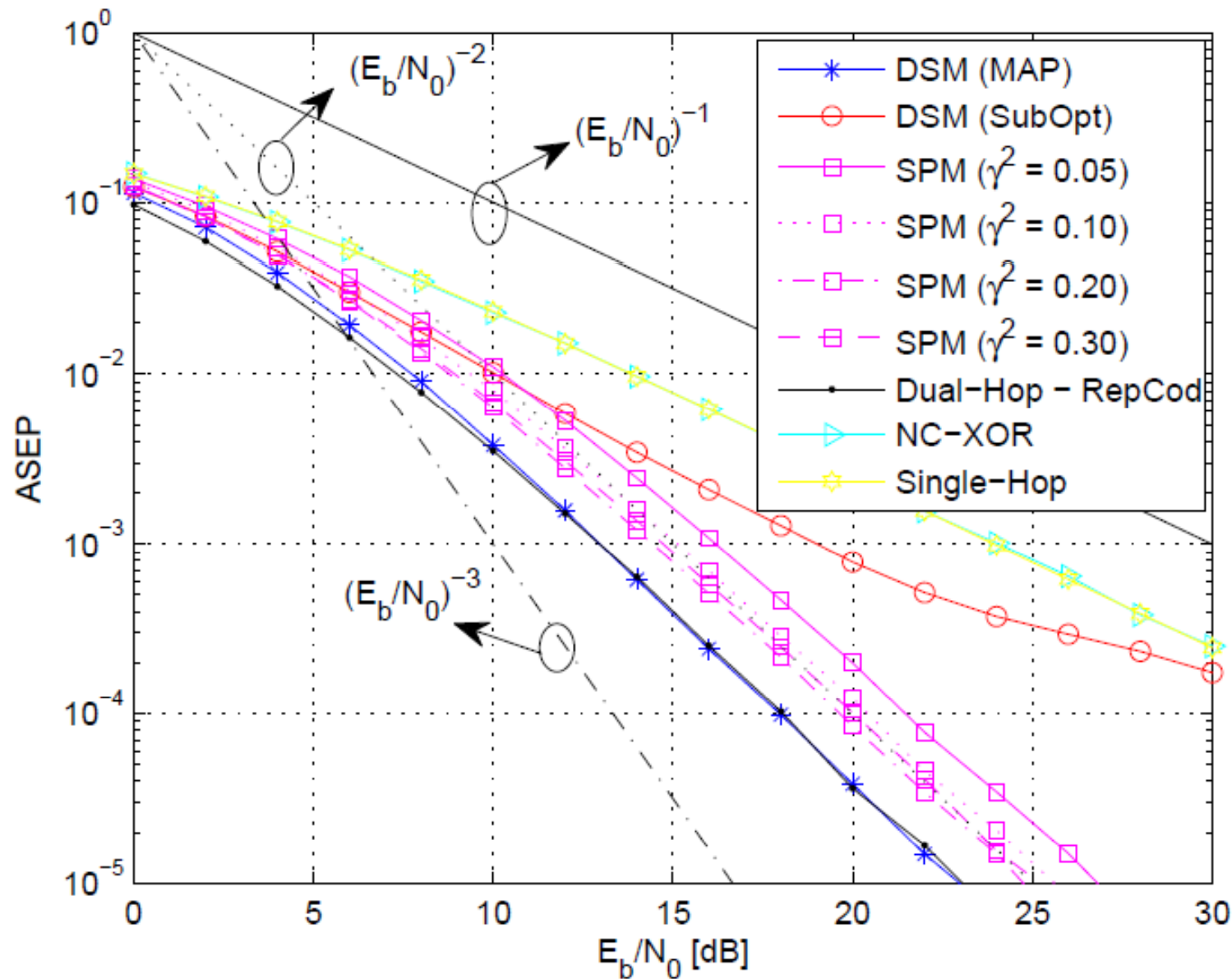
$$w_{SR_r} \left( \mathbf{x}_S^{(D)}, \mathbf{x}_{R_r}^{(D)} \right) = \begin{cases} 1 - Q \left( \sqrt{2 |h_{SR_r}|^2 (E_S/N_0)} \right) & \text{if } \left( \mathbf{x}_S^{(D)} = r-1 \text{ and } \mathbf{x}_{R_r}^{(D)} \neq \mathcal{N} \right) \text{ or } \left( \mathbf{x}_S^{(D)} \neq r-1 \text{ and } \mathbf{x}_{R_r}^{(D)} = \mathcal{N} \right) \\ Q \left( \sqrt{2 |h_{SR_r}|^2 (E_S/N_0)} \right) & \text{otherwise} \end{cases}$$



## Relay-Aided SM (17/24)

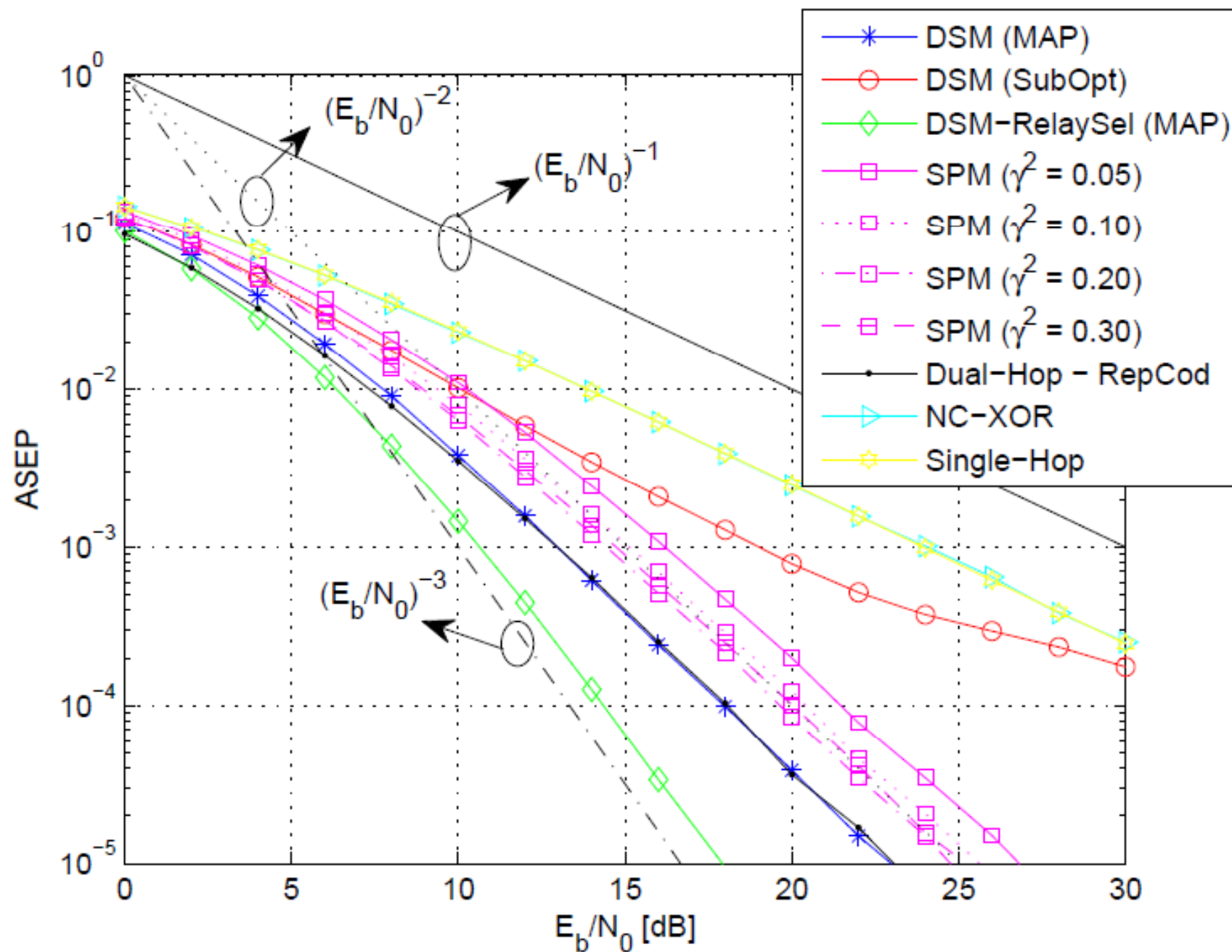


# Relay-Aided SM (18/24)



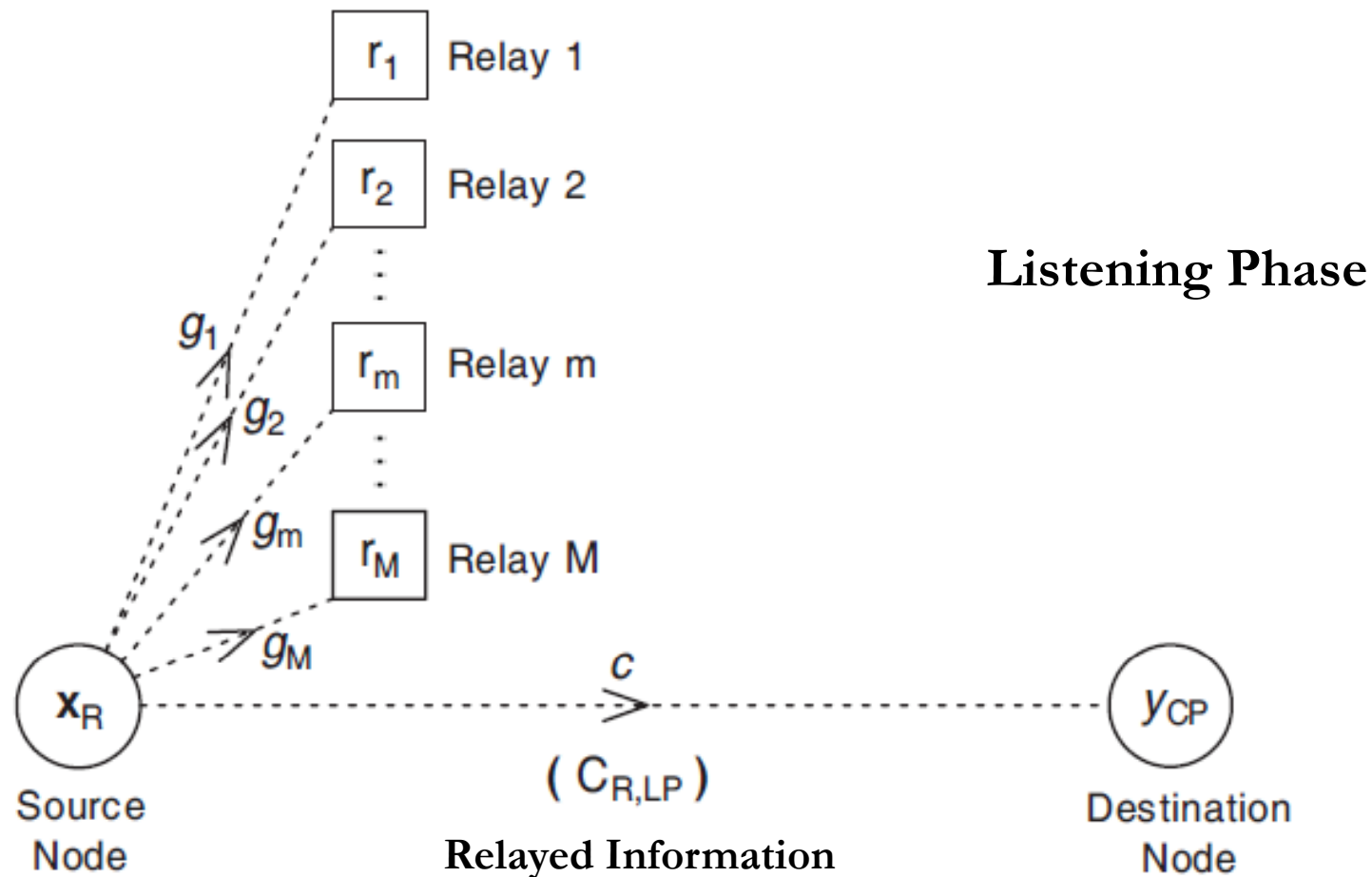
$$y_{RD}^{\text{SPM}} = \sqrt{E_{R_1}} h_{R_1 D} \left( \sqrt{1 - \gamma^2} \mathfrak{M}_R(\mathbf{x}_{R_1}) + \gamma \mathfrak{M}_S(\hat{\mathbf{x}}_S^{(R_1)}) \right) + n_{RD}$$

## Relay-Aided SM (19/24)



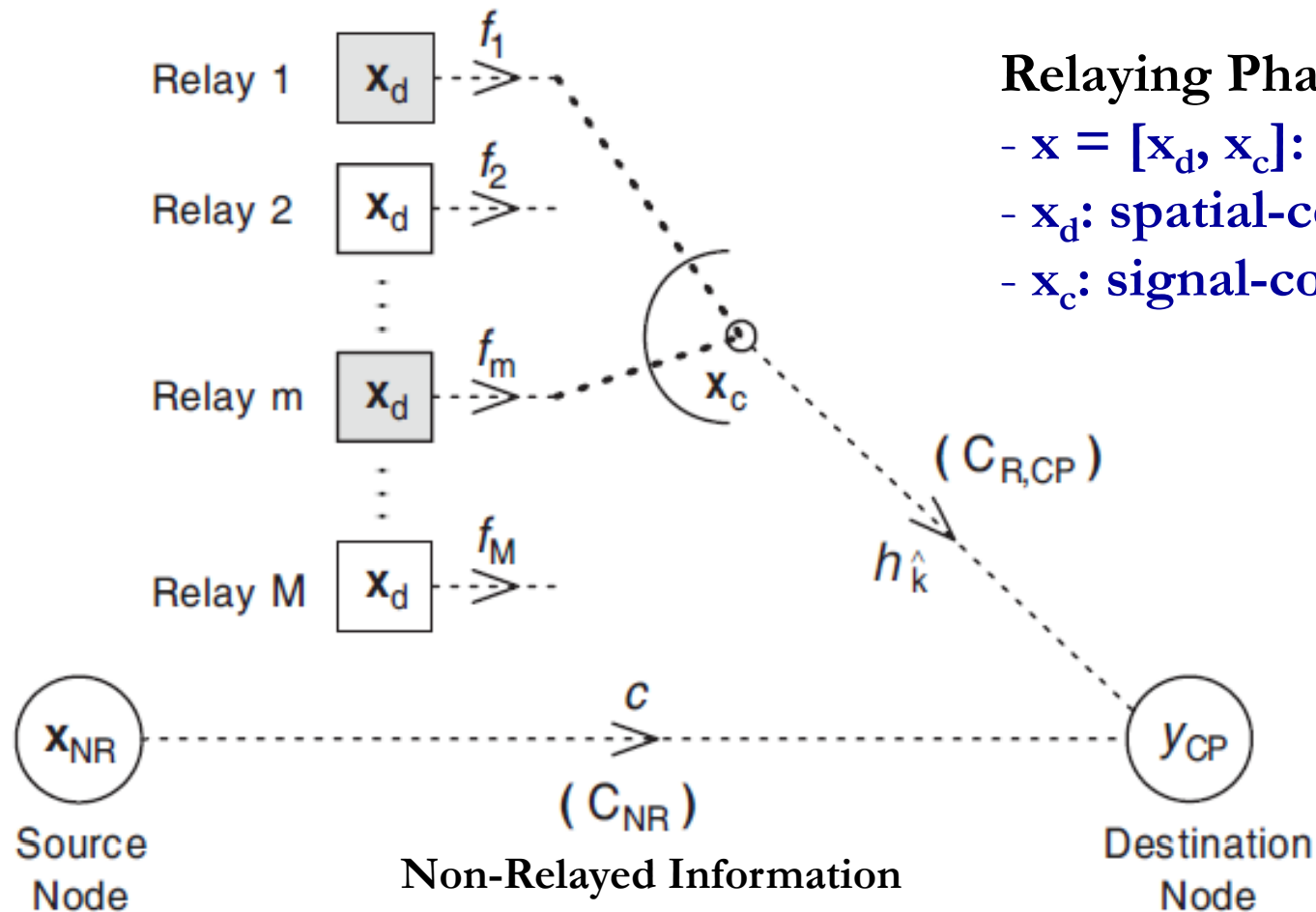
## Relay-Aided SM (20/24)

### Decode-and-Forward (DF) Non-Orthogonal Relaying



## Relay-Aided SM (21/24)

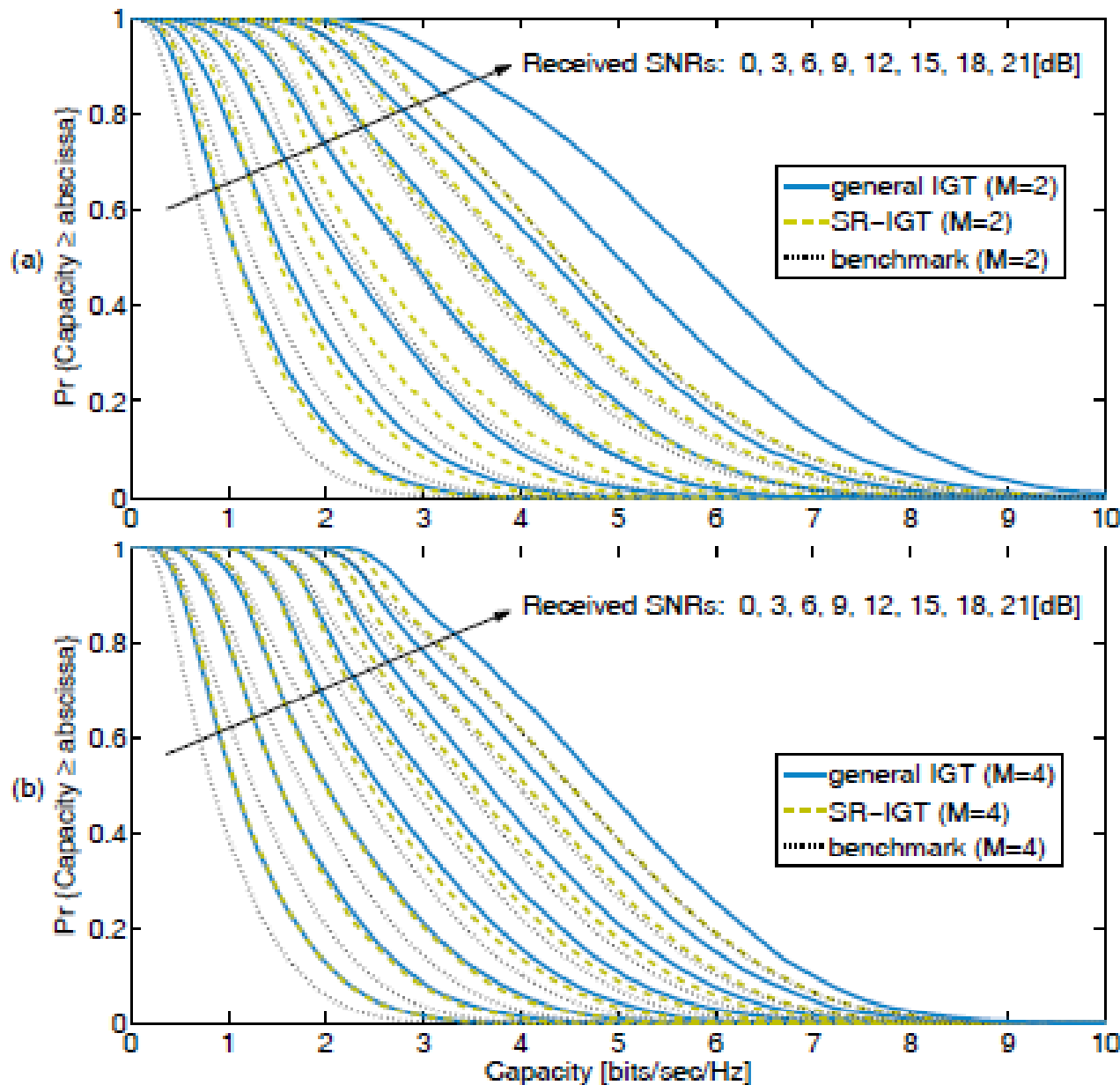
### Decode-and-Forward (DF) Non-Orthogonal Relaying



#### Relaying Phase

- $x = [x_d, x_c]$ : received from the source
- $x_d$ : spatial-constellation diagram
- $x_c$ : signal-constellation diagram

# Relay-Aided SM (22/24)



Capacity complementary cumulative distribution function (CCDF)

comparison among:

- The general IGT scheme (**general IGT**)
- The specific IGT case with single-relay selection (**SR-IGT**)
- The **benchmark** in [\*]

(a)  $M = 2$  relay nodes

(b)  $M = 4$  relay nodes

[\*] K. Azarian, H. El Gamal, and P. Schniter, "On the achievable diversity-multiplexing tradeoff in half-duplex cooperative channels," IEEE Trans. Inf. Theory, vol. 51, no. 12, pp. 4152–4172, Dec. 2005.

## Relay-Aided SM (23/24)

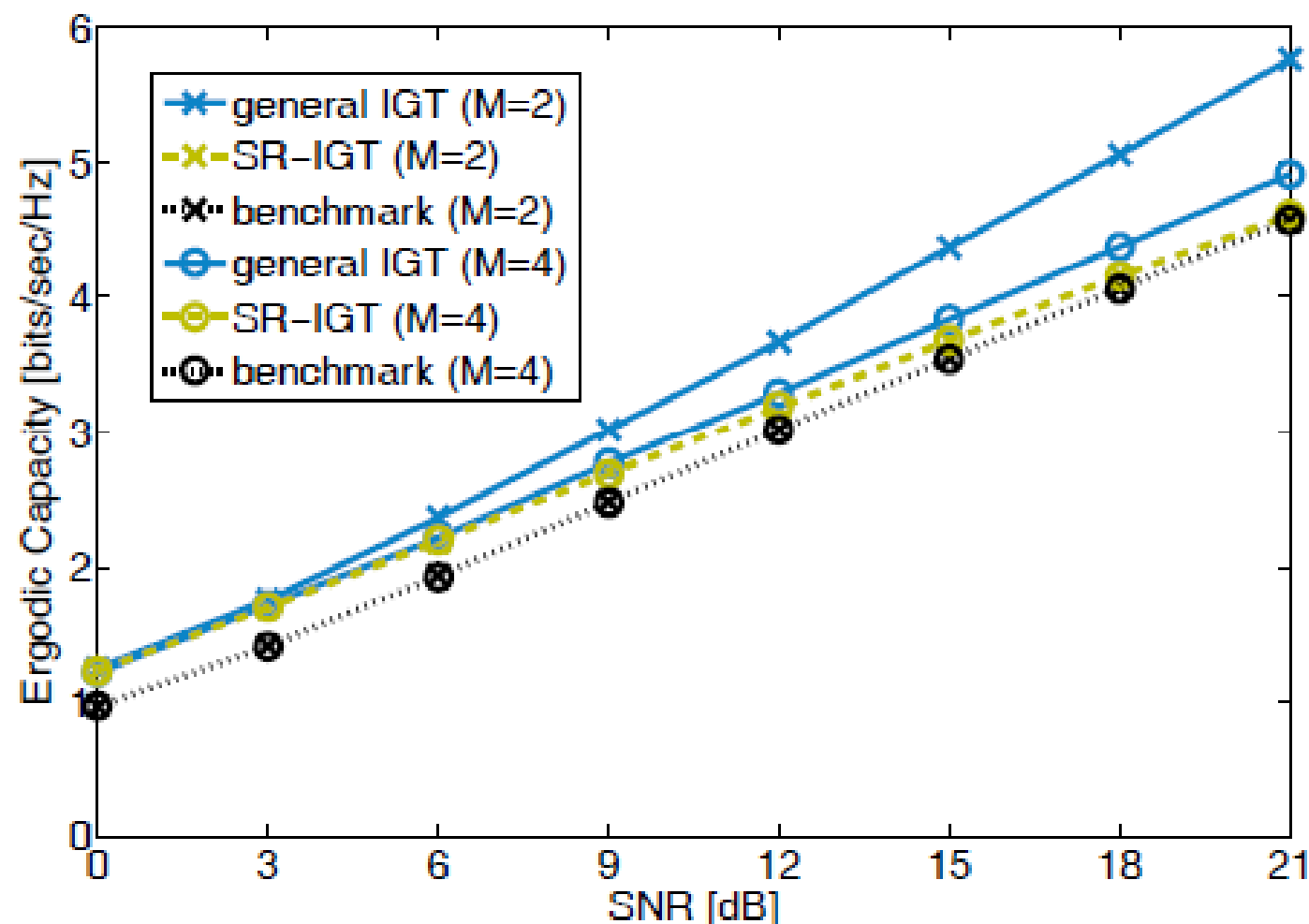
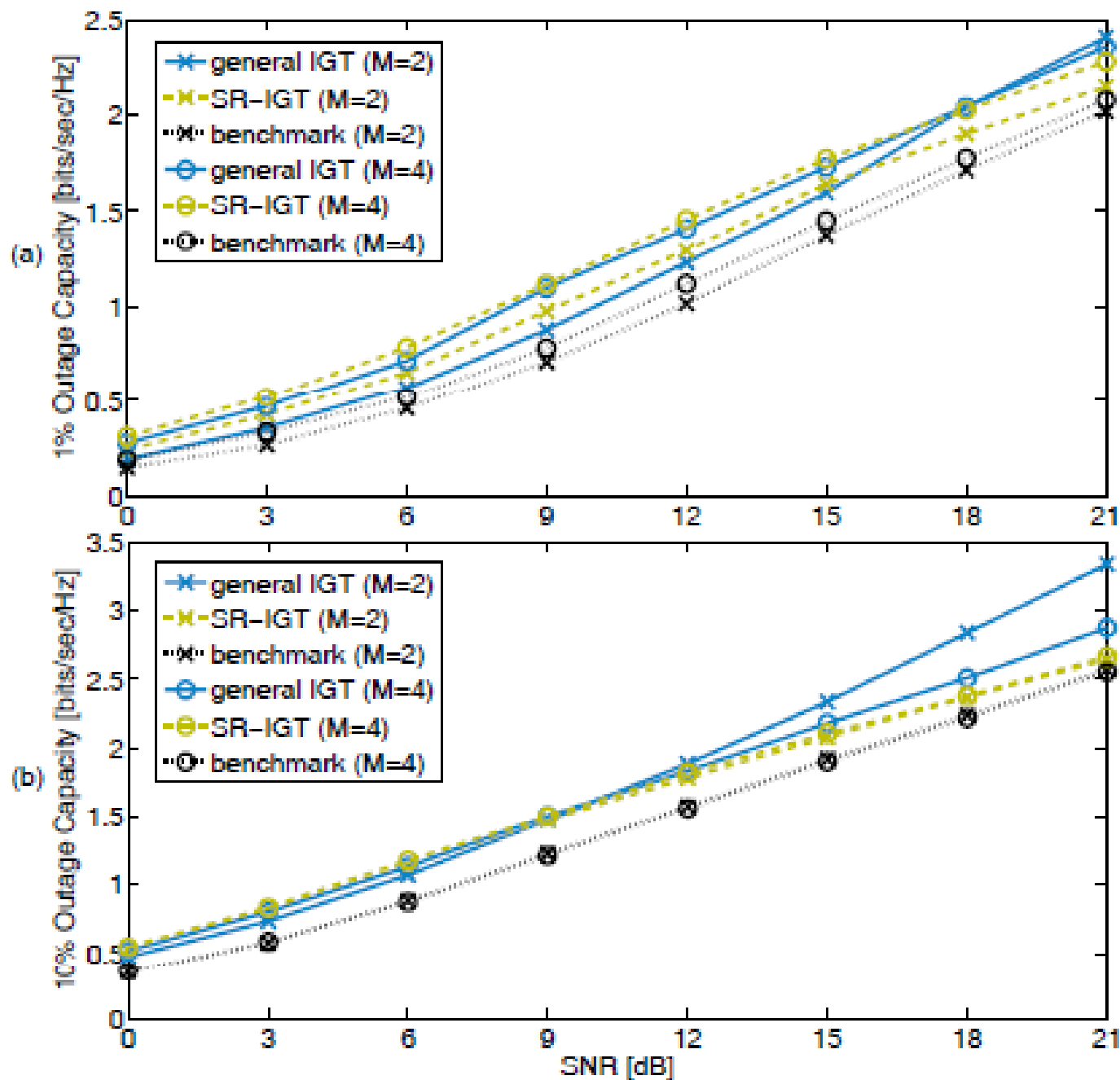


Fig. 6. Ergodic capacity vs. SNR comparisons among the general IGT scheme (general IGT), the specific IGT case with single-relay selection (SR-IGT), and the benchmark.

## Relay-Aided SM (24/24)



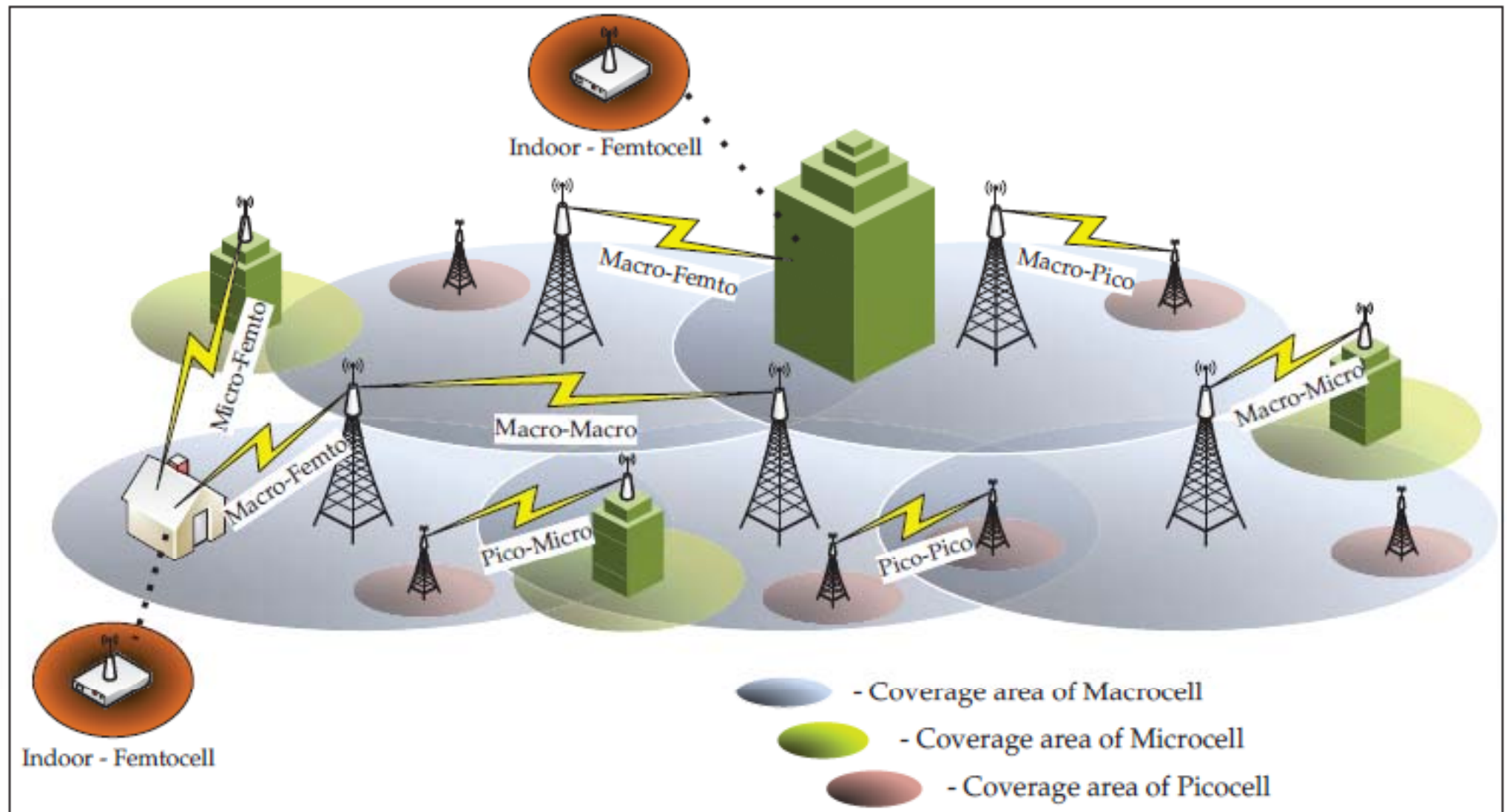


# *Outline*

---

1. Introduction and Motivation behind SM-MIMO
2. History of SM Research and Research Groups Working on SM
3. Transmitter Design – Encoding
4. Receiver Design – Demodulation
5. Error Performance (Numerical Results and Main Trends)
6. Achievable Capacity
7. Channel State Information at the Transmitter
8. Imperfect Channel State Information at the Receiver
9. Multiple Access Interference
10. Energy Efficiency
11. Transmit-Diversity for SM
12. Spatially-Modulated Space-Time-Coded MIMO
13. Relay-Aided SM
14. **SM in Heterogeneous Cellular Networks**
15. SM for Visible Light Communications
16. Experimental Evaluation of SM
17. The Road Ahead – Open Research Challenges/Opportunities
18. Implementation Challenges of SM-MIMO

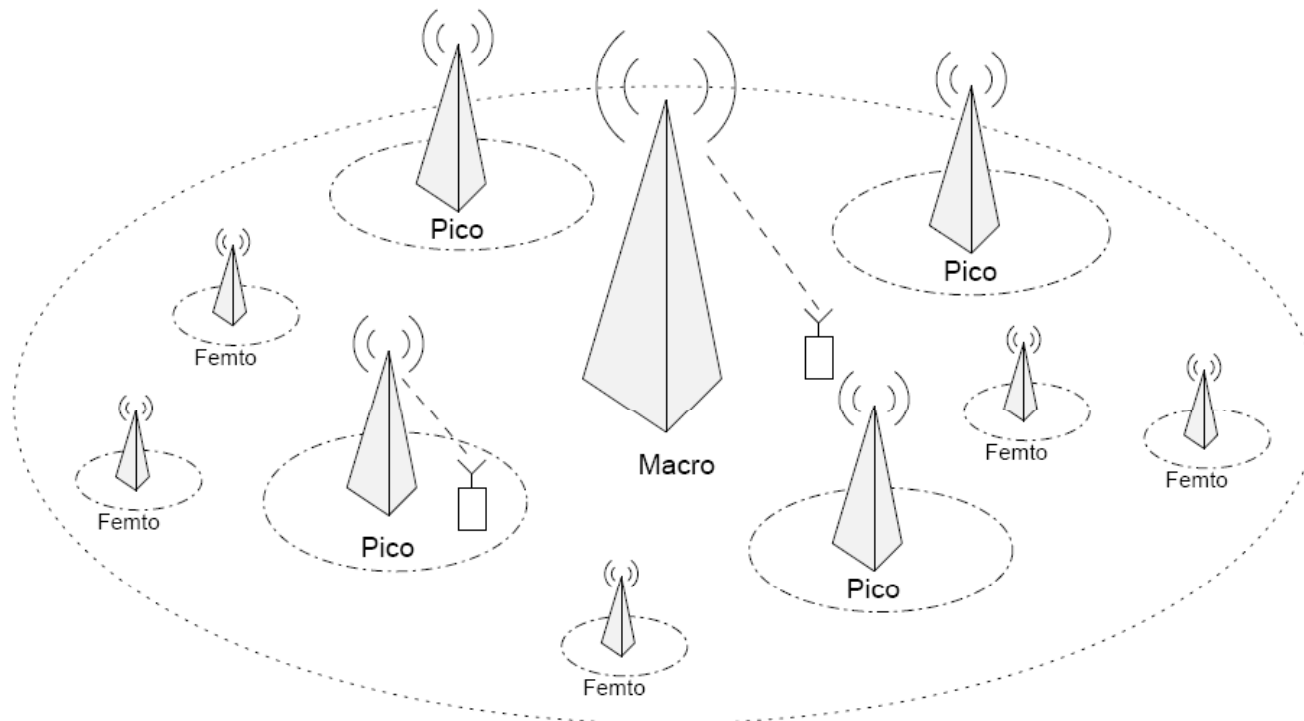
# *SM in Heterogeneous Cellular Networks (1/22)*



## *SM in Heterogeneous Cellular Networks (2/22)*

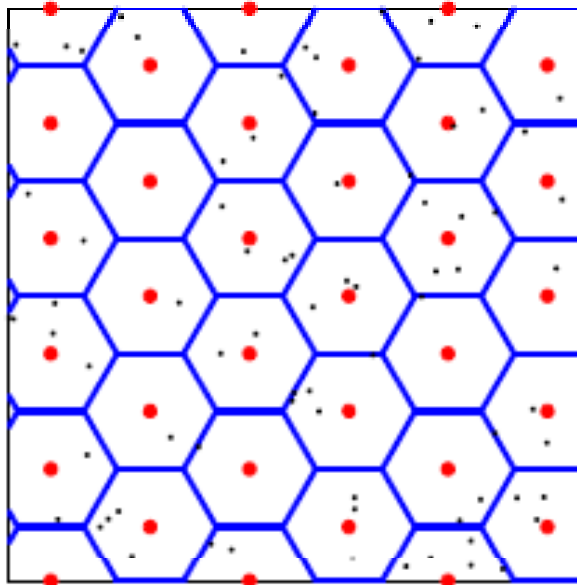
- ❑ Heterogeneous cellular systems are networks with different types of cells providing different QoS requirements to the users, which coexist and contend the wireless medium (macro, pico, femto, relays, DAEs, cognitive radios, etc.)
- ❑ Thus, interference should be properly managed and/or exploited for reliable communications and energy efficiency

### Overlaid multi-tier heterogeneous scenario

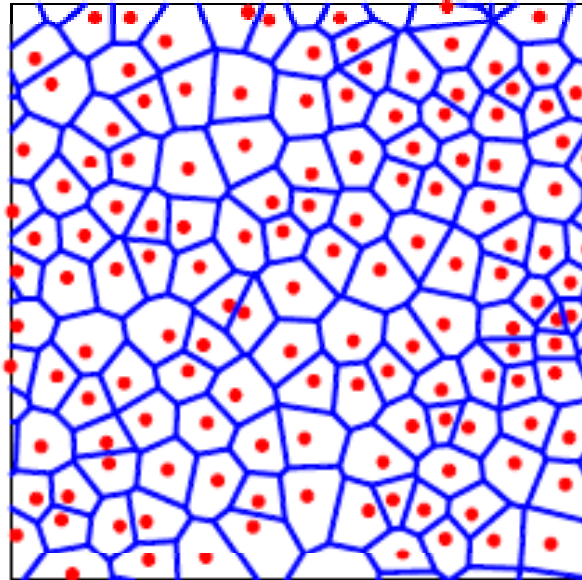


# *SM in Heterogeneous Cellular Networks (3/22)*

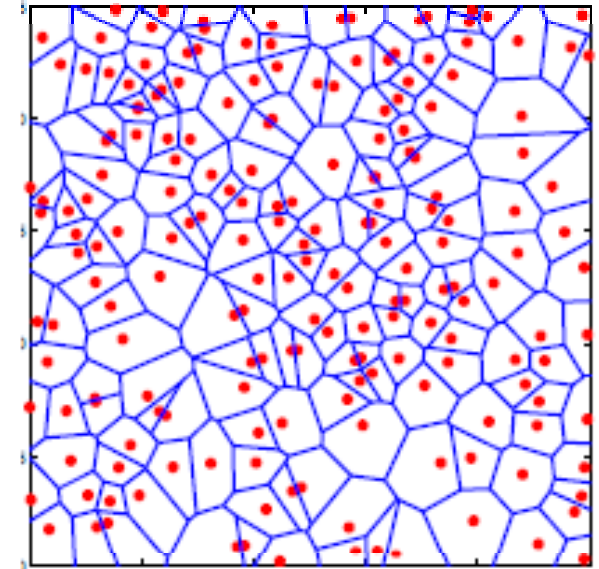
...what cellular will migrate to (Prof. Jeff Andrews, UT Austin)...



Traditional grid model

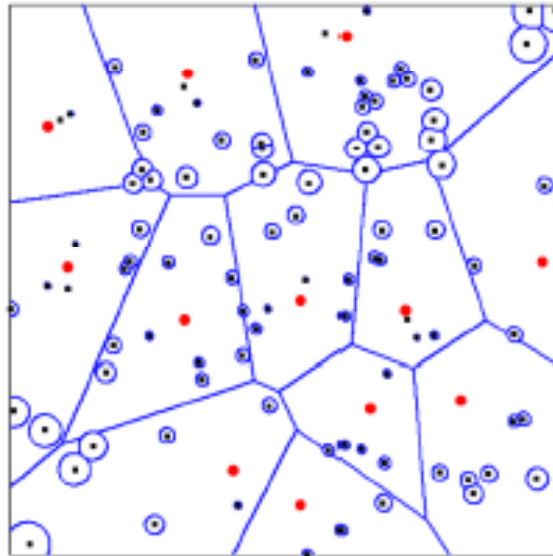


Actual 4G network today



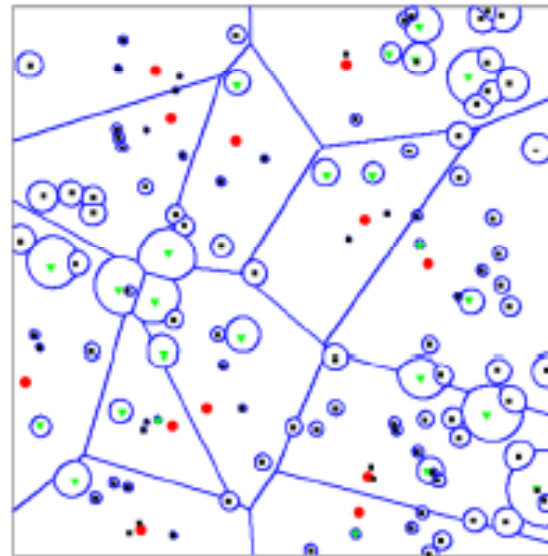
Completely random BSs

Zoom w/ femtocells



4

Zoom w/ picocells too



## *SM in Heterogeneous Cellular Networks (4/22)*

- ❑ Conventional approaches for the analysis and design of (heterogeneous) cellular networks (**abstraction models**) are:
  - The Wyner model
  - The single-cell interfering model
  - The regular hexagonal or square grid model
  
- ❑ However, these abstraction models:
  - **Are over-simplistic and/or inaccurate**
  - **Require intensive numerical simulations and/or integrations**
  - **Provide information only for specific BSs deployments**
  - **No closed-form solutions and/or insights**

J. G. Andrews, F. Baccelli, and R. K. Ganti, “A Tractable Approach to Coverage and Rate in Cellular Networks”, **IEEE Trans. Commun.**, vol. 59, no. 11, pp. 3122–3134, Nov. 2011.

M. Di Renzo, C. Merola, A. Guidotti, F. Santucci, and G. E. Corazza, “Error Performance of Multi-Antenna Receivers in a Poisson Field of Interferers – A Stochastic Geometry Approach”, **IEEE Trans. Commun.**, Vol. 61, No. 5, pp. 2025–2047, May 2013.

M. Di Renzo, A. Guidotti, and G. E. Corazza, “Average Rate of Downlink Heterogeneous Cellular Networks over Generalized Fading Channels – A Stochastic Geometry Approach”, **IEEE Trans. Commun.**, Vol. 61, No. 7, pp. 3050-3071, July 2013.

# *SM in Heterogeneous Cellular Networks (5/22)*

---

## **An Emerging (Tractable) Approach**

### **□ RANDOM SPATIAL MODEL for Heterogeneous Cellular Networks (HCNs):**

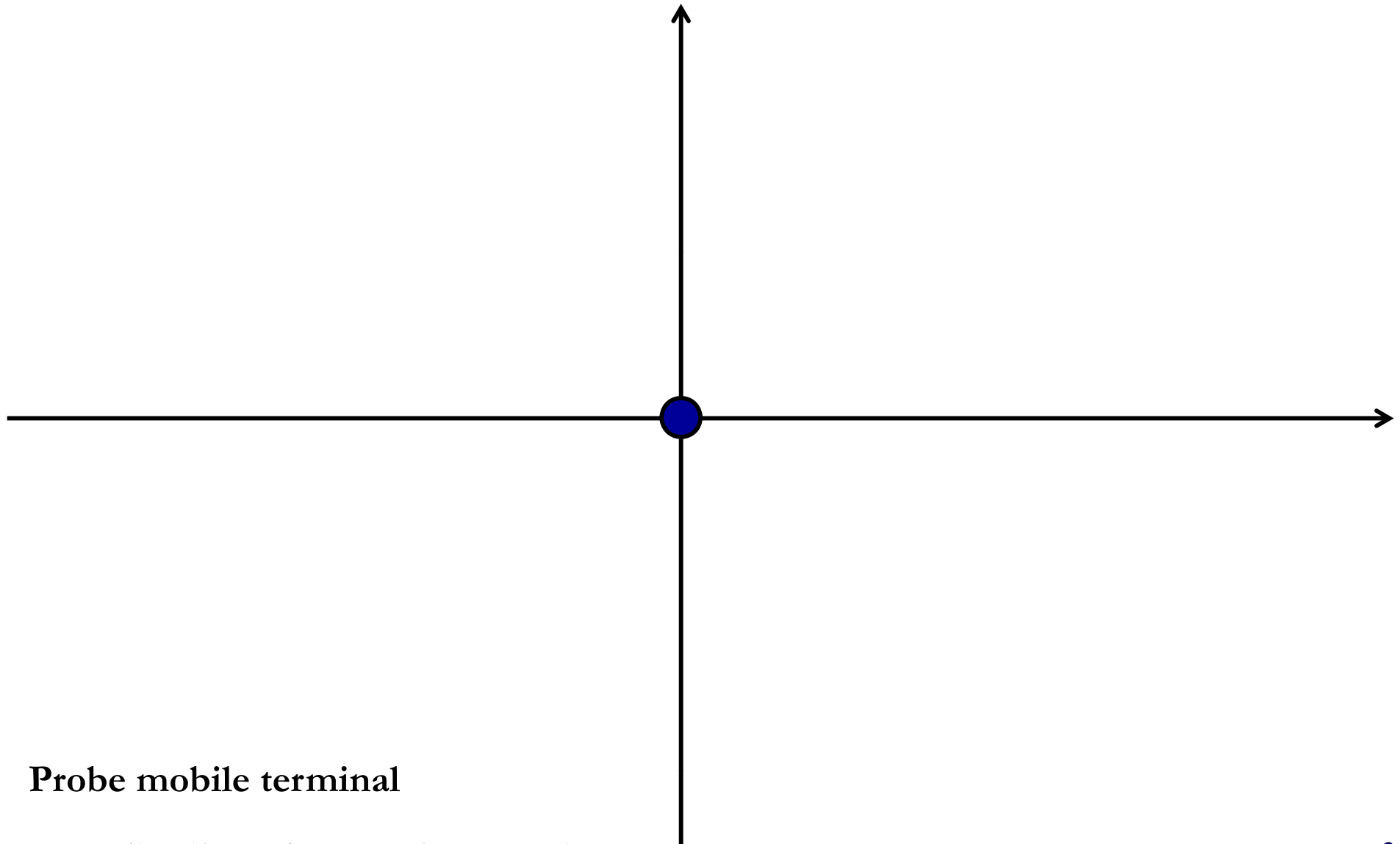
- **K-tier network with BS locations modeled as independent marked Poisson Point Processes (PPPs)**
- **PPP model is surprisingly good for 1-tier as well (macro BSs): lower bound to reality and trends still hold**
- **PPP makes even more sense for HCNs due to less regular BSs placements for lower tiers (femto, etc.)**

**Stochastic Geometry  
emerges as an effective tool for  
analysis, design, and optimization  
of HCNs**

# *SM in Heterogeneous Cellular Networks (6/22)*

---

## How It Works (Downlink – 1-tier)



Probe mobile terminal

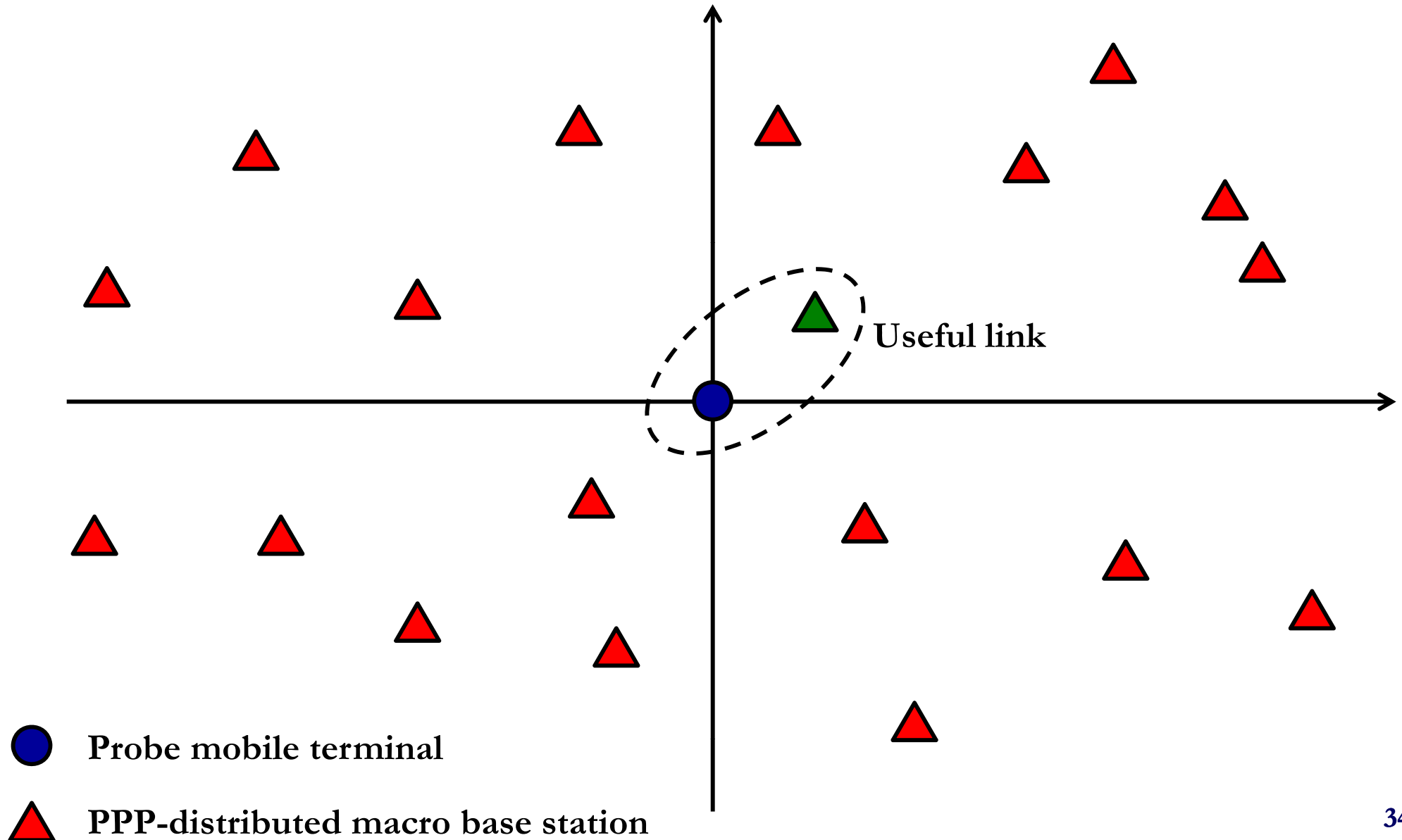


PPP-distributed macro base station



# *SM in Heterogeneous Cellular Networks (7/22)*

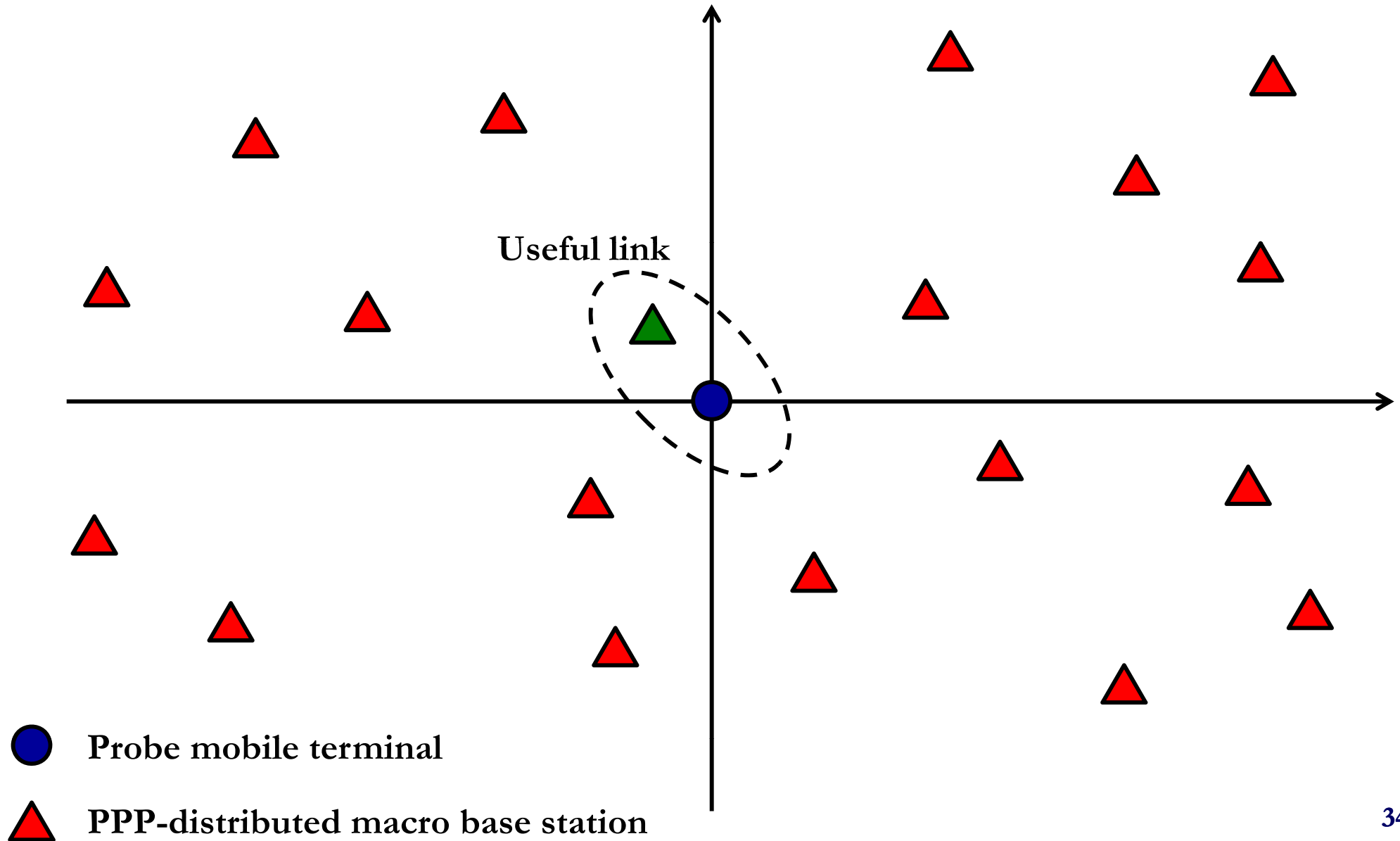
## How It Works (Downlink – 1-tier)





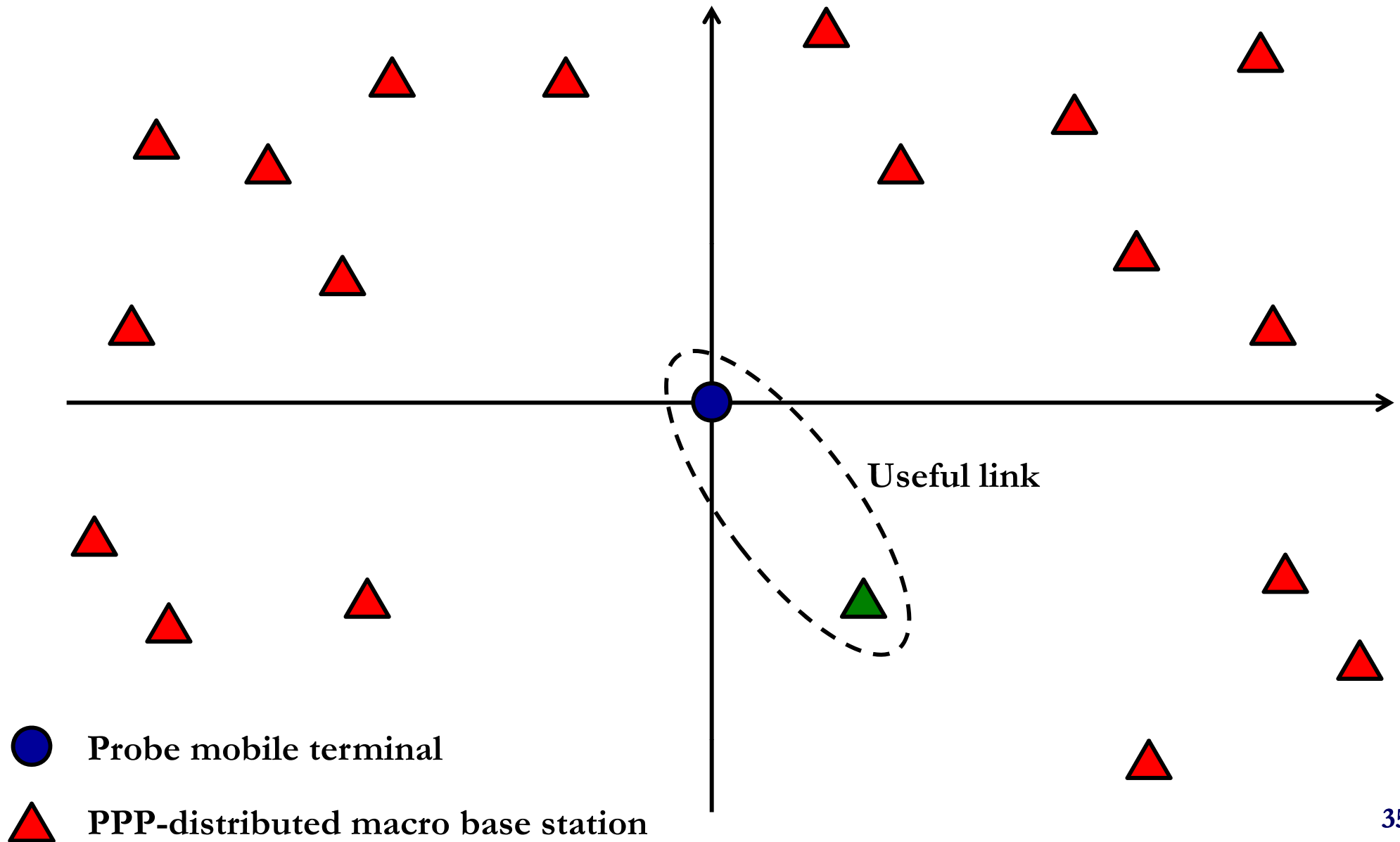
# *SM in Heterogeneous Cellular Networks (8/22)*

## How It Works (Downlink – 1-tier)



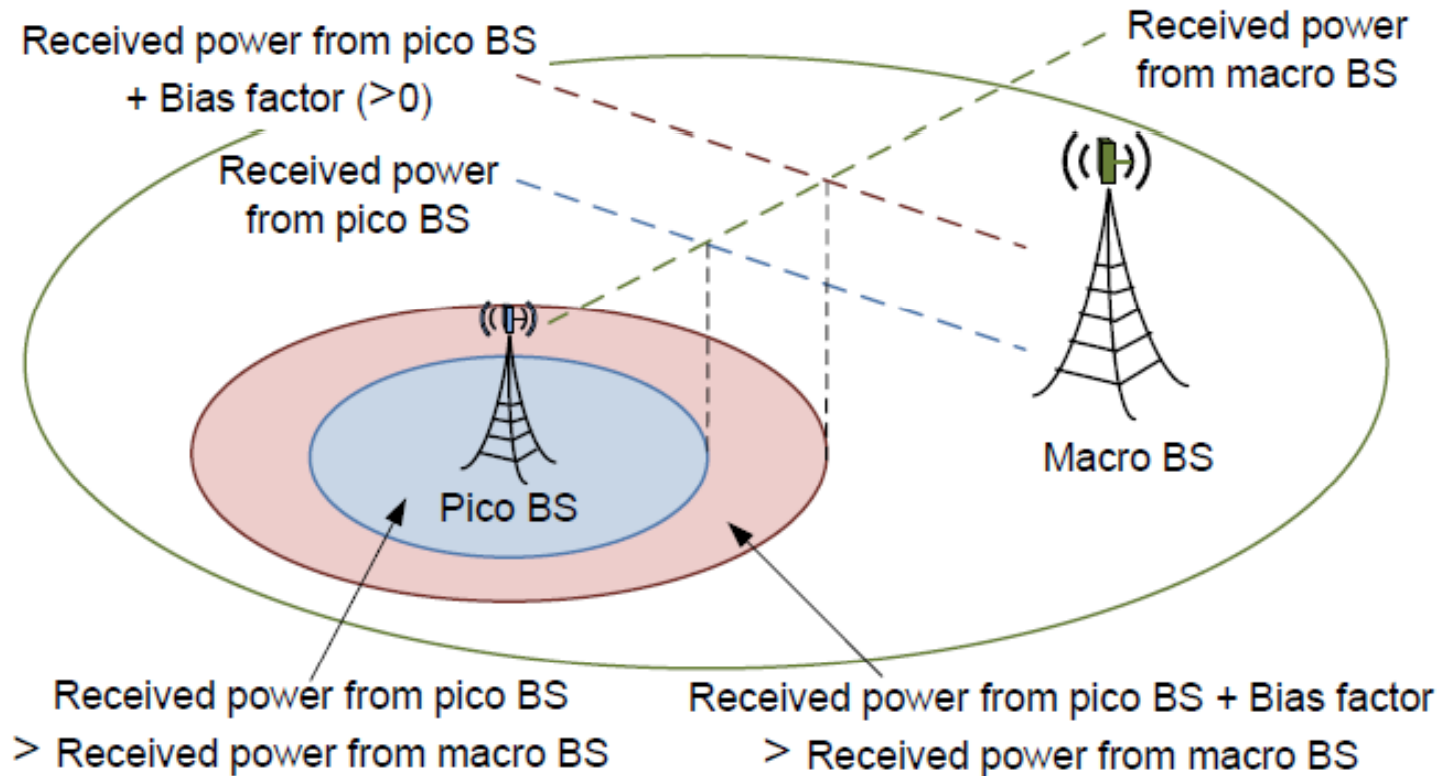
# *SM in Heterogeneous Cellular Networks (9/22)*

## How It Works (Downlink – 1-tier)



# *SM in Heterogeneous Cellular Networks (10/22)*

## How It Works (Downlink – 2-tier)



J. G. Andrews et al., “Heterogeneous Cellular Networks with Flexible Cell Association: A Comprehensive Downlink SINR Analysis”, *IEEE Trans. Wireless Commun.*, vol. 11, no. 10, pp. 3484–3495, Oct. 2012.

M. Di Renzo, A. Guidotti, and G. E. Corazza, “Average Rate of Downlink Heterogeneous Cellular Networks over Generalized Fading Channels – A Stochastic Geometry Approach”, *IEEE Trans. Commun.*, Vol. 61, No. 7, pp. 3050–3071, July 2013.

# *SM in Heterogeneous Cellular Networks (11/22)*

## Worldwide Base Station Locations Available via OpenCellID



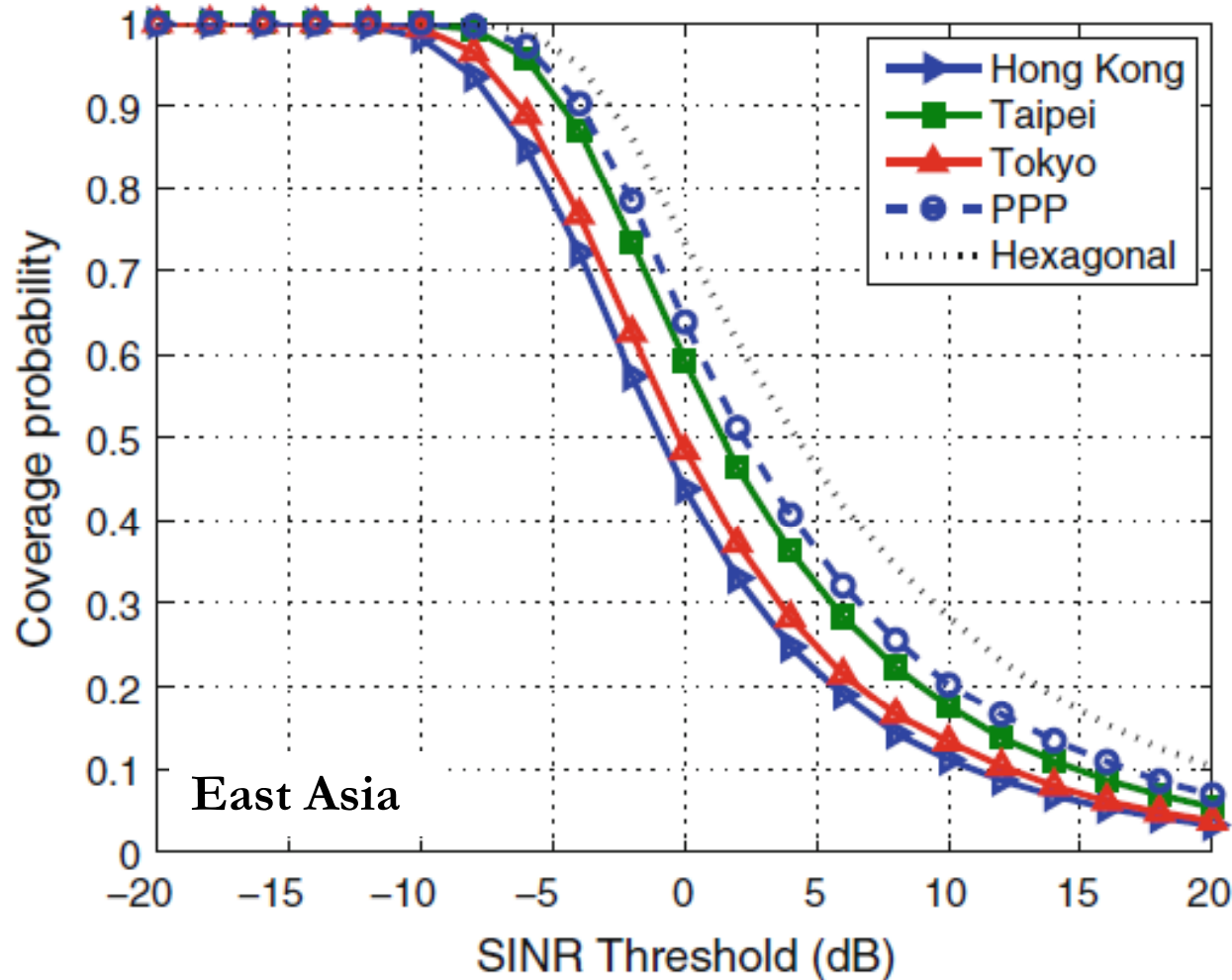
Base station distribution in Taipei City, Taiwan, shown on Google Map. Blue  $\Delta$ 's are the locations of base stations

C.-H. Lee, C.-Y. Shihet, and Y.-S. Chen, "Stochastic geometry based models for modeling cellular networks in urban areas", *Springer Wireless Netw.*, 10 pages, Oct. 2012.

Open source project OpenCellID: <http://www.opencellid.org/>

# *SM in Heterogeneous Cellular Networks (12/22)*

PPP better than (or same accuracy as) Hexagonal



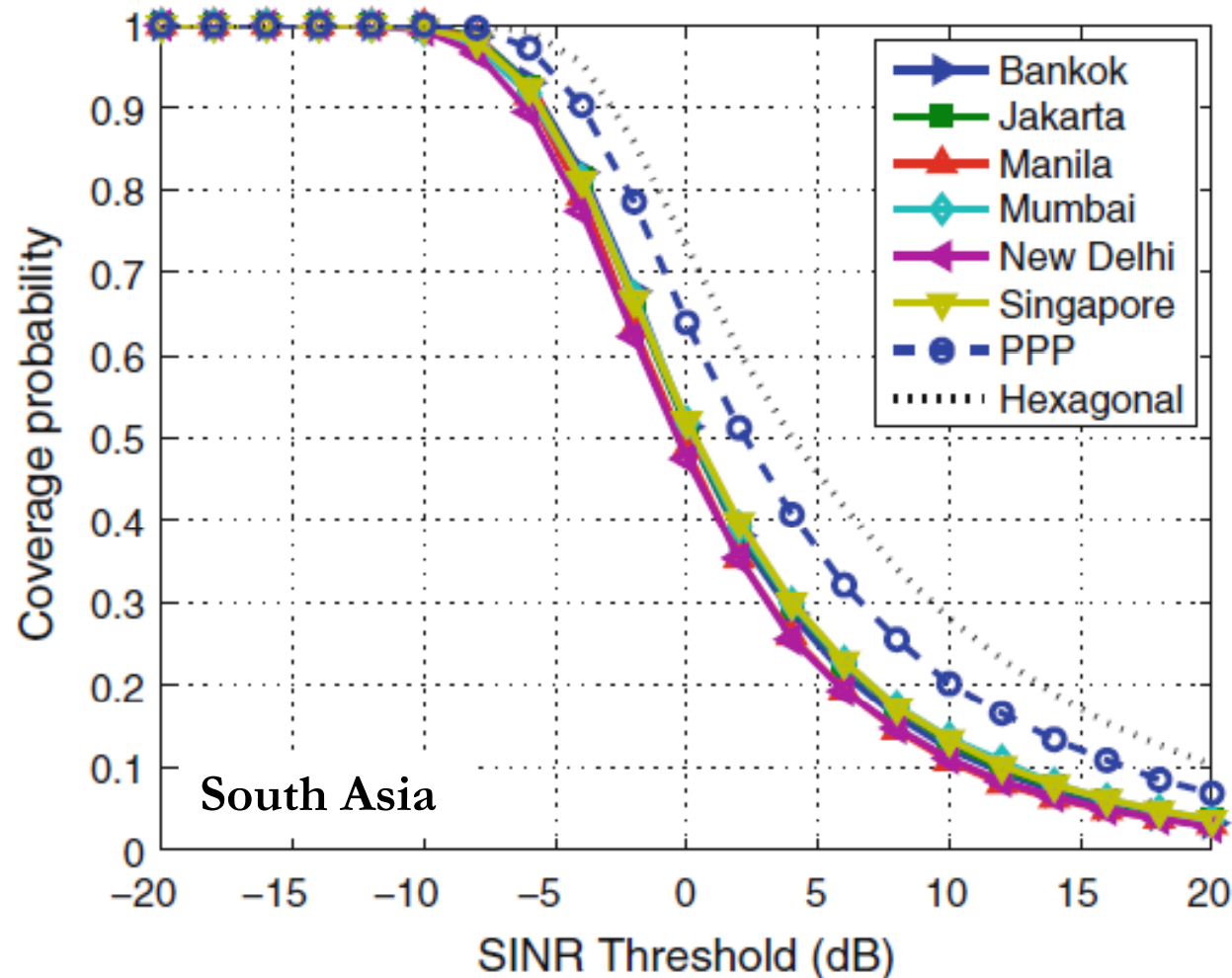
C.-H. Lee, C.-Y. Shihet, and Y.-S. Chen, “Stochastic geometry based models for modeling cellular networks in urban areas”, *Springer Wireless Netw.*, 10 pages, Oct. 2012.

Open source project OpenCellID: <http://www.opencellid.org/>



# *SM in Heterogeneous Cellular Networks (13/22)*

**PPP better than (or same accuracy as) Hexagonal**

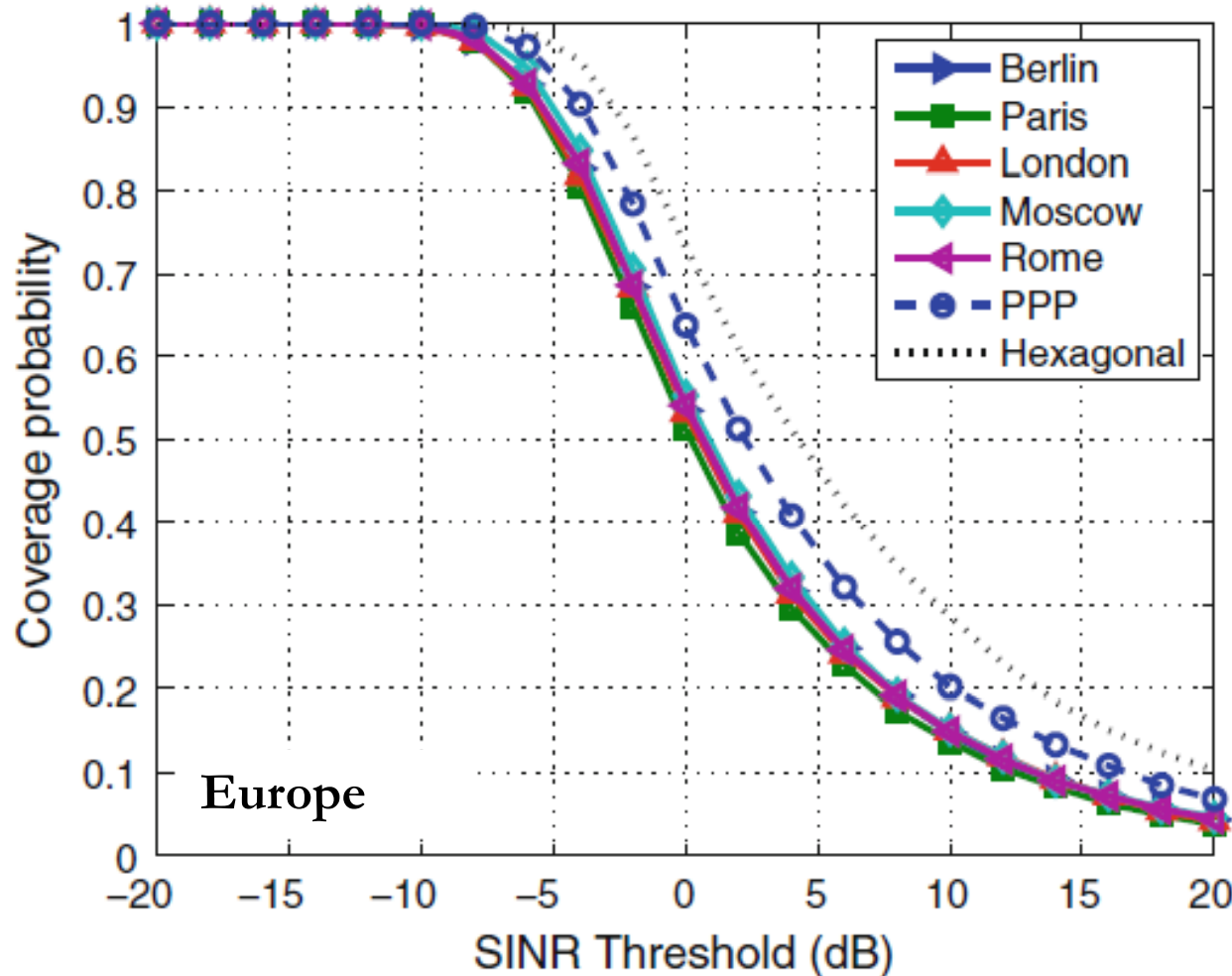


C.-H. Lee, C.-Y. Shihet, and Y.-S. Chen, “Stochastic geometry based models for modeling cellular networks in urban areas”, **Springer Wireless Netw.**, 10 pages, Oct. 2012.

Open source project OpenCellID: <http://www.opencellid.org/>

# *SM in Heterogeneous Cellular Networks (14/22)*

**PPP better than (or same accuracy as) Hexagonal**

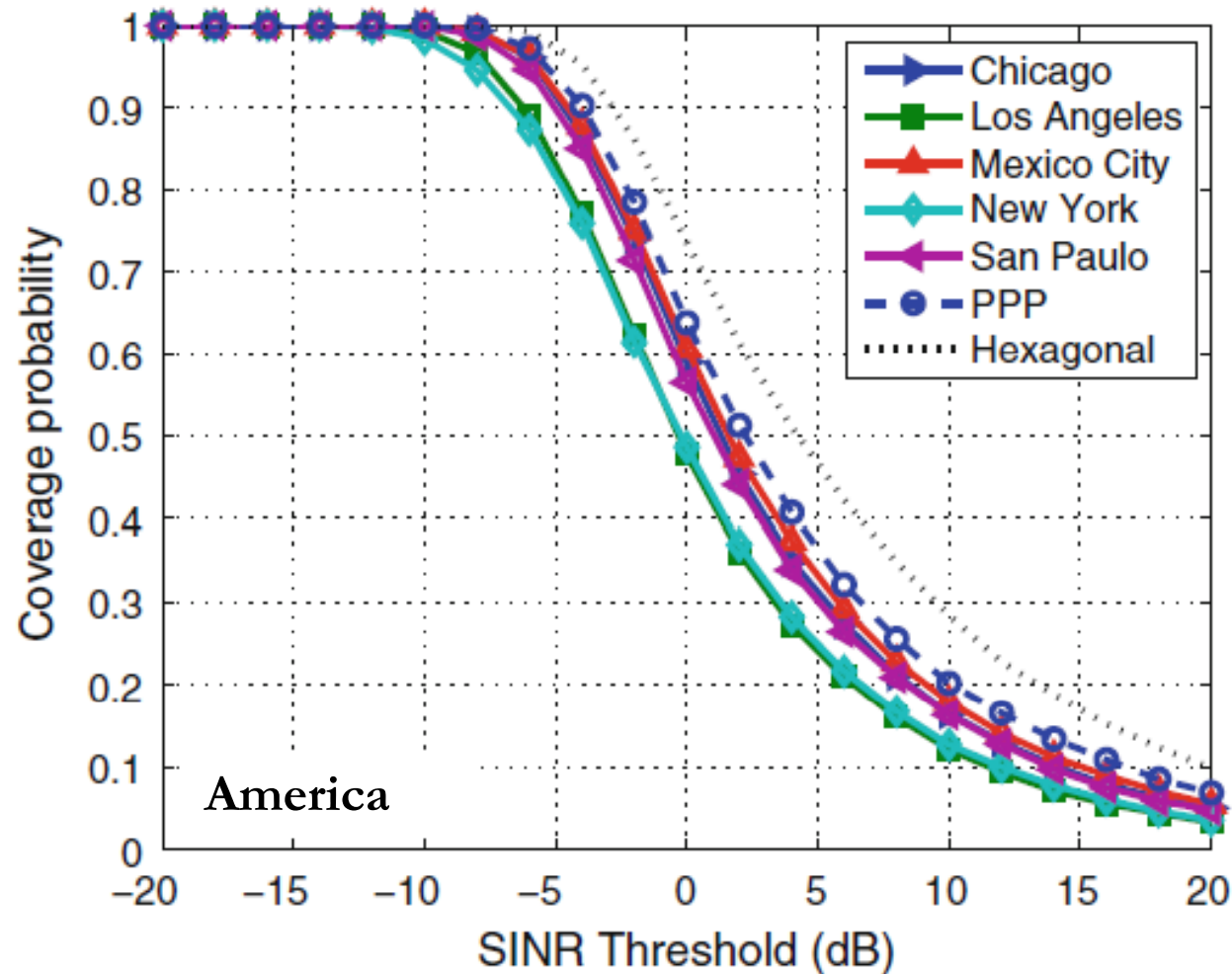


C.-H. Lee, C.-Y. Shihet, and Y.-S. Chen, “Stochastic geometry based models for modeling cellular networks in urban areas”, **Springer Wireless Netw.**, 10 pages, Oct. 2012.

Open source project OpenCellID: <http://www.opencellid.org/>

# *SM in Heterogeneous Cellular Networks (15/22)*

PPP better than (or same accuracy as) Hexagonal



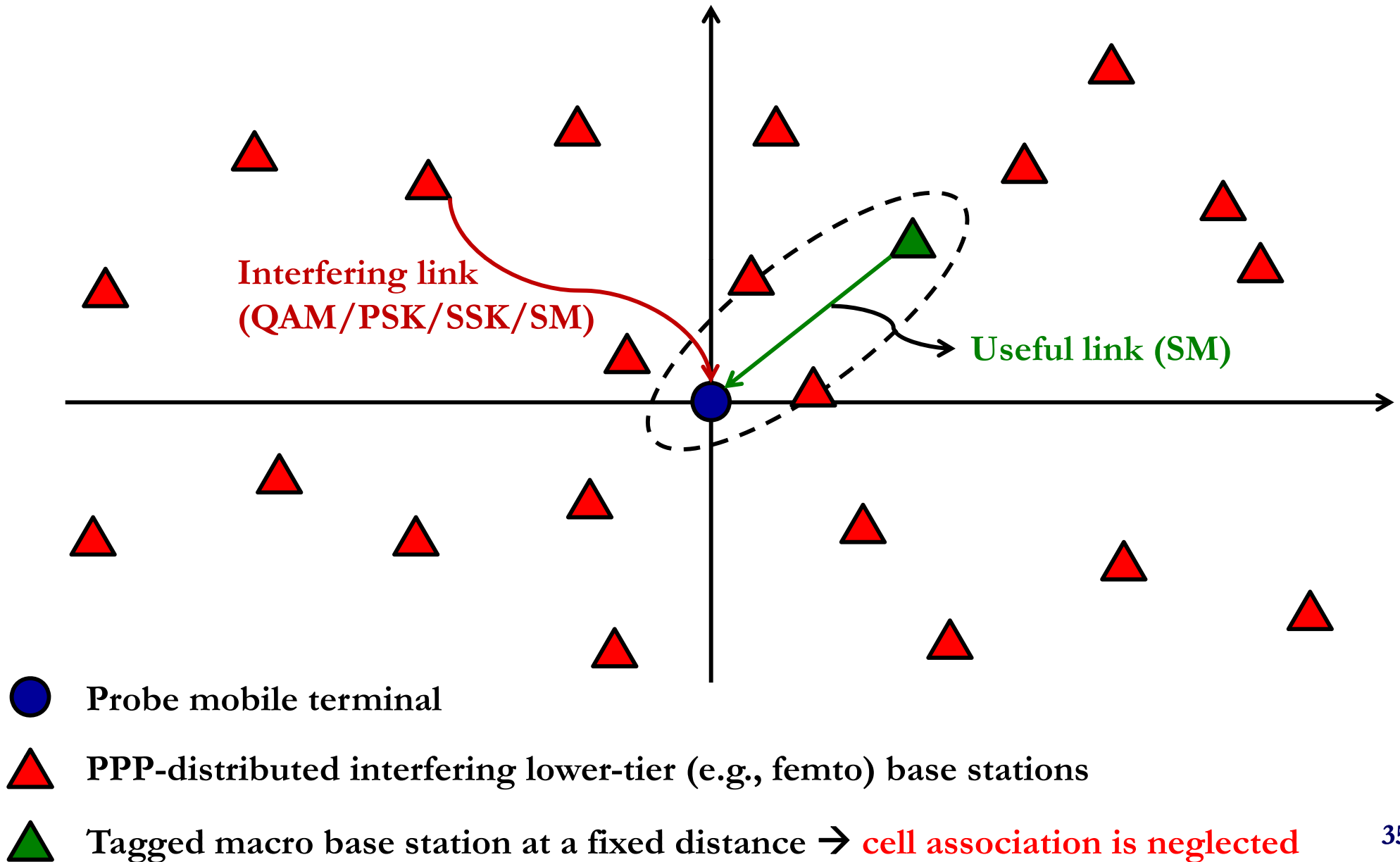
C.-H. Lee, C.-Y. Shihet, and Y.-S. Chen, “Stochastic geometry based models for modeling cellular networks in urban areas”, *Springer Wireless Netw.*, 10 pages, Oct. 2012.

Open source project OpenCellID: <http://www.opencellid.org/>



# *SM in Heterogeneous Cellular Networks (16/22)*

## Preliminary Reference Scenario



# SM in Heterogeneous Cellular Networks (17/22)

## A Key Result from Stochastic Geometry and PPP Theory

$$\underbrace{\Delta}_{\text{Decision Metric}} \propto \underbrace{|\Delta_0|^2 U}_{\text{Useful Signal}} + \underbrace{2 \operatorname{Re}\{\Delta_0^* \bar{N}\}}_{\text{AWGN}} + \underbrace{2 \operatorname{Re}\{\Delta_0^* \bar{I}_{\text{AGG}}\}}_{\text{Aggregate Interference}}$$



$$\bar{I}_{\text{AGG}} = \sum_{i \in \Phi_{\text{PPP}}} \left( \frac{\bar{Z}_i}{d_i^{b_I}} \right) \Rightarrow \bar{I}_{\text{AGG}} = B_I^{1/2} \bar{G}_I \sim S\alpha S(\alpha_I = 2/b_I, \gamma_I)$$



$$\begin{cases} B_I \sim S(1/b_I, 1, \cos^{b_I}(\pi/2b_I)) \\ M_{B_I}(s) = E_{B_I} \{ \exp(-sB_I) \} = \exp(-s^{1/b_I}) \\ \bar{G}_I \sim CN(0, 4\gamma_I^{b_I}) \end{cases}$$

# *SM in Heterogeneous Cellular Networks (18/22)*

## Equivalent AWGN Channel

$$\underbrace{\Delta}_{\text{Decision Metric}} \propto \underbrace{|\Delta_0|^2 U}_{\text{Useful Signal}} + \underbrace{2 \operatorname{Re} \{ \Delta_0^* \bar{N} \}}_{\text{AWGN}} + \underbrace{2 \operatorname{Re} \{ \Delta_0^* (B_I^{1/2} \bar{G}_I) \}}_{\text{Aggregate Interference}}$$

Equivalent AWGN  
conditioning upon  $B_I$



**STEP 1:** The frameworks developed without interference can be applied by conditioning upon  $B_I$

**STEP 2:** The conditioning can be removed either numerically or analytically (preferred)

# *SM in Heterogeneous Cellular Networks (19/22)*

## **The Bottom Line**

□ Closed-form results in **STEP 1** can be obtained from:

- M. Di Renzo and H. Haas, “Bit Error Probability of Spatial Modulation (SM-) MIMO over Generalized Fading Channels”, **IEEE Trans. Veh. Technol.**, Vol. 61, No. 3, pp. 1124-1144, Mar. 2012.

$$\text{ABEP}(B_I) \leq \text{ABEP}_{\text{signal}}(B_I) + \text{ABEP}_{\text{spatial}}(B_I) + \text{ABEP}_{\text{joint}}(B_I)$$

□ The average over  $B_I$  in **STEP 2** can be computed using (e.g., for Nakagami-m fading):

- M. Di Renzo, C. Merola, A. Guidotti, F. Santucci, G. E. Corazza, “Error Performance of Multi-Antenna Receivers in a Poisson Field of Interferers – A Stochastic Geometry Approach”, **IEEE Trans. Commun.**, Vol. 61, No. 5, pp. 2025–2047, May 2013.

$$\begin{aligned} \mathcal{J}(\eta_p^2; \psi_p; \theta_p) &= \mathcal{J}(\mathbf{v}_p) \\ &= \int_0^{\mu_p} \mathbb{E}_{\mathcal{B}_I} \left\{ \left( 1 + \frac{\chi_{\mathcal{B}_I}^{(p)}}{\sin^2(\omega)} \right)^{-m_0 N_r} \right\} d\omega \end{aligned}$$

# *SM in Heterogeneous Cellular Networks (20/22)*

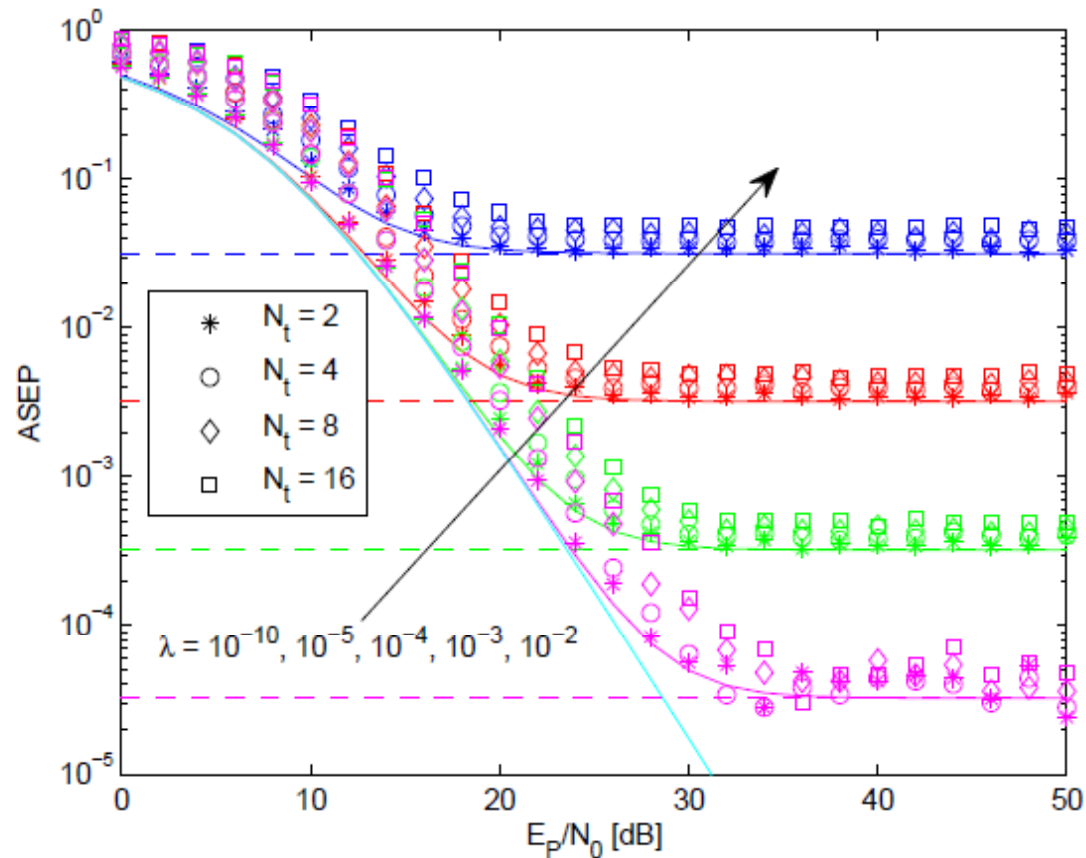


Fig. 1. ASEP as a function of  $E_P/N_0$ ,  $N_t$  and  $\lambda$ . Setup:  $\Omega_P = \Omega_I = 1$ ;  $b = 4$ ;  $X_0^2 = 1$ ;  $N_r = 2$ ;  $E_P = E_I$ ; PSK modulation with  $M = 8$ . The solid lines show the framework in (21), (23) and (26), the dashed lines the asymptotic framework in (29), and the markers the Monte Carlo simulations.

# *SM in Heterogeneous Cellular Networks (21/22)*

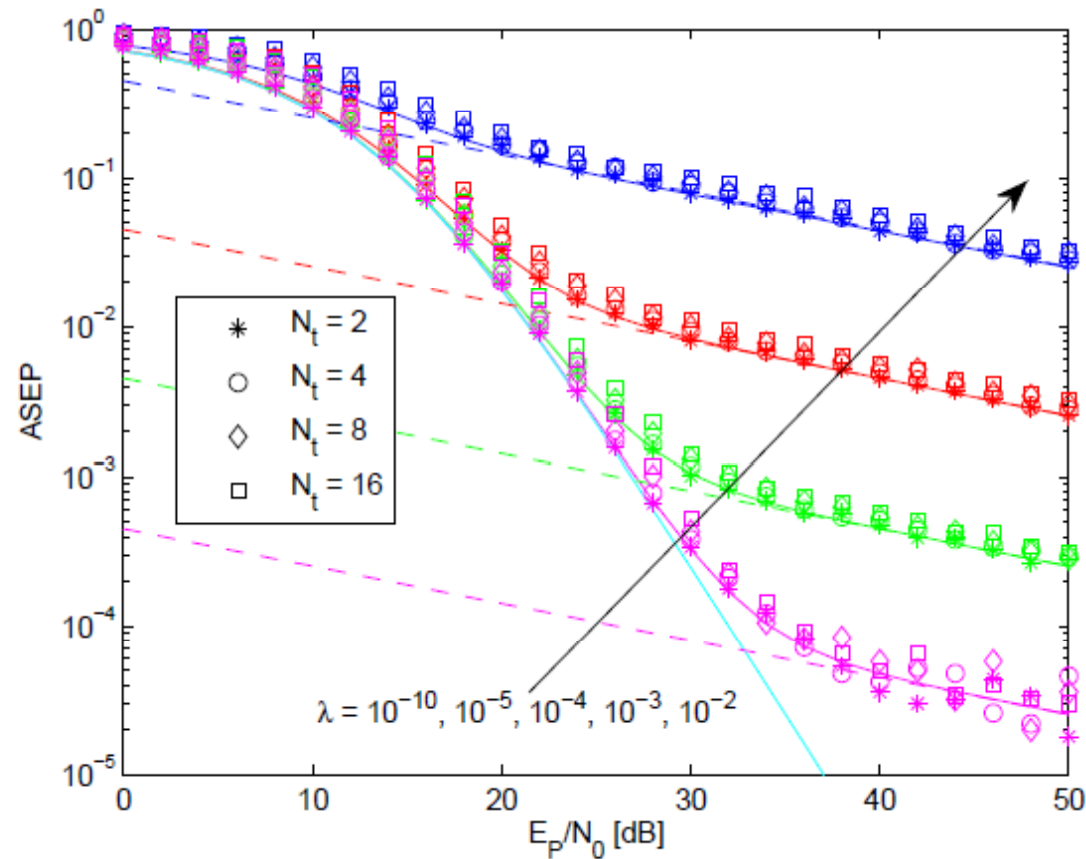


Fig. 2. ASEP as a function of  $E_P/N_0$ ,  $N_t$  and  $\lambda$ . Setup:  $\Omega_P = \Omega_I = 1$ ;  $b = 4$ ;  $X_0^2 = 1$ ;  $N_r = 2$ ;  $E_I/N_0 = 40\text{dB}$ ; PSK modulation with  $M = 16$ . The solid lines show the framework in (21), (23) and (26), the dashed lines the asymptotic framework in (23), and the markers the Monte Carlo simulations.

# *SM in Heterogeneous Cellular Networks (22/22)*

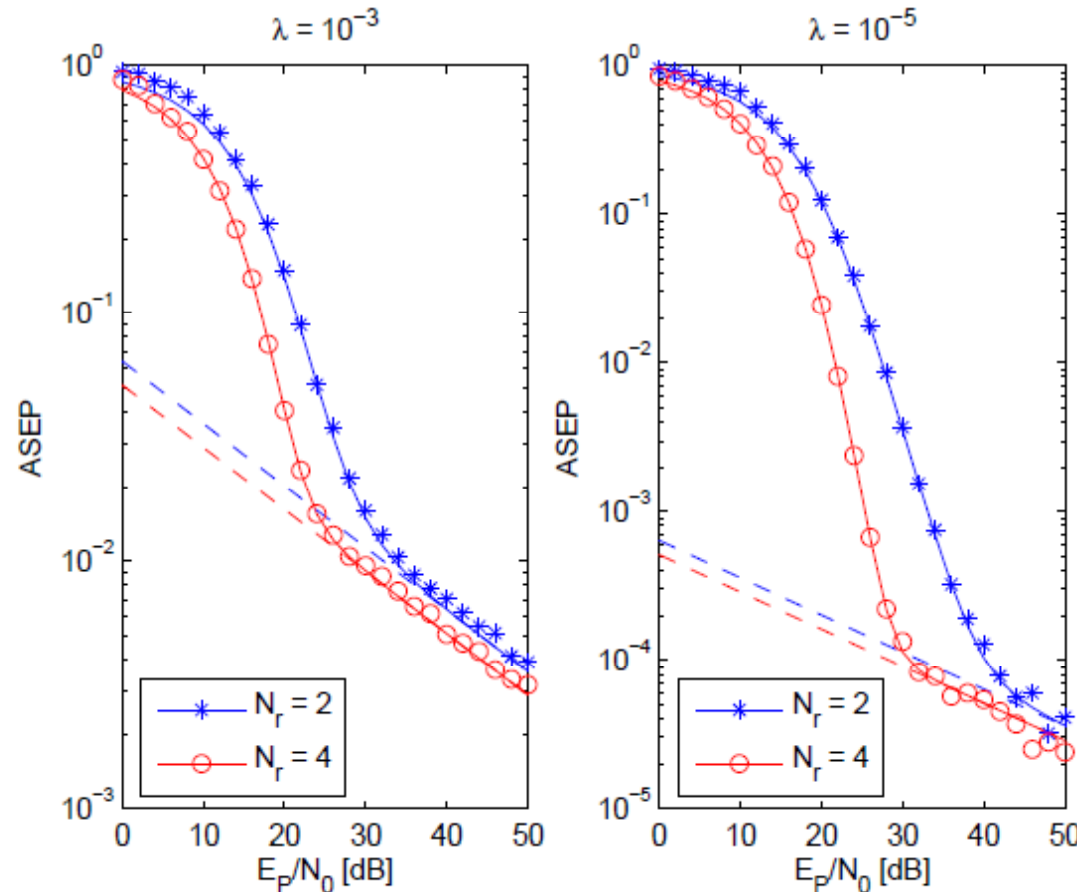


Fig. 3. ASEP as a function of  $E_P/N_0$ ,  $N_r$  and  $\lambda$ . Setup:  $\Omega_P = \Omega_I = 1$ ;  $b = 4$ ;  $X_0^2 = 1$ ;  $N_t = 8$ ;  $E_I/N_0 = 40\text{dB}$ ; PSK modulation with  $M = 32$ . The solid lines show the framework in (21), (23) and (26), the dashed lines the asymptotic framework in (30), and the markers the Monte Carlo simulations.

# *Outline*

---

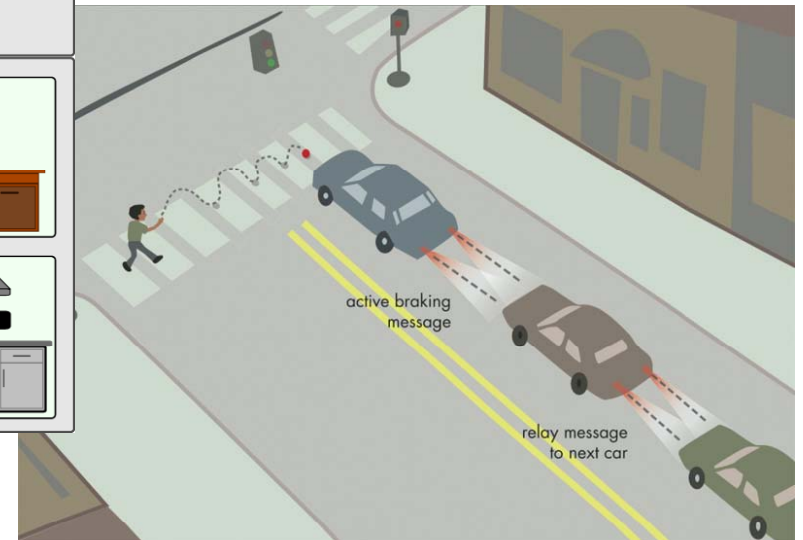
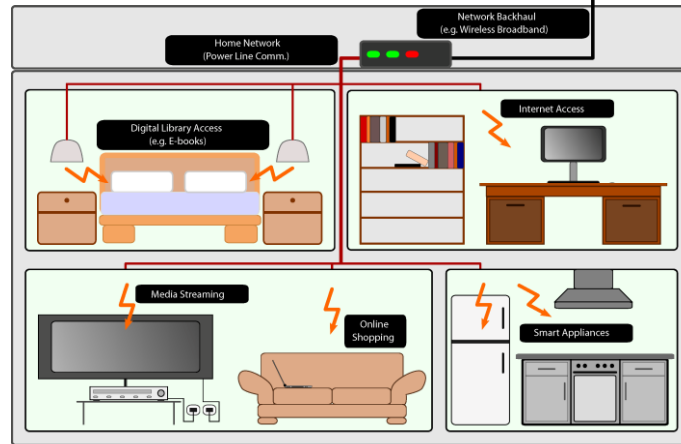
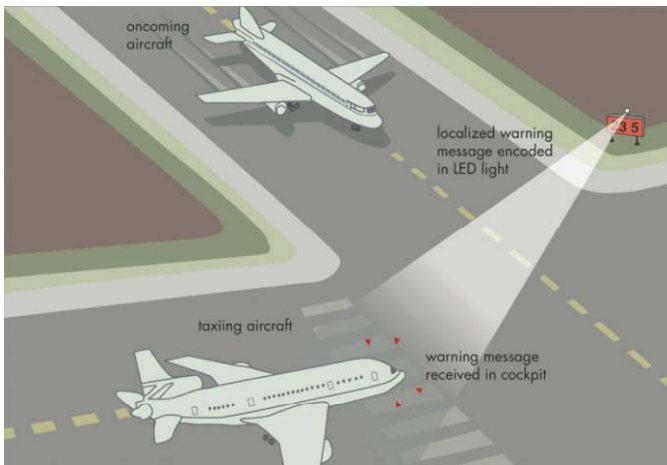
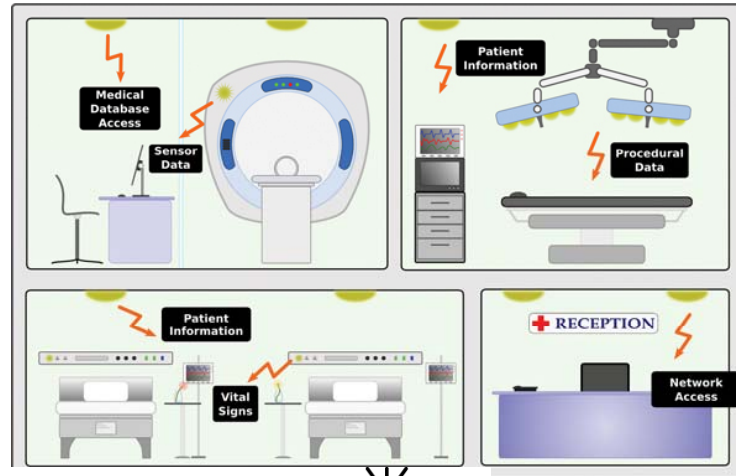
1. Introduction and Motivation behind SM-MIMO
2. History of SM Research and Research Groups Working on SM
3. Transmitter Design – Encoding
4. Receiver Design – Demodulation
5. Error Performance (Numerical Results and Main Trends)
6. Achievable Capacity
7. Channel State Information at the Transmitter
8. Imperfect Channel State Information at the Receiver
9. Multiple Access Interference
10. Energy Efficiency
11. Transmit-Diversity for SM
12. Spatially-Modulated Space-Time-Coded MIMO
13. Relay-Aided SM
14. SM in Heterogeneous Cellular Networks
15. **SM for Visible Light Communications**
16. Experimental Evaluation of SM
17. The Road Ahead – Open Research Challenges/Opportunities
18. Implementation Challenges of SM-MIMO



# *SM for Visible Light Communications (1/13)*

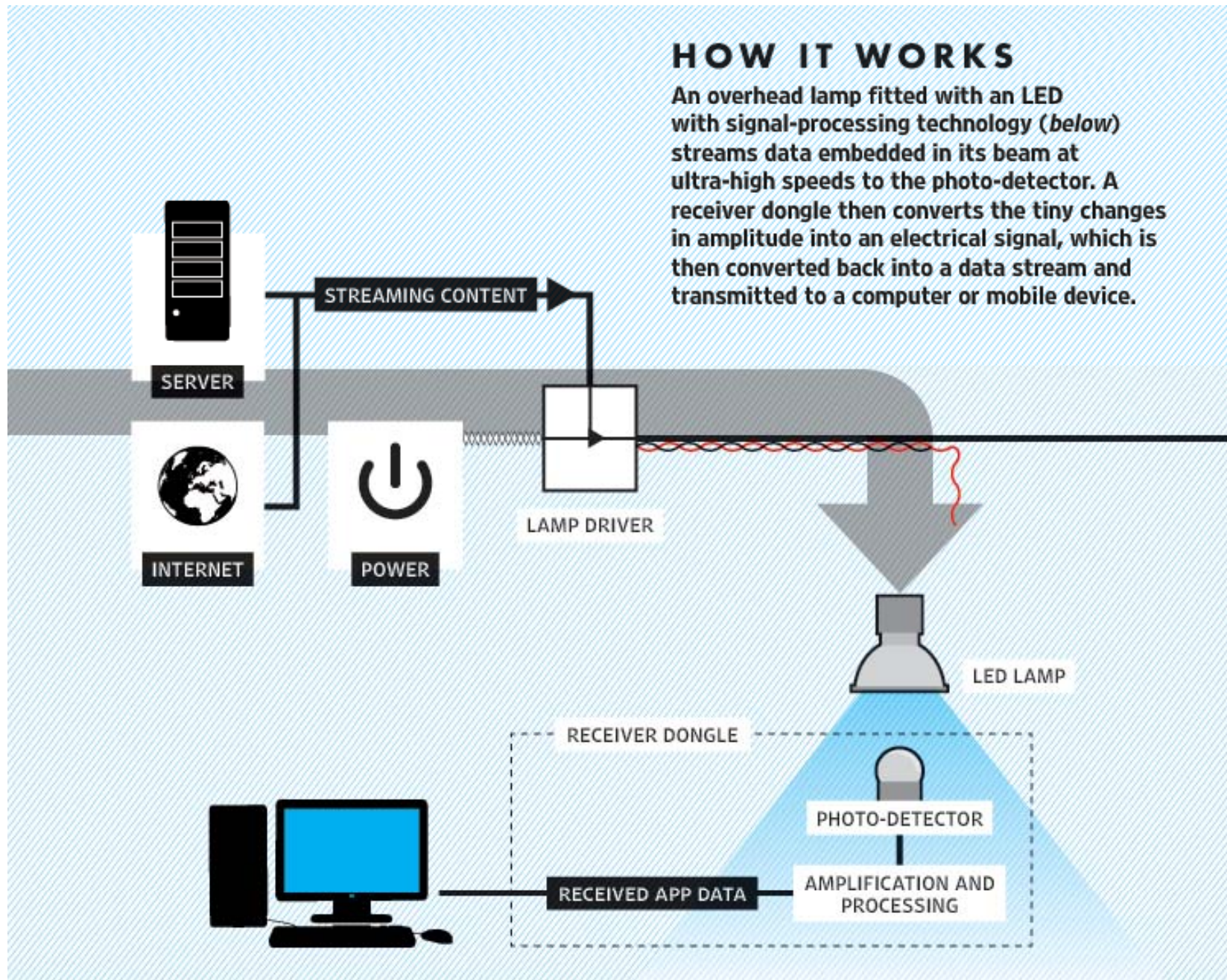


# SM for Visible Light Communications (2/13)



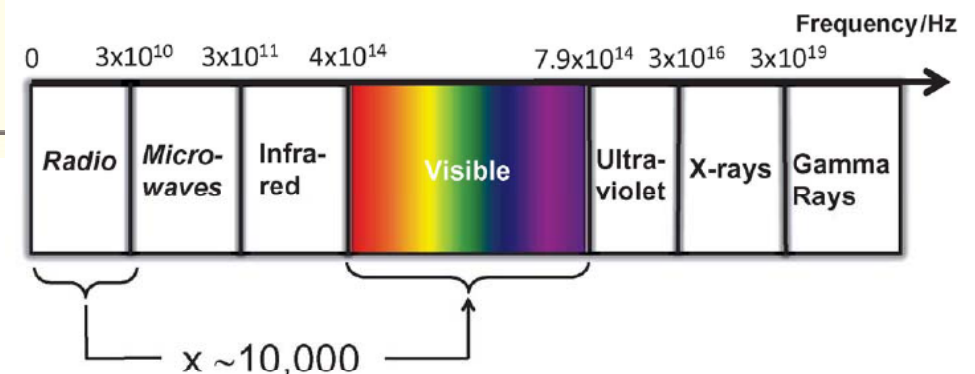


# SM for Visible Light Communications (3/13)

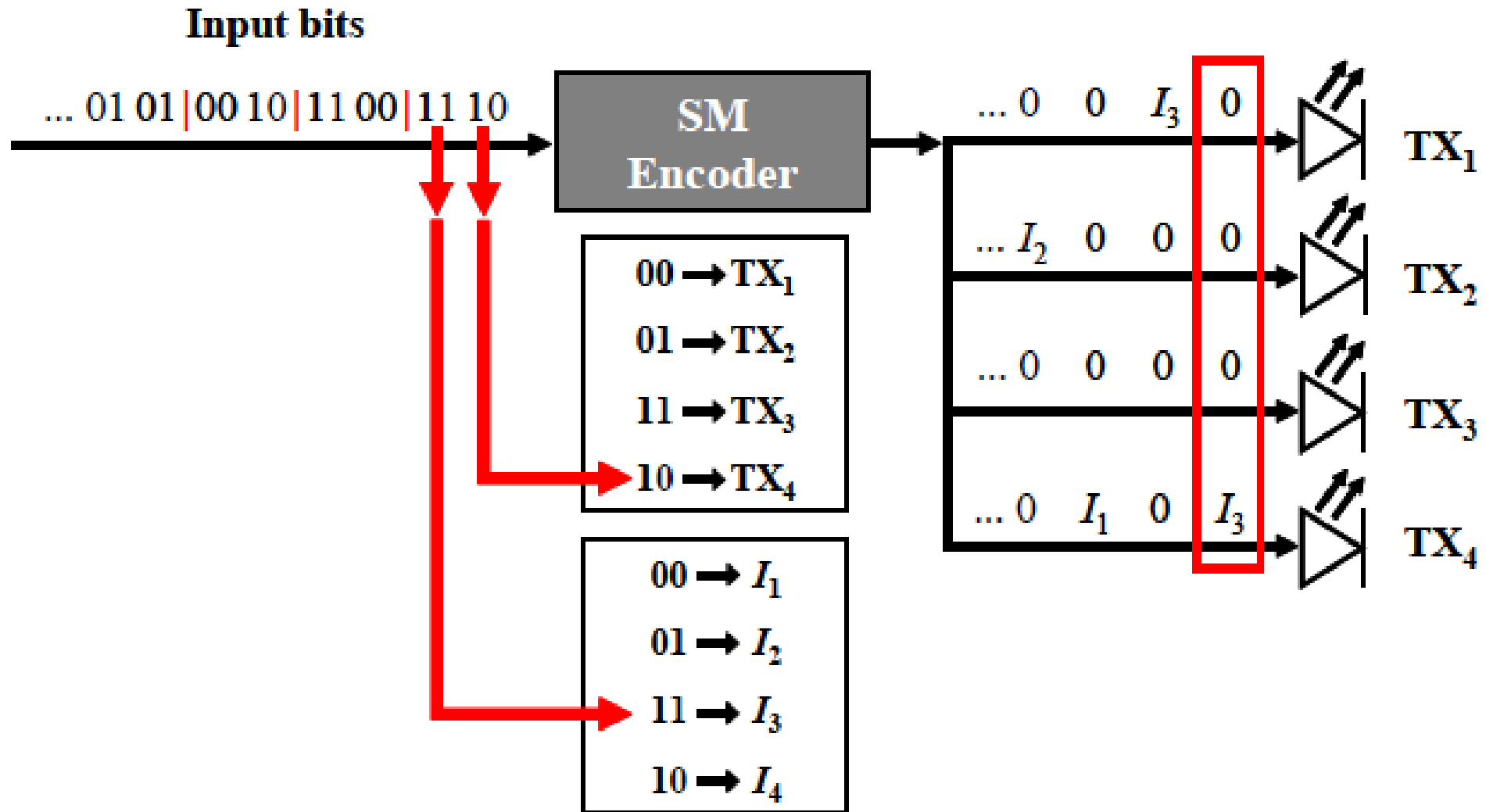


# *SM for Visible Light Communications (4/13)*

Attribute	RF wireless	Optical Wireless
Link margin	Excellent, due to coherent detection and noise processes	Poor due to incoherent detection at receiver and noise mechanisms
Signal confinement	Typical propagation loss through walls: 1dB/cm	Confined by internal spaces
Regulation	Subject to licensing and regulation	Subject to eye safety regulation, currently no licensing
Availability of spectrum	Limited and expensive	1000s of THz of spectrum available
Ability to control radiation patterns	Challenging owing to constraints on antenna size in most appliances	High degree of control using lenses and diffractive elements
Propagation	Scattering/reflection and diffraction create broad area coverage	Ray propagation allows very tight confinement of radiation
Interface with fixed network	Need optoelectronic interface of directed RF to connect with fibre network	Possibility of using light from fiber network to create transparent interface



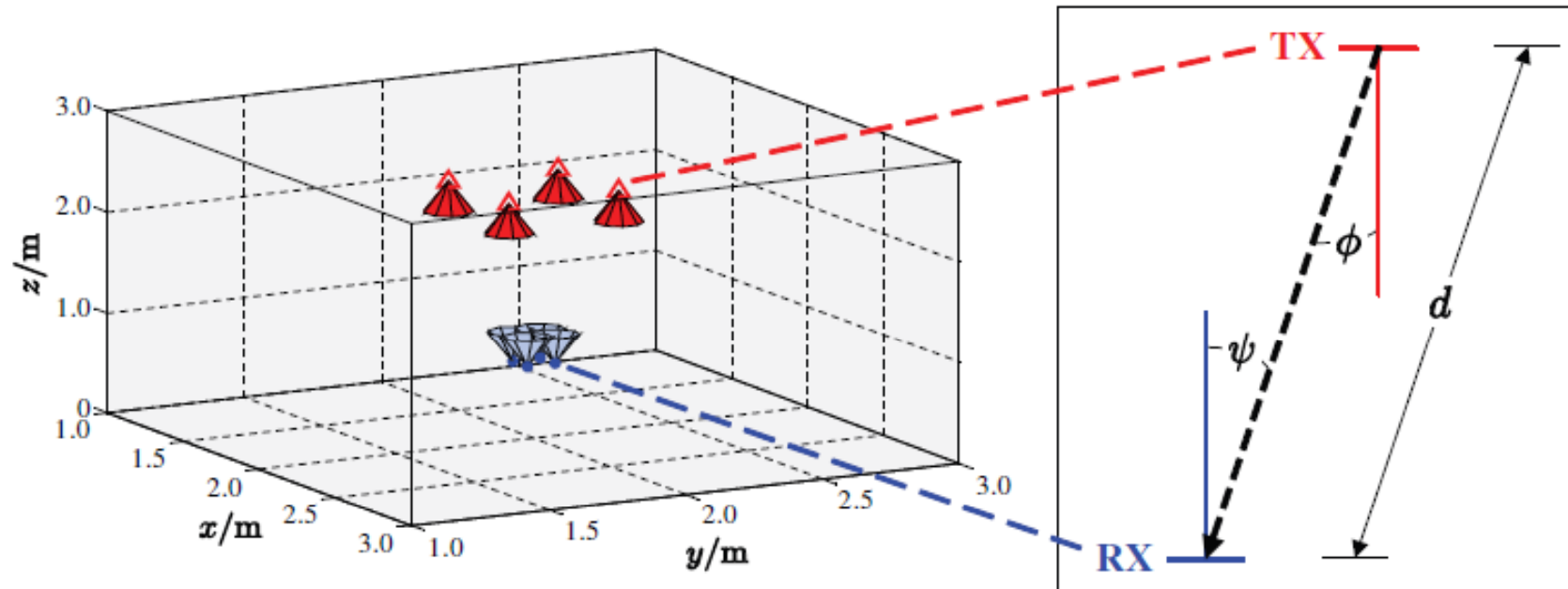
# SM for Visible Light Communications (5/13)





# *SM for Visible Light Communications (6/13)*

## Optical Wireless Setup and Channel



$$h = \begin{cases} \frac{(k+1) A}{2 \pi d^2} \cos^k \phi \cos \psi & 0 \leq \psi \leq \Psi_{\frac{1}{2}} \\ 0 & \psi > \Psi_{\frac{1}{2}} \end{cases}$$
$$k = \frac{-\ln(2)}{\ln(\cos \Phi_{\frac{1}{2}})}$$

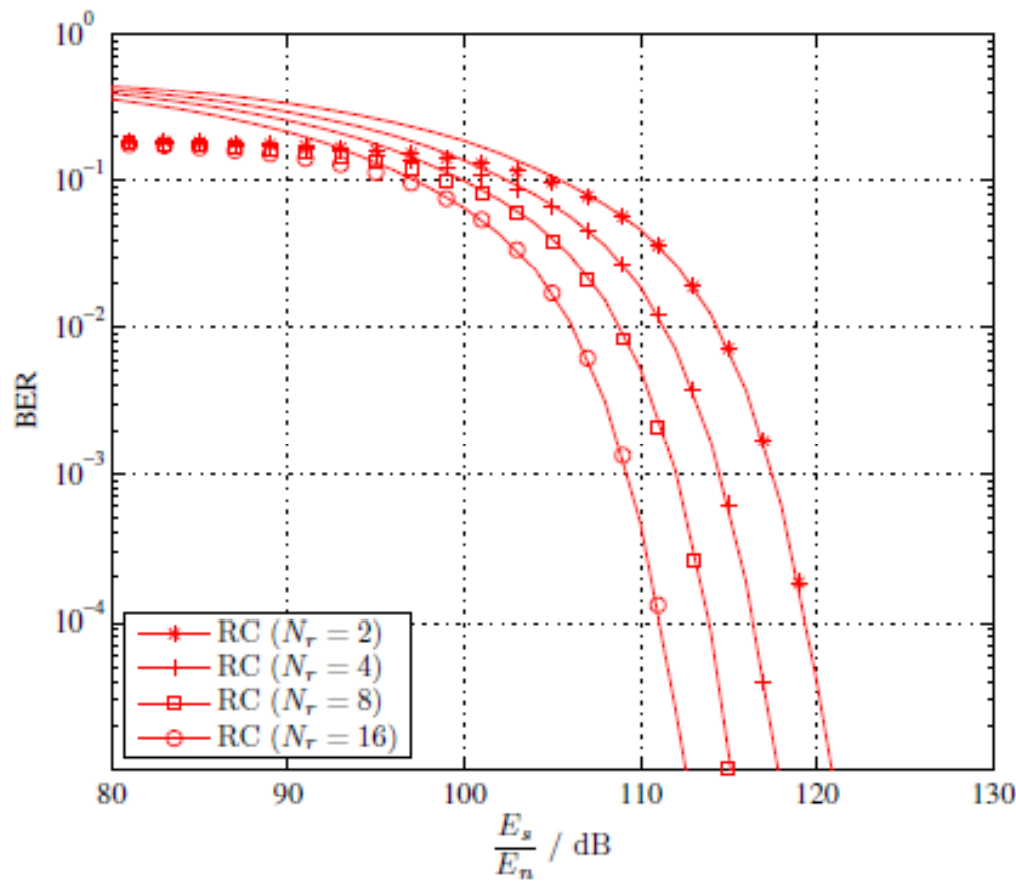
$\Phi_{1/2} = 15^\circ$ : Tx semi-angle

$\Psi_{1/2} = 15^\circ$ : Rx semi-angle

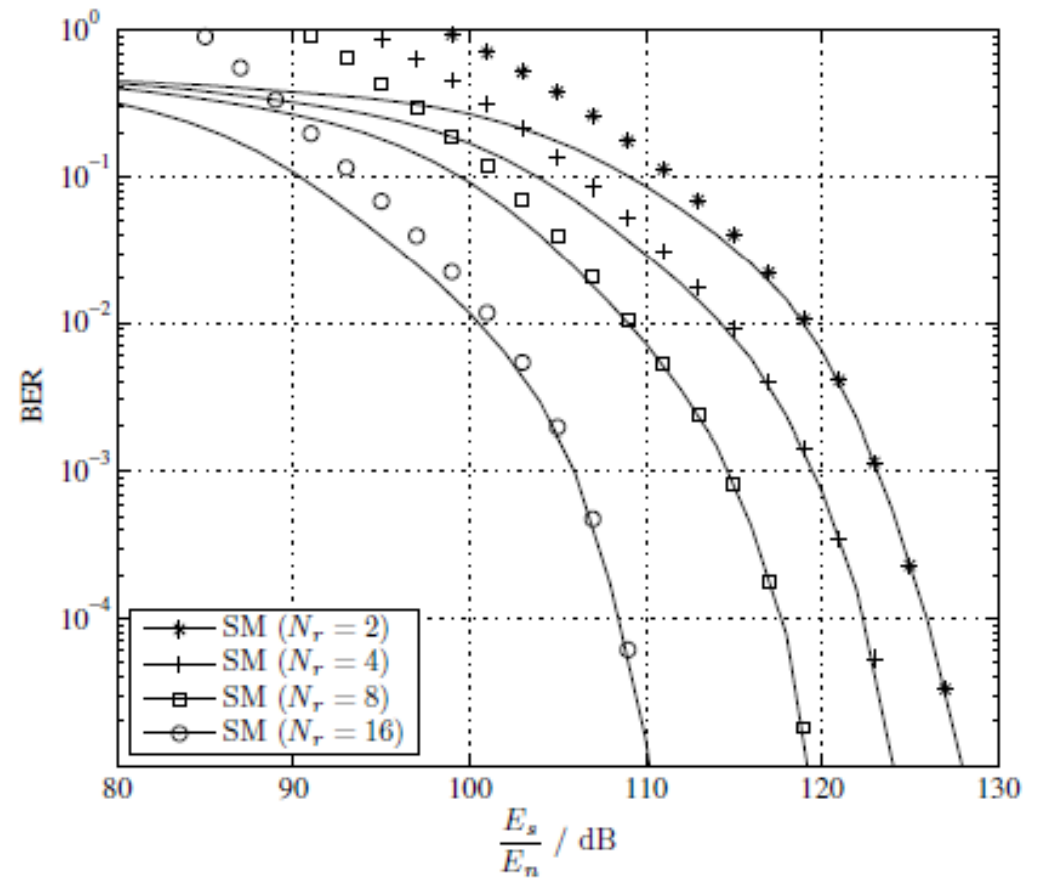
$A = 1\text{cm}^2$ : receiver detector area

# *SM for Visible Light Communications (7/13)*

$N_t = 8$ , Rate = 5 bpcu



(a) 32-PAM RC



(b) SM with  $M = 4$

## *SM for Visible Light Communications (8/13)*

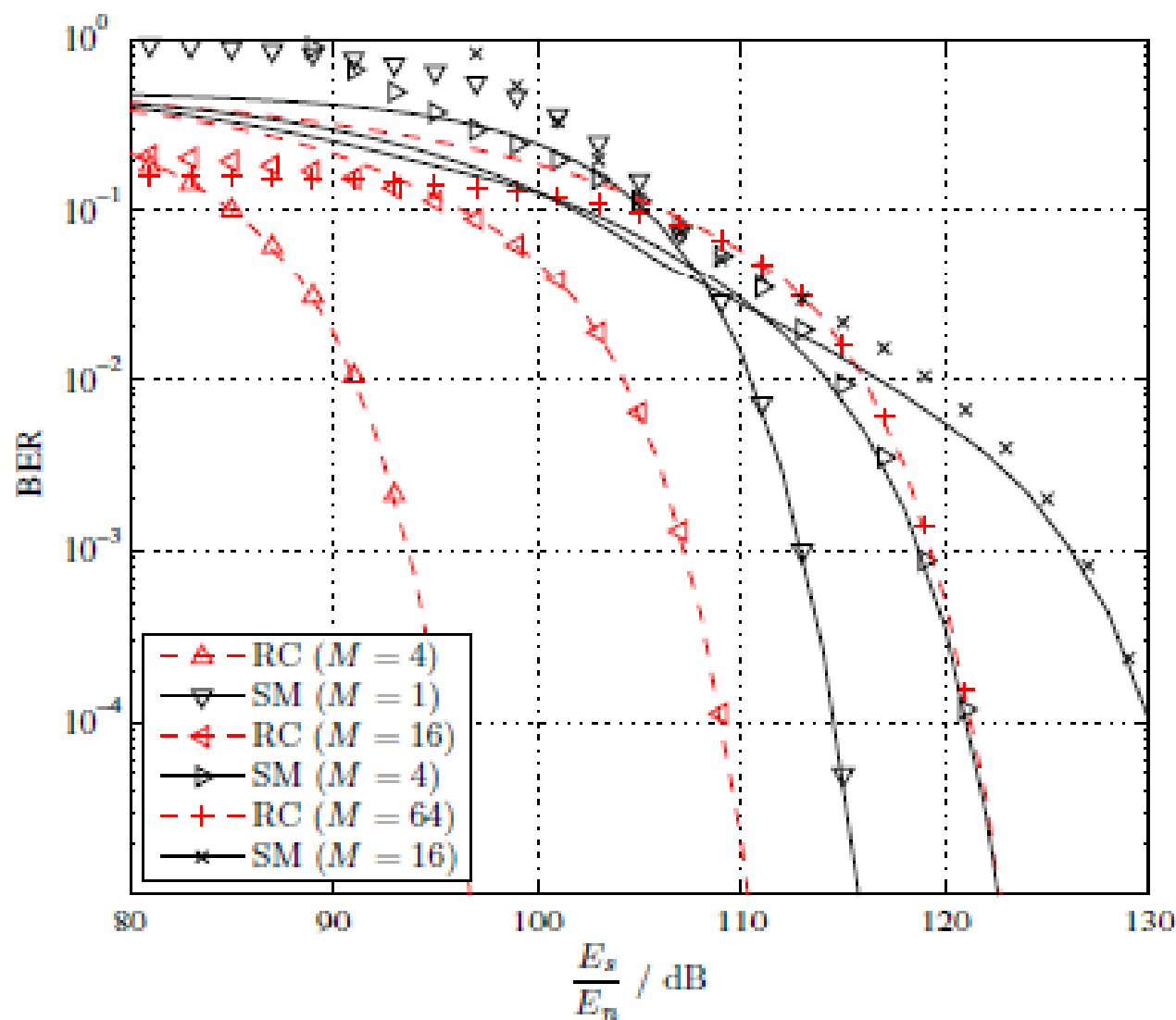


Fig. 4. Comparison of SM and RC for spectral efficiency of 2, 4 and 6 bit/s/Hz in  $4 \times 4$  setup scenario (lines show simulation results and markers numerical ABEP results).



## *SM for Visible Light Communications (9/13)*

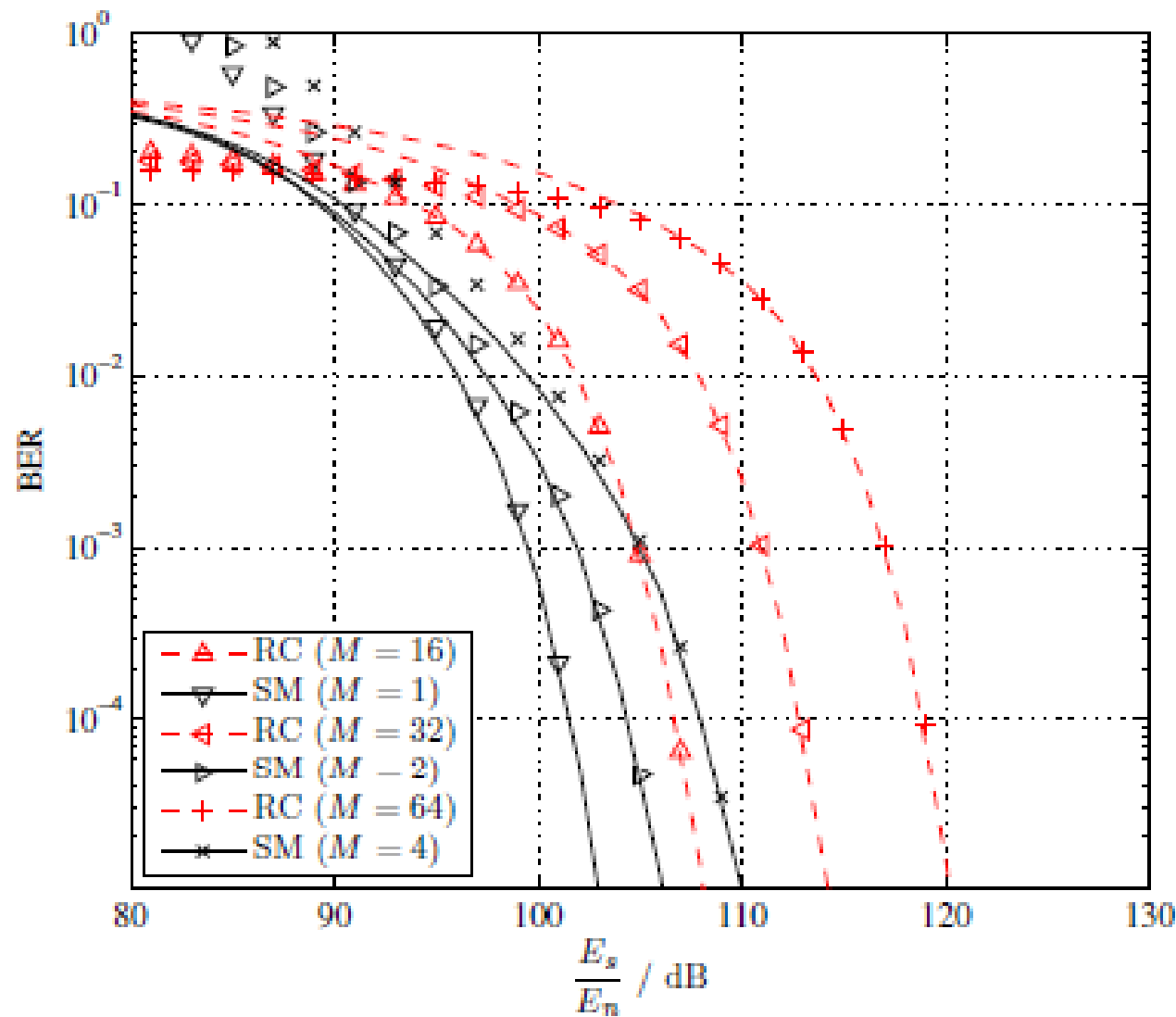
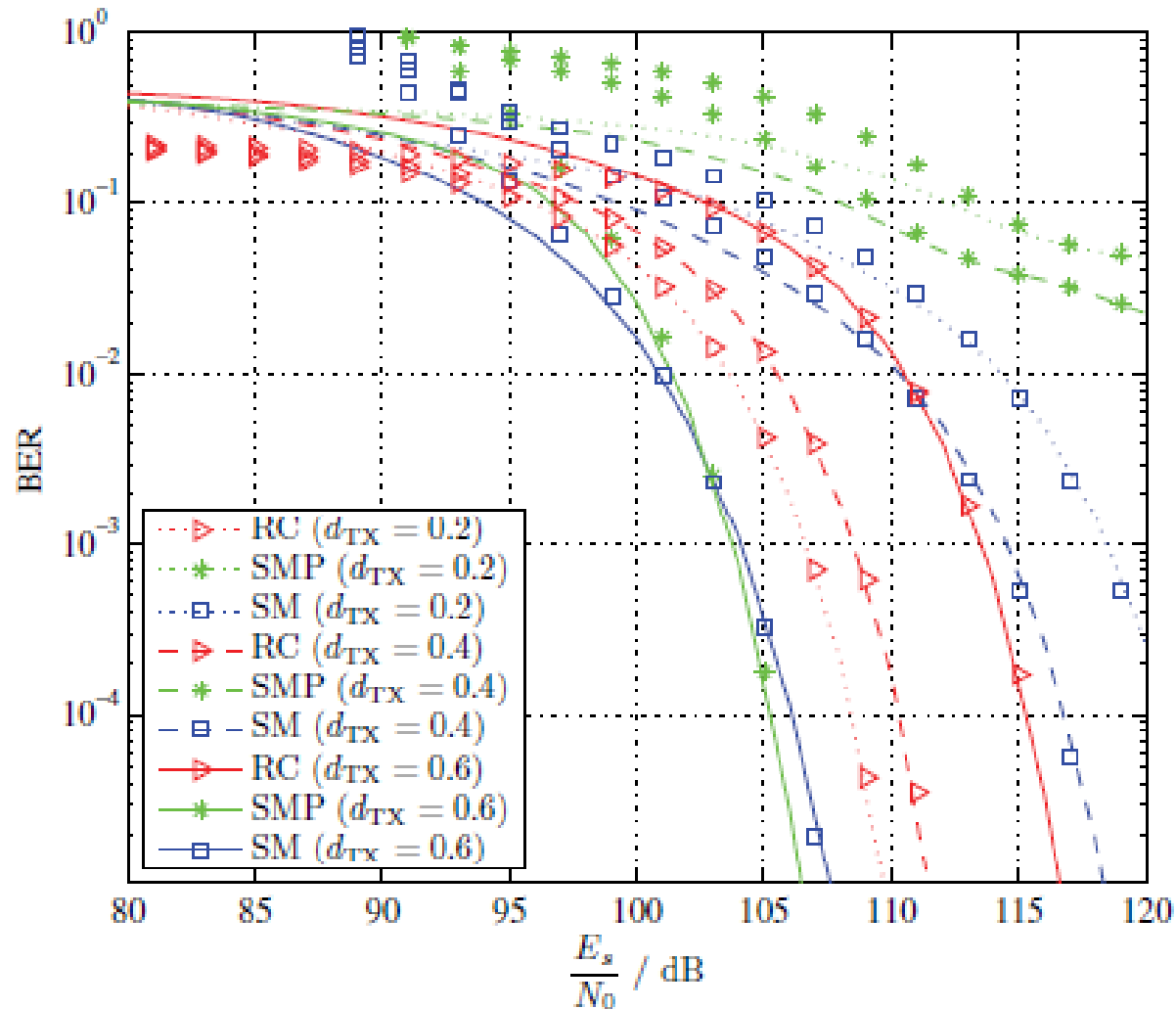


Fig. 6. Comparison of SM and RC for spectral efficiency of 4, 5 and 6 bit/s/Hz in 16x16 setup scenario (lines show simulation results and markers numerical ABEP results).

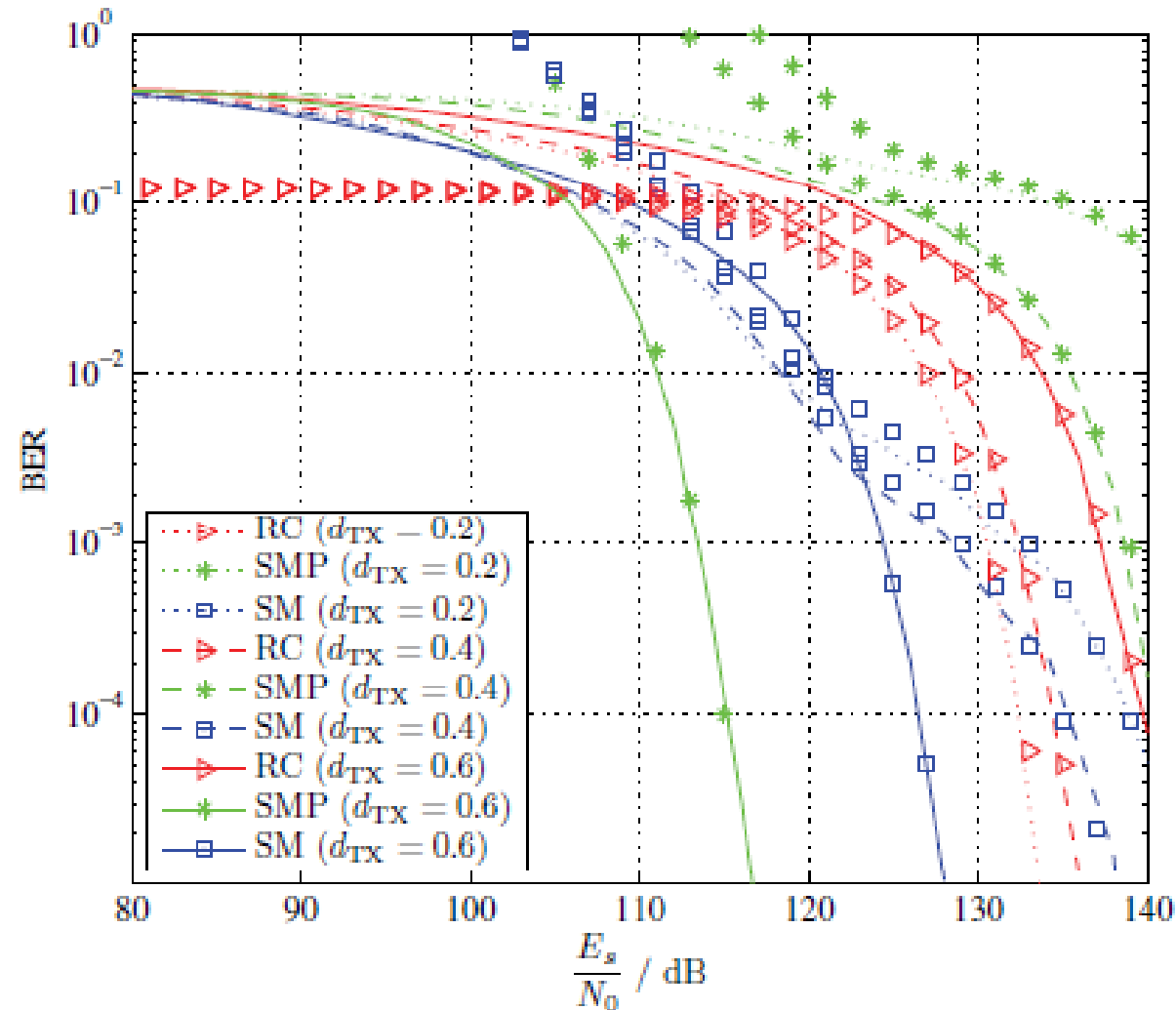
# *SM for Visible Light Communications (10/13)*

$$N_t = N_r = 4, \text{ Rate} = 4 \text{ bpcu}$$



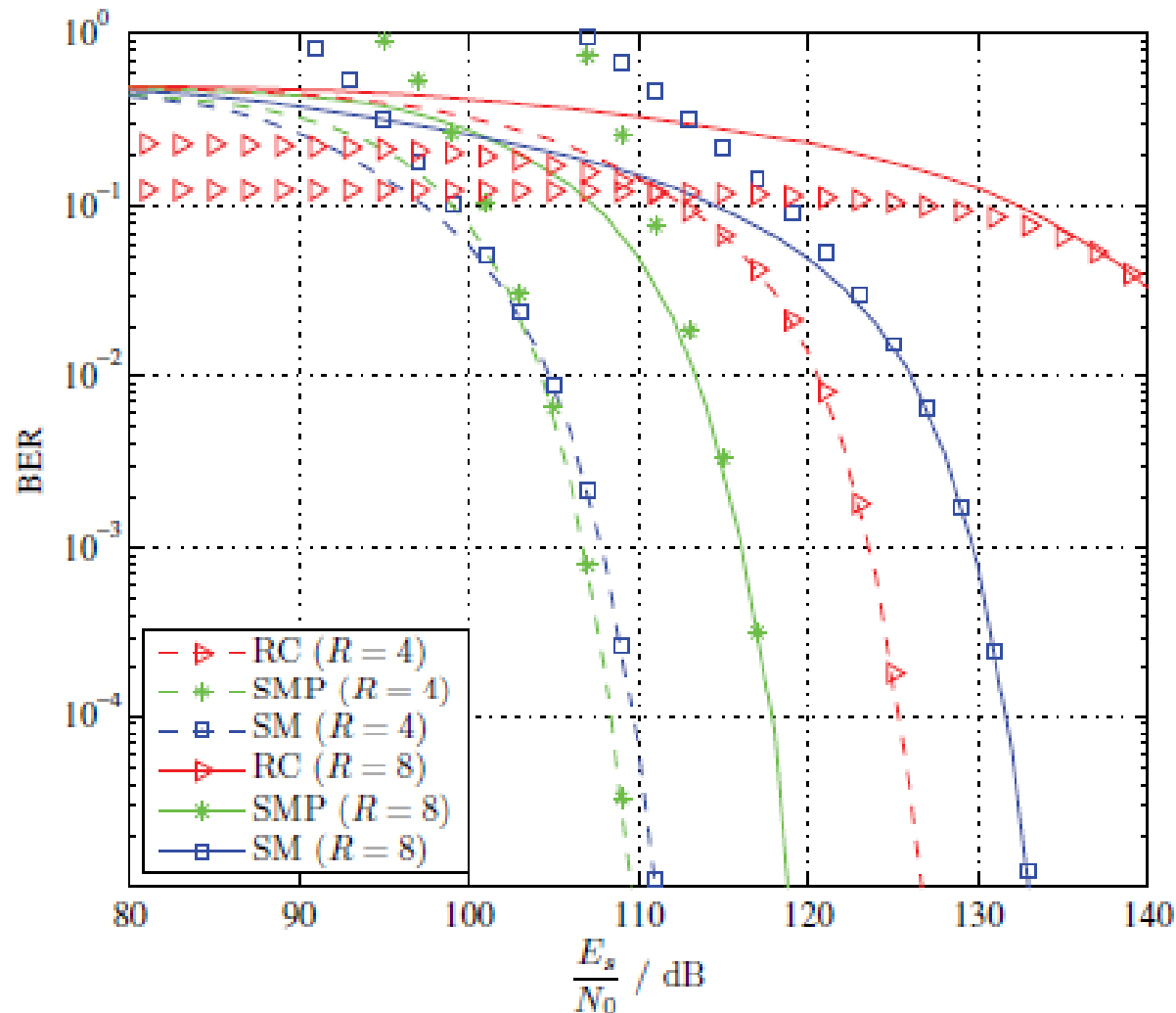
# *SM for Visible Light Communications (11/13)*

$$N_t = N_r = 4, \text{ Rate} = 8 \text{ bpcu}$$

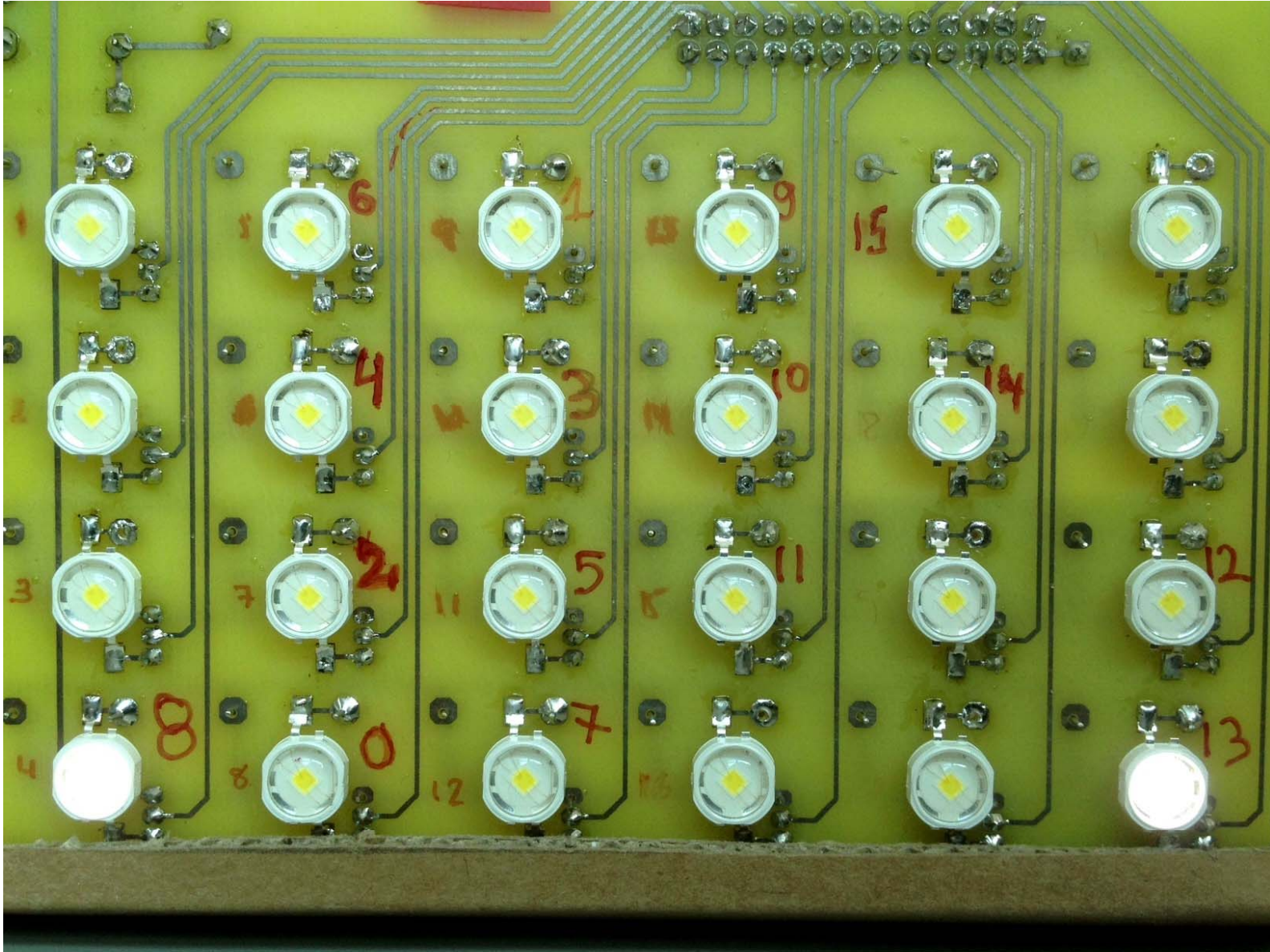


# *SM for Visible Light Communications (12/13)*

$N_t = N_r = 4$ , Rate = 4, 8 bpcu,  $d_{TX} = 0.7$



## *SM for Visible Light Communications (13/13)*



GSSK –VLC transmitter developed by the startup PureVLC

<http://purevlc.com/>

# *Outline*

---

1. Introduction and Motivation behind SM-MIMO
2. History of SM Research and Research Groups Working on SM
3. Transmitter Design – Encoding
4. Receiver Design – Demodulation
5. Error Performance (Numerical Results and Main Trends)
6. Achievable Capacity
7. Channel State Information at the Transmitter
8. Imperfect Channel State Information at the Receiver
9. Multiple Access Interference
10. Energy Efficiency
11. Transmit-Diversity for SM
12. Spatially-Modulated Space-Time-Coded MIMO
13. Relay-Aided SM
14. SM in Heterogeneous Cellular Networks
15. SM for Visible Light Communications
16. **Experimental Evaluation of SM**
17. The Road Ahead – Open Research Challenges/Opportunities
18. Implementation Challenges of SM-MIMO

# Experimental Evaluation of SM (1/31)

- Performance assessment via channel measurements
  - Urban scenario (Bristol/UK) @ 2GHz carrier frequency

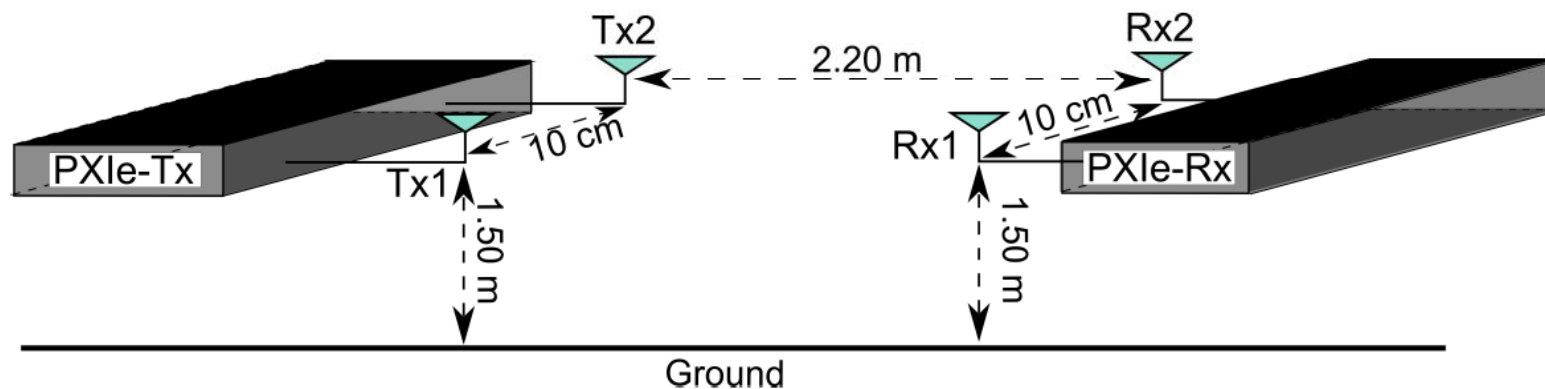


MIMO channel sounder



Post-processing

- Testbed implementation (NI-PXIe-1075 @ Heriot-Watt Univ. / UK)
  - Laboratory environment: 2x2 MIMO @ 2.3GHz carrier frequency

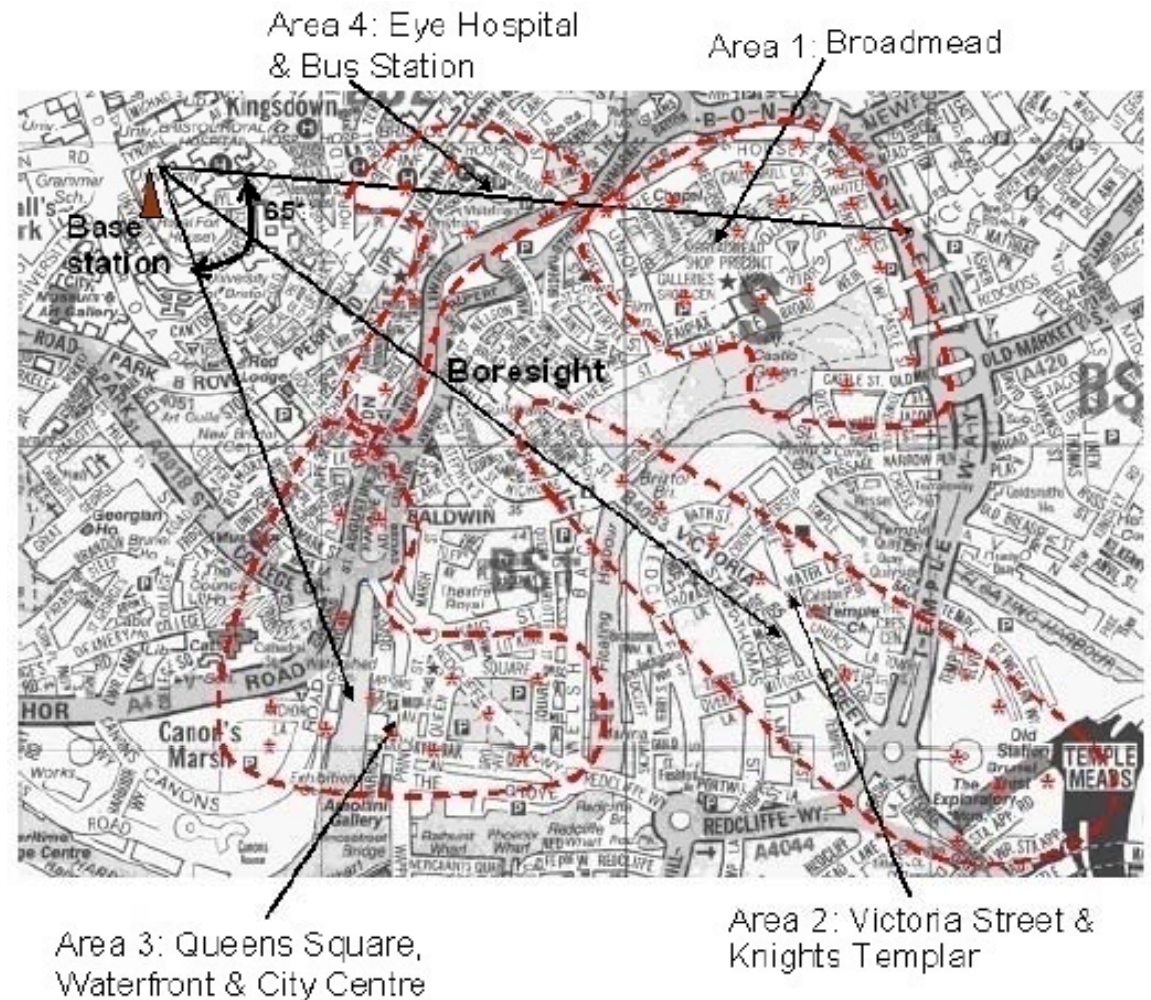




# Experimental Evaluation of SM (2/31)

## Channel Measurements

- ❑ MIMO channel measurements are taken around the center of Bristol city (UK), using a MEDAV RUSK channel sounder
- ❑ The setup consists of a 4×4 MIMO, with 20 MHz bandwidth centered at 2 GHz
- ❑ The transmitter consists of a pair of dual polarized ( $\pm 45^\circ$ ) Racal Xp651772 antennas separated by 2m, positioned atop a building, providing elevated coverage of central business and commercial districts of Bristol city





# *Experimental Evaluation of SM (3/31)*

## Channel Measurements

- ❑ At the receiver, two different receiver devices are used, both equipped with four antennas:
  - A reference headset, which is based on 4-dipoles mounted on a cycle helmet, thus avoiding any shadowing by the user
  - A laptop, which is equipped with 4 Printed Inverted F Antennas (PIFA) fitted inside the back of the display panel



A. Younis, W. Thompson, M. Di Renzo, C.-X. Wang, M. A. Beach, H. Haas, and P. M. Grant, "Performance of Spatial Modulation over Correlated and Uncorrelated Urban Channel Measurements", **IEEE VTC-Fall**, 2013.

# *Experimental Evaluation of SM (4/31)*

---

## **Channel Measurements**

- ❑ 58 measurement locations are chosen around the city
- ❑ At each location the user walked, holding the laptop in front of him and the reference device on his head, in a straight line roughly 6 m long, until 4096 channel snapshots were recorded
- ❑ A second measurement is then taken with the user walking a second path perpendicular to the first
- ❑ As the measurement speed is significantly faster than the coherence time of the channel, the measurements are averaged in groups of four to reduce measurement noise
- ❑ One set of measurement results with the laptop and reference device, and a second set of only the reference device measurements taken at the same locations, but on different days

# *Experimental Evaluation of SM (5/31)*

---

## Channel Measurements

- ❑ This provides a total of 348 different measurement sets, each containing 1024 snapshots of a 4×4 MIMO channel, with 128 frequency bins spanning the 20 MHz bandwidth
- ❑ As the simulations are carried out using flat fading channels, a single frequency bin centered around 2 GHz, is chosen from each measurement snapshot to create the narrowband channel
  
- ❑ Two MIMO test cases are investigated:
  - “**Small-scale**” MIMO, which are the original 4x4 channel measurements
  - “**Large-scale**” MIMO, where, by manipulating the original measurements, larger virtual MIMO systems are created

# *Experimental Evaluation of SM (6/31)*

## Small-Scale MIMO

- ❑ For small-scale MIMO, locations whose channel taps experienced Rayleigh fading are used
- ❑ The chi-squared goodness of fit test, with a significance level of 1%, is used to identify Rayleigh fading channels
- ❑ 20 out of the 348 measurement sets (each containing 1024 snapshots), fulfilled this requirement and are kept for further processing
- ❑ For each location the transmit and receive correlation matrices are estimated, then the decay of the correlation, based on the antenna indices, is fitted to an exponential decay model ( $\gamma$  is the correlation decay coefficient):

$$\mathbf{R} = \begin{bmatrix} 1 & \exp(-\gamma) & \exp(-2\gamma) & \exp(-3\gamma) \\ \exp(-\gamma) & 1 & \exp(-\gamma) & \exp(-2\gamma) \\ \exp(-2\gamma) & \exp(-\gamma) & 1 & \exp(-\gamma) \\ \exp(-3\gamma) & \exp(-2\gamma) & \exp(-\gamma) & 1 \end{bmatrix}$$

# *Experimental Evaluation of SM (7/31)*

---

## Small-Scale MIMO

### ❑ Correlated channels:

- Two measurement sets with the lowest mean square error between the model and the actual correlation matrices are retained. Both of them are from the laptop device
- The measured decay coefficients for the transmitter and receiver are 0.41 and 0.99 for the first channel and 0.36 and 0.75 for the second channel, respectively

### ❑ Uncorrelated channels:

- The two measurement sets with the lowest average correlation coefficient are kept
- One is from the laptop and the other from the reference device



# *Experimental Evaluation of SM (8/31)*

---

## Large-Scale MIMO

- The following post-processing steps are used to create the large-scale channel measurements from the original channel measurements:
  - 1) The original channels are reversed, such that the mobile terminal becomes the transmitting device
  - 2) One channel from each snapshot is kept to form a transmitter of the virtual array. This results in a virtual array with 1024 elements
  - 3) To reduce the correlation between adjacent channels, only 256 elements are kept using a down-sampling factor of 4
  - 4) Only the locations passing the chi-squared goodness of fit test for the Rayleigh fading distribution are kept

## Experimental Evaluation of SM (9/31)

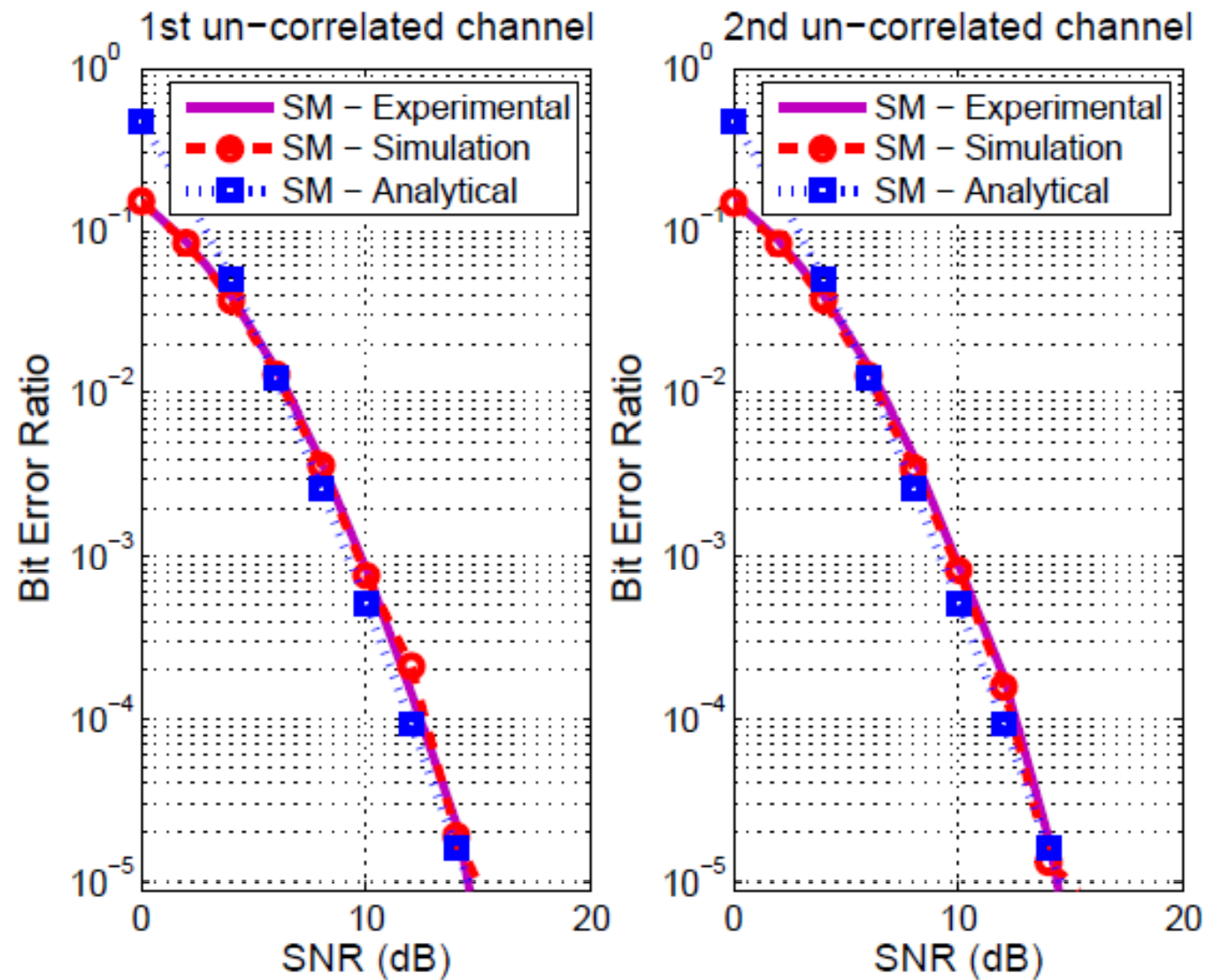


Fig. 1. ABER versus the SNR for SM over an uncorrelated channel.  $m = 4$ ,  $N_t = N_r = 4$ .

## *Experimental Evaluation of SM (10/31)*

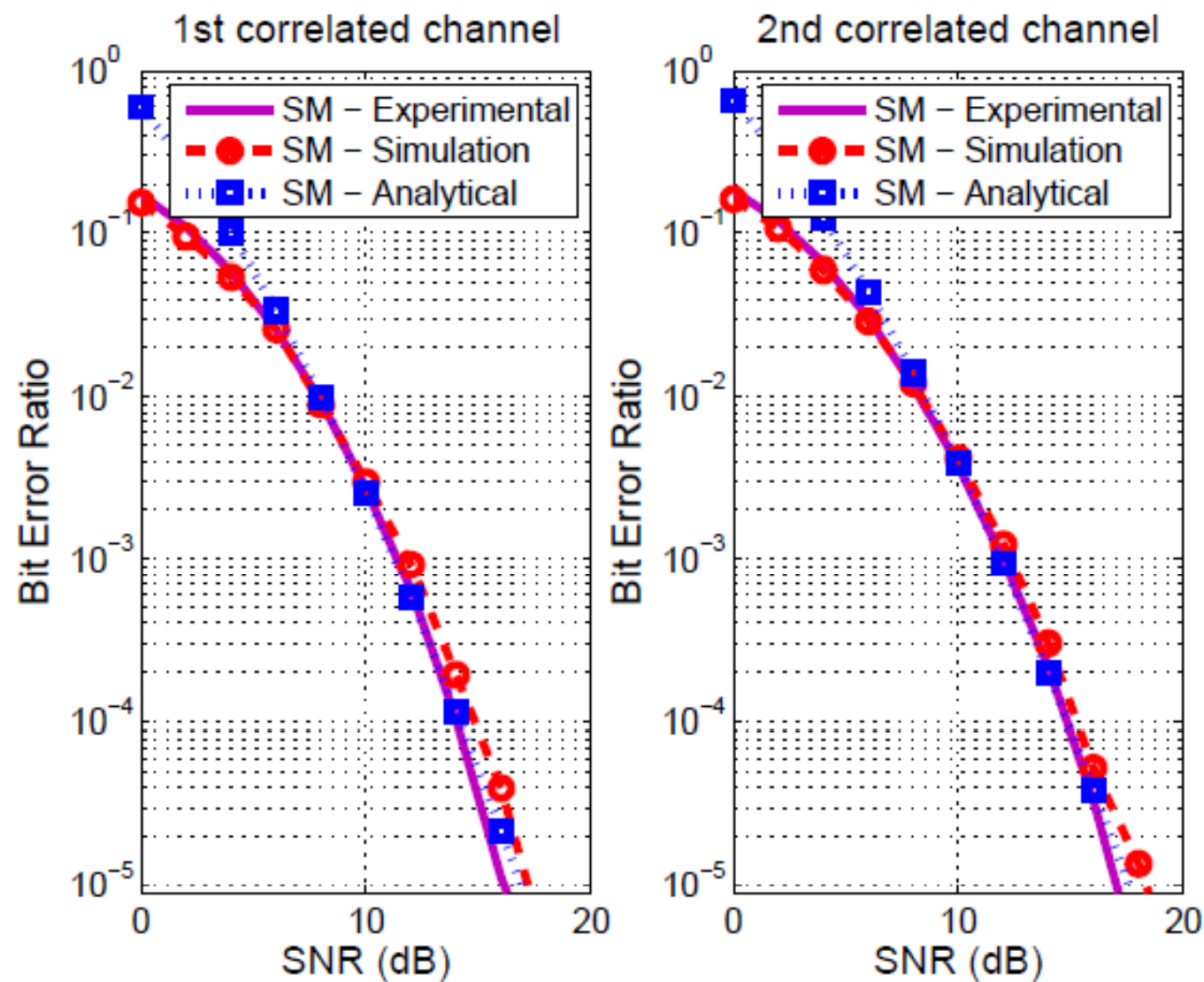


Fig. 2. ABER versus the SNR for SM over a correlated channel.  $m = 4$ ,  $N_t = N_r = 4$ .



## *Experimental Evaluation of SM (11/31)*

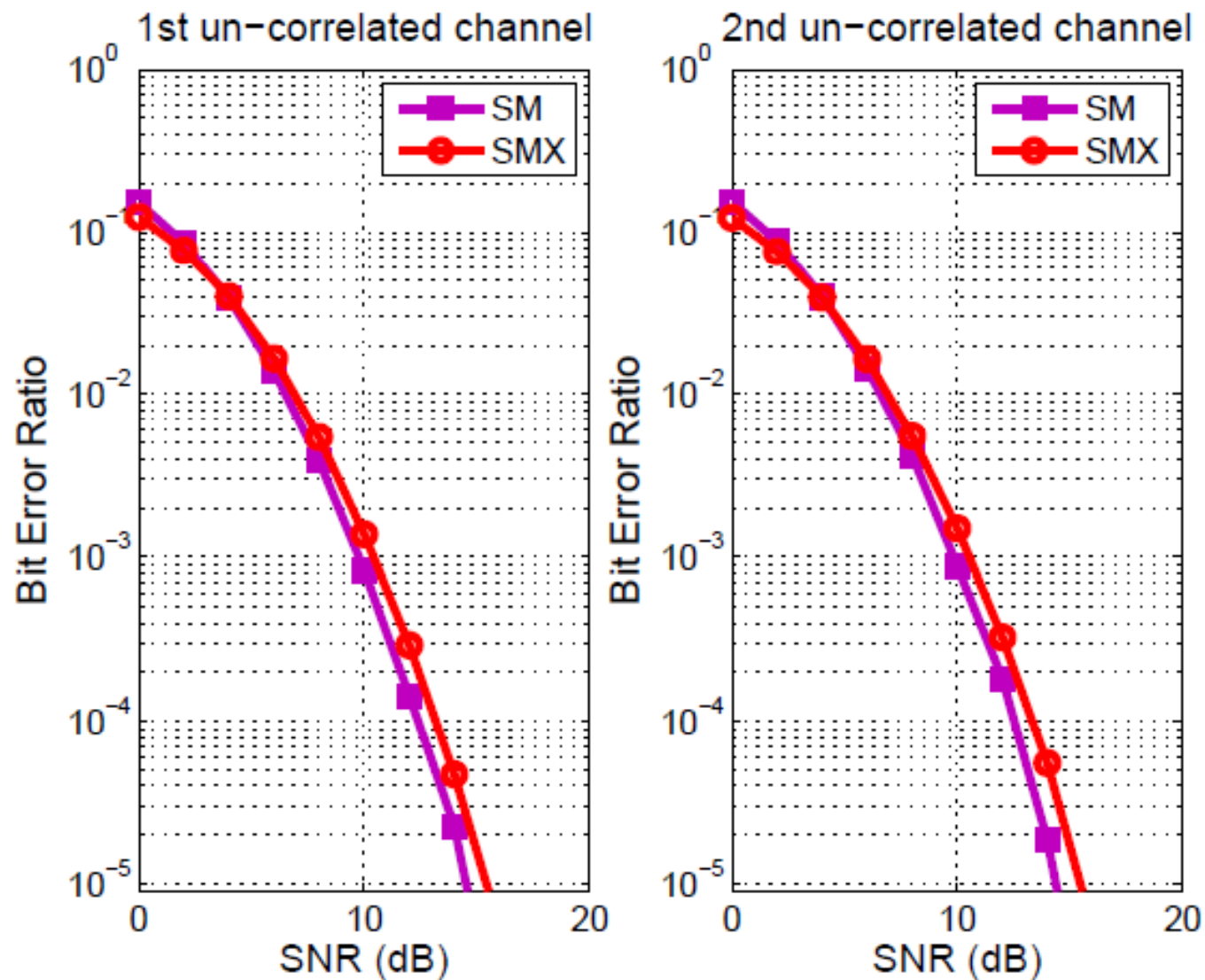


Fig. 3. ABER versus the SNR for SM and SMX over an uncorrelated channel.  $m = 4$ ,  $N_t = N_r = 4$ .

## *Experimental Evaluation of SM (12/31)*

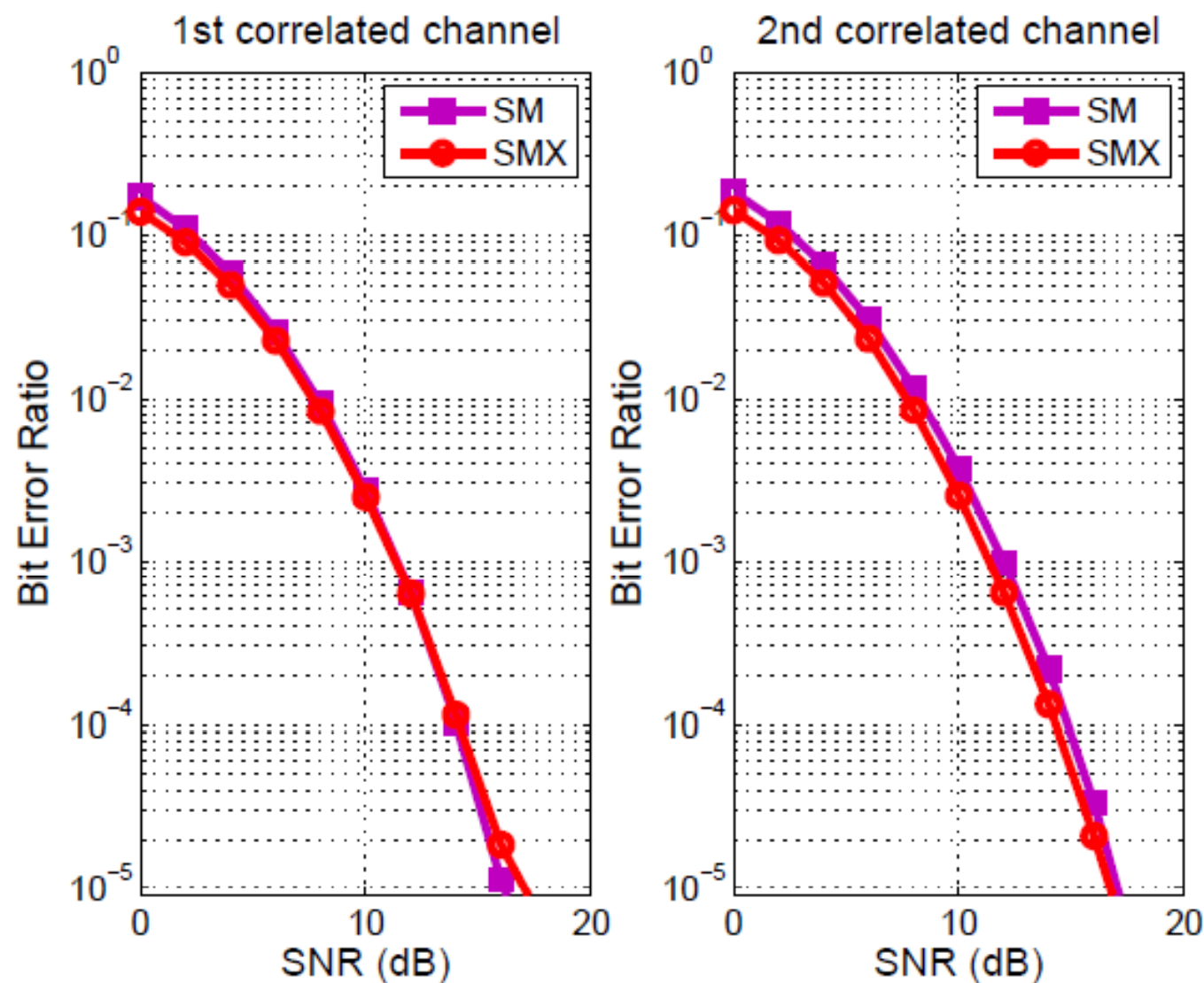


Fig. 4. ABER versus the SNR for SM and SMX over a correlated channel.  
 $m = 4$ ,  $N_t = N_r = 4$ .

# Experimental Evaluation of SM (13/31)

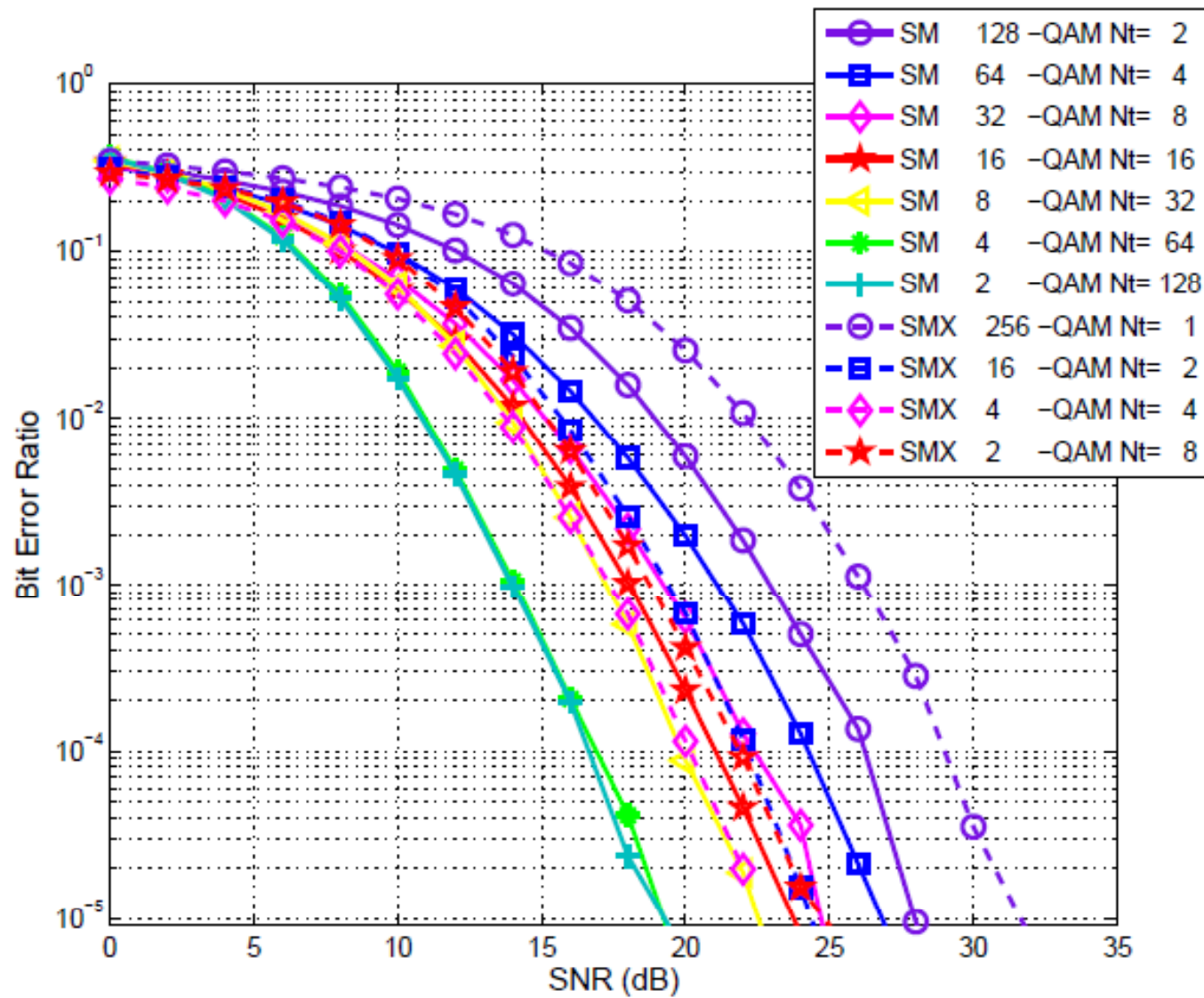
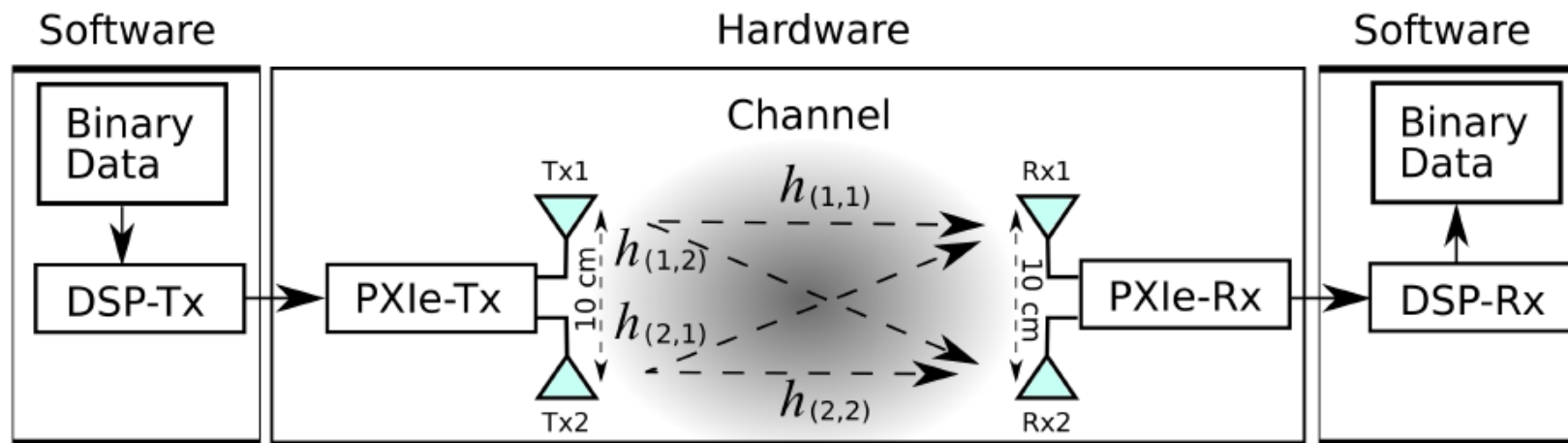


Fig. 5. ABER versus the SNR for SM and SMX over real measured channels.  $m = 8$ ,  $N_r = 4$ .

# Experimental Evaluation of SM (14/31)

## Indoor Testbed



- ❑ The binary data to be broadcast is first passed through the digital signal processing algorithm at the transmitter (DSP-Tx)
- ❑ The processed data is then passed to the physical transmitter on the National Instruments (NI)-PXIe chassis (PXIe-Tx)
- ❑ Each transmit antenna ('Tx1' and 'Tx2') is then activated according to the SM principle at a carrier frequency of 2.3 GHz
- ❑ The receiver then detects and processes the radio frequency (RF) signal in PXIe-Rx. Lastly, the receive side digital signal processing algorithm (DSP-Rx) recovers the original data stream

## *Experimental Evaluation of SM (15/31)*

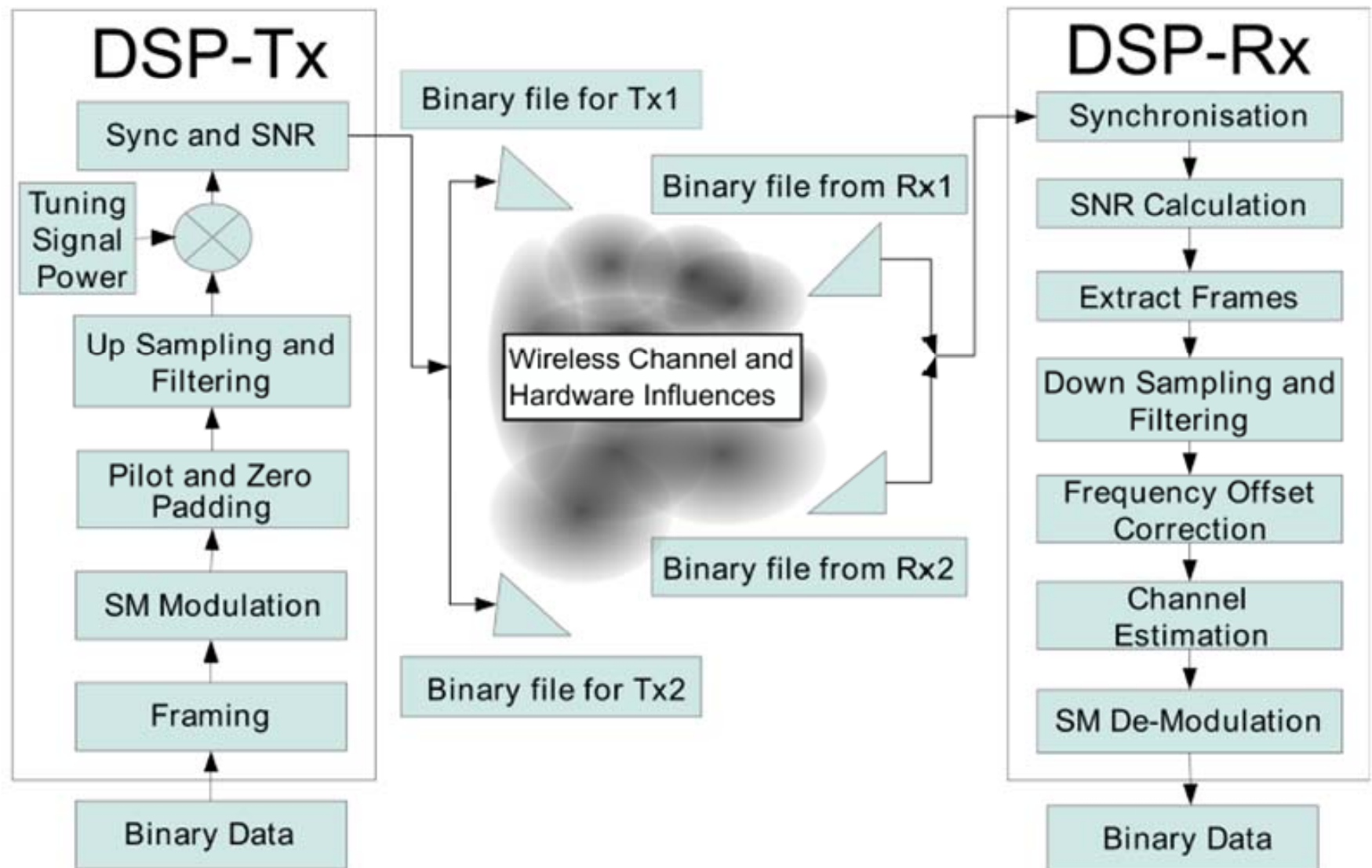


Fig. 3. Binary data encoder (DSP-Tx) and decoder (DSP-Rx) algorithms for SM.

# *Experimental Evaluation of SM (16/31)*

## Antenna Spacing (Line-of-Sight Scenario)

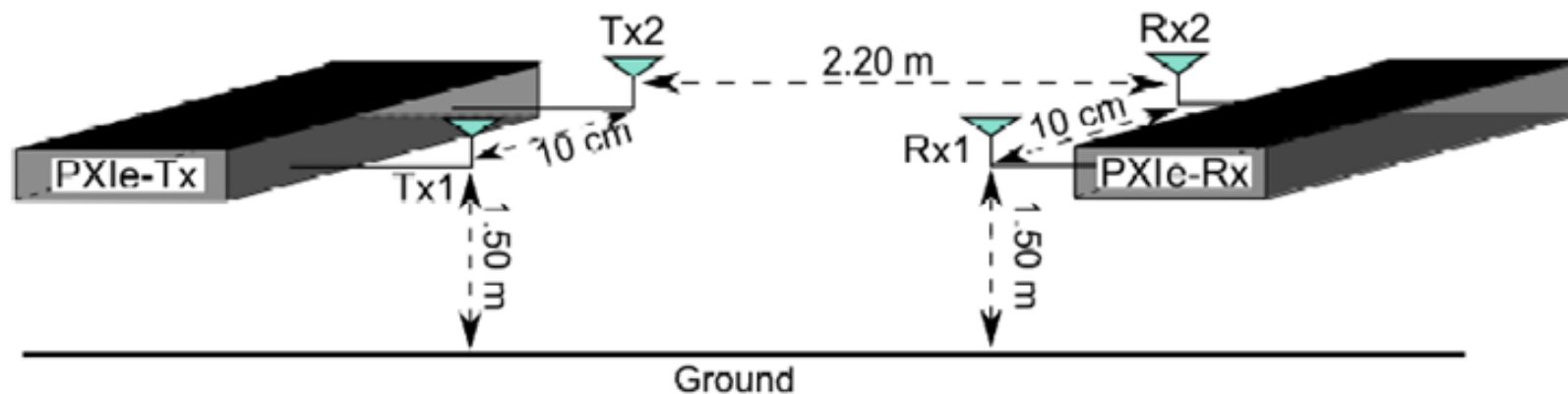


Fig. 4. Physical experimental layout: A pair of receive and a pair of transmit antennas are set 2.2 m apart from each other with a direct line of sight. Each pair of antennas is 1.5 m from the ground and there is a 10 cm spacing between the antennas in a pair corresponding to 0.77 times the wavelength at 2.3 GHz. All antennas are omnidirectional.



# *Experimental Evaluation of SM (17/31)*

---

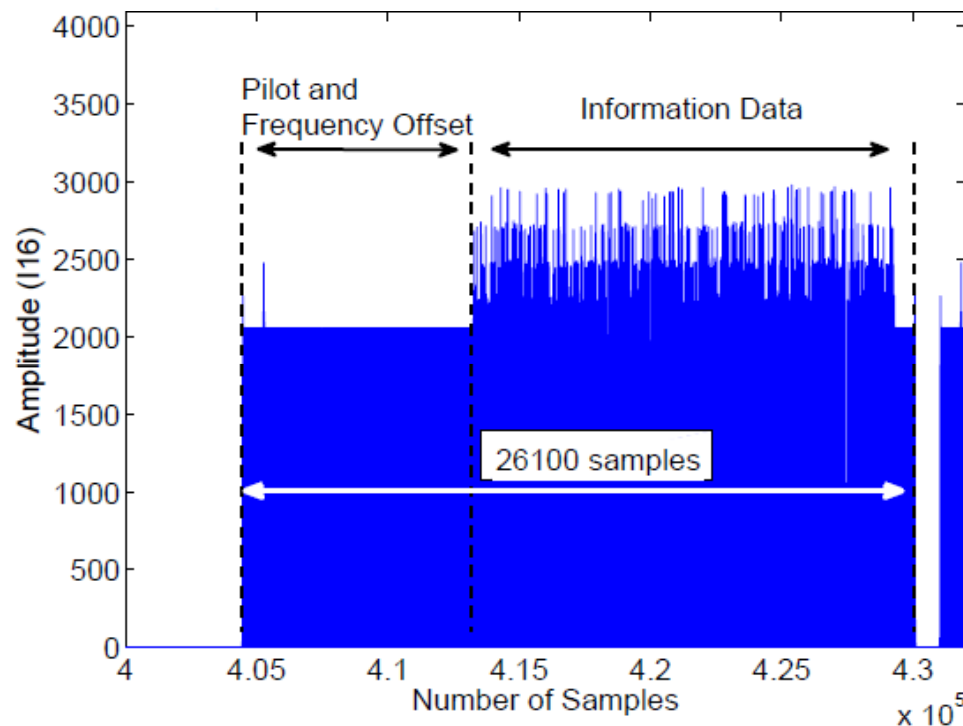
## **Digital Signal Processing for Transmission (DSP-Tx)**

- ❑ The binary data is first split into information segments of appropriate size
- ❑ The information data in each segment is then modulated using SM
- ❑ A pilot signal used for channel estimation is then added, along with a frequency offset estimation section
- ❑ In addition, zero-padding is performed which permits up-sampling of the data while maintaining the same signal power. The up-sampling ratio is set to four and the up-sampled data is then passed through a root raised cosine (RRC) finite impulse response (FIR) filter with 40 taps and a roll-off factor of 0.75. **A large roll-off factor and a long tap-delay are necessary to ensure that the power is focused in a short time, i.e., ensure that only a single RF chain is active**
- ❑ The resulting vector is multiplied with a factor labelled ‘Tuning Signal Power’ to obtain the desired transmit power for the information sequence
- ❑ Frames are created such that the frame length multiplied by the sampling rate is less than the coherence time of the channel which is typically  $\sim 7$  ms for a stationary indoor environment. This ensures that all channel estimations at the receiver are valid for the frame duration

# *Experimental Evaluation of SM (18/31)*

## Digital Signal Processing for Transmission (DSP-Tx)

- A frame includes the frequency offset estimation sequence, the pilot and up-sampled data sequences, as shown below:



- The I16 data format is used, which is a signed 16 bit representation of an integer number
- Each frame has at most 26100 samples

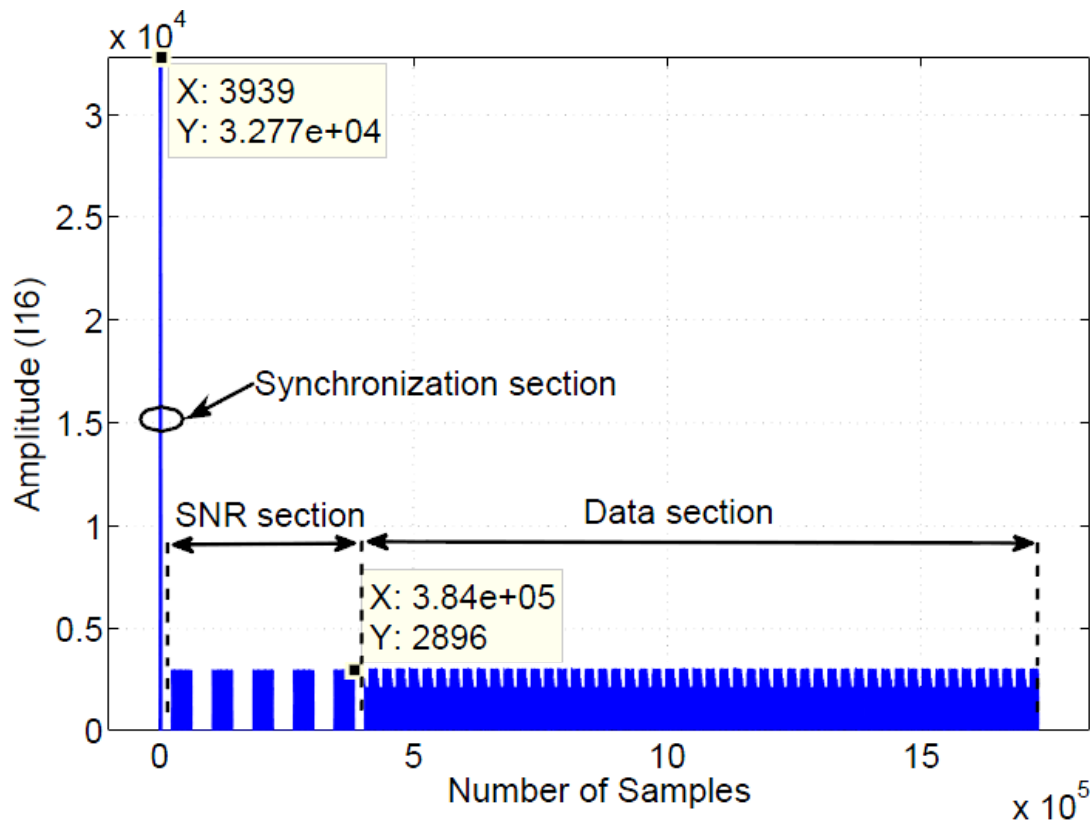
- The 'Data section' is formed from a series of concatenated frames



# Experimental Evaluation of SM (19/31)

## Digital Signal Processing for Transmission (DSP-Tx)

- In particular, the differences between the amplitude of the ‘Pilot and Frequency Offset’ estimation section and the amplitude of the ‘Information Data’ is clearly observable in the figure below:

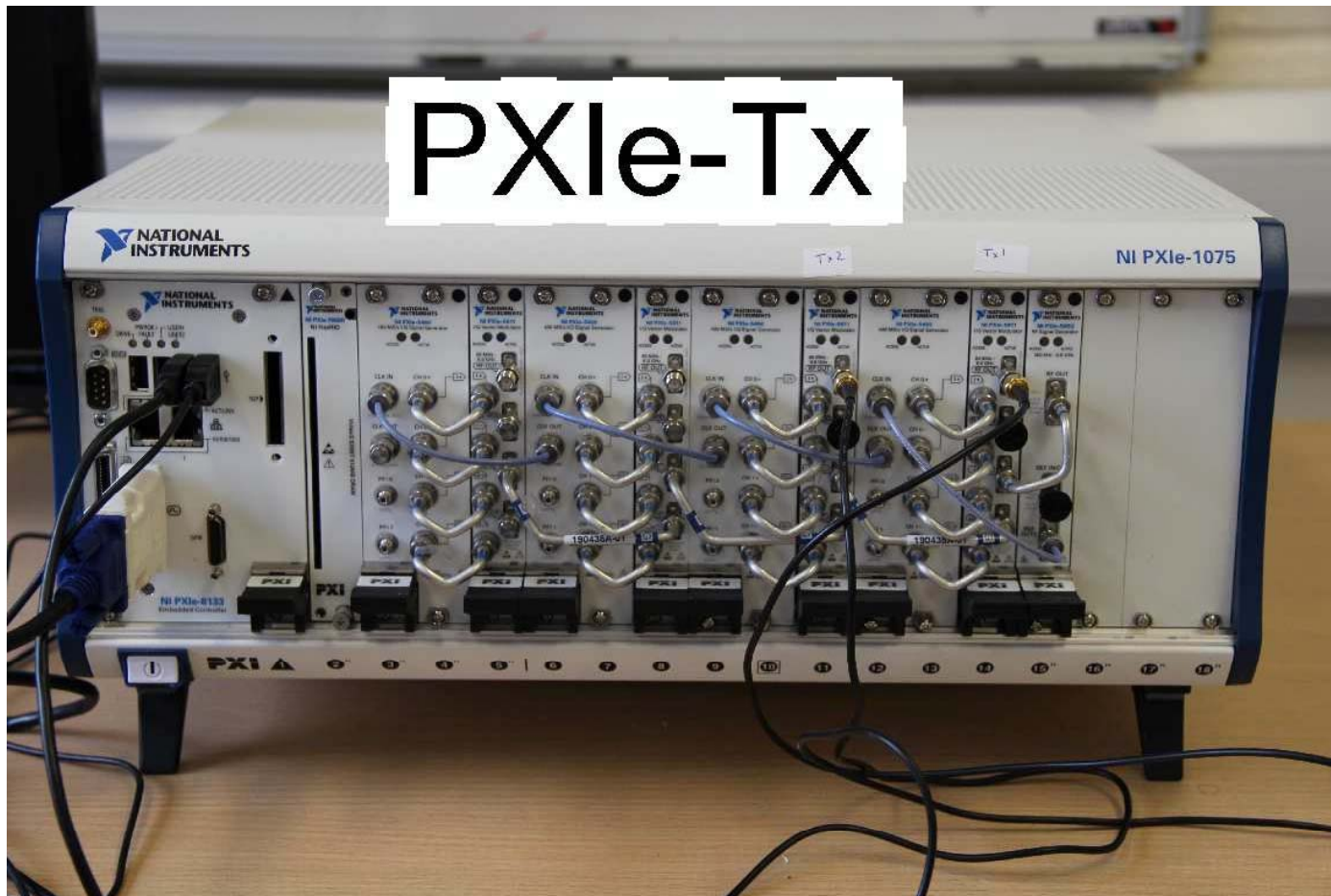


- The synchronization, SNR estimation and data sections are shown
- There is approximately a 21.1 dB difference between the peak power in the synchronization section and the peak power in the SNR estimation and data sections

# *Experimental Evaluation of SM (20/31)*

## Transmission Hardware (PXIe-Tx)

- ❑ NI-PXIe-1075 chassis having on-board an Intel-i7 processor operating at 1.8 GHz with 4GB of RAM



# *Experimental Evaluation of SM (21/31)*

---

## **Transmission Hardware (PXIe-Tx)**

### **❑ NI-PXIe-5450 I/Q Signal Generator**

- 400 Mega samples (Ms)/s, 16-Bit I/Q Signal Generator
- Dual-channel, differential I/Q signal generation
- 512 MB of deep on-board memory
- 16-bit resolution
- 400 Ms/s sampling rate per channel
- $\pm 0.15$  dB flatness to 120 MHz with digital flatness correction
- 140 dBc/Hz phase noise density
- $-160$  dBm/Hz average noise density
- 25 ps channel-to-channel skew

### **❑ NI-PXIe-5652 RF Signal Generator**

- $-110$  dBc/Hz phase noise at 1 GHz and 10 kHz offset typical
- 500 kHz to 6.6 GHz frequency range
- Typically less than 2 ms frequency sweep tuning speed

### **❑ NI-PXIe-5611 intermediate frequency (IF) to carrier RF up-converter**

# *Experimental Evaluation of SM (22/31)*

---

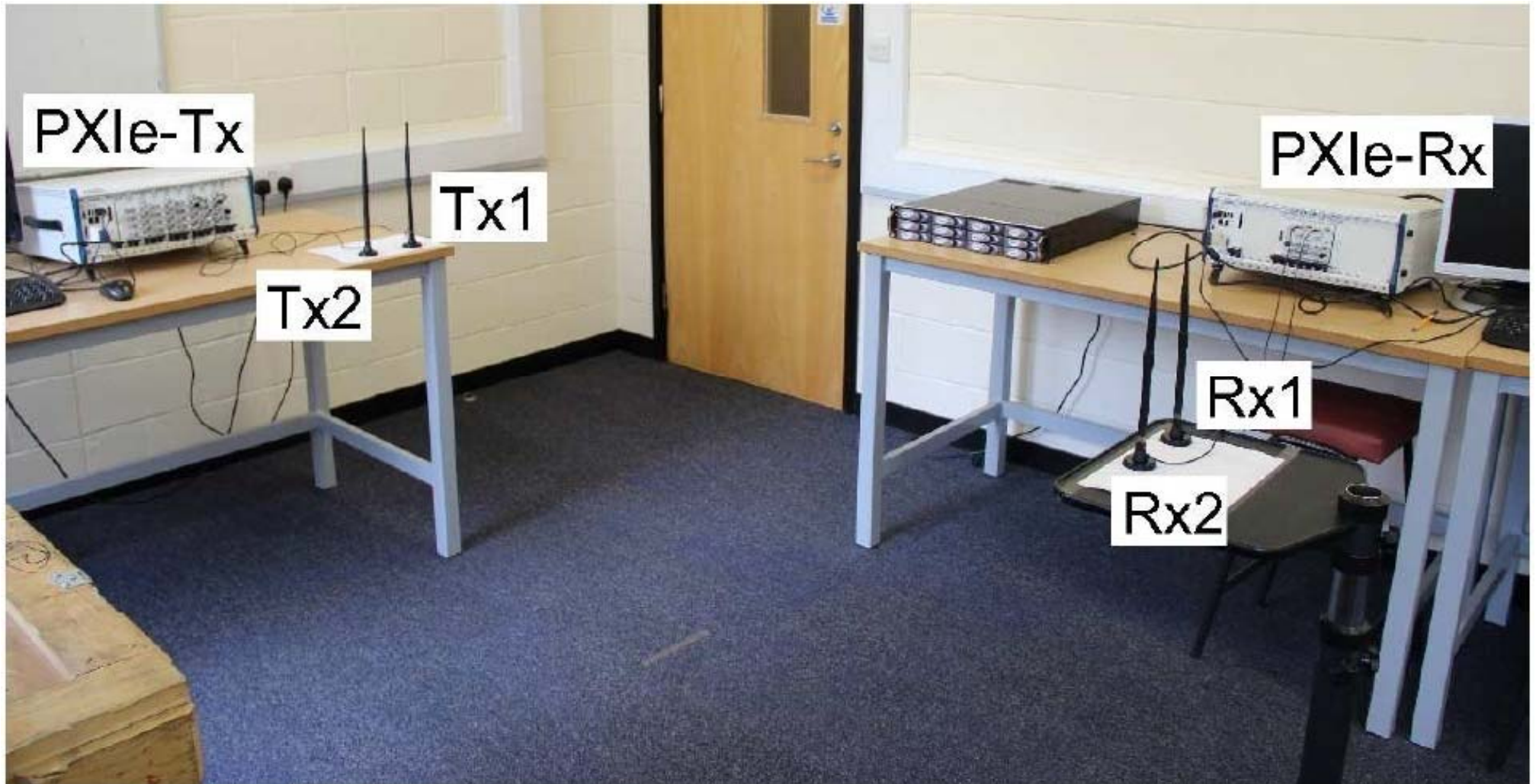
## **Transmission Hardware (PXIe-Tx)**

- ❑ The NI-PXIe-5450 I/Q signal generator is fed with the transmit vector from the binary file generated in Matlab by the encoding DSP-Tx algorithm
- ❑ In particular, the NI-PXIe-5450 I/Q signal generator performs a linear mapping of the signed 16-bit range to the output power and polarization, i.e., peak voltage amplitude is assigned to any value equal to 215 and a linear scale of the voltage amplitude down to zero
- ❑ The output from the NI-PXIe-5450 I/Q signal generator then goes to the NI-PXIe-5652 RF signal generator which is connected to the NI-PXIe-5611 frequency converter
- ❑ The NI-PXIe-5611 outputs the analogue waveform corresponding to the binary data at a carrier frequency of 2.3 GHz
- ❑ Each antenna at the transmitter and receiver contains two quarter-wave dipoles, and one half-wave dipole placed in the middle. All three dipoles are vertically polarized
- ❑ Each antenna has a peak gain of 7 dBi in the azimuth plane, with an omnidirectional radiation pattern. The 10 cm inter-antenna separation is sufficient to guarantee very low, if any, spatial correlation when broadcasting at 2.3 GHz with a 2.2 m separation between the transmitter and receiver



# *Experimental Evaluation of SM (23/31)*

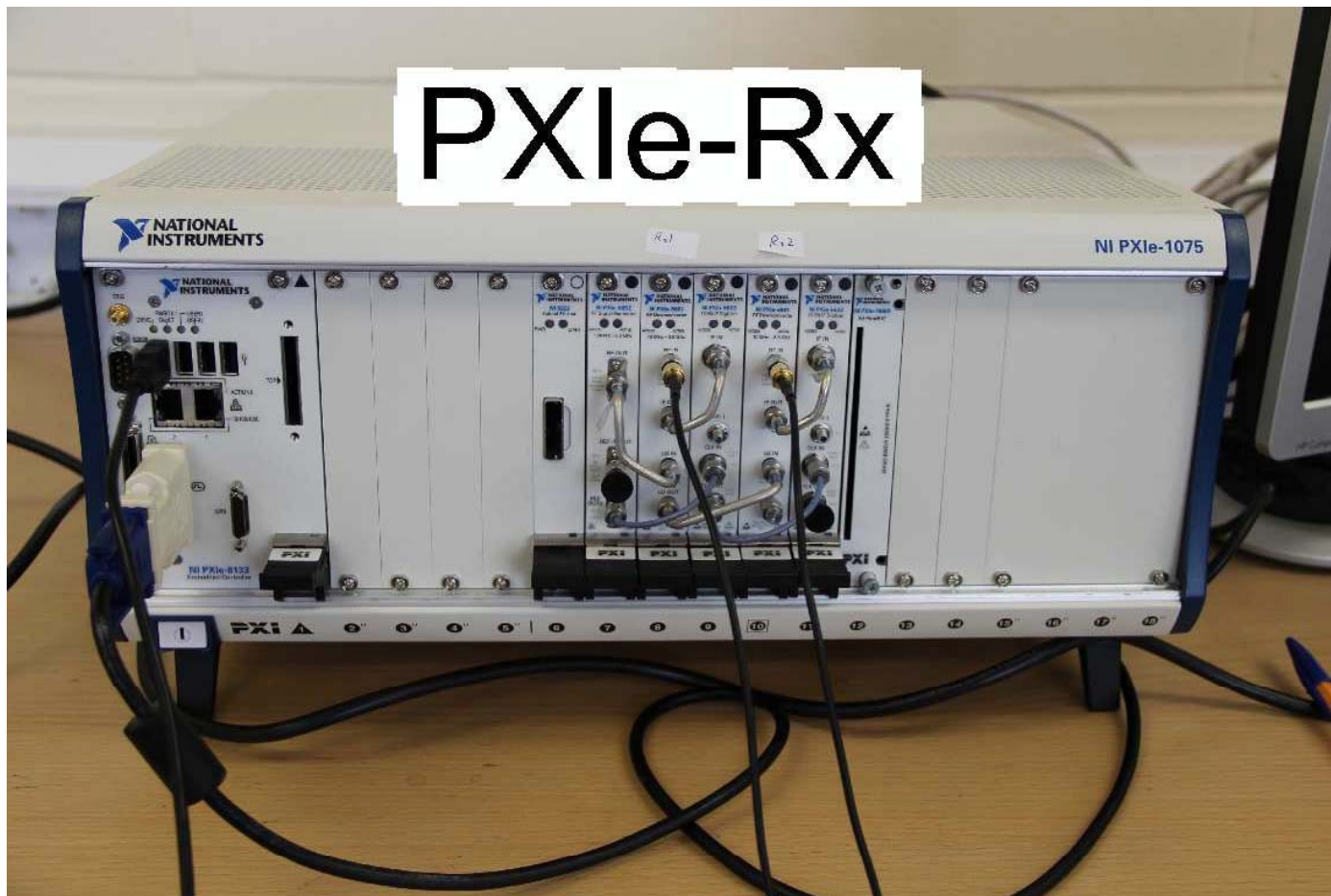
## Laboratory Setup



# *Experimental Evaluation of SM (24/31)*

## Receiver Hardware (PXIe-Rx)

- ❑ **NI-PXIe-1075 chassis** having on-board an Intel-i7 processor operating at 1.8 GHz with 4GB of RAM



# *Experimental Evaluation of SM (25/31)*

---

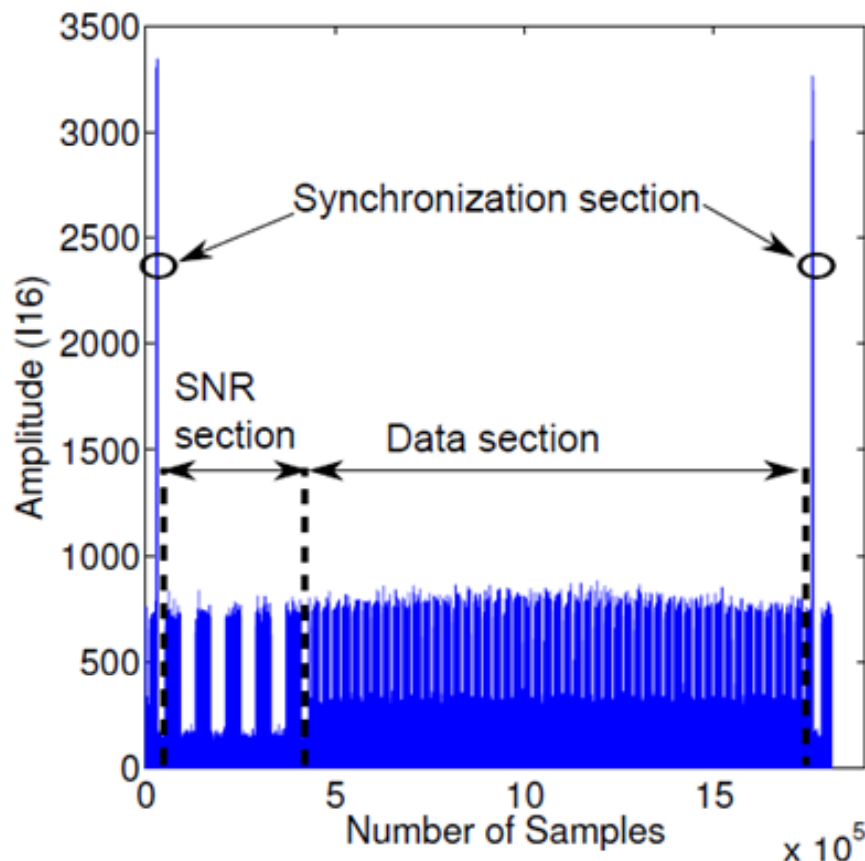
## **Receiver Hardware (PXIe-Rx)**

- ❑ NI-PXIe-5652 on-board reference clock
- ❑ NI-PXIe-5622 16-Bit Digitizer (I16)
  - 150 Ms/s real-time sampling
  - 3 to 250 MHz band in direct path mode, or 50 MHz bandwidth centered at 187.5 MHz
- ❑ NI-PXIe-5601 RF down-converter
- ❑ The receiving antennas are the same as those used for transmission
- ❑ The NIPXIe-5601 RF down-converter is used to detect the analogue RF signal from the antennas
- ❑ The signal is then sent to the NI-PXIe-5622 IF digitizer, which applies its own bandpass filter with a real flat bandwidth equal to  $0.4 \times \text{SampleRate}$ . The sampling rate in the experiment is 10 Ms/s which results in a real flat bandwidth of 4 MHz
- ❑ The NI-PXIe-5622 digitizer is synchronized with the NI-PXIe-5652 on-board reference clock and writes the received binary files
- ❑ The recorded binary files are then processed according to 'DSP-Rx'

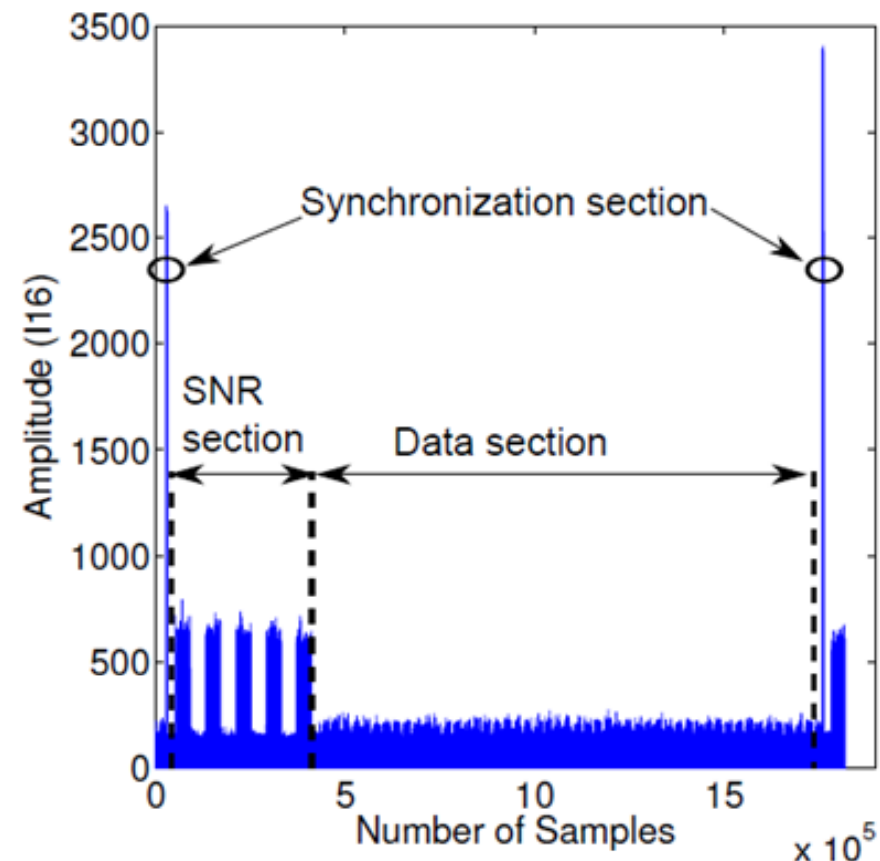
# Experimental Evaluation of SM (26/31)

## Digital Signal Processing for Reception (DSP-Rx)

- ❑ The binary files recorded by the NI-PXIe-5622 digitizer on the PXIe-Rx are converted to Matlab vectors
- ❑ In particular, a sample received vector detected by PXIe-Rx on Rx1 is as follows:



(a) SNR = 30 dB



(b) SNR = 14 dB



# *Experimental Evaluation of SM (27/31)*

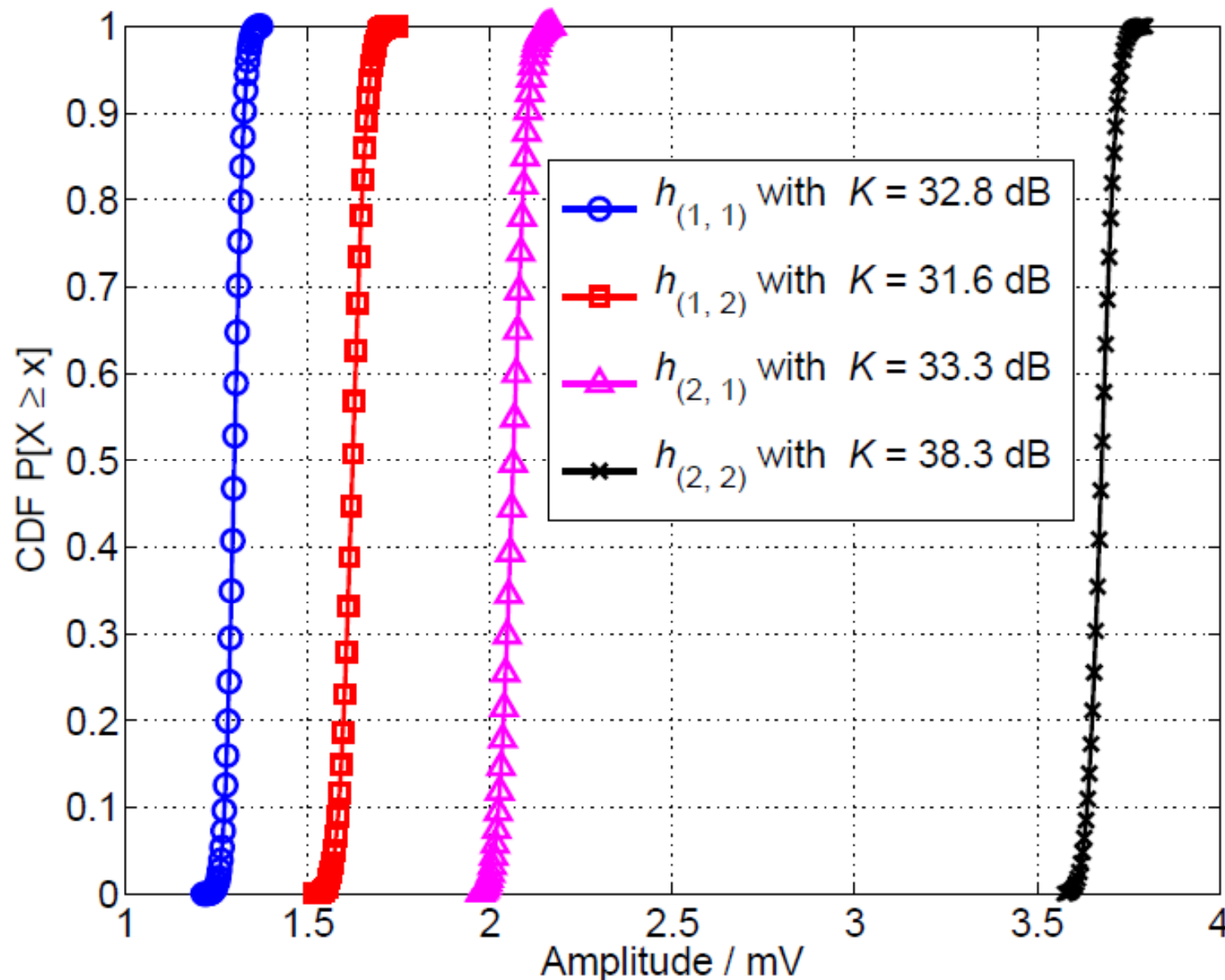
---

## **Digital Signal Processing for Reception (DSP-Rx)**

- ❑ The Matlab vectors are then combined to form a received matrix
- ❑ The detector first finds the beginning of the transmitted sequence by using the synchronization sequence (based on an autocorrelation algorithm)
- ❑ The SNR is then calculated using the 'SNR section'
- ❑ After the SNR for that vector has been determined, each vector is decomposed into its underlying frames
- ❑ Each frame is then down-sampled and passed through the RRC filter which completes the matched-filtering
- ❑ The frequency offset estimation, timing recovery and correction of each frame follows and are performed using state-of-the-art algorithms
- ❑ The pilot signal is then used for channel estimation
- ❑ The remaining data, along with the estimated channels, is finally used to recover an estimated binary sequence (SM maximum-likelihood demodulation )

# Experimental Evaluation of SM (28/31)

## Wireless Channel Characterization



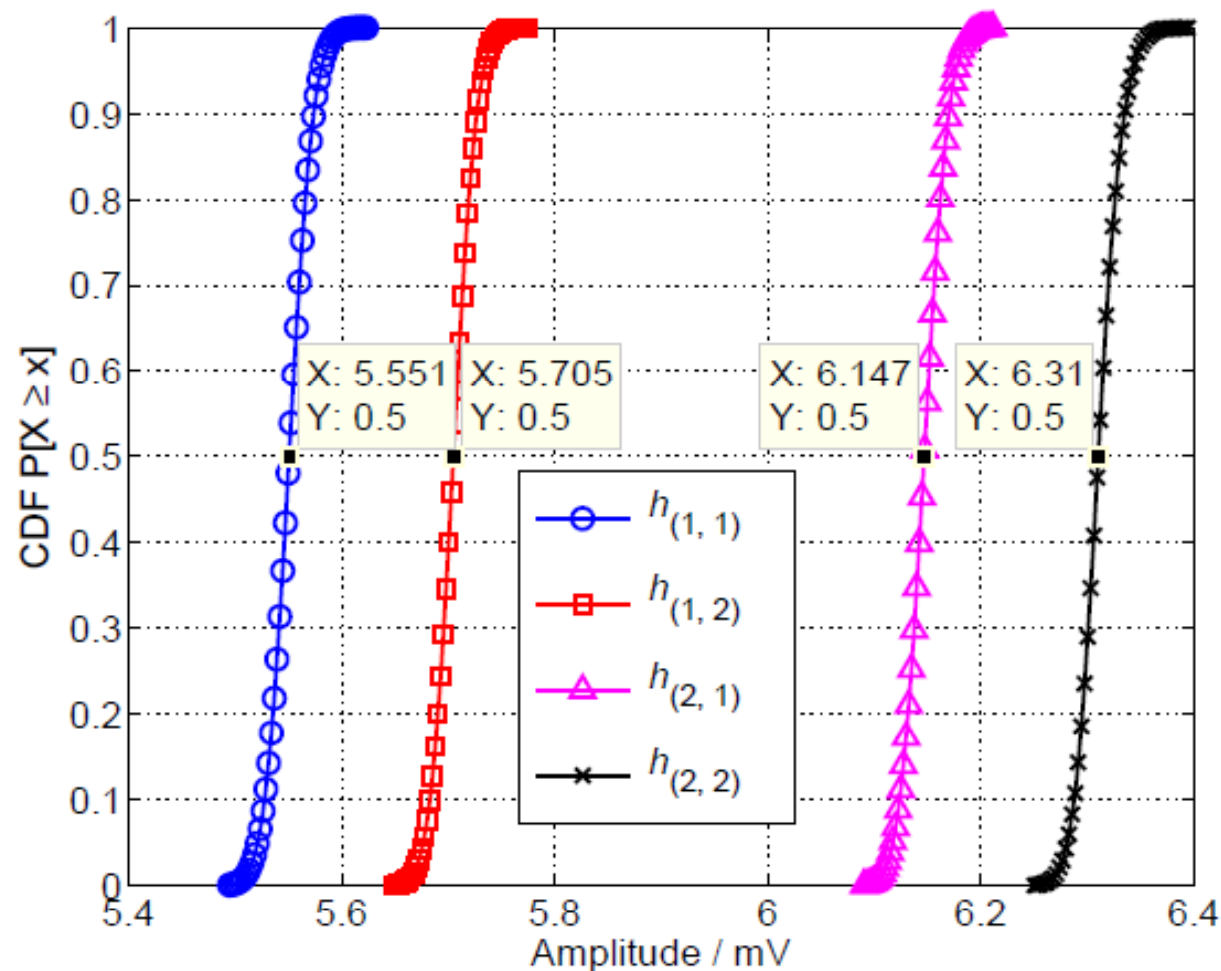
CDFs of the channel coefficients

Each is defined by a Rician distribution with a unique K-factor

The markers denote the measurement points while the lines denote the best fit approximation

## *Experimental Evaluation of SM (29/31)*

### The Wireline Test: RF Chain Mismatch



(b) A coaxial cable with a loss of 10 dB is connected between the transmit and receive antennas.

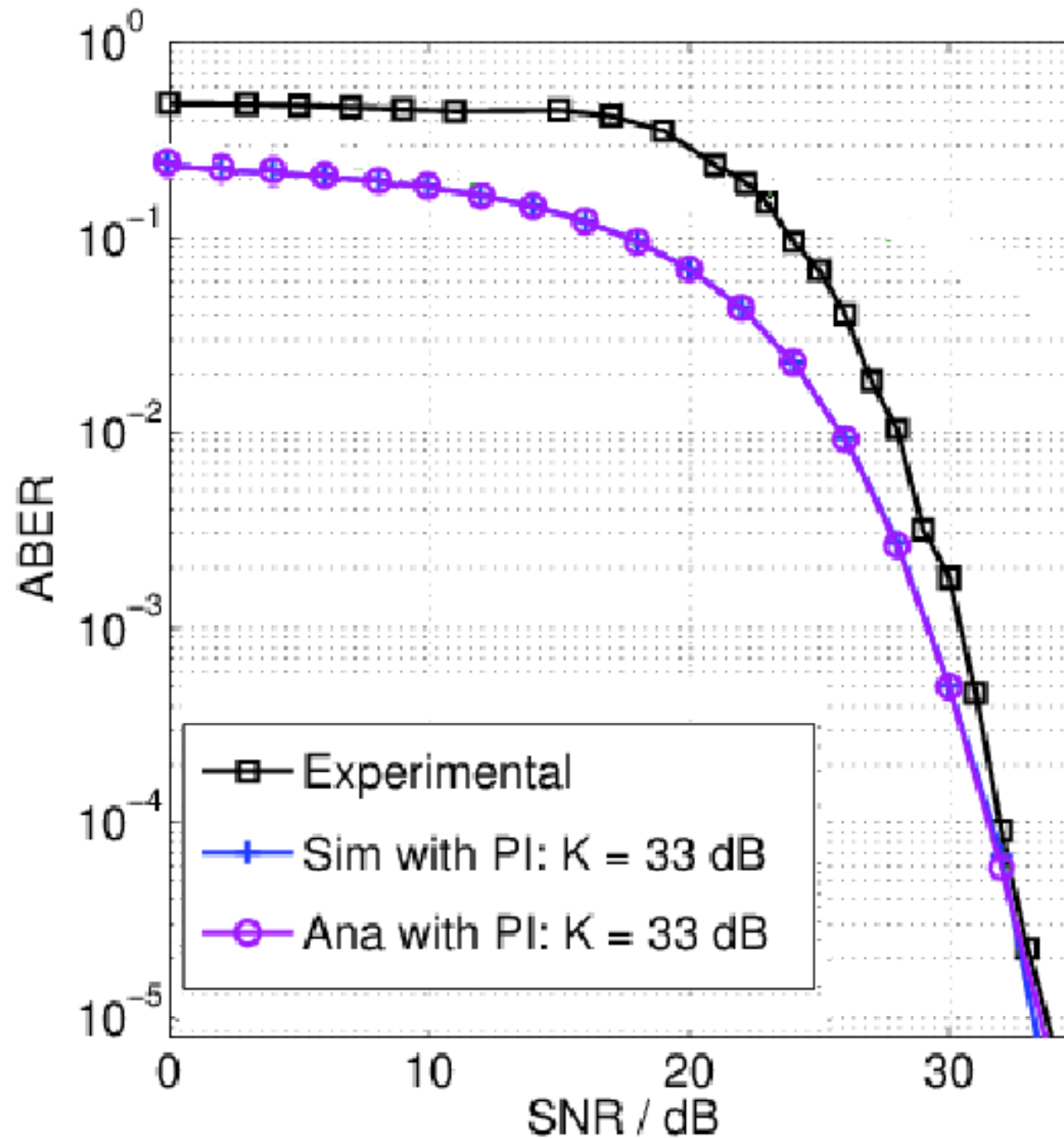
# *Experimental Evaluation of SM (30/31)*

---

## Results

- ❑ A stream of  $10^5$  information bits is sent per transmission to obtain the experimental results
- ❑ The information data is put in 50, 2000 bit, frames
- ❑ The channel is estimated at the beginning and at the end of every frame resulting in 100 channel estimations per transmission
- ❑ The experiment is repeated 1000 times for every SNR point

## *Experimental Evaluation of SM (31/31)*



# *Outline*

---

1. Introduction and Motivation behind SM-MIMO
2. History of SM Research and Research Groups Working on SM
3. Transmitter Design – Encoding
4. Receiver Design – Demodulation
5. Error Performance (Numerical Results and Main Trends)
6. Achievable Capacity
7. Channel State Information at the Transmitter
8. Imperfect Channel State Information at the Receiver
9. Multiple Access Interference
10. Energy Efficiency
11. Transmit-Diversity for SM
12. Spatially-Modulated Space-Time-Coded MIMO
13. Relay-Aided SM
14. SM in Heterogeneous Cellular Networks
15. SM for Visible Light Communications
16. Experimental Evaluation of SM
17. The Road Ahead – Open Research Challenges/Opportunities
18. Implementation Challenges of SM-MIMO

## *The Road Ahead – Open Research Challenges/Opportunities*

---

- ❑ Appraising the Fundamental Trade-Offs of Single- vs. Multi-RF MIMO Designs
- ❑ Large-Scale Implementations: Training Overhead for CSIT/CSIR Acquisition
- ❑ From Single-User Point-to-Point to Multi-User Multi-Cell SM-MIMO Communications
- ❑ Millimeter-Wave Communications: The Need for Beamforming Gains
- ❑ Small Cell Heterogeneous Cellular Networks: Towards Interference Engineering
- ❑ Radio Frequency Energy Harvesting: Taking Advantage of the Idle Antennas
- ❑ Leveraging the Antenna Modulation Principle to a Larger Extent
- ❑ Open Physical-Layer Research Issues

## *The Road Ahead – Open Research Challenges/Opportunities*

---

- ❑ **Point-to-point SM-MIMO** has been studied extensively and little room for significant steps forwards can be expected. However, some important aspects are still not completely understood:
  - Transmit-diversity with single-RF base stations
  - Precoding and CSIT
  - Application to the uplink (co-located antennas)
  - etc...
  
- ❑ **Multi-user SM-MIMO** and understanding the potential of SM in cellular networks have almost been neglected so far. Here major research opportunities can be found:
  - Precoding for multi-user SM-MIMO
  - Application of stochastic geometry and random matrix theory to the analysis and the design of SM in HCNs
  - (Low-complexity) Interference-aware SM-MIMO
  - etc...



## *The Road Ahead – Open Research Challenges/Opportunities*

---

- ❑ Distributed SM-MIMO for uplink applications is still almost unexplored:
  - Advantages and disadvantages against state-of-the-art relaying
  - End-to-end achievable diversity is unknown
  - Error propagation and related low-complexity receiver design
  - etc...
- ❑ Energy efficiency assessment and optimization:
  - The number of RF chains vs. the total number of antennas trade-off is still unclear
  - Fair performance assessment and optimization against state-of-the-art
  - Realistic/fair comparison with massive MIMO
  - etc...
- ❑ Testbed/practical implementation and measurements...

# *Implementation Challenges of SM-MIMO*

---

- ❑ Antenna switching at the symbol time
- ❑ Switching loss characterization
- ❑ Reconfigurable single-RF antenna design to create unique channel signatures
- ❑ Bandwidth efficient finite-duration pulse shaping
- ❑ Large-scale antenna-array implementation and electromagnetic compatibility assessment
- ❑ Multi-carrier SM-MIMO
- ❑ Efficient channel estimation with single-RF transmitters
- ❑ Sampling time and quantization errors if orthogonal shaping filters are used
- ❑ etc...

# *Thank You for Your Attention*

---

□ We gratefully acknowledge the support of:

- The European Union (ITN-GREENET project, grant 264759)
- The Engineering and Physical Sciences Research Council (EPSRC), UK
- The Laboratory of Signals and Systems (“Jeunes Chercheurs 2010”), France
- The UK-China Science Bridges: R&D on (B)4G Wireless Mobile Communications
- The Italian Inter-University Consortium for Telecommunications (CNIT), Italy
- The European Union (ITN-CROSSFIRE project, grant 317126)
- EADS Deutschland GmbH, Germany



M. Di Renzo



H. Haas



A. Ghrayeb

## *Further Readings (1/3)*

---

- ❑ R. Y. Mesleh, H. Haas, S. Sinanovic, C. W. Ahn, and S. Yun, “Spatial modulation”, IEEE Trans. Veh. Technol., vol. 57, no. 4, pp. 2228-2241, July 2008.
- ❑ J. Jeganathan, A. Ghrayeb, and L. Szczecinski, “Spatial modulation: Optimal detection and performance analysis”, IEEE Commun. Lett., vol. 12, no. 8, pp. 545-547, Aug. 2008.
- ❑ J. Jeganathan, A. Ghrayeb, L. Szczecinski, and A. Ceron, “Space shift keying modulation for MIMO channels”, IEEE Trans. Wireless Commun., vol. 8, no. 7, pp. 3692-3703, July 2009.
- ❑ N. Serafimovski, M. Di Renzo, S. Sinanovic, R. Y. Mesleh, and H. Haas, “Fractional bit encoded spatial modulation (FBE-SM)”, IEEE Commun. Lett., vol. 14, no. 5, pp. 429-431, May 2010.
- ❑ M. Di Renzo and H. Haas, “Improving the performance of space shift keying (SSK) modulation via opportunistic power allocation”, IEEE Commun. Lett., vol. 14, no. 6, pp. 500-502, June 2010.
- ❑ R. Y. Mesleh, M. Di Renzo, H. Haas, and P. M. Grant, “Trellis coded spatial modulation”, IEEE Trans. Wireless Commun., vol. 9, no. 7, pp. 2349-2361, July 2010.
- ❑ M. Di Renzo and H. Haas, “A general framework for performance analysis of space shift keying (SSK) modulation for MISO correlated Nakagami-m fading channels”, IEEE Trans. Commun., vol. 58, no. 9, pp. 2590-2603, Sep. 2010.
- ❑ M. Di Renzo and H. Haas, “Space shift keying (SSK) modulation with partial channel state information: Optimal detector and performance analysis over fading channels”, IEEE Trans. Commun., vol. 58, no. 11, pp. 3196-3210, Nov. 2010.
- ❑ M. Di Renzo and H. Haas, “Space shift keying (SSK-) MIMO over correlated Rician fading channels: Performance analysis and a new method for transmit-diversity”, IEEE Trans. Commun., vol. 59, no. 1, pp. 116-129, Jan. 2011.

## *Further Readings (2/3)*

---

- ❑ M. Di Renzo and H. Haas, “Bit error probability of space shift keying MIMO over multiple-access independent fading channels”, *IEEE Trans. Veh. Technol.*, vol. 60, no. 8, pp. 3694-3711, Oct. 2011.
- ❑ M. Di Renzo and H. Haas, “Bit error probability of space modulation over Nakagami-m fading: Asymptotic analysis”, *IEEE Commun. Lett.*, vol. 15, no. 10, pp. 1026-1028, Oct. 2011.
- ❑ M. Di Renzo, H. Haas, and P. M. Grant, “Spatial modulation for multiple-antenna wireless systems: A survey”, *IEEE Commun. Mag.*, vol. 49, no. 12, pp. 182-191, Dec. 2011.
- ❑ M. Di Renzo and H. Haas, “Bit error probability of SM-MIMO over generalized fading channels”, *IEEE Trans. Veh. Technol.*, vol. 61, no. 3, pp. 1124-1144, Mar. 2012.
- ❑ M. Di Renzo, D. De Leonardis, F. Graziosi, and H. Haas, “Space shift keying (SSK-) MIMO with practical channel estimates”, *IEEE Trans. Commun.*, vol. 60, no. 4, pp. 998-1012, Apr. 2012.
- ❑ N. Serafimovski, S. Sinanovic, M. Di Renzo, and H. Haas, “Multiple Access Spatial Modulation”, *EURASIP J. Wireless Communications and Networking*, September 2012.
- ❑ K. Ntontin, M. Di Renzo, A. Perez-Neira and C. Verikoukis, “Adaptive Generalized Space Shift Keying”, *EURASIP J. Wireless Communications and Networking*, vol 2013, Feb. 2013.
- ❑ M. Di Renzo and H. Haas, “On Transmit–Diversity for Spatial Modulation MIMO: Impact of Spatial–Constellation Diagram and Shaping Filters at the Transmitter”, *IEEE Trans. Veh. Technol.*, vol. 62, no. 6, pp. 2507–2531, July 2013
- ❑ A. Younis, S. Sinanovic, M. Di Renzo, and H. Haas, “Generalized Sphere Decoding for Spatial Modulation”, *IEEE Trans. Commun.*, Vol. 61, No. 7, pp. 2805–2815, July 2013.
- ❑ N. Serafimovski, A. Younis, R. Mesleh, P. Chambers, M. Di Renzo, C.–X. Wang, P. M. Grant, M. A. Beach, H. Haas, “Practical Implementation of Spatial Modulation”, *IEEE Trans. Veh. Technol.*, 2013, to appear. [Online]. Available: IEEE Xplore Early Access.

## *Further Readings (3/3)*

---

- ❑ W. Thompson, M. Beach, J. McGeehan, A. Younis, H. Haas, P. Grant, P. Chambers, Z. Chen, C.-X. Wang, and M. Di Renzo, “Spatial modulation explained and routes for practical evaluation”, COST 2100 TD(11)02047, Lisbon, Portugal, Oct. 19-21, 2011. [Online]. Available: [http://www.ukchinab4g.ac.uk/sites/default/files/5\\_Achievements/conference/TD\(11\)02047.pdf](http://www.ukchinab4g.ac.uk/sites/default/files/5_Achievements/conference/TD(11)02047.pdf).

### ❑ YouTube:

- Spatial Modulation  
(<http://www.youtube.com/watch?v=cPKIbxrEDho>)
- The Advantages of Spatial Modulation  
(<http://www.youtube.com/watch?v=baKkBxzf4fY>)
- The World's First Spatial Modulation Demonstration  
(<http://www.youtube.com/watch?v=a6yUuJFUtZ4>)

## *Further Readings – From Other Research Groups (1/3)*

---

- ❑ Y. Yang and B. Jiao, “Information-guided channel-hopping for high data rate wireless communication”, *IEEE Commun. Lett.*, vol. 12, no. 4, pp. 225–227, Apr. 2008.
- ❑ S. Sugiura, S. Chen, and L. Hanzo, “Coherent and differential space-time shift keying: A dispersion matrix approach”, *IEEE Trans. Commun.*, vol. 58, no. 11, pp. 3219–3230, Nov. 2010.
- ❑ S. Chen, S. Sugiura, and L. Hanzo, “Semi-blind joint channel estimation and data detection for space-time shift keying systems”, *IEEE Sig. Process. Lett.*, vol. 17, no. 12, pp. 993–996, Dec. 2010.
- ❑ Y. Yang and S. Aissa, “Bit-padding information guided channel hopping”, *IEEE Commun. Lett.*, vol. 15, no. 2, pp. 163–165, Feb. 2011.
- ❑ C. Xu, S. Sugiura, S. X. Ng, and L. Hanzo, “Reduced-complexity noncoherently detected differential space-time shift keying”, *IEEE Sig. Process. Lett.*, vol. 18, no. 3, pp. 153–156, Mar. 2011.
- ❑ H. A. Ngo, C. Xu, S. Sugiura, and L. Hanzo, “Space-time-frequency shift keying for dispersive channels”, *IEEE Sig. Process. Lett.*, vol. 18, no. 3, pp. 177–180, Mar. 2011.
- ❑ E. Basar, U. Aygolu, E. Panayirci, and H. V. Poor, “Space-time block coded spatial modulation”, *IEEE Trans. Commun.*, vol. 59, no. 3, pp. 823–832, Mar. 2011.
- ❑ S. Sugiura, S. Chen, and L. Hanzo, “Generalized space-time shift keying designed for flexible diversity-, multiplexing- and complexity-tradeoffs”, *IEEE Trans. Wireless Commun.*, vol. 10, no. 4, pp. 1144–1153, Apr. 2011.
- ❑ S. Sugiura, S. Chen, H. Haas, P. M. Grant, and L. Hanzo, “Coherent versus non-coherent decode-and-forward relaying aided cooperative space-time shift keying”, *IEEE Trans. Commun.*, vol. 59, no. 6, pp. 1707–1719, June 2011.



## *Further Readings – From Other Research Groups (2/3)*

---

- ❑ P. Yang, Y. Xiao, Yi Y., and S. Li, “Adaptive spatial modulation for wireless MIMO transmission systems”, *IEEE Commun. Lett.*, vol. 15, no. 6, pp. 602–604, June 2011.
- ❑ D. Yang, C. Xu, L.–L. Yang, and L. Hanzo, “Transmit–diversity–assisted space–shift keying for colocated and distributed/cooperative MIMO elements”, *IEEE Trans. Veh. Technol.*, vol. 60, no. 6, pp. 2864–2869, July 2011.
- ❑ E. Basar, U. Aygolu, E. Panayirci, and H. V. Poor, “New trellis code design for spatial modulation”, *IEEE Trans. Wireless Commun.*, vol. 10, no. 8, pp. 2670–2680, Aug. 2011.
- ❑ C. Xu, S. Sugiura, S. X. Ng, and L. Hanzo, “Reduced–complexity soft–decision aided space–time shift keying”, *IEEE Sig. Proces. Lett.*, vol. 18, no. 10, pp. 547–550, Oct. 2011.
- ❑ S. Sugiura, C. Xu, S. X. Ng, and L. Hanzo, “Reduced–complexity coherent versus non–coherent QAM–aided space–time shift keying”, *IEEE Trans. Commun.*, vol. 59, no. 11, pp. 3090–3101, Nov. 2011.
- ❑ J. Wang, S. Jia, and J. Song, “Signal vector based detection scheme for spatial modulation”, *IEEE Commun. Lett.*, vol. 16, no. 1, pp. 19–21, Jan. 2012.
- ❑ L.–L. Yang, “Signal detection in antenna–hopping space–division multiple–access systems with space–shift keying modulation”, *IEEE Trans. Sig. Process.*, vol. 60, no. 1, pp. 351–366, Jan. 2012.
- ❑ E. Basar, U. Aygolu, E. Panayirci, and H. V. Poor, “Performance of spatial modulation in the presence of channel estimation errors”, *IEEE Commun. Lett.*, vol. 16, no. 2, pp. 176–179, Feb. 2012.
- ❑ S. S. Ikki and R. Mesleh, “A general framework for performance analysis of space shift keying (SSK) modulation in the presence of gaussian imperfect estimations”, *IEEE Commun. Lett.*, vol. 16, no. 2, pp. 228–230, Feb. 2012.



## *Further Readings – From Other Research Groups (3/3)*

---

- ❑ R. Y. Chang, S.-J. Lin, and W.-H. Chung, “New space shift keying modulation with hamming code-aided constellation design”, *IEEE Wireless Commun. Lett.*, vol. 1, no. 1, pp. 2–5, Feb. 2012.
- ❑ J. Wang, S. Jia, and J. Song, “Generalised spatial modulation system with multiple active transmit antennas and low complexity detection scheme”, *IEEE Trans. Wireless Commun.*, vol. 11, no. 4, pp. 1605–1615, Apr. 2012.
- ❑ S. Sugiura, S. Chen, and L. Hanzo, “A universal space-time architecture for multiple-antenna aided systems”, *IEEE Commun. Surveys Tuts.*, vol. 14, no. 2, pp. 401–420, 2nd quarter 2012.